

**COLOUR REMOVAL FROM DYE HOUSE  
EFFLUENTS USING ZERO VALENT IRON  
AND FENTON OXIDATION**

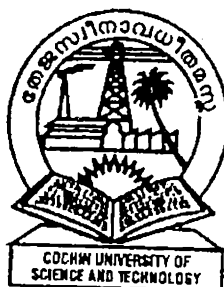
**THESIS SUBMITTED TO THE  
COCHIN UNIVERSITY OF SCIENCE AND  
TECHNOLOGY**

**IN PARTIAL FULFILLMENT OF THE REQUIREMENTS**

**FOR THE DEGREE OF  
DOCTOR OF PHILOSOPHY**

**BY**

**V.G.RAJESH BABU**



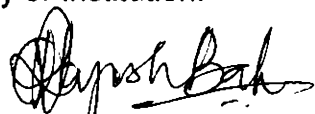
**SCHOOL OF ENVIRONMENTAL STUDIES  
COCHIN UNIVERSITY OF SCIENCE AND TECHNOLOGY  
COCHIN - 682016  
DECEMBER 2003**

*Dedicated to my beloved parents...*

## DECLARATION

I, V.G.Rajesh Babu do hereby declare that the thesis entitled “ **Colour Removal From Dye-House Effluents Using Zero-Valent Iron and Fenton Oxidation**” is a genuine record of research work done by me under the supervision of Dr. V.N.Sivasankara Pillai, Professor, School of Environmental Studies, Cochin University of Science and Technology and has not been previously, formed a basis for the award of any degree, diploma, associate ship, fellowship or other similar title of any University or Institution.

Cochin – 16  
December 2003



V.G. Rajesh Babu

## **CERTIFICATE**

This is to certify that the thesis is an authentic record of the research work carried out by Sri. V.G.Rajesh Babu, under my supervision and guidance in the School of Environmental Studies, Cochin University of Science and Technology in partial fulfillment of the requirement for the degree of Doctor of Philosophy and no part thereof has been submitted for any other degree.



Dr.V.N.Sivasankara Pillai

(Supervising Teacher)

Professor  
School of Environmental Studies  
Cochin University of Science and Technology  
Cochin – 682016.

December 2003



*To those who made it possible....*

*To those who inspired, encouraged, supported and stood with faith I remain indebted. To Prof. (Dr.) V.N.Sivasankara Pillai who gave me the courage, opportunity and freedom to explore my ideas. Thank You, Sir, You have been supportive and patient with a research topic that initially did not seem to work and when it did, kept throwing up surprises! Your knowledge has always been a source of inspiration and I will try that I know, if not more, at least half as much as you do. From You, I have learnt both the Do's and Don'ts. These lessons that I learnt from you, will be of great help all my life. To my parents who gave me a dream, who believed that I could and who stood by me with faith and admiration. I guess I would not have been writing this page without them.*

*I thank Dr.N.Sridevi, Dept. of applied chemistry, C.U.S.A.T. for all her help and guidance rendered during the course of my research work. I shall always remember you for your patience, support and encouragement. In spite of being busy you have always given me the time to clarify my doubts. Thank You Madam!*

*I thank Dr. Ammini Joseph, Director, School of Environmental Studies for all her unconditional help and guidance through out my research tenure, particularly during my tryst with Daphnia and Chlorella.*

*I express my deepest sense of gratitude to Dr.A.Mohandas and Dr.I.S.Bright Singh whose attitude has taught me how one can be supportive and encouraging.*

*I thank Dr.Harindranathan Nair, Dr.Suguna Yashodharan and Dr.S.Rajathy for their help rendered during the course of my research.*

*I would like to use this opportunity to thank Dr.V.S. Achari who has been helpful with his suggestions during the course of this work.*

*I thank Dr. Rajalakshmi Subramaniam for her patience and her constant encouragement. Thank you madam for your patience in explaining things to me when I did not understand them. At times when situations were tough it was your support and encouragement that kept me going.*

*I thank Mr.H.Krishna Iyer for all the help rendered towards statistical Analysis of my data.*

*My lab mates I guess, these are the people who have seen me through the ups and downs. I have been lucky to have a bunch of caring people as my colleagues, not many are fortunate like me. They have always helped me in innumerable ways, be it a request or just silly queries, experiments, discussions or be it just a patient hearing when I needed to vent. Balu, Suja, Alex, Manu and Surekha have made Water Quality and Water Treatment laboratory, the wonderful place that it is. They have all taken keen interest in my work and their suggestions have been of great help. THANKS GUYS!*

*I thank all the members of CFDDM especially Jay Prakash, Anas, Ranjit K and Somnath Pai for the help rendered when I needed it the most. Thank you friends.*

*I thank all the research scholars of the Environmental biology and toxicology laboratory for being ever so willing to help me during my research.*

*The Directors office staff have been extremely helpful with all the paper work, especially since I always found it hard to figure out what needs to be done and when!*

*My friends they form my support system and have helped me smile! I owe much to them than words can express. Thank you all...*

*My family- I guess they just hopelessly love me and that explains their undying faith in me. My fathers confidence, my mothers constant support and encouragement and my brothers understanding nature have kept me afloat. It is with them that I have shared the excitement of small experiments, to the fathomless depression when things went out of my control. They believed and made me believe when I almost thought I couldn't. I don't want to belittle them by even trying to say THANK YOU. This thesis is dedicated to them.*

*Rajesh Babu V.G.*

## Contents

Sl. No.	Topic	Page No.
	Preface	i
<b>Chapter I</b>		
1.	Treatment options for colour removal	
1.1.	Introduction	1
1.2.	Technology for colour removal	
1.2.1	Adsorption	7
1.2.2.	Reduction	16
1.2.3.	Oxidation	22
1.2.4.	Electrochemical technology	28
1.2.5.	Pretreatment	36
1.2.6.	Aerobic biological treatment	40
1.2.7.	Anaerobic biological treatment	47
1.2.8.	Anaerobic-aerobic sequence	52
1.2.9.	Fungal treatment	56
1.2.10.	PACT system	58
1.2.11.	Membrane filtration	59
<b>Chapter II</b>		
	Iron mediated reductive transformation of Azo dyes	
2.	Zero Valent Iron – A review.	66
(i)	Reduction of Dyes	67
(ii)	Reduction of Nitrobenzene	88
(iii)	Dechlorination of aromatic compounds	92
(iv)	Dechlorination of pesticides	104
(v)	Heavy metal removal	106
(vi)	Removal of radioactive substances	113
(vii)	Permeable reactive barriers	116
(viii)	Dechlorination of carbon tetrachloride	118
(ix)	Treatment of explosives	119
(x)	Related works	121

Sl. No.	Topic	Page No.
	Abstract	124
2.1.	Introduction	126
2.2.	Materials and methods	128
2.3.	Experimental procedure	131
2.4.	Results and Discussion	137
2.4.1.	Molecular structure	137
2.5.	UV-Vis spectrum	139
2.6.	Calibration curves	141
2.7.	Kinetics of transformation	143
2.8.	Effect of flow rate	149
2.8.1.	Direct Sky Blue	153
2.8.2.	Direct Black EG	158
2.8.3.	Direct Catachine Brown	163
2.8.4.	Direct Green B	166
2.8.5.	Direct Yellow – 5GL	170
2.9.	Effect of concentration	
2.9.1.	Direct Sky Blue	175
2.9.2.	Direct Black EG	183
2.9.3.	Direct Catachine Brown	185
2.9.4.	Direct Green B	193
2.9.5.	Direct Yellow – 5GL	200
2.10.	Influence of pH	
2.10.1.	Direct Sky Blue	206
2.10.2.	Direct Black EG	212
2.10.3.	Direct Catachine Brown	216
2.10.4.	Direct Green B	221
2.10.5.	Direct Yellow – 5GL	229
2.11.	Statistical analysis and conclusions	236

Sl. No.	Topic	Page No.
	<b>Chapter III</b>	
	Fenton oxidation of dyes	
3.1.	Introduction	267
3.2.	Review on Fenton oxidation	284
3.3.	Fenton Oxidation of dyes	331
3.3.1.	Materials and methods	334
3.3.2.	Experimental procedure	335
3.4.	Results and Discussion	
3.4.1.	Molecular structures	338
3.4.2.	UV-Vis spectrum	340
3.5.	Optimization studies	
3.5.1.	Optimization of hydrogen peroxide	342
3.5.2.	Optimization of ferrous sulphate	349
3.5.3.	Optimization of dye concentration	353
3.6.	Kinetic studies	361
3.6.1.	Influence of hydrogen peroxide	365
3.6.2.	Influence of ferrous sulphate	373
3.6.3.	Influence of dye concentration	385
3.6.4.	Reaction mechanism	388
3.6.5.	Conclusions	391
	References	394

## *PREFACE*

Environmental issues associated with residual colour in dye house effluents are not new. Over the past few decades manufacturers and users of synthetic colorants have faced increasingly stringent regulations promulgated by agencies established to safe guard human health and environment. This has meant that much of the emerging technology in these two areas arose as a need to comply with regulation. A significant proportion of this technology has been directed specifically to analyze for and remove colour and priority pollutants from effluents to circumvent pollution problems by eliminating their source.

The global consumption of textiles is currently around 30 million tones, with expected growth at 3% per annum. The coloration of this total needs approximately 800,000 tones of dye, promoting an industry of 2500 million pound per annum (Glover and Pierce, 1992). In the dye stuff market the textile industry shares a whopping 2/3 of the total synthetic organic dyestuff production; making it the largest consumer of synthetic coloring material (Kulkarni et al., 1985). The huge quantities of water employed in the dyeing and finishing operation associated with the dye house processes provides the textile industry with another dubious distinction of being one of the largest water consuming industry. According to an estimate made by the internal technical report, 1994, 100 L of water is consumed for every tonne of cloth processed. This calls for a serious

approach to environmental issues associated with residual colour in the dye house effluents.

The long-standing dyers goal has been to evenly achieve and consistently produce specific color at low costs in a safe, timely and efficient manner. Thus, if it were possible to achieve quantitatively 100% dye bath exhaustion with no wash off the problem of residual colour would not have gained prominence.

Despite efforts to improve the fixation of dyes on specific substrates, enhance biodegradability by affecting changes through modification in the chemical structure of dyes and achieve better control over dye manufacturing and dye consumption, the reactions that bind dyes on to a substrate do not always run to completion. An equilibrium will be established between the dye bath and the fabric after which no further binding of the dye to the fabric can occur. Residual dyes, auxiliaries and chemicals are often left in the process water and discharged with the wastewater. Therefore the wash off from the dye house invariably contains large amount of residual dye. Estimates indicate that approximately 12% of the synthetic textile dyes used each year are lost to waste streams during manufacturing and processing operations and that 20% of these losses would enter the environment through effluents from wastewater treatment plants (Brown, et al., 1981). According to another estimate over  $7 \times 10^5$  tonnes and approximately 10,000 dyes are produced annually worldwide, of which about 10% is lost in the industrial effluents (Vaidya et al., 1982). The three major chromophores of various commercial dyes are Azo,



Antraquinone and Indigo (Rattee., 1995). These effluents are discharged to sewers from where they enter into the Municipal wastewater treatment plants.

In the dye-manufacturing units there is considerable debate on the level of environmental hazard produced by colored effluents. Many of them have stated that there are no tenable arguments for the classification of dyestuffs as dangerous substances in the effluent. They go even further to say that dye stuffs should not be regarded as water pollutants since their harmful effects are negligible. Nonetheless, although the problem of color could be argued as only aesthetic, it is accepted that the problem has to be rectified. Thus, the mounting pressure on the industry to treat the dye house effluents have led to a host of new and old technologies competing to provide cost effective solution to the problem of residual color imparted by dyes.

Dyes are highly structured polymers required to exhibit a high degree of chemical, photolytic and microbiological stability in order to fulfill the fastness requirements. Consequently, the dyes are so structured that they do not degrade under typical usage conditions. Constant product changes and batch dyeing operations could cause considerable swings in the wastewater characteristics thereby presenting difficulty in acclimating the microorganisms to the substrate. Synthetic dyes are therefore not uniformly susceptible to degradation in conventional biological wastewater treatment processes because of their resistance to microbial attack. Attempts to develop aerobic bacterial strains for dye degradation often

resulted in a very specific organism, which showed strict degradation ability on individual dyes (Kulla., 1981). Hence, these dyes pass through the treatment systems virtually undegraded. These synthetic colorants although impart only a small fraction of the total organic load, the high degree of color that they impart is very detectable. To make matters worse the human eye can detect dyes at concentrations as low as 0.005 mg/L in clear river water.

Of the dyes commercially available, approximately 50% are azo compounds (Kulkarni et al., 1985). These compounds are characterized by aromatic moieties linked together with azo group ( $N=N$ ). These azo dyes can be divided into monoazo, diazo and triazo classes and are found in six application categories acid, basic, direct, disperse, azoic and pigments. These azo dyes are wide spread class of environmental pollutants that find wide applications in textile, cosmetic, food colorants, printing and pharmaceutical industries (Ryan et al.,). These synthetic compounds have been identified as the most problematic compounds in the textile effluents due to their high water solubility and low exhaustion rate leading to elevated dye concentrations in the spent dye bath. The strong electron withdrawing character of the azo group generates electron deficiency, thus stabilizing these aromatic pollutants against conversion by oxygenases (Kulla et al., 1983). As a consequence these compounds are less susceptible to oxidative catabolism and many of them tend to persist under aerobic environmental conditions. This statement is supported through the studies conducted by Shaul and coworkers (1987) in which more than a

hundred azo dyes were tested in aerobic activated sludge systems of which only a few were actually biodegraded. A literature review indicated that adsorption to the sludge is the primary removal mechanism for dyes in a biological wastewater treatment and that factors inhibiting permeation of the dye through the microbial cell membrane like increased water solubility and increased molecular weight reduce the effectiveness of biological degradation (M.Dohanyos, V. Medera, H.R.Hitz, W.Huber and R.H. Reed., W.C.Tincher, K.Wuhrmann, K.Mechener (1978) and T.Kappeler ( 1980).). The results from such studies reveal that the dyes were removed from wastewater via physical and physico-chemical processes such as diffusion, adsorption and chemical reaction. The dyes that adsorbed to the sludge had fewer sulfonic acid groups and were of higher molecular weight both of which are features that tend to reduce water solubility. Further more, the coupling components that go into the synthesis of azo dyes like naphthalene-sulfonic acids as well as aromatic amino derivatives represent an extensive non-biodegradable class of compounds (Krull, R and Hempel, D.C. (1994). Due to their recalcitrance in aerobic environment's they pass through the aerobic treatment systems virtually undegraded and eventually end up in anaerobic sediments, shallow aquifers and ground waters (Braughmann et al.,). All these findings substantiate the view that the conventional aerobic treatment systems such as the activated sludge process are grossly inadequate in meeting the present standards for acceptable effluent making the dye related industries incapable of responding to stringent legislation.

In the recent years concern over the environmental fate of these azo dyes have grown. This can be partly attributed to the intense coloration, which they impart to the natural water bodies on discharge, and largely to the fact that these dye partition strongly to the bottom sediments where under anaerobic conditions they undergo reductive cleavage via a four electron reduction at the azo linkage generating aromatic amines (Brown et al., 1983). Unfortunately, as suspect mutagens and carcinogens, these aromatic amines cannot be regarded as environmentally safe end products (Chung, K.T.,(1992) and Ames, B.N.,( 1975)).

Research by Huag (1991) and Field, J.A.,(1995) report that these aromatic amines are more amenable to treatment under aerobic conditions provided the co-substrate and the oxygen are in balance. Literature reviews indicate that the aromatic amines generated as a result of reduction of the N=N bond are in most cases benzene or naphthalene derivatives, which can be rapidly oxidized by aerobic microorganisms in oxic environs. This study throws up a new option of utilizing integrated and sequential anaerobic – aerobic system to achieve complete biodegradation of azo dyes. Microbial anaerobic processes capable of producing and maintaining low oxidation reduction potential cleaves the chromophore N=N generating stoichiometric amounts of amines to be further metabolized by the aerobes under oxic environs. Some studies also reveal that some nitro-aromatic compounds and azo dyes could be completely mineralized and serve as a carbon, energy and nitrogen source for anaerobic bacteria in contrast to the common assumption that they are only

biotransformed to mutagenic and carcinogenic aromatic amines. Although the use of microbial consortium does provide a very interesting treatment option towards achieving biodegradation of dyes; isolation of specific microorganism that degrade one or more dyes and application of this technology to a textile dye wastewater that contains many dyes and varies in composition may pose practical difficulties. Moreover, such systems require an acclimatized microbial consortium, which could be time consuming under the event of constant product changes and batch dyeing operations prevalent in the dye house. Eliaz et al., (1997) reports complete biodegradation of the azo dye azodisalicylate under anaerobic conditions taking up to 50 days. Thus it is accepted that the azo dyes are non-specifically reduced under anaerobic conditions, but the slow rates at which many dyes react may present a serious problem for the application of anaerobic technology as a first stage in the complete biodegradation of these compounds. Therefore, it is significant to explore an alternative cost effective treatment option to achieve a faster and more efficient abiotic cleavage of azo linkages. Towards this direction, the second part of this study explores the possibility of utilizing the reduction chemistry provided by Zero Valent Iron (ZVI) in decolorizing azo dyes.

The first part of this study brings to light a host of various treatment options (both old and new) competing with one another to provide cost effective solutions for the dye-house towards effective colour removal. The number of different wastewater treatment methods that have emerged in the recent past is clearly indicative of magnitude of the problem and the

diversity of types of wastewater encountered. However, one major factor that offsets many of their applications is their associated costs for installation and maintenance.

Historically the Fenton's reagent has been of interest mostly from a synthetic or a mechanistic perspective, for their relevance to enzyme reactions or free radical damage to cells. However, it is only recently that the potential of this seemingly simple reagent that generates highly reactive hydroxyl radicals at low temperature has attracted the attention of several researchers towards destruction of refractory organics. The second chapter of this study investigates the performance of Fenton's reagent towards the oxidation of selected dyes that find wide application in the textile and carpet dyeing units (particularly in the Alapuzha District, Kerala).

## **Chapter I**

### **Treatment Options For Colour Removal – An Overview**

## 1.1. Introduction

The proper use of dyes, auxiliaries, energy and water are required to obtain the desired color, handle, wearing comfort and design of textile. For many years, achieving a certain finishing effect was the main consideration, but recently due to the change in values in our society, environmental protection has become the focal point of attention.

Almost every industry uses dyes and pigments, many of which are inert and non-toxic at the concentrations discharged into receiving waters. However, some are not so innocuous and, in either case, the color they impart is very undesirable and is easily detectable. These commercial dyes are usually mixtures of large complex molecules and often-uncertain molecular structures and properties. Of the various classes of dyes investigated, basic dyes were found to be the brightest class of soluble dyes used by the textile industry, with a high tinctorial value and concentrations even less than  $1 \text{ mg L}^{-1}$  produces obvious water coloration (Gordon McKay (1980)). The current annual world production of dyestuffs is about 640,000 tons of active substance. Of this total some 56% are textile dyes, 23.5% pigments, 14% dyes for paper and 6.5% others. The long-standing dyers goal has been to evenly and consistently produce specific colors at low costs in a safe, timely and an efficient manner. Thus if it were possible to achieve quantitatively 100% dye bath exhaustion with no wash off; then the problems associated with colored effluent would be reduced to controlling handling spills and clean-up. In addition this could also be an ideal way to ensure a maximum shade reproducibility, and the problem of



shade repeats would be a simple matter of settling the correct amount of dye and substrate into the bath. However, quantitative dye bath exhaustion is not possible with most systems. This is because an equilibrium is established in the dyeing and washing off, that always leaves some amount of the dye in wastewater. In commercial processes, there may be from almost none to over 50% of the total dye left in the dye bath. In the textile sector an estimated 10-20% of the 360,000 tons of dyes (active substances) used is lost in residual liquors through incomplete exhaustion and washing process. For pigments the rate of loss is about 1-2%, and for paper and leather dyes, it is 10%. These brightly colored unfixed dyes are highly water-soluble and to make matters worse, the human eye can detect dyes (particularly reactive dyes) at concentrations as low as 0.005 mg/L (Willmott et al., 1989). Many of the dyes used in textile industry are particularly difficult to remove by conventional waste treatment methods because by design they are stable to light and oxidizing agents and are resistant to aerobic digestion. Other factors involved in reducing the biodegradation of dyes include properties such as high water solubility and high molecular weight, which inhibit permeation through biological cell membranes. Many dyestuffs, in particular disperse, direct and basic dyes are expected to be removed from wastewaters via adsorption on to activated sludge. Acid dyes and reactive dyes, however, exhibit low adsorption values and thus pass through activated sludge processes largely unaffected. Effluent treatment processes for dye-containing effluents are capable of removing about half of the lost 94,000 tons leaving

about 47,000 tons per year or 128 tons daily to find its way into the environment. Colored organic substances generally impart only a small fraction of the total organic load in a wastewater but their high degree of color is easily detectable and detracts from the aesthetic value of the water bodies. As far as the public is concerned the removal of color from wastewaters is often more important than the removal of the soluble colorless organic substances which usually contribute to the major fraction of the biochemical oxygen demand (BOD). Therefore, color at least from the viewpoint of aesthetics is one of the first parameters considered in the field of pollution prevention. However, there is a lack of understanding about the problem of color in many aspects. Stringent standards sometimes require significant additional treatment or up gradation of the existing plant. There are difficulties in defining a common or collective parameter such as BOD<sub>5</sub> or COD with which the magnitude or the strength of the additive substances could be expressed or the potential impact of this strength be predicted. The treatability information especially for textile dyes is considerable, though a system of utilizing this information judiciously is missing. This section attempts to evaluate the various treatment options available for color removal and to discuss the applicability of a systematic approach.

Textile, pulp and paper, tannery and dye manufacturing units are among the most important sources of colored effluents. The textile processing industry is characterized by its fairly high specific water consumption and its large amount of wastewater discharges. Dyeing and

finishing are two integral parts in the textile manufacturing process. However, due to processing in aqueous solutions or suspensions, generates considerable amount of wastewater. The quantity and quality of wastewater depends primarily on the substrate – such as cotton or wool and also the production method used. The specific wastewater discharge could vary according to the production method, between 40m<sup>3</sup> and 300 m<sup>3</sup> per ton of finished substrate (Rott and Minke (1999)). The large quantity of aqueous waste generated by the textile industry is a major source of considerable pollution. According to Rott and Minke (1999), the composition of raw mixed wastewater in the textile processing industry include the following characteristics:

- (a) Intense coloring due to large amounts of unfixed dyes.
- (b) High temperatures, as required by many of the processing reactions.
- (c) On an average pollution with organic materials corresponds to the pollution of domestic wastewater.
- (d) High-molecular synthetic textile auxiliaries and dyes leading to a large amount of refractory COD and high conductivity.
- (e) High AOX, sulphide and heavy metal concentrations due to chlorinated bleaching agents and halogen, sulphur or heavy metal contained in dyes.
- (f) Addition of polyphosphates for conditioning of hard water used in the process leads to high phosphate content.

Dye house effluents are not only aesthetic pollutants by nature of their intensity but may also undergo chemical as well as biological changes, consume dissolved oxygen from the stream, interfere with light penetration in the receiving water bodies and destroy aquatic life, as these dyes are mostly toxic in nature (Ajmal and Khan, 1985 and Walsh et al., 1980). The recent high profile of colour pollution is mainly the result of increasing public awareness and expectations of the environment, coinciding with rising levels of colored discharges. Therefore, it is of paramount importance to minimize pollution and to know its exact nature, in order to implement an appropriate treatment process. There is currently no single economically feasible method of treating textile effluent, which would reliably remove its color. Conventional biological processes have not proven to be particularly effective. In a study of various dyes it was shown that, for disperse dyes, carbon adsorption and ozonation resulted in poor color removal. Chemical coagulation and reverse osmosis resulted in a large proportion of the color being removed, with reverse osmosis being the most effective. But the major limitation that offsets the application of reverse osmosis is its high capital costs. Furthermore, the large variability in composition of textile wastewaters makes color removal a challenging problem in environmental pollution control. It is now a more or less an accepted fact that application and manufacture of dyestuffs create substantial quantities of wastewater that calls for the implementation of regulatory standards prior to discharge. Aggressive wastewater minimization programmes have been implemented at various units to

process the dye house effluents and to meet the regulatory standards prior to discharge.

The multitude of commercial dyes and dyeing systems makes it highly unlikely that any one single method will alone meet the demands of every situation, as each of them have their own set of specific problems depending on the dyeing system. For example, the coagulation process can effectively decolorize the wastewater containing insoluble dyes such as disperse dyes. However it does not work well for soluble dyes such as reactive dyes. Soluble dyes can be effectively decolorized by oxidation process such as ozonation (Perkins et al., 1980). However it cannot decolorize insoluble dyes. Fenton's reagent has shown be effective in decolorizing both soluble and insoluble dyes (Kuo, 1992) however in the process, a large volume of sludge is generated by the ferrous ions during coagulation. Hence, search for cost effective treatment methods is in order. The mounting pressure on the textile industry to treat dye house effluents, has led to a host of new and old technologies competing to provide cost effective solutions.

All the treatment methods for reducing pollution at source have advantages and disadvantages, however, they become increasingly important as methods for minimizing waste streams, reducing effluent treatment costs and reducing resource consumption. The following sections provide a brief insight into the various treatment options available towards decolorizing colored effluents particularly with special emphasis to the textile industry.

## 1.2. Technology of colour removal

### 1.2.1. Adsorption

Organic substances such as dyes that are difficult or impossible to degrade biologically can be removed from wastewater by adsorption on to suitable adsorbents. Adsorption is a physico-chemical process, which offers great potential as a means of producing quality effluent. The various adsorbents used in colour removal operations have been reviewed by Poots et al., (1976 a, b). Of these adsorbents the most well known adsorbent is activated carbon. There are essentially four stages in the adsorption process by porous adsorbents:

- (i) Transport of dye from the bulk solution to the exterior surface of the adsorbent;
- (ii) Movement of dye across the interface and adsorption onto external surface sites;
- (iii) Migration of dye molecules within the pores of the adsorbent, and
- (iv) Interaction of dye molecules with the available sites on the interior surfaces, bonding the pore and capillary spaces of the adsorbent.

One or more of the above steps controls the rate at which dye is adsorbed and the quantity of dye adsorbed onto the solid particle. At low degrees of agitation the boundary layer resistance will be significant and step (ii) will be the rate-controlling step.

Adsorption is an effective treatment option for lowering the concentration of Dissolved organics in an effluent. Commercial activated carbon is one of the most widely used adsorbents; usually prepared from lignite and bituminous coal, wood, pulp mill residue, coconut shell and blood and has a surface area ranging from 500 to 1400 m<sup>2</sup> gm<sup>-1</sup>. Adsorption on activated carbon is an area that has been extensively studied as a wastewater treatment option for the removal of different classes of dyes ranging from acid, direct, basic, and reactive to disperse dyes (Cheremisinoff and Ellerburch, 1978) making it one of the most favored adsorbent for removal of dyes from the effluent (Hall, 1975 and Davies et al., 1973).

The feasibility of adsorption on activated carbon for the removal of dissolved organic pollutants is demonstrated by carbon adsorption isotherms generated by contacting a fixed quantity of dye wastewater with different amounts of activated carbon for a fixed length of time. Of the various adsorption isotherms the Freundlich isotherm is used to express the mathematical relationship between the quantities of impurity remaining in solution versus the quantity adsorbed. The mathematical equation representing the Freundlich isotherm is given as

$$X / M = KC^{1/n}$$

Where,

X = Amount of impurity adsorbed

M = Mass of carbon

C = Equilibrium concentration of the impurity in solution

K, n = Constants.

A logarithmic plot of the data gives the capacity of activated carbon to adsorb the particular impurity at a specified equilibrium concentration and the quantity of adsorbate remaining in solution can be determined by total organic carbon (TOC), COD, BOD, HPLC etc. By applying the Freundlich equation to the analyzed values on a log-to-log paper, a carbon adsorption isotherm can be obtained which enable us to evaluate the theoretical capacity of the activated carbon to achieve a desired degree of treatment.

The theoretical quantity of liquid (Litres<sup>-1</sup>) that can be treated per gram of carbon can be calculated from the following formula :

$$V_{C_0} = \frac{(X/M) C_0 (V)}{C_0}$$

Where,

$C_0$  = Influent concentration (mg L<sup>-1</sup>).

$(X/M) C_0$  = Ultimate capacity per gram of carbon at influent concentration  $C_0$  in mg g<sup>-1</sup>.

$V$  = Volume of the liquid used in the isotherm test.

Therefore, if one liter of a solution is divided by  $V/C_0$ , carbon column dosage or usage rate required to treat each liter of wastewater may be obtained. This figure when multiplied by the conversion factor 8.337, gives the carbon exhaustion rate in pounds per 100 gallons. The adsorption intensity can be obtained from the slope of a linear plot of  $X/M$  Vs  $C_0$ .

The success achieved with the use of activated carbon as an adsorbent for the removal of dissolved organics in laboratory scale batch processes have led to the development of activated carbon adsorption columns for treating dye house effluents on a commercial scale however,



such systems have met with limited success in the treatment of Disperse cationic dyes and anionic dyes. Hall (1975) studied the adsorption characteristics of three disperse dyes choosing concentration, pH, surfactants and alkali salts as variables that influence dye removal from the effluent and concluded that a high degree of adsorption was possible by controlling these variables. McKay et al (1980) has reported that the rate processes for the adsorption of a disperse dye (Disperse Blue 7) on activated carbon was found to vary with agitation, initial dye concentration, carbon particle size and temperature of the dye solution. Reife and Freeman (1996) studied a group of disperse and basic dyes (Basic yellow 11, Basic blue 3, Basic blue 9, Disperse Red 78 and Disperse blue 64) to define factors affecting the removal of textiles dyes from wastewater by carbon adsorption. It was shown that the dyes of the same application class exhibit similar adsorption characteristics. Differences in chemical structure (e.g. oxazine, methane, thiazine, azo or anthraquinone) influence the affinity of specific dyes for the adsorbent. In the case of the basic dyes, the enhanced affinity to activated carbon has been correlated to its basicity however, the lower affinity of disperse dyes could be attributed to its colloidal nature. Carbon adsorption isotherms generated from the disperse dyes often resulted in steeply sloped lines indicating low adsorbability. However, the adsorptive capacity of the disperse dyes could be enhanced to the level of basic dyes in the presence of a dye carrier. An important and effective application of the dye-carrier interaction is observed in the dyeing of hydrophobic fibres, where a sparingly soluble disperse dye must

be blended with anionic surfactants to reduce agglomeration and solubilize the dye and keep the disperse dye well dispersed. Result of the study showed an 88.4-95.7% reduction in colour using 0.5 & 10% activated carbon. It was inferred that these dye carriers enhance adsorption by increasing the solubility of disperse dyes in the bulk solution & in the immediate area surrounding the carbon granules, thereby reducing the repulsive forces between the colloidal dye and the carbon surface allowing adsorption to take place.

Variation in the adsorption properties of the dye can also be attributed to the differences in the chemical structure. Carbon adsorption is relatively ineffective in removing disperse dyes, vat dyes and pigments (Porter and Sneider., 1976). This has been attributed to the low solubility and colloidal dispersion properties of the dyes, which prevent the adsorption and migration of the dye particles to the carbon surface; thereby their rate of adsorption on to carbon becomes prohibitively slow at room temperature. Water-soluble dyes such as acid, basic, direct, metallized, mordant and reactive dyes are also not readily adsorbed. This could be attributed to the polar nature of the dyes versus the non-polar nature of carbon.

Some of the factors that need to be considered when generating carbon adsorption isotherms on wastewater are temperature, pH, contact time, carbon dosage and choice of activated carbon. To illustrate the point that the choice of carbon is also of immense importance (De John and

Hutchins., 1975) it was observed that carbon adsorption isotherms when generated using a single dye on activated carbon from different sources (from bituminous coal), from wood and from pulp mill residue showed marked differences with respect to the amount of carbon required to treat 1 L of solution and carbon exhaustion rates. Examination of the adsorption isotherms of the different carbons showed differences in the efficiency of the carbon for adsorption of the dye. The slope of these adsorption isotherms is an indicator of the relative absorbability of the carbon. The slightly sloped lines reflect high absorbability, a horizontal line would represent infinite absorbability and a steeply sloped lines indicate low absorbability.

Regeneration of the carbon has a marked influence on the adsorptive capacity. Studies conducted by DeJohn & Hutchins (1975) reveal that when granular activated carbon is regenerated, the surface area in the micro pore range is drastically reduced and the transitional pore surface is slightly increased. This change in the pore structure changes the adsorptive performance of a regenerated carbon, with the degree of change dependent on the substance to be adsorbed. If the compound is a relatively large molecule, the adsorptive performance of the regenerated carbon is equal to or better than that of the virgin carbon. This is because dyes of high molecular weight are adsorbed on to the transitional pores of an activated. On the other hand if the organic compound is a relatively small molecule, the absorbability of the regenerated carbon decreases substantially when large molecules are adsorbed into transitional pores,

that are essentially unaffected by the thermal regeneration process, small molecules are adsorbed into the micro pores, a good portion of which is lost during carbon activation.

The molecular structure of a compound also has a significant effect on the extent to which it will be adsorbed on carbon. In general it has been observed that the adsorbability of a compound is enhanced by increasing size and aromaticity and by decreasing solubility, polarity and carbon chain branching. Adsorption is also influenced by the presence of specific functional groups on the adsorbate. For e.g. adsorption is increased by the presence of hydroxy, nitro and azo groups but decreased by sulfonic acid groups.

In a study conducted by R.H.Horning (1997) powdered activated carbon was generally found effective in removing color but required large doses relative to the amount of wastewater treated. For e.g., although color reductions to less than 100 ADMI units could be achieved, PAC doses from, 400 – 2500 mg/L were required. The average percent color reduction for the eight dyes evaluated with PAC treatment was 94%. Therefore, a combination of PAC & alum could be a potential cost effective solution to the problem of high PAC dose requirements. Horning (1978) based on the results from the evaluation of seventeen dyes found that carbon treatment did not perform well with Vat and disperse dyes but performed better for reactive and basic dyes.

Nicolet and Rott (1999) used a peculiar mode of advanced treatment for color removal in which PAC was not disposed of before being

recirculated several times thereby enabling the use of a great part of the total adsorption capacity. A added advantage of this treatment was that halogenated and refractory org. compounds., which were not degraded by microorganisms in a conventional municipal wastewater treatment plant, were also removed.

Ince et al., (2002) studied a combination of adsorption and advanced oxidation for the removal of a reactive dye Everzol Black-GSP (EBG). In this method aqueous solutions of the dye containing hydrogen peroxide and granules of activated carbon were irradiated with UV light. The effectiveness of the system was tested by monitoring the rate of decolorization and degree of carbon mineralization in the effluent. Results of the study revealed that color was principally removed by oxidative degradation while adsorption contributed to the longer process of dye mineralization. The proposed combination provided 25 and 35% reduction in  $H_2O_2$  and energy consumption relative to the UV/ $H_2O_2$  system.

Taebi et al., (2000) observes that chitosan could be used as an appropriate and comprehensive adsorbent agent for the treatment of textile wastewaters, and could also be substituted for other adsorbents. The authors explored the feasibility of applying chitosan, derived from chitin (a natural biopolymer found in the shells of crustaceans), for the adsorption of soluble dyes from textile industry wastewaters was assessed. The objectives of the experiments were to compare color removal efficiencies of chitosan and that of activated carbon; in addition to study factors affecting adsorption by chitosan such as pH, temperature, contact time, and

adsorbent concentration. Results showed that chitosan has more efficient for the removal acid, direct, and reactive dyes while activated carbon was efficient in removing basic dyes. Moreover, the study reported that the removal by chitosan is higher than activated carbon for all dyes.

One of the major disadvantages of Activated carbon is its high price, which calls for regeneration. Because of their high solubility, most of the dyes are very difficult to remove by adsorption. Their high positive charge means that they could be scarcely adsorbed. Although carbon adsorption of dyes is neither efficient nor economical when used alone, when used in tandem with polymer flocculation, chemical reduction or biodegradation it becomes a very useful polishing step for efficient dye removal. This throws up a whole new possibility to evaluate the effectiveness of inexpensive alternative materials as potential adsorbent for dyes using activated carbon as a reference. A look into literature indicates that the alternatives considered include a wide array of substances. Just to name a few they include cellulose derivatives (Youssef, 1993) peat (Coupal and Lalancette, 1976), Wheat bran, sawdust, tree barks (Michelsen et al., 1992; Khattri and Singh, 2000; Kadirvelu et al., 2000 and Sharma et al., 1999), chitin (Laszlo, 1994 and Figueiredo et al., 2000), fly ash (Gupta et al., 1990) Cement kiln dust (Ibrahim et al., 1998), mixed adsorbents (Gupta et al., 1990) baggasse pith (McKay et al., 1988) Wood (Poots et al., 1976) Bentonite (McKay et al., (1986), clays & Fuller's earth (McKay et al., (1985) ), pig and human hair, meat, bone meal, wheat and rice bran and turkey feathers (McKay et al.,

1987), burnt brick particles (Priyantha et al., (2000) activated sludge (Pagga and Taeger. 1994) and coal (Gupta et al., 1990). The adsorption properties of activated sludge were found to be similar to activated carbon in studies involving acid, direct, reactive, disperse and basic dyes. The adsorption capacity of activated sludge for acid, direct, reactive, disperse and basic dyes have been determined by the Freundlich equation and adsorption isotherms (Hitz et al., 1978).

### **1.2.2. Reduction**

D. Brown and B. Hamburger (1987) report that azo dyes undergo conversion to aromatic amines via reductive cleavage of the azo bond under reducing environments. Similar mechanism is also observed under anaerobic biological degradation.

Chemical reduction of the azo dyes also causes the cleavage of the azo bond, generating aromatic amines that are more amenable to subsequent aerobic biological treatment than the parent dye structure.

For many dyes, particularly azo dyes, chemical reduction is an effective decolorization technique. Sodium hydrosulfite (also known as sodium dithionite), Thiourea dioxide (formamidine sulfinic (FAS) acid), sodium borohydride, sodium formaldehyde sulfoxylate and tin (II) chloride are some of the most commonly used chemical reducing agent for treating dye wastewater.

M.W.McCurdy and coworkers (1991) evaluated the effectiveness of three reducing agents sodium hydrosulfite, thiourea dioxide and sodium

borohydride in decolorizing Navy 106 (a mixture of three azo dyes) wash water generated from a textile plant and the percent removals were calculated based on the influent to the entire system. However, chemical reduction using the three reducing agents resulted in the generation of wastewater that was inhibitory or toxic to the subsequent aerobic biological system. The authors suggested that either the reducing agents or the aromatic amines generated from the reductive cleavage of the azo bonds might have been toxic to the microorganisms in the biological treatment plant. In a second experiment, McCurdy and coworkers evaluated the effect of chemical reduction followed by peroxide addition and aerobic biological treatment. The hydrogen peroxide addition following chemical reduction created an oxidized environment that was more conducive to aerobic biological treatment than the environment resulting from chemical reduction alone. Moreover, the toxic aromatic amines generated by chemical reduction may be oxidized to aromatic amine oxides or aromatic quinones that are no longer toxic to the microorganisms in the biological systems.

The reducing agents sodium hydrosulfite, thiourea dioxide and sodium formaldehyde sulfoxylate was evaluated at various pH levels by Michelsen (1992). After considering color reduction efficiency, dosage requirement and cost it was found that sodium hydrosulfite was most effective at pH 4 achieving 71% color removal at a dose of 400 mg/L. Thiourea dioxide was most efficient at a pH of 10.7 achieving 63% color

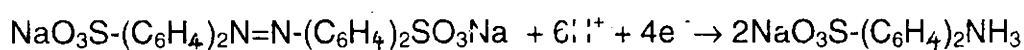


removal at a dose of 100 mg L<sup>-1</sup>. However, of the two, sodium hydrosulfite due to its lower cost is preferred over thiourea dioxide.

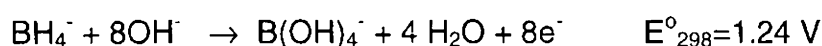
McCurdy, Powell and Michelsen designed, fabricated and tested a 1L/min. pilot plant using a sequence of two continuously stirred tank reactors in an attempt to treat, decolorize, remove metals and TOC from selected reactive dye bath concentrates using Fenton's reagent, thiourea dioxide and sodium hydrosulfite. The results show that reductive pretreatment resulted in 92.2% color removal, with partial color regeneration upon aeration. Thereby reducing the net color removal to 76.6%. Oxidative pretreatment resulted in 98.8% color removal, with a net color removal after aerobic treatment of 96.8%. The TOC removal during aerobic treatment was greater for the oxidized wastewater than the reduced wastewater.

(i) Reduction using Sodium Borohydride

Water soluble dyes and closely related by products containing azo groups can be chemically reduced by a variety of agents like dithionite, formamidine sulfonic acid (FAS) (Reife A. Kirk – Othmer, 1993) or tin chloride (Voyksner, 1993) to the corresponding aromatic amines according to the following equation

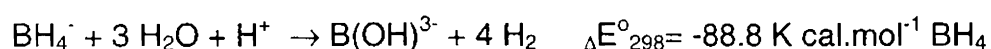


Sodium borohydride is one of the strongest water-soluble reducing agents commercially available.

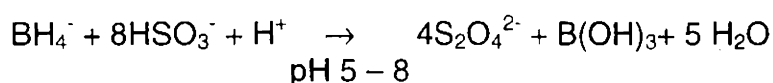


Wastewater treatments utilizing sodium borohydride reduction has been commercialized for the removal various metal cations such as copper, nickel, lead, mercury and silver. These chemical reductions occur with both complexed and non-complexed metal cations.

However, one of the major factors hindering the extensive application of sodium borohydride in dye wastewater decolorization is due to its rapid reaction with water at pH<8 (Sanglet, 1989) and its tendency to reduce via a hydride transfer mechanistic pathway.

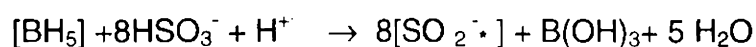
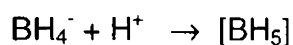


However, this deficiency can be overcome by employing an effective level of bisulfite in conjunction with borohydride. In the absence of other reducible species, borohydride quantitatively and rapidly reduces bisulfite to dithionite in the pH range of 5-8.

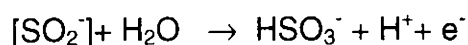


Hence, by employing bisulfite in conjunction with borohydride at reaction pH in the 4-7 range has been shown to dramatically improve the efficiency of sodium borohydride in wastewater treatment (Sanglet, 1989).

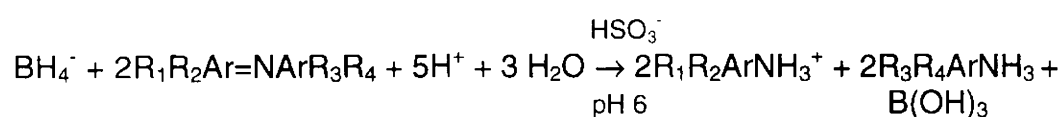
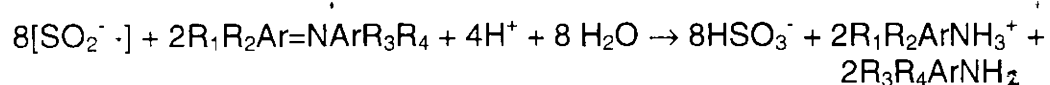
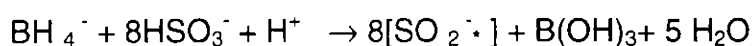
Although, the exact mechanism of this reaction has not been fully characterized, the  $[\text{BH}_5]$  and  $[\text{SO}_2^-]$  species are likely intermediates (Chou et al., 1984)



The  $\text{SO}_2$  radical anion is also a very strong single electron reducing agent whose oxidation product is bisulfite (Friar, (1981).



Thus, in the overall borohydride reduction chemistry bisulfite is not consumed but acts as a regenerable co-reagent or catalyst (Lores and Moore, 1974).



Technologies based on bisulfite catalyzed borohydride reduction have been applied to water soluble dyes containing azo or other reducible groups and to copper based metallized dyes (Reife and Freeman, 1996). This particular reductive treatment chemically cleaves the dye into smaller molecules which in comparison to the parent compounds are virtually colorless and can be more readily metabolized by activated sludge, chemically oxidized, adsorbed on carbon or precipitated by polycationic agents. A review of literature shows that bisulfite catalyzed sodium borohydride reduction was found to show encouraging results both when applied under laboratory conditions as well as on field trials. Experiments on industrial dye wastewaters carried out by Cook et al., 1992, using bisulfite catalyzed borohydride reduction followed by precipitation with a cationic coagulant brought about over 90% colour reduction. Under field

conditions, the optimum pH was observed at 5-6 and the optimum dosage of bisulfite was approximately 200 – 500  $\text{Na}_2\text{S}_2\text{O}_5 \text{ L}^{-1}$  (Reife and Freeman, 1996). The borohydride solution is added in slight excess relative to the requirements of the solution. This can be conveniently monitored in the field using an oxidation-reduction probe ORP. At a pH of around 5.5-7 the presence of bisulfite ion ( $\text{HSO}_3^-$ ) and dithionite ion ( $\text{S}_2\text{O}_4^{2-}$ ) formed by the reduction of bisulfite with the slight excess of borohydride gives a stable negative ORP reading at approximately -500 to -600 mV.

Cook et al., 1992, used the bisulfite catalyzed sodium borohydride reductive technology to reduce a direct dye (Direct Red 254) and the toxicity of the resulting biologically active amine species was tested on a 48 hr activated sludge respiration inhibition test. The control, the sample containing the untreated dye had similar pH,  $\text{O}_2$  and  $\text{BOD}_5$  levels after 48 hrs. This indicates that there was no adverse effect of the reduction treatment on the subsequent activated sludge process.

This treatment process can be widely used either in batch or continuous application. The byproducts produced in the process, boric acid and sodium bisulfite can be discharged without any further treatment. ORP controllers can be installed for the automated borohydride feed. The reduced species can be separated and removed as solids or in the case of the byproduct amines, be adsorbed on carbon, oxidized or safely treated biologically.

### 1.2.3. Oxidation

Many dyes can be effectively decolorized using chemical oxidizing agents. Chlorine in the form of a liquid or gas, chlorine water or hypochlorite is often used to decolorize wastewater. However, the generation of toxic chlorinated organics disfavors the use of chlorine.

Gosh and co-workers (1978) evaluated the effectiveness of chlorination in color removal and found that 77% decolorization was achieved at a chlorine level of 150 mg/L but detected a residual chlorine of 110 mg/L. No residual chlorine was detected at doses below 100 mg/L but only 50% decolorization could be achieved.

Ozone is another oxidant more powerful than chlorine with the added advantage of oxidizing dye e wastewater without the generation of chlorinated organics. Horning (1997) as a part of an ADMI study found ozone to be effective in decolorizing dye baths containing basic and reactive dyes but ineffective in the case of disperse dyes. In the case of direct dyes the ozone treatment had a variable efficiency. Cost efficiency is one of the major factors that hinder the wide application of ozone. Ozone is one of the most active oxidants. Ozone is generated from oxygen by methods such as corona discharge and ultraviolet radiation. Highly concentrated ozone is generated using the corona discharge process. However, ozone is highly unstable. The half-life of ozone in the vapor phase at room temperature is known to be about 16 hrs. The stability of dissolved ozone in water depends on the pH value of the solution. Under acidic conditions, ozone is stable while under alkaline conditions it is very

unstable. The half-life of ozone in distilled water at room temperature is known to be about 20 min. (Masaki Matsui, 1981).

The chemistry of ozone has been widely studied and ozone has been used for the treatment of drinking water for disinfection. However, no commercial method for ozone treatment of dye wastewater has been reported. Most of the literature that is available with respect to the ozone dye interaction is based primarily on batch and laboratory studies.

The reactivity of ozone with an organic compound can be classified into

- (1) 1,3-Addition reaction: This is the most widely known and studied reaction of ozone. Ozone reacts with olefins to give a primary ozonide, which decomposes into carbonyl oxide and carboxyl compounds (Bailey, 1978). In the case of unsymmetric olefins, the primary ozonide can decompose in two ways. The primary ozonide decomposes in a manner that stabilizes the positive charge on the carbon atoms of the carbonyl oxide. The reactivity of carbonyl oxides depends on the solvent and reaction temperature. Being unstable, the carbonyl oxide will recombine with the carbonyl compound to yield ozonide, which dimerize and react with water to give a second carbonyl compound.
- (2) 1,3-Insertion reaction: Ozone reacts with aldehydes and acetals to give unstable hydro trioxides (Bailey, 1982). The hydro trioxides then decompose to give the corresponding carboxylic acid and singlet oxygen.

- (3) Electrophilic attack of ozone: Ozone easily reacts with amines, sulfides and ethers, each of which contains a lone pair of electrons on the heteroatoms (Bailey, 1982). The adducts are converted into oxidation products of the alkyl side chains.
- (4) Nucleophilic attack of ozone: (Bailey, 1982) indicates the reaction of ozone with isatin to give isatoic anhydride. In this reaction ozone has been reported to act as a nucleophile to attack the carbonyl carbon in the 3-position of isatin.
- (5) Electron transfer reaction of ozone: (Bailey, 1982) indicates that organic compounds having low oxidation potential such nitrogen containing substrates, transfer a single electron to ozone to form the radical cation of the substrate and radical anion of ozone.

#### Ozone dye Interaction:

Ozone fading of the dye occurs by the oxidative cleavage of the conjugated system of the molecule (Matsui, (1981)., Sneider and Porter, (1974)., Lopez, (1998)..

- (i) Stilbene Dyes: Chrysophenine-G reacts quantitatively with ozone to give the corresponding aldehydes. Ozone attacks the central olefinic bond of the dye by a 1,3-addition reaction. The azo linkage of the dye remains intact under the conditions of the reaction, as the reactivity of the olefinic bond towards ozone is higher than that of the azo bond.

- (ii) **Indigoid Dyes:** Indigo reacts with ozone to give isatin. This reaction is a useful method for the quantitative analysis of ozone. Ozone attacks the central olefinic bond of Indigo by a 1,3-addition reaction to generate two molecules of isatin per molecule of indigo.
- (iii) **Azomethine Dyes:** Ozone attacks the azo methane and dimethylamino moieties of the dye to give corresponding oxaziridine and N-dealkylated derivatives. The mechanism for the formation of the oxaziridine ring is by an electrophilic reaction of ozone at the azo methane nitrogen atom followed by loss of molecular oxygen. The formation of the N-methyl amino moiety by the ozone attack of ozone at the nitrogen atom from the identical intermediate, the formyl methyl amino derivative is obtained.
- (iv) **Azo dyes:** the reactivity of an azo linkage with ozone is very low compared to an olefinic or azo methane group. In the ozonization of azo benzene, both azoxy benzene and glyoxal are formed. The aromatic rings are more reactive toward ozone than an azo linkage.
- (v) **Diphenyl methane Dyes:** Auramine O reacts with ozone to give Michler's ketone accompanied by monoformyl methyl amino derivative.
- (vi) **Triphenyl methane Dyes:** Malachite Green reacts with ozone to give formylmethylamino derivative, di-arylketones and p-



dimethylamino phenol. The selectivity of ozone attack at an N-dimethylamino group versus carbon skeleton depends on the substituent functional group. Electron donating groups such as dimethylamino (Crystal violet) and methoxy groups accelerate ozone attack at the dimethylamino groups; while an electron withdrawing nitro group activates the carbon skeleton. The ozonization of phenolphthalein depends on the pH of the solution. Under acidic conditions, the reactivity is very low, because of the presence of the lactone structure. However, under alkaline conditions, the dye reacts readily to give ketone, phthalic acid and hydroquinone. In alkaline solution the carbon skeleton of the quinonoid structure is easily attacked by ozone.

- (vii) Anthraquinone Dyes: Ozonation of alizarin and Alizarin crimson gives phthalic acid.
- (viii) Metal containing dye: Ozone reacts with copper complex dye to give phenol, 2-naphthol and phthalic anhydride.
- (ix) Xanthenes: Xanthene reacts with ozone to give xanthone by way of xanthidrol accompanied by the formation of singlet oxygen. This suggests a 1,3-insertion reaction at the C-H bond of the 9-position of xanthene and xanthidrol to give corresponding hydro trioxide.
- (x) Phenothiazines and Phenoxazines: the reactions of phenothiazines and phenoxazines having low ionization potential with ozone in dichloromethane has been reported to exhibit

single electron transfer from the dye to ozone to give the radical cation of the dye and the radical anion of ozone.

Powell and coworkers (1992) evaluated the effectiveness of ozone and Fenton's reagent on the effluent from a textile slack washer and jet dye bath using a semi batch method. The dyes present were reactive azo and anthraquinone dyes containing a vinylsulfone reactive group. The reactor column was filled with a known amount of wastewater and ozone was bubbled through the wastewater solution at a constant rate. Fenton's reagent was conducted on a batch basis. Iron and peroxide were added at a specific rate and allowed to react until no further reaction was observed. The results of the ozone pretreatment indicate that ozone was ineffective in removing color from dye waste streams and the color removal efficiency ranged between 86%, 68% and 63% at ozone concentrations of 100 ppm, 250 ppm, 570 ppm and 725 ppm although no significant reduction in dissolved organic carbon could be observed. The variation in removal efficiency could be caused by competition and selective oxidation of chemicals.

Matsui et al., (1981) examined the reaction of various kinds of water-soluble dyes with ozone. It was observed that ozonation not only improved the biodegradability of all types of dyes but in addition, the azo dyes had a tendency to be easily decomposed with ozone and the decomposition being accelerated when accompanied by ultra-violet radiation. Tzitzis et al., (1994) studied the application of ozone to both raw and chemically precipitated textile wastewater. The authors observed that when 50% color

removal was obtained for raw wastewater, in the case of chemically precipitated wastewater, the percentage decolorization increased to 90%. In general the reactivity of ozone with dyes, in solution is evaluated by subjecting the decrease in the absorption maximum to first order rate kinetics. Dyes having olefinic and hydrazone groups react readily with ozone. Metal-containing and anthraquinone dyes are rather stable towards ozone. The introduction of an electron withdrawing or bulky substituent in the dye structure in the 2-position of the diazo component depresses ozonization.

Fenton's reagent reduced color to low level but the removal efficiency was dependent on the initial dissolved organic carbon of the waste streams, with higher initial DOC resulting in lesser color removal. Powell and coworkers (1992) recommended a ratio of peroxide to iron of 10 to 1 from 20 to 1, with the higher ratio being used when solids generation present a problem.

#### **1.2.4. Electrochemical Technology for Colour Removal**

The commercial development of electrochemical technology for treating contaminated water dates back to the early 1970's when the process was initially applied to the chemical reduction and removal of hexavalent chromium from cooling tower blow down water. Sung Ki Lee (1973) first patented this technology. However, when toxicity concerns discouraged the use of chromates in cooling tower water, the process found application in the treatment of wastewater from electroplating surface

finishing and printed circuit board operations where it was primarily applied for the removal of heavy metals from the wastewater of various industries and for the treatment of ground water. Several patent modifications and improvements have been made since then. This success in the treatment of heavy metals in wastewater paved path for utilizing this method as a treatment option for the removal of metallized dyestuffs. This method when applied performs a dual function of not only the removal of heavy metals but also achieves color removal from the dye liquor. In 1989, Andco Environmental Processes bagged the first (Uhrich, 1989) patent on the application of this process for the treatment of textile wastewater.

Uhrich (1989) in focused on the treatment of effluent from dye baths containing a variety of classes of dyestuffs using an iron cell were the first to put the Andco electrochemical system to use. Efficiency as high as 90% was achieved in terms of reductions in BOD, COD, TSS, Heavy metals and color.

Another similar study was carried out by Tincher, Weinberg and Stephens (1988) and Weinberg (1989) to study the decontamination of simulated acid dye baths, simulated solutions of stain blocking agents and effluent from a carpet dyeing facility reported a 80% efficiency in the removal of acid dyes from dye baths.

Wilcock et al., (1992) studied the potential for recycling electrochemically treated (using iron electrode) disperse dye effluents and reported a substantial degree of decolorization and detoxification could be achieved. Reuse of the electrochemically treated effluent resulted in first

quality dyeing. The authors reported results of five case studies applying Andco system to decolorize effluents containing metal complex disperse and acid dyestuffs, confirmed the ability of the electrochemical system to remove both the heavy metal (chromium) as well as the dyestuff. The study also report the success of reusing the electrochemically treated dye baths which is remarkable in the sense that they minimize the quantity of the effluent discharged without compromising the dyeing quality.

McClung and Lemley (1992) studied the mechanism behind electrochemical treatment and identified the breakdown products that could be released into the environment or be contained in the recycled decolorized effluent using HPLC. They report that adsorption and degradation of the dyestuff following interaction with the iron electrodes was the principal mechanism for the removal of dyestuff from the aqueous solution. In the case of azo dyes the study confirmed the formation of aniline.

When the iron cell was replaced by an Aluminium cell by Wilcock and co-workers (1992) to treat disperse dye effluent reported that physical adsorption rather than dye degradation was the principal mechanism behind decolorization. The difference in the results obtained by McClung and Lemley (1992) and Wilcock and co-workers (1992) could be explained by making a comparison of the two electrodes being used.

The Aluminium electrode cannot act as a reducing agent since Aluminium enters solution in a single valence state. In contrast when an iron electrode is used ferrous iron is released, which is capable of acting as

reducing agent cause dye degradation. The results also suggest that Quinolone dyes were easier to decolorize than either anthraquinone or azo dyes and that dyes with similar chemical structures react in a similar manner to electrochemical treatment. Thus, the nature of the dye, dispersing agent and other components of the commercial dye bath formulations are some of the factors that influence the efficiency of electrochemical treatment. Removal efficiencies are also dependent on the type (iron or Aluminium) and the quantity of absorbing matrix introduced.

The dye house effluents apart from containing dyes also contain heavy metals (chromium, copper, molybdenum and zinc), organic contaminants, BOD, COD, TOC, TDS and TSS. The dyes, heavy metals and organic contaminant although can be removed from the aqueous phase through physical methods such as adsorption and co precipitation, a large portion of the other contaminants would still remain the effluent. It is in this regard that the electrochemical technology offers a more superior treatment option in the sense that in addition to achieving a high efficiency in the removal of dyes, heavy metals and organic contaminants it will also remove BOD, COD, TOC, TDS and TSS.

The system utilizes an electrochemical cell to generate ferrous hydroxide directly from steel electrodes. The electrochemical cell consists of a fibreglass body containing a number of electrodes separated from each other by small gaps. The electrochemical cell could be iron electrodes or aluminium electrode. Wastewater flows through the gaps and comes in contact with the electrodes. A direct current power supply is

connected between the two end electrodes of the cell and the treatment level is controlled by the potential provided by the cell. As the current flows from one electrode to another through the process water, the positively charged sides of the electrode (the anodes) give off ferrous ions. At the negative side (the cathodes), water decomposes into hydrogen gas and hydroxyl ions. When iron electrodes are used, the overall reaction results in the formation of a combination of one or more of the following hydrous iron oxides: ferrous hydroxide, ferric oxyhydroxide and ferrous oxyhydroxide. On the contrary, when aluminium electrodes are used the end products are a combination of aluminium hydroxide and aluminium oxyhydroxide. The dissolved organics are removed through the generation of iron, aluminium or combined iron and aluminium matrix. The electrodes are slowly consumed as the metal hydroxide matrix is generated. Faraday's law is used to determine the generation time for a specific sample volume at controlled amperage. Since, hydrogen is formed during the process it is necessary that the effluent must be degassed. Hence, the effluent passes through a degassing tank where the dissolved gases are allowed to dissipate. During degassing it is necessary that the pH must be monitored. In the liquors in which the pH is less than 7 or greater than 11 (the range at which satisfactory  $\text{Fe}^{2+}$  precipitation occurs) the pH needs to be adjusted to maximize precipitation and ensure dye removal by adsorption. The water is then pumped from the reactor tank followed by a prior addition of a small amount of polymer flocculant to a clarifier where the newly forming solids settle. The clarifier supernatant then flows to a polishing filter before

leaving the system. Surface complexation and electrostatic attraction are the two most commonly used adsorption mechanisms (Buffle, 1988). Soluble inorganic heavy metal contaminants can exist either as cations ( $\text{Cr}^{3+}$ ,  $\text{Cd}^{2+}$ ,  $\text{Pb}^{2+}$ ,  $\text{Cu}^{2+}$ ) or anions (e.g.  $\text{MoO}_4^{2-}$ ). After forming all possible surface complexes, contaminants may be removed by simple electrostatic attraction.  $\text{Fe}(\text{OH})_2$  or  $\text{Al}(\text{OH})_3$  in combination with various surface complexes, contains areas of apparent positive or negative charge. The opposite charges attract and are capable of removing some dissolved species for aqueous phase.

The two most important factors to consider when adsorptive removal of heavy metals is desired are pH and the absorbing matrix to contaminant weight ratio. Careful control of the pH is critical if adequate adsorbing matrix is to be provided for complete adsorption. An increase in the pH improves adsorption of cations while a decrease in the pH forms adsorption of anions.

Wilcock et al., (1992) studied the performance of a 700 gal/min full-scale system located in Kentucky. The wastewater containing Vat and direct dyes when subjected to electrochemical treatment produced treated water of which 70-80% was suitable for reuse.

Szpyrkowicz et al., (2000) studied the electrochemical oxidation of synthetic textile wastewater containing partially soluble disperse dyes using seven different anode materials and 0.1 M NaCl as the supporting electrolyte. Among the anode materials tested, Ti/Pt-Ir anode displayed the best performance. Results indicated that pollutant removal was mediated



by active  $\text{Cl}_2$  generated by electrochemical oxidation of  $\text{Cl}^-$  or by other mediator's generated in-situ and not by a direct discharge of pollutants at the anode.

Vlyssides (1999) carried out electrochemical oxidation of textile dye wastewater from a reactive azo dyeing process using Ti/Pt as anode and Stainless Steel 304 as cathode. When the wastewater was passed through the electrolytic cell strong oxidants like  $\text{Cl}_2$ ,  $\text{O}_2$ ,  $\text{OH}^\cdot$  that were produced oxidized organic pollutants to  $\text{CO}_2$  and water. With the addition of 2 mL of HCl (36%) and after 18 min of electrolysis at  $0.89 \text{ A/cm}^2$ , COD was reduced by 86%, BOD was reduced by 71%, ADMI color units were reduced by 100%, and TKN was reduced by 35%. Wastewater biodegradability improved as indicated by the decrease in COD: BOD ratio from 2.16 to 1.52. At the same time, the mean energy consumption was  $21 \text{ kWh kg}^{-1} \text{ COD}$ .

Ciorba et al., (2001) studied color removal from simulated wastewaters containing direct (Direct Red 4A) and fiber reactive (Reactive Red M3A, Reactive Orange MG and Reactive Blue 4) dyes by aluminum based coagulant generated in an electrochemical cell with horizontal electrodes. The extent of color removal depended on the nature of the dye (89% for direct red, about 70% for reactive orange and reactive red and 94% for reactive blue) and occurred mainly in the bulk of solution.

When judiciously used the electrochemical ion generation (Fe or Al) is a proven cost effective technology for the removal of color, BOD, COD,

TOC, TSS, TDS and heavy metals from the dye house effluents. However, this electrochemical ion generation must be coupled with a conventional process such as clarification and filtration. This technology also reduces toxicity and produce clean water for reuse. Although not a major contributor to waste stream dyes often receive the most attention in textile wastewater treatment processes because of their color and toxicity of the raw materials like aromatic amines that go into the synthesis of dyes. Park and Shore (1984) indicated that the over 90% of the COD load from a typical plant that dyes and finishes woven cotton fabrics included desizing, scouring reducing agents and bleaches rather than the dyeing operation that contributed only 10 – 20% of the COD load. Shriver and Dague (1978) evaluated the characteristics of process wastewater and reported that the major waste source arise from sizing, dyes, soap, oils and other products typical of the industry. Textile dye wastewater is generally nutrient deficient however nutrient input can be provided by mixing the dye wastewater with municipal wastewater. Dyes exhibit different chemical characteristics and consequently respond differently to treatments aimed at their removal moreover, the arrival of numerous dyestuffs in the local market makes optimizing procedures for treatment of dye containing wastewater a horrendous task. The wide variety of dyes and other chemicals used in the dyeing operations provide an extremely variable composition to the dye wastewater. Detailed wastewater characterization is therefore an integral step in selecting wastewater treatment methodologies.

### 1.2.5. Pretreatment

Prior to discharge into an aerobic biological treatment system the dye house effluents are generally exposed to a wide array of pretreatment process such as coagulation and flocculation using lime, alum, ferric salts or polyelectrolytes followed by sedimentation or dissolved air flotation (DAF). However, generation of large amounts of sludge is one factor that tends to offset the use of coagulation and flocculation.

In a study conducted by Horning (1997) alum achieved average color reduction of 82% for the nine dyes in the study with doses ranging from 8-80 mg L<sup>-1</sup>. Although both alum and Powdered activate carbon was effective in reducing color, the average TOC reduction was 43% for PAC and 33% for alum. Boe (1993) found alum more efficient in removing color than ferric sulfate or polyaluminium chloride. 37.8%, 40.7% and 23.5% reductions were achieved with respect to color, COD and BOD using an alum dose of 400 mg L<sup>-1</sup>.

Stahr et al., (1980) conducted chemical precipitation experiments on sulfur, vat and acid dyes and found that alum at doses between 100-500 mg/L effectively removed color. Color removal increased with a cationic polymer at a dosage of 10 mg L<sup>-1</sup>.

Mehrotra et al., (1995) applied coagulation to remove color from textile dyeing effluents. MgCO<sub>3</sub> was found to be effective at 1000 mg L<sup>-1</sup> and at pH 10 providing over 90% removal of sulfur dye. FeSO<sub>4</sub> removed color only at a high dosage of 14000 mg L<sup>-1</sup> for vat dye.

Panswad and Wongchaisuwan (1986) examined capability of magnesium carbonate-hydrated basic ( $3 \text{MgCO}_3 \cdot \text{Mg}(\text{OH})_2 \cdot 3\text{H}_2\text{O}$ ; MCHB) in terms of color reduction from a reactive red dye wastewater. Their study indicated over 90% color removal when MCHB was combined with lime.

Poon and Virgadamo (1973) put into use a combination of activated carbon and biological treatment at dyeing and finishing operation. The system consisted of an aeration basin, two activated carbon columns operating in parallel with an anaerobic biological regeneration phase and a second part of the parallel activated carbon columns with an aerobic biological regeneration phase. This plant produced 53-67% reduction in TOC, 55-70% reduction in COD and 66-73% reduction in  $\text{BOD}_5$  at an average flow rate of 75,000 gal/day. The efficiency of treatment was found to dependent on the flow rate with a lesser degree of treatment being achieved at lower flow rate. The system when modified through increased size of the aeration basin, three additional carbon columns and increased carbon regeneration times increased the TOC reduction by 91%, COD by 92% and  $\text{BOD}_5$  by 94% at a flow rate of 75,000 gallons per day.

Grau (1991) observed that although chlorination and ozonation was effective in decolorizing reactive and acid dyes, chlorine was more efficient at lower pH while the efficiency of ozone was found to be pH independent.

Kabdash et al., (1995) reported that when hydrogen peroxide was not effective in decolorizing acrylic dyeing wastewaters at both acid and alkali pH values for raw and biologically treated wastewaters, sodium hypochlorite resulted in complete decolorization. The dosages required

varied between 500-2000 mg L<sup>-1</sup> as Cl<sub>2</sub> with lower dosages being required under acidic conditions.

Davis et al., (1982) oxidized the textile wastewater with hydrogen peroxide and found no decoloration at neutral pH values. A significant color removal was obtained with hydrogen peroxide at pH 12 only after 24 hours. Chemically precipitated wastewater samples were subjected to calcium hypochlorite and at a dosage of 100 mg L<sup>-1</sup> the color changed to pale yellow. Michelsen et al (1992) evaluated the efficiency of various adsorbents (32 different adsorbents including rice, grain, chitin and coal), flocculants and reducing agents in removing color from Navy 106 slack washer water. The adsorbents were found to be generally effective however, disintegrated adsorbents contributed to increased TOC. The authors however concluded that the use of adsorbents do not appear to be a practical mechanism for the removal of reactive dyes from wastewater since large amounts of expensive adsorbents were required to achieve a high degree of color removal. Of the fifteen polymers that was evaluated very little color removal was achieved. While adsorbents performed better at lower pH, there was no observable trend in flocculant performance versus pH. The results suggest that the use of polymer flocculant cannot be considered as a practical treatment option to decolorize wastewater containing hydrolyzed reactive dyes.

Coagulation/flocculation could be a viable method for treating dye wastewater particularly those containing reactive dyes as shown by Koprivanac et al., (1998). The authors evaluated the possible use of

coagulation/flocculation process for the removal wastewater containing monochlorotriazine reactive dyes with azo and anthraquinone chromophoric groups. The ability of  $AlCl_3$  to remove various reactive dyes from aqueous solutions was examined using a certain stirring tank configuration, which involved rapid and slow mixing. Optimum pH and coagulant concentration and sludge characteristics were also determined. Dye removals >99.5% was achieved. The quality of treated dye wastewater was evaluated using several ecological parameters like COD, BOD, total organic carbon, adsorbable organic halides and IC50.

Ganjidoust et al., (2000) compared the effect of natural and synthetic polymers vs. chem. coagulants on COD, turbidity and color removal from wastewater. Results indicated that among polymeric coagulants, chitosan with a minimum dosage removed 46, 19, 50% of COD, turbidity and color, respectively while among chemical coagulants, Lime removed 33, 57, 40% of COD, turbidity and color, respectively.

Malik et al., (2001) carried out coagulation-flocculation experiments using two inorganic coagulants (aluminum sulfate and ferric chloride) and a cationic organic polyelectrolyte. pH, coagulation-flocculation time and coagulant dose were optimized. Results indicated that under optimum conditions when the wastewater samples were treated using only inorganic coagulant, 92% decolorization was observed and a combination of inorganic-organic coagulants increased the percentage decolorization to 96. The removal of TSS and COD by these processes under the optimum

conditions for color removal were 48-70%, 55-75% and 40-50%, 46-54% respectively.

Carvalho et al., (2002) reports that the process performance of coagulation to remove reactive dyes from dye-house effluent is affected by multiple factors, which can be best examined in factorially designed experiments. An inorganic salt (ferrous sulfate) and an organic polymer (DEC 50) was selected for the study. Factorially designed jar-test experiments were performed with different compounds of a synthetic cotton processing wastewater to identify the factors that most affected color removal and highlight interactions between them. Results indicated that some additives, such as an oxidative desizing agent and a peroxide stabilizer, favored color removal within specific concentration ranges, while the presence of sizing agents and surfactants reduced process efficiency. This could be counteracted using high concentrations of ferrous sulfate, but it would result in higher sludge disposal costs.

#### **1.2.6. Aerobic Biological Treatment**

Aerobic biological degradation and in that the activated sludge treatment system which also happens to be the most traditional and widely used secondary treatment process is being viewed today as being grossly inadequate in meeting the present standard for effluent discharge. The issue of toxicity of effluents is also gaining prominence with improvements in analytical methodologies and sophisticated instruments to analyze toxic compounds, in water, sludge and sediment BOD<sub>5</sub> no longer happens to be

the only criteria for evaluating the effectiveness of a particular treatment process.

The inefficiencies of such system in effectively addressing the problem of residual color have caused aesthetic problems in the receiving waters and encourage alternative treatment options. One of the most important properties that are built into commercial dyes is its resistance to fading caused by chemical and light induced oxidation. In other words, the dyes are by themselves resistant to oxidative biodegradation.

The dye house effluents due to constant product changes and batch dyeing operation present wide variations in composition; as a result one of the major factors that contribute to the ineffectiveness of the aerobic biological treatment of dye wastewater is the difficulty in acclimating the organisms to the substrate.

Porter and Snider (1976) conducted studies on the aerobic biological degradation of dyes have revealed that the dyes are slow to degrade by this method and a non-biodegradable fraction remains in the dye wastewater following treatment. This is supported by the studies on  $BOD_5$  versus the ultimate biodegradability of the waste; which indicate that:

- (i) The  $BOD_5$  for textile dye wastewater is a relatively small fraction of the 30-day BOD. This indicates that the 30-day BOD tests demonstrate much greater biodegradability of the dye wastes than the standard 5 day BOD test.
- (ii) The textile dye degradation is much slower than the degradation of biodegradable wastes found in the domestic



wastewater. Porter and Snider (1976) found that of the eight commercial textile dyes that included direct, disperse, reactive and vat dyes, the average  $BOD_5$  was found to be  $20,000 \text{ mg L}^{-1}$ , which was 38% of the 30 day BOD load of  $53,000 \text{ mg L}^{-1}$ . In addition, the study also found that the BOD curves for some of the dyes tested continued to rise increased beyond 30 days, which indicate that the dye wastes require long periods of acclimation and are slow to degrade. On the other hand,  $BOD_5$  values for readily biodegradable wastewater such as a domestic wastewater is 60-70% of the ultimate BOD.

Moreover, in spite of achieving moderate reduction in  $BOD_5$  significant amounts of TOC and COD still remain in the effluent; this could be explained by the fraction of organics present in waste stream that is either non-biodegradable or difficult to biodegrade. This is not measured by  $BOD_5$ . Porter and Snider (1976) therefore concluded that  $BOD_5$  is therefore not an accurate measurement of the ultimate biodegradability.

In the BOD tests conducted by Shriver and Dague (1978) after ten days the biodegradation of the textile wastewater was 31% while the biodegradation of colored domestic water was 92% complete. The study indicates that in comparison to the domestic wastewater the textile wastewater undergo a slower rate of biodegradation. They observed a high COD to BOD ratio (average 135:1) indicating that a non-biodegradable fraction of organics remained in the effluent even after aerobic treatment.

Shaul and coworkers (1987) have also shown that dyes degrade slowly under aerobic conditions.

The results of all these studies show that there is a need to identify alternative treatment technologies that would perform better than the aerobic biological treatment in reducing organic loadings, color and toxicity of wastewater effluent.

Shriver and Dague (1978) constructed four pilot scale activated sludge units with detention times of 12, 24, 36 and 48 hrs and a MLSS concentration of  $200 \text{ mg L}^{-1}$  and observed that a substantial decrease in color and COD with increase in detention time. For a 12 hr detention time, the BOD, COD and Color reductions were 84%, 41% and 22% respectively whereas for a 48 hr detention time increased the reduction by 92%, 74% and 50%.

Scientists at the EPA's water Engineering Research Laboratory in Cincinnati, Ohio, (Shaul and coworkers, 1987) studied the fate of water-soluble acid and direct azo dyes in the activated sludge process. Screened raw wastewater was used from a local sewage treatment plant as an influent to a three pilot scale activated sludge biological treatment system operated in parallel. The wastewater influent to the treatment system was then spiked with commercial dye of varying concentrations. Dye analysis was then conducted on the wastewater effluent and activated sludge. Data obtained from the study demonstrated that eleven out of eighteen dyes passed through the system untreated, four adsorbed on to the activated sludge and three underwent biodegradation.

Literature survey conducted by Shaul and coworkers (1987) indicate that adsorption to the sludge was the primary removal mechanism for dyes in a biological wastewater treatment system. The authors report that there are several factors that inhibit the permeation of dye through the microbial cell membrane, such as increased water solubility and increased molecular weight, which reduce the effectiveness of biological degradation. These reports further strengthen the view that the activated sludge process does not decolorize wastewater-containing dyes of high water solubility, effectively. The four dyes that were adsorbed on to the activated sludge had fewer sulfonic acid groups and were of higher molecular weight, features that reduce water solubility.

Dohanyos and coworkers (1978) evaluated the treatment efficiency of twenty textile dyes including azo acid, direct and reactive dyes in a laboratory scale activated sludge system. The results of the study reveal that physical and physico-chemical processes such as diffusion, adsorption and chemical reaction were the prime mechanisms for dye removal. With the presence of hydroxyl, nitro and azo groups in the dye structure and the decreased size of the dye molecule favoring increased removal and decreased by the presence of sulfonic acid groups. These results also indicate that dyes having high water solubility are less likely to be removed by the activated sludge process. A comparison of the batch and continuous flow activated sludge treatment systems reveal that dye removal occurred via similar mechanisms, the concentration of the dye (10

– 240 g/m<sup>3</sup>/day) had no effect on the treatment efficiency and the amount of dye removed was directly proportional to the sludge production.

Gardner and coworkers investigated the fate of a water-insoluble monoazo dye (Disperse blue 79) in a continuous feed pilot-scale wastewater treatment system. Since, the dye house effluents are nutrient deficient; screened raw wastewater from a local municipal wastewater treatment plant was spiked with 5 mg L<sup>-1</sup> of the dye. Unspiked municipal wastewater served as a control. The fate of the dye in the effluent, primary and waste activated sludge; digester supernatant and digester effluent was evaluated. The results of this study revealed that on an average 20.4% of the dye remained in the effluent from the activated sludge system, 3.6% was found in the primary sludge and 62.3% was present in the waste activated sludge. A mass balance around the entire system accounted for 86.3% of the dye present in the influent. The authors did not detect any compound related to the dye so as to provide evidence of biodegradation in the activated sludge process and account for the remaining 13.7%. This result indicates that although 62.3% of the dye was removed by the activated sludge treatment the primary removal mechanism was adsorption to the sludge.

The Ecological and Toxicological Association of the dyestuffs Manufacturing Industry (ETAD), a trade association representing dyestuff manufacturers, developed a test method to evaluate the tendency of a particular dye to be treated by the activated sludge process (1978). In the test the dye solution was added to activated sludge suspension, the treated

sludge was then centrifuged and the absorbance of the supernatant was measured using a colorimeter. The amount of the dye adsorbed on the sludge is determined by comparing the absorbance of the supernatant to that of a blank solution (prepared in the absence of the dye) and a standard dye solution (of a known concentration). This test method was applied to six classes of dyes and the test results were found to be consistent among six laboratories using two types of activated sludge. ETAD found that the presence of a sufficient amount of activated sludge is critical to the effective adsorption and successful dye removal. The class of the dye and structural differences within each class determines the suitability of the dye to the activated sludge treatment. The test results indicate that low adsorption occurs with acid and reactive dyes, high adsorption occurs with the basic and direct dyes and high to medium adsorption occurs with disperse dyes. Within the class of acid dyes the degree of adsorption was partly related to the number of sulfonic acid groups in the dye molecule.

In contrast to the general conclusion from the above studies which show that little degradation of dyestuffs occur in aerobic biological treatment system; in a study conducted by H.D. Pratt (1968) involving the degradation of two Disperse dyes show that Disperse Red 5 was degraded under aerobic conditions, whereas Disperse Orange 5 required anaerobic conditions for degradation.

Walker and Weatherley (2000) examined aerobic biodegradation of an acid anthraquinone dye, Tectilon Blue (TB4R) a major colored component from the aqueous effluent of a carpet printing plant using 3

bacterial strains: *Bacillus gordonae* (NCIMB 12553), *Bacillus benzeovorans* (NCIMB 12555), and *Pseudomonas putida* (NCIMB 9776). All 3 strains successfully decolorised the dye and results were correlated using Michaelis-Menten kinetic theory. Biosorption of the dye onto the biomass attributed to 19% decolorization while majority of decolorization was caused by dye utilization by bacteria. The reaction rate was intermediate between zero and first order at dye concentrations of 200-1000 mg L<sup>-1</sup>.

### **1.2.7. Anaerobic Biological Treatment**

Anaerobic biological treatment studies on textile wastewater have yielded encouraging results. Significant color reductions and breakdown of azo dye molecule have been demonstrated under anaerobic conditions. The anaerobic biological reduction of azo dyes have been investigated from many perspectives; some have been primarily concerned with the treatment option that this method offers to color removal and chemical degradation. Others have studied the potential generation of toxic amines and the consequences of their release to the environment.

Brown and Hamburger (1987) carried out anaerobic digestion of fourteen solutions of commercial azo dyes, which included acid, direct and mordant dyes; observed that 90% of the dyes were degraded. Cleavage of the azo bond and formation of the corresponding aromatic amines was the primary degradation step. Other pathways contributing to dye degradation include sludge adsorption and reduction of the functional groups.

Walker and Weatherley (2000) examined aerobic biodegradation of an acid anthraquinone dye, Tectilon Blue (TB4R) a major colored component from the aqueous effluent of a carpet printing plant using 3 bacterial strains: *Bacillus gordonae* (NCIMB 12553), *Bacillus benzeovorans* (NCIMB 12555), and *Pseudomonas putida* (NCIMB 9776). All 3 strains successfully decolorised the dye and results were correlated using Michaelis-Menten kinetic theory. Biosorption of the dye onto the biomass attributed to 19% decolorization while majority of decolorization was caused by dye utilization by bacteria. The reaction rate was intermediate between zero and first order at dye concentrations of 200-1000 mg/L.

Hu (1998) studied the decolorization of three Azo dyes V<sub>2</sub>RP, RP<sub>2</sub>B and Y<sub>3</sub>GP by *P.luteola*. They observed that *P.luteola* grew well even in medium containing 300 mg/L of the dye at low glucose concentration and without nitrogen source achieving up to 95% decolorization within 5 days. The reduction was mediated by an inducible enzyme azoreductase, which was found to be substrate specific. The reduction followed first order kinetics and the metabolic product was identified as orthanilic acid.

Minke R. and Rott U. (1999) carried out bench scale biodegradability tests. The authors observed that anaerobic processes could be used to treat highly loaded split flows and concentrates from the textile processing industry as many dyes that were refractory under aerobic conditions underwent almost complete decolorization under anaerobic conditions with efficient COD removal rates.

Willettts and Ashbolt (2000) studied the decolorization of Reactive Red 235 under batch conditions under both thermophilic and mesophilic conditions with intact and autoclaved biomass and also using the pre-reduced supernatant from a spent culture. The decolorization followed first-order kinetics. The availability of the reducing power was considered to be the rate limiting factor and that the dye reduction occurred extracellularly. The authors observed that active anaerobic cells give the most efficient and complete decolorization especially under thermophilic conditions where the rate was three times higher under thermophilic conditions as compared with mesophilic conditions.

Krull et al., (1998) studied the combined biological and chemical treatment of highly concentrated reactive azo dye-containing residual dye house liquors with recalcitrant compounds using a sequencing batch reactor (SBR) consisting of both anoxic and aerobic phases. Complete decolorization and mineralization without the addition of external auxiliary substrate occurred under anoxic conditions up to a dye concentration of 20 g L<sup>-1</sup>. Revitalization and production of biomass, which acts as an internal hydrogen-donor in the anoxic phase, took place in the aerobic phase from split flows with readily biodegradable compounds. Mineralization of the remaining recalcitrant organic compounds was improved by partial oxidation with ozone in a circulating process, simultaneously performed to the aerobic phase. The authors report that the combined biological and chemical treatment resulted in complete decolorization and an overall COD and DOC elimination of 90%.



Beydilli et al., (1998) developed a fixed-film anaerobic reactor using anaerobic, methanogenic culture enriched from municipal sewage sludge to renovate reactive textile dye baths and reuse the high salt-containing mixture in the dyeing process. Bioassays performed to evaluate potential toxicity of the selected dyes to the anaerobic microorganisms indicated that no significant toxic effects were observed up to a dye concentration of 300 mg L<sup>-1</sup>. On the contrary, gas production was found to be higher than that of the control cultures. Percentage decolorization ranged from 77.8 to 97.1%. Despite continued decolorization higher dye concentrations had slight inhibitory effects on methanogenesis with the total gas and methane production decreasing to 66.5% and 56.6% at a dye concentration of 2000 mg/L. The authors report that under the low redox potential maintained by the methanogenic culture, color removal occurs irrespective of the culture activity level.

Wang and Yu (1998) investigated the adsorption and degradation of three synthetic dyes with representative chromophores of azo, anthraquinone and indigo on the mycelium of *Trametes versicolor*. The maximum adsorption capacity ( $Q_{max}$ ) and adsorption affinity ( $K$ ) of dead and living fungal mycelia to the three dyes were measured and estimated using the Langmuir model. The authors observed that the adsorption capacity and affinity of fungal hyphae to the dyes depended on the structure of individual dyes. Intracellular or extra cellular enzymatic degradation of adsorbed dyes was found to be the major mechanism of decolorization by the fungal mycelium. The authors reported that T.

versicolor produces little extra cellular enzymes in its primary growth phase, but releases the enzymes as secondary metabolites in stationary phase. The sequential adsorption and degradation of dye molecules on living fungal hyphae provides a feasible application of white rot fungi as a treatment option for decolorization.

Several studies have indicated that rather than biodegradation, adsorption was the primary mechanism that contributed to colour removal. Singer and Little (1975) conducted biodegradability studies on textile wastewaters and observed that during an extended 21 day BOD test the color removal in general was less than 50%. Porter and Snider (1976) reported that no significant loss of color occurred even after 30 days for 8 dyes in a long-term BOD test. The authors attributed limited removal of color in biological treatment mainly to flocculation and adsorption on mixed-liquor suspended solids. Weeter and Hodgson (1977) studied the biodegradability of six textile dyes and showed that dyes were very slightly degradable on an extended time period with the removal mechanism being primarily adsorption on microorganisms. Contact time was found to have no influence on color removal and adsorption capacity was found to have a limit. The sludge acclimated to dyes were found to give better color removal. Pagga and Brown (1986) conducted short-term aerobic biodegradation tests on 87 dyestuffs and found that dyestuffs were most unlikely to show any biodegradation and color removal may be attributed to adsorption. Similar findings have also been reported by Grau (1991) who stated that partial decoloration in biological treatment was achieved by

adsorption of dyes on activated sludge. Davis et al., (1982) studied the biodegradability of several textile-dyeing wastewaters and found that there is a trend of more color removal with increased organic loading probably due to the high cellular growth rate and associated color adsorption at higher organic loading rates. The authors also indicated that color desorption could also occur during sludge handling.

#### **1.2.8. Anaerobic-Aerobic Sequence**

Anaerobic-aerobic sequence can be considered as a potential treatment option for the dye house effluents. This is because although the anaerobic treatment degrade the azo dyes to their corresponding amines achieving decolorization the potential toxicity of these amines call for a high efficiency subsequent aerobic treatment in order to prevent the release of toxic compounds into the environment.

Lloyd and coworkers (1992) evaluated an anaerobic-aerobic treatment sequence on dye house effluents containing reactive azo dyes. The study was conducted using an acclimated seed and varying ratio of the dye and sanitary effluent solutions in 300 ml BOD bottles. Color measurements were taken in each of the seven intermittent days, including the 21<sup>st</sup> day. Results show that the dyestuff degraded from 31% to 86% depending on the concentration of the dyestuff present in the solution. At high dye concentration less overall color degradation and slow rate of color loss was observed. This has been attributed to the high dye-

microorganism ratio and due to the inhibition caused by the dye molecules or the reduction metabolites.

In a similar study Lloyd and coworkers (1992) carried out decolorization experiments using an aerobic biological treatment and anaerobic biological pretreatment followed by aerobic treatment. When the aerobic treatment alone produced 28% decolorization; the anaerobic-aerobic sequence achieved 88% color reduction. Similarly when the anaerobic-aerobic sequence achieved a 79% TOC reduction, the aerobic treatment alone achieved only 69% reduction. Thus, the anaerobic-aerobic sequence was approximately 10% more effective in reducing TOC than aerobic treatment alone. Similarly in the case of BOD<sub>5</sub> when 96% reduction was obtained from aerobic treatment process 98% reduction was obtained from anaerobic -aerobic treatment. In the case of COD reduction; when the aerobic treatment achieved 78% reduction, the anaerobic-aerobic sequence achieved 88% reduction in COD.

Similarly, when the BOD<sub>5</sub>: COD ratio was calculated at several points as a measure of the biodegradation potential of the wastewater show that the anaerobic pretreatment step increased the ratio and the subsequent aerobic treatment reduced it.

Weber and wolfe (1987) report that the anaerobic degradation of azo dyes may be abiotic in nature and the primary removal mechanism could be sorption to the sludge; but, they identified that sorption was the first step in the anaerobic degradation of dye stuffs and developed a kinetic model based on abiotic anaerobic degradation of soluble azo dye in sediment-

water systems where transport to the sediment site is the rate determining step.

Thus, the results indicate that the anaerobic-aerobic sequence show a significant improvement over aerobic treatment alone by not only achieving greater color reductions but also improves the removal of organics as well. In a pilot study conducted by Boe and coworkers (1993) report 65-70% decolorization and 70-75% reduction in TOC using an anaerobic system with only 200 mg L<sup>-1</sup> biomass.

Microorganisms that are not acclimated to the substrate are likely to inhibit the biodegradation process. In some cases acclimation could also be a primary requirement in biological wastewater treatment but the textile mills may not have the luxury of acclimating and maintaining the system to treat specific components of the waste due to the batch nature of the dyeing process and large number of dyes being used in the dyeing operations.

Shaul and coworkers (1987) indicate that sulfonic acid groups, which are widely used to increase the water solubility of dyes, inhibit aerobic biological degradation of dye wastewater.

Lloyd and coworkers (1992) indicate that dyes by themselves are often inhibitory to the activated sludge process.

Gardiner and coworkers (1978) indicate that the presence of toxic metals in the dye could inhibit microorganisms.

Brown and Hamburger (1987) indicated that some dyes could be structurally altered under anaerobic conditions, which could influence its

biodegradability. The types of dyes and substituent groups found in the wastewater greatly influence their treatment.

Investigations into the rate-determining factors in the anaerobic reduction of azo dyes reveal that the optimum pH range for the azo reductase enzyme is 5-8 and that the reduction rate increases exponentially as that pH is lowered within the range (1982). They report that the transport of the dye through the cell wall may be a rate-determining factor. Increased cell age and reduced food-microorganism ration increase cell permeability and improves the rate of dye reduction.

Luangdilok W and Panswad T. (2000) used an Anaerobic/Aerobic sequence sequential batch reactor system to treat synthetic dye wastewater. Glucose and acetic acid were used as the carbon sources together with four different reactive dyes over the concentration range of 20-100 mg L<sup>-1</sup>. The authors observed that there was a decrease in the decolorization rates with an increase in dye concentration. Of the dyes studied decolorization of disazo dye resulted from the cleavage of the azo bond while, the decolorization of anthraquinone dye was believed to be through direct adsorption of the dyes on to the floc materials. Different types of dyes had different impacts on phosphorous removal rates, while the dye type did not greatly affect the COD or TKN removal. Moreover, when the phosphorous removal rates ranged from 40-50% the COD and TKN removal rates were 90-99%.

Some researchers (Huag et al., (1991)) have studied the influence of enzyme-generated flavins and cofactors NADP<sup>+</sup> and FAD<sup>+</sup>, glucose 6-

phosphate on the rate of azo bond cleavage initiated by azo reductase enzyme. The position and types of substituent groups (e.g., amino, hydroxy, methyl and sulfonic acid) and the relative positions on the aromatic rings of the dye molecule affect the availability of the substrate and consequently, the rate of biological anaerobic reduction.

### 1.2.9. Fungal treatment

White-rot fungi is reported to have decomposing effect on variety of materials such as lignin, cellulose, and toxic chemicals. Cho et al., (1999) investigated decolorization characteristics of effluents from bleaching plant of pulp mill with three white-rot fungi (*Trametes versicolor*, *Ganoderma applanatum*, and *Pleurotus ostreatus*). In addition, the effect of carbon and nitrogen resources was also identified. Stationary cultures were more effective at decolorization compared to the shaking culture. The optimum inoculum weight based on dry weight of mycelia was 1.0 g. The addn. of nitrogen source was found more efficient than that of carbon source. The authors observe that Mn peroxidase (MnP) and laccase activity play an important role in decolorization of the effluent. Similar experiments were carried out by Srinivasan and Murthy, (1999) using mycelial pellets of *Trametes (Coriolus) versicolor*. The variables studied were pH, glucose (substrate) concentration, initial effluent color, and ammonium chloride (nutrient). The maximum color removal efficiency was 82.5% obtained with an optimal glucose and ammonium chloride concentrations of 15 g L<sup>-1</sup> and 0.5 g L<sup>-1</sup>, respectively at pH of 4.5 without

diluting the effluent. On the other hand Shintani et al., (2002) observed that a newly isolated fungus *Geotrichum candidum* Dec 1 decolorized Kraft pulp bleaching effluent when supplemented with glucose. The fungus showed decolorizing potential for a wide spectrum of synthetic dyes. The authors observed that Dec 1 had a different mechanism of decolorizing kraft pulp bleaching effluent, as the contribution of extracellular enzymes such as peroxidase (DyP), manganese peroxidase, and laccase to the decolorization process was small. This is contrary to the observations made by Cho et al., (1999).

Mohan and Karthikeyan (2000) investigated removal a diazo dye (Direct Brown 2) using viable algae *Spirogyra* species. Color removal was found to be dependent on the contact time and biomass. Color removal mechanism was attributed to biosorption and/or bioconversion and/or biocoagulation.

Sumathi and Manju (2000) observed that *Aspergillus foetidus* (an isolated fungus) was found to effectively decolorize media containing azo reactive dyes namely, Drimarene dyes. The extent of color removal was greater than 95% within 48 h of growth of the fungus. The process of decolorization was found concomitant with the exponential growth phase of the fungus and needed the presence of a biodegradable substrate such as glucose. The mechanism was reported to be bioadsorption to the rapidly settling fungal biomass pellets. Biotransformation was found to be insignificant. The process was time dependent and followed first order



kinetics with respect to initial dye concentration. The rates of color uptake (k values) decreased significantly with increasing initial dye concentration.

#### **1.2.10. PACT system for treatment of dye house effluents**

A combination of the powdered activated carbon and activated sludge system is known as PACT system. The development of the PACT system dates back to 1960's. In the Delaware River in 1960's numerous incidents of fish kills were reported in summer. Low dissolved oxygen concentrations were identified as the major cause for the fish kills. The regulating authorities on the basis of a river model study directed all the discharges to reduce their BOD load to the river by 85%. However, modification in the activated sludge plant could not meet the required standard. It was then that the idea of adding powdered activated carbon to the activated sludge system occurred and within a week the effects of the carbon addition was observed; as the BOD removal increased from 79% to 96% (Hutton and Robertaccio, 1975). The PACT system is used to treat aqueous waste streams that are too dilute for oxidation technologies, such as wet air oxidation or incineration and for waste streams that are too strong to economically treated with GAC. Depending on the waste characteristics, the carbon dosage may range from 10 to over 1000 mg of powdered carbon added per liter of wastewater flow. Although the point of addition of the PAC generally makes little difference in the overall results the common points of application include directly to the waste stream before treatment. to the recycle sludge or to the aeration tank. PACT

systems can treat aqueous waste streams having a strength of 50-50,000 mg/L COD (Meidl and Wilhelmi, 1986).

Since the origin, several modifications have been introduced into the PACT system. In 1991, the original single stage process has been upgraded to the two stages to enhance the removal efficiency of the pollutants.

The batch aerobic PACT system was developed by Zimpus Environmental mainly to handle less (1,50,000 gpd) wastewater flows. In this system the same tank is used to create and to settle. Wastewater would be first pumped into an aeration tank where it comes in contact with a mixture of biological solids and PAC and the flow is stopped. The contents of the aeration tank are then aerated during which the biodegradable portion of the waste degrades, while the non-biodegradable components get adsorbed on the activated carbon particles.

#### **1.2.11. Membrane Filtration**

It has been established beyond doubt that the biological treatment system although widely used falls short of meeting the stringent environmental regulations, particularly with respect to the residual color. This fact has forced several industrial units to install advanced physical or chemical methods.

Several studies report that through the membrane filtration technique it was possible to produce stable liquid reactive dyestuffs through the removal of dissolved electrolytes. (Kroll et al., 1983, Pohlmann et al.,

1983, Lacroix R., 1985 and Hugelshofer et al., 1985). According to Irvine et al., (2000) Nanofiltration has proved to be a cost effective method for color removal by small treatment works and tubular membranes have proved to be ideally suited as routine mechanical cleaning can be automated, thereby reducing operator attendance and costs.

Koyuncu et al., (1999) used a two-stage membrane treatment ultra filtration [UF] and reverse osmosis [RO], (brackish water [BW] and seawater [SW] membranes) to treat a biologically treated effluent from pulp and paper and fermentation industry. In the first part of the study, UF and RO combined treatment resulted in very high removal of COD, color, and conductivity from pulp and paper effluent. Almost complete color removal was achieved in RO experiments with SW membranes. In the second part of the study, UF and RO membranes were evaluated for their suitability to separate color and COD from different wastewater streams generated by the fermentation industry. Overall removal efficiency for COD, color, conductivity, and  $\text{NH}_3\text{-N}$  were 90-95%, 95-97%, 85-90%, and 80-90%, respectively. The study clearly reveals that color in complex industrial wastewater could be effectively solved using membrane technology.

Polysulfone membranes have gained prominence in the field of textile effluent treatment due to their high resistance to strong acids and bases, solvents and elevated temperatures. Alves et al., (2000) Investigated the performance of ultra filtration (UF) for color removal from 3 different effluents coming from the dyeing cycle of a tannery industry using 4 polyethersulfone (PES) membranes with molecular weight cut-offs

(MWCO) of 40, 10, 5, and 3 kDa. A closed-loop recycle (CLR) and batch (B) modes of operation were used. Membranes with higher MWCO showed the occurrence of concentration polarization and adsorptive fouling. The results indicated High-color and low-solids rejections for all the experiments.

Ribeiro et al., (2002) studied the use of asymmetric polymeric membranes synthesized by phase inversion process for color and turbidity removal from an industrial textile wastewater. A 23 factorial planning was carried out using 2 levels (- and +), together with the factors: polymer type (polysulfone and polyvinylidene fluoride), polymer concentration and salt concentration (KCl 0% and 5%). Best results of these parameters were obtained with the membranes: M1 (polysulfone 13% and salt 0%), M2 (polysulfone 13% and salt 5%) and M3 (polysulfone 18% salt 5%).

Porter (1990) described an Indigo recovery process using a multi stage feed and bleed ultra filtration system with vinyl-sulfone membranes. Each stage automatically establishes a steady state concentration that becomes progressively higher as the dye concentration increases. The final stage achieves the maximum concentration of Indigo needed for reuse.

Hobbs (1989) estimate that about 20-50% of the reactive dyes used initially would be present in the exhaust liquor; this is because during the application of reactive dyes to cellulosic fibers a competing hydrolysis reaction occurs inactivating some of the reactive dye stuff, thereby resulting in unfixed hydrolyzed dye stuff producing unacceptable levels of color in

the effluents. Such effluents can be effectively treated by reverse osmosis and ultra filtration where the percentage decolorization achieved range between 95-100%.

Tegtmeyer (1993) and Sewekow (1993) studied the application of membrane filtration for the treatment of reactive dye baths using nano-filtration membrane. The results show that the dyestuff could be concentrated to about 0.5-1% of its initial volume. The resulting permeate stream was almost colorless, containing salt and low molecular weight impurities that could be discharged or reused. The report demonstrate that the total reactive dyestuff wastewater can be separated into two streams one having low salt content that could be treated by reverse osmosis and one having high salt content which can be concentrated by nano-filtration.

Erswell and coworkers (1988) report that the reactive dye liquors can be effectively decolorized in a closed loop recycle system using ultra-filtration membrane carrying ionic charges. The system produced decolorized permeates with over 90% water recoveries which could be reused in the dye house.

Groves and coworkers (1988) using dual layered zirconium based dynamic membrane successfully treated dye containing effluents from both alkaline viscose and acidic polyester dyeing units, achieved a 99% color removal at pH-4.3 with a 70% water recovery. The same membrane achieved a 99% color removal, 97% reduction for TOC and an overall water recovery of over 80% at pH range of 7.8-9.3.

According to Irvine et al., (2000) Nanofiltration has proved to be a cost effective method for color removal by small treatment works and tubular membranes have proved to be ideally suited as routine mechanical cleaning can be automated, thereby reducing operator attendance and costs.

Hugelshofer et al., (1984) and Kroll et al., (1982) report that reverse osmosis or ultra filtration could be used for the preparation of highly concentrated dispersions of vat and disperse dyestuffs in the production of liquid basic dye stuffs, leather dye stuffs and food colorants.

A.Henz and H.Pfenninger (1987) developed a two stage ultra filtration reverse osmosis system to treat about 500 m<sup>3</sup> /day of wastewater from dyestuff manufacturing units utilizing polysulfone or polyacrylonitrile modified with cationic or anionic groups. The color removal efficiency was 99% and the retention of heavy metals such as copper and chromium was in the range of 75-99% and 85-99% respectively. The removal of azo dyes using ultra filtration using cellulose acetate membrane indicated that the structural features of the dyestuff such as arrangement of sulfonic acid groups and the presence of heterocycles in the conjugated system have a greater influence on their selective removal and the membrane than molecular weight.

Membrane filtration is well known in electroplating industries where it is used for the recovery of heavy metals (Kosarek., 1981).

Gaddis and Spencer (1979) showed that reverse osmosis membrane effectively reduced color; salts, organic species and toxic metals present even in low concentrations in textile process water.

Henz and Pfenninger (1987) showed that a multi-stage ultra filtration-reverse osmosis membrane unit with modified polysulfone membrane plants was effective in the removal of copper and chromium from effluents arising from the manufacture of copper complexed direct and reactive dyestuffs.

The membrane filtration technology is a viable technique that significantly reduces the volume of wastewater and provides possibilities for the reuse of dyestuffs, chemical and water. However, the main factor that offsets its application is the high capital investment that is associated with this mode of treatment. Porter and Rozelle (1990) report that ultra filtration has been used successfully to recover the expensive dye Indigo (recovery >98%) for reuse and at the same time reduce the pollution load on the wastewater treatment systems.

Membrane filtration has been demonstrated as a commercially viable technology for the effective technology for the removal of residual color arising from both the manufacture and application of the dyestuffs. This is due to its ability to separate various types of wastewater into two streams; concentrate and permeate. An added advantage of this technology is its effectiveness with which it produces water of reusable quality.

Carriere and coworkers (1993) showed that the use of integrated systems such as combined ultra filtration-reverse osmosis membrane system coupled with an activated sludge bioreactor may have significant technical and economical benefits for the textile industry.



## **Chapter II**

### **Iron Mediated Reductive Transformation Of Azo Dyes**

## Zero-Valent Iron-A Review

Weber E.J. (1995) reported that approximately 12% of the synthetic textile dyes used each year are lost to waste streams during manufacturing and processing operations and that 20% of these losses will enter the environment through effluents from wastewater treatment plants. Kulkarni et al., (1985) report that textile industry is the largest consumer of dyes accounting for two-thirds of the dyestuff market. Of the azo dyes available in the market, approx. 50% is azo compounds. Azo dyes can be divided into monoazo, diazo and triazo classes and are found in six application categories: acid, basic, direct, disperse, azoic and pigments. Clarke and Anilker (1980) report that textile dyes are of environmental interest because of their wide spread use, their potential for formation of toxic aromatic amines and their low removal rate during aerobic waste treatment. Baughman and Weber (1994) report that roughly 80% of the dyes in use are azo compounds and, of the remainder, 15-20% contain the anthraquinone moiety. Yoshida et al., (1981) report that in natural systems the formation of aromatic amines could result either from *in vivo* metabolism of azo dyes or by the action of bacteria in river water or soil. There have been many laboratory studies on the microbial transformation, mostly with regard to waste treatment of anionic azo dyes. Reductive cleavage of azo dyes results in irreversible formation of aromatic amine products. Azo dyes are among the largest group of colorants used in a variety of industries ranging from textile to paper. The effluent streams are highly colored. Therefore, there is a reasonable urgency for developing a

treatment process that decolorizes the dye (Naomi et al., 2000). These dyes are of great environmental concern due to their potential to form carcinogenic aromatic amines under reducing conditions (Hudlicky, 1986). Genotoxicity among azo dyes and their synthetic intermediates has been well documented (Searle, 1976). For instance Hueper (1969) identified 2-naphthylamine, 4-aminobiphenyl, benzidine Acid red 27 as actual or potential carcinogens, although evidence suggests that metabolites of some of the azo compounds are the actual genotoxic agents. According to IARC Monographs, (1975) aromatic amines used in the past as precursors of synthetic dyes posed a potential risk to human health. This point was initially thought to be important only if workers were exposed to a genotoxic precursor during dye manufacture or when handling an impure dye containing the unreacted genotoxic parent arylamine. It was later found that even a commercially available and a highly purified dye such as Congo red could generate the carcinogen benzidine in the presence of mammalian enzymes. The fact that numerous dyes are non-volatile, are thermally unstable and are active carcinogens in the ppt-ppb range places an enormous burden on the environment (Voyksner et al., 1993).

- (i) The following sections give a brief review of works carried out on the reduction of dyes using zero valent iron.

Over the recent years, there has been an increased concern over the environmental fate of azo dyes in natural water systems. The concern arises from the fact that these dyes are highly water-soluble and some hydrophobic dyes like disperse dyes will partition strongly to bottom

sediments where reductive cleavage of the azo linkages may occur. This transformation process could result in the release of potentially hazardous aromatic amines to the water column. Decolorization of textile effluents is a worldwide problem to which many diverse technologies have been applied. Common methods of decolorization include physical adsorption or flocculation, chemical destruction by oxidation or reduction and biodegradation. To gain acceptance, an ideal treatment option would be one that should decolorize a broad range of dyes at an economic cost and in an environmentally benign manner. However, the technologies currently available lack one or more of these features.

Weber E.J. (1996) report that textile dyes are typically recalcitrant chemicals that are not readily degraded in conventional wastewater treatment plants. Prior treatment of dissolved azo dyes with zero valent iron would result in aromatic amines that are generally more susceptible to biodegradation than the parent dye and colourless. The disappearance of the dye was concurrent with the formation of aromatic amines that were consistent with a reaction pathway involving the reduction of azo linkage and the aromatic nitro groups.

Phillips et al., (2000) report that recently zero-valent iron based permeable reactive barrier technology has received much interest as an alternative to pump and treat systems because  $\text{Fe}^0$  is a readily available medium that is cost saving over a long term and has shown encouraging results in the remediation a wider variety of redox labile contaminants. However a major factor that limits the long-term performance of such zero-

valent iron based columns is the depletion of the reactive media through corrosion. The accumulation of corrosion products either individually or as a mixture, such as iron and calcium carbonate, green rust and iron oxyhydroxides, may restrict flow or eventually leads to clogging of the system.

Zero-valent iron has been extensively used for remediating both organic and inorganic contaminants. This is because being inexpensive and readily available makes  $\text{Fe}^0$  filings one of the most promising permeable barrier materials. According to Sherman et al., (2000) the three important factors that determine the utility of zero valent iron material as a treatment option are:

- (i) There must be sufficient quantity of iron to react stoichiometrically with the contaminant.
- (ii) Efficient utilization of the reductant i.e. ability to reduce greater amount of contaminant for the same amount of iron.
- (iii) Corrosion rate of iron.

Joseph et al., 1998 state that there can be three possible mechanisms by which organics could be removed through ZVI

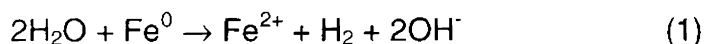
- (i) Reduction
- (ii) Sorption onto iron oxide corrosion products by ion exchange with hydroxyl sites
- (iii) A combination of reduction and precipitation.

The contaminants could also be removed by ZVI via a heterogeneous surface reaction (reduction, adsorption or coprecipitation),

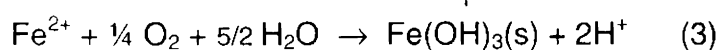
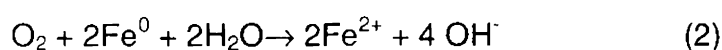
which could render the contaminants insoluble and immobilize them onto the ZVI or iron oxide surface.

$\text{Fe}^0$  in contact with water could undergo the following processes:

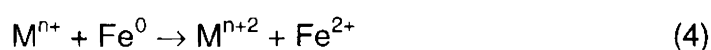
Anaerobic corrosion



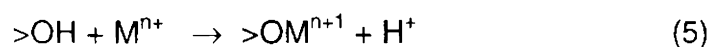
Aerobic corrosion



Cementation



Sorption / ion exchange

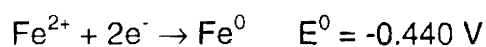
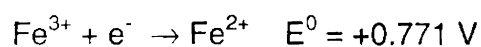


Under aerobic conditions, equations 2, 3 and 5 represent the most likely mechanisms.  $\text{Fe}^0$  is first oxidized to ferrous. The ferrous iron in turn gets rapidly oxidized to form a high surface area and highly porous layer of hydrolyzed ferric oxide. Hydrolyzed ferric iron [ $\text{Fe}(\text{OH})_3(\text{s})$ ] and its polymer, ferrihydrate, are active sorption sites (Hakanen and Lindberg, 1992). The  $\text{>OH}$  in equation 5 represents an exchangeable site on the hydrous metal oxide at the hydrous iron substrate or on its detached corrosion product. Depending on the pH of the solution pH, the surface site may have a net positive charge ( $\text{>OH}_2^+$ ) or negative ( $\text{>O}^-$ ) charge. The exchange of protons to and from the oxide surface creates specific sorption sites. For most iron containing minerals, the solution pH value that results in no net charge on the mineral (i.e., point of zero charge or pzc) is in the

range of approx. 6-8. As the solution pH falls below the pzc of the substrate, the net surface charge becomes positive, favoring the sorption of anionic species. On the other hand as the pH is increased above the pzc of the substrate, the net surface charge becomes negatively charged favoring the sorption of cationic species. At pH 6, the iron surface would contain equal amounts of negative and positive charge because the pH is close to the pzc of the iron substrate. Since both charges exist on the iron surface at this pH, sorption of a positively charged species can occur on the negatively charged oxide layer. When pH is higher than 6, the conditions become detrimental due to the production of hydroxyl ions and favors sorption. Under such conditions sorption becomes the most significant removal mechanism rather than reduction.

Demirer and Bowers., (2000) observed that the surface area of acid-washed Fe<sup>0</sup> particles was lower than that of the unamended Fe<sup>0</sup> particles due to the more porous structure of the oxide layer and loss of very fine Fe<sup>0</sup> particles during the washing procedure.

Gu et al., (1998) report that It is unclear whether the removal of contaminants is through physical processes such as adsorption or chemical reduction. Fe<sup>0</sup> is a much stronger reductant than Fe<sup>2+</sup>.



The authors report that electrochemical corrosion of iron is the main driving force, producing electrons for reduction and removal from aqueous phase.

Therefore, as long as the corrosion proceeds, the redox labile compounds would be reduced and removed from aqueous phase

Uhlig and Revie., (1985) state that at low ionic strengths, the high electrical resistivity of the solution requires small separations between anodic and cathodic sites on the iron surface. This allows the  $\text{Fe}^{2+}$  released at anodic sites to combine with the  $\text{OH}^-$  released at cathodic sites to precipitate as  $\text{Fe}(\text{OH})_2(\text{s})$  on the iron surface.

Farrell et al., (2001) report that the ferrous hydroxide produced by corroding iron ages to form magnetite ( $\text{Fe}_3\text{O}_4$ ) over a period of hours to days. The authors report that the measured  $E_{\text{corr}}$  values were in the range of  $-520 \pm 5$  mV. This corresponds to the equilibrium potential between zero-valent iron and magnetite, indicating that the zero-valent iron was in contact with a magnetite phase.

Passive films on iron have an Fe(II)/Fe(III) gradient consistent with an inner layer of magnetite and an outer layer of maghemite. Both these layers are thermodynamically stable due to the redox potential gradient and could serve as active sites for complexation with organic compounds.

At low concentrations, the ratio of dissolved compounds to the available (uncomplexed) iron hydroxide is sufficiently low. As a result there is no competition between the dissolved substances for the complexation sites. Under such conditions the removal kinetics follows first order and may be representative of both complex formation, or may result from diffusional mass transfer limitations within the iron oxide phase. As the concentration is increased, the ratio of the dissolved organics to the



complexation sites increases, leading to competition for the complexation sites. With increasing competition, the generation of new sites for complexation becomes the rate-limiting step. Under such conditions the reaction would follow zero order kinetics.

At low pH values,  $\text{Fe}(\text{OH})_2$ , magnetite and maghemite will not form on the zero-valent iron. Therefore, the physical barrier limiting the access of the dissolved compounds to the zero-valent iron is essentially eliminated. At neutral pH values although the iron oxide layer coats the zero-valent phase, the oxides are porous and only partially protect the underlying iron from the oxidant in solution.

The potential of zero surface charge is  $-370$  mV for iron Bockris and Reddy (1970) and is in the range of  $-70$  to  $+80$  mV for mixed valent iron corrosion products.

Studies of adsorption on iron oxides indicate that freshly formed ferric hydroxide has a greater adsorption capacity per unit mass than aged oxides, such as akaganeite or goethite (Cornell and Schwertmann, 1996). Therefore, the advantage of zero-valent iron may be that its corrosion continuously generates high specific surface area iron oxides that are more reactive than aged materials.

Hung et al., (2000) suggested that heterogeneous reactions involve five steps:

- (i) Mass transfer of the reactant to the metal surface from the bulk solution.
- (ii) Adsorption of the reactant on the surface.

- (iii) Chemical reaction at the surface
- (iv) Desorption of the products from the surface.
- (v) Mass transfer of the products into the bulk solution.

Any one of these steps may be rate limiting. To properly interpret trends in observed reaction rates, it is important to decouple the observed kinetics into mass transport and reaction-limited kinetics. This has practical implications for developing models to optimize the design of Permeable Reactive Barriers (PRBs).

Li and Farrell., (2000) state that zero-valent iron is thermodynamically unstable in water and must be cathodically protected in order to prevent anodic solution of the iron. Although iron is a base metal that forms an oxide coating even under cathodic polarization it may be a practical electrode material due to its low cost and high over potential for hydrogen (value/reference).

Su and Puls., (2001) observed that corrosion products of  $\text{Fe}^0$  such as magnetite, hematite and goethite form a passivated layer on the  $\text{Fe}^0$  surface, thus affecting the behavior of its interaction with organic compounds.

pH plays an important role in the adsorption on iron hydroxide. The pH effect is described in terms of the zero point of charge (zpc) of the adsorbent. Hematite a common iron oxide has a zpc of 7.1. Under low pH conditions, the iron oxide undergoes surface protonation. Surface protonation diminishes as the pH increases to above 5, and approaches 0 at pH 7 resulting in maximum adsorption. When the pH is

above 9 the oxide surface becomes negatively charged, resulting in electrostatic repulsion and decreased adsorption.

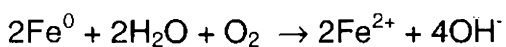
Abinash and Tratnyek., (1996) report that Zero-valent iron metal,  $\text{Fe}^0$  is readily oxidized to ferrous iron by many substances. In aqueous systems this phenomenon leads to dissolution of the solid, which is the primary cause of metal corrosion. Metal corrosion is an electrochemical process in which the oxidation of  $\text{Fe}^0$  to  $\text{Fe}^{2+}$  is the anodic half-reaction. The cathodic reaction may vary with the reactivity of available electron acceptors. Under anoxic conditions the electron acceptors include  $\text{H}^+$  and  $\text{H}_2\text{O}$ , the reduction of which gives  $\text{OH}^-$  and  $\text{H}_2$ . The cathodic half reaction involves oxygen as the electron acceptor and the primary reaction yields only  $\text{OH}^-$ . Several other strong organic and inorganic electron acceptors may offer additional cathodic reactions that contribute to iron corrosion.

During the  $\text{Fe}^0$  mediated reactions an increase in pH is expected because of water decomposition by  $\text{Fe}^0$  and adsorption reactions, which release  $\text{OH}^-$  groups from adsorbents as a result of exchange of ligands. Water undergoes decomposition by  $\text{Fe}^0$  by two pathways:

Anaerobic corrosion:



Aerobic corrosion:



The layer of oxides formed at the iron-water interface mediates the aqueous corrosion of iron. The incoherent and porous nature of oxide film on iron allows adequate and continuous adsorption.

Johnson et al., (1996) observed that acid washing increased the specific surface area concentration of  $\text{Fe}^0$ , but to highly variable degrees. The most important factors influencing the reductive dechlorination reaction are the reactivity of the substrate, and the iron surface area concentration. Other factors include the surface condition of  $\text{Fe}^0$ , pH, initial contaminant concentration and flow or mixing rate.

Farrell et al., (2000) reported that the rates on freshly acid-washed surfaces were considerably faster than those on surfaces with aged iron oxide layers. This indicates that the condition of iron surfaces have a significant influence on the reaction rate.

Cornell and Schwertmann (1996) report that under anaerobic conditions, amorphous ferrous hydroxide,  $(\text{Fe}(\text{OH})_2)$ , is the first corrosion product formed. This is further oxidized to form Magnetite ( $\text{Fe}_3\text{O}_4$ ). At neutral pH intermediate to the formation of magnetite, mixed-valent Fe(II)/Fe(III) salts, known as green rusts, may be formed. Green rusts are stable only at low redox potentials, and their oxidation commonly leads to the formation of maghemite or lepidocrocite. Spectroscopic analysis of aged iron surfaces have found that iron becomes coated with an inner layer of magnetite and an outer layer of maghemite. Magnetite being a semiconductor, the band gap between its valence and conduction bands are small giving it an electrical conductivity close to that of metals. Therefore, magnetite is not considered to be a passivating oxide. However, in the case of maghemite the band gap is large and is considered passivating.

Gillham and O'Hannesin (1994) observed up to 10-fold increase

in the rates for a decrease in 2 pH units, indicating that the reduction rates were strongly influenced by pH. A heterogeneous reaction is indicated by both the strong dependence of reaction rate on the iron surface area and the lack of reaction when water is removed.

Burris et al., (1995) state that a heterogeneous reaction requires that the reactant molecules reach the solid surface. They then associate with the surface at sites that may be either reactive or non-reactive. The 'reactive sites' are the seat of chemical reaction where the cleavage of bonds of the reactant solute molecules takes place. Non-reactive sites are those with which the solute molecules associate by sorption in which the molecules remain intact. When the process involved is chemical reaction it is necessary that the product must dissociate from the surface site before the site becomes available for further reaction with the reactant solute molecules. A reaction could be zero order with respect to the reactant solute if the capacity of the available reactive sites is exceeded. Competition could also occur between solutes for the reactive or non-reactive sites.

A first order process with respect to aqueous phase concentrations implies that mass of the aqueous phase is of particular importance to the reaction, since it is that portion of mass, which is accessible to the reactive sites.

Scherer et al., (2001) have reported that the degree to which mass transport determines the overall rate of reduction by  $\text{Fe}^0$ , difficult to resolve because of a multitude of indirect effects (both physical and chemical

processes) that may occur in batch and column reactors. The layer of granular  $\text{Fe}^0$  becomes covered by a layer of oxide formed by the accumulation of corrosion products at the metal surface. Mass transport through the oxide layer as well as external diffusion give rise to three potential domains:

- i. Mass transport limited kinetics, where  $\text{ArNO}_2$  diffuses to the surface more slowly than it reacts at the surface.
- ii. Reaction limited kinetics, where  $\text{ArNO}_2$  reacts at the surface more slowly than it diffuses to the surface.
- iii. Intermediate kinetics, where mass transport and surface reaction occur on similar time-scales.

Behaviour typical of mass transport limited kinetics (e.g. faster rates with increased mixing intensity) may occur from indirect physical effects such as abrasion of the oxide layer making it difficult to confirm whether the observed kinetics are measuring diffusion rates, reaction rates, or a combination of both (Devlin et al., 1998).

To overcome these difficulties an alternative experimental approach that avoids the formation of an oxide layer and separates mass transport rates from surface reaction rates have been developed. The experimental design consists of an electrochemical cell with an oxide-free  $\text{Fe}^0$  rotating disk electrode (RDE). Since no oxide forms on the  $\text{Fe}^0$  RDE (in the potential range of active corrosion), pore diffusion is eliminated as a potential mass transport process. These conditions create a system where external mass transport and surface reaction (which includes sorption

processes, such as surface attachment and rear arrangement, as well as electron transfer) are the dominant processes. The controlled hydrodynamics of an RDE can be used to quantify the external mass transport and surface reaction contributions to the observed reduction rate.

Farrell et al., (2000) report that there are both direct and indirect mechanisms for reduction by zero-valent metals. Direct reduction may occur by electron tunneling or via the formation of a chemisorption complex of the organic compound with surface metal atoms. Electron tunneling may occur to compounds that are physically adsorbed at the metal surface or to compounds that are separated from the surface by adsorbed water or corrosion products. Indirect reduction of the organic compound involves atomic hydrogen. Atomic hydrogen adsorbed at the metal surface may reduce the organic compounds through the formation of chemisorbed hydride complexes. This mechanism is fast on metals with low hydrogen overpotentials, such as platinum and palladium, but is much slower on metals with high hydrogen overpotentials such as iron.

Agrawal and Tratnyek., (1996) report that changes in pH can cause changes in the nitro reduction rates through,

- (i) Direct involvement of  $H^+$  in the contributing reactions
- (ii) Mass transport limitations imposed by the precipitation of a passive film on the metal surface, or
- (iii) Mass transport limitations determined by the thickness of the Nernst layer between the passive film and the bulk electrolyte.

The authors also report that aniline cannot be further reduced by Iron as it is a well-known corrosion inhibitor. The mechanism of inhibition is believed to be simple interference with mass transport of the oxidant to the metal surface, which is in turn influenced by the orientation of aniline adsorption. Competitive inhibition by this mechanism implies that contaminant reduction rate may also be limited by competition for reactive sites on the metal.

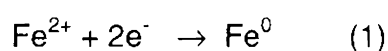
Agarwal and Tratnyek (1996) report that the effect of HCl pretreatment may be due to cleaning of the surface by dissolution of metal and breakdown of the passivating oxide layer; increasing the metal surface by etching and pitting through corrosion; increase in the density of highly reactive sites consisting of steps, edges, and kinks, following corrosion by acid; and increased concentrations of adsorbed  $H^+$  and  $Cl^-$  that persists after pretreatment with HCl.

Mantha et al., (2001) report that the amino group of aniline (in the neutral, free-base form) acts as a ligand in complex formation with the metal. Mantha et al., (2001) and Orth and Gillham., (1996) suggest that reduction by zero-valent iron involves adsorption of halogenated organic compounds to the metal surface. For heterogeneous reactions to take place, it is necessary that the reactant molecules reach the solid surface. They in turn combine with "reactive" or "nonreactive" sites present on the surface. Burriss et al., (1995) states that reactive sites are those where the breaking of bonds in the reactant molecules takes place, while the nonreactive sites are those where only sorption interactions occur and the

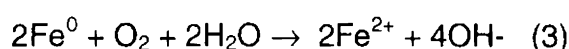
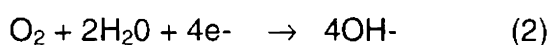


solute molecules remains intact. They speculated that bulk of the sorption occurred at the nonreactive sites and sorption kinetics fitted the generalized Langmuir isotherm expression.

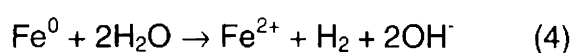
According to Matheson and Tratnyek., (1994) the redox couple formed by zero-valent iron and dissolved aqueous ferrous iron has a standard reduction potential of  $-0.44$  V.



This makes  $\text{Fe}^0$  a reducing agent relative to many redox-labile substances. Iron corrosion results in oxidative dissolution of the metal near neutral pH. In the absence of strongly oxidizing solutes, there are two reduction half-reactions that can be coupled with the above equation to produce spontaneous corrosion reaction in water. Dissolved oxygen, when present, is the preferred oxidant resulting in rapid corrosion according to the equation



The ferrous iron so produced can undergo further oxidation to form ferric hydroxides (rust). However, under anaerobic conditions, water alone can serve as an oxidant, resulting in anaerobic corrosion according to the reaction



Equations 3 and 4 result in increased pH in weakly buffered systems, although the effect is more pronounced under aerobic conditions as the corrosion is much more rapid. This pH increase favors the formation

of iron hydroxide precipitates, which may eventually form a surface layer on the metal that inhibits its further dissolution. Therefore, the three major reductants associated with an  $\text{Fe}^0\text{-H}_2\text{O}$  system are iron metal, ferrous iron and hydrogen that result from corrosion. The entire process can therefore involve three major pathways:

- (i) Involves the metal directly and implies that the reduction occurs by direct electron transfer from the metal surface to the adsorbed compound.
- (ii) Involves ferrous which is an immediate product of corrosion in aqueous systems. Although such reactions are slow they depend on the ligands present in the system because speciation of ferrous iron has a significant effect on its strength as a reductant. Inner species complexation of  $\text{Fe}^{2+}$  to metal oxides creates more reducing species. However, the reactivity of such species are uncertain.
- (iii) Involving hydrogen, which is produced by the reduction of water during anaerobic corrosion. This phenomenon is known as hydrogenolysis. In the absence of an effective catalyst hydrogen is not a facile reductant. On the other hand, excessive accumulation of hydrogen can inhibit the continuation of corrosion and the reduction reactions.

Singh et al., (1999) observed that lowering of the oxygen concentration or reducing or buffering the pH of the  $\text{Fe}^0 - \text{H}_2\text{O}$  suspension

prior to the addition of  $\text{Fe}^0$  could result in increased contaminant destruction rates because less  $\text{Fe}(\text{OH})_3(\text{s})$  would precipitate and protons are provided for reductive transformations.

Wust et al., (1999) reports that kinetics of the processes involved are of paramount importance for the design of iron walls. Iron surface area concentration was found to be the most important parameter on which the rate constant depend and proportionality could be established over a wide range. The linear relationship indicates that dehalogenation with commercial iron is a heterogeneous reaction. It is however less evident which step is rate controlling and therefore the determining factor behind the overall kinetics of the heterogeneous dehalogenation reaction. Results of batch experiments indicate that transport of the chlorinated compounds to the iron surface may contribute to the kinetic control. In column experiments, the effect of flow velocity on the degradation rate varied from insignificant to a 3-fold increase with doubling of the flow rate. All these evidence indicate that iron mediated reduction could be a surface process.

Richardson and Nicklow., (2002) report that In-situ permeable reactive barriers (PBRs) consists of zones of reactive material, such as granular iron or other typically reduced metal, lime, electron donor-releasing compounds, or electron acceptor-releasing compounds, installed in path of a plume of contaminated groundwater. As the groundwater flows through this zone, contaminants are degraded to innocuous components through chemical or biological reactions, adsorbed, or chemically altered to form insoluble precipitates. The characteristics in favor of PBRs are it is an

alternative to pump and treat option since it does not need pumps or treatment vessels, thereby saving operation and maintenance costs. However, some of the disadvantages associated with such treatment processes could be that they rely on natural advective processes to move contaminants through the treatment zone, resulting in long treatment time frames. Another disadvantage is uncertainties over the long-term effectiveness of the reactive media used in such systems. Ritter et al., (2002) state that this could be because the permeable walls are usually made of impure commercial material that is covered with a passive layer of  $\text{Fe}_2\text{O}_3$ , magnetite or green rust, formed as a result of corrosion of the metal surface. The  $\text{Fe}_2\text{O}_3$  layer is passivating as it inhibits the mechanisms such as electron transfer and catalytic hydrogenation behind contaminant reduction. However, magnetite and green rust would not inhibit contaminant reduction and their formation is beneficial in the long run.

Nam and Tratnyek., (2000) studied the reduction of azo dyes by zero valent iron in aqueous anaerobic batch systems. All the dyes were reduced with first-order kinetics. The degradation of dyes produced stoichiometric amounts of sulfanilic acid indicating reductive cleavage at the azo group. Extraction of the  $\text{Fe}^0$  with methanol recovered only < 4% of the original dye indicating that reduction and not adsorption was the major process involved.

At increased dye concentrations a shift from first order to zero order kinetics is reported. This behavior was attributed to site saturation. The

rate of the reaction was found to increase linearly with the square root of rpm. This indicates that the system was limited by mass transport at low dye concentrations and by saturation of surface sites at high dye concentrations. No strong trends were observed to derive structure activity relationships.

Cao et al., (1999) studied the degradation kinetics of five azo dyes by zero-valent iron powder in aqueous solution. The authors observed that the reaction was a two-step process, with the first step being reversible. The degradation rates increased with an increase in solution acidity and iron surface area. The authors observed that the reaction was by the cleavage of azo bond and as the reaction continued the characteristic absorption of the products (aromatic amine) appear and become prominent. This was indicated by the wavelength shift and decrease in absorbance at  $\lambda_{\max}$  of the dye. Disappearance of the dye fitted well with the Langmuir model. The rate coefficients were determined using first order rate equation.

Weber E.J. (1995) studied the chemical (using sodium dithionite) and sediment (3- anoxic sediment-water systems) associated reduction of Disperse Blue 79 and BDNA (an important intermediate in the preparation of Disperse Blue 79). The study was carried out mainly to determine if Disperse Blue 79 when reduced formed BDNA and the degree to which BDNA persists in anoxic sediment-water system. The reduction of Disperse Blue 79 followed pseudo-first order kinetics. The reduction of the dye with sodium dithionite and with iron yielded the same aromatic amines

establishing that the reduction was at the azo linkages. A significant decrease in the rate of disappearance of the dye was observed after 1-1.5 half-lives. This indicated that after its initial rapid loss there was a change in the rate-limiting step controlling disappearance of the dye. Two possible scenarios that could account for such a behavior was saturation of the reductive sites associated with the sediment or sorption of the dye to the sediment such that only the dissolved fraction of the dye could be reduced. The results suggested that the azo dyes could undergo rapid reductive transformation in anoxic bottom sediments, resulting in the release of aromatic amines to the water column. The authors observed that the data did not indicate simple first-order kinetics.

Weber E.J. (1996) observed that the primary question concerning iron mediated reduction studies is whether the reduction by zero-valent iron is a surface-process involving direct electron transfer by  $\text{Fe}^0$  or complexation of a product of iron corrosion, or in the aqueous phase by release of a water-soluble reductant. If the reduction is surface mediated, transport of the contaminant to the iron surface would be the rate limiting step. To determine whether the reaction was surface-mediated, the reduction of a probe molecule (4-aminoazobenzene) was studied. The results indicated that reductive transformation is a surface mediated process and direct contact of the substrate with the iron surface is necessary for electron transfer to occur.

Baughman and Weber., (1994) studied the reduction of several azo, anthraquinone and Quinoline dyes in settled sediments. Several 1-

substituted anthraquinones were lost from sediment with half-lives less than 10 days. The authors observed that in most anoxic sediment environments, uncharged azo and simple anthraquinone dyes would not persist. The azo dyes reacted by reductive cleavage of azo bonds. Quinoline dyes were found to be more stable than azo and anthraquinone dyes. The products were found to be much more stable than the parent molecules.

Voyksner et al., (1993) studied the reduction of 16 commercial azo dyes using sodium hydrosulfite and tin(II) chloride. The authors observed the formation of similar reduction products under both aerobic and anaerobic conditions. The PB HPLC/MS analysis of the reduced azo dyes indicated that the major degradation products formed were aromatic amines generated through the cleavage of azo linkages. These aromatic amines were not detected in intact dye prior to reduction. The presence of numerous substituent groups in addition to the azo linkages increased the number of components among the reductive-cleavage products. The common reduction products were aniline, aminonaphthol, diamino benzene and 4-nitroaniline. Depending on the identity of azo dyes, the aromatic reduction products are more harmful to the environment than the original untreated dye. Tin(II) chloride was found to be more powerful as a reducing agent than sodium hydrosulfite.

Xiong and Karlsson., (2001) studied the decolorization of an Acid dye Acid Scarlet BS in a two step process. The dye wastewater was first pretreated with Fe(II) followed by electrochemical oxidation with a three-

phase three-dimensional electrodes. The system not only effectively reduced COD but also resulted in decolorization. This was attributed chiefly to the reductive destruction of the dye at its azo linkages rather than adsorption or flocculation. The authors observe that it was easier to reduce COD of the decolorized wastewater rather than in the presence of original dye.

Perey et al., (2001) report that zero-valent iron could be used to effectively decolorize azo dyes through cleavage at the azo linkages into products that are more amenable to biological treatment systems such as activated sludge systems. The study carried out in batch systems indicated that the reduction products formed were mainly aniline and sulfanilic acid, which was degraded within 24 hours by acclimated bacterial cultures. Respirometric data indicated that iron treated dye solutions exerted a significantly higher BOD than the solutions containing the undegraded dye molecule indicating that although the azo dyes were recalcitrant their reduction products could be aerobically degraded.

(ii) A brief review of works carried out on the reduction of nitrobenzene using zero valent iron is reported in the following section of review.

Schultz and Grundl., (2000) studied the reduction of 4-chloronitrobenzene by Fe(II)/Montmorillonite in batch systems over the range of pHs from 6 to 8. The authors observed that the reduction process followed first order kinetics. The reaction rates increased with an increase in pH from 6 to 8. This was found to correlate to the increase in  $\text{FeOH}^+$



which was found to be the primary reductant at high pH. This was attributed to both an increase in concentration of the  $\text{FeOH}^+$  ion and to the sorption of  $\text{Fe(II)}$  at high pH. Ferrous=ferric oxide sorption complexes on the surface of ferric oxides are analogous to  $\text{FeOH}^+$  complexes in aqueous phase. The authors state that ferric oxyhydroxide precipitates formed during the reaction are a source of mediating surfaces that could potentially control the reaction.

Mantha et al., (2001) used zero-valent iron to reduce nitrobenzene to aniline in both batch and continuous flow reactors. Anaerobic conditions were maintained in the reactor by using  $\text{CoCl}_2$  (0.1% of  $\text{Na}_2\text{S}_2\text{O}_3$  by weight) catalyzed sodium bisulfite as an oxygen scavenger instead of degassing. Ionizable nitrophenols exhibited a strong pH dependence of the distribution coefficient value in the pH region corresponding to the  $\text{pK}_a$  of the compound. Batch experiments indicated adsorption of aniline on  $\text{Fe}^0$ . The adsorption could be described by Langmuir isotherm. In some of their experiments, aniline desorption curves were recorded which confirmed that aniline had deposited on  $\text{Fe}^0$ . Iron corrosion products in the form of black precipitates identified as maghemite were formed at the influent, excessive accumulation of which resulted in reduced flow rates due to clogging. The change in height of the precipitate front from the influent end of the column with time was linear indicating that the rate of formation of corrosion products is directly proportional to the rate of conversion reaction.

Mantha et al., (2002) carried out flow through column studies to establish that aniline formed during the zero-valent iron mediated reduction

of nitroaromatics could be effectively captured through peroxidase catalyzed oxidative polymerization. Complete reaction time for two-step process was 5 to 5.5 hours. Neutral pH and a hydrogen peroxide to substrate molar ratio of 1.5 was found optimum for all the nitroaromatics tested.

Klausen et al., (2001) evaluated the importance of groundwater composition on the long-term performance of  $\text{Fe}^0$  based reactive permeable barrier. 2-nitrotoluene (2-NT) was the model contaminant used in the study. The authors observed that although there is a rapid reduction of 2-NT to 2-aminotoluene in the column through mass transport controlled conditions, the reactivity of iron decreased with time. This phenomenon of decreased reactivity was decreased in the presence of chloride, and increased in the presence of silicate.

Hung et al., (2000) studied the reduction of nitrobenzene and aniline in water using sonolysis, reduction by elemental iron and a combination of sonolysis and reduction by elemental iron. The reaction rate for nitrobenzene degradation was found to be first order at low  $\text{Fe}^0$  loadings, at higher concentrations of iron the second order polynomial function was found give a better fit than a simple first order relationship. The rate of reduction of nitrobenzene by  $\text{Fe}^0$  was enhanced in the presence of ultrasound. This was attributed to the continuous cleaning and activation of the  $\text{Fe}^0$  surface by the chemical and physical effects of sound. The rate of the reaction increased with increase in mixing indicating that the influence

of mass transfer kinetics. As the reaction proceeds an increase in pH is reported.

Scherer et al., (2001) studied the influence of mass transport on the reduction kinetics of Nitrobenzene using rotating disk electrode (RDE) in an electrochemical cell. The kinetics was studied at a pH of 8.4 at a potential below, which an oxide film would form. The cathodic current measured in this system was dependent on the electrode rotation rate. The measured first order heterogeneous rate coefficient for surface reaction was about 10 times faster than the first order mass transport rate coefficients measured in permeable reactive barriers. The findings suggested that mass transport was an important parameter to be considered in the design of reactive barriers.

Agrawal and Tratnyek., (1996) observed that nitro aromatic compounds (NAC) nitrobenzene could be reduced by iron under anaerobic conditions to aniline with nitrosobenzene as an intermediate product. The reduction rates of nitrobenzene and nitrosobenzene followed first order reduction kinetics while the appearance of aniline was slow. The suggested reaction mechanism includes coupling of nitro reduction intermediates to form azo and azoxy compounds or cleavage at the azo linkages to form amines. The authors report a linear increase in the reduction rate with iron surface area. A linear correlation was observed with square root of mixing rates indicating that mass transfer of NAC to the metal surface controlled the reaction rates. pH did not have any significant effect on the nitro reduction rates. Rate of the reduction reaction

decreased with increased concentration of dissolved carbonates. Siderite precipitated on the metal surface could be a possible site for adsorption. According to the authors, the adsorbed molecule must undergo a series of electron transfers, proton transfers and dehydrations to achieve complete reduction. The precise sequence would vary depending on the pH, solvent properties and composition of the surface where adsorption and reaction occur.

Hozalski et al., (2001) used batch experiments to investigate the reactions of four trihaloacetic acids, trichloroacetic acid, tribromoacetic acid, chlorodibromoacetic acid and bromodichloroacetic acid with  $\text{Fe}^0$ . The investigation revealed that the reactions proceeded via hydrogenolysis. The removal of these trihaloacetic acid followed pseudo-first-order kinetics.

(iii) Zero valent iron has also been used in the dechlorination of several aromatic compounds as indicated by the works discussed below.

Kim and Carraway., (2000) studied the dechlorination of pentachlorophenol (PCP) by zero valent iron and modified zero valent irons in batch reactors. The disappearance of PCP from aqueous solutions in contact with zero valent metals was attributed to dechlorination reactions or sorption to zero valent metal related surfaces. The dechlorination of PCP was confirmed by following the appearance of tetrachlorophenol isomers and fits to a first order model. The authors observe that both sorption and reaction at the metal surface could be an important process in the application of zero valent metals, as sorption accounted more than 50% of

the initial mass of PCP. The study demonstrated the dechlorination of PCP and indicates that it is necessary to separate reaction and sorption processes.

Agrawal et al., (2002) studied the reduction of 1,1,1-trichloroethane by zero-valent iron in batch systems. The study was carried out to determine the influence of precipitate formation and groundwater composition (containing dissolved carbonate species in the form of Cr(IV)) on the reactivity of iron. The authors observed that Cr(IV) precipitated mainly in the form of siderite and in the form of green rust. The reduction of TCA was accelerated by Fe<sup>0</sup> in the presence of dissolved Cr(IV). The products formed were mainly ethane and ethene with minor amounts of several butenes. The kinetics of TCA reduction followed first order until Cr(IV) enhanced corrosion after which they become zero order, when Cr(IV) caused surface passivation. The data fitted Michaelis-Menten type kinetic model.

Lien and Zhang., (2002) observed that a copper and aluminium bimetal system was effective in enhancing the dechlorination of halogenated methanes. The results obtained were comparable to that of iron based bimetals (e.g., palladized iron) and zero valent iron.

Arnold and Roberts., (2000) through batch tests investigated the pathways and kinetics of Fe<sup>0</sup> mediated reduction of chlorinated ethylene and their daughter products. The authors observed that the linear relationship between the reaction rates and iron loading holds good only over a limited range. No significant influence of mass transport was

observed. The pseudo-first order rate coefficients were found to decrease with increase in initial concentration. The authors observed a decrease in the reactivity of chlorinated ethylenes with increasing halogenation. Competitive experiments indicated both interspecies and intraspecies competition for reactive sites at the metal surface.

Farrell et al., (2000) investigated the long-term performance of zero-valent iron for the reductive dechlorination of trichloroethylene (TCE) over a two year period. Initially the reduction followed first order kinetics, which at later stages shifted to zero order kinetics indicating saturation of the reactive sites. The reaction rate constant was uniform along the length of the column indicating that TCE reaction rates were independent of the pH of the bulk solution. This was attributed to the fact that the surface of the corroding iron is in contact with a saturated solution of hydrous ferrous oxide, which had a pH of approx. 9.5. Therefore, unless the solution pH is low enough to dissolve the surface hydroxide layer, the bulk solution pH would have little effect on the reduction rates. Towards the end of the column an increased passivation of iron surface is reported. The extent of surface passivation was dependent on the TCE concentration, the background electrolyte solution and the adhering tendency of corrosion products. A comparison of the corrosion rates induced by nitrate and chloride indicated that the former contributed to enhanced surface passivation. Corrosion current measurements indicated that on fresh iron surfaces the halocarbon reduction was cathodically controlled, while on aged iron surfaces the reduction was anodically controlled. Anodic control

of corrosion contributed to reactive site saturation. The author's state that the decrease in the TCE reaction rates over time could be attributed to the anodic control of corrosion and not by mass transfer limitations.

Zhang et al., (2002) observed through dynamic flow through studies that the reduction rates of perchloroethylene could be enhanced by using surfactant-modified zeolite on zero-valent iron pellets. The reduction rates of surfactant-modified pellets were three times higher than the reduction rates with unmodified  $\text{Fe}^0$  pellets. The authors observed that the PCE reduction rate constants increased with an increase in the flow rate suggesting that in flow through systems reduction of PCE was a surface phenomenon limited by mass transport.

Li and Farrell., (2000) investigated the effectiveness of electrochemical reduction for the removal of trichloroethene (TCE) and carbon tetrachloride ( $\text{CCl}_4$ ). The study was conducted using flow through, iron electrode reactors and with amperometric measurement of reduction rates. The variables studied were flow rates, pH, ionic strength, dissolved oxygen concentration and working electrode potentials. Studying the effect of electrode potential, the authors report that the TCE reduction rates showed a small potential dependence, indicating that the rate-limiting step was indirect and did not involve electron transfer. With respect to pH the authors observed that the half-lives increased by a factor of three between a pH of 4 and 10. This indicates that hydrogen was involved in the TCE reduction by iron electrode. Dissolved oxygen did not affect the reduction of TCE or  $\text{CCl}_4$  indicating that there was no competitive effects with

dissolved oxygen for reactive sites on the electrode surface. The effect of carbonates on palladium deactivation was studied by comparing the TCE reaction rates in fee waters with and without dissolved carbon dioxide. The addition of carbon dioxide increased the cell current mostly due to increased hydrogen evolution resulting from the lower pH value of the influent solution. Some increase in the current was attributed to reduction of carbon dioxide itself. Slower reaction rate was observed in the presence of sulfide. This was attributed to the competitive adsorption of H<sub>2</sub>S on palladium.

Alessi and Li., (2001) in Fe<sup>0</sup> based systems the authors evaluated the use of cationic surfactants. The authors observed that irrespective of the presence or absence of these surfactants the reduction of both PCE and TCE followed pseudo-first-order kinetics. In comparison to the unmodified Fe<sup>0</sup> the rate of the reduction reaction increased by one order of magnitude when Fe<sup>0</sup> coated with a cationic surfactant was used. Reduction rates were not affected by ionic strength of the solution but high pH was found to significantly reduce the PCE degradation rate.

Li and Farrell., (2001) studied the reduction of trichloroethylene (TCE) and carbon tetrachloride (CT) at iron surfaces using rotating disk electrode. The objective was to determine if the reaction was influenced by rate of electron transfer. The rate constants for TCE and CT dechlorination were measured as a function of the electrode potential over a temperature range from 2 to 42°C. Changes in the dechlorination rate constants with electrode potential were used to determine the apparent electron-transfer



coefficient at each temperature. The transfer coefficient for CT dechlorination was found to be independent of temperature indicating that the rate-limiting mechanism involved an outer-sphere electron-transfer. However, in the case of TCE the transfer coefficient was found to be temperature dependent indicating that electron transfer was not the only step and that the reduction rate was also influenced by chemical dependent factors.

Johnson et al., (1996) observed that the first order rate constants derived from batch and column experiments carried out by many independent investigators varied widely without meaningful correlation. Some of the factors that influenced the degradation kinetics by modifying the interfacial region include dissolved oxygen, chloride, pH, carbonate alkalinity and sulfur. However, these data when normalized to the surface area of iron yielded a specific rate coefficient that varied only by one order of magnitude for individual halocarbons. A kinetic model to account for the experimental factors that contributed to variability in  $k_{obs}$  is presented in this paper.

Orth and Gillham., (1996) studied the degradation of TCE in the presence of iron powder. Column experiments were carried out with the objective of identifying the reaction products and the degradation pathway involved. The authors observed an increase in pH and occasional gas bubbles were on the interior wall of the column indicating evolution of hydrogen gas. The rates of TCE degradation was very fast and the reaction followed pseudo-first order kinetics with respect to TCE

concentration. The rate constants were found to be independent of concentration. The authors observe that it could be a surface process also. There would be some upper limit in the concentration of the substrate where the reactive sites get saturated and then the reaction would no longer be pseudo-first order. The principal degradation product was ethene and ethane in the ratio of 2:1, followed by smaller amounts of other C1-C4 hydrocarbons. The hydrocarbons appeared to be produced simultaneously rather than sequentially. Simultaneous reactions i.e. oxidation of iron by water and TCE produced  $\text{Fe}^{2+}$  possibly as siderite ( $\text{FeCO}_3$ ) or as  $\text{Fe}(\text{OH})_2$  on which the TCE remains sorbed until complete dechlorination. Less than 10% of the initial TCE was detected in solution indicating that TCE was completely dechlorinated in a single step. The authors state that the reaction could involve multiple degradation pathways, as a large number of hydrocarbons were detected in the solution phase.

Farrell et al., (2000) investigated the long-term effectiveness of zero-valent iron barriers for reductive dechlorination of trichloroethylene (TCE) and perchloroethylene (PCE). The dechlorination rates followed pseudo-first order kinetics, with an observed increase in rates during initial operation. Passivation of iron surfaces was observed at high TCE concentrations, and the reaction was found to deviate from pseudo first order kinetics. Surface passivation was slowly reversible as the concentration of TCE was lowered. The reaction rate of TCE was found to be 2-3 times faster than

G8955

PCE. The results indicated that zero-valent iron systems were capable of maintaining their reactivity over a long period of operation.

Scherer et al., (1998) observes that despite all the work done in the kinetics of dehalogenation, there were very few Linear Free Energy Relationships (LFERs) that could explain or predict the rates of reductive dehalogenation. In this paper, the authors report a LFER based on estimated Lowest unoccupied molecular orbital energies calculated from semi-empirical and *ab initio* methods and one-electron reduction potentials.

Matheson and Tratnyek., (1994) studied the reductive dechlorination of chlorinated solvents in well mixed anaerobic batch systems. Zero-valent iron sequentially dechlorinated carbon tetrachloride via chloroform to methylene chloride. The reduction followed pseudo-first order kinetics initially but then became slow as dehalogenation progressed. pH had a significant influence with the rate constants decreasing linearly with increased pH. Low pH results in increased aqueous corrosion, while at high pH ranges iron hydroxide precipitates formed on the metal surface. The condition and quantity of the metal surface was found to significantly influence the rate of dehalogenation. Rinsing the metal with dilute HCl provided well-defined and reproducible surface that produced faster dechlorination. This was attributed to the effect that acid washing dissolved the surface layer on the iron grains leaving clean reduced metal relatively free of unreactive oxide or organic coatings. The corrosion pits formed as a result of the acid pretreatment of Fe<sup>0</sup> could contribute to its greater reactivity. Another factor influencing the reaction was the amount of iron

metal available to react with the organic substrate. Mass transport of the substrate to the iron surface appeared to be an important determinant of the dechlorination rate.

Wust et al., (1999) investigated whether pseudo-first order kinetics was sufficient to describe the degradation kinetics of TCE and cis-DCE with commercial over a wide concentration range using both batch and flow through systems. The authors observed that the data could not be explained using pseudo-first order kinetics. At high aqueous concentrations, the degradation kinetics became pure zero-order whereas for low concentrations the kinetics was first order. The observed zero-order was attributed to the build up of iron oxides. This called for an enhanced model and it was observed that a combined zero and first order model could successfully account for their observations. This was attributed to the reason that pure order fits partially account for the mixed kinetics in the transition zone. Increase in flow rates resulted in an increase in the rate constant indicating that diffusion from bulk solution to the iron surface contributed to the overall kinetics. Variations in the kinetic parameters of combined zero-and first-order model suggested that both transport and sorption to reactive sites contributed to kinetic control.

Su and Puls., (1999) investigated the reduction of trichloroethene (TCE) by zero-valent iron and tin in batch tests. The reduction followed pseudo first order kinetics with respect to the substrate and iron surface area concentration. The authors observed that the amount of available surface area under effectively constant metal surface condition is one of

the most significant variables that influence the reduction of TCE. The rate coefficients increased linearly with an increase in the iron surface area. However, the regression line does not pass through origin, implying that other processes such as adsorption probably contributed to substrate disappearance. The authors observed that  $\text{Fe}^0$  when treated with HCl resulted in an increase in the specific area, which in turn led to greater observed rate constants. The authors report that a few steps are involved in the  $\text{Fe}^0$  reduction of TCE. First, TCE diffused through the solution to a metal particle, which is usually coated by a hydroxide layer. Second, TCE is adsorbed to a favorable reaction site on the metal particle. Third, electrons are transferred from the metal to the TCE molecule forming intermediate products such as metal hydroxides. Fourth, the intermediate and final products diffuse from the metal surface to the solution. This is the slowest step and determines the rate of the reaction.

Grittini et al., (1995) studied the dechlorination of polychlorinated biphenyls on the surface of palladized iron. The authors observed that the bimetallic system could rapidly dechlorinate PCBs in an aqueous methanol solution. Palladium on the iron surface would act as a collector of the hydrogen gas produced by the corrosion of  $\text{Fe}^0$ . Dechlorination occurred on the metal surface and all the chlorine atoms were replaced by hydrogen to form biphenyl. Condition of the iron surface had a significant influence on the reduction reaction. Despite all attempts to remove the surface oxide layers, an iron surface when exposed to air and an aqueous solution will

form oxide layers in which the ratio of oxygen to iron would vary as a function of depth from the surface.

Demirer and Bowers (2001) studied the reduction of trichloroethylene (TCE) by zero-valent iron in batch reactors. The study was carried out in solid, aqueous and gaseous phase. There were two processes operating in the system. The first step was adsorption of TCE onto the  $\text{Fe}^0$  surface under conditions of low humidity. This was followed by chemical reaction with  $\text{Fe}^0$  to form organic compounds like ethylene, isomers of dichloroethylene and vinyl chloride. The initial adsorption of TCE on to  $\text{Fe}^0$  was fast and highest at low temperatures. The reduction reaction was found to be first order with respect to TCE concentration. The rate of chemical reaction was high at elevated temperatures.

Demirer and Bowers., (2000) investigated the interactions of Trichloroethylene (TCE) with “clean” and “partially oxidized”  $\text{Fe}^0$  in gas phase. The authors observed that TCE removal proceeded by adsorption onto the  $\text{Fe}^0$  surface or by dechlorination reactions with  $\text{Fe}^0$  depending on the moisture content of the reaction medium. Water was found to be a critical component competing with TCE for the adsorption sites and above a critical limit serves as a proton donor for the hydrogenolysis of TCE.

Burris et al., (1995) studied the sorption behaviour and reduction kinetics of trichloroethylene (TCE) and tetrachloroethylene (PCE) with zero-valent iron in a closed anaerobic batch system. The study was carried out to delineate chemical reaction and sorption. Both aqueous and total phase concentrations were determined as a function of time and their difference

gave the sorbed phase concentrations. The reaction orders with respect to TCE and PCE total system concentrations were found to be 2.7 and 1.3 indicating the complexity of the reaction. Both the compounds exhibited non-linear sorption behavior that fitted to the generalized Langmuir isotherm. After sorption, at low solute concentrations the reduction rate of both the compounds were found to follow first-order kinetics. The first order behavior could be representative of the intrinsic chemical reaction or the diffusion limited access to the reactive sites. The authors observed competition for sorption, but not for chemical reaction indicating that sorption was mainly to the non-reactive sites. The experiments conducted could not differentiate between chemical reaction and mass transfer-limited access to the reactive sites. The authors conclude by stating that degradation was dependent on aqueous phase concentration and the mass balance of such systems is given as the sum of the decrease in concentration due to sorption plus the gain due to desorption.

Cassey et al., (2000) observed that the fate and transport of chlorinated solvents (TCE) flowing through reactive barriers containing zero-valent metals were influenced by several factors like advection, dispersion, adsorption and transformation reactions. The authors state that although batch systems have been extensively used to study  $\text{Fe}^0$  mediated reduction of several redox sensitive compounds, extending the results from batch to flow-through systems could be challenging due to the simultaneous occurrence of sorption and degradation which are indistinguishable. Moreover, adsorption-desorption phenomenon may also

occur. Results of the experiment indicated that sorption on to the zero-valent iron was an important process in the degradation of TCE in flow through processes.

Kim and Carraway., (2003) tested the dechlorination of Trichloroethene (TCE) using six zero-valent bimetal combinations. Palladium, Nickel and copper were coated on zero-valent iron and zinc. The authors observed that in general iron metals and bimetals exhibit faster reaction rates than zinc reductants. Bimetals were found to exhibit faster reaction rates than pure metals. Metal coatings enhanced reactivity in the order of Pd>Ni>Cu. Iron showed small amounts of chlorinated intermediate products, which was not observed for zinc.

Uludag and Bowers (2003) studied the reduction of trichloroethylene (TCE) in gas phase by Fedegrees under water vapor saturated conditions. Fedegrees pretreated with acid showed faster reduction rates and followed first order kinetics. The reaction occurred in two stages. The first stage was rapid. The second stage on the other hand was a slow step. The slow step was attributed to the formation of an oxide layer as a result of iron corrosion. The surface of Fedegrees was saturated at high TCE concentrations.

(iv) Zero-valent iron has also been used to dechlorinate several pesticides as indicted by the studies below.

Eykholt and Davenport., (1998) evaluated whether the reduction chemistry provided by zero-valent iron could be used for the remediation of



herbicides like alachlor and Metolachlor. The authors report that the reaction occurred in two stages. A fraction of the organic compound underwent instantaneous sorption and the remaining fraction showed rate limited sorption and first-order degradation. The reductive dechlorination of Alachlor and Metolachlor occurs by hydrogenolysis at the chloroacetyl group. The reduction was provided at the iron surface by oxidation of the iron metal. The half-lives were 5.8 and 6.9 for Alachlor and Metolachlor respectively indicating that there was only slight difference in the reaction rate constants. Metalochlor was found to be more reactive and more freely associated with the aqueous phase. This was because the products formed from the alachlor reaction do not interfere with its subsequent sorption, whereas the product formed from metolachlor competes for nonreactive sorption sites with metolachlor leaving it more readily available for reaction on the active iron sites.

Sayles et al., (1997) investigated the Dechlorination of DDT, DDD and DDE by zero-valent iron in the presence and absence of nonionic surfactant Triton X-114. The study indicated that zero-valent could successfully transform DDT with over 90% of the original mass removed within 20 days. Initial first order transformation rates were used since the data set did not fit satisfactorily to either zero or first order or Langmuir adsorption isotherm. The rate of the reaction in the presence of the surfactant was greater than during its absence. This was because, the transfer of DDT from solid to surfactant micelles to the aqueous phase was found to be faster than its direct dissolution into the aqueous phase. The

rate of dechlorination was independent of the specific surface area of iron. This indicates that the reaction was limited by mass transfer due to the slow dissolution of DDT. The authors reported that despite buffering, the pH increased with time in all reactors containing iron.

Ghauch. (2001) studied the degradation of some pesticides like benomyl, picloram and dicamba in a batch experiments by zero-valent iron powder. The decrease in pesticide concentration was monitored using HPLC. The  $t_{1/2}$  values ranged from 3 to 5.5 minutes.

(v) Zero-valent iron has also been used in the removal of heavy metals.

Ponder et al., (2000) studied the reduction of Cr(VI) and Pb(II) in aqueous solutions using "Ferragels". The kinetics of reduction was complex and included both reaction and adsorption. Once the active sites on the metal surface were saturated, the reduction reaction tends to proceed at slower rates, limited by mass transfer. The authors observed that the reaction was dependent both on the initial iron concentration as well as the concentration of the substrate. The reaction was found to be complicated. At times irrespective of the contaminant species or concentration the sorption of the contaminant on to the iron occurred at a much faster rate than the rate at which it was reduced. This indicates that the mechanism is physical. As a result the reaction could not be accounted by the simple first order kinetics alone and required complicated mixed order models to explain the observed trends. XRD of  $\text{Fe}^0$  indicated the presence of iron oxides and oxyhydroxides. The high surface area of these

deposits could favor adsorption. The apparent rate constants increased linearly with increase in the amount of iron (i.e., 10 times the number of moles of the contaminant). At low iron contents the surface sites were saturated and mass transfer of the contaminant on to the iron surface becomes the rate-limiting step. The apparent rate constants decreased with increased concentrations of the metal contaminant.

Pratt et al., (1997) used flow through columns to study the kinetics of chromate reduction using iron filings and quartz grains. The study involved identification of the mineralogical and geochemical nature of secondary reaction products formed on the barrier material. Surface analysis revealed that coatings on the iron surface and quartz grains were goethite, with the highest amount of chromium found at the outermost edges of the coatings. Within these regions chromium had a highly heterogeneous distribution. Near the iron surface the coatings were identified as ferric and hematite. The coatings had a botryoidal appearance. Majority of oxygen occurred as hydroxyl species. pH of the aqueous medium had a strong effect on the degree of protonation of water molecules coordinated with the oxide surface. As the pH increased there was a tendency of water molecules bound to the metal oxide surface to dissociate. Chromium occurred chiefly in the form of Cr (III) species. As the concentration of Cr (III) increased goethite underwent phase transformation into solid species that structurally and chemically resembled hematite. High concentrations of chromium were associated with the particulates.

Melitas et al., (2001) investigated the passivating effect of chromium on zero-valent iron. In contrast to many catalytic systems where the activity of reactive sites was independent of the reactant concentration, the reactivity of sites on zero-valent iron decreased with increasing concentration of chromium. This was attributed to the passivating effect of a corrosion inhibitor like chromium. However, in column studies the surface passivation reached a steady state. The chromium removal rates was affected by both the ability of Cr(VI) to penetrate the passivating oxides and by the ability of iron to release  $\text{Fe}^{2+}$  at the anodic site. The removal kinetics although fitted well to zero-order rate law the authors suggest that the process cannot be described by simple zero, first or fractional order kinetic models as they do not account for surface passivation of iron.

Melitas and Farrell., (2002) observed that the condition of the iron surface at the time of their exposure to chromate determined the effectiveness of iron for chromate removal. Both oxide free iron and iron coated with water-formed oxide were initially effective for chromate removal. However, iron coated with air-formed oxide was an order of magnitude less effective for removing soluble chromium. Increased concentrations of chromium resulted in decreased removal due to increased corrosion potential and anodic charge resistance.

Farrell et al., (2001) investigated the mechanisms involved in the removal of arsenate using zero-valent iron in batch experiments. The removal rates followed pseudo-first order kinetics at low concentrations and

approached zero order at high concentrations. The corrosion rates of iron wires were determined as a function of time using Tafel analysis. Although initially the presence of arsenate decreased the iron corrosion rates, at later stages it became steady indicating that the passivation had approached a steady state. The authors report that the primary mechanism behind arsenate removal was complexation of arsenate with Fe(III) on the surface of magnetite or maghemite.

Su and Puls (2001) through batch tests studied the influence of different types of iron filings on the removal of arsenate (As(V)) and arsenite (As(III)). The authors observed an exponential decrease in arsenate concentration in all the Fe<sup>0</sup> systems with time. The removal followed first order kinetics with R<sup>2</sup> values ranging from 0.85 to 0.98. The adsorption of As on iron oxides the possible corrosion products, could be the primary removal mechanism rather than chemical reaction with Fe<sup>0</sup>. pH had a significant influence, with the adsorption of As(V) by iron oxide decreasing for an increase in the pH. The adsorption of As(III) was maximum at pH 9 and equal amounts of As(V) and As(III) were adsorbed at pH below 7. The adsorption process could be described using the Langmuir adsorption isotherm. As the reaction progressed an increase in the pH is observed.

Su and Puls., (2001) studied the removal of arsenate and arsenite by zero-valent iron in batch systems in the presence of several anions. The authors observed that when phosphate, silicate, carbonate, borate and sulfate underwent sorption-dominated reactions, other anions like chromate, molybdate and nitrate showed reduction-dominated reactions.

In the presence of each of these variables, the reduction of As(V) to As(III) followed pseudo-first-order kinetics. Each of the anions were found to inhibit the reduction reactions, however, inhibition was maximum in the presence of phosphate and chloride. The results showed that  $\text{Fe}^0$  could serve as excellent barrier material that can remove a wide range of inorganic contaminants. However, the competing influence of certain anions must be considered when designing ZVI based reactive barriers.

Martin and Kempton (2000) investigated a new in-situ method for remediating groundwater contaminated with metals. The contaminated aquifers are coated with an adsorptive substrate by injecting solutes that react as they mix in the aquifer to form a sparingly soluble solid having a high metal-adsorption capacity. Ferrous sulphate and oxygen solutions were injected into a column of unconsolidated sand. The unretarded oxygen then reacts with Fe(II) bound to the sand to produce a coating of hydrous ferrous oxide (HFO). The effectiveness of this method was proved when the HFO delayed the breakthrough of Cr(VI) and As(V) by 8 and 30 pore volumes, respectively in comparison to the unamended material. Some potential advantages of this method suggested by the authors are

- (i) The problem of aquifer heterogeneity could be overcome as the coatings are emplaced preferentially in high-conductivity zones,
- (ii) Minimal surface disturbance.
- (iii) Straightforward regeneration of coating.
- (iv) No hazardous materials are generated.

Ramaswami et al., (2001) presents the results of a study using zero-valent iron to remove arsenic from water stored within rural homes in Bangladesh and West Bengal. The study observes that zero-valent iron added in the form of iron filings could remove >93% arsenic from waters containing up to  $2000\text{mg L}^{-1}$  over short contact times (0.5 – 3h). Arsenic removal was more rapid with sulphates while phosphate buffers were observed to inhibit arsenic removal by iron. The authors observed that arsenic removed was strongly bound to the  $\text{Fe}^0$  filings and the treated water could be decanted and the iron could be used repeatedly.

Astrup et al., (2000) investigated the feasibility of an attenuating barrier containing 5%  $\text{Fe}^0$  for removing Cr(VI) that arise from the storage or disposal of coal fly ash. The study also involved determining the geochemical processes that control chromium behavior. The study indicated that Cr mobility was significantly retarded in the presence of  $\text{Fe}^0$ . Color of the barrier material changed to dark green a few minutes after it came into contact with the aqueous solution, indicating the formation of corrosion products on  $\text{Fe}^0$ .  $\text{Fe(II)}$  enters solution through the initial oxidation of  $\text{Fe}^0$  and comes to equilibrium through the precipitation of  $\text{Fe(II)}$ -oxyhydroxides (Green rust). Further oxidation of  $\text{Fe}^{2+}$  and  $\text{Fe}^0$  resulted in the formation of ferric oxyhydroxides and colour of the surface later on changed to red-brown and the pH increased from 8.5 to 10.5. Under such conditions chromium does not have any direct access to the metal surface and the reaction becomes diffusion-limited when the oxide coating reaches

a certain thickness.. At high pH the build up of oxide layer depletes the capacity of  $\text{Fe}^0$  and results in decreased chromium removal.

Blowes et al., (1997) assessed the ability of four different types of iron bearing solids, siderite, pyrite, coarse grained elemental iron and fine grained  $\text{Fe}^0$  to remove dissolved Cr(VI) from solution at different flow rates. The primary reaction that occurred was the reduction of Cr(VI) to Cr(III) coupled with the oxidation of  $\text{Fe}^0$  to Fe(II) and Fe(III), and a subsequent precipitation of a sparingly soluble Fe-(III) – Cr(III) (oxy)hydroxide phase. Mineralogical analysis showed that chromium was associated with goethite. Results suggested that chromium was removed either through the formation of a solid solution or by the adsorption of Cr(III) onto the goethite surface. Roh et al., (2000) studied the mineralogical characteristics in a  $\text{Fe}^0$  based permeable reactive barrier and observed that major phases in the reactive iron barrier included iron oxides, carbonates, iron sulfides and elemental sulfur depending on the degree of iron corrosion, ground water chemistry and microbial activity.

Williams and Scherer., (2001) studied the kinetics of Cr(VI) to Cr(III) using carbonate green rust over a range of chromium concentrations and pH. Carbonate green rust was synthesized by induced hydrolysis of an Fe (II)/Fe (III) solution held at a constant pH of 8. Heterogeneous reduction by Fe (II) associated with the carbonate green rust appeared to be the dominant pathway controlling the reduction of Cr (VI). The reduction process followed pseudo-first-order kinetics and was proportional to the surface area concentration of green rust. An increase in pH from 5-9



showed a 5-fold decrease in the rate of the reaction. The reduction followed first order kinetics at low COD concentrations (<200 m $\mu$ M) while they deviated from first order at high COD values and approached a constant value. This deviation was attributed to the exhaustion of available Fe (II).

Nikolaidis et al., (2003) Observed that iron filings could effectively remove arsenic from aqueous solutions to levels less than 10 m $\mu$ g/L. Hydraulic detention time was a critical factor that influenced treatment efficiency. Precipitation of corrosion products was observed which became irreversible with time.

(vi) Several studies have also been carried out with respect to removal of radioactive substances using zero valent iron.

Fiedor et al., (1998) investigated the removal mechanism of soluble uranium from groundwater. X-ray photoelectron spectroscopy was used to determine the uranium oxidation state at the Fe<sup>0</sup> or iron oxide surface. The authors postulated the formation of a highly hydroxylated layer of iron oxide where U<sup>6+</sup> could be actively adsorbed to form U-O-Fe bonds. Upon adsorption in this manner, Uranium becomes immobilized long enough during which there is a transfer of electrons from the electron rich layer of iron oxide or the bulk Fe<sup>0</sup>. The study also involves determining product speciation and the relative removal kinetics for the removal of soluble uranium under aerobic and anaerobic conditions with ZVI. The authors reported that under aerobic conditions copious amounts of ferric corrosion

products were formed. Under such conditions  $U^{6+}$  gets actively sorbed on to the highly hydrated  $Fe^{3+}$  corrosion products through proton exchange with the hydroxyl sites. These  $Fe^{3+}$  corrosion products are loosely bound to the ZVI matrix and sloughs off through simple rinsing or agitation. However, under anaerobic conditions they get slowly and incompletely reduced to  $U^{4+}$ . The authors observed a lag period in the anaerobic experiment, and attributed it to the formation of sorptive sites. This lag phase was eliminated in the case of oxide coated iron indicating that the reduction was surface mediated. X-ray diffraction analysis of these sorptive sites indicated that they were thin and highly porous layer of iron oxides primarily magnetite ( $Fe_3O_4$ ) and hematite ( $Fe_2O_3$ ).

Gu et al., (1998) investigated the rates and mechanisms involved in the removal of uranium from contaminated ground water using  $Fe^0$  and other adsorbent materials like peat, iron oxides and bone char. The results indicated that  $Fe^0$  was the most efficient of the materials tested. Batch adsorption-desorption studies and spectrophotometric studies indicate that reductive precipitation of Uranium on  $Fe^0$  was the major reaction pathway. Less than 4% of  $UO_2^{2+}$  appeared to be adsorbed on the corrosion products of iron. The study showed that the reaction was reversible, as the reduced U(IV) species on the  $Fe^0$  surfaces could be reoxidized and remobilized when the reduced systems become more oxidized. However, the reoxidation rate is a much slower process compared to the reduction process. The authors observed that iron oxide materials strongly adsorb dissolved uranyl species at about pH 5-10. Adsorption was greatest on

amorphous ferric oxyhydroxide and least on hematite. The adsorption mechanism exhibited relatively fast reaction kinetics and was attributed to surface complexation between  $\text{UO}_2^{2+}$  and iron oxyhydroxide. Incomplete removal of U was due to the limited availability of surface sites. The adsorption could be described by Langmuir adsorption isotherm. The adsorption isotherms indicated a relatively rapid increase in adsorption initially but decreased for an increase in the solution concentration. The adsorption process would dominate only when  $\text{Fe}^0$  was consumed and the corrosion products (Iron oxyhydroxides) are formed. The  $\text{UO}_2^{2+}$  reduction could be by direct electron transfer at the  $\text{Fe}^0$  surface following electrochemical corrosion. However the electrochemical process takes longer than the adsorption process because it involves corrosion of  $\text{Fe}^0$  and an electron transfer from  $\text{Fe}^0$  to  $\text{UO}_2^{2+}$ . As long as there is sufficient iron present in the system to maintain an electron flow the reduction process would continue. The results indicated apparent pseudo-first order kinetics. As the reaction progressed an increase in pH was observed.

Schneider et al.,(2001) used columns filled with  $\text{Fe}^0$ , waste sludge containing Fe/Mn and peat for treatment of water from Uranium ore mines. The authors observed that the primary mechanism behind the removal of uranium was adsorption in the case of waste sludge containing Fe/Mn and peat. However,  $\text{Fe}^0$  was found to be the most efficient (resulting in 96% Uranium removal) where the removal was chiefly chemical reduction. Fe/Mn-sludge adsorbed 60% of radium and 70% of arsenic.

Morrison et al., (2001) carried out studies on  $\text{Fe}^0$  based permeable reactive barrier to remove Uranium contaminated waters. The authors report that longer residence time in the PRB compared to shorter residence time resulted in better treatment efficiency.

(vii) The following studies are related to the evaluation of Zero-valent iron based permeable reactive barriers.

Phillips et al., (2000) studied the mineralogical characteristics and evaluated the effects of cementation and corrosion of  $\text{Fe}^0$  on the long-term performance of in situ  $\text{Fe}^0$  reactive barriers. Analysis of the core material from a 15-month-old reactive barrier by XRD and SEM-EDX showed the presence of iron oxyhydroxides. Of the minerals found Aragonite ( $\text{CaCO}_3$ ), siderite ( $\text{FeCO}_3$ ) and Iron Sulfide ( $\text{FeS}$ ) were dominant in the shallow regions while aragonite ( $\text{CaCO}_3$ ) and  $\text{FeS}$  were present in the deeper zones. The authors reported corrosion and subsequent cementation as some of the factors that affected the long-term performance of the barrier.

Chew and Zhang., (1998) investigated the feasibility of using electrokinetics coupled with zero-valent iron treatment to abiotically remediate nitrate-contaminated soils and operational conditions under which the process can achieve their optimal operational effects is presented. The results obtained indicate that the process increased nitrate transformation efficiencies by 2 to 4 times. The highest removal efficiency

of nitrate was close to 90% at a pH ranging from 4 to 10. The major transformation products were ammonia-nitrogen and nitrogen gas.

Tratnyek et al., (2001) have indicated that a variety of organic surface-active substances can enhance or inhibit contaminant degradation, depending on the degree to which they promote solubilization, sorption, and/or reaction. Of these natural organic matter and certain quinones (juglone, lawsone and anthraquinone disulfonate), which represent the redox-active functional groups associated with NOM, is of particular importance. Studies on carbon tetrachloride showed that the inhibitory effect of humic acid was more pronounced than that of fulvic acid. Isotherms for adsorption of TCE and NOM onto  $\text{Fe}^0$  showed evidence of competition for surface sites.

Cunningham and Reinhard (2002) observed that a permeable reactive barrier based on zero-valent iron had several disadvantages. High capital cost especially when the installation is below ground surface and uncertainty regarding its long-term performance are some of the disadvantages just to name a few. An injection-extraction treatment well pair (IETWP) for the capture and treatment of contaminated groundwater could effectively overcome some of the practical limitations. This paper compares the hydraulics of a permeable reactive barrier to that of an IETWP. The authors observed that although hydraulics of both the systems was similar IETWP provided excellent plume capture and was better suited than PRB for a particular contaminated site.

(viii) The following studies review investigations carried out on the dechlorination of carbon tetrachloride using zero valent iron.

Scherer et al., (1997) studied the kinetics of carbon tetrachloride dechlorination by a polished  $\text{Fe}^0$  rotating disk electrode in an electrochemical cell. The reduction kinetics was studied at a pH of 8.4 in borate buffer and a potential at which an oxide layer would not be formed. At high rotation rates, the reactant was transported to the surface faster than it could be consumed, and the current density reached a value that was limited by chemical reaction and independent of the disk rotation rate. The authors found the rate of  $\text{CCl}_4$  reduction by oxide-free  $\text{Fe}^0$  to be dominated by chemical reaction at the metal-water interface rather than mass transport to the metal surface.

Devlin et al., (1998) Used granular iron to study the reduction kinetics of nitroaromatic compounds like 4-chloronitrobenzene, 4-acetylnitrobenzene, nitrobenzene, 2-methylnitrobenzene and 2,4,6-trinitrotoluene. None of the nitroaromatic compounds tested strictly followed pseudo-first-order kinetics. Although the iron was flushed between experiments to desorb the reduction products only partial recovery of iron reactivity was observed and the rates declined as the reaction progressed. The apparent pseudo-first order rate coefficients were found to decrease with increase in the concentration of nitroaromatic compounds up to a certain limit after which at higher concentrations the rate coefficients began to plateau, which indicated the saturation of reactive sites.

(ix) Investigations carried out on the mineralization of explosives by Zero-valent iron are discussed in the following sections.

Oh et al., (2001) evaluated the potential benefit of an integrated microbial-Fe<sup>0</sup> system to treat groundwater contaminated with RDX. The combination resulted in faster mineralization than separate treatments indicating that the treatment efficiency could be enhanced by biogeochemical interactions through bioaugmentation.

Oh et al., (2002) through batch experiments studied the adsorption of 2,4,6-trinitrotoluene (TNT) and hexahydro-1,3,5-triazine (RDX) in aqueous solution with scarp iron and high-purity iron. The authors observed that when high purity iron was used TNT was reduced to 2,4,6-triaminotoluene (TAT) with little accumulation of intermediate at the surface. However, with scarp iron the reduction of TNT was slower and the extent of adsorption was more significant. In either case, the reaction occurred primarily through reduction of the ortho nitro group. Kinetic analysis indicated that the process was surface mediated, with mass transfer controlling the overall rate of reduction. However, the reduction of RDX was less rapid and independent of the type of iron used.

Oh et al., (2002) studied the mechanism behind reduction of 2,4-dinitrotoluene (2,4-DNT) in batch systems using iron powder and scrap iron. The authors observed differences in kinetics, adsorption patterns and the distribution of intermediates with respect to the different forms of iron. This indicated that differences in reaction mechanism could occur with the type of iron used for the study.

Hofstetter et al., (1999) reported that explosives like trinitrotoluene (TNT) could be completely reduced to their corresponding aromatic polyamines by Fe(II) present at the surface of Fe(III)hydroxides or less efficiently by hydroquinone moieties of natural organic matter in the presence of H<sub>2</sub>S. The reduction kinetics was investigated through batch and column studies using FeOOH coated sand or a pure culture of the iron-reducing bacterium *Geobacter metallireducens* or ferrogenic consortia in aquifer sediments. The reduction followed zero-order kinetics. The study showed that one-electron reduction potential was an appropriate parameter for relating and evaluating the reduction rates of a series of nitroaromatic compounds. The rate constants of the most and least reactive poly nitroaromatic compounds (TNT and DANT respectively) was 3 orders of magnitude smaller with surface-bound Fe(II) than with hydroquinone moieties of NOM. This indicates that complete abiotic reduction of (P) NACs to the corresponding aromatic polyamines can be achieved easier by surface-bound Fe(II) rather than by reduced NOM. The results indicate that ferrous iron species play an important role in the reduction of a variety of organic and inorganic pollutants in natural and engineered systems.

Singh et al., (1999) showed that zero-valent iron could effectively remediate soil and water contaminated with RDX. pH showed a steady increase, which was attributed to the oxidative dissolution of iron metal resulting from the reaction with Fe<sup>0</sup> and dissolved oxygen. The Eh of the solution indicated a rapid drop followed by an increase, after which it became relatively constant. The authors observed that a slight decrease in



Eh resulted in a one-unit rise in pH. The rapid drop in Eh was attributed to the oxidation of  $\text{Fe}^0$  during aerobic corrosion because if the solution pH is greater than 6, dissolved oxygen causes rapid oxidation of  $\text{Fe}^{2+}$  and precipitation of ferric hydroxide. The rate of oxidation of ferrous iron was first-order with respect to oxygen and  $\text{Fe}^{2+}$  and second order with respect to  $\text{OH}^-$ . The results indicate that lowering the Eh and maintaining a neutral pH could enhance removal of RDX by  $\text{Fe}^0$ .

Wildman and Alvarez., (2001) used permeable reactive iron barriers (packed with iron powder or iron wool) to intercept and degrade RDX plumes. The study indicated that the rate and extent of RDX mineralization was enhanced by the presence of anaerobic bacteria that fed on cathodically produced hydrogen. Reductive treatment of RDX with  $\text{Fe}^0$  had the twin advantages of reducing toxicity as well as increasing the biodegradability under both aerobic and anaerobic conditions.

(x) A few other related works using zero-valent iron is discussed below.

Huang and Zhang., (2002) studied the kinetics of nitrate reduction using two types of zero valent iron at neutral pH. The authors observed that although the values of the kinetic parameters change with the type of iron used, the experimental data fitted well with a double-Langmuir-adsorption model that represented site saturation.

Alowitz and Scherer (2002) studied the reduction kinetics of nitrate, nitrite and Cr(VI) using three different types of iron metal in batch reactors. The variables studied were iron surface area concentrations and solution

pH over a range of 5.5 to 9. The reduction followed pseudo-first order kinetics with no significant variation in rate coefficients at pH above 7. Nitrite and Cr(VI) reduction was first order with respect to iron surface area concentration. However, surface area concentration did not have any significant influence on nitrate reduction. An increase in pH resulted in a decrease in the reduction rates with buffering effects being minimal. Under high pH conditions reduction ceased and became negligible. These observations indicate that pH was a major factor responsible for driving the reduction reaction.

Westerhoff and James., (2003) Evaluated the influence of different influent water quality parameters like pH, dissolved oxygen and nitrate concentration on the removal of nitrate in both continuous and packed bed columns containing zero valent iron. The efficiency of  $\text{Fe}^0$  for nitrate removal was tested over both short and long term periods. The results indicated a 70% conversion of the applied nitrogen to nitrate under short-term studies while it was less than 25% for long-term. Nitrate removal was accompanied by an increase in pH. Long-term studies showed cementation that resulted in reduced permeability of the  $\text{Fe}^0$  in packed columns.

Geiger et al., (2002) observed that the first order rate constants showed a 78% increase when the iron was pretreated with ultrasound for 2h. The kinetic improvement indicated that ultrasound pretreatment brought about physical and chemical changes at the iron surface. SEM and surface area analysis showed that ultrasound increased the iron

surface area by up to 169%. Ultrasound pretreatment was found to enhance the reactivity of iron by altering ratios of surface species, such as adventitious carbon to carbonyl carbon and iron to oxygen.

Loraine et al., (2002) studied the reduction kinetics of 1,2-dibromoethane (EDB) reduction by zero-valent iron in batch reactors. Ethylene and Bromide were identified as the reduction products. EDB sorption on to the cast iron surface was nonlinear and could be described by Langmuir equation. The results showed two distinct removal processes, an initial rapid phase dominated by mass transfer followed by a slower phase where surface reactions dominated.

**Abstract**

The objective of this study is to explore the possibility of utilizing the reduction chemistry provided by zero valent iron, as a viable treatment option to achieve decolorization of selected azo dyes that find wide application in the carpet dyeing units of the Alappuzha district in Kerala, India.

The study also involves investigating the influence of different operating variables that affect the kinetics of iron mediated reductive transformation of azo dyes. The dyes chosen for the study although belong to the chemical classification of azo dyes, one of the largest groups of dyes commercially available; still differ from one another with respect to the number of azo linkages separating the aromatic moieties. Therefore, results of the study would indicate if azo dyes could be reduced by elemental iron irrespective of the number of azo linkages. The study could provide insight on the influence of molecular structure of azo dyes during the use of elemental iron as a cost effective treatment option for the decolorization of spent dye baths containing azo dyes.

Although well-mixed batch systems usually examined in the laboratories do meet the academic requirements the transfer of such technologies to the field or onsite situation, demands further information. Therefore, from a practical point of view flow-through systems would be a much more attractive option compared to well-mixed batch systems. Hence, in the present study all observations are based on dynamic flow through columns packed with mild steel wire cuttings.

Prominent advantages associated with such flow through systems is that since iron in the form of  $\text{Fe}^0$  is present in far excess than the amount stoichiometrically required to cleave the azo linkages such systems not only bring about complete decolorization but also holds the potential of being functional over repeated runs before they require recharging or their reactivity diminish. However, when used repeatedly it was observed that there is a possible decrease in the treatment efficiency; due to the formation of organic coatings of associated corrosion products or ferric hydroxide layers which inhibits the reduction process. However, these disadvantages do not seem large as they can be easily overcome by rinsing iron metal with dilute hydrochloric acid thus maintaining the reactivity over long periods of operation.

In all, four variables were chosen to optimize the treatment efficiency of such flow through columns with packed iron metal viz., column height, flow rate, pH and concentrations of the dye. However, of the four variables in the later part of the experiment column height and flow rates were grouped together as residence time. This leaves only three effective variables namely flow rate, pH and dye concentration.

## 2.1. Introduction

There is an amount of increasing evidence indicating the role of  $\text{Fe}^{2+}$  in chemical reduction of organic pollutants through the reduction of critical functional groups. This principle paved the path for the emergence of a cost effective technology for the remediation of environmental contaminants. The technology is based on utilizing zero valent metals such as iron, tin and zinc, which are moderately strong reducing agents as a viable pretreatment option for enhancing biodegradability of refractory organics in wastewater. Of these metals zero valent iron has received a great deal of attention partly due to its abundance (fourth most abundant element making up Approx. 5.5% of the earths crust) and being environmentally benign iron is used in all the three valence states  $\text{Fe}^0$ ,  $\text{Fe}^{2+}$  and  $\text{Fe}^{3+}$  in a variety of physico-chemical processes for the treatment of water and wastewater taking advantage of its innocuous nature.

The effluent produced by the carpet dyeing process contains numerous contaminants, such as dyestuffs, surfactants, thickeners and finishing agents (Walker and Weatherley, 1997). Many of these dyeing units in the Alapuzha District of Kerala are either small or medium scale industries that are not in a position to install exorbitant treatment facilities that involve huge capital investments. As a result many of these units run without adequate treatment facilities and the colored effluents are indiscriminately let into the adjacent water bodies without prior treatment. These freshwater bodies in turn form valuable source of drinking water. The menace of residual color has restricted the utility of these resources in an area, which often faces acute water scarcity problems. Towards this direction the objective of our study is to

- (i) Explore the possibility of utilizing Zero Valent Iron as a viable treatment option to achieve decolorization of selected azo dyes, which finds wide application in the carpet dyeing units of Alappuzha District, in Kerala

- (ii) Study the operating characteristics that affect the reaction mechanism and kinetics of iron mediated reductive transformation of azo dyes taking place in dynamic flow through column tests in the presence of granular iron.

Although well-mixed batch systems usually examined in the laboratories meet the academic requirements; the transfer of such technologies to the field or onsite situations could be a difficult task. Therefore, dynamic flow through systems with stationary iron would be a more practical treatment application unlike well-mixed batch systems. Hence, dynamic flow through column was used in our study. An advantage of the column systems is that as the zero valent iron is present in far excess than the amount actually required to cleave the N=N bonds and hence bring about complete decolorization; the column may function for many repeated runs before it requires recharging. Another added advantage of such zero valent iron based technology is the in-situ generation of  $\text{Fe}^{2+}$  resulting from the oxidation of  $\text{Fe}^0$  which binds to the surface of the iron metal and is considered much stronger reductants than the solution phase  $\text{Fe}^{2+}$ .

In this study the efficiency of the zero valent iron to achieve dye reductions were examined at various concentrations of the dye , pH and flow rates. The results of this study demonstrates the effectiveness and applicability of the zero valent Iron option as a cost effective decolorization technology for spent dye baths.

## 2. 2. Materials and Methods

### 2.2.1. Reagents and supplies

The molecular structures and related features of the five dyes chosen for the study shown in figures 2.1 to 2.5 was obtained from Ms. Dhaval Dye Chem., Mumbai, India. The criteria behind the choice of these dyes is that they find wide spread application both in the textile as well as in the carpet making coir dyeing units of Alappuzha district, Kerala, India. All dye samples for the study was commercially available and hence used without any further purification.

Mild steel wire with a diameter of 0.25 mm was cut into pieces of uniform length. The average length was 2 cm.

Hydrochloric acid and sodium hydroxide used for pH adjustments were analytical grade.

Buffer tablets used to calibrate the pH meter were reagent grade and was obtained from Qualigens.

### 2.2.2. Instruments and experimental set up

Optical spectrum of the dye (200 to 800 nm) in dilute solutions was recorded using a Varian UV-Vis. Cary – 50 single beam spectrophotometer and  $\lambda_{\text{max}}$  of the dye was determined. The residual dye concentration was determined using a 1 cm quartz cell against a calibration diagram.

pH measurements have been made using a Systronics pH meter.



### 2.2.3. Column description

All observations have been drawn from dynamic flow through column experiments. The column was fabricated in the laboratory using PVC tubing with an inner diameter of 50 mm and a length of 110 cms provided with an inlet and an outlet. The length of the column from the inlet to the outlet was 80 cms. A strainer with a length of 13 cms was placed at the bottom of the column to prevent the loss of iron filings. This strainer formed a cup just beneath the inlet ensuring that the packing of iron filings began above the point of inlet. The sample port located in line with the inlet is considered as the initial port since; the dye solution does not come in contact with the iron filings. There were eight sampling ports located at equal distance of 10 cms along the entire length of the column. This makes column height one of the variables. The sample ports were made of threaded PVC caps that had an outer diameter of 1 cm, which was screw-fitted and then sealed on to the body of the column. These caps were in turn covered with another bored cap which could be screw fitted or removed according to convenience from the fixed sample ports. Thus, there was a small gap between the sample port fixed to the column and the detachable bored cap. Between this gap a self-sealing rubber septum was introduced. Bore on the cap was just sufficient for the entry of a hypodermic needle. The column packing consisted of commercial mild steel wire of 0.25 mm cut into pieces of uniform length. The average length of the cut wire was 2 cms. The column could on an average hold 2.4 kg of these iron filings and when packed the column had a bed volume of 1.5 L.



### 2.3. Experimental procedure

Stock solution of the dye was prepared by weighing out appropriate amounts of the dye and dissolving it in distilled water. The solution was then heated to near boiling to promote maximum dissolution of the dye, which was then cooled to room temperature. All standard solutions for the calibration diagram and all the stock solutions to carry out experiments were prepared from this hydrolyzed dye solution.

Spectrum of the acidified dye in the UV-visible range was recorded in aqueous medium and the absorption maximum of the dye in the visible region (wavelength in the visible region where the dye gave a maximum absorbance) was identified. A calibration diagram for the dye was then prepared at this wavelength. The hydrolyzed stock dye solutions were appropriately diluted to obtain a range of working standards of known concentrations for which the experiments had to be conducted. From these working standards of the dye 1 mL was drawn and transferred into 15 mL test tubes containing 9 mL distilled water. The solution was then acidified using 1 mL, 1N HCl and the calibration curve for the dye was prepared thereby directly relating the decrease in absorbance to dye concentration.

#### 2.3.1. Sampling

During a typical run, the column was packed with approx. 2.4 kg of mild steel wire cuttings. Once packed the dye solution of known concentrations (ranging from 50 mg/L to 200 mg/L) was adjusted to the desired pH (ranging from pH 2 to pH 8 covering both acidic and alkaline

range). Dye solution of the desired concentration and pH was then pumped through the column in an up-flow mode using a Miclins variable speed peristaltic pump at predetermined flow rates. Flow rate was one of the variables (ranging from  $20 \text{ mL min}^{-1}$  to  $60 \text{ mL min}^{-1}$ ). Actual flow rates were determined by measuring discharge at the outlet. Residence time was calculated from the measured flow rates and cross sectional area of the column. The reduced dye solution from the column was channeled into a separate glass bottle until a volume corresponding to two bed volumes of the column (3L) was collected. Under such conditions it is assumed that a steady-state is reached after which there would not be any significant variation in the concentration profile along the length of the column. At this juncture, reactant concentration profiles were measured by withdrawing 10 mL samples through the sampling ports using a syringe with a stainless steel needle having a length of 5 cms. This enabled the sample to be drawn right from the middle of the column. Between samples, the sampling syringe was rinsed first with distilled water and then with the samples from the respective ports. The samples so drawn were centrifuged at 4000 rpm for 10 minutes. 1 mL of the centrifugate was then drawn into 15 mL test tubes containing 9 mL distilled water. The solution was then acidified using 1 mL 1N HCl which was then thoroughly mixed using a cyclomixer. The residual dye concentrations were determined through comparison with the calibration curve.

All experiments were triplicated to ward off randomness and the average of these values have been considered for interpretations. Good

agreement between the triplicates within any particular experiment performed on different days indicated that the protocol was an acceptable one.

### 2.3.2. Iron pretreatment and analysis

The direct role of iron metal as a reactant implies the involvement of reactive sites on the metal and therefore the condition and quantity of metal surface in a reaction system should strongly influence the rate of the reduction reactions in any zero valent iron based treatment system. Despite all attempts to remove the surface oxide layers, an iron surface when exposed to air and an aqueous solution will form oxide layers depending on the variation in the ratio of oxygen to iron which is in turn a function of the column depth from the surface (Carina et al., 1995). These factors could lead to reactivity loss due to reversibly sorbed residues and surface oxides. Matheson and Tratnyek, (1994) showed that preceding each experiment by rinsing the metal in dilute hydrochloric acid produced faster dechlorination and that this pretreatment was necessary to obtain any appreciable reaction at all for some iron samples. Treating zero-valent iron in this way provided a well-defined and reproducible surface (Metals Handbook, (1982). The most likely explanation for the effect of acid washing is that it dissolves the surface layer on the iron grains, leaving clean reduced metal, which is relatively free from unreactive oxide or organic coatings. Increased iron surface area due to corrosion pits may also contribute to the greater reactivity of the acid washed iron. Therefore, at the end of each experiment the reacted iron filings were soaked in 0.1N

Hydrochloric acid as a step towards minimizing the reactivity loss due to reversibly sorbed residues or reduction products. Before the next experiment these filings were thoroughly washed with copious amounts of distilled water to remove any traces of residual acidity. This was ensured through subsequent pH measurement of the washings. This pretreatment of iron was adopted as a standard procedure to all experiments. Farrell et al., (2000) reported that the rates on freshly acid-washed iron surfaces were considerably faster than those on surfaces with aged iron oxide layers. This indicated that the condition of iron surfaces had a significant influence on the reaction rate. Similar studies by Johnson et al., (1996) observed that acid washing increased the specific surface area concentration of  $\text{Fe}^0$ , but to highly variable degrees. The most important factors that influenced the reductive dechlorination reaction were reactivity of the substrate, and the iron surface area concentration. Other factors include the surface condition of  $\text{Fe}^0$ , pH, initial contaminant concentration and flow or mixing rate. Agrawal and Tratnyek., (1996) reported that the effect of HCl pretreatment may be due to cleaning of the surface by dissolution of metal and breakdown of the passivating oxide layer; increasing the metal surface by etching and pitting through corrosion; increase in the density of highly reactive sites consisting of steps, edges, and kinks, following corrosion by acid; and increased concentrations of adsorbed  $\text{H}^+$  and  $\text{Cl}^-$  that persists after pretreatment with HCl.

Matheson and Tratnyek, (1994) report that although about 15% of the iron used initially at the start of the experiment was lost due to corrosion

during the pretreatment step, Corrosion continued to occur after rinsing the iron and stabilizing the system with circum-neutral pH. However, the iron dissolution under these conditions was much slower as evidenced by the lack of measurable decrease in iron by weight (production of  $< 400 \mu\text{g/L Fe}^{2+}$ ) but the corrosion of iron taking place by the reduction of water was confirmed as the concentration of hydrogen increased to  $>400 \text{ mg/L}$  within 1hr. Matheson and Tratnyek., (1994) reported that rinsing the metal with dilute HCl provided well-defined and reproducible surface that produced faster dechlorination. This was attributed to the effect that acid washing dissolved the surface layer on the iron grains leaving clean reduced metal relatively free of unreactive oxide or organic coatings. The corrosion pits formed as a result of the acid pretreatment of  $\text{Fe}^0$  could contribute to its greater reactivity. Su and Puls., (1999) observed that  $\text{Fe}^0$  when treated with HCl resulted in an increase in the specific area, which in turn led to greater observed rate constants

During the course of the experiment it was observed that copious amounts of ferrous corrosion products were produced and these sloughed off into solution. Since, all the experiments are based on flow-through column studies it is observed that these corrosion products that were formed were only loosely bound to the zero valent iron matrix and was easily removed at all flow rates. However, since the samples were drawn from the middle of the column, substantial quantities of corrosion products in the form of fine powder was visible which if not removed was found to interfere with spectrophotometric measurements. Hence, as a standard

procedure, all samples were centrifuged at 4000 rpm for ten minutes and 1mL of the centrifugate was taken for analysis. However, under acidic pH conditions (pH 2) significant quantities of dissolved iron was detected in the samples drawn for analysis. Such samples although freed of suspended iron particles through centrifugation contained copious amounts of colloidal iron that do not separate out. These samples with the passage of time developed a pale yellow color that progressively intensified. This could be attributed to the fact that the experiments being carried out under aerobic conditions, the dissolved oxygen in the samples was causing the dissolved iron to precipitate into the difficult to settle colloidal iron, imparting the pale yellow color. Such samples when analyzed gave erroneous results as the recorded absorbance values corresponds to both the residual dye in solution, as well as the absorbance imparted by the colloidal iron. During the course of our study it was observed that this problem could be overcome by ensuring that the solution remained acidified at  $\text{pH} < 2$ . For this reason, as a standard procedure the samples were acidified using 1mL 1N HCl before analysis. This step prevented the precipitation of colloidal iron by maintaining it in the dissolved state.



## 2.4. Results and Discussion

2.4.1. Molecular structures and other related features of various dyes used in the study are shown in figures 2.1 to 2.5.

(i) Molecular structure of Direct Sky Blue is shown in figure 2.1.

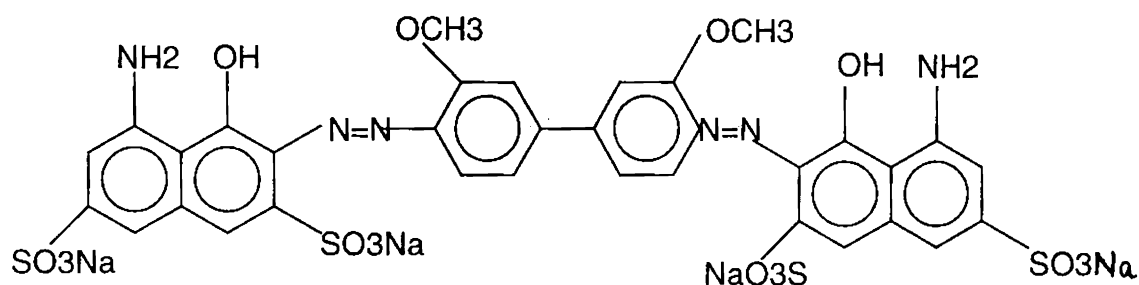


Figure 2.1. Molecular structure of Direct Sky Blue (DSB)

C.I. Generic name: Direct Blue- 15

C.I. Constitution Number: 24400

Commercial Name: Sky Blue

Application class: Direct

Chemical classification: Diazo

Wavelength of maximum absorbance: 605 nm

(ii) Molecular structure of Direct Black-EG is shown in figure 2.2.

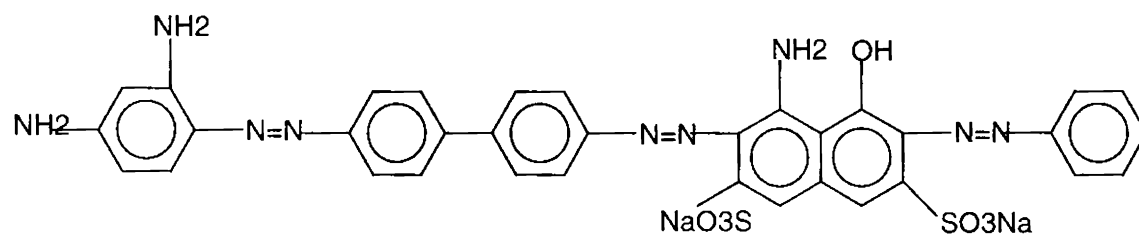


Figure 2.2. Molecular structure of Direct Black-EG (BEG)

C.I. Generic name: C.I. Direct Black 38

C.I. Constitution Number: 30235

Commercial Name: Black - EG

Application class: Direct

Chemical classification: Tri azo

Wavelength of maximum absorbance: 530 nm

(iii) Molecular structure of Direct Catechine Brown is shown in figure 2.3.

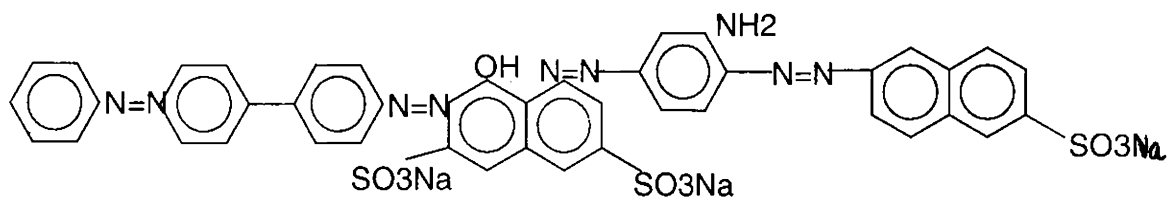


Figure 2.3. Molecular structure of Direct Catechine Brown (DCB)

C.I. Generic Name: CI Direct Brown- 3B

C.I. Constitution Number: 35520

Commercial Name: Catechine Brown

Application class: Direct

Chemical classification: Tetra azo

Wavelength of maximum absorbance: 487 nm

(iv) Molecular structure of Direct Green B is shown in figure 2.4.

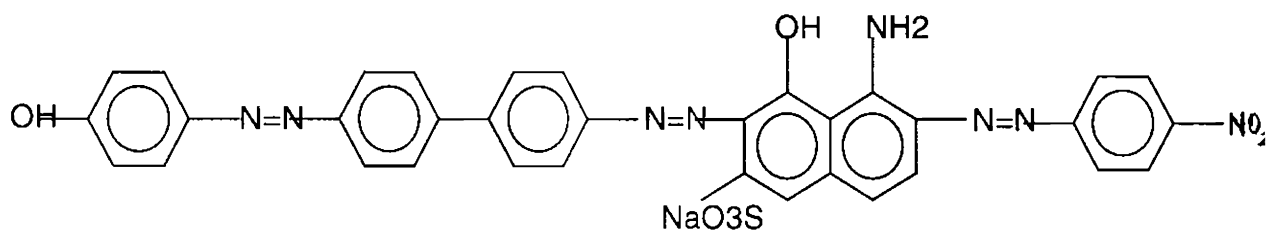


Figure 2.4. Molecular structure of Direct Green-B (DGB)

C.I. Generic name: C.I.Green-6

C.I. Constitution Number: 30295

Commercial Name: Green-B

Application class: Direct

Chemical classification: Tri azo

Wavelength of maximum absorbance: 620 nm.

(v) Molecular structure of Direct Yellow-5GL is shown in figure 2.5.

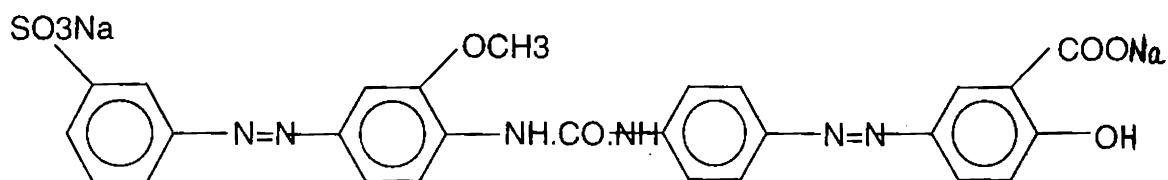


Figure.2.5. Molecular structure of Direct Yellow 5GL (Y-5GL)

C.I. Generic name: C.I. Direct Yellow 44

C.I. Constitution Number: 2900

Commercial Name: Yellow – 5GL

Application class: Direct

Chemical classification: Diazo

Wavelength of maximum absorbance: 401 nm.

## 2.5. UV-Vis. Spectrum

UV-Vis spectrum of the different dyes studied is shown in figures 2.6 to 2.10.

2.5.1. The absorption spectrum of an acidified solution of Direct Sky Blue is shown in figure 2.6. The spectrum is characterized by a single peak in the visible range ( $\lambda_{\max}$ : 605 nm, Abs: 0.055). The peak in the visible region could be attributed to the conjugated  $\pi$  system of aromatic rings connected by two azo groups. A small peak that was not very significant observed in the UV region could be attributed to the two adjacent rings (Ince and Tezcanli, 1999).

2.5.2. Absorption spectrum of an acidified solution of Direct Black-EG is shown in figure 2.7 and is characterized by a peak in the visible range ( $\lambda_{\max}$ : 530 nm, Abs: 0.310).

- 2.5.3. The absorption spectrum of an acidified solution of Direct Catachine Brown is shown in figure 2.8 and is characterized by a peak in the visible range ( $\lambda_{\max}$ : 416.9 nm, Abs: 0.160).
- 2.5.4. The absorption spectrum of an acidified solution of Direct Green-B is characterized by two peaks in the visible range ( $\lambda_{\max}$ : 620 nm, Abs: 0.072 and ( $\lambda_{\max}$ : 377 nm; Abs.0.070) as shown in figure 2.9. However, calibration curve for the dye has been prepared at 620 nm.
- 2.5.5. The absorption spectrum of an acidified dye solution of Yellow-5GL is shown in figure 2.10. The spectrum is characterized by a single peak in the visible region ( $\lambda_{\max}$ : 401 nm, Abs: 0.12).

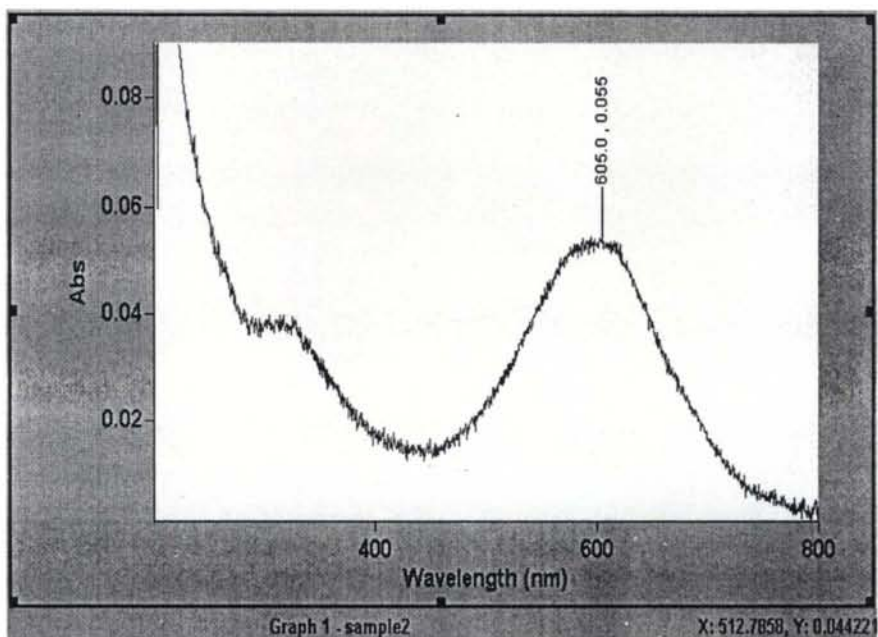


Figure 2.6.  
 UV-Vis absorption spectrum of Direct Sky Blue (DSB) in water.  
 Dye concentration  $100 \text{ mg L}^{-1}$ , path length 10 mm

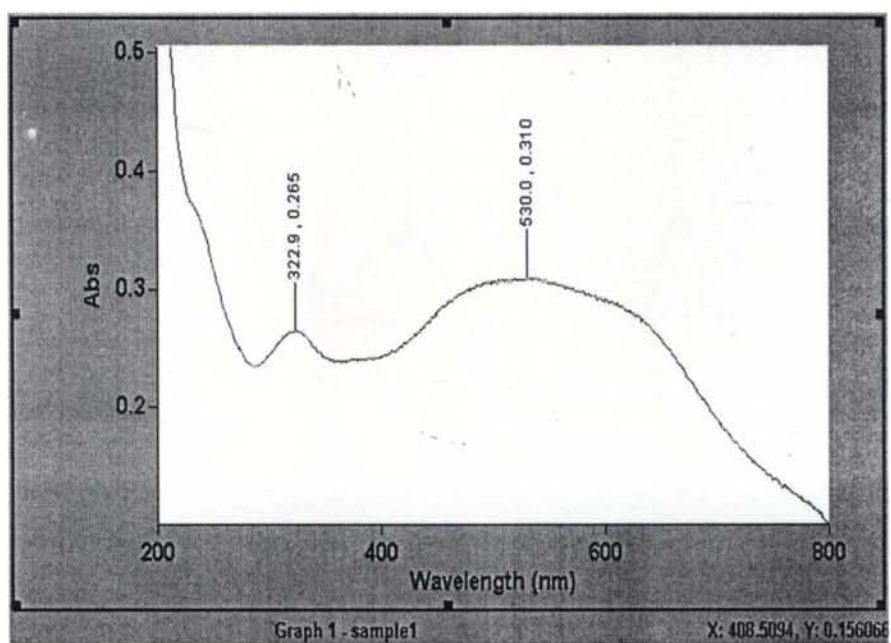


Figure 2.7.  
 UV-Vis absorption spectrum of Direct Black-EG (BEG) in water.  
 Dye concentration  $100 \text{ mg L}^{-1}$ , path length 10 mm

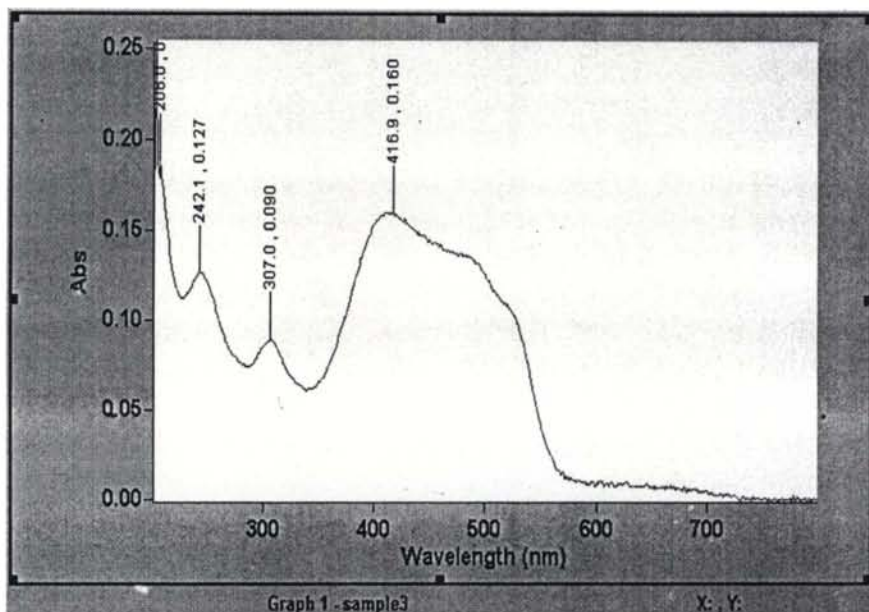


Figure 2.8.  
 UV-Vis absorption spectrum of Direct Catachine Brown (DCB) in water.  
 Dye concentration  $100 \text{ mg L}^{-1}$ , path length 10 mm

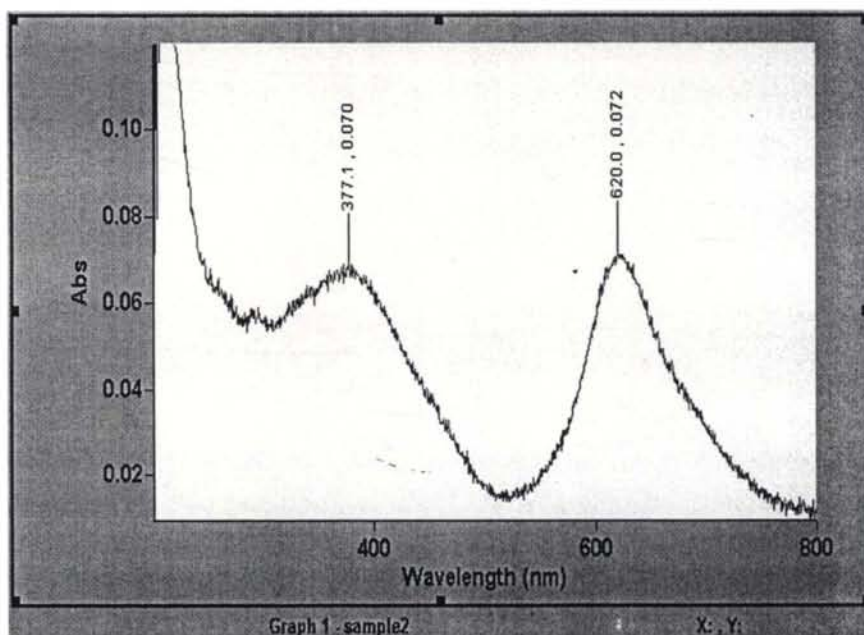


Figure 2.9.  
 UV-Vis absorption spectrum of Direct Green-B (DGB) in water.  
 Dye concentration  $100 \text{ mg L}^{-1}$ , path length 10 mm

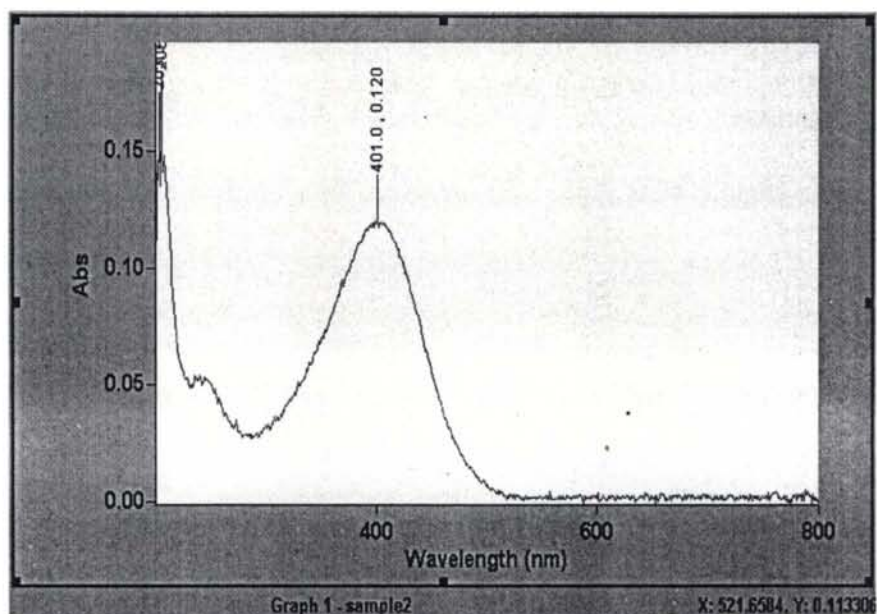


Figure 2.10.  
UV-Vis absorption spectrum of Direct Yellow-5GL (Y-5GL) in water.  
Dye concentration  $100 \text{ mg L}^{-1}$ , path length 10 mm

## 2.6. Calibration curve

2.6.1. A calibration curve for Direct Sky Blue was prepared at a wavelength of 605 nm. The dye solution was found to obey Beer Lambert's law up to 300 mg L<sup>-1</sup> however; experiments have been conducted at concentrations ranging from 50 to 200 mg L<sup>-1</sup>. The calibration curve is shown in figure 2.11.

The residual dye concentration was determined by comparison with the calibration curve.

2.6.2. A calibration curve for Direct Black-EG was prepared at the observed  $\lambda_{\max}$  of 605 nm. The dye solution was found to obey Beer Lambert's law up to 300 mg L<sup>-1</sup> however; experiments have been conducted at concentrations ranging from 50 to 200 mg L<sup>-1</sup>. The calibration curve is shown in figure 2.12.

The residual dye concentration was determined by comparison with the calibration curve.

2.6.3. A calibration curve for Direct Catachine Brown was prepared at the observed  $\lambda_{\max}$  of 416.9 nm. The dye solution was found to obey Beer Lambert's law up to 300 mg L<sup>-1</sup> however; experiments have been conducted at concentrations ranging from 50 to 200 mg L<sup>-1</sup>. The calibration curve is shown in figure 2.13.

The residual dye concentration was determined by comparison with the calibration curve.



2.6.4. A calibration curve for Direct Green-B was prepared at the observed  $\lambda_{\max}$  of 620 nm. The dye solution was found to obey Beer Lambert's law up to 300 mg L<sup>-1</sup> however; experiments have been conducted at concentrations ranging from 50 to 200 mg L<sup>-1</sup>. The calibration curve is shown in figure 2.14.

The residual dye concentration was determined by comparison with the calibration curve.

2.6.5. A calibration curve for Direct Yellow 5GL was prepared at the observed  $\lambda_{\max}$  of 401 nm. The dye solution was found to obey Beer Lambert's law up to 300 mg/L however; experiments have been conducted at concentrations ranging from 50 to 200 mg L<sup>-1</sup>. The calibration curve is shown in figure 2.15.

The residual dye concentration was determined by comparison with the calibration curve.

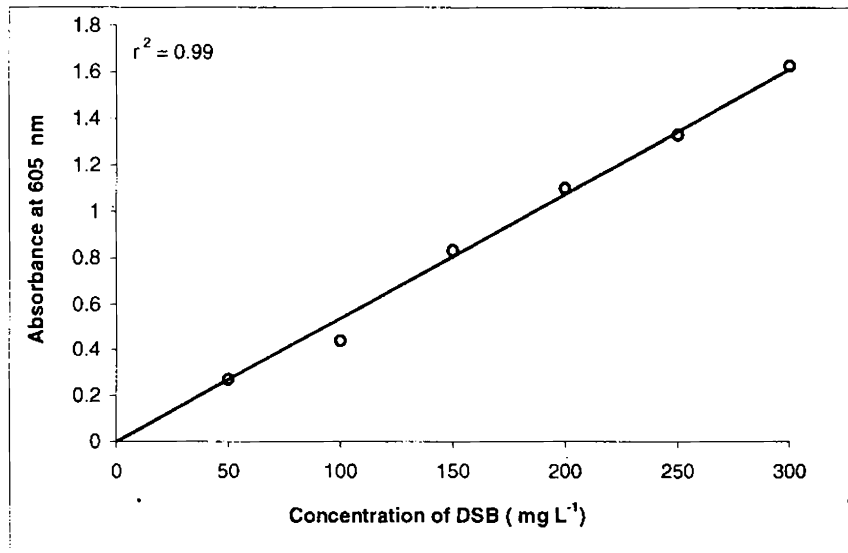


Figure 2.11  
 Calibration curve according to Beer-Lamberts law for Direct Sky Blue(DSB)  
 Conc. range 0 to 300 mg/L, path length 10 mm and analytical wavelength 605 nm

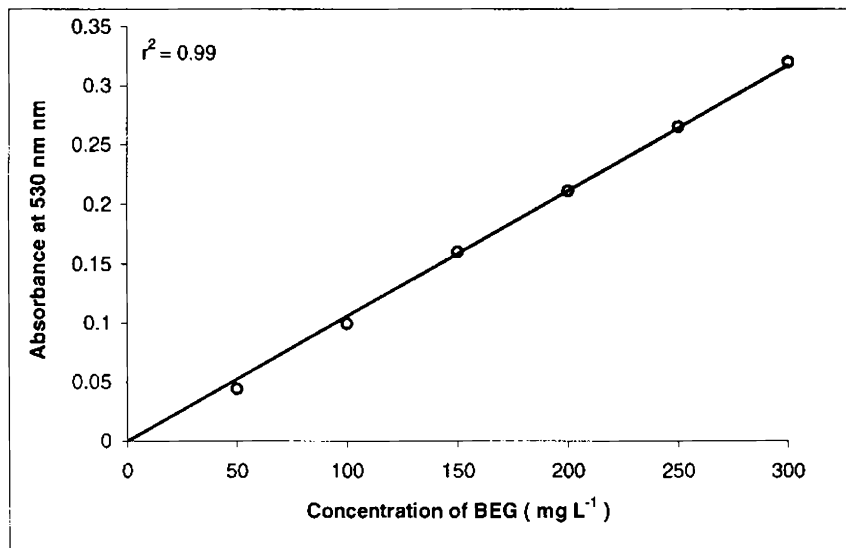


Figure 2.12  
 Calibration curve according to Beer-Lamberts law for Direct Black EG (BEG)  
 Conc. range 0 to 300 mg/L, path length 10 mm and analytical wavelength 530 nm

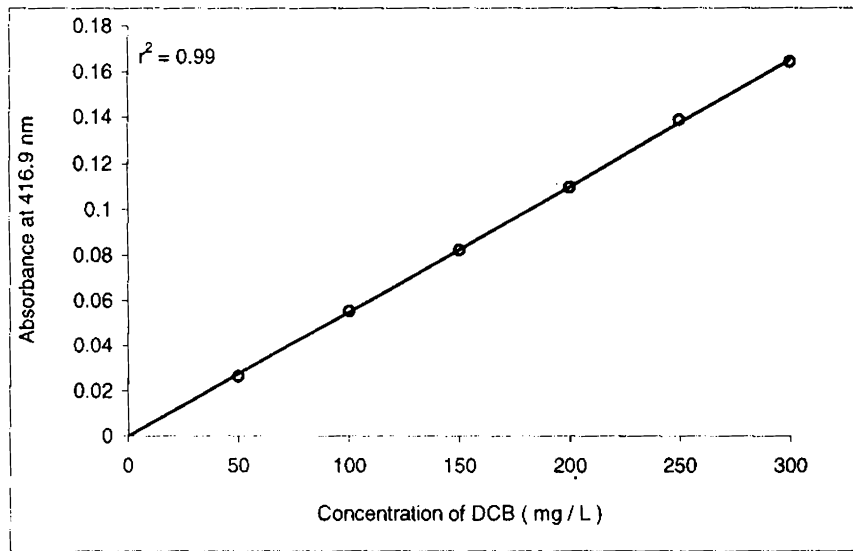


Figure 2.13  
 Calibration curve according to Beer-Lamberts law for Direct Catachine Brown  
 Conc. range 0 to 300 mg/L, path length 10 mm and analytical wavelength 416.9 nm

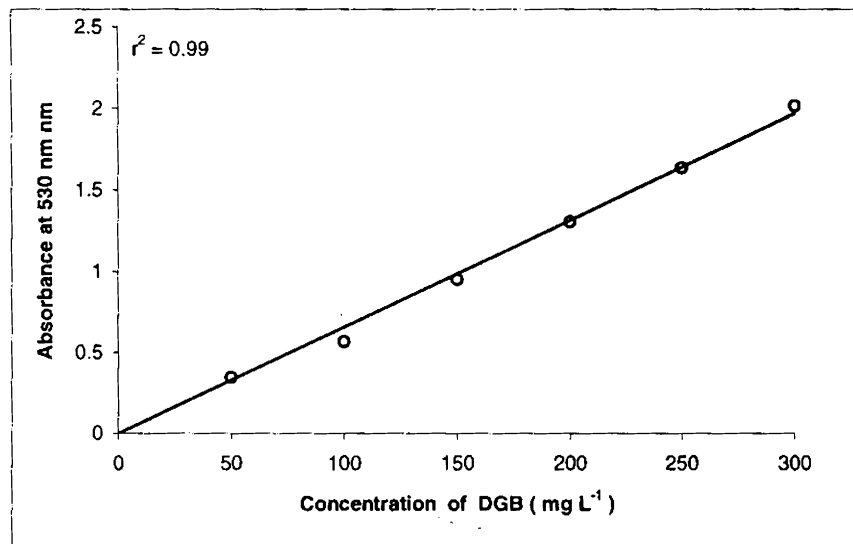


Figure 2.14  
 Calibration curve according to Beer-Lamberts law for Direct Green B  
 Conc. range 0 to 300 mg/L, path length 10 mm and analytical wavelength 530 nm

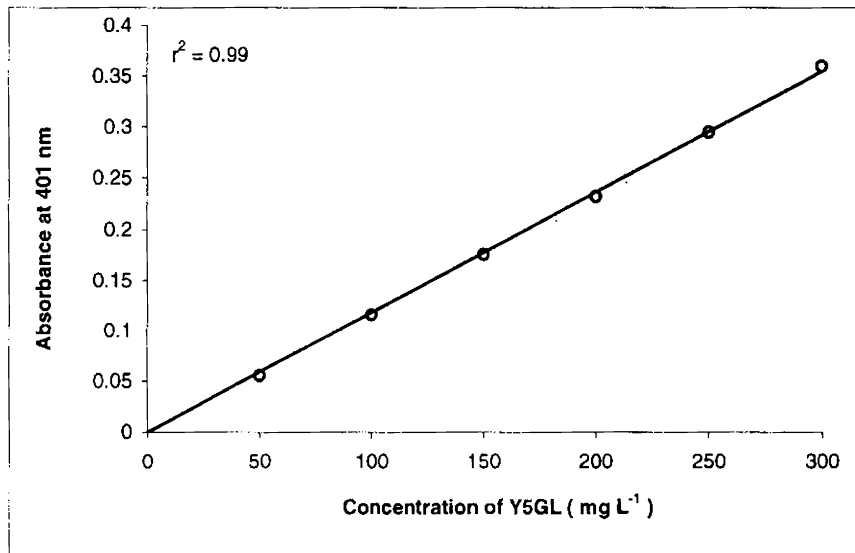


Figure 2.15  
Calibration curve according to Beer-Lamberts law for Direct Yellow 5GL (Y5GL)  
Conc. range 0 to 300 mg/L, path length 10 mm and analytical wavelength 401 nm

## 2.7. Kinetics of transformation

A heterogeneous reaction is indicated by both the strong dependence of the reaction rate on the iron surface area and the lack of the reaction when water is removed from the presence of iron surfaces. Heterogeneous reactions require that the reactant molecules reach the solid surface. At the surface of the metal it is necessary that the dye molecules have to associate with at two sites, which can be either reactive or non-reactive. The term 'reactive sites' refers to those sites involved in the breaking of the bonds. It is at these sites, the azo bonds present in the dye molecule would be cleaved to result in the formation of the corresponding reaction products, which could be either hydrazo derivatives or amines depending on the number of electrons transferred during the reaction. However, in either case the reaction products formed is colour less when compared to their parent dye molecule. This clearly indicates that for decolorization of the dye it is not necessary that the entire molecule should be destroyed; cleavage of the chromophore groups is all that is necessary to achieve decolorization. Such a process is irreversible as the dye molecule loses their identity through the breakage of the azo linkages. On the other hand the 'non-reactive sites' refer to those sites where the dyes would remain adsorbed on the surface of a layer of corrosion products accumulated at the metal surface. In such sites the dye molecule would not lose their identity, as they simply remain adsorbed without undergoing any chemical transformation. Such a process is reversible as the adsorbed dye molecule could also become desorbed.

Hung et al., (2000) suggested that heterogeneous reactions involve five steps:

- (i) Mass transfer of the reactant to the metal surface from the bulk solution.
- (ii) Adsorption of the reactant on the surface i.e. the molecules associate with the surface at sites that may be either reactive or non-reactive.
- (iii) Chemical reaction at the surface i.e. transfer of electrons from the metal surface to the reactant leading to the formation of intermediate products.
- (iv) Desorption of the products from the surface.
- (v) Mass transfer of the products into the bulk solution i.e. some intermediate and final products could diffuse from the metal surface to the solution.

Any one of these steps may be rate limiting.

A major issue in such systems is the extent to which the overall reaction rate is controlled by chemical reaction (i.e. electron transfer) versus the extent to which it is controlled by mass transport for the well-mixed bulk solution to the iron surface. To properly interpret trends in the reaction rate, it is especially important to decouple the observations into mass transport and reaction-limited kinetics.

There are views, which suggest the direct influence of zero-valent iron as a reactant. This means that reactive sites of the metal plays a prominent role in the overall reaction kinetics associated with the system.

Following electrochemical corrosion of  $\text{Fe}^0$  there would be a continuous generation of electrons, which could be transferred to the organic compound (dye), which in turn would be reduced. Under such conditions direct electron transfer at the metal surface to the organic compound can be the primary reaction mechanism. Such reactions have been strongly correlated to the specific surface area of  $\text{Fe}^0$ . Although the iron surface when exposed to air and an aqueous solution will form oxide layers, we have attempted to minimize the problem by rinsing the metal in dilute HCl. Such a pre-treatment would provide a well defined surface free from oxide film on the metal surface as it dissolves the surface layer on the iron grains leaving clean, reduced metal that is relatively free of unreactive oxide or organic coatings. However, before the experiments the iron filings were washed with copious amounts of distilled water so that there is no possibility of attributing the decolorization of the dye on acid washed iron to the effect of residual acidity, as confirmed by pH measurements.

The principle behind monitoring reactions in flow systems is that the reactant, which in this case is the aqueous dye solutions, is led at a known flow rate through a reaction column of known volume. As it was not possible to maintain the column at a constant temperature, all reactions have been carried out at room temperature and the influence of variations in the ambient room temperature on the reaction kinetics was overlooked assuming that these variations were not significant. Since, the sampling ports were located at equal distances, from the reactor volume and the flow rate, it is possible to calculate the mean time spent by the reaction mixture

(residence time) at each of these ports. The difference between the concentrations at each of these sampling ports represents the amount of reaction that has occurred. This difference divided by the time of contact is therefore the rate of the reaction. The order of the reaction can be determined by varying the different operating parameters, which in this study are column height, flow rates, concentration and pH.

As previously stated, the results of the study are based on a dynamic flow through column that does not involve any stirring, and hence the flow through the column can be considered to be plug flow.

Suppose, the reaction mixture is passed through the reactor at a volume rate of flow (expressed in mL min<sup>-1</sup>) is  $u$ . Consider an element of volume  $dV$  in the reactor, and suppose for simplicity that the reaction rate depends upon the concentration  $c$  of a single reactant. For a reaction of the  $n$ th order, the rate of disappearance of the substance is given by

$$V = -dc/dt = kc^n$$

The rate of disappearance of reactant in a volume  $dV$  is therefore  $kc^n dV$ .

After the system has been operating for a sufficient period of time (which in this study is 3L corresponding to two bed volumes), a steady state is established; this means that there is no change, with time, in the concentration of the reactant in the volume element. Three processes contribute to the steady state, as follows:

1. Molecules of reactant enter the column through the inlet, the number of moles entering in time  $dt$  being  $uc dt$ .



2. Molecules leave the column through the outlet, the number of moles leaving in time  $dt$  being  $u(c+dc) dt$ .
3. Molecules that disappear by chemical reaction; for a reaction of the  $n$ th order the number of moles  $(-dn)$  disappearing in time  $dt$  is  $kc^n dV dt$ .

The steady-state equation is obtained by equating the rate of entry of reactant into the column (by process 1) to the sum of the rates of removal (by process 2 and 3). The result is

$$uc dt = u(c+dc) dt + kc^n dV dt$$

or 
$$-dc / c^n = k / u dV$$

This equation must be integrated over the reactor volume  $V_0$ ; at the entrance to the reactor  $V = 0$  and  $c = c_i$  (the initial concentration), while at the exit  $V = V_0$  and  $c = c_f$  (the final concentration of the reactant).

For a particular case in which  $n=1$ , integration gives

$$\ln c_f / c_i = k V_0 / u$$

The above equation is the same as the first order rate equation for a static system and the two are equivalent if  $V_0 / u$  is replaced by  $t$ . This quantity  $V_0 / u$  is known as the contact time or the residence time of the reaction; and is the average time that a molecule takes to pass through the reactor. Unlike the static system where the above equation is tested by varying the time, in our study the above equation has been tested by varying the  $V_0 / u$  which can be achieved by either varying the volume of the reactor or the flow rate (Keith J. Laidler, 1990).

Therefore, in such systems, plots of the natural logarithm of the substrate concentration versus time gives a linear plot from their initial concentrations to the concentration profile along the length of the column (followed in most cases to up to two half lives with the average  $r^2$  values being 0.95) indicating that the kinetics of the azo dye reduction in such columns follow first order. The slope of the lines regressed to natural logarithm of concentration versus time data were used to obtain the first order rate coefficients. However, because  $\text{Fe}^0$  in the column is present in far excess in comparison to the dye concentration this reaction can be considered to be pseudo first order and the observed rate coefficients, pseudo-first order rate coefficients.

## 2.8: Effect of flow rate

A common criterion adopted to differentiate between surface processes and mass transport limited processes in batch systems, is to monitor the variation in the rate coefficients with the intensity of stirring or mixing. Rates controlled by chemical reaction step should not be affected; however, if it is a mass transport mediated process there would be an increase in the diffusion-controlled rates due to the decrease in the thickness of the diffusion layer at the particle surface (Spiro, M. 1989). However, Agarwal and Tratnyek (1996), has pointed out that an increasing surface reactivity with increasing stirring rate could also be due to indirect effects such as increasing abrasion of the agitated particles or the oxide layer. Therefore in order to overcome the potential interference of particle abrasion on interpretation of mass transport effects, the present study is based on dynamic flow through columns in which the mild steel filings were held stationary. Flow rate has been chosen as one of the variables to investigate its influence on the kinetics of iron mediated reduction of azo dyes and to evaluate whether mass transport effects need to be considered when designing an iron metal based permeable reactor barrier for redox labile contaminants such as azo dyes.

Scherer et al., (1998) report that the degree to which mass transport determines the overall rate of reduction of organic compounds by iron metal however, is difficult to resolve because of a multitude of indirect effects that may occur in the reactor. Surface of the metal gets covered by

an oxide layer, which is formed by the accumulation of corrosion products at the iron metal-water interface, which is accompanied by external diffusion. This could give rise to three potential kinetic domains:

- i Mass transport limited kinetics, where the substrate diffuses to the surface more slowly than it reacts at the surface.
- ii Reaction limited kinetics where the substrate reacts at the surface more slowly than it diffuses to the surface.
- iii Intermediate kinetics, where mass transport and surface reaction occur on similar time scales.

All these factors could make it difficult to confirm whether the observed kinetics is measuring diffusion rates, reaction rates or a combination of both.

The pretreatment of iron metal with dilute acid therefore is a bid to overcome these difficulties in the interpretation of the data.

Sivavec et al., (1995) and Burris et al., (1995) indicate that transport of the compounds to the iron surface may contribute to the kinetic control. Column experiments carried out by Thomas et al., (1995) showed that the effect of flow velocity on the degradation rate of TCE varied from insignificant to a three-fold increase with the doubling of flow rate. This clearly indicates the influence of mass transfer of the organic compounds from bulk solution to the reactive iron sites as a rate-determining step in the overall kinetics. Agrawal and Tratnyek, (1996) have reported a linear correlation between the observed rate constants for the

reduction of organic compounds and the square root of mixing rate (rpm) indicating that the observed reaction rates were controlled by mass transfer of the substrates to the surface of the iron metal.

Additional support for the importance of mass transport to the iron mediated reduction kinetics comes from the effect of temperature on the observed rate coefficients. Reaction rates that are limited by diffusion typically have low activation energies and, therefore, a weak dependence on temperature relative to the rates that are limited by chemical reaction Spiro, M.(1989). Matheson and Tratnyek (1994) have found that the observed rate of the reaction was unaffected by temperature over the range from 4 to 35°C, and fitting the data to the Arrhenius equation gave a slope that was not significantly different from zero. The result clearly indicated that the reductive dehalogenation of chlorinated methanes by iron metal could be a surface mediated process

In this part of the study since all the observations are based on dynamic flow through column, the influence of mass transport on the reduction of azo dye has been studied by monitoring variation in the pseudo-first order rate coefficients with flow rates. The influence of flow rate on the reaction kinetics has been studied by maintaining a constant dye concentration and pH but for varying flow rates.

Having established that the reaction does fit well into pseudo first order kinetics the influence of flow rate on reaction kinetics has been interpreted by observing the variation in pseudo-first order rate coefficients with flow rate.

The influence of flow rate on pseudo first order rate coefficients has been studied in two ways:

- (i) By following the variation in rate coefficients derived for each pH chosen for the study at a fixed concentration and then comparing it with varying flow rates. This comparison would give the relation between flow rates with respect to pH at constant concentration.
- (ii) By following the variation in rate coefficients derived for each concentration chosen for the study at a fixed pH and then comparing it to varying flow rates. This comparison would give the relation between flow rates with respect to concentration at constant pH.

### 2.8.1. Direct Sky Blue

Figures 2.17 to 2.20 indicate that the variation in dye concentration with flow rates fits into a linear first order model.

(i) Comparison between flow rate and pH at constant concentration

The variation in pseudo-first order rate coefficients with respect to flow rates at a dye concentration of  $50 \text{ mg L}^{-1}$  for a constant pH is shown in figure 2.21.

A comparison of the pseudo-first order rate constants derived for each pH chosen for the study at fixed concentration against flow rates indicate that the rate of the reaction was found to increase with an increase in the flow rate; however, this behavior was found to be dependent on the pH of the dye solution. For a dye concentration of  $50 \text{ mg L}^{-1}$  it was observed that irrespective of the flow rates in the range studied the rate of the reaction is maximum at pH 2 with a subsequent decrease as the pH is increased attaining a minimum at pH 8. Between these pH the rate of the reaction increased linearly for increase in flow rates at pH 4 and pH 6, but at both pH 2 and pH 8 the linear increase was observed only up to a flow rate of  $50 \text{ mL min}^{-1}$ . This observation indicates that at these pH there exists an effective flow rate above which the lack of adequate contact time between the dye molecules and the metal surface can lead to a decrease in the rate coefficients. Moreover, at low initial dye concentrations ( $50 \text{ mg L}^{-1}$ ) there is a significant difference between the rate coefficients with respect to flow rates under all pH conditions.

The variation in pseudo-first order rate coefficients with respect to flow rates at a dye concentration of  $100 \text{ mg L}^{-1}$  for a constant pH is shown in figure 2.22.

For a further increase in the dye concentration to  $100 \text{ mg L}^{-1}$  the rate of the reaction was found to increase linearly with increase in flow rates except at pH 8 where the linear increase has been observed only up to  $50 \text{ mL min}^{-1}$ . This increase in the concentration of the dye reduced the difference between the rate coefficients derived for different solution pH, in contrast to the observation made at lower concentrations where the difference was quite apparent.

The variation in pseudo-first order rate coefficients with respect to flow rates at a dye concentration of 150 and  $200 \text{ mg/L}$  for a constant pH is shown in figures 2.23 and 2.24. The results indicate similar trends for higher dye concentrations ( $150$  and  $200 \text{ mg L}^{-1}$ ) where although there is an increase in the rate coefficients with increase in flow rates, the difference between pH for varying flow rates tend to decrease.

Another observation made is that at a low dye concentration of  $50 \text{ mg/L}$  the rate of the reaction was maximum at pH 2 and then decreased subsequently for increase in pH, this trend was not found to hold good at higher concentrations where the maximum rate coefficients varied between all the pH ranges under study.



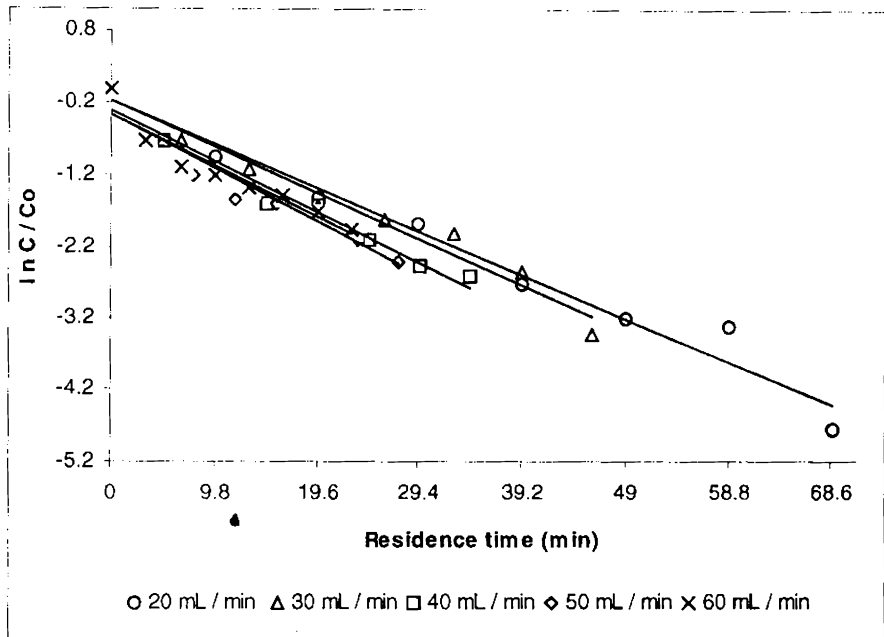


Figure 2.17  
 Direct Sky Blue  
 Plots confirming first order with respect to flow rates at pH 2 and at a dye concentration of  $50 \text{ mg L}^{-1}$

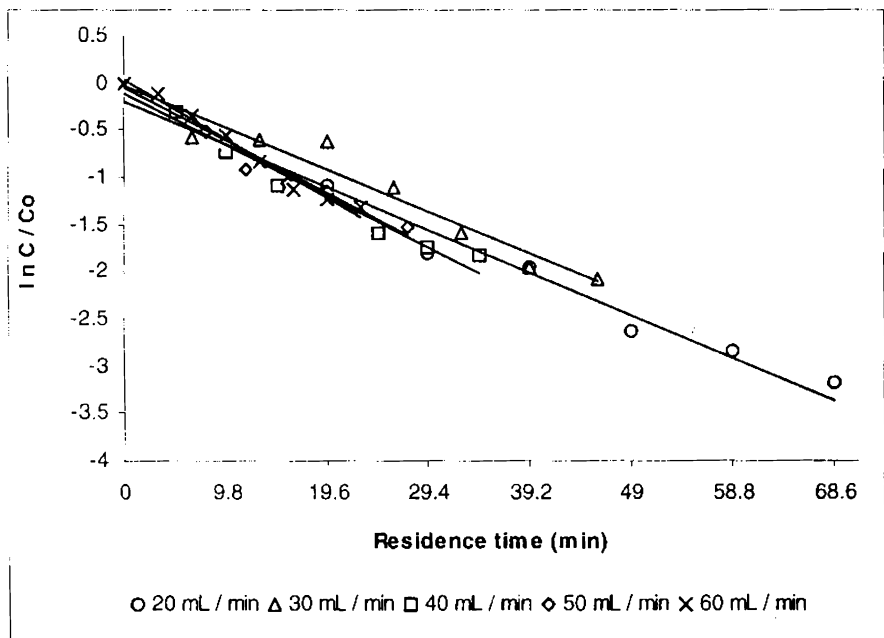


Figure 2.18  
 Direct Sky Blue  
 Plots confirming first order with respect to flow rates at pH 4 and at a dye concentration of  $50 \text{ mg L}^{-1}$

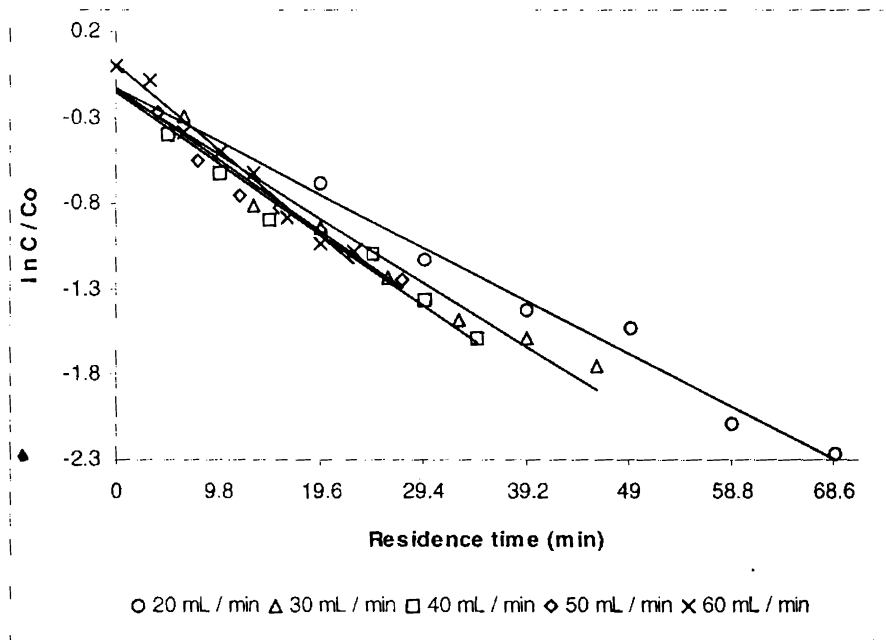


Figure 2.19  
 Direct Sky Blue  
 Plots confirming first order with respect to flow rates at pH 6 and at a dye concentration of  $50 \text{ mg L}^{-1}$

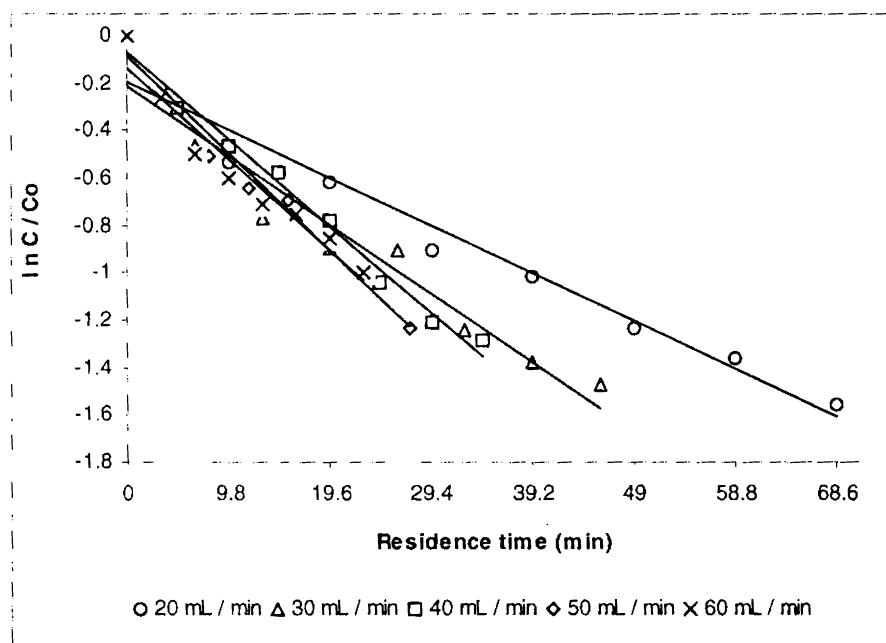


Figure 2.20  
 Direct Sky Blue  
 Plots confirming first order with respect to flow rates at pH 8 and at a dye concentration of  $50 \text{ mg L}^{-1}$

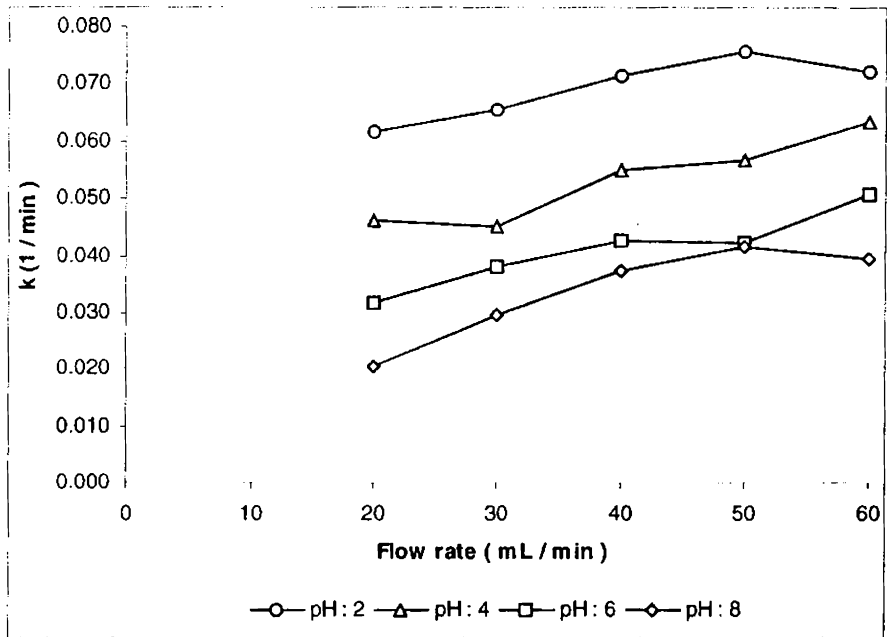


Figure 2.21  
 Direct Sky Blue  
 Influence of flow rates on the pseudo first order rate coefficients at a dye concentration of 50 mg L<sup>-1</sup> and at constant pH.

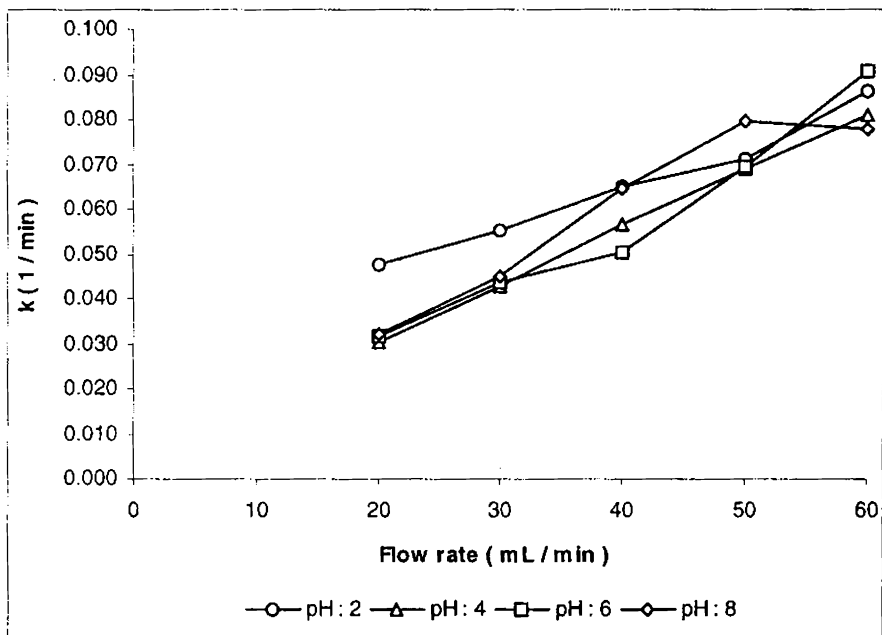


Figure 2.22  
 Direct Sky Blue  
 Influence of flow rates on the pseudo first order rate coefficients at a dye concentration of 100 mg L<sup>-1</sup> and at constant pH.

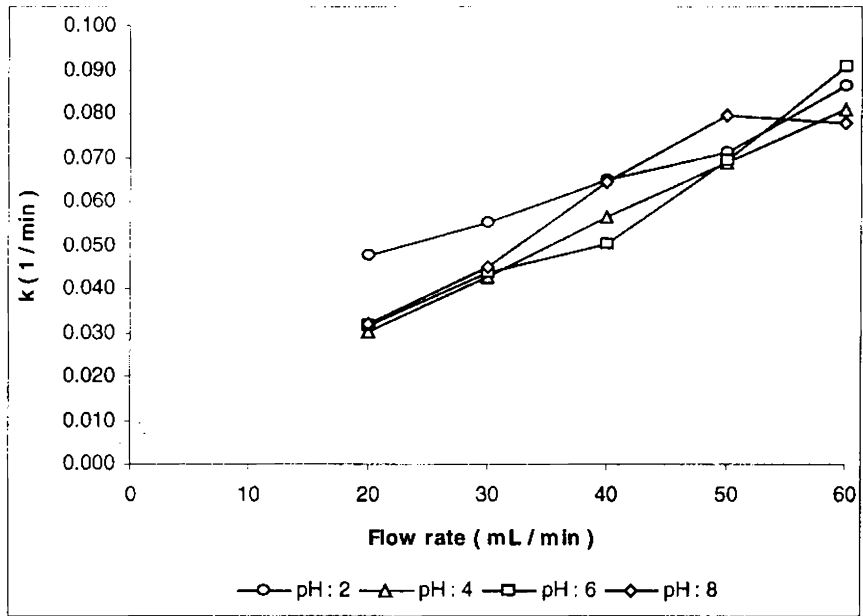


Figure 2.23  
 Direct Sky Blue  
 Influence of flow rates on the pseudo first order rate coefficients at a dye concentration of 150 mg L<sup>-1</sup> and at constant pH.

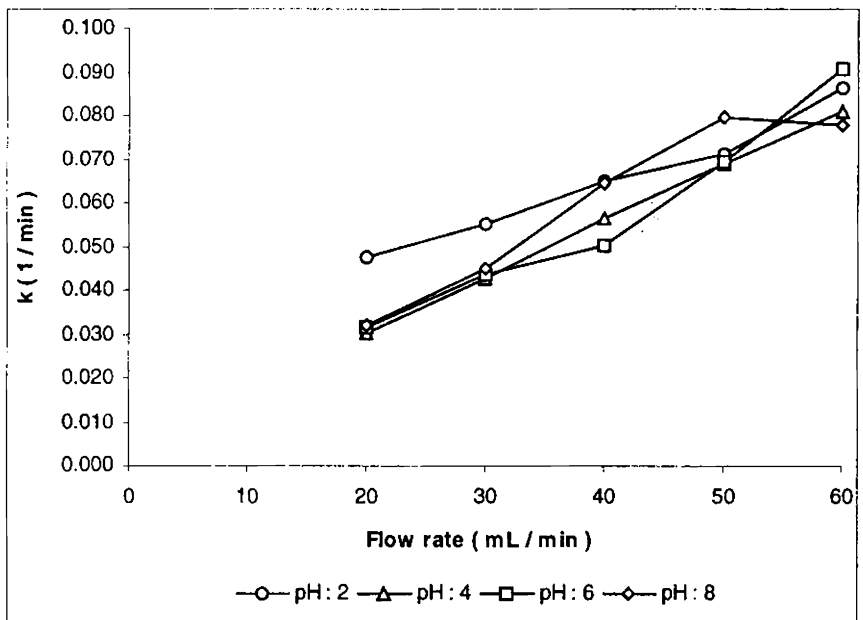


Figure 2.24  
 Direct Sky Blue  
 Influence of flow rates on the pseudo first order rate coefficients at a dye concentration of 200 mg L<sup>-1</sup>.

(ii) Comparison between flow rate and concentration at constant pH

To determine the influence of flow rate, the variation in pseudo first order rate coefficients derived for each concentration at a fixed pH was compared for varying flow rates. The observations are summarized below.

The variation in pseudo-first order rate coefficients with respect to flow rates at pH 2 and for fixed dye concentrations are shown in figure 2.25. At pH 2 it is observed that the rate coefficients were found to increase with an increase in flow rates for all concentrations studied. However, at an initial dye concentration of  $200 \text{ mg L}^{-1}$  a linear increase with an increase in flow rate is observed only up to a flow rate of  $50 \text{ mL min}^{-1}$ . This probably means that at high concentrations an increase in the flow rate would bring about a decrease in the rate coefficient due to the lesser contact time between the dye molecule and the  $\text{Fe}^0$  surface.

The variation in pseudo-first order rate coefficients with respect to flow rates at pH 4 and for fixed dye concentrations is shown in figure 2.26. As the pH was raised to 4, for an initial dye concentration of  $50 \text{ mg L}^{-1}$  it was observed that the rate coefficients were found to be almost independent of flow rates between  $20$  and  $30 \text{ mL min}^{-1}$  as indicated by only a marginal difference between them. At concentrations of  $100$  and  $200 \text{ mg L}^{-1}$  a linear increase in the rate coefficients with increase in flow rates is observed. However, at  $150 \text{ mg L}^{-1}$  the linear increase with flow rates was observed only up to a flow rate of  $50 \text{ mL min}^{-1}$  after, which it becomes independent of flow rate.

Figure 2.27 shows variation in pseudo-first order rate coefficients with respect to flow rates at pH 6 and for fixed dye concentrations.

At pH 6, the rate coefficients showed an increase with an increase in flow rates for all the dye concentrations studied with the rate coefficients increasing linearly for dye concentrations of 150 and 200 mg L<sup>-1</sup>.

Figure 2.28 shows variation in pseudo-first order rate coefficients with respect to flow rates at pH 8 and for fixed dye concentrations. For a further increase in pH to 8, for an initial dye concentration of 50 mg/L the rate coefficients showed a linear increase with an increase in flow rate up to 50 mL min<sup>-1</sup> after which it tends to decrease for a further increase in flow rate. At the same pH higher initial dye concentrations up to 200 mg L<sup>-1</sup> become independent of concentration up to a flow rate of 50 mL min<sup>-1</sup>. As the flow rate was raised further to 60 mL min<sup>-1</sup> the rate coefficients of 150 mg/L continued to increase however that of 100 and 200 mg/L showed a decrease.

A general conclusion that can be drawn from a majority of the experimental results is that there is an increase in the observed pseudo-first order rate coefficients with an increase in the flow rates suggesting that the reaction is mediated by mass-transport. In some cases the increase has been linear. However in a few runs with no specific relation to concentration or pH it has been observed that beyond a flow rate of 50 mL min<sup>-1</sup> the rate of the reaction was found to decrease. This probably indicates that under such conditions the effective flow rate up to which the mass transport becomes limiting is 50 mL min<sup>-1</sup>. At high dye

concentrations the decrease at high flow rates could be attributed to the decrease in the residence time thereby decreasing the contact time between the dye molecule and the metal surface resulting in the observed decrease in the rate coefficient values.

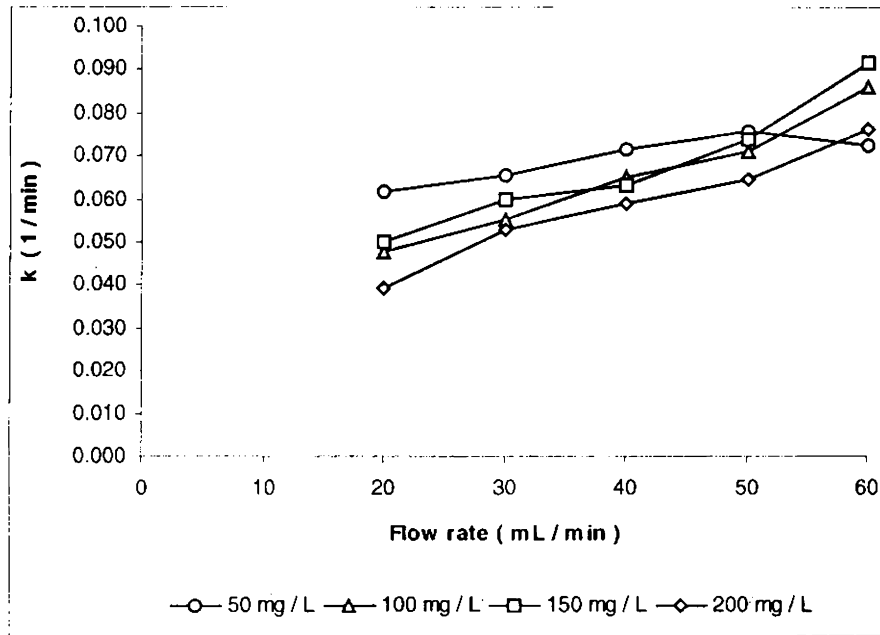


Figure 2.25  
Direct Sky Blue  
Influence of flow rates on pseudo first order rate coefficients at pH 2 and at constant concentration.

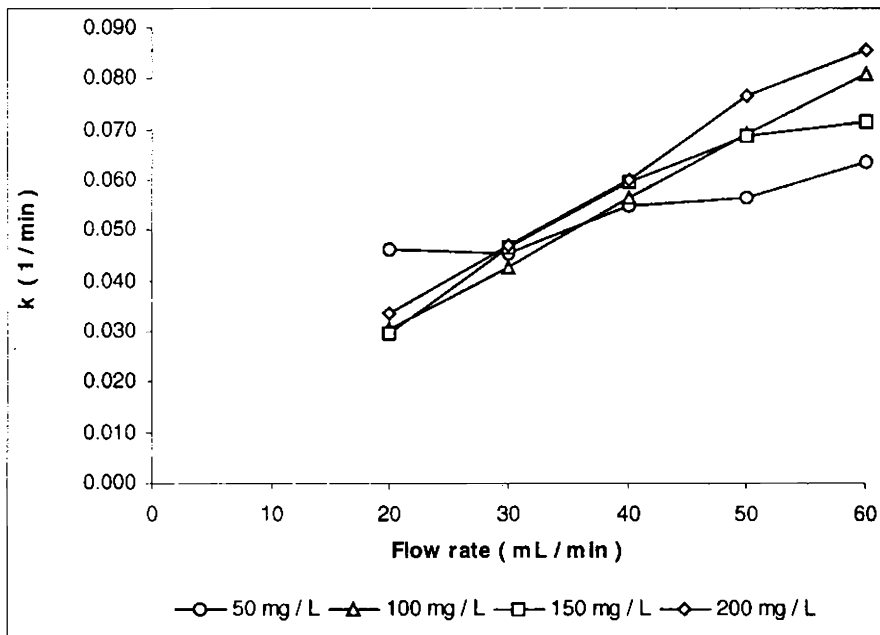


Figure 2.26  
Direct Sky Blue  
Influence of flow rates on pseudo first order rate coefficients at pH 4 and at constant concentration.



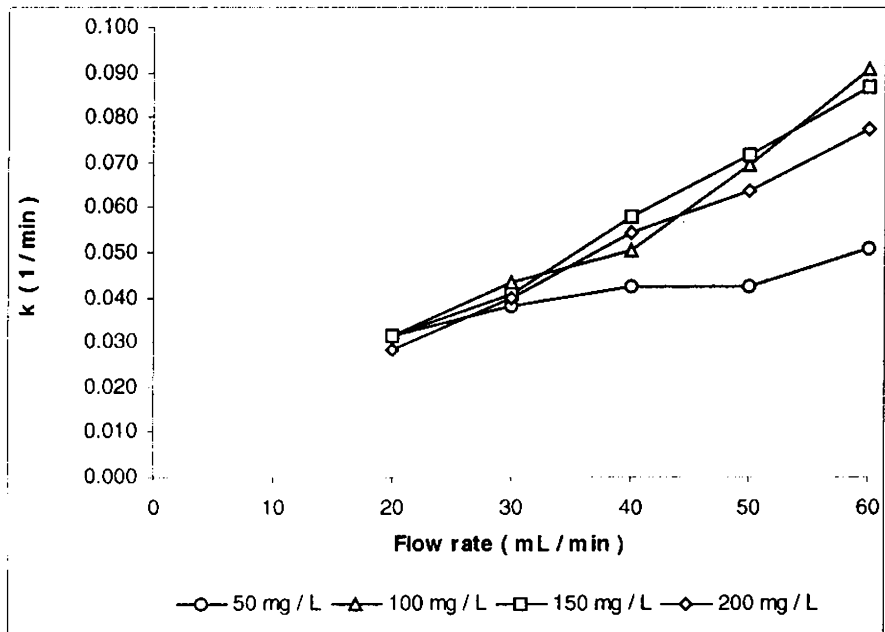


Figure 2.27  
Direct Sky Blue  
Influence of flow rates on pseudo first order rate coefficients at pH 6 and at constant concentration.

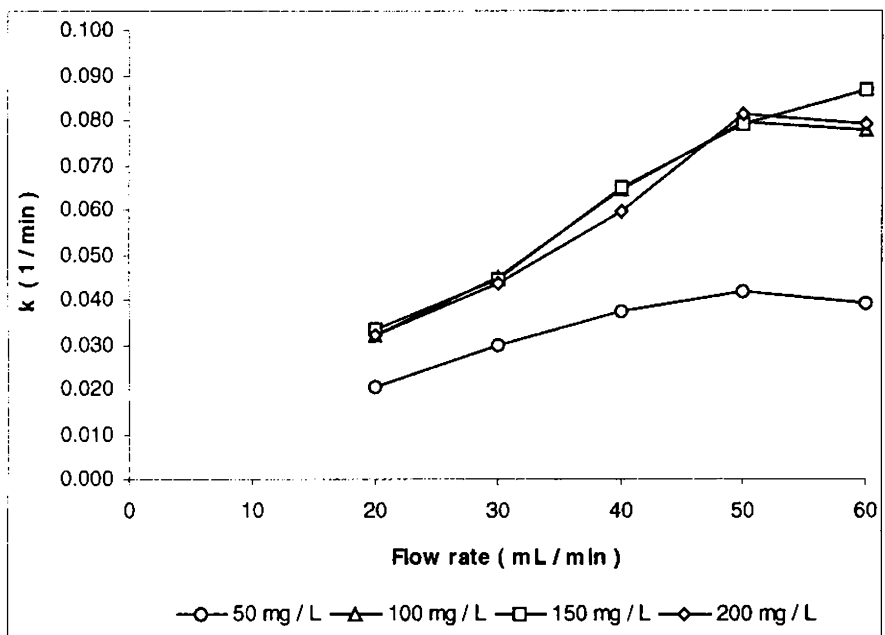


Figure 2.28  
Direct Sky Blue  
Influence of flow rates on pseudo first order rate coefficients at pH 8 and at constant concentration.

### 2.8.2. Direct Black EG

Figures 2.29 to 2.32 indicate that the variation in dye concentration with flow rates fits into a linear first order model.

(i) Comparison between flow rate and pH at constant concentration

The variation in pseudo-first order rate coefficients with respect to flow rates at pH 2 and for fixed pH is shown in figure 2.33. At a concentration of  $50 \text{ mg L}^{-1}$ , but for the rate coefficients remaining steady at flow rates of  $50$  and  $60 \text{ mL min}^{-1}$  there is an observed increase in the rate coefficients with increase in flow rates at all pH. Although the rate coefficients were found comparable the influence of pH is very apparent with being maximum at pH 2 and minimum at pH 8.

Figure 2.34 shows variation in pseudo-first order rate coefficients with respect to flow rates at a dye concentration of  $100 \text{ mg L}^{-1}$  and at constant pH. For an initial concentration of  $100 \text{ mg L}^{-1}$ , the rate coefficients at pH 2 were found to increase linearly with flow rate up to  $40 \text{ mL min}^{-1}$  after which it becomes random (decrease at  $50 \text{ mL min}^{-1}$  and again increases at a flow rate of  $60 \text{ mL min}^{-1}$ ). However, between pH 4, 6 and 8, the increase is linear with flow rates with out any significant difference in the rate coefficients between them. The rate coefficients for pH 2 was found to be exceedingly higher than the lower pH under all flow rates in spite of its random variation.

Figure 2.35 shows variation in pseudo-first order rate coefficients with respect to flow rates at a dye concentration of  $150 \text{ mg L}^{-1}$  and for fixed pH. With an increase in the concentration to  $150 \text{ mg L}^{-1}$ , similar trends of

increased rate coefficients with increase in flow rate are observed for the entire range of pH studied. Comparisons between pH indicate that at pH 2 the rate coefficients was found to increase linearly with an increase in the flow rate up to  $50 \text{ mL min}^{-1}$ , after which a decrease is observed. Rate coefficients at pH 4, 6 and 8 increased linearly with an increase in flow rate with no significant difference between them. However, the rate coefficients at pH 2 continued to remain significantly different from the rest.

Figure 2.36 shows variation in pseudo-first order rate coefficients with respect to flow rates at a constant dye concentration of  $200 \text{ mg L}^{-1}$  and pH. For an initial concentration of  $200 \text{ mg L}^{-1}$ , the rate coefficients increased with an increase in the flow rate under all pH conditions. Comparison between pH and flow rate indicate that the rate of the reaction at pH 2 was found significantly higher than the rest. However, the difference was found to decrease when compared to the difference between them at lower dye concentrations. Although at pH 2 there is an increase in the rate coefficients with flow rate a linear increase has been observed only at lower pH.

(ii) Comparison between flow rate and concentration at constant pH

The variation in pseudo-first order rate coefficients with respect to flow rates at pH 2 and for fixed dye concentrations is shown in figure 2.37. At pH 2 concentrations of  $50$  and  $100 \text{ mg L}^{-1}$  showed an increase in the rate coefficients with increase in flow rates up to a flow rate of  $50 \text{ mL min}^{-1}$ , after which a decrease is observed for a dye concentration of  $50 \text{ mg L}^{-1}$ , while that for  $100 \text{ mg L}^{-1}$  showed an increase. Rate coefficients at a

concentration of  $150 \text{ mg L}^{-1}$ , after an initial decrease with an increase in the flow rate from  $20$  to  $30 \text{ mL min}^{-1}$ , for the rest of the flow rates, the rate coefficients increase with an increase in flow rate. At a dye concentration of  $200 \text{ mg L}^{-1}$ , a linear increase in the rate coefficient with an increase in the flow rate is observed.

The variation in pseudo-first order rate coefficients with respect to flow rates at pH 4 and for fixed dye concentrations is shown in figure 2.38.

Figure 2.39 shows variation in pseudo-first order rate coefficients with respect to flow rates at pH 6 and for fixed dye concentrations.

Figure 2.40 show the variation in pseudo-first order rate coefficients with respect to flow rates at pH 8 and for fixed dye concentrations.

Figures 2.38, 2.39 and 2.40 indicates that an increase in the rate coefficient with an increase in the flow rate is observed irrespective of the concentrations for all further increase in pH.

On the basis of the above observations the general conclusion that can be drawn is that the rate coefficients recorded a linear increase with an increase in flow rates clearly indicating the influence of hydrodynamic mass transport limitations imposed on the system. Relating the rate coefficients for different flow rates for a particular pH reveal that the values are high at pH 2 and then subsequently decreases with an increase in pH. At low dye concentrations the gradation follows a definite pattern with the rate coefficients being maximum at lower pH before recording a minimum value at pH 8. At higher concentrations rate coefficients with respect to flow rates

at pH 2 becomes significantly higher than that for higher pH where they become comparable.

In some cases there is an observed increase in the rate coefficients at pH 6 and 8, which although become comparable was found higher than that at pH 4. These observations suggest that there are two processes operating in the reduction kinetics. At pH 2, the apparently increased rate coefficients can be related to chemical reaction mediated by direct electron transfer from the metal surface to the dye molecules in the bulk solution. Under such conditions it is the reactive sites present at the metal surface that tends to influence the overall reduction kinetics. The decreased rate coefficients at all higher pH suggests that under such conditions the reaction mechanism switches over from chemical reaction to a surface mediated process where mass transport of the dye molecules from the bulk solution to the metal surface becomes the limiting process. Under such conditions the non-reactive sites present at the metal surface (in the form of the oxide layer as a result of metal corrosion) influence the decolorization process by serving as sites where the dye molecules can become adsorbed. However, the rate of such surface phenomenon in comparison to the chemical reduction process is much lower as reflected by the decreased rate coefficients at higher pH conditions. pH 4 probably represents the transition pH below which the reaction mechanism is chemical reduction (involving electron transfer) becomes prominent and above which the reaction mechanism is predominantly adsorption on to the

exchangeable sites present in the form of a layer of corrosion products at the metal surface.

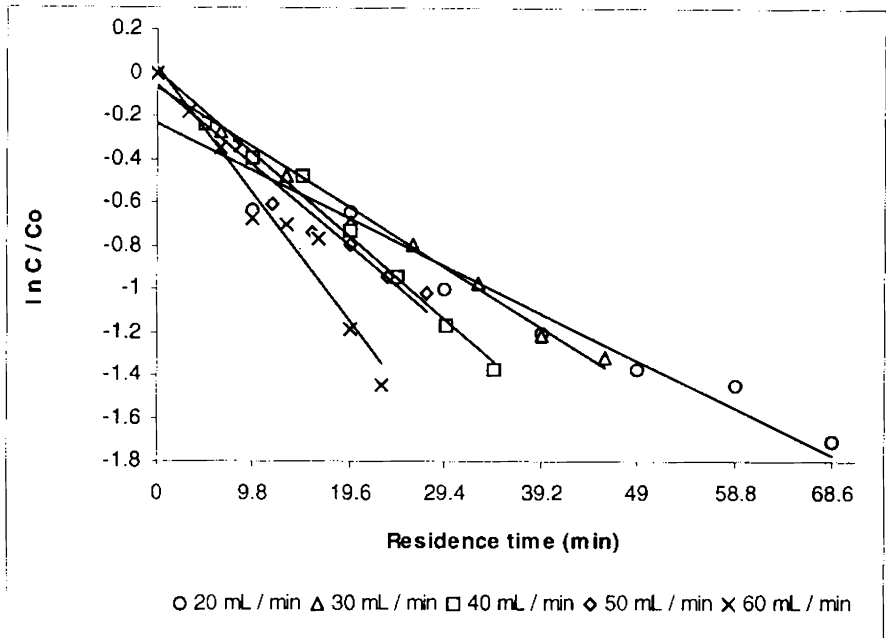


Figure 2.29  
 Direct Black EG  
 Plots confirming first order with respect to flow rates at pH 2 and at a  
 Dye concentration of  $50 \text{ mg L}^{-1}$

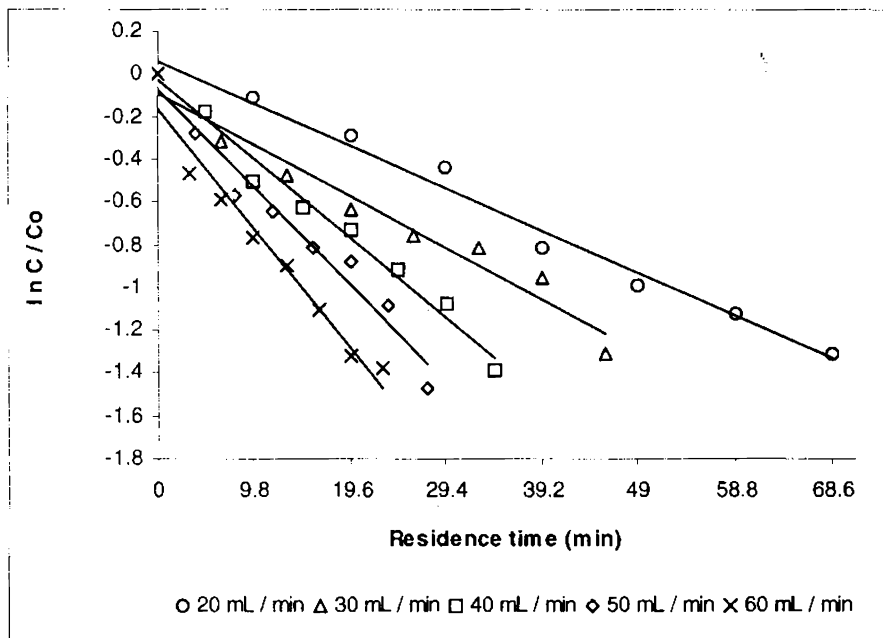


Figure 2.30  
 Direct Black EG  
 Plots confirming first order with respect to flow rates at pH 4 and at a  
 Dye concentration of  $50 \text{ mg L}^{-1}$

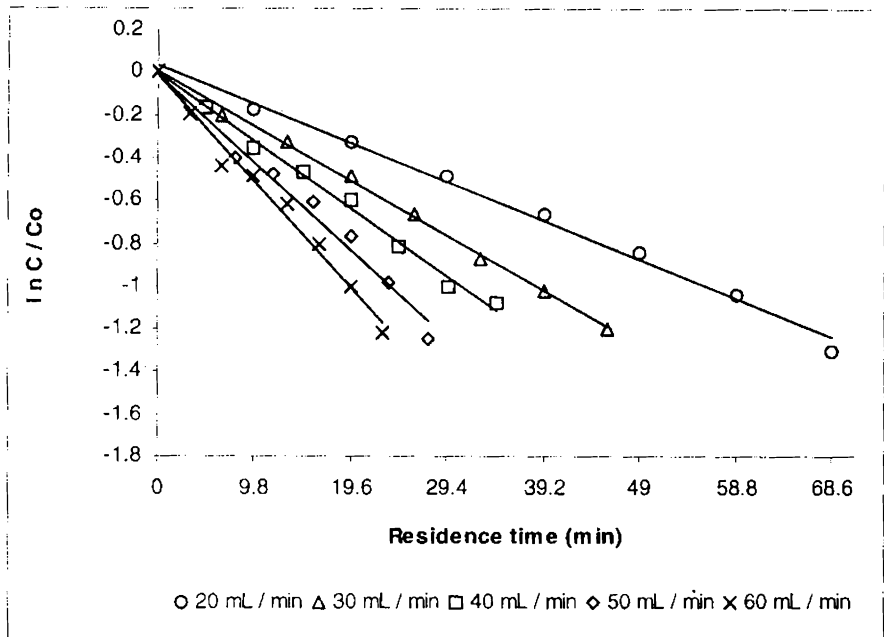


Figure 2.31  
 Direct Black EG  
 Plots confirming first order with respect to flow rates at pH 6 and at a  
 Dye concentration of  $50 \text{ mg L}^{-1}$

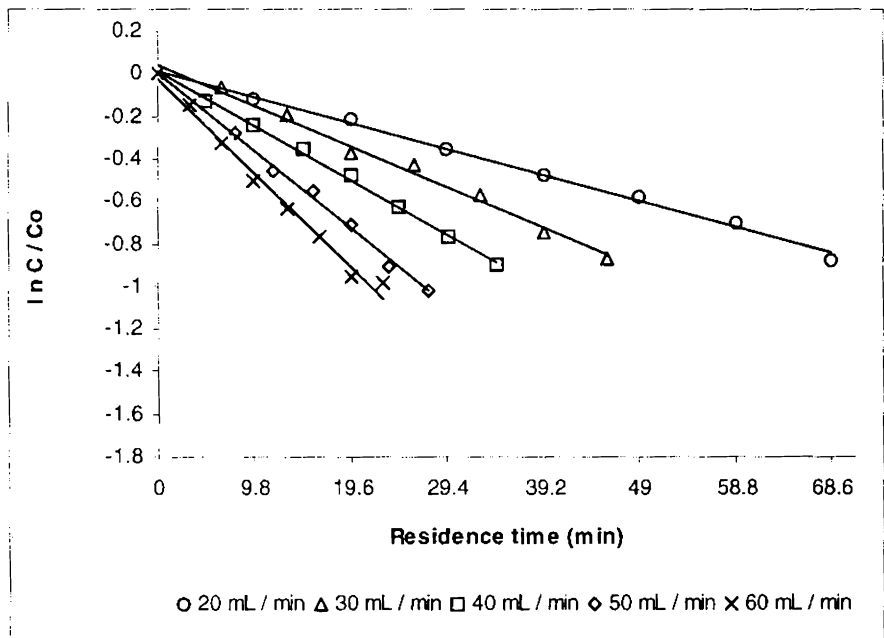


Figure 2.32  
 Direct Black EG  
 Plots confirming first order with respect to flow rates at pH 8 and at a  
 Dye concentration of  $50 \text{ mg L}^{-1}$



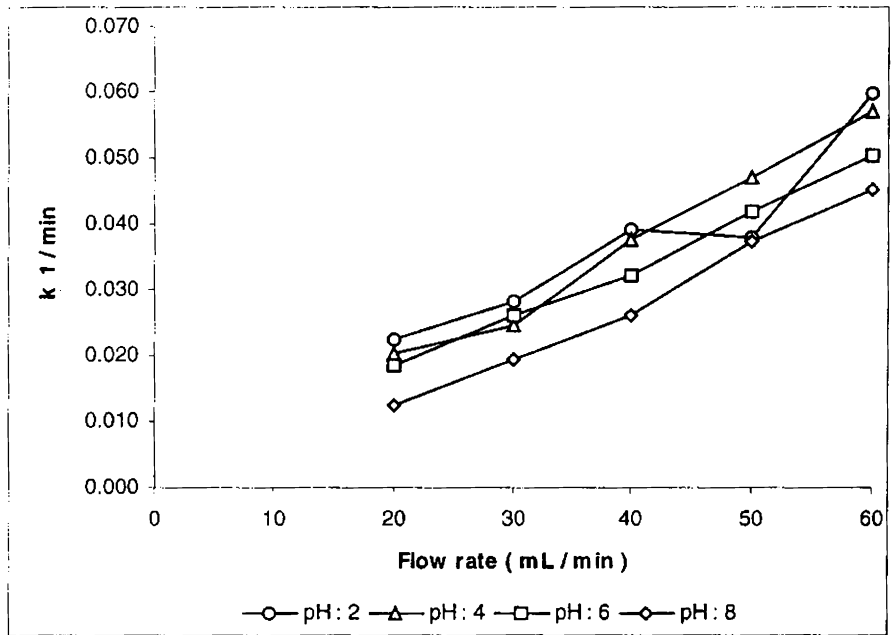


Figure 2.33  
 Direct Black EG  
 Influence of flow rates on the pseudo first order rate coefficients at a dye concentration of 50 mg L<sup>-1</sup> and at constant pH.

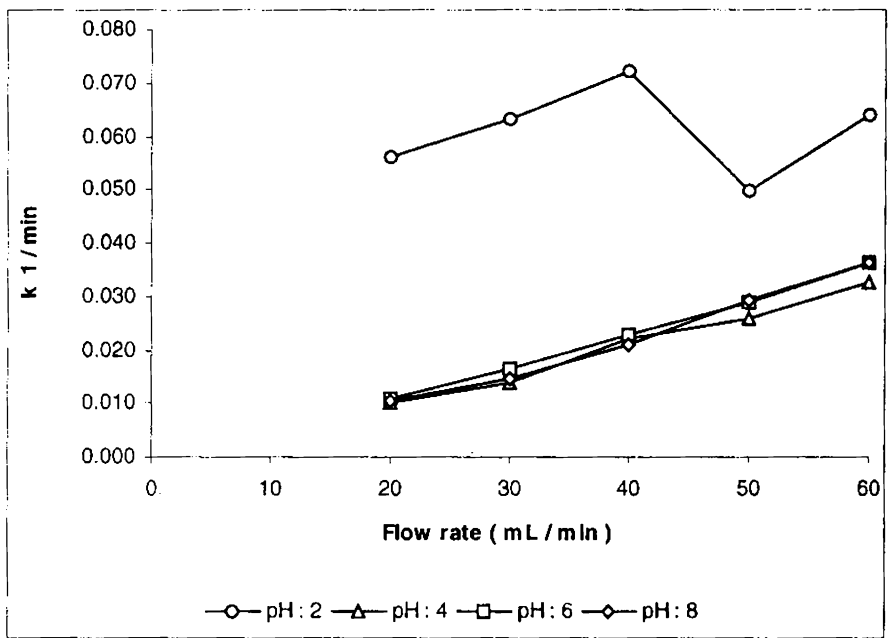


Figure 2.34  
 Direct Black EG  
 Influence of flow rates on the pseudo first order rate coefficients at a dye concentration of 100 mg L<sup>-1</sup> and at constant pH.

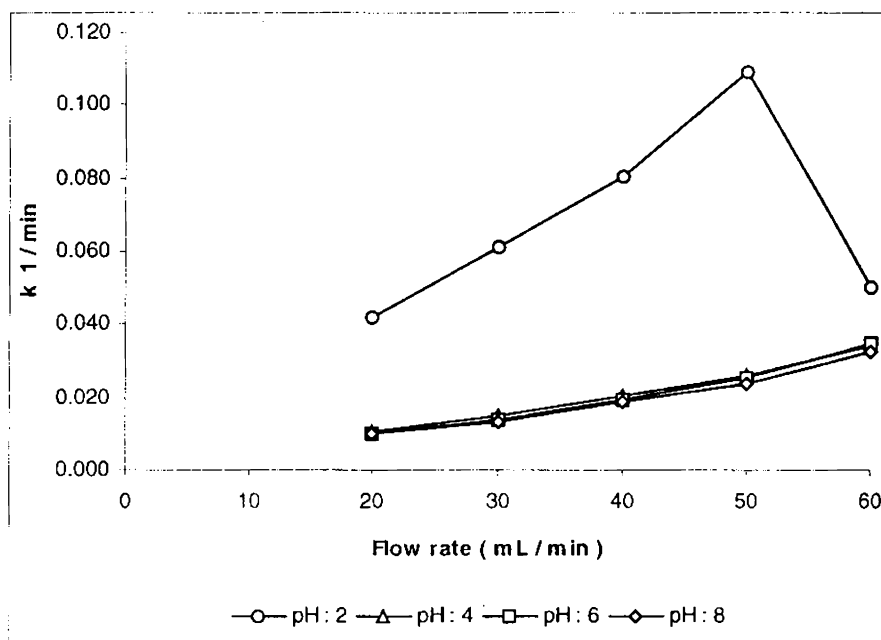


Figure 2.35  
Direct Black EG  
Influence of flow rates on the pseudo first order rate coefficients at a dye concentration of 150 mg L<sup>-1</sup> and at constant pH.

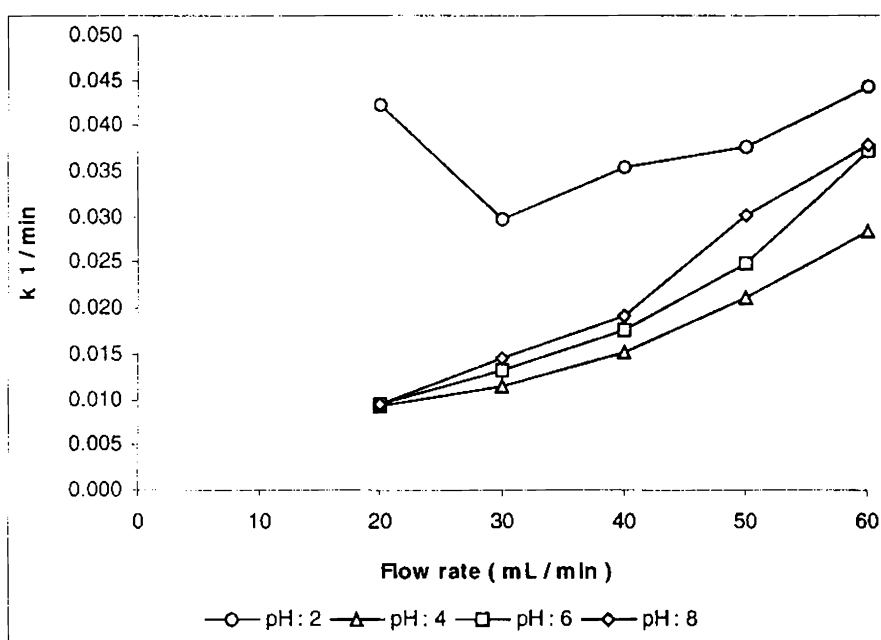


Figure 2.36  
Direct Black EG  
Influence of flow rates on the pseudo first order rate coefficients at a dye concentration of 200 mg L<sup>-1</sup> and at constant pH.

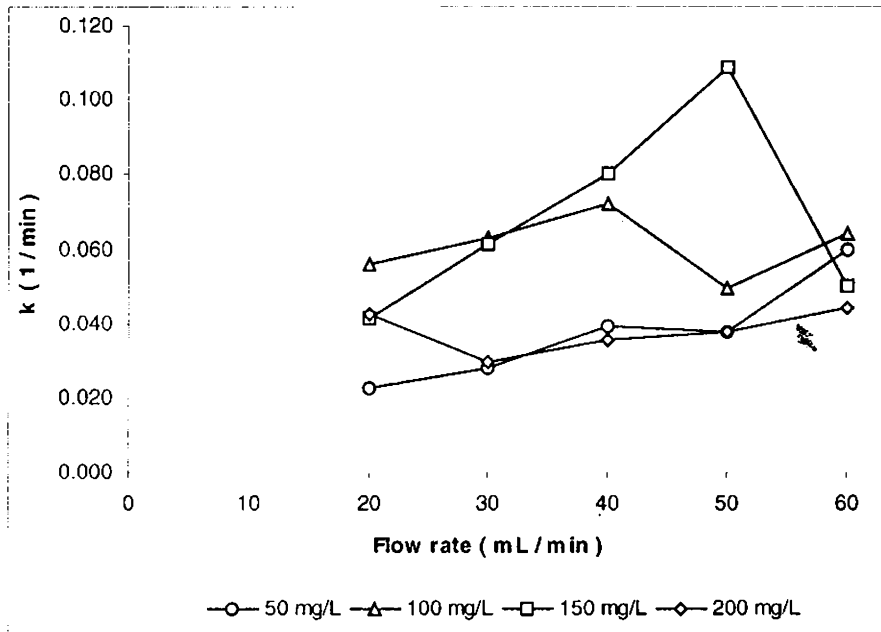


Figure 2.37  
 Direct Black EG  
 Influence of flow rates on pseudo first order rate coefficients at pH 2 and at constant concentration.

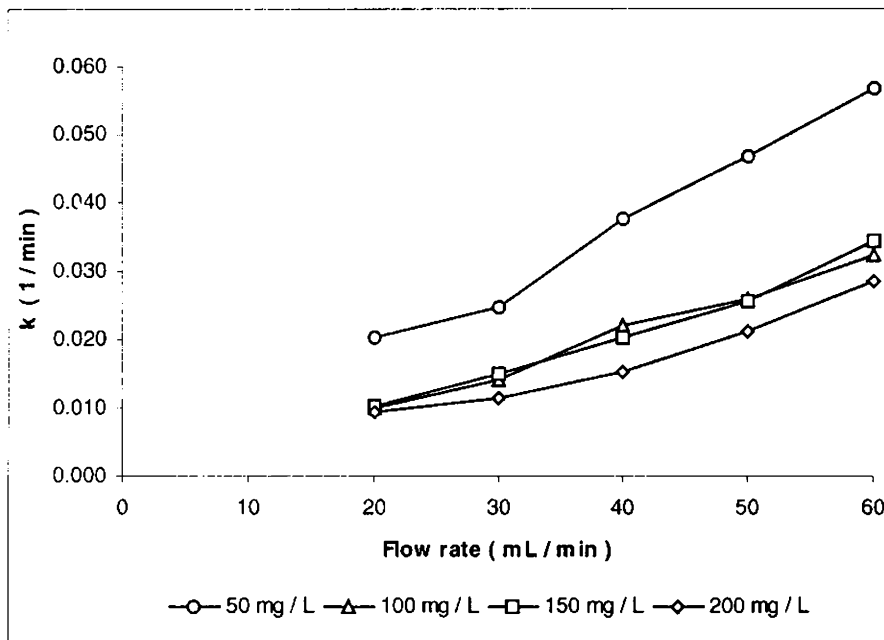


Figure 2.38  
 Direct Black EG  
 Influence of flow rates on pseudo first order rate coefficients at pH 4 and at constant concentration.

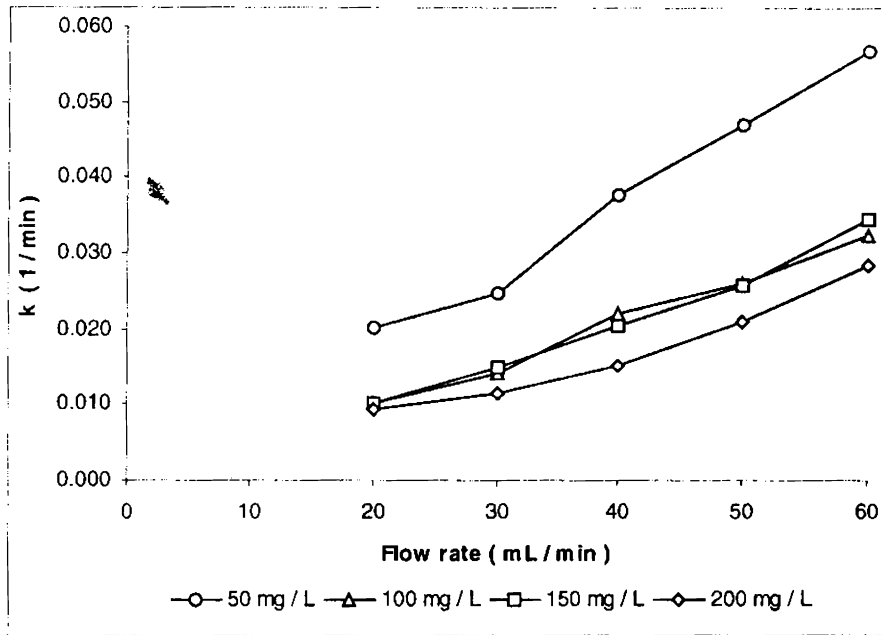


Figure 2.39  
Direct Black EG  
Influence of flow rates on pseudo first order rate coefficients at pH 6 and at constant concentration.

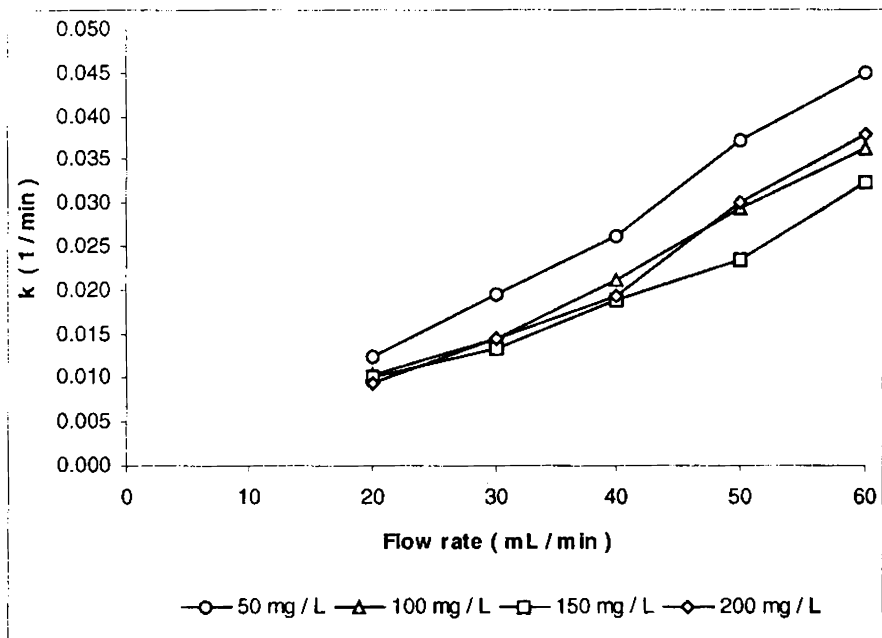


Figure 2.40  
Direct Black EG  
Influence of flow rates on pseudo first order rate coefficients at pH 8 and at constant concentration.

### 2.8.3. Direct Catachine Brown

Figures 2.41 to 2.44 indicate that the variation in dye concentration with flow rates fits into a linear first order model.

(i) Comparison between flow rate and pH at constant concentration

In general the rate coefficients were found to increase with an increase in flow rate; however, this behavior shows dependence on pH of the dye solution.

The variation in pseudo-first order rate coefficients with respect to flow rate at a dye concentration of  $50 \text{ mg L}^{-1}$  and for fixed pH is shown in figure 2.45. At a dye concentration of  $50 \text{ mg L}^{-1}$ , it is observed that there is a linear increase in the rate coefficient with an increase in the flow rates at pH 4, 6 and 8. However, at pH 2 the increase was observed only up to a flow rate of  $50 \text{ mL min}^{-1}$ . This observation indicates that there exists an effective flow rate above which the lack of adequate contact time between the dye solution and the metal surface can lead to a decrease in the rate coefficient.

Figure 2.46 shows variation in pseudo-first order rate coefficients with respect to flow rates at a dye concentration of  $100 \text{ mg L}^{-1}$  and at constant pH. As the initial dye concentration was raised to  $100 \text{ mg L}^{-1}$ , the rate coefficient was found to increase with an increase in flow rate except at pH 6 and 8 where the rate coefficients become more or less independent at high flow rates. However, increase in the dye concentration reduced the difference between the rate coefficients for the different pH, which was very apparent at the lower concentration.

Figure 2.47 shows variation in pseudo-first order rate coefficients with respect to flow rates at a dye concentration of  $150 \text{ mg L}^{-1}$  and for fixed pH.

Figure 2.48 shows variation in pseudo-first order rate coefficients with respect to flow rates at a constant dye concentration of  $200 \text{ mg L}^{-1}$  and pH.

Figures 2.47 and 2.48 indicate similar trends of increase in rate coefficients with increase in flow rate have also been observed for higher dye concentrations. Although at low initial dye concentration (at  $50 \text{ mg L}^{-1}$ ), the rate of the reaction was maximum at pH 2 and then subsequently decreased for increase in pH, this trend was not found to continue at higher concentrations.

(ii) Comparison between flow rate and concentration at constant pH

The rate coefficients obtained at a fixed pH has been compared with that for various concentrations against varying flow rates.

The variation in pseudo-first order rate coefficients with respect to flow rates at pH 2 and for fixed dye concentrations is shown in figure 2.49. At pH 2 comparison of the rate coefficients indicate that, but for concentrations of 100 and  $200 \text{ mg L}^{-1}$  which showed a decrease in the rate coefficients at flow rates above  $50 \text{ mL min}^{-1}$ , for all the remaining dye concentrations an increase in the rate coefficient with an increase in flow rate is observed.

The variation in pseudo-first order rate coefficients at pH 4 and

for fixed dye concentrations is shown in figure 2.50. As the pH was raised to 4, a linear increase in the rate coefficients with increase in flow rate is observed only at a dye concentration of  $50 \text{ mg L}^{-1}$  (similar observation is also made at pH 6), after which at  $100 \text{ mg L}^{-1}$  the increase is observed only between flow rates of  $30$  and  $50 \text{ mL min}^{-1}$ . At a dye concentration of  $150 \text{ mg L}^{-1}$ , the rate coefficients after showing an initial increase become independent of flow rates up to  $50 \text{ mL min}^{-1}$  before decreasing for a further increase in flow rate. For a concentration of  $200 \text{ mg L}^{-1}$  the rate coefficients after showing an initial decrease become independent of flow rates.

Figure 2.51 shows variation in pseudo-first order rate coefficients at pH 6 and for fixed dye concentrations. But for an initial decrease in the rate coefficient at  $100 \text{ mg L}^{-1}$  for all higher concentrations beyond  $50 \text{ mg L}^{-1}$  the rate coefficients at pH 6 become independent of flow rate.

The variation in pseudo-first order rate coefficients at pH 8 and for fixed dye concentrations is shown in figure 2.52. Except for some random variations the trends observed at pH 8 remains more or less similar to the trends observed at pH 6 as indicated in figure 2.52.

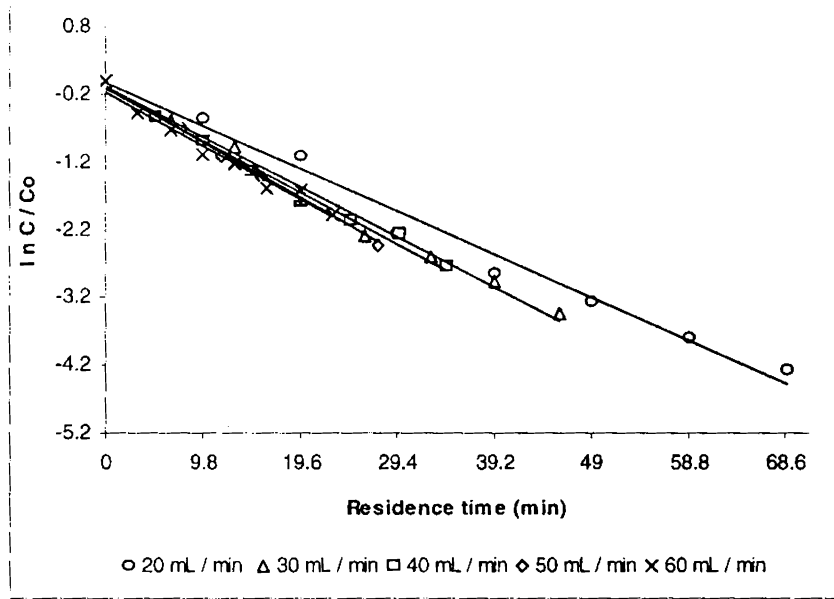


Figure 2.41  
 Direct Catachine Brown (DCB)  
 Plots confirming first order reaction with respect to flow rates at pH 2 and at a  
 Dye concentration of  $50 \text{ mg L}^{-1}$

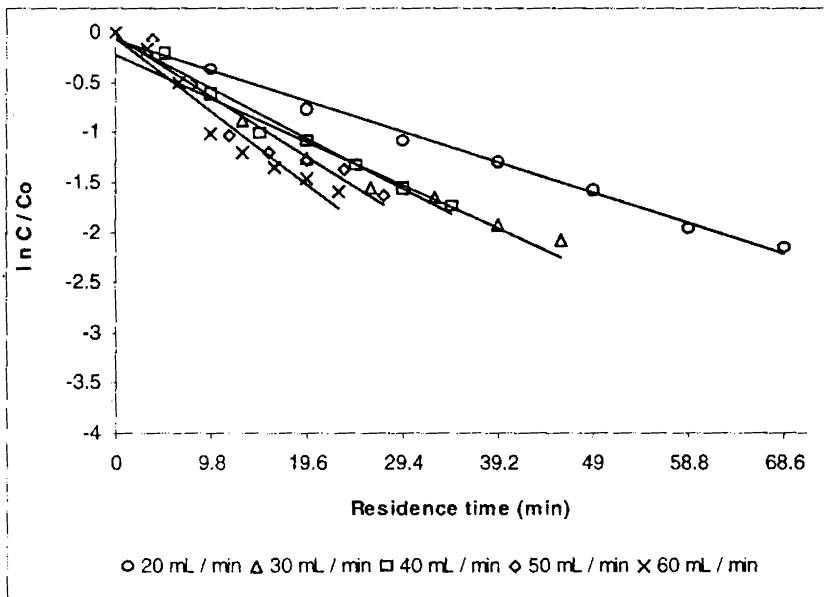


Figure 2.42  
 Direct Catachine Brown  
 Plots confirming first order with respect to flow rates at pH 4 and at a  
 Dye concentration of  $50 \text{ mg L}^{-1}$



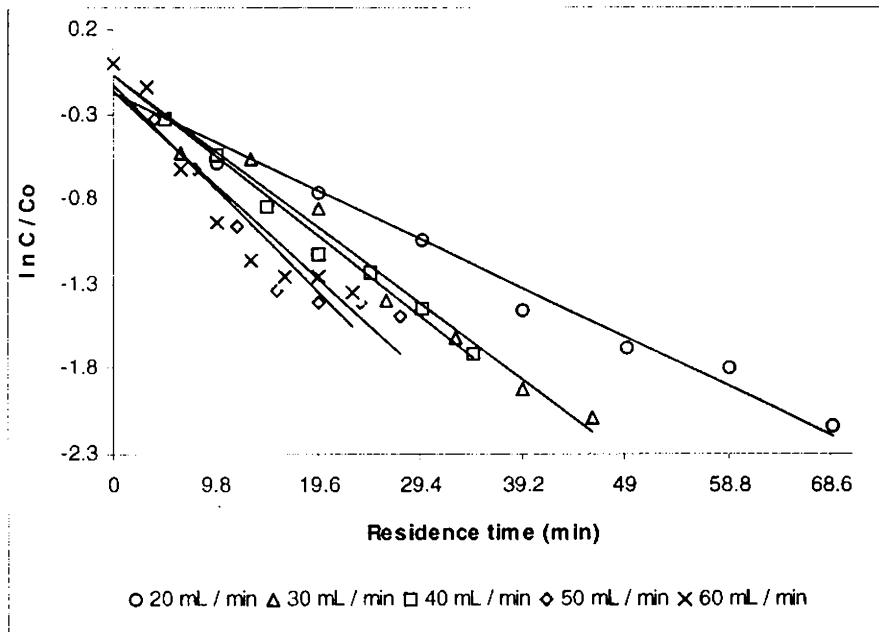


Figure 2.43  
 Direct Catachine Brown  
 Plots confirming first order with respect to flow rates at pH 6 and at a  
 Dye concentration of  $50 \text{ mg L}^{-1}$

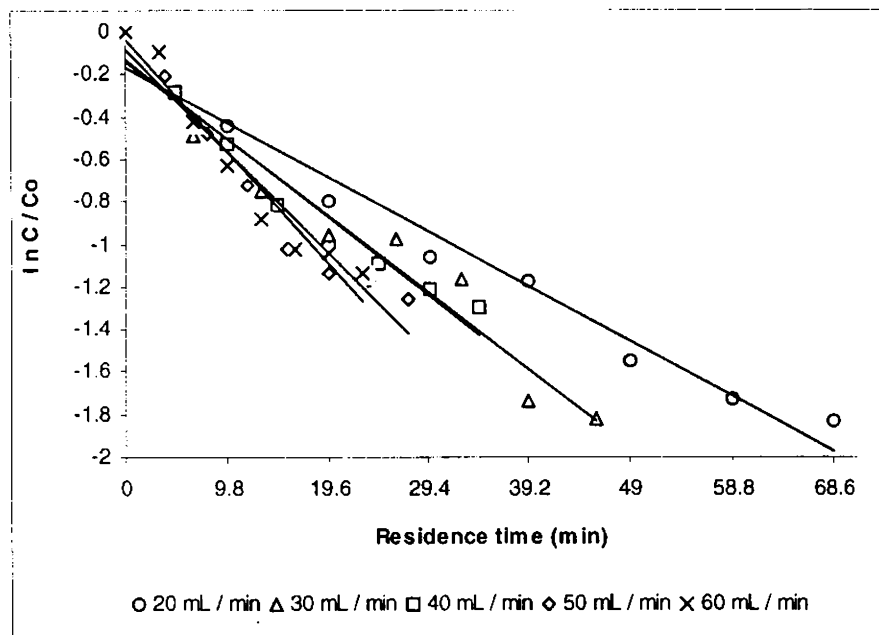


Figure 2.44  
 Direct Catachine Brown  
 Plots confirming first order with respect to flow rates at pH 8 and at a  
 Dye concentration of  $50 \text{ mg L}^{-1}$

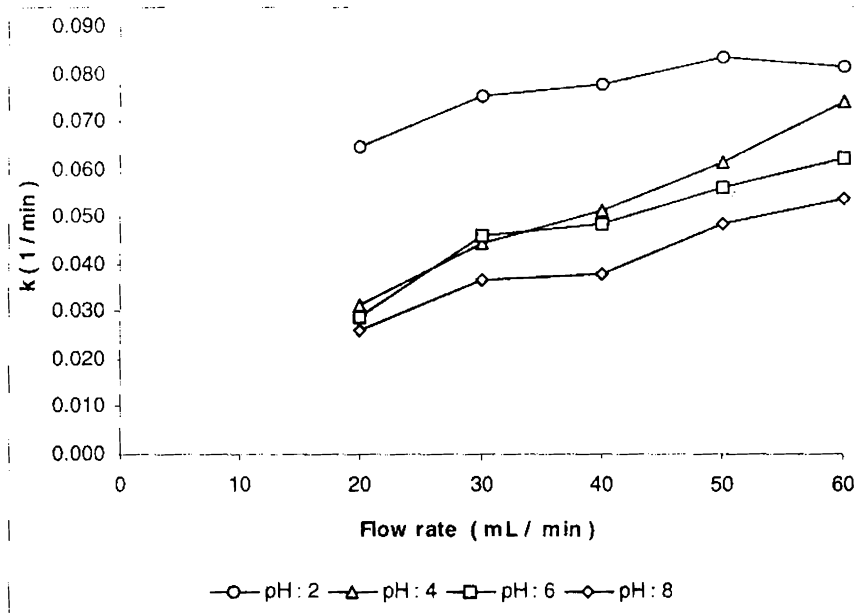


Figure 2.45  
Direct Catachine Brown  
Influence of flow rates on the pseudo first order rate coefficients at a dye concentration of 50 mg L<sup>-1</sup> and at constant pH

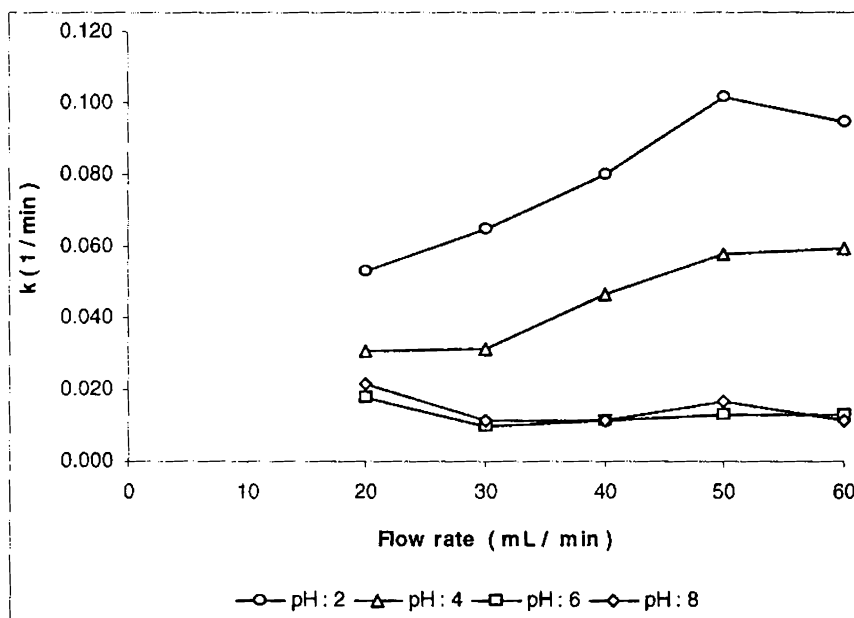


Figure 2.46  
Direct Catachine Brown  
Influence of flow rates on the pseudo first order rate coefficients at a dye concentration of 100 mg L<sup>-1</sup> and at constant pH

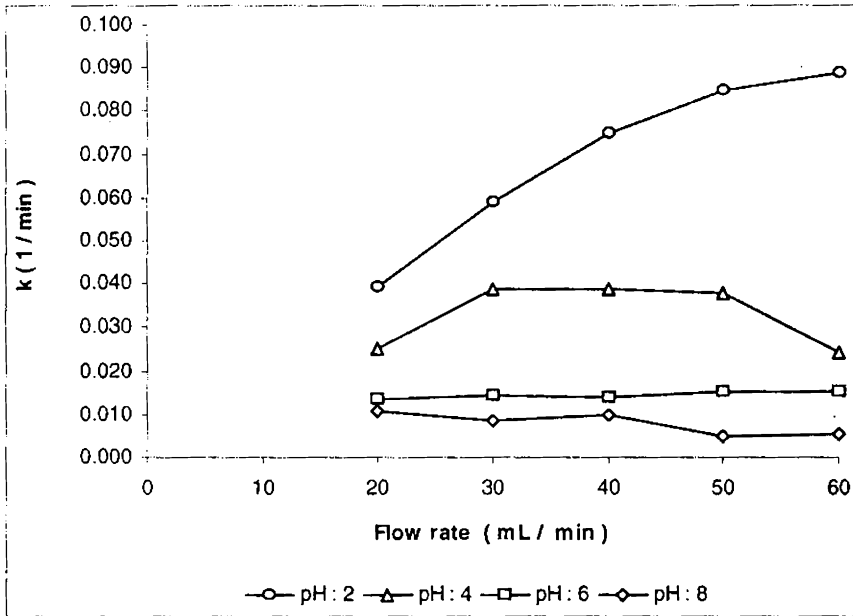


Figure 2.47  
 Direct Catachine Brown  
 Influence of flow rates on the pseudo first order rate coefficients at a dye concentration of 150 mg L<sup>-1</sup> and at constant pH.

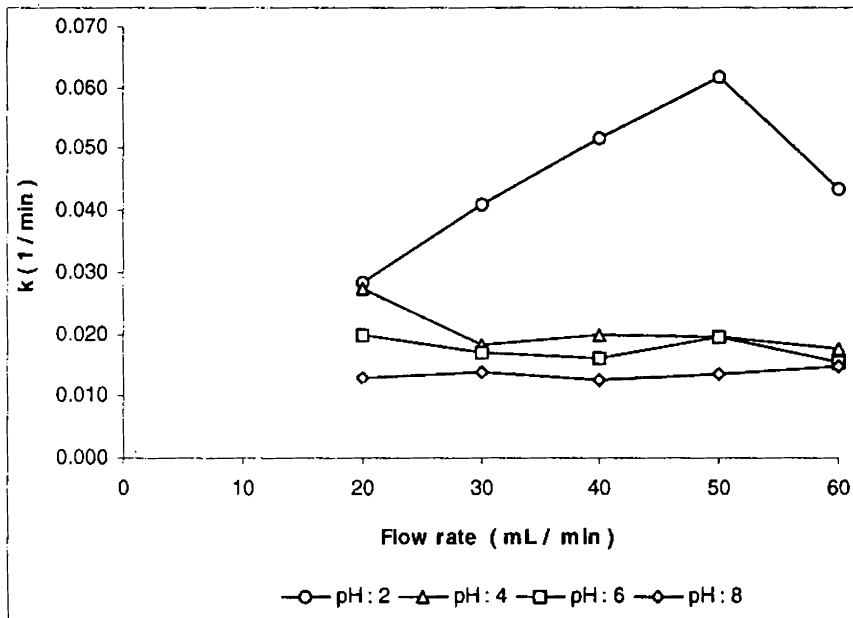


Figure 2.48  
 Direct Catachine Brown  
 Influence of flow rates on the pseudo first order rate coefficients at a dye concentration of 200 mg L<sup>-1</sup> and at constant pH.

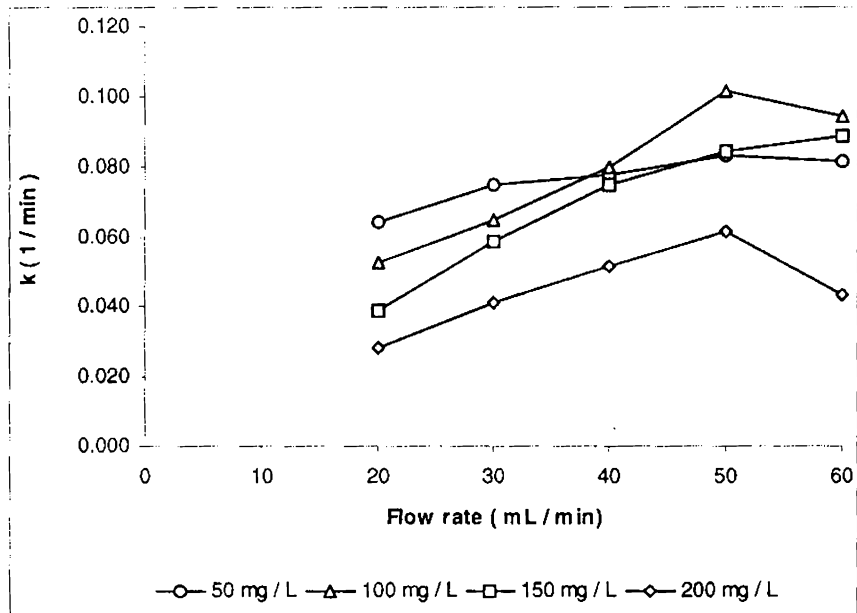


Figure 2.49  
Direct Catachine Brown  
Influence of flow rates on pseudo first order rate coefficients at pH 2 and at constant Concentration.

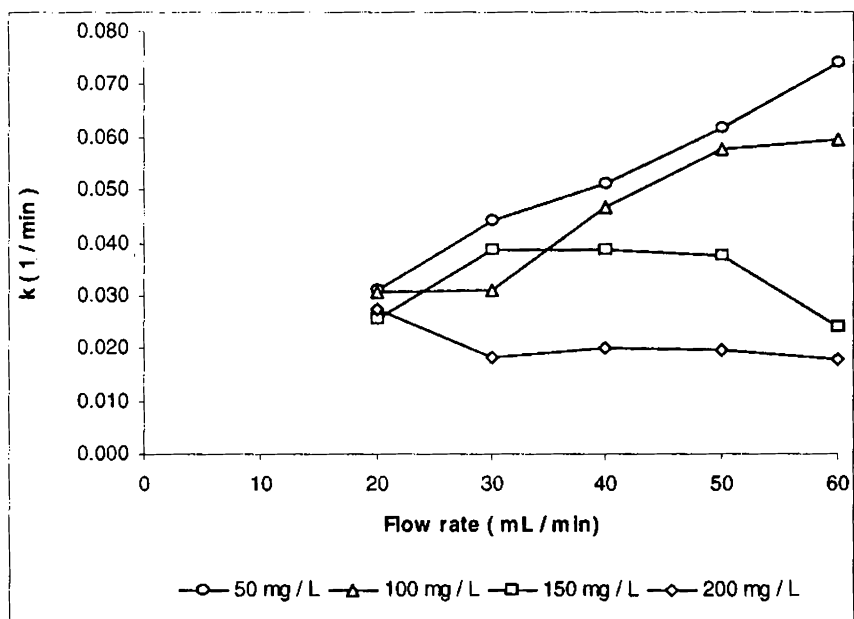


Figure 2.50  
Direct Catachine Brown  
Influence of flow rates on pseudo first order rate coefficients at pH 4 and at constant Concentration.

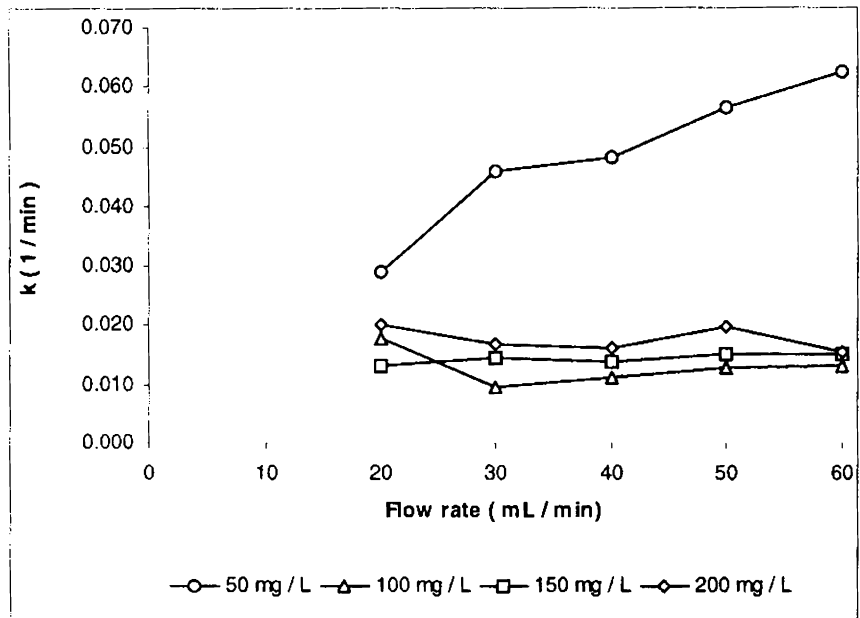


Figure 2.51  
Direct Catachine Brown  
Influence of flow rates on pseudo first order rate coefficients at pH 6 and at constant concentration.

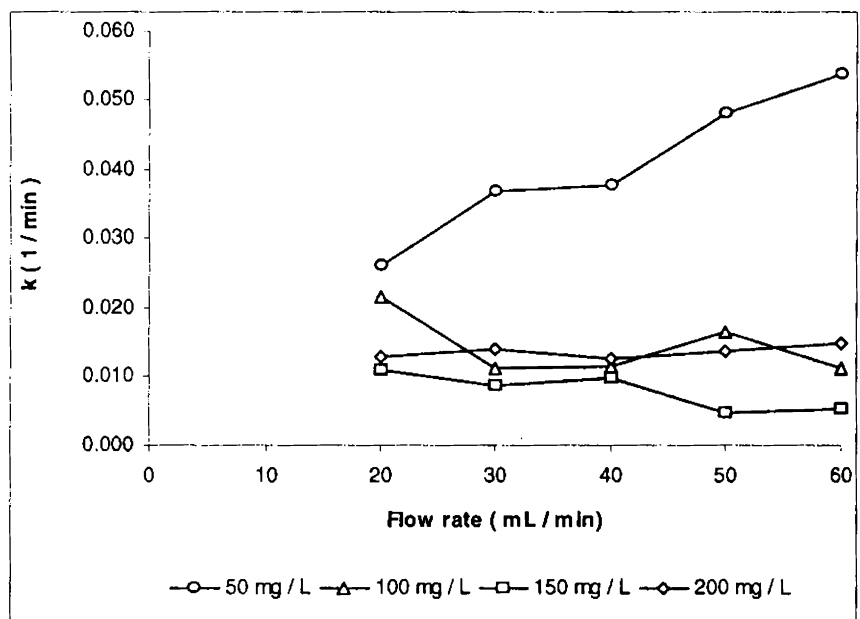


Figure 2.52  
Direct Catachine Brown  
Influence of flow rates on pseudo first order rate coefficients at pH 8 and at constant concentration.

#### 2.8.4. Direct Green - B

Figures 2.53 to 2.56 indicate that the variation in dye concentration with flow rates fits into a linear first order model.

(i) Comparison between flow rate and pH at constant concentration

The variation in pseudo-first order rate coefficients at a dye concentration of  $50 \text{ mg L}^{-1}$  and for fixed pH with respect to flow rates is shown in figure 2.57. For an initial dye concentration of  $50 \text{ mg L}^{-1}$ , an increase in the pseudo first order rate coefficients with an increase in flow rate has been observed. However, there is an observed dependence of this variation on the pH of the solution with the rate coefficients being maximum at pH 2 followed by pH 4 and pH 6, before attaining a minimum at pH 8. At the lowest flow rate ( $20 \text{ mL min}^{-1}$ ) it is observed that there is a significant difference in the rate coefficients between pH 2 and the rest. There is a marginal increase in the rate coefficients at pH 4 for the same flow rate over pH 6 and 8. However, the rate coefficients at both pH 6 and 8 are the same indicating that at low flow rate they become independent of pH over 6. As the flow rate is increased the rate coefficients at pH 4 begin to show a progressive increase over pH 6 and 8. However, between pH 6 and 8, the difference between the rate coefficients get narrowed considerably, indicating that at low dye concentrations there is a tendency of the rate coefficients to become almost independent of pH above 6.

Figure 2.58 shows variation in pseudo-first order rate coefficients with respect to flow rates at a dye concentration of  $100 \text{ mg L}^{-1}$  and at constant pH. As the initial dye concentration was raised to  $100 \text{ mg L}^{-1}$ , the

general trend of increase in rate coefficients with an increase in flow rate continues showing dependence on pH except for pH 4 where a decrease in the rate coefficient is observed at flow rate over  $50 \text{ mL min}^{-1}$ . Confirming with the previously observed trend the rate coefficients at pH 2 is found greater than the higher pH with the values becoming comparable at pH 6 and 8.

Figure 2.59 shows variation in pseudo-first order rate coefficients with respect to flow rates at a dye concentration of  $150 \text{ mg L}^{-1}$  and for fixed pH. Results indicate that with an increase in the dye concentration to  $150 \text{ mg L}^{-1}$  it is observed that the argument of mass transport does not hold good at both the extremes of pH, where a decrease in the rate coefficient with an increase in the flow rate is observed. However, in the middle pH ranges of 4 and 6 an increase in the rate coefficient with an increase in the flow rate is observed. At both pH 2 and pH 4, the rate coefficients remain more or less steady after a flow rate of  $50 \text{ mL min}^{-1}$ . However, at pH 4, a linear increase in the rate coefficients for an increase in flow rate is recorded up to a flow rate of  $40 \text{ mL min}^{-1}$  after which the rate coefficients increase before becoming independent of flow rate.

Figure 2.60 shows variation in pseudo-first order rate coefficients with respect to flow rates at a constant dye concentration of  $200 \text{ mg L}^{-1}$  and pH. At a concentration of  $200 \text{ mg L}^{-1}$ , at pH 2, the rate coefficient become independent of flow rate while at all higher pH, the general trend followed is an increase in the rate coefficient with increase in flow rate up to  $40 \text{ mL}$

$\text{min}^{-1}$  after which the values become independent of flow rate if minor variations are overlooked.

(ii) Comparison between flow rate and concentration at constant pH

The variation in pseudo-first order rate coefficients with respect to flow rates at pH 2 and for fixed dye concentrations is shown in figure 2.61. At pH 2, the increase in rate coefficients for an increase in flow rate is observed only at low concentrations of 50 and 100  $\text{mg L}^{-1}$ . Higher concentrations of 150 and 200  $\text{mg L}^{-1}$  showed almost similar trends with the rate coefficient becoming independent of flow rates except for an initial decrease with an increase in flow rate observed at a concentration of 150  $\text{mg L}^{-1}$ .

The variation in pseudo-first order rate coefficients with respect to flow rates at pH 4 and for fixed dye concentrations is shown in figure 2.62.

At pH 4, the rate coefficients showed an increase with increase in flow rates at low initial dye concentrations of 50 and 100  $\text{mg L}^{-1}$ , however, at 100  $\text{mg L}^{-1}$ , the rate coefficients were found to increase with an increase in flow rate only up to a flow rate of 50  $\text{mL min}^{-1}$ . Similar observations were also observed at higher dye concentrations of 150 and 200  $\text{mg L}^{-1}$  with the rate coefficients becoming independent of flow rate for further increase over a flow rate of 50  $\text{mL min}^{-1}$ , while for 200  $\text{mg L}^{-1}$  the rate coefficients were found independent of flow rates over 40  $\text{mL min}^{-1}$ .

Figure 2.63 shows variation in pseudo-first order rate coefficients with respect to flow rates at pH 6 and for fixed dye concentrations.



The variation in pseudo-first order rate coefficients with respect to flow rates at pH 8 and for fixed dye concentrations is shown in figure 2.64. From figure 2.63 and 2.64, it can be observed that at higher pH of 6 and 8, the values began to fluctuate randomly as a result of which it was not possible to arrive at any definite interpretation of the observed trends.

The general conclusion that can be drawn is that the variation in the rate coefficients with flow rate is dependent on both pH and the initial dye concentration. At low concentrations an increase in the rate coefficients with increase in flow rates, indicative of mass transport limited kinetics is observed. In all cases, the rate coefficients were found maximum at pH 2 clearly indicating the influence of hydrogen ion participation in the reduction process. However, no apparent trend has been observed between pH 4, 6 and 8 with the rate coefficients varying between them.

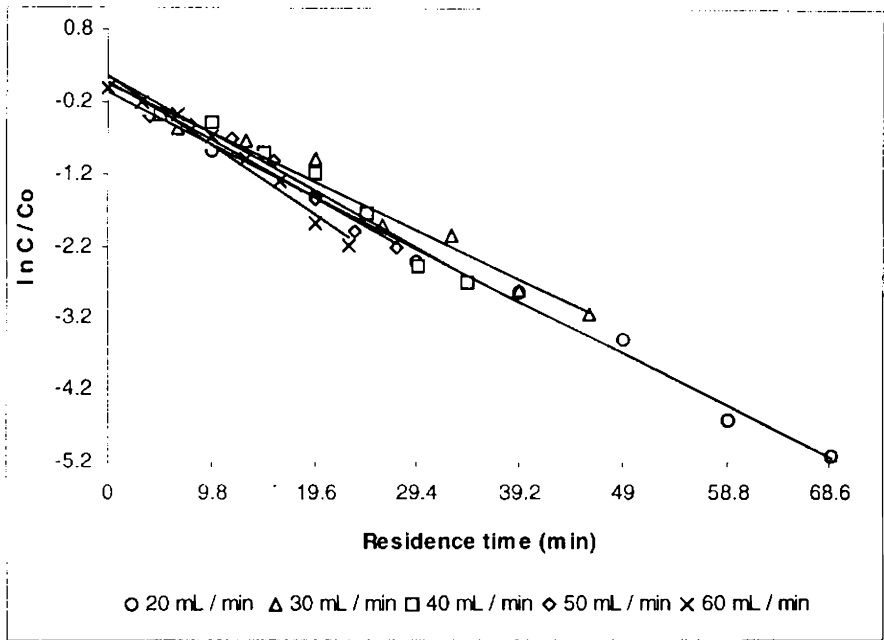


Figure 2.53  
 Direct Green - B  
 Plots confirming first order with respect to flow rates at pH 2 and at a  
 Dye concentration of  $50 \text{ mg L}^{-1}$

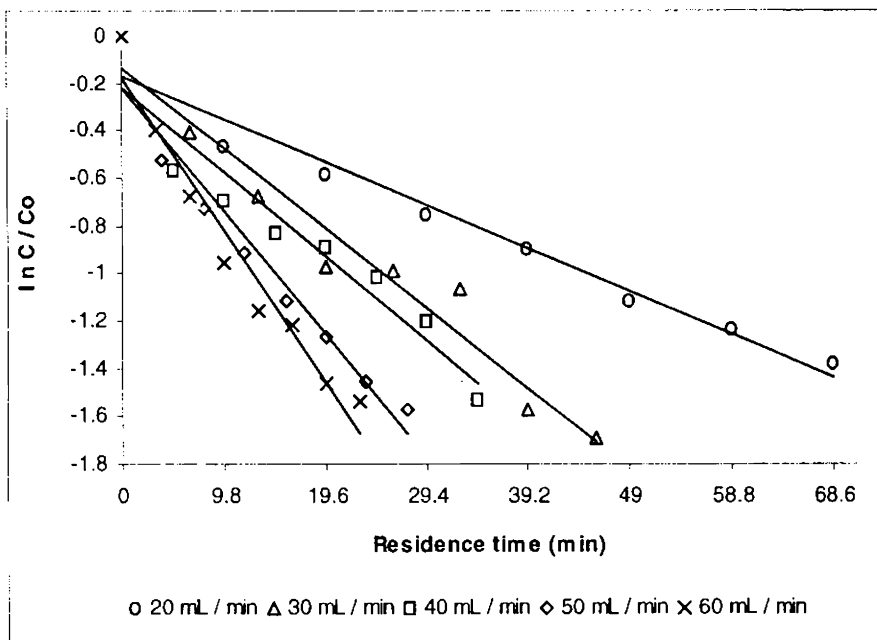


Figure 2.54  
 Direct Green - B  
 Plots confirming first order with respect to flow rates at pH 4 and at a  
 Dye concentration of  $50 \text{ mg L}^{-1}$

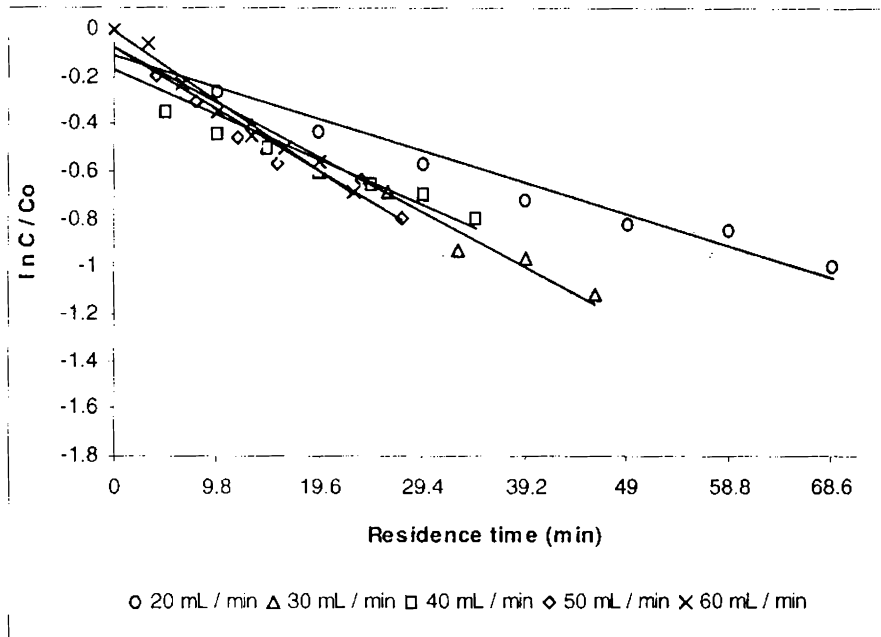


Figure 2.55  
 Direct Black EG  
 Plots confirming first order with respect to flow rates at pH 6 and at a  
 Dye concentration of  $50 \text{ mg L}^{-1}$

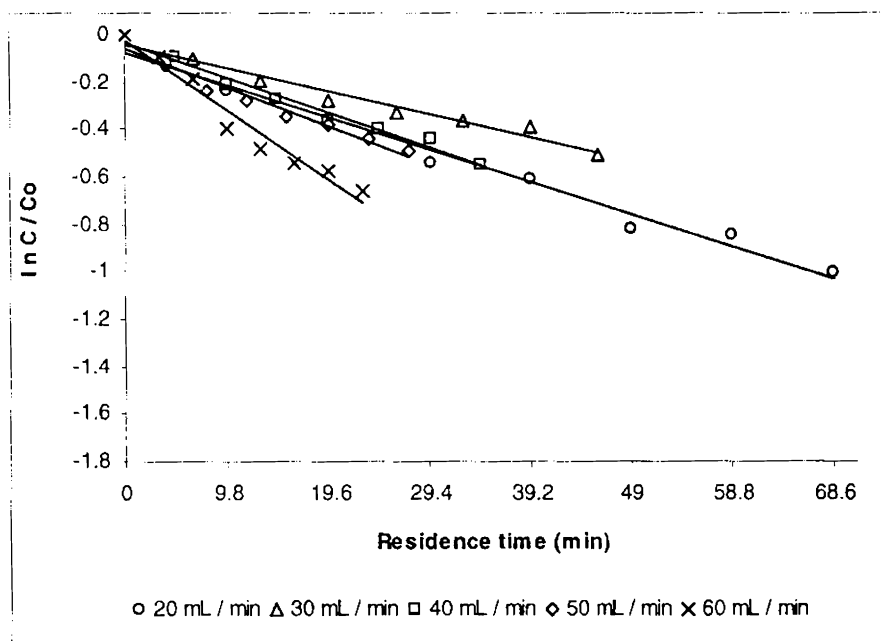


Figure 2.56  
 Direct Black EG  
 Plots confirming first order with respect to flow rates at pH 8 and at a  
 Dye concentration of  $50 \text{ mg L}^{-1}$

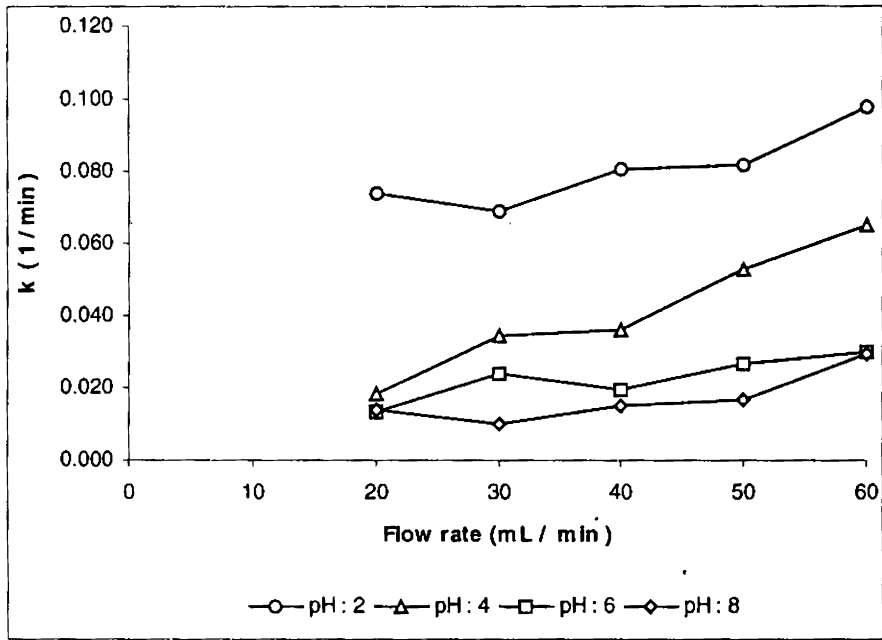


Figure 2.57  
 Direct Green - B  
 Influence of flow rates on the pseudo first order rate coefficients at a dye concentration of 50 mg L<sup>-1</sup> and at constant pH

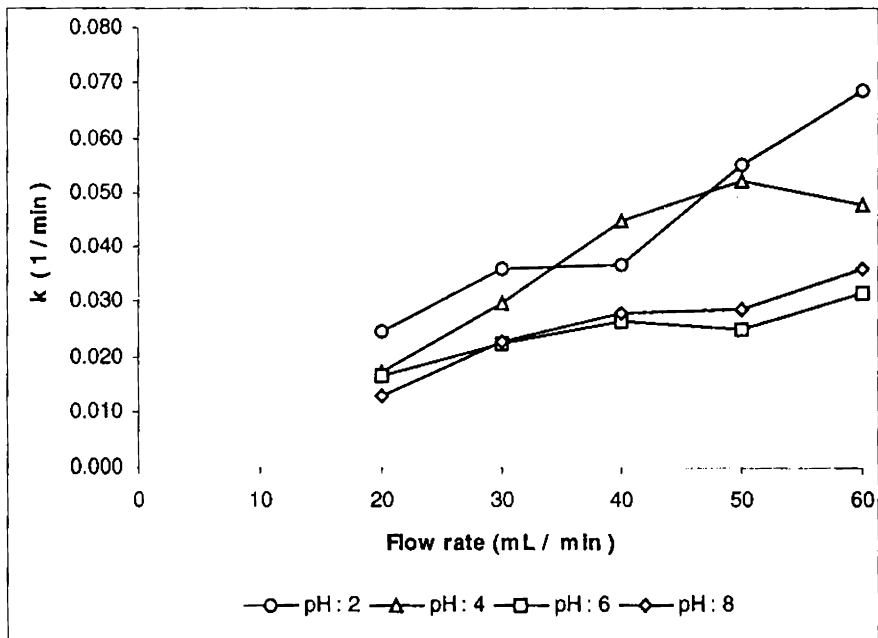


Figure 2.58  
 Direct Green - B  
 Influence of flow rates on the pseudo first order rate coefficients at a dye concentration of 100 mg L<sup>-1</sup> and at constant pH

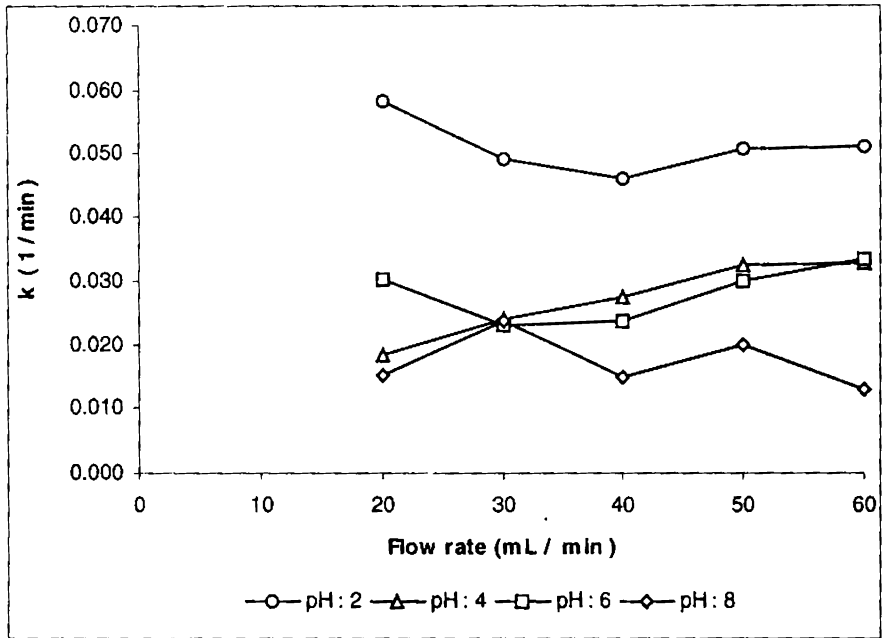


Figure 2.59  
 Direct Green - B  
 Influence of flow rates on the pseudo first order rate coefficients at a dye concentration of  $150 \text{ mg L}^{-1}$  and at constant pH.

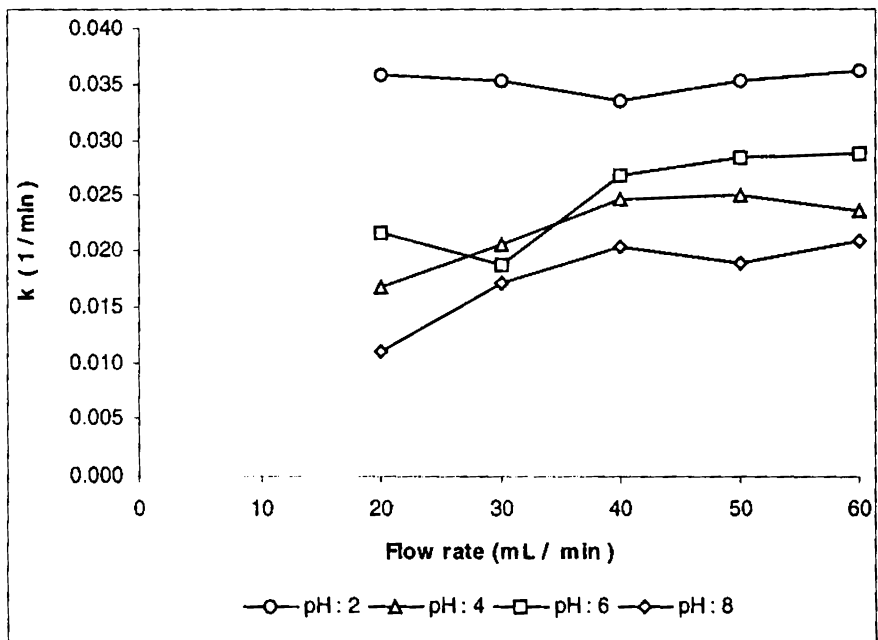


Figure 2.60  
 Direct Green - B  
 Influence of flow rates on the pseudo first order rate coefficients at a dye concentration of  $200 \text{ mg L}^{-1}$  and at constant pH.

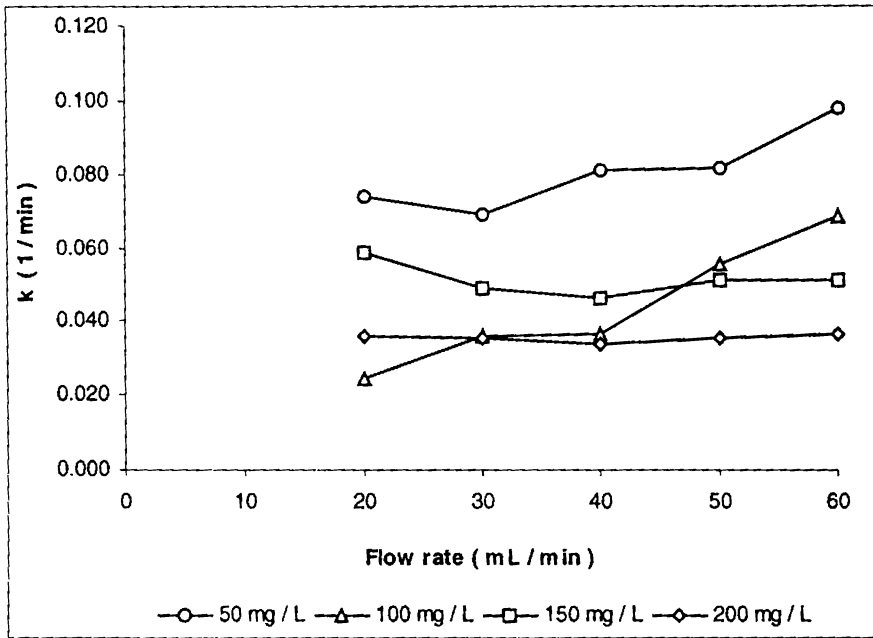


Figure 2.61  
Direct Green - B  
Influence of flow rates on pseudo first order rate coefficients at pH 2 and at constant concentration.

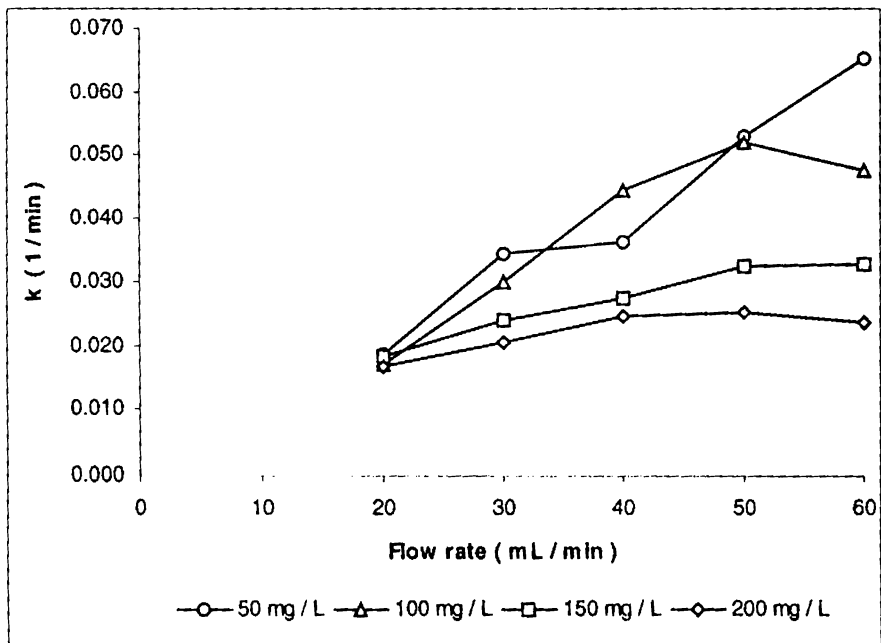


Figure 2.62  
Direct Green - B  
Influence of flow rates on pseudo first order rate coefficients at pH 4 and at constant concentration.

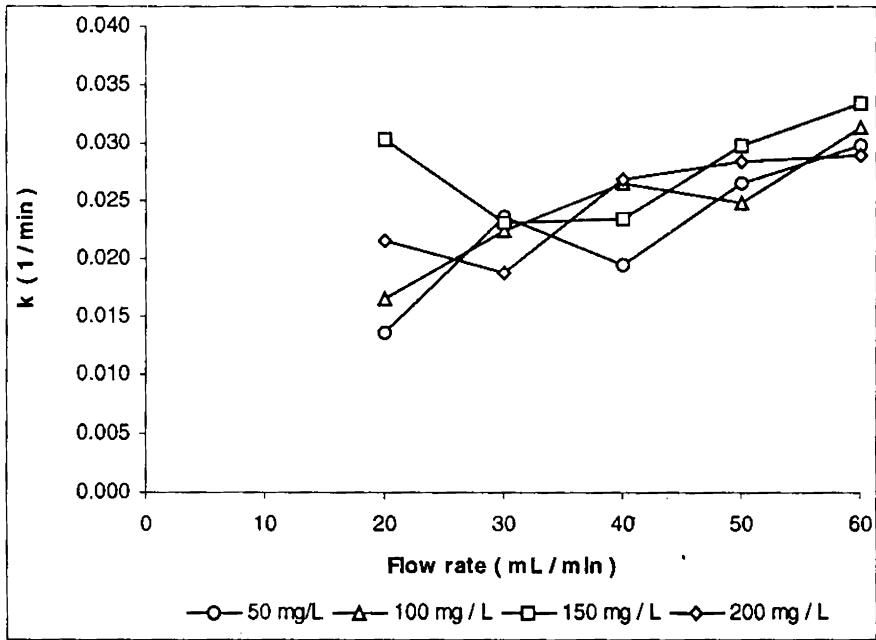


Figure 2.63  
 Direct Green - B  
 Influence of flow rates on pseudo first order rate coefficients at pH 6 and at constant concentration.

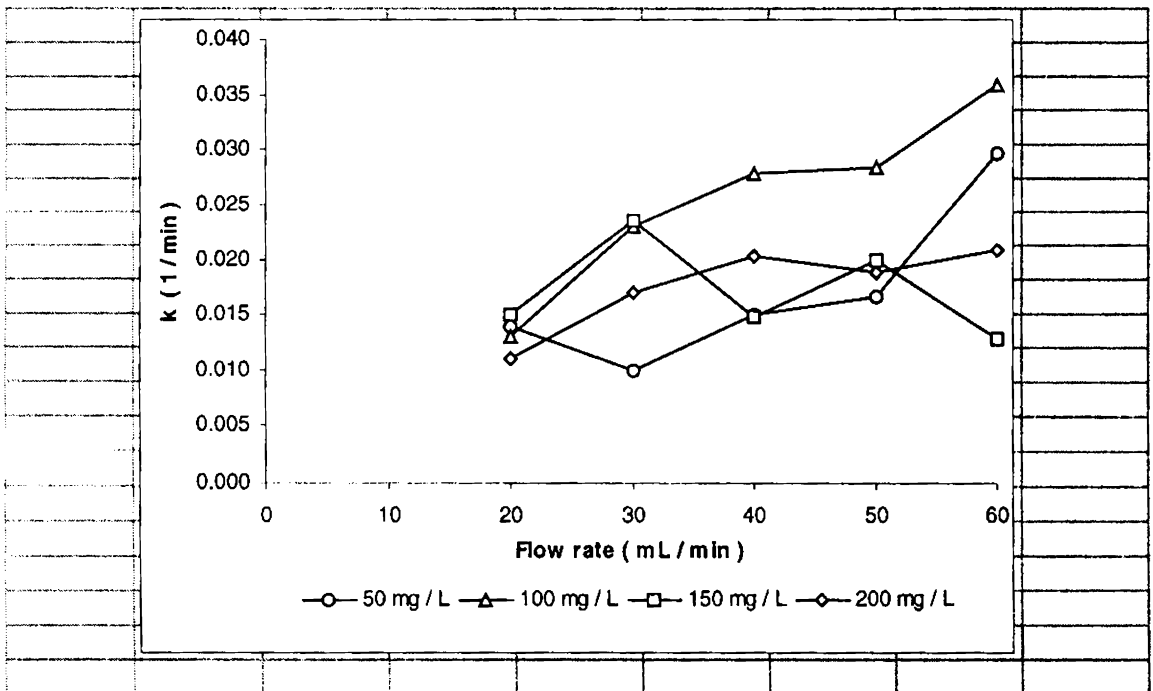


Figure 2.64  
 Direct Green - B  
 Influence of flow rates on pseudo first order rate coefficients at pH 8 and at constant concentration.

### 2.8.5. Yellow- 5GL

Figures 2.65 to 2.68 indicate that the variation in dye concentration with flow rates fits into a linear first order model

(i) Comparison between flow rate and pH at constant concentration

The variation in pseudo-first order rate coefficients at a dye concentration of  $50 \text{ mg L}^{-1}$  and for fixed pH with respect to flow rates is shown in figure 2.69. For an initial dye concentration of  $50 \text{ mg L}^{-1}$ , it is observed that the rate coefficients increase with an increase in flow rates for the entire range of pH studied. However, this increase has been observed only up to a flow rate of  $50 \text{ mL min}^{-1}$ , after which the rate coefficients was found to decrease, indicating that the effective flow rate for reducing the dye up to which the phenomenon of mass transport mediates the reduction process is a flow rate of  $50 \text{ mL min}^{-1}$  where the average residence time is 3.9 min. For a further increase in flow rates, the decreased residence time could be a major factor that results in the observed decrease in rate coefficients. At a low flow rate of  $20 \text{ mL min}^{-1}$ , the difference between the rate coefficients for the different pH under study is small, however, as the flow rate is increased the difference in rate coefficients become apparent with maximum rate coefficients being recorded at pH 2. For the entire range of flow rate studied, the rate coefficients at pH 8 was found greater than that at pH 6 which at a flow rate of  $60 \text{ mL min}^{-1}$  was found to be even greater than the rate coefficients obtained for pH 4 indicating that at high flow rates and for low concentrations the rate of the reaction could be higher at pH 8 than at pH 4.



In the case of the former, the process involved is chiefly adsorption while in the case of the latter the rate coefficient is a sum of the two processes namely adsorption and chemical reaction. It could be a case of the rate of physical processes such as adsorption, becoming greater than a combination of both adsorption and chemical reaction.

Figure 2.70 shows variation in pseudo-first order rate coefficients with respect to flow rates at a dye concentration of  $100 \text{ mg L}^{-1}$  and at constant pH. As the concentration was raised to  $100 \text{ mg L}^{-1}$ , it is observed that the rate coefficients were found to increase linearly with an increase in flow rate for pH 4, 6 and 8. However, at pH 2 this increase in rate coefficients is observed only up to  $50 \text{ mL min}^{-1}$  similar to the observation made at the lower concentration ( $50 \text{ mg L}^{-1}$ ). Between pH the rate coefficients were found to significantly higher at pH 2, when compared to the rest. However, depending on the flow rate it is observed that at flow rates of 30 and  $40 \text{ mL min}^{-1}$  the rate coefficients of pH 6 and 8 become comparable indicating that at these flow rates the rate coefficients were found to become independent of pH above 6. At flow rates of 50 and  $60 \text{ mL min}^{-1}$ , there is no significant difference between the rate coefficients at pH 4, 6 and 8, indicating that at flow rates above  $50 \text{ mL min}^{-1}$ , the rate coefficients can be considered independent of pH.

Figure 2.71 shows variation in pseudo-first order rate coefficients with respect to flow rates at a dye concentration of  $150 \text{ mg L}^{-1}$  and for fixed pH. With an increase in concentration to  $150 \text{ mg L}^{-1}$ , pH 2 continued to show similar trends observed at lower dye concentrations, with pH 4 and 6

showing a linear increase in the rate coefficient with an increase in flow rate. However at pH 8, there is no significant difference between the rate coefficients at flow rates of 20 and 30 mL min<sup>-1</sup>, after which there is a linear increase in rate coefficients for increase in flow rate. This indicates that at a dye concentration of 150 mg L<sup>-1</sup> and at pH 8, the rate coefficients become independent of flow rates between 20 and 30 mL min<sup>-1</sup>. Therefore, but for a small decrease in the rate coefficients of pH 4 at a flow rate of 40 mL min<sup>-1</sup>, the rate coefficients at pH 4 and 6 were found to become comparable indicating that after pH 2, the rate coefficients become independent of pH between 4 and 6 for the entire range of flow rate studied, before showing dependence at pH 8.

Figure 2.72 shows variation in pseudo-first order rate coefficients with respect to flow rates at a constant dye concentration of 200 mg L<sup>-1</sup> and pH. As the concentration was raised to 200 mg L<sup>-1</sup>, a linear increase in the rate coefficient for an increase in flow rate is observed only up to 40 mL min<sup>-1</sup> for pH 2, after which the value decreased at 50ml/min before becoming independent of flow rate. pH 4, 6 and 8 showed a linear increase in rate coefficients with increase in flow rate, with the rate coefficients of pH 4 and 8 becoming comparable.

(ii) Comparison between flow rate and concentration at constant pH

The variation in pseudo-first order rate coefficients with respect to flow rates at pH 2 and for fixed dye concentrations is shown in figure 2.73.

At pH 2, for a dye concentration of  $50 \text{ mg L}^{-1}$  the rate coefficient was found to increase linearly with an increase in flow rate up to  $40 \text{ mL min}^{-1}$ , after which it decreases as the flow rate is increased to  $50 \text{ mL min}^{-1}$  and then becomes independent of flow rate. The rate coefficients for all higher concentrations was found to increase linearly with increase in flow rates up to  $50 \text{ mL min}^{-1}$  after which it decreased for an increase in flow rate to  $60 \text{ mL min}^{-1}$ . At the lowest flow rate ( $20 \text{ mL min}^{-1}$ ), the rate coefficients of  $50$ ,  $100$  and  $200 \text{ mg L}^{-1}$  show no significant difference between them indicating that at low flow rate there is a tendency of the rate coefficient to become independent of concentration. The rate coefficient for  $150 \text{ mg L}^{-1}$  was found to be higher than the rest.

The variation in pseudo-first order rate coefficients with respect to flow rates at pH 4 and for fixed dye concentrations is shown in figure 2.74. As the pH was raised to 4, the rate coefficients showed dependence on the initial dye concentration. At a concentration of  $50 \text{ mg L}^{-1}$ , the rate coefficient showed a linear increase with increase in flow rate up to  $50 \text{ mL min}^{-1}$ , before decreasing for a further increase in flow rate. For all the remaining dye concentrations the rate coefficients showed a linear increase with increase in flow rate confirming the influence of mass transport. Between concentrations, no significant difference is observed between the rate coefficients at a flow rate of  $30 \text{ mL min}^{-1}$ , after which the difference seemed to become apparent and at a flow rate of  $60 \text{ mL min}^{-1}$ , the rate coefficient was lowest for a concentration of  $50 \text{ mg L}^{-1}$  followed by  $100$  and  $150 \text{ mg L}^{-1}$  with a maximum at  $200 \text{ mg L}^{-1}$ .

Figure 2.75 shows variation in pseudo-first order rate coefficients with respect to flow rates at pH 6 and for fixed dye concentrations. As the pH was raised to 6, the observations were similar to that at pH 4 except that the rate coefficients were significantly different for all concentrations with the rate coefficients increasing for an increase in concentration.

The variation in pseudo-first order rate coefficients with respect to flow rates at pH 8 and for fixed dye concentrations is shown in figure 2.76. At pH 8 the rate coefficients was found to increase with an increase in flow rate for all concentrations, except at 50 mg L<sup>-1</sup>, where it was found to decrease after a flow rate of 50 mL min<sup>-1</sup>.

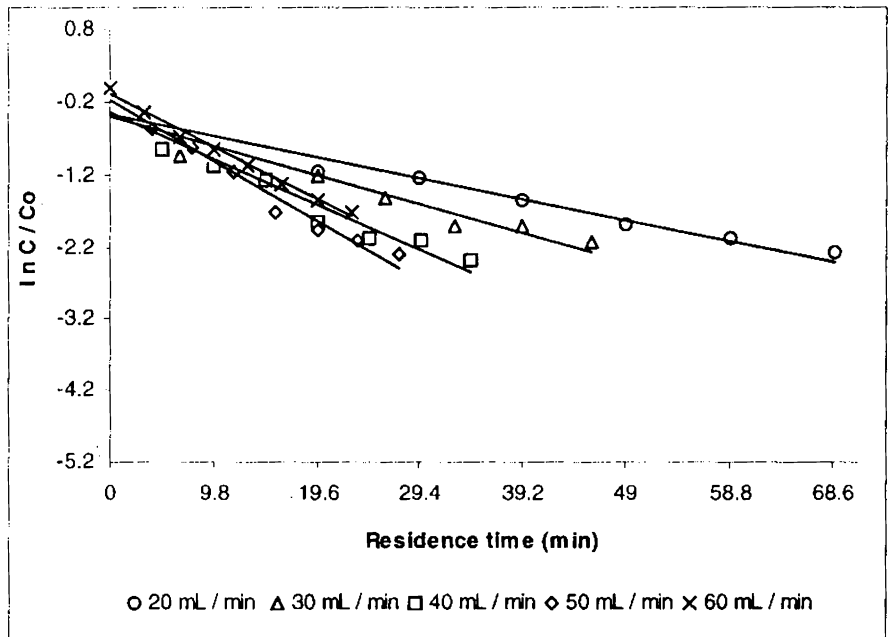


Figure 2.65  
 Yellow - 5GL  
 Plots confirming first order with respect to flow rates at pH 2 and at a  
 Dye concentration of  $50 \text{ mg L}^{-1}$

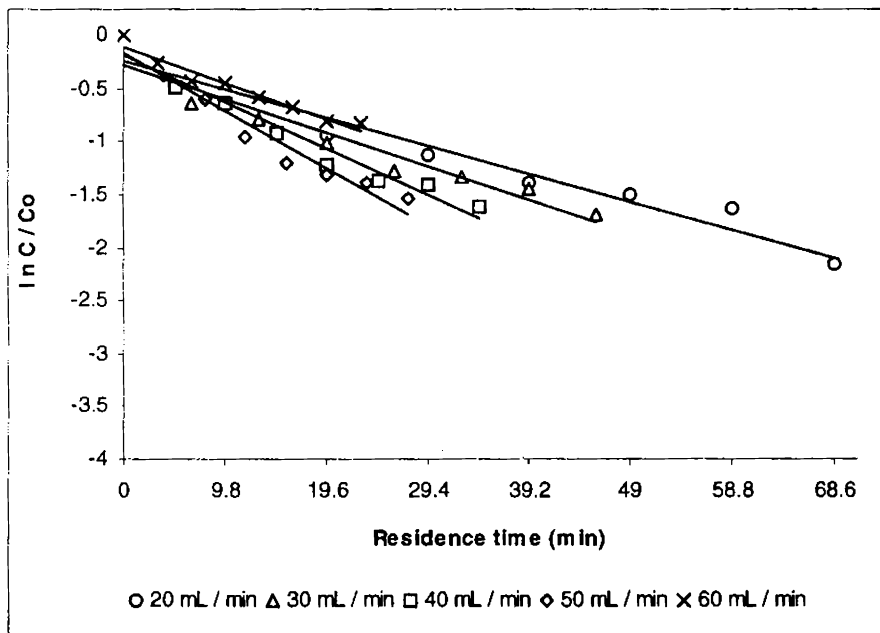


Figure 2.66  
 Yellow - 5GL  
 Plots confirming first order with respect to flow rates at pH 4 and at a  
 Dye concentration of  $50 \text{ mg L}^{-1}$

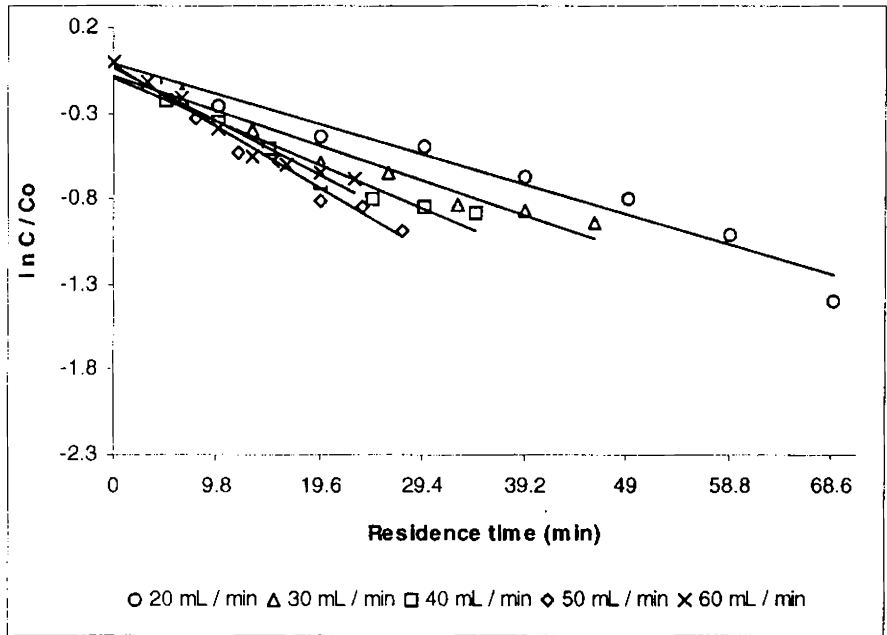


Figure 2.67  
 Yellow - 5GL  
 Plots confirming first order with respect to flow rates at pH 6 and at a  
 Dye concentration of  $50 \text{ mg L}^{-1}$

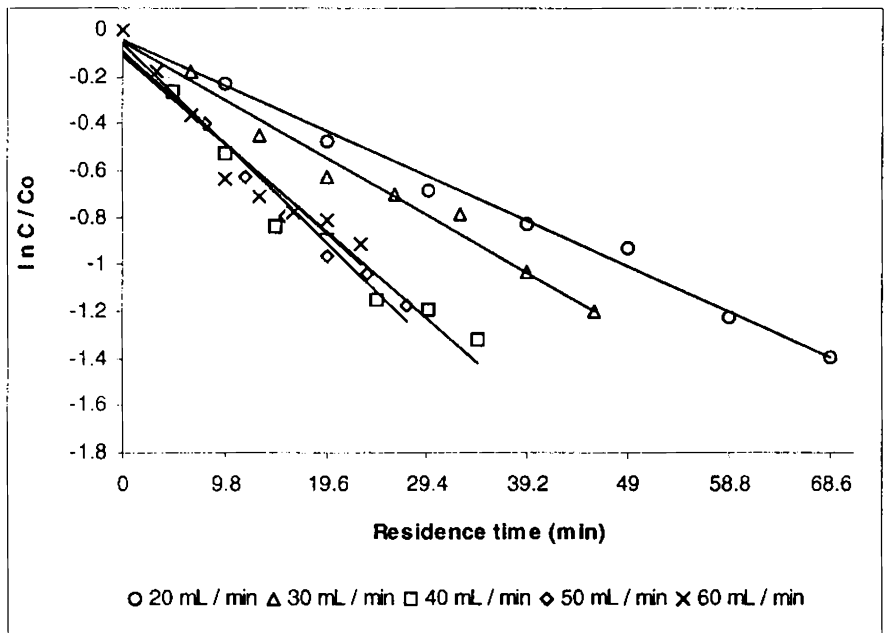


Figure 2.68  
 Yellow - 5GL  
 Plots confirming first order with respect to flow rates at pH 8 and at a  
 Dye concentration of  $50 \text{ mg L}^{-1}$

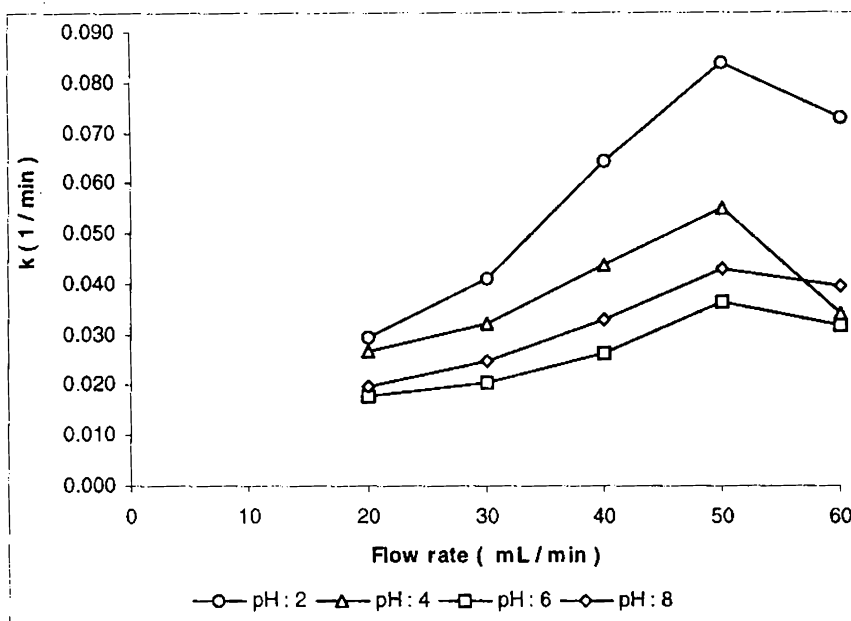


Figure 2.69  
Direct Yellow 5GL  
Influence of flow rates on the pseudo first order rate coefficients at a dye concentration of 50 mg L<sup>-1</sup> and at constant pH.

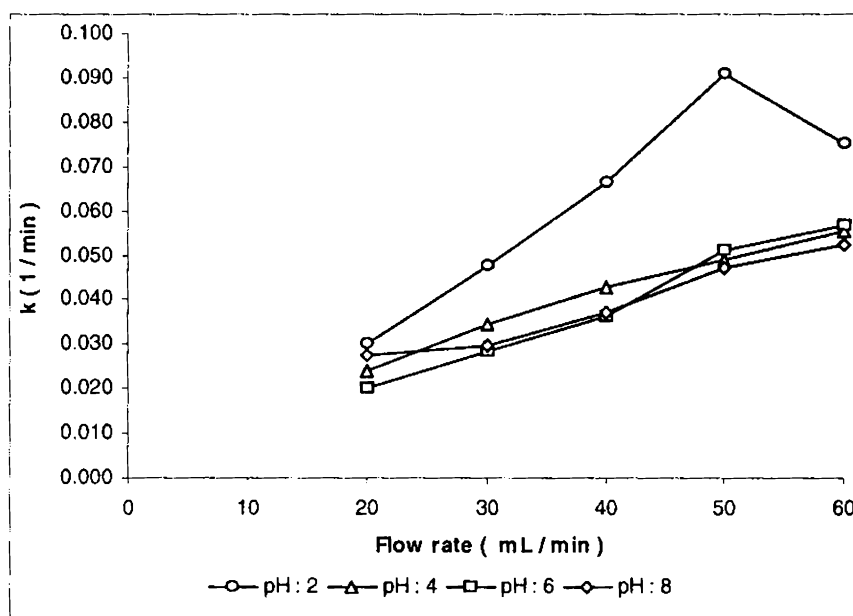


Figure 2.70  
Direct Yellow 5GL  
Influence of flow rates on the pseudo first order rate coefficients at a dye concentration of 100 mg L<sup>-1</sup> and at constant pH.

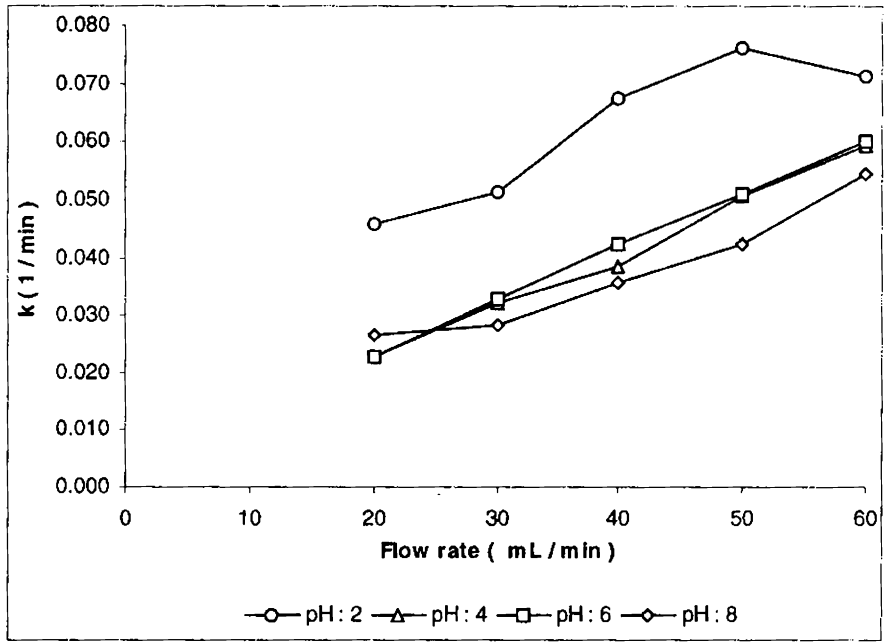


Figure 2.71  
Direct Yellow 5GL  
Influence of flow rates on the pseudo first order rate coefficients at a dye concentration of 150 mg L<sup>-1</sup> and at constant pH.

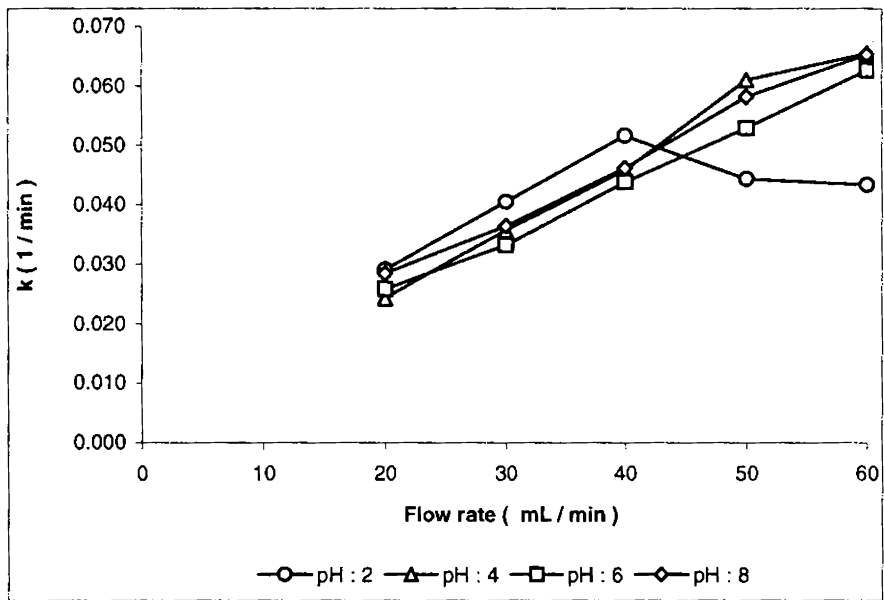


Figure 2.72  
Direct Yellow 5GL  
Influence of flow rates on the pseudo first order rate coefficients at a dye concentration of 200 mg L<sup>-1</sup>.



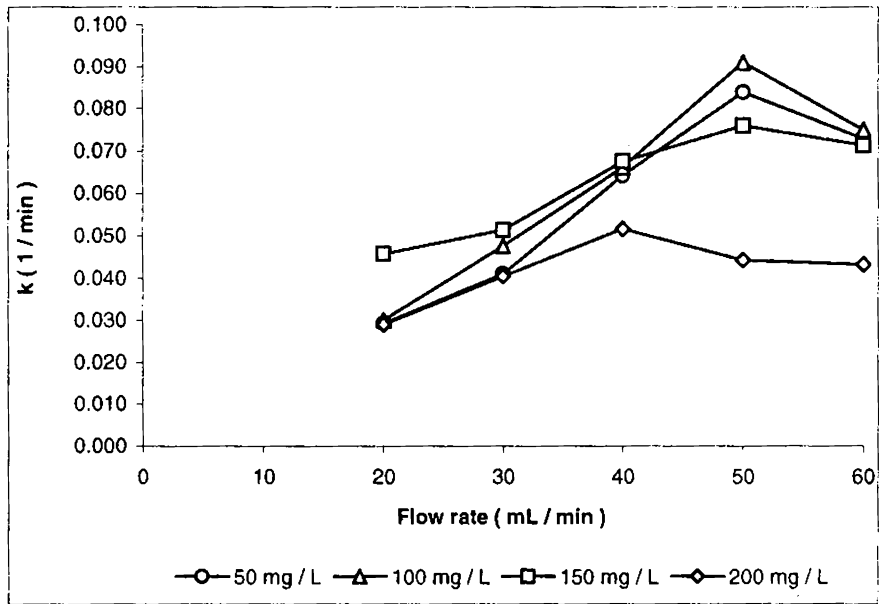


Figure 2.73  
Direct Yellow 5GL  
Influence of flow rates on pseudo first order rate coefficients at pH 2 and at constant concentration.

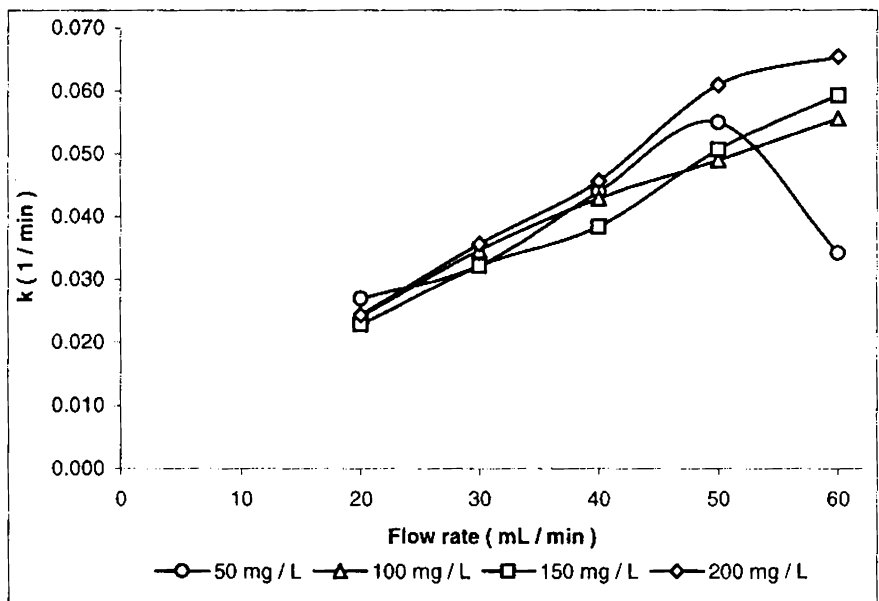


Figure 2.74  
Direct Yellow 5GL  
Influence of flow rates on pseudo first order rate coefficients at pH 4 and at constant concentration.

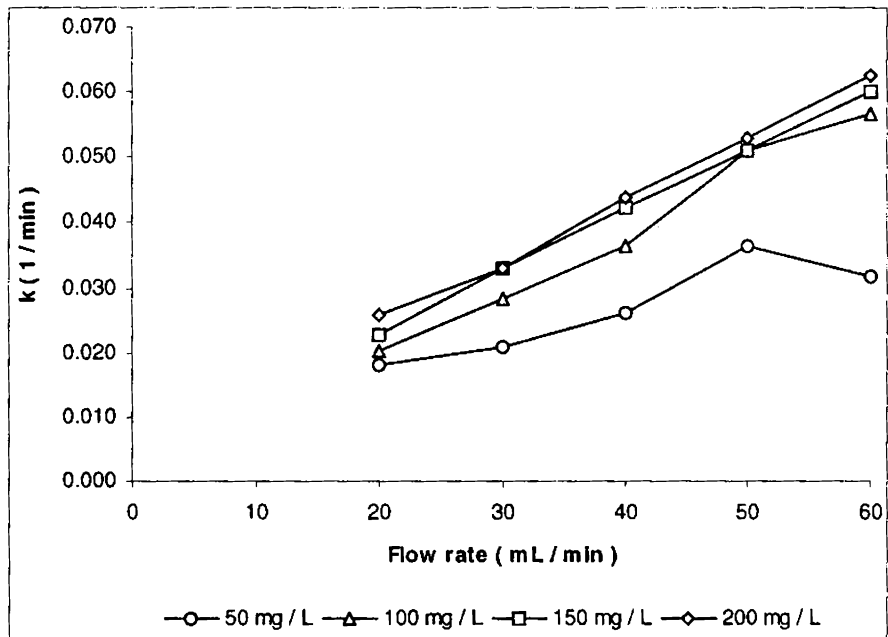


Figure 2.75  
Direct Yellow 5GL  
influence of flow rates on pseudo first order rate coefficients at pH 6 and at constant concentration.

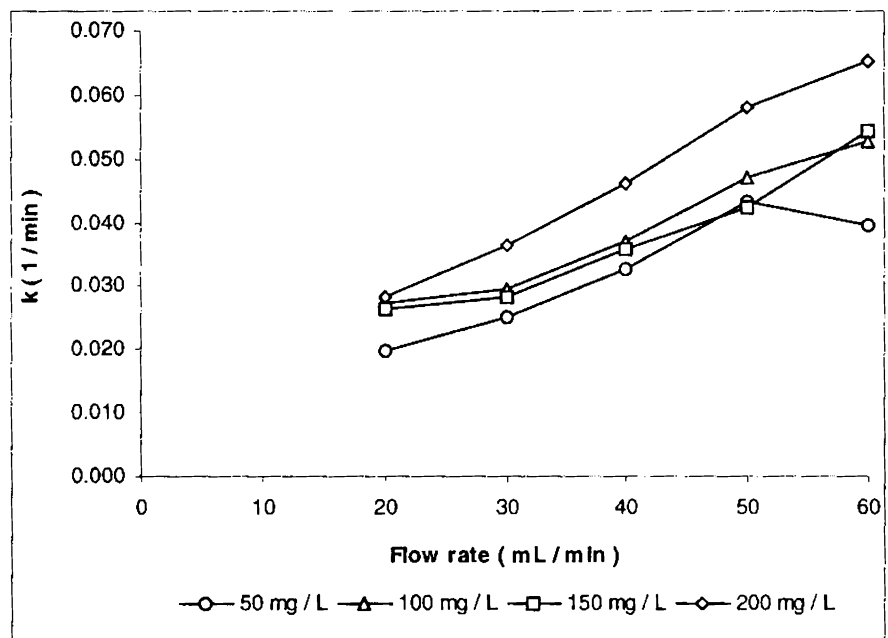


Figure 2.76  
Direct Yellow 5GL  
influence of flow rates on pseudo first order rate coefficients at pH 8 and at constant concentration.

## 2.9. Effect of concentration

### 2.9.1. Direct Sky Blue

It was observed that the data fit well into linear first order plots and the influence of the initial dye concentrations has been studied by monitoring the variation in the pseudo-first order rate coefficients. Figures 2.77 to 2.81 presents the first order fit of the observations.

The objective behind the choice of concentration as a variable was to determine if the dye could be reduced irrespective of its initial concentration. The influence of concentration on the reaction kinetics has been studied by monitoring the variation in the pseudo-first order rate coefficients for a constant pH and flow rate but for varying concentrations. The influence has been studied in two ways:

- (i) Monitoring the variation in the pseudo first order rate coefficients derived for the various flow rates for a specific pH against the concentration range studied. This gives us the relationship between concentration and flow rate.
  - (ii) Monitoring the variation in the pseudo first order rate coefficients derived for the various pH for a specific flow rate against the concentration range studied. This gives us the relationship between concentration and pH.
- (i) Comparison between concentration and flow rates at constant pH

Figure 2.82 illustrates the influence of dye concentration on pseudo-first order rate coefficients at pH 2 and fixed flow rates. The inference drawn is that under acidic conditions when the pH is 2 at flow rates of 20,

30 and 40 mL min<sup>-1</sup> there is a decrease in the rate coefficient values with an increase in concentration. As the flow rate is increased, the intensity of this decrease tends to wear off and at a flow rate of 60 mL min<sup>-1</sup> it is observed that the rate coefficient values increase with an increase in the dye concentration up to 150 mg L<sup>-1</sup> after which the value decreases.

Figure 2.83 is a representation of influence of dye concentration on pseudo first order rate coefficients at pH 4 and fixed flow rates. At pH 4 for a low flow rate of 20 mL min<sup>-1</sup> there is a decrease in the rate coefficient values as the concentration is raised from 50 mg L<sup>-1</sup> to 100 mg L<sup>-1</sup> beyond which the values remain more or less steady. However, as the flow rate is increased to 30 mL min<sup>-1</sup> and 40 mL min<sup>-1</sup> the rate coefficient values become independent of concentration. For a further increase in the flow rate to 50 and 60 mL min<sup>-1</sup> the rate coefficient values were found to increase with an increase in the concentration.

Figure 2.84 illustrates the influence of dye concentration on pseudo-first order rate coefficients at pH 6 and fixed flow rates. At pH 6 the rate coefficient values were found to remain more or less steady for a flow rate of 20 mL min<sup>-1</sup> and 30 mL min<sup>-1</sup> but for a further increase in the flow rates the pseudo first order rate coefficients were found to increase with an increase in the dye concentration up to 100 mg L<sup>-1</sup> after which it remains steady up to 150 mg L<sup>-1</sup> and then drops.

Figure 2.85 is a representation of influence of dye concentration on pseudo first order rate coefficients at pH 8 and fixed flow rates. At pH 8 a steady increase in the rate coefficient values was observed with an

increase in flow rates up to  $100 \text{ mg L}^{-1}$  after which the rate coefficient values decrease. At flow rates of  $50$  and  $60 \text{ mL min}^{-1}$  it is observed that the variation in the rate coefficients become comparable with a significant increase up to  $150 \text{ mg L}^{-1}$  followed by a decrease for a further increase in the dye concentration.

(ii) Comparison between concentration and pH at constant flow rates.

Influence of dye concentration on the pseudo first order rate coefficients at a flow rate of  $20 \text{ mL min}^{-1}$  and fixed pH is shown in figure 2.86. At a flow rate of  $20 \text{ mL min}^{-1}$  the rate coefficients derived for pH 2 and 4 was found to decrease with an increase in concentration up to  $100 \text{ mg L}^{-1}$  after which it becomes independent of concentration up to  $150 \text{ mg L}^{-1}$  before decreasing at  $200 \text{ mg L}^{-1}$  for pH 2 and increasing for pH 4. pH 6 was found independent of concentration up to  $150 \text{ mg L}^{-1}$  after which the rate coefficients showed a decrease as the concentration was raised to  $200 \text{ mg L}^{-1}$ . pH 8 showed an increase in the rate coefficient as the concentration was increased from  $50$  to  $100 \text{ mg L}^{-1}$  after which the values become independent of concentration.

Figure 2.87 is a representation of the influence of dye concentration on pseudo first order rate coefficients at a flow rate of  $30 \text{ mL min}^{-1}$  and fixed pH. With an increase in flow rate to  $30 \text{ mL min}^{-1}$ , the rate coefficients at pH 2 was found to decrease as the concentration was raised from  $50$  to  $100 \text{ mg L}^{-1}$ , for a further increase in concentration to  $150 \text{ mg L}^{-1}$  an increase in the rate coefficient is observed which then decreases again as the concentration is raised to  $200 \text{ mg L}^{-1}$ . At pH 4 the rate coefficients was

found to decrease marginally, however, at pH 6 there was an increase as the concentration was raised from 50 to 100 mg L<sup>-1</sup> after which since, the difference in rate coefficients at concentrations of 100 and 150 mg L<sup>-1</sup> is small they are considered independent of concentrations above 100 mg L<sup>-1</sup> at pH 4 and 6. With respect to pH 8 the rate coefficients showed a prominent increase as the concentration was raised from 50 to 100 mg L<sup>-1</sup> after the rate coefficients become independent of concentration.

Influence of dye concentration on the pseudo first order rate coefficients at a flow rate of 40 mL min<sup>-1</sup> and fixed pH is shown in figure 2.88. At a flow rate of 40 mL min<sup>-1</sup> rate coefficients for pH 2 decreased with an increase in concentration from 50 to 100 mg L<sup>-1</sup> after which it remains more or less independent of concentrations between 100 and 150 mg L<sup>-1</sup> before recording a marginal decrease for a concentration of 200 mg L<sup>-1</sup>. After 100 mg L<sup>-1</sup> since, there is only a small difference between the rate coefficients they are considered independent of concentration above 100 mg L<sup>-1</sup>. pH 4 and 6 showed almost similar trends with the rate coefficients increasing with an increase in concentration ( linearly for pH 6) up to 150 mg L<sup>-1</sup> after which pH 4 becomes independent of concentration while pH 6 shows a decrease in rate coefficients as the concentration was raised from 150 mg L<sup>-1</sup> to 200 mg L<sup>-1</sup>. For a higher pH at 8, the rate coefficients showed an increase with an increase in concentration from 50 to 100 mg L<sup>-1</sup> after which they remain independent of concentration between 100 and 150 mg L<sup>-1</sup> before showing a decrease at 200 mg L<sup>-1</sup>.

Figure 2.89 is a representation of the influence of dye concentration on pseudo first order rate coefficients at a flow rate of  $50 \text{ mL min}^{-1}$  and fixed pH.

At a flow rate of  $50 \text{ mL min}^{-1}$ , the rate coefficients for pH 2 was found to decrease with an increase in concentration up to  $100 \text{ mg L}^{-1}$  after which remaining more or less independent of concentration up  $150 \text{ mg L}^{-1}$  the rate coefficients decrease as the concentration is raised to  $200 \text{ mg L}^{-1}$ . pH 4 and 6 showed trends similar to pH 2 except that an increase in the rate coefficients is observed with an increase in concentration from 50 to  $100 \text{ mg L}^{-1}$ . This trend of increase in rate coefficient for an increase in concentration from 50 to  $100 \text{ mg L}^{-1}$  is also observed at pH 8 however, after this the rate coefficients become independent of concentration.

Influence of dye concentration on the pseudo first order rate coefficients at a flow rate of  $60 \text{ mL min}^{-1}$  and fixed pH is shown in figure 2.90.

At a flow rate of  $60 \text{ mL min}^{-1}$  the rate coefficients at pH 2 increased linearly with an increased in concentration up to  $150 \text{ mg L}^{-1}$  after which for a higher concentration at  $200 \text{ mg L}^{-1}$  a decrease is observed. pH 4 showed random variations in rate coefficients as a result showing trends that could not be interpreted. Rate coefficients were found to increase with an increase in concentration from 50 to  $100 \text{ mg L}^{-1}$  at both pH 6 and pH 8, after which all further increase in concentrations lead to a decrease in the rate coefficients. If the trend observed at pH 4 is considered random, it is

observed that at a concentration of  $200 \text{ mg L}^{-1}$  and at a flow rate of  $60 \text{ mL min}^{-1}$  the rate coefficients was found to become independent of pH.

All these features suggest that there is a strong relationship between flow rate, pH and concentration. At low pH and flow rates the decrease in the rate coefficient values with increase in concentration can be attributed to the fact that under acidic condition the process involved is chemical reaction involving direct electron transfer between the metal surface to the dye molecule. Under such conditions there is no scope for the formation of oxide layers at the metal surface as the corrosion products that is formed is being continuously dissociated from the metal surface partly through dissolution and moreover, being a flow through system, washing away the corrosion products. An increased build up of the dye molecules at higher concentrations forms a passivating layer at the metal surface thereby preventing the electron transfer required to carry out the reduction of the dye molecule, thus decreasing the rate of the reaction as the dye molecule assumes the role of a corrosion inhibitor. However, at higher flow rates even at pH 2 mass transfer phenomenon do occur as indicated by an increase in the rate coefficient values for increased concentration. However, even this phenomenon reach a limit after which for a further increase in the concentration the rate of the reaction shows a decrease. At pH 4 the observed pseudo-first order rate coefficient could be a sum of both the chemical reaction as well as the surface phenomenon such as adsorption. Therefore, initially when the surface of the metal is free from an oxide layer and when the flow rate and the dye concentration is low the



removal is attributed to chemical reaction after which it remains steady at higher concentrations as now the dye has formed a layer over the surface of the metal preventing electron transfer. However at higher concentrations a slight increase in the rate coefficients could be attributed to the adsorption phenomenon occurring at the metal surface. As the flow rate is increased the rate coefficient values was found to become independent of concentration. This step probably indicates the transition from processes mediated by chemical reaction to surface mediated processes. Above such transition flow rates, a linear increase in the rate of the reaction at higher flow rates with increase in concentrations confirms the involvement of processes mediated by mass transfer. The regions beyond the linear increase is indicated by higher pH where the linear increase begin to give way to curves that approach a limiting concentration beyond which the features of increased pH increased concentration and increased flow rates together results in conditions leading to decreased rates of dye reduction.

Therefore, the influence of concentration on the pseudo first order rate coefficients can be summed into the following four type of behaviors:

- (i) A decrease in the rate coefficients with increase in dye concentration can be attributed to corrosion inhibition.
- (ii) A transition stage, when the rate coefficients become independent of the dye concentrations.
- (iii) Above the transition stage there is a region of linear increase in the rate coefficient values with increase in concentration indicating the influence of mass transport

due to increased transport of the dye molecules at the metal surface.

- (iv) Beyond this region of linear increase is the region where the variation in the rate coefficient attains a limiting value and then falls fitting a curve.

Each of these conditions is strongly influenced by the variables of pH and flow rate.

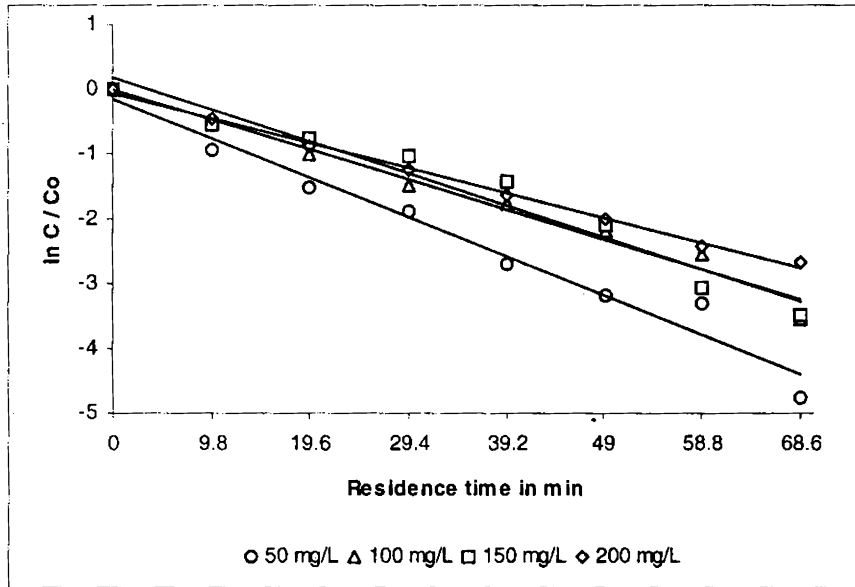


Figure 2.77  
 Direct Sky Blue  
 Plots confirming first order with respect to concentration at pH 2 and at a flow rate of 20 mL min<sup>-1</sup>

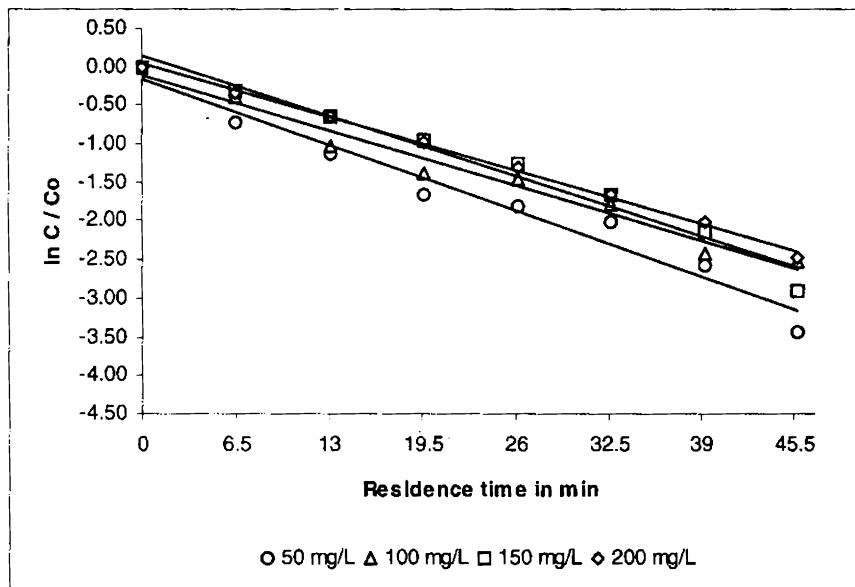


Figure 2.78  
 Direct Sky Blue  
 Plots confirming first order with respect to concentration at pH 2 and at a flow rate of 30 mL min<sup>-1</sup>

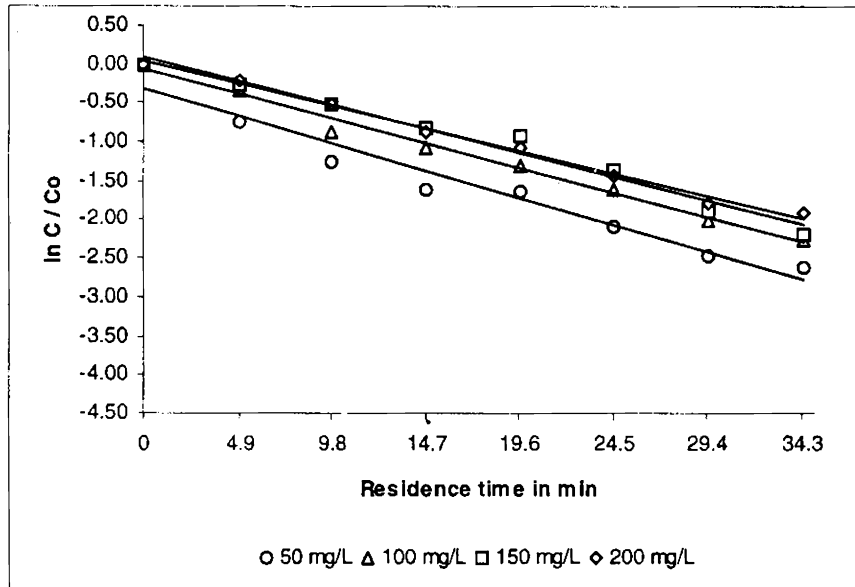


Figure 2.79  
 Direct Sky Blue  
 Plots confirming first order with respect to concentration at pH 2 and at a flow rate of 40 mL min<sup>-1</sup>

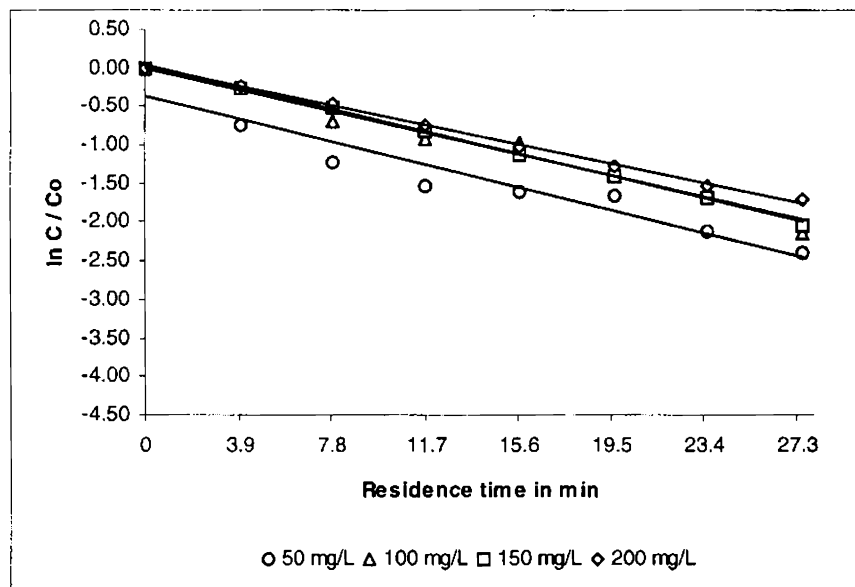


Figure 2.80  
 Direct Sky Blue  
 Plots confirming first order with respect to concentration at pH 2 and at a flow rate of 50 mL min<sup>-1</sup>

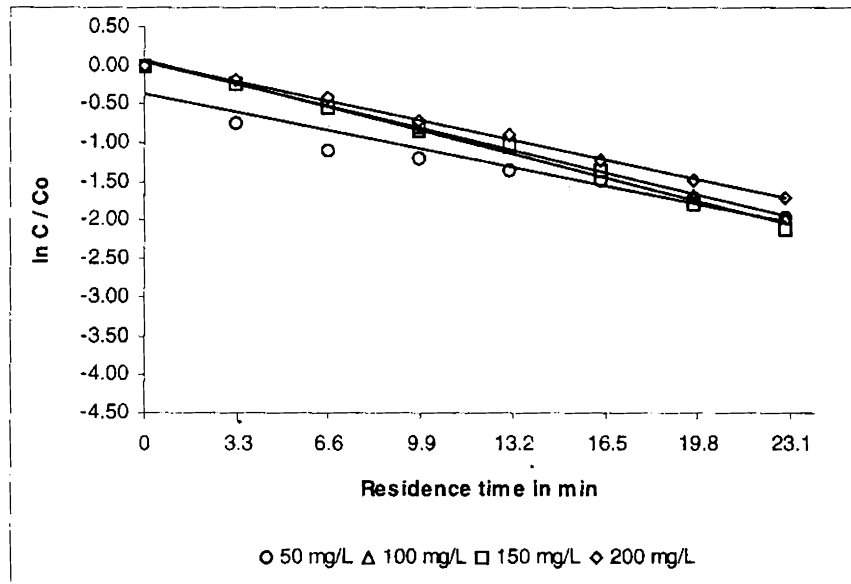


Figure 2.81  
Direct Sky Blue  
Plots confirming first order with respect to concentration at pH 2 and at a flow rate of  $60 \text{ mL min}^{-1}$

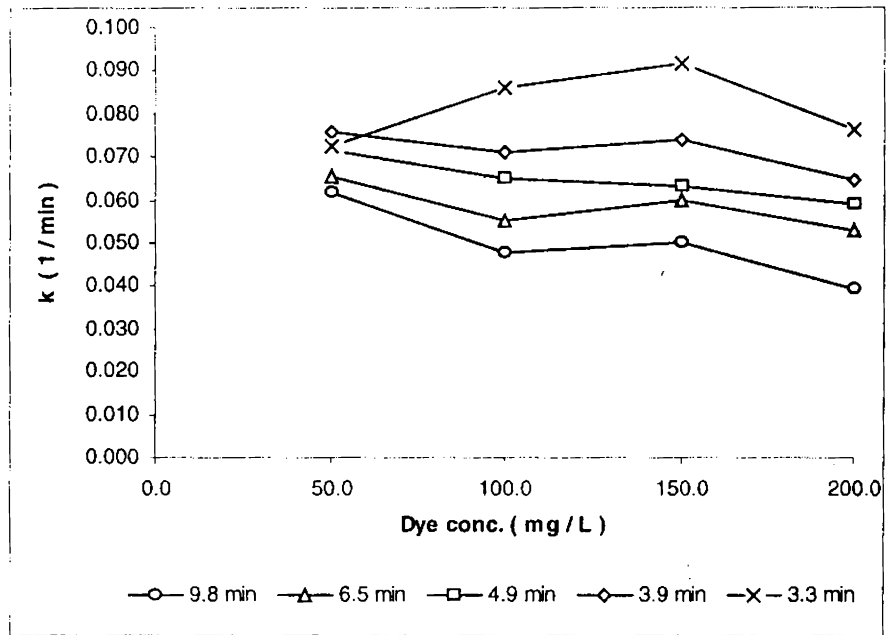


Figure 2.82.  
Direct Sky Blue  
Influence of dye concentration on pseudo first order rate coefficients at pH 2 and at fixed flow rates.

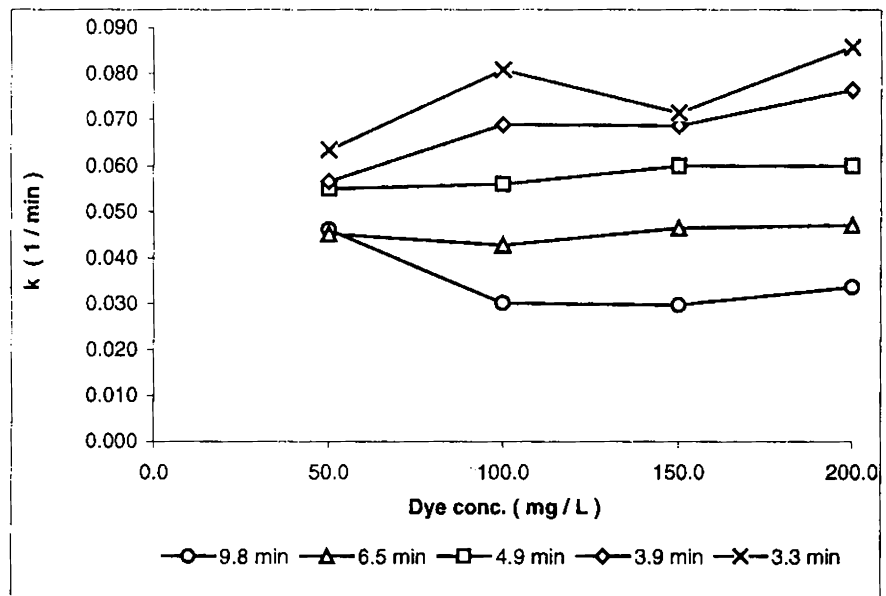


Figure 2.83  
Direct Sky Blue  
Influence of dye concentration on pseudo first order rate coefficients at pH 4 and at fixed flow rates.

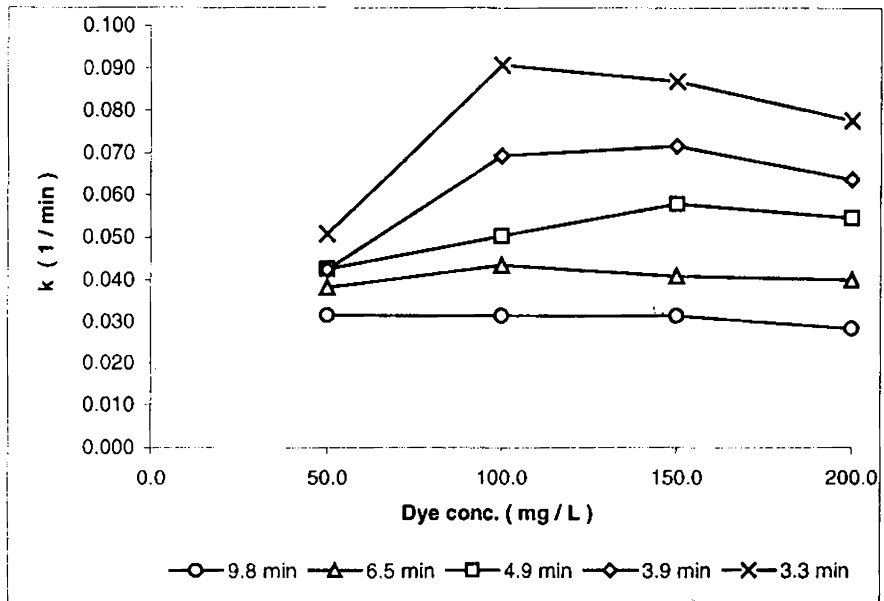


Figure 2.84  
 Direct Sky Blue  
 Influence of dye concentration on pseudo first order rate coefficients at pH 6 and at fixed flow rates.

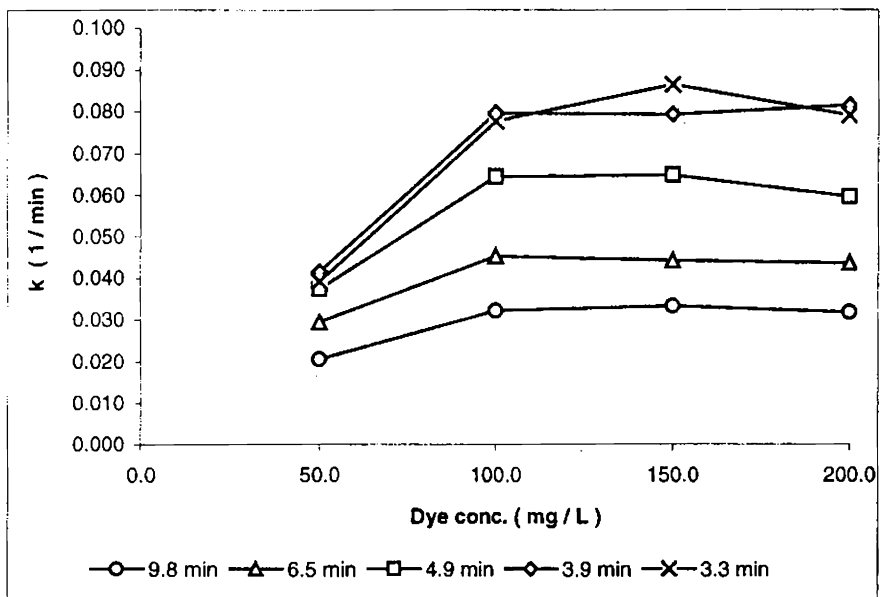


Figure 2.85  
 Direct Sky Blue  
 Influence of dye concentration on pseudo first order rate coefficients at pH 8 and at fixed flow rates.

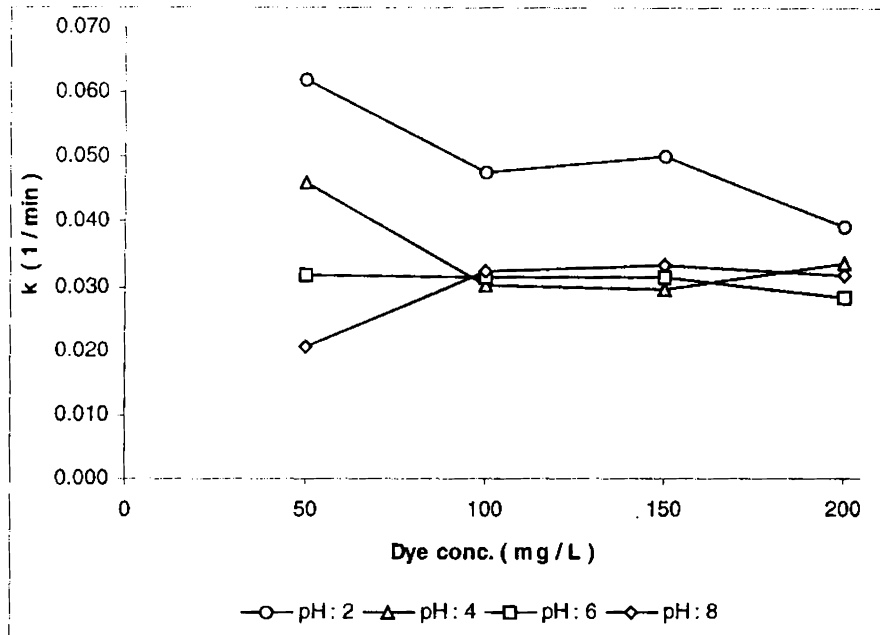


Figure 2.86  
Direct Sky Blue  
Influence of dye concentration on pseudo first order rate coefficients at a flow rate of  $20 \text{ mL min}^{-1}$  and at fixed pH

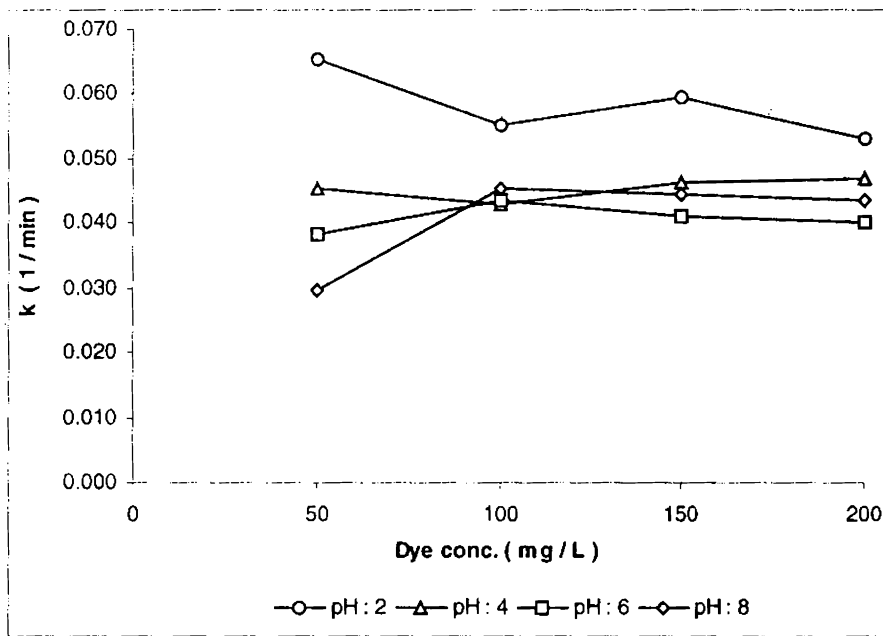


Figure 2.87  
Direct Sky Blue  
Influence of dye concentration on pseudo first order rate coefficients at a flow rate of  $30 \text{ mL min}^{-1}$  and at fixed pH



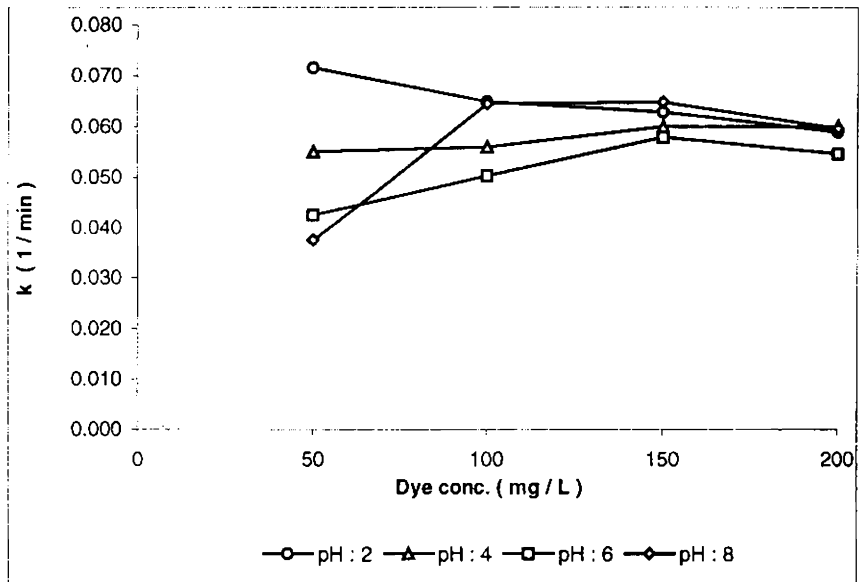


Figure 2.88  
 Direct Sky Blue  
 Influence of dye concentration on pseudo first order rate coefficients at a flow rate of  $40 \text{ mL min}^{-1}$  and at fixed pH.

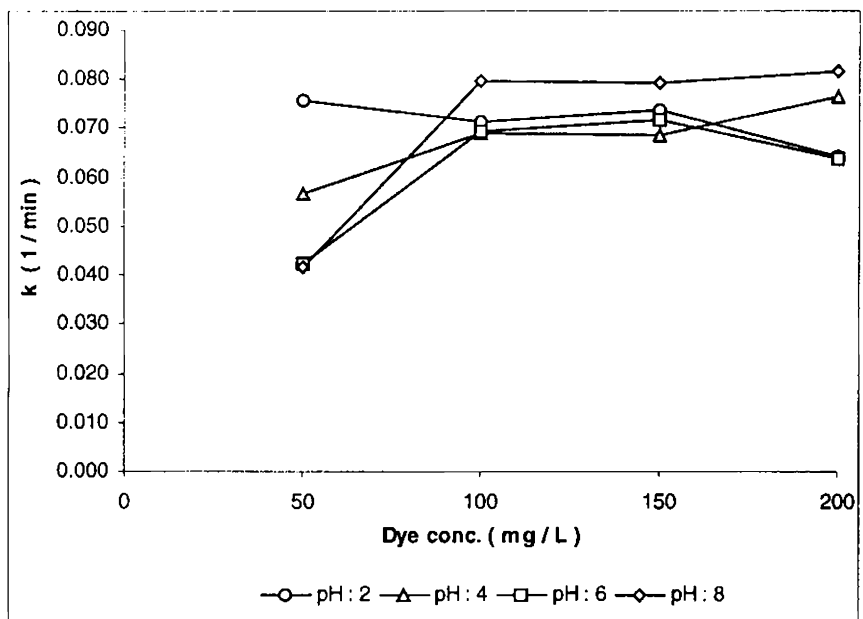


Figure 2.89  
 Direct Sky Blue  
 Influence of dye concentration on pseudo first order rate coefficients at a flow rate of  $50 \text{ mL min}^{-1}$  and at fixed pH.

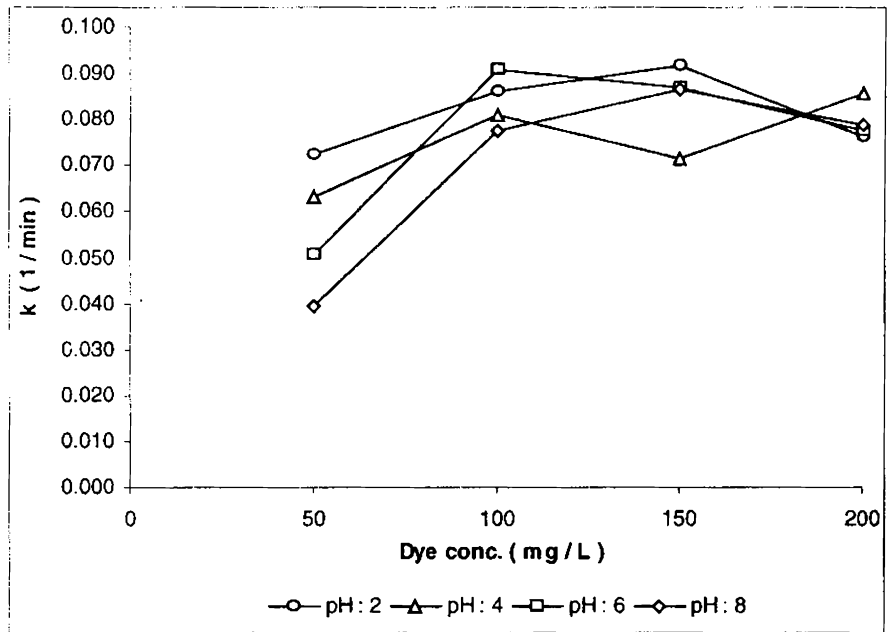


Figure 2.90  
Direct Sky Blue  
Influence of dye concentration on pseudo first order rate coefficients at a flow rate of  $60 \text{ mL min}^{-1}$  and at fixed pH.

### 2.9.2. Direct Black EG

It was observed that the data fit well into linear first order plots and the influence of the initial dye concentrations has been studied by monitoring the variation in the pseudo-first order rate coefficients. The following figures (from 2.91 to 2.94) presents the first order fit of the observations.

(i) Comparison between concentration and flow rate at constant pH

Figure 2.95 illustrates the influence of dye concentration on pseudo-first order rate coefficients at pH 2 and fixed flow rates. At pH 2, the rate coefficients were found to increase with an increase in the concentration from 50 to 100 mg L<sup>-1</sup> at flow rates of 20 and 30 mL min<sup>-1</sup>, after which the a decrease in the rate coefficient is observed. But at flow rates of 40 and 50 mL min<sup>-1</sup> the rate coefficient increased up to 150 mg L<sup>-1</sup> after which there is a drop. For flow rates beyond 50 mL min<sup>-1</sup> the rate coefficient remained steady up to a concentration of 100 mg L<sup>-1</sup> and then decreased. Thus, for an increase in flow rate there is an increase in the rate of the reaction at higher concentrations, however, there appears to be a limiting flow rate above which this observation does not hold good as indicated at a flow rate of 60 mL min<sup>-1</sup>.

Figure 2.96 is a representation of influence of dye concentration on pseudo first order rate coefficients at pH 4 and fixed flow rates. As the pH was raised to 4, the rate coefficients were found to decrease with an increase in concentration, with the rate coefficients increasing with an increase in flow rate emphasizing the influence of mass transport.

Between flow rates, at low flow rates (20 and 30 mL min<sup>-1</sup>) after the initial decrease for an increase in the concentration from 50 to 100 mg L<sup>-1</sup>, the rate of the reaction become independent of concentration. However, as the flow rate is increased (40 mL min<sup>-1</sup> and beyond), although the general trend is a decrease with increase in concentration, the rate coefficients show a small dependence on concentration. Since, there is no major difference in the rate coefficients between concentrations at 100 and 150 mg L<sup>-1</sup>, it is considered independent at these concentrations after which a decrease is observed at a concentration of 200 mg L<sup>-1</sup>.

Figure 2.97 illustrates the influence of dye concentration on pseudo-first order rate coefficients at pH 6 and fixed flow rates. At pH 6, low flow rates (20 and 30 mL min<sup>-1</sup>) become independent of concentration after an initial decrease with an increase in concentration from 50 to 100 mg L<sup>-1</sup>. However, at higher flow rates (40 mL min<sup>-1</sup>) the rate coefficient decreases progressively with increase in concentration or become independent of concentration above 150 mg L<sup>-1</sup> (at 50 mL min<sup>-1</sup>) or become independent of concentration from 100 to 150 mg L<sup>-1</sup> with an increase in the rate coefficient at 200 mg L<sup>-1</sup> (at 60 mL min<sup>-1</sup>).

Figure 2.98 is a representation of influence of dye concentration on pseudo first order rate coefficients at pH 8 and fixed flow rates. At pH 8, flow rates up to 40 mL min<sup>-1</sup> is found independent of concentration above 100 mg L<sup>-1</sup>, while at higher flow rates the rate coefficients decrease with an increase in concentration up to 150 mg L<sup>-1</sup>, after which an increase in the

rate coefficient is observed. However, between 100 and 200 mg L<sup>-1</sup> the difference in rate coefficients is marginal.

(ii) Comparison between concentration and pH at constant flow rate

Influence of dye concentration on the pseudo first order rate coefficients at a flow rate of 20 mL min<sup>-1</sup> and fixed pH is shown in figure 2.99. At a flow rate of 20 mL min<sup>-1</sup>, pH 2 the general observation was that there was an increase in the rate coefficient with an increase in the concentration from 50 to 100 mg L<sup>-1</sup>, after which a further increase in concentration to 150 mg L<sup>-1</sup> resulted in a decrease in the rate coefficient which later becomes independent of concentration. However, for all further increase in pH, the rate coefficients showed similar trends of decrease with increase in concentration from 50 to 100 mg L<sup>-1</sup> and from thereon becoming independent of concentration.

Figure 2.100 is a representation of the influence of dye concentration on pseudo first order rate coefficients at a flow rate of 30 mL min<sup>-1</sup> and fixed pH.

Influence of dye concentration on the pseudo first order rate coefficients at a flow rate of 40 mL min<sup>-1</sup> and fixed pH is shown in figure 2.101. Figures 2.100 and 2.101 indicate similar observations at flow rates of 30 and 40 mL min<sup>-1</sup> with random variations observed at pH 2.

Figure 2.102 is a representation of the influence of dye concentration on pseudo first order rate coefficients at a flow rate of 50 mL min<sup>-1</sup> and fixed pH. As the flow rate was raised to 50 mL min<sup>-1</sup> although the observations at flow rates pH 4, 6 and 8 remain similar to that of the

previous flow rates, at pH 2, an increase in the rate coefficient is observed as the concentration was raised up to  $150 \text{ mg L}^{-1}$ , after a decrease is observed.

Influence of dye concentration on the pseudo first order rate coefficients at a flow rate of  $60 \text{ mL min}^{-1}$  and fixed pH is shown in figure 2.103. At a flow rate of  $60 \text{ mL min}^{-1}$ , the rate coefficients of pH 2 after an initial increase with an increase in concentration from  $50$  to  $100 \text{ mg L}^{-1}$  was found to decrease while pH 6 and 8 became independent of concentration above  $100 \text{ mg L}^{-1}$  after an initial decrease with an increase in concentration from  $50$  to  $100 \text{ mg L}^{-1}$ . However, in the case of pH 4, the rate coefficients after remaining independent of concentration from  $100$  to  $150 \text{ mg L}^{-1}$  showed a decrease as the concentration was raised to  $200 \text{ mg L}^{-1}$ . In all the cases it is observed that the rate coefficient at pH 2 is found higher than all the other pH over the entire range of flow rate studied.

One possible explanation to the decrease in the rate coefficient with an increase in the dye concentration is that the dye under study could be a corrosion inhibitor. As a result of which an increase in the dye concentration leads to an increased build up of the dye molecules at the metal surface forming a passivating layer that prevents electron transfer from the metal surface necessary to drive the reduction reaction. Furthermore, the reduction products of the azo dyes namely, the amines could also inhibit the reduction process by functioning as a corrosion inhibitor as amines such as aniline, which could be generated through the cleavage of the azo linkages, are established corrosion inhibitors. Hence,

leading to a decrease in the rate coefficients with increase in dye concentration.

As far as the increase in the rate coefficients after an initial decrease is concerned, this phenomenon is frequently observed only under conditions of high dye concentrations or at high flow rates (particularly at flow rates over  $40 \text{ mL min}^{-1}$ ) or at high pH (especially above 4), all these conditions favour adsorption and the increase can be attributed to the adsorption phenomenon gaining prominence over chemical reduction.

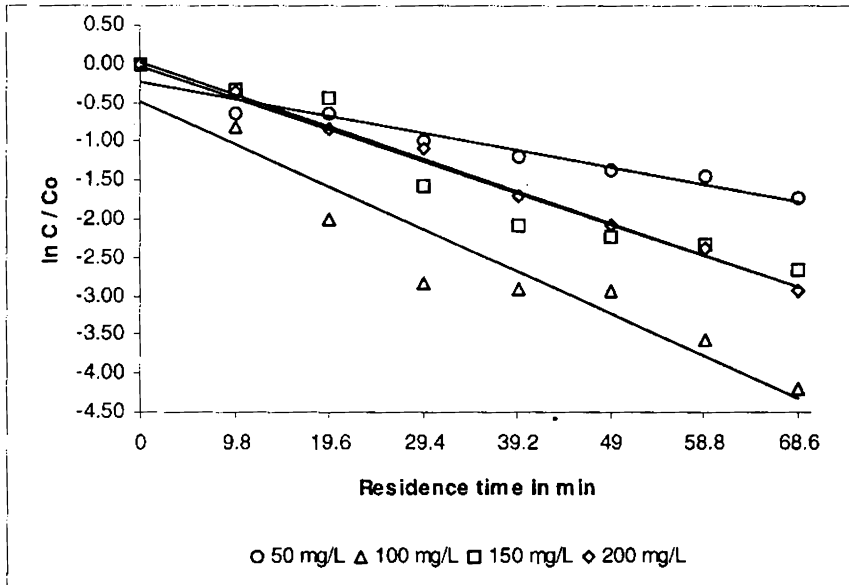


Figure 2.91  
 Black EG  
 Plots confirming first order with respect to concentration at pH 2 and at a flow rate of 20 mL min<sup>-1</sup>

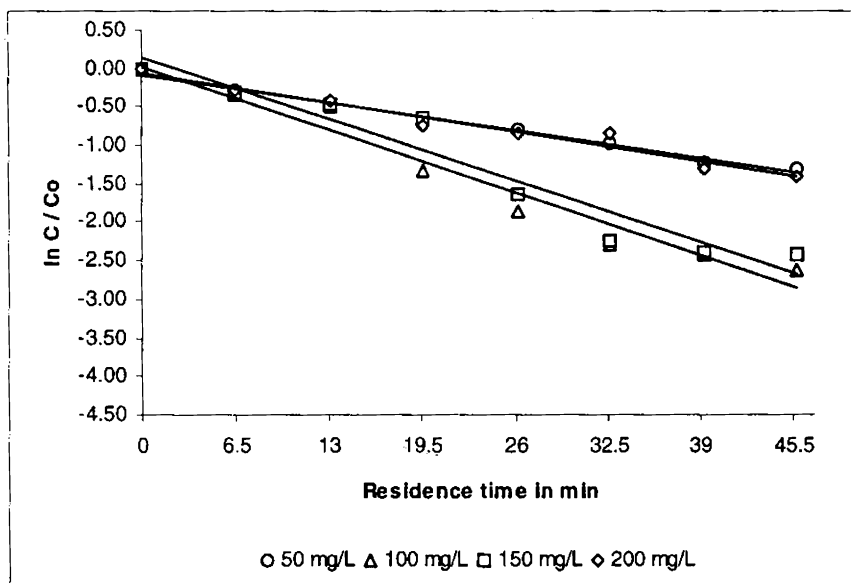


Figure 2.92  
 Black EG  
 Plots confirming first order with respect to concentration at pH 2 and at a flow rate of 30 mL min<sup>-1</sup>



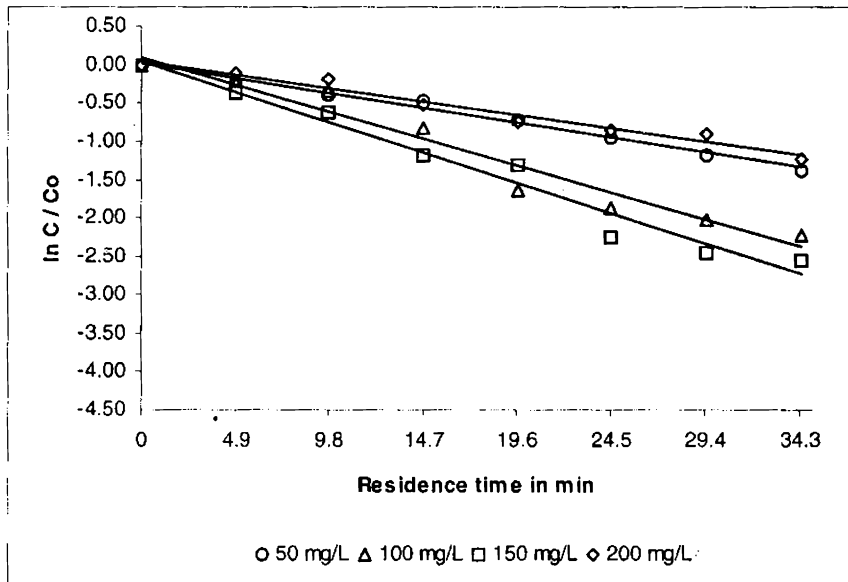


Figure 2.93  
 Black EG  
 Plots confirming first order with respect to concentration at pH 2 and at a flow rate of 40 mL min<sup>-1</sup>

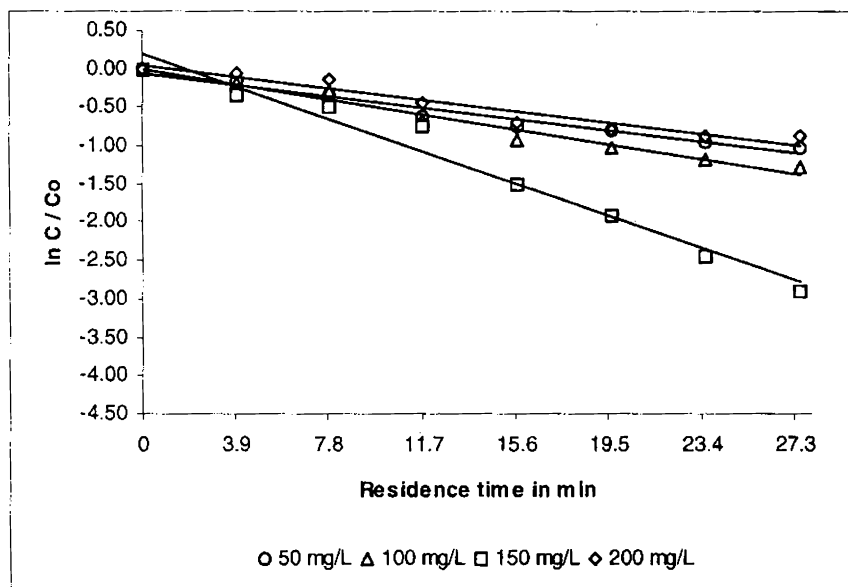


Figure 2.94  
 Black EG  
 Plots confirming first order with respect to concentration at pH 2 and at a flow rate of 50 mL min<sup>-1</sup>

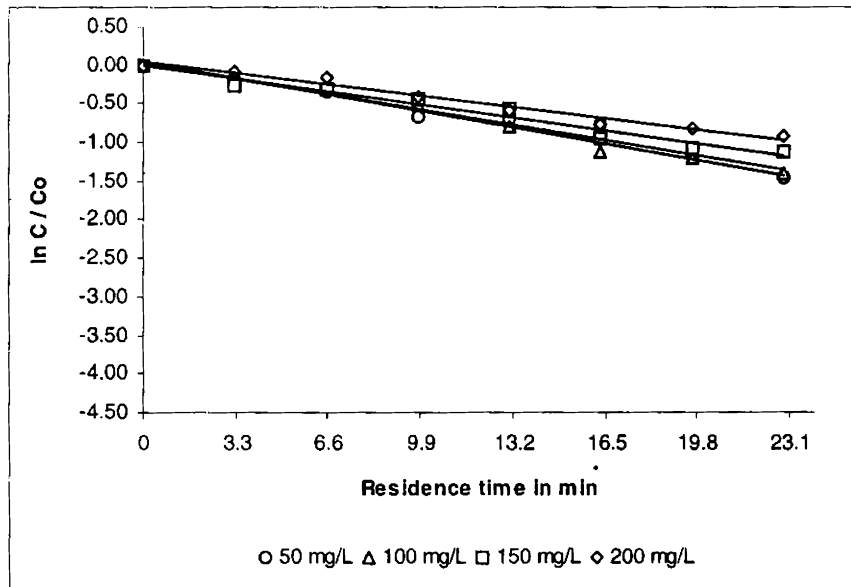


Figure 2.95  
Black EG  
Plots confirming first order with respect to concentration at pH 2 and at a flow rate of  $60 \text{ mL min}^{-1}$

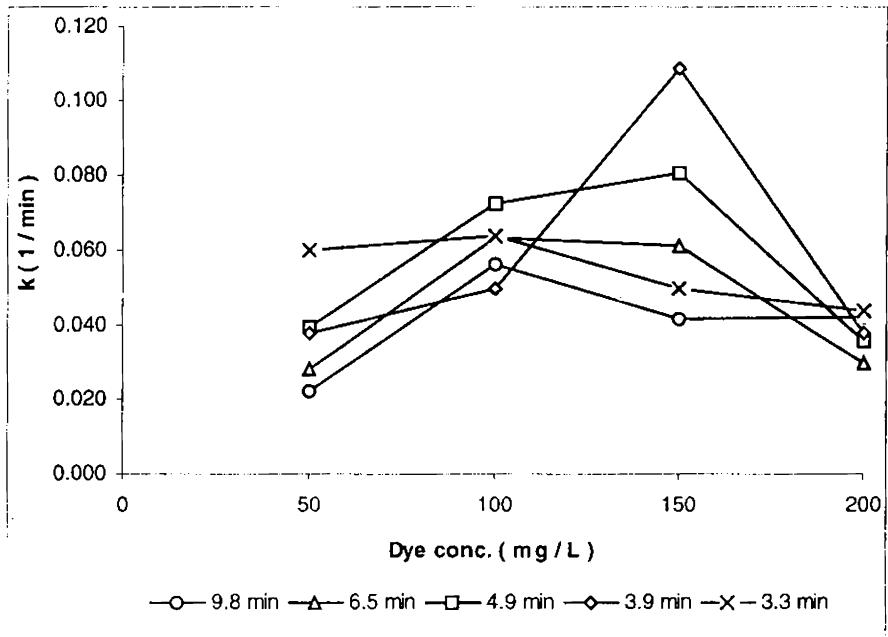


Figure 2.95.  
 Direct Black EG  
 Influence of dye concentration on pseudo first order rate coefficients at pH 2 and at fixed flow rates.

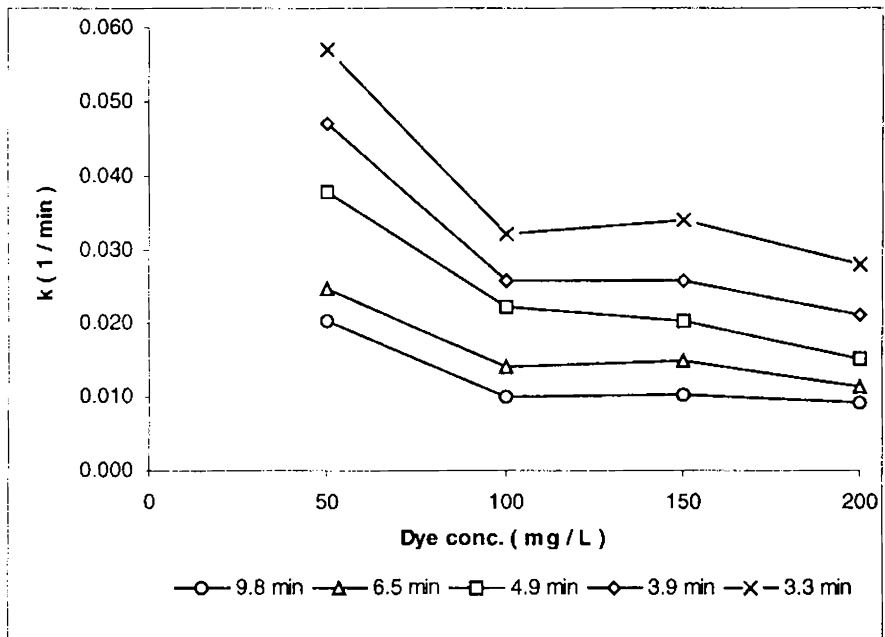


Figure 2.96  
 Direct Black EG  
 Influence of dye concentration on pseudo first order rate coefficients at pH 4 and at fixed flow rates.

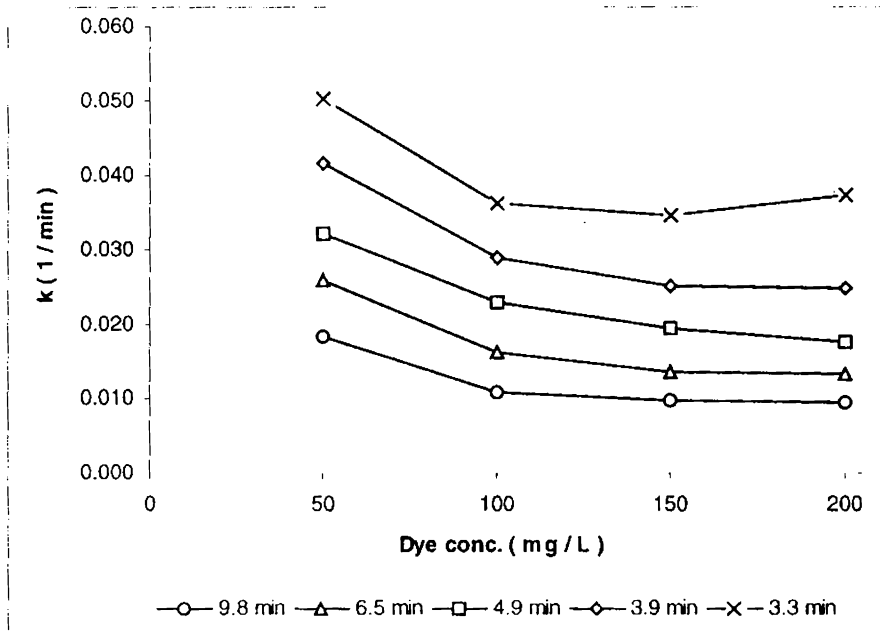


Figure 2.97  
 Direct Black EG  
 Influence of dye concentration on pseudo first order rate coefficients at pH 6 and at fixed flow rates.

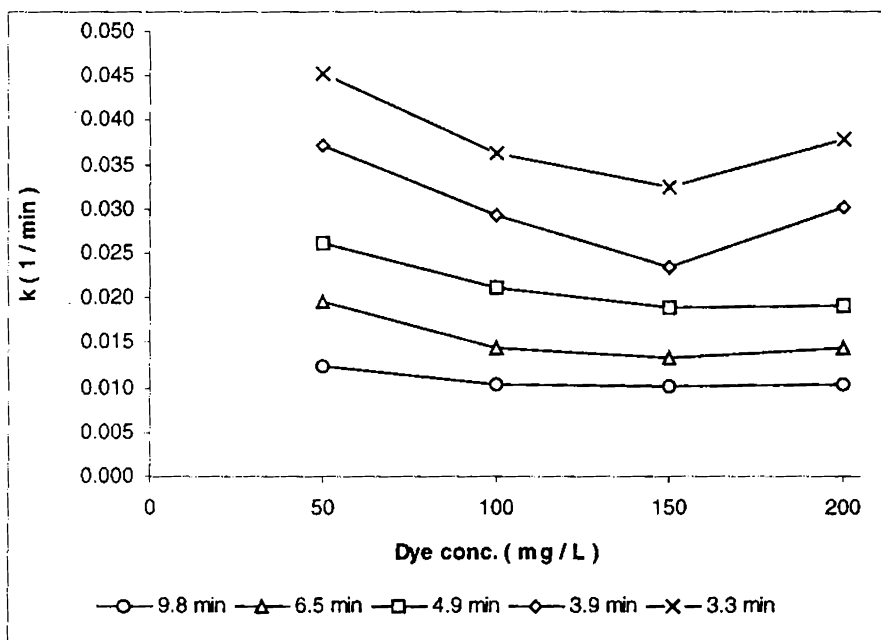


Figure 2.98  
 Direct Black EG  
 Influence of dye concentration on pseudo first order rate coefficients at pH 8 and at fixed flow rates.

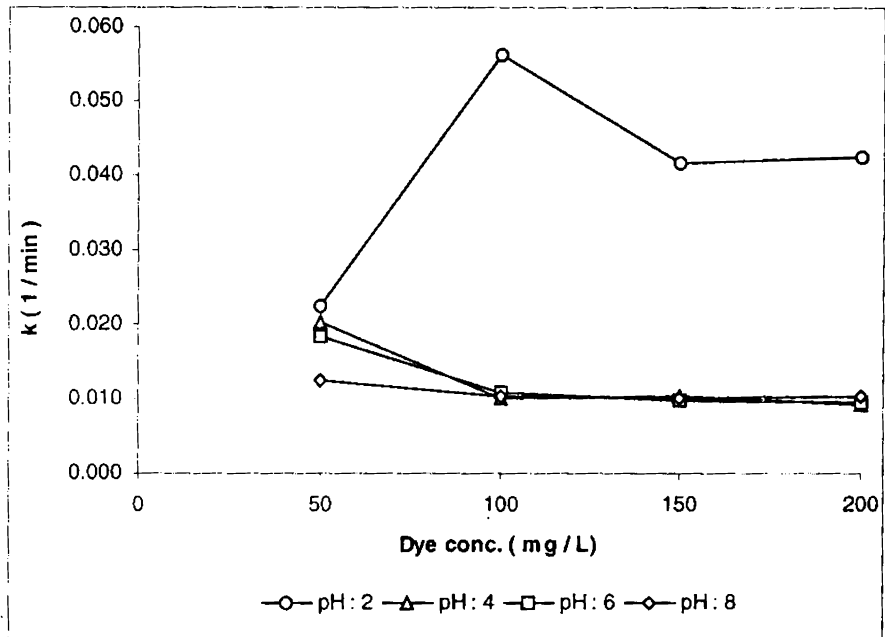


Figure 2.99  
 Direct Black EG  
 Influence of dye concentration on pseudo first order rate coefficients at a flow rate of  $20 \text{ mL min}^{-1}$  and at fixed pH.

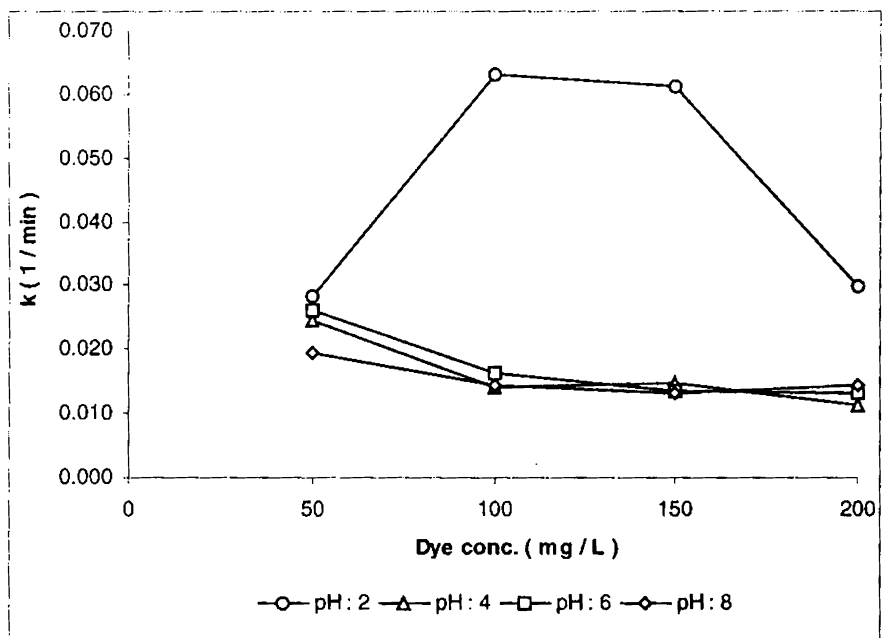


Figure 2.100  
 Direct Black EG  
 Influence of dye concentration on pseudo first order rate coefficients at a flow rate of  $30 \text{ mL min}^{-1}$  and at fixed pH.

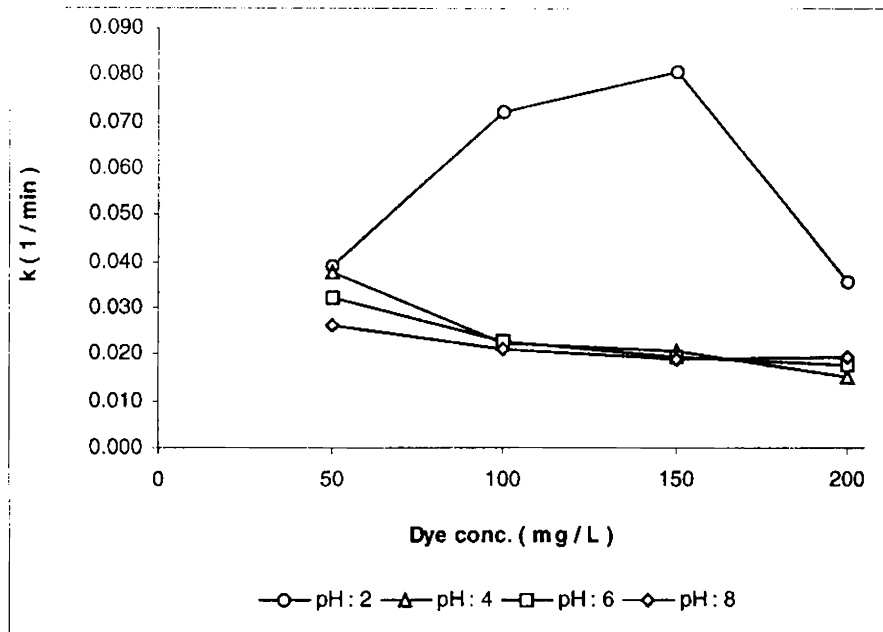


Figure 2.101  
 Direct Black EG  
 Influence of dye concentration on pseudo first order rate coefficients at a flow rate of  $40 \text{ mL min}^{-1}$  and at fixed pH.

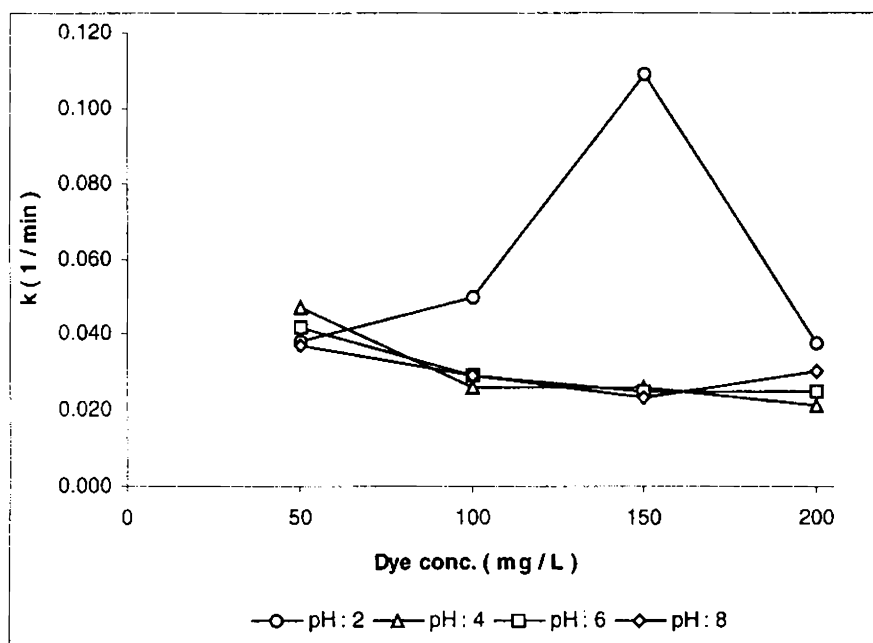


Figure 2.102  
 Direct Black EG  
 Influence of dye concentration on pseudo first order rate coefficients at a flow rate of  $50 \text{ mL min}^{-1}$  and at fixed pH.

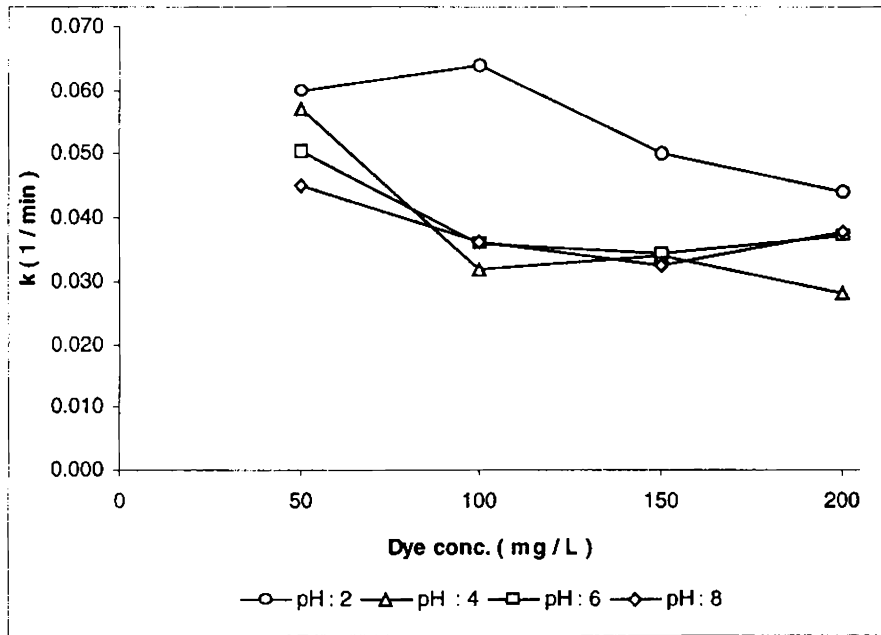


Figure 2.103  
Direct Black EG  
Influence of dye concentration on pseudo first order rate coefficients at a flow rate of  $60 \text{ mL min}^{-1}$  and at fixed pH.

### 2.9.3. Direct Catachine Brown

It was observed that the data fit well into linear first order plots and the influence of the initial dye concentrations has been studied by monitoring the variation in the pseudo-first order rate coefficients. Figures 2.104 to 2.108 presents the first order fit of the observations.

(i) Comparison between concentration and flow rate at constant pH

Figure 2.109 illustrates the influence of dye concentration on pseudo-first order rate coefficients at pH 2 and fixed flow rates. At pH 2, it is observed that there is a decrease in the rate coefficient with an increase in concentration. However, the behavior of the pseudo first order rate coefficient was strongly influenced by flow rate. Under low flow rates (20 and 30 mL min<sup>-1</sup>), a linear decrease in the rate coefficients for an increase in concentration is observed. With an increase in flow rates the rate coefficients were found to increase as the concentration was raised from 50 to 100 mg L<sup>-1</sup>, after which the rate coefficients were found to decrease.

Figure 2.110 is a representation of influence of dye concentration on pseudo first order rate coefficients at pH 4 and fixed flow rates. At pH 4 the general trend observed is a decrease in the rate coefficient with an increase in concentration.

Figure 2.111 illustrates the influence of dye concentration on pseudo-first order rate coefficients at pH 6 and fixed flow rates. As the pH is raised to 6, for a flow rate of 20 mL min<sup>-1</sup> the rate coefficient showed an initial decrease with an increase in concentration from 50 to 100 mg L<sup>-1</sup> after which for a further increase in concentration, the rate coefficient was



found to increase. However, since there is no major difference in the rate coefficients after a concentration of  $100 \text{ mg L}^{-1}$  the rate coefficients can be considered independent of concentration.

Figure 2.112 is a representation of influence of dye concentration on pseudo first order rate coefficients at pH 8 and fixed flow rates. With an increase in pH to 8, rate coefficients for flow rates of 20, 30 and  $60 \text{ mL min}^{-1}$ , showed similar trends of decrease with an increase in concentration up to  $150 \text{ mg L}^{-1}$  after which the lowest flow rate became independent of concentration, while that of the higher flow rates recorded an increase in rate coefficient for a further increase in concentration. However, rate coefficients for flow rates of 30 and  $40 \text{ mL min}^{-1}$  become independent of concentration above  $100 \text{ mg L}^{-1}$ .

(ii) Comparison between concentration and pH at constant flow rate

Comparisons were made between the rate coefficients of the different pH at a specific flow rate against the range of concentrations studied.

Influence of dye concentration on the pseudo first order rate coefficients at a flow rate of  $20 \text{ mL min}^{-1}$  and fixed pH is shown in figure 2.113. At a flow rate of  $20 \text{ mL min}^{-1}$  the general trend observed is a decrease in the rate coefficients for increase in concentration. However, the variation of the pseudo first order rate coefficient was found pH dependent. At pH 2, a linear decrease in the rate coefficients with increase in concentration is observed. At pH 4, the rate coefficients were found independent of concentration up to  $100 \text{ mg L}^{-1}$ , after which a decrease is

observed at  $150 \text{ mg L}^{-1}$  before showing an increase at  $200 \text{ mg L}^{-1}$ . pH 6 and 8 show similar trends of decrease in rate coefficients up to a concentration of  $150 \text{ mg L}^{-1}$ , after which an increase is observed at concentration of  $200 \text{ mg L}^{-1}$  for pH 6, while at pH 8 the rate coefficients become independent of concentrations above  $150 \text{ mg L}^{-1}$ .

Figure 2.114 is a representation of the influence of dye concentration on pseudo first order rate coefficients at a flow rate of  $30 \text{ mL min}^{-1}$  and fixed pH. With an increase in the flow rate to  $30 \text{ mL min}^{-1}$ , pH 2 and 4 showed similar trends of decrease in the rate coefficient with increase in concentration (except for a random value observed at a concentration of  $150 \text{ mg L}^{-1}$  for pH 4). At pH 6, after an initial decrease the rate coefficients were found to increase steadily with increase in concentration. However, at pH 8, the decrease continued up to a concentration of  $150 \text{ mg L}^{-1}$  after which an increase in the rate coefficient is observed at  $200 \text{ mg L}^{-1}$ .

Influence of dye concentration on the pseudo first order rate coefficients at a flow rate of  $40 \text{ mL min}^{-1}$  and fixed pH is shown in figure 2.115. As the flow rate was raised to  $40 \text{ mL min}^{-1}$ , pH 2 and 4, showed a decrease in the rate coefficients for an increase in concentration, while pH 6, after an initial decrease continued to show a marginal increase with increase in concentration, while pH 8, can be considered more or less independent of concentration beyond  $100 \text{ mg L}^{-1}$ .

Figure 2.116 is a representation of the influence of dye concentration on pseudo first order rate coefficients at a flow rate of  $50 \text{ mL}$

$\text{min}^{-1}$  and fixed pH. Influence of dye concentration on the pseudo first order rate coefficients at a flow rate of  $60 \text{ mL min}^{-1}$  and fixed pH is shown in figure 2.117. Higher flow rates of both  $50$  and  $60 \text{ mL min}^{-1}$  showed similar trends (as shown in figure 2.116 and 2.117). pH 2 showed an increase in the rate coefficient with an increase in concentration from  $50$  to  $100 \text{ mg L}^{-1}$  while for the same concentration, pH 4 showed a decrease; after which the rate coefficients for both pH 2 and 4 was found to decrease with an increase in concentration. pH 6 continued to show similar characteristics observed at the lower flow rate ( $40 \text{ mL min}^{-1}$ ) while at pH 8, a decrease in the rate coefficients is observed up to  $150 \text{ mg L}^{-1}$ , after which the rate coefficient increases for a further increase in concentration. However, in all cases, the increase in rate coefficients after an initial decrease is found marginal.

The general trend observed is that the rate coefficients decrease with an increase in concentration. The variation in rate coefficients with concentration is a function of both flow rates and pH, with a significant difference between the rate coefficients at all flow rates for all the concentration range studied under acidic conditions (pH 2). However, at higher pH (4 and above) a significant difference in the rate coefficients is observed only at low concentrations.

The decrease in the rate coefficients at high dye concentrations can be attributed to the dye molecule exerting its influence as a corrosion inhibitor, forming an oxidized layer of corrosion products over the metal surface, thereby preventing the electron transfer required for the reduction

reaction to occur. This argument is justified from the plots indicating a significant difference in the rate coefficients at low dye concentrations, with the difference decreasing as the concentration is raised and then becoming comparable with out any major difference at higher dye concentrations.

In some cases it is observed that there is an increase in the rate coefficients after an initial decrease. This trend is observed either at high concentrations (above  $100 \text{ mg L}^{-1}$ ) or at high pH (above 4) or at high flow rates (above  $40 \text{ mL min}^{-1}$ ). Under each of these conditions the primary mechanism involved behind the observed decrease in the dye concentration is chiefly attributed to the physical processes such as adsorption, where mass transport of the dye molecules from the bulk solution to the metal surface becomes the limiting factor influencing the decolorization mechanism. Under such conditions, the column being a flow through system results in the partial removal of the dye layer formed over the metal surface through the shear force created by the increased flow rates. The random behavior is observed only between pH 4, 6 and 8 where the decrease in dye concentration could be chiefly attributed to adsorption. The rate coefficients although tend to fluctuate between these pH ranges, the values were in most cases found lower than that at pH 2, indicating that the discrepancies observed could be due to similar phenomenon occurring at these pH ranges in solutions that are not strongly buffered.

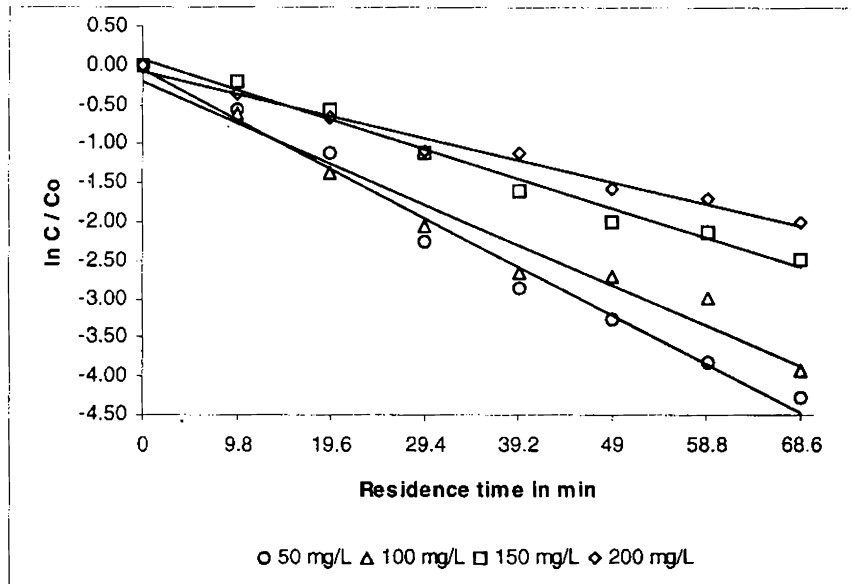


Figure 2.104  
 Direct Catachine Brown  
 Plots confirming first order with respect to concentration at pH 2 and at a flow rate of 20 mL min<sup>-1</sup>

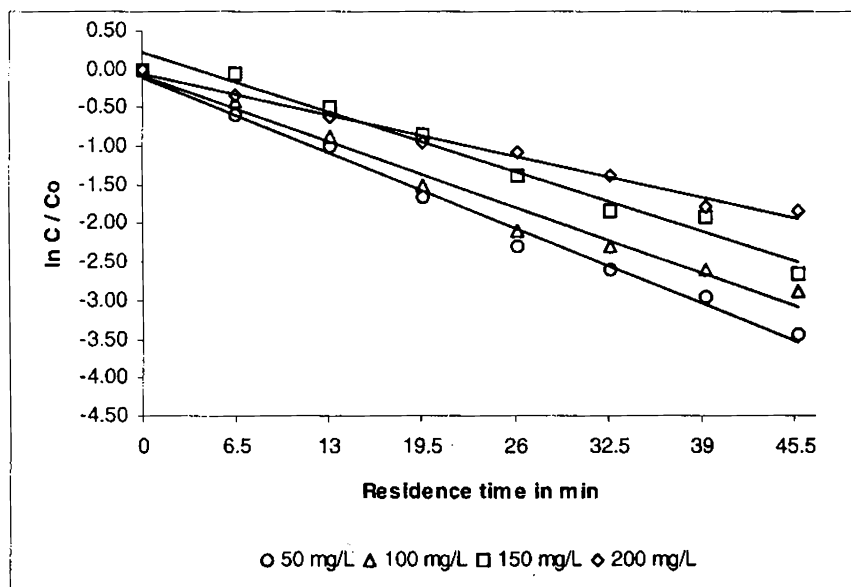


Figure 2.105  
 Direct Catachine Brown  
 Plots confirming first order with respect to concentration at pH 2 and at a flow rate of 30 mL min<sup>-1</sup>

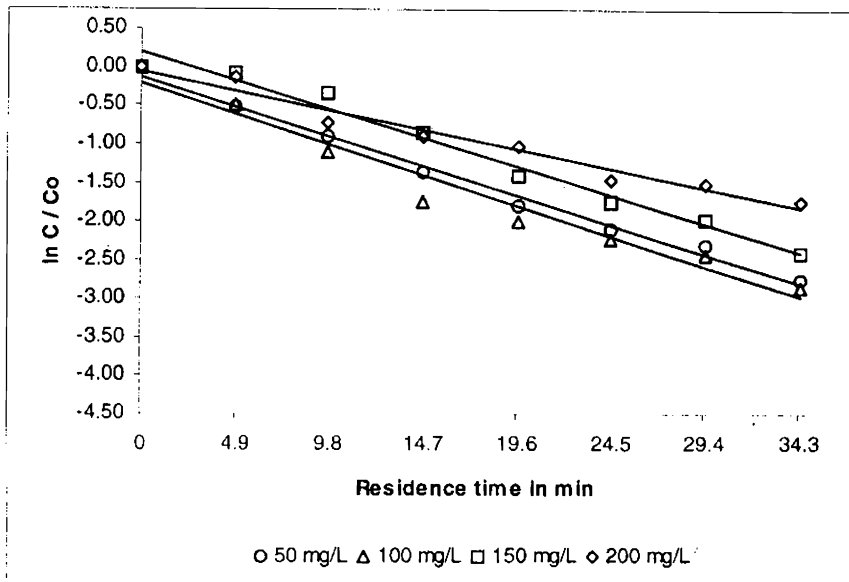


Figure 2.106  
 Direct Catachine Brown  
 Plots confirming first order with respect to concentration at pH 2 and at a flow rate of 40 mL min<sup>-1</sup>

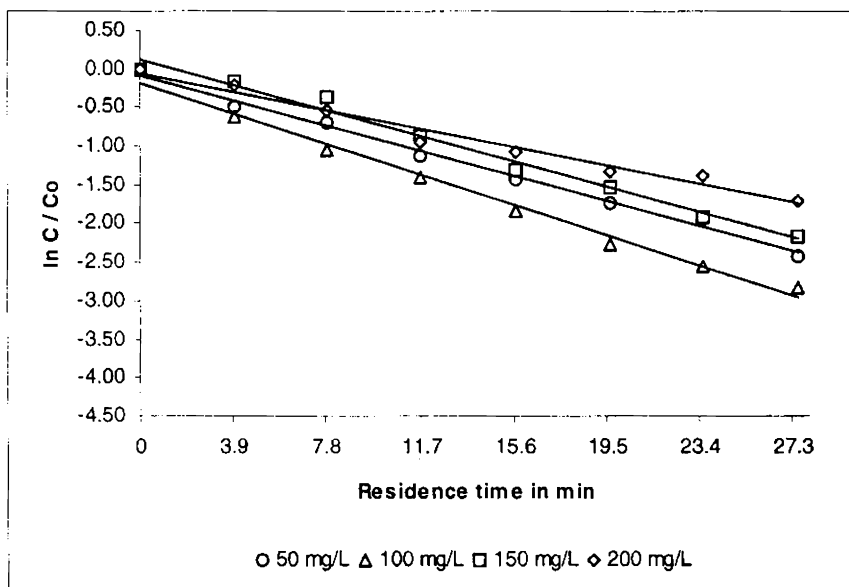


Figure 2.107  
 Direct Catachine Brown  
 Plots confirming first order with respect to concentration at pH 2 and at a flow rate of 50 mL min<sup>-1</sup>

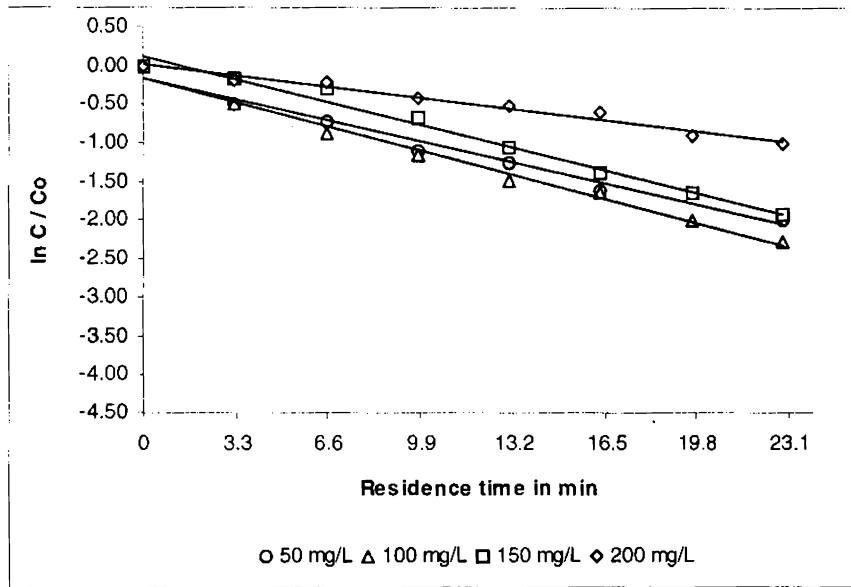


Figure 2.108  
Direct Catachine Brown  
Plots confirming first order with respect to concentration at pH 2 and at a flow rate of  $60 \text{ mL min}^{-1}$

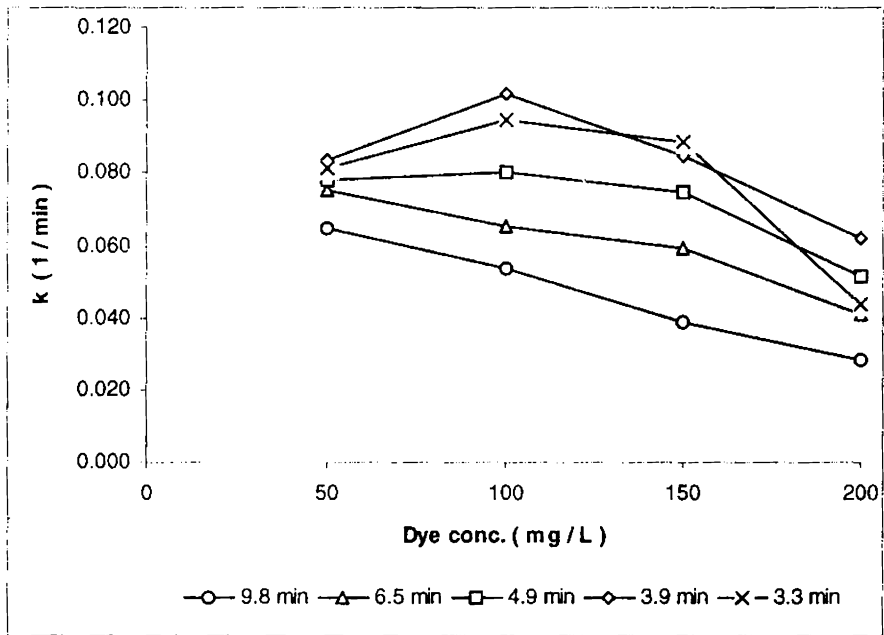


Figure 2.109  
 Direct Catachine Brown  
 Influence of dye concentration on pseudo first order rate coefficients at pH 2 and at Fixed flow rates.

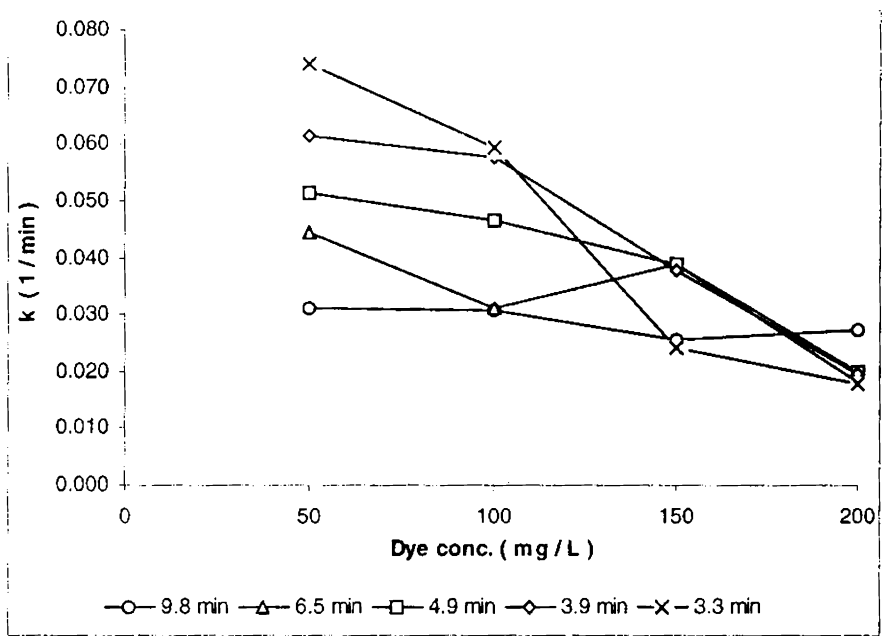


Figure 2.110  
 Direct Catachine Brown  
 Influence of dye concentration on pseudo first order rate coefficients at pH 4 and at Fixed flow rates.



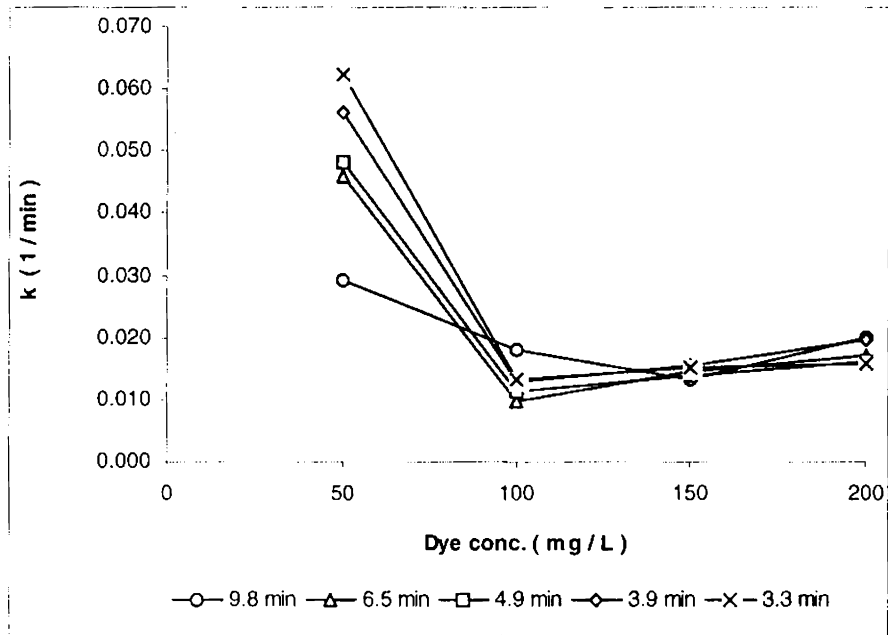


Figure 2.111  
 Direct Catachine Brown  
 Influence of dye concentration on pseudo first order rate coefficients at pH 6 and at fixed flow rates.

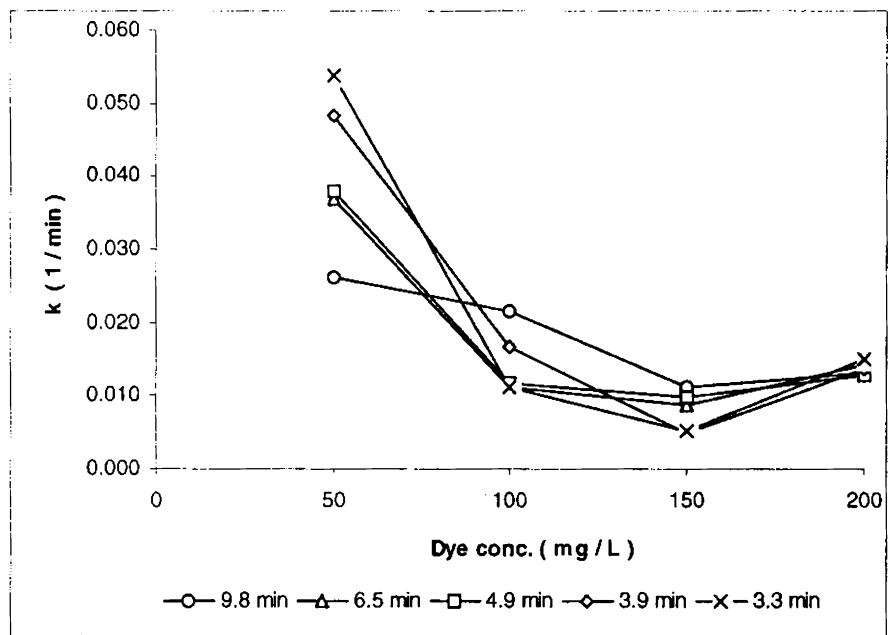


Figure 2.112  
 Direct Catachine Brown  
 Influence of dye concentration on pseudo first order rate coefficients at pH 8 and at fixed flow rates.

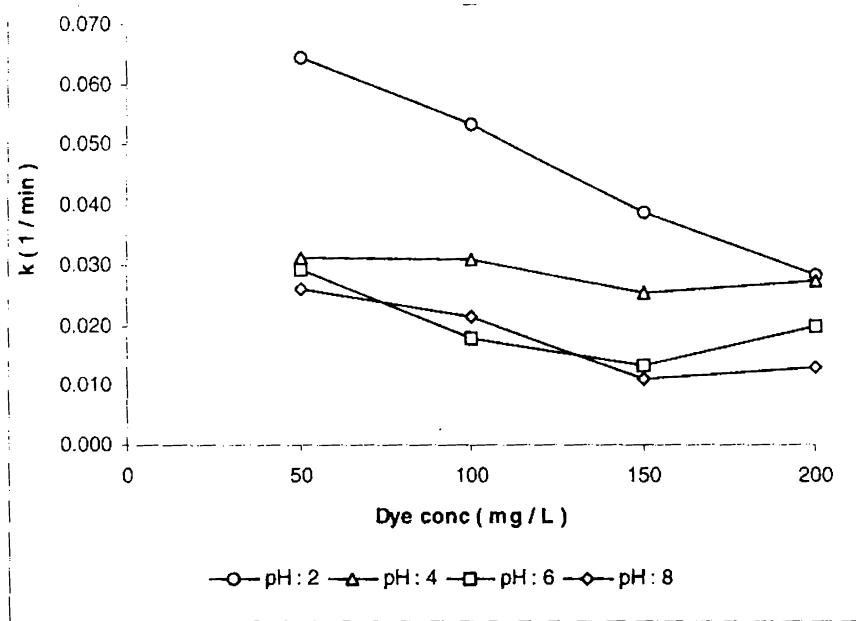


Figure 2.113  
 Direct Catachine Brown  
 Influence of dye concentration on pseudo first order rate coefficients at a flow rate of 20 mL min<sup>-1</sup> and at fixed pH.

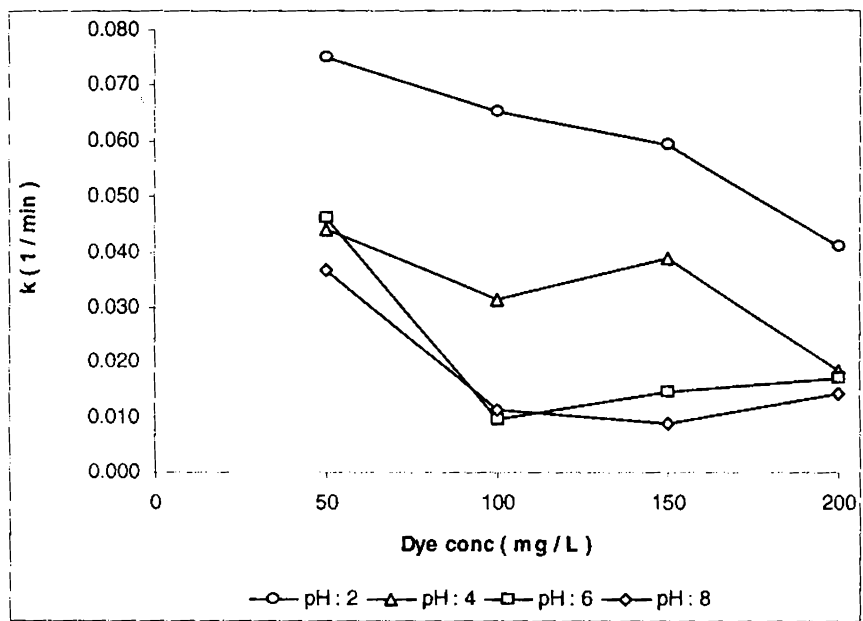


Figure 2.114  
 Direct Catachine Brown  
 Influence of dye concentration on pseudo first order rate coefficients at a flow rate of 30 mL min<sup>-1</sup> and at fixed pH.

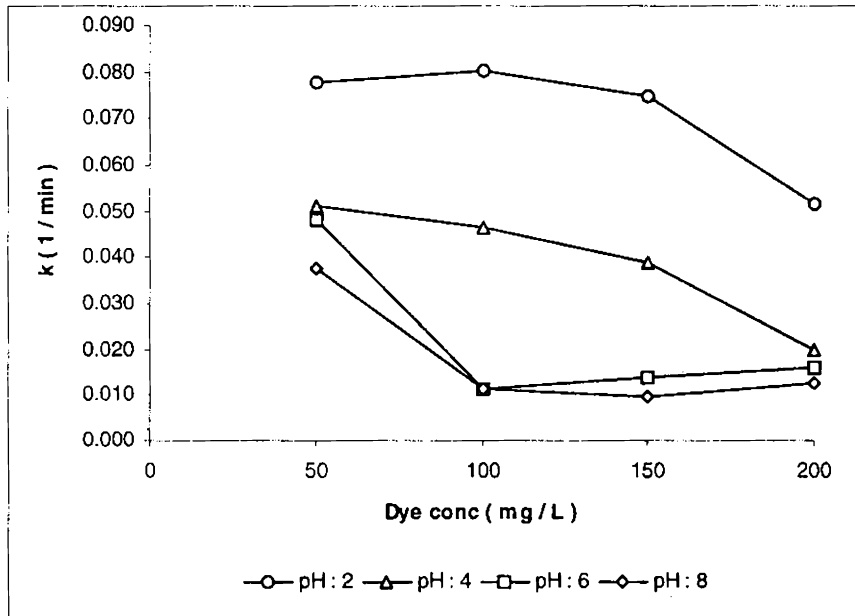


Figure 2.115  
 Direct Catachine Brown  
 Influence of dye concentration on pseudo first order rate coefficients at a flow rate of  $40 \text{ mL min}^{-1}$  and at fixed pH.

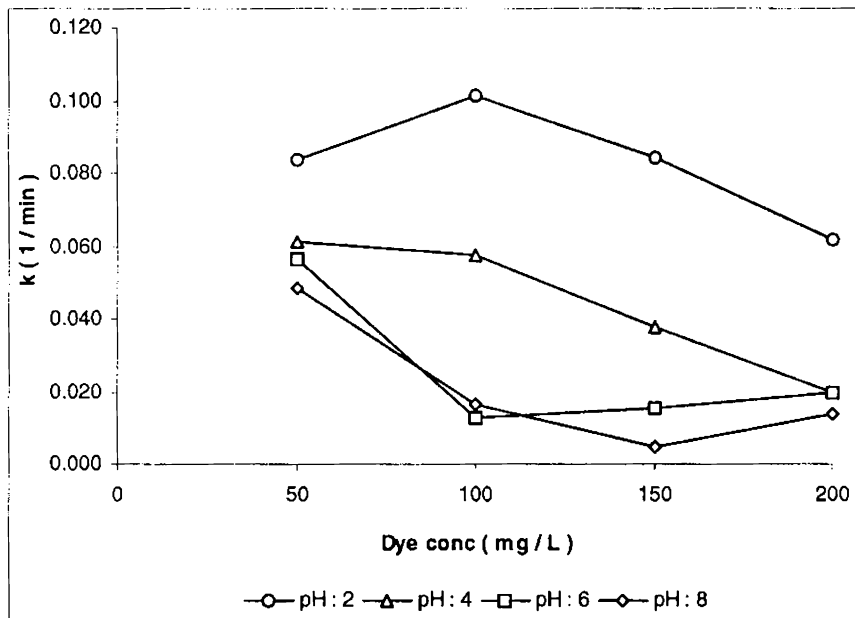


Figure 2.116  
 Direct Catachine Brown  
 Influence of dye concentration on pseudo first order rate coefficients at a flow rate of  $50 \text{ mL min}^{-1}$  and at fixed pH.

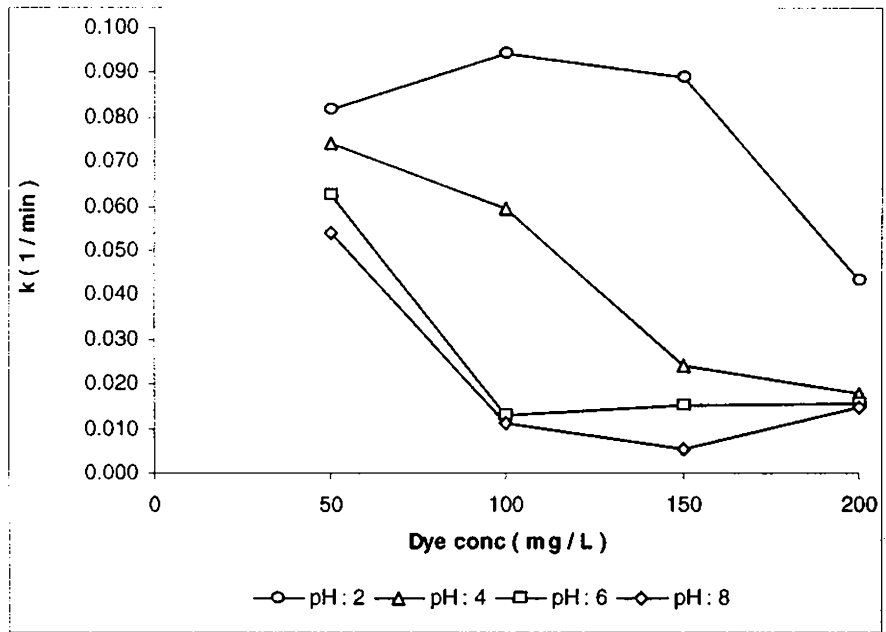


Figure 2.117  
Direct Catachine Brown  
Influence of dye concentration on pseudo first order rate coefficients at a flow rate of  $60 \text{ mL min}^{-1}$  and at fixed pH.

#### 2.9.4. Direct Green-B

It was observed that the data fit well into linear first order plots and the influence of the initial dye concentrations has been studied by monitoring the variation in the pseudo-first order rate coefficients. The following figures 2.118 to 2.122 presents the first order fit of the observations.

(i) Comparison between concentration and flow rate at constant pH

Figure 2.123 illustrates the influence of dye concentration on pseudo-first order rate coefficients at pH 2 and fixed flow rates. At pH 2, the rate coefficients was found to decrease with an increase in concentration from 50 to 100 mg L<sup>-1</sup> for flow rates up to 40 mL min<sup>-1</sup>. However, an increase in the rate coefficients is observed at a concentration of 150 mg L<sup>-1</sup> before decreasing again for a further increase in concentration. However, as the flow rate was increased it is observed that the magnitude of increase in the rate coefficient at this concentration (150 mg L<sup>-1</sup>) was found to decrease. At a flow rate of 50 mL min<sup>-1</sup>, the rate coefficients was found to decrease over the entire concentration range studied, before showing a linear decrease in the rate coefficient for a higher flow rate of 60 mL min<sup>-1</sup>.

Figure 2.124 is a representation of influence of dye concentration on pseudo first order rate coefficients at pH 4 and fixed flow rates. With an increase in pH to 4, it is observed that the rate coefficients become independent of concentration at a flow rate of 20 mL min<sup>-1</sup>, while at a flow rate of 30 mL min<sup>-1</sup>, a linear decrease in the rate coefficient for an increase

in concentration is observed. However, flow rates at 40 and 50 mL min<sup>-1</sup> showed similar trends of an initial increase in rate coefficient as the concentration was raised from 50 to 100 mg L<sup>-1</sup> followed by a decrease at 150 mg L<sup>-1</sup>, after which it becomes independent of concentration at flow rate of 40 ml/min while a continued decrease is observed at a flow rate of 50 mL min<sup>-1</sup>. With a further increase in flow rate to 60 mL min<sup>-1</sup>, a linear decrease in the rate coefficient for an increase in concentration is observed.

Figure 2.125 illustrates the influence of dye concentration on pseudo-first order rate coefficients at pH 6 and fixed flow rates. As the pH was raised to 6, for a flow rate of 20 mL min<sup>-1</sup>, the rate coefficient was found to increase with an increase in concentration up to 150 mg L<sup>-1</sup> after which a decrease is observed for a further increase to 200 mg L<sup>-1</sup>. At a flow rate of 30 mL min<sup>-1</sup> the rate coefficient was found independent of concentration up to 150 mg L<sup>-1</sup> after that a decrease is observed. The rate coefficient was found to behave randomly with no apparent trend at a flow rate of 40 mL min<sup>-1</sup>. For a flow rate of 50 mL min<sup>-1</sup> the rate coefficient after an initial decrease in concentration from 50 to 100 mg L<sup>-1</sup> was found to increase at 150 mg L<sup>-1</sup>, before becoming independent of concentration. At a higher flow rate of 60 mL min<sup>-1</sup> the rate coefficient was found to increase linearly with an increase in concentration up to 150 mg L<sup>-1</sup> after which a decrease is observed.

Figure 2.126 is a representation of influence of dye concentration on pseudo first order rate coefficients at pH 8 and fixed flow rates. As the pH

was raised to 8, for a flow rate of  $20 \text{ mL min}^{-1}$ , the rate coefficient was found to become independent of concentration up to  $150 \text{ mg L}^{-1}$  before recording a decrease at  $200 \text{ mg L}^{-1}$ . All higher flow rates showed similar trends of increase in rate coefficient as the concentration was raised from 50 to  $100 \text{ mg L}^{-1}$  after that a decrease in the rate coefficient is observed at  $150 \text{ mg L}^{-1}$ . At a concentration of  $200 \text{ mg L}^{-1}$  all flow rates except  $50 \text{ mL min}^{-1}$  (where the rate coefficient was found to become independent of concentration above  $150 \text{ mg L}^{-1}$ ), the rate coefficients was found to increase as the concentration was increased to  $200 \text{ mg L}^{-1}$ .

(ii) Comparison between concentration and pH at constant flow rate

Observations were made by comparing the rate coefficients obtained for the various pH at specific flow rate over the range of concentrations.

Influence of dye concentration on the pseudo first order rate coefficients at a flow rate of  $20 \text{ mL min}^{-1}$  and fixed pH is shown in figure 2.127. At a flow rate of  $20 \text{ mL min}^{-1}$ , it is observed that the rate coefficients become independent of concentration at pH 2 and 4. As the pH was raised to 6, an increase in the rate coefficient is observed as the concentration was raised from 50 to  $150 \text{ mg L}^{-1}$ , after which the values decreased at  $200 \text{ mg L}^{-1}$ . However, at pH 8 the rate coefficient was found to behave randomly with out any apparent trend.

Figure 2.128 is a representation of the influence of dye concentration on pseudo first order rate coefficients at a flow rate of  $30 \text{ mL min}^{-1}$  and fixed pH. As the flow rate was raised to  $30 \text{ mL min}^{-1}$ , rate

coefficients at pH 2 showed random behavior showing trends that were not interpretable. pH 4 and 8 showed similar characteristics of increase in the rate coefficient with an increase in concentration up to  $100 \text{ mg L}^{-1}$ , after which it decreases with an increase in concentration to  $150 \text{ mg L}^{-1}$  before becoming independent of concentration for pH 4, while at pH 8, after an initial increase in the rate coefficient with increase in concentration to  $100 \text{ mg L}^{-1}$ , the rate coefficient become independent of concentration up to  $150 \text{ mg L}^{-1}$ , before decreasing at  $200 \text{ mg L}^{-1}$ . While pH 6 was found independent of concentration over the range studied.

Influence of dye concentration on the pseudo first order rate coefficients at a flow rate of  $40 \text{ mL min}^{-1}$  and fixed pH is shown in figure 2.129. At a flow rate of  $40 \text{ mL min}^{-1}$ , pH 2 showed trends similar to the observation made at the lower flow rate. pH 4 and 8, showed an increase in the rate coefficient for an increase in concentration from  $50$  to  $100 \text{ mg L}^{-1}$ , while a further increase in concentration to  $150 \text{ mg L}^{-1}$  resulted in a decrease. Increase in concentration to  $200 \text{ mg L}^{-1}$  resulted in pH 4 showing a marginal decrease in the rate coefficient, while an increase is observed for pH 8. But for an initial increase in rate coefficients as the concentration was raised from  $50$  to  $100 \text{ mg L}^{-1}$ , they were found independent of concentration for pH 6.

Figure 2.130 is a representation of the influence of dye concentration on pseudo first order rate coefficients at a flow rate of  $50 \text{ mL min}^{-1}$  and fixed pH. As the flow rate was raised to  $50 \text{ mL min}^{-1}$ , at pH 2, a decrease in the rate coefficient with an increase in concentration is



observed. At pH 4, the rate coefficient was found independent of concentration up to  $100 \text{ mg L}^{-1}$ , after which a decrease is observed for an increase in concentration. At pH 6, the rate coefficients can be considered independent of concentration, as the difference between them does not appear significant. At pH 8, the rate coefficients were found to increase with an increase in concentration from 50 to  $100 \text{ mg L}^{-1}$  followed by a decrease in rate coefficient as the concentration was raised to  $150 \text{ mg L}^{-1}$  and then becomes independent.

Influence of dye concentration on the pseudo first order rate coefficients at a flow rate of  $60 \text{ mL min}^{-1}$  and fixed pH is shown in figure 2.131. At a higher flow rate of  $60 \text{ mL min}^{-1}$ , pH 2 and 4, showed a linear decrease in the rate coefficients for an increase in concentration. pH 6 continued to remain independent of concentration, while pH 8 showed an increase in the rate coefficient as the concentration was raised from 50 to  $100 \text{ mg L}^{-1}$ , after which it decreased for a further increase in concentration to  $150 \text{ mg L}^{-1}$ , before showing an increase in the rate coefficient with an increase in concentration to  $200 \text{ mg L}^{-1}$ .

Going by the trends observed with respect to concentration, the general conclusion that can be drawn is that the behavior of the pseudo first order rate coefficients with respect to concentration is highly influenced both by flow rates as well as the pH of the dye solution. The observations can be grouped into the following:

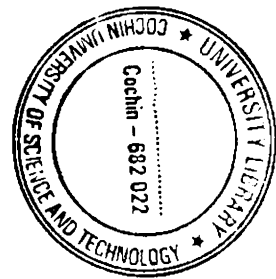
- (a) The rate coefficients decrease with an increase in concentration.

This trend indicates that the dye could be exerting its influence

as a corrosion inhibitor. The increased accumulation of the dye at the surface of the metal forms a passivating layer that prevents the transfer of electrons at the metal surface needed to reduce the dye. Moreover, it is established that amines such as aniline, which could be formed as a result of the cleavage of the azo linkages, can function as effective corrosion inhibitors. Therefore, an increased accumulation of both dye as well as its reduction product (amines), over the metal surface can result in a decrease in the rate of the reaction.

- (b) The rate coefficients increase as the concentration is raised from 50 to 100 mg L<sup>-1</sup>, after which a decrease is observed. This probably suggests that up to a concentration of 100 mg L<sup>-1</sup>, the dyes are not inhibitory and it is only over this concentration that the molecules become inhibiting.
- (c) Random behavior of the rate coefficients particularly at pH 6 and 8, with no apparent trends. Being a heterogeneous system, it is apparent that the system involves many inherent errors. Therefore, the data has been subjected to statistical analysis and attempt made to account for the observations.
- (d) Rate coefficients becoming independent of concentration particularly at concentrations greater than 150 mg L<sup>-1</sup>. This trend suggest that the dyes can function as corrosion inhibitors beyond certain concentrations after which, once a passivating layer of

the dye has been formed over the metal surface the rate coefficients become independent of concentration.



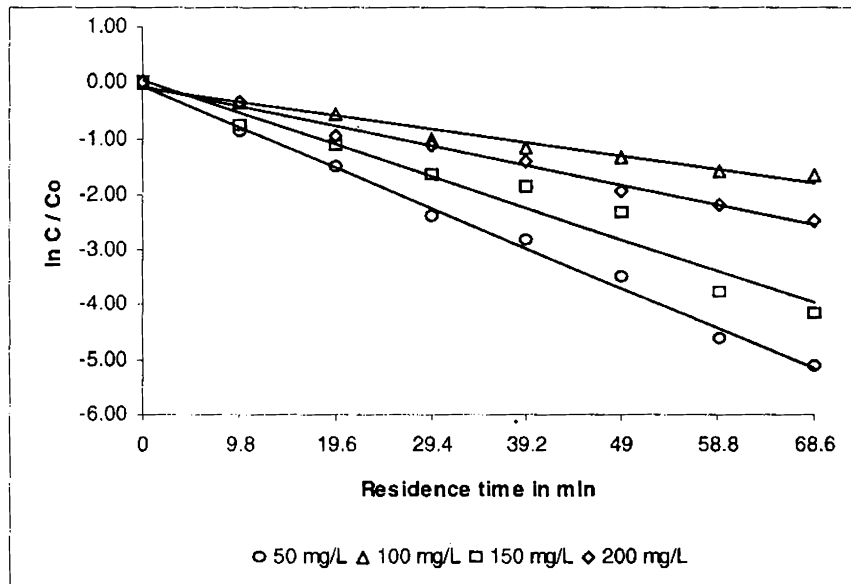


Figure 2.118  
 Direct Green - B  
 Plots confirming first order with respect to concentration at pH 2 and at a flow rate of 20 mL min<sup>-1</sup>

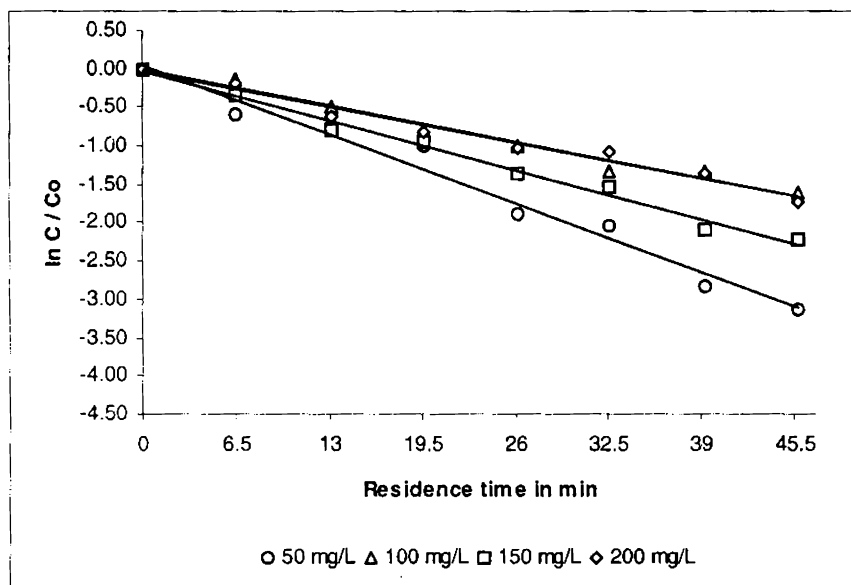


Figure 2.119  
 Direct Green - B  
 Plots confirming first order with respect to concentration at pH 2 and at a flow rate of 30 mL min<sup>-1</sup>

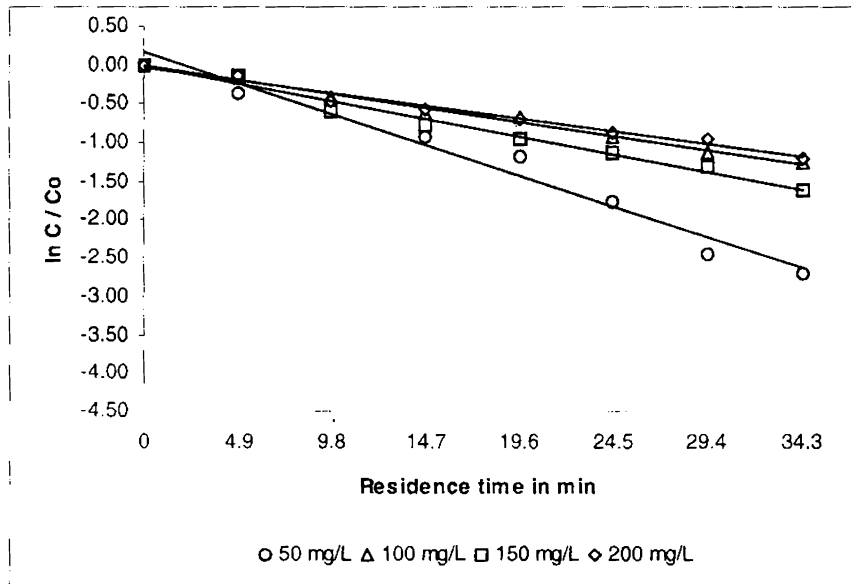


Figure 2.120  
Direct Green - B  
Plots confirming first order with respect to concentration at pH 2 and at a flow rate of 40 mL min<sup>-1</sup>

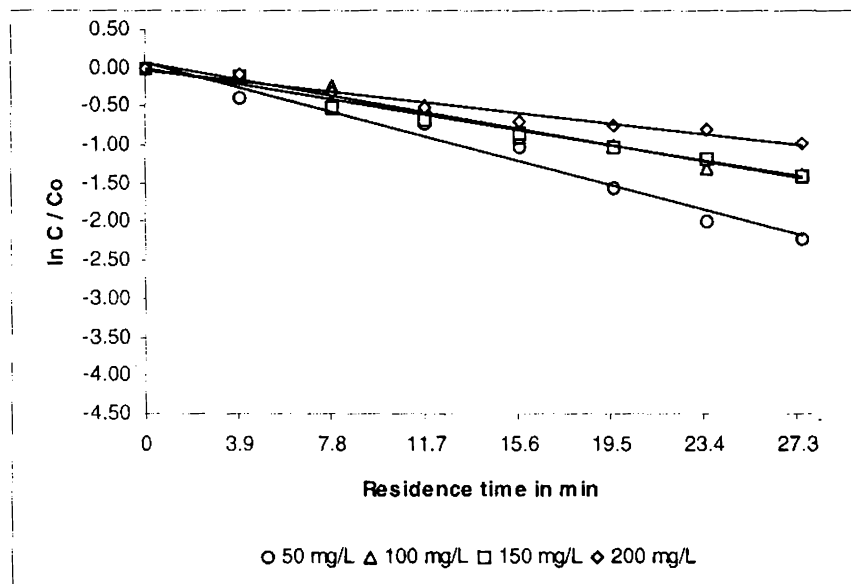


Figure 2.121  
Direct Green - B  
Plots confirming first order with respect to concentration at pH 2 and at a flow rate of 50 mL min<sup>-1</sup>

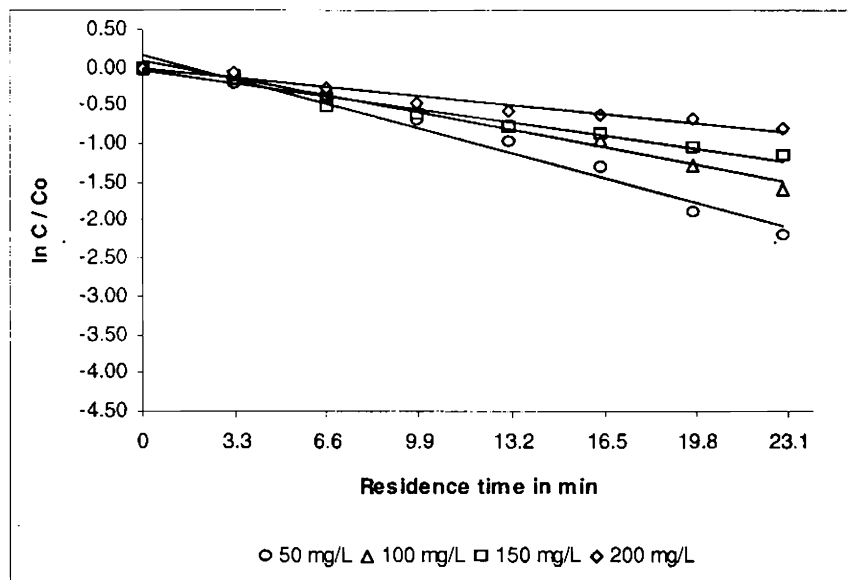


Figure 2.122  
Direct Green - B  
Plots confirming first order with respect to concentration at pH 2 and at a flow rate of  $60 \text{ mL min}^{-1}$

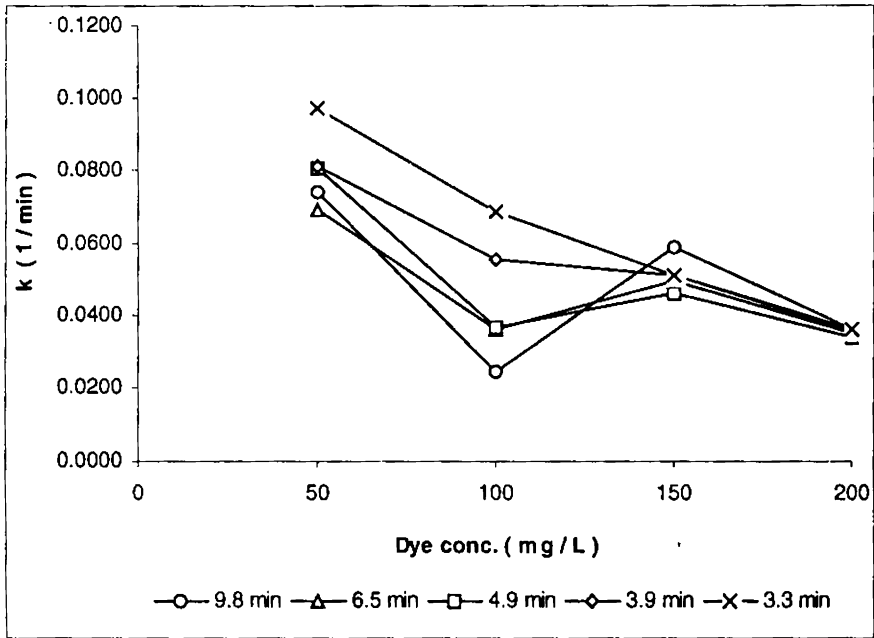


Figure 2.123  
 Direct Green - B  
 Influence of dye concentration on pseudo first order rate coefficients at pH 2 and at fixed flow rates.

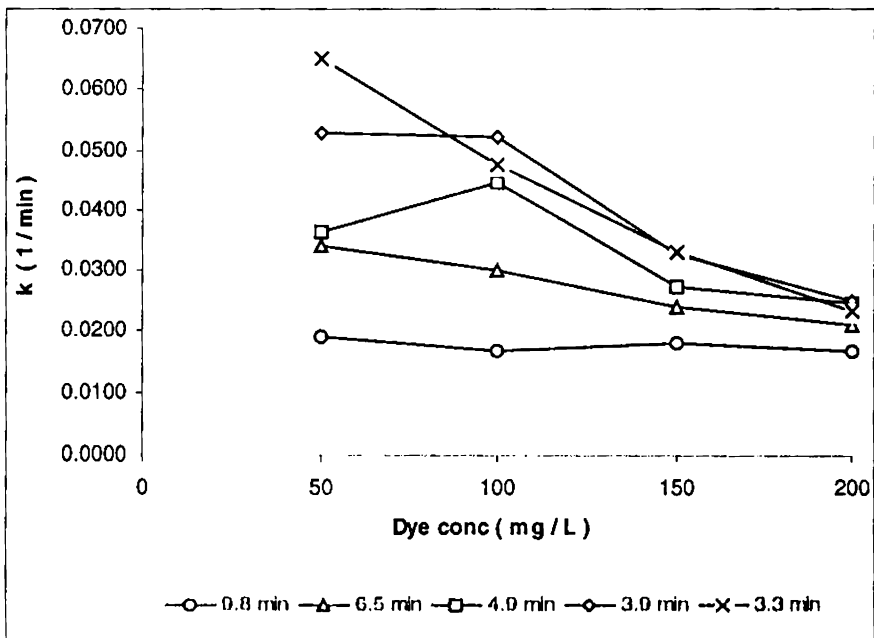


Figure 2.124  
 Direct Green - B  
 Influence of dye concentration on pseudo first order rate coefficients at pH 4 and at Fixed flow rates.

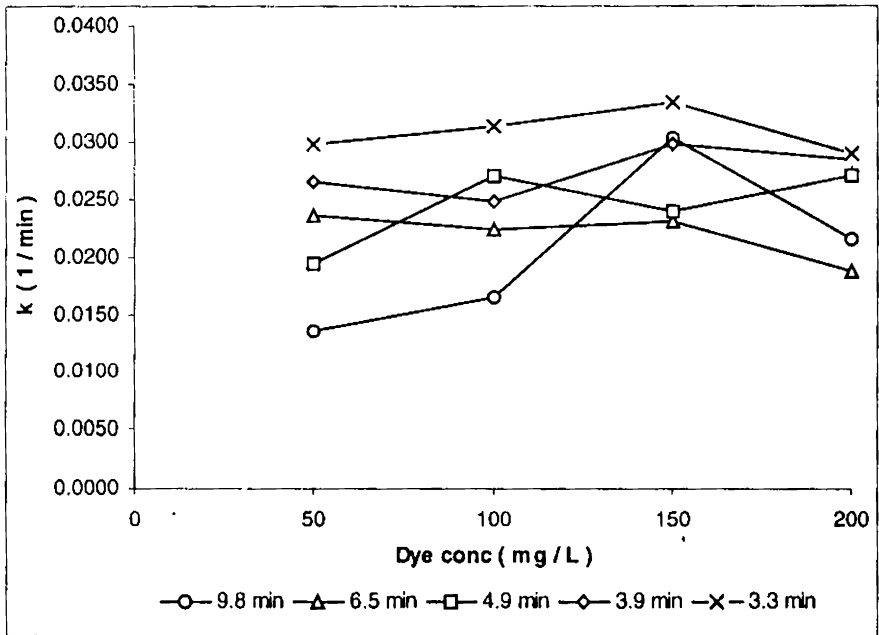


Figure 2.125  
Direct Green - B  
Influence of dye concentration on pseudo first order rate coefficients at pH 6 and at fixed flow rates.

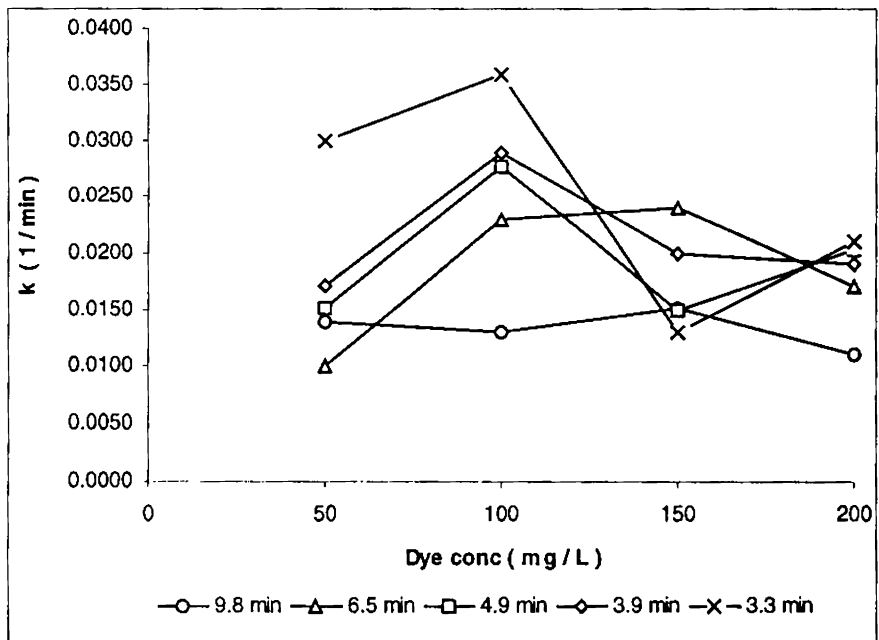


Figure 2.126  
Direct Green - B  
Influence of dye concentration on pseudo first order rate coefficients at pH 8 and at fixed flow rates.



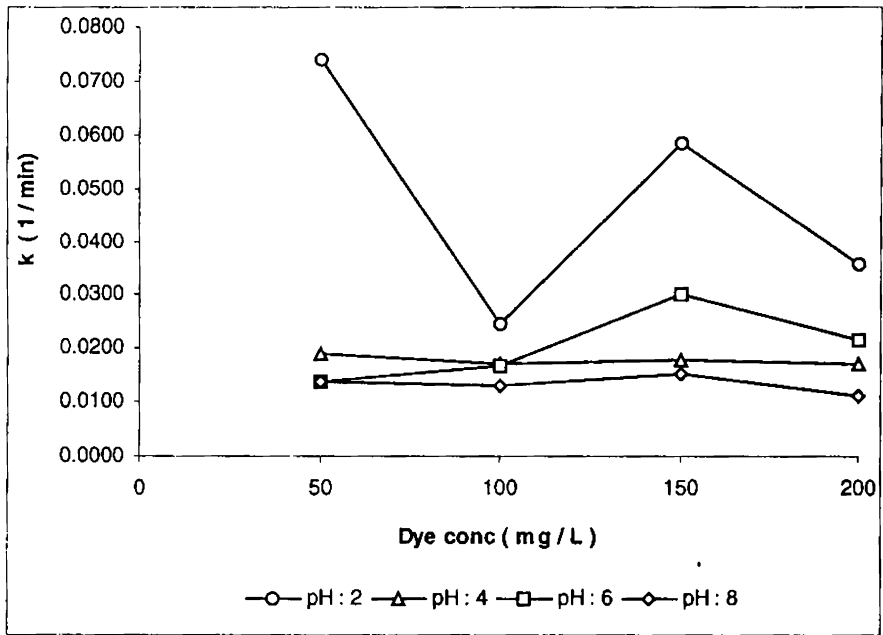


Figure 2.127  
 Direct Green - B  
 Influence of dye concentration on pseudo first order rate coefficients at a flow rate of  $20 \text{ mL min}^{-1}$  and at fixed pH.

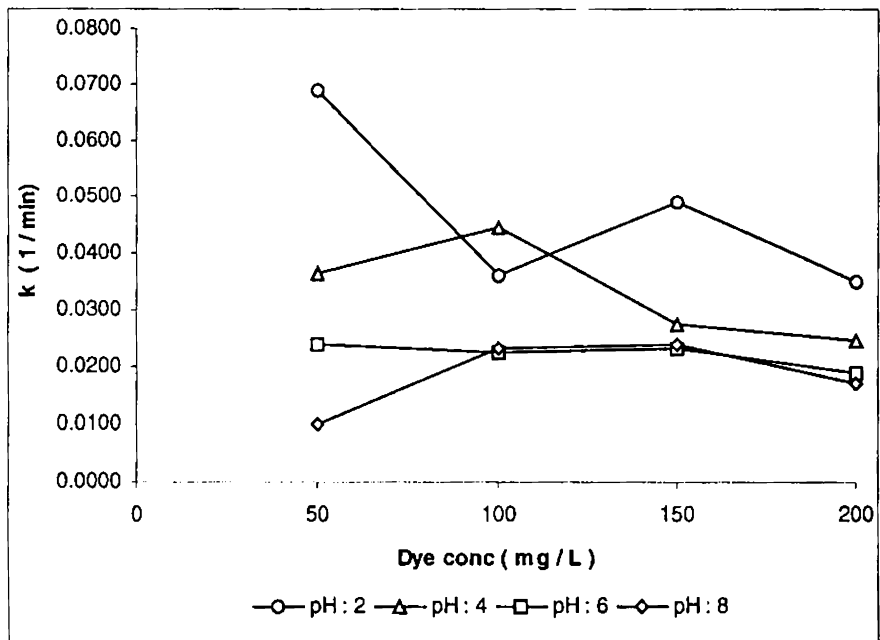


Figure 2.128  
 Direct Green - B  
 Influence of dye concentration on pseudo first order rate coefficients at a flow rate of  $30 \text{ mL min}^{-1}$  and at fixed pH.

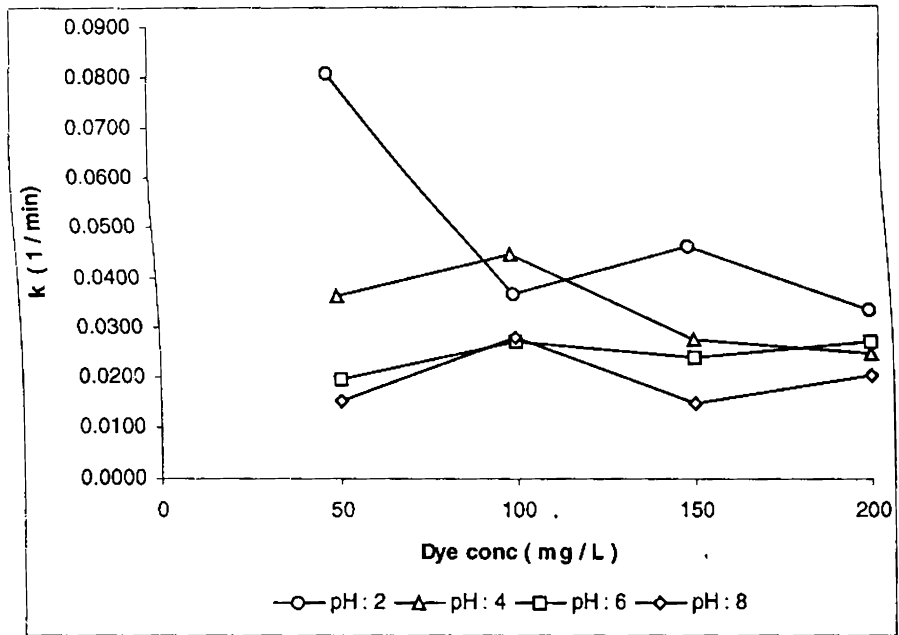


Figure 2.129  
Direct Green - B  
Influence of dye concentration on pseudo first order rate coefficients at a flow rate of 40 mL min<sup>-1</sup> and at fixed pH.

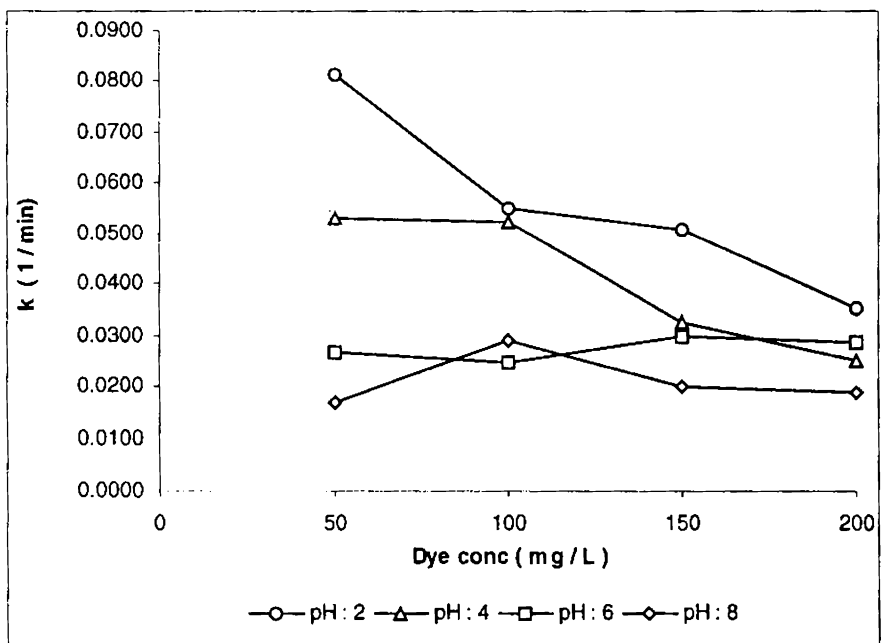


Figure 2.130  
Direct Green - B  
Influence of dye concentration on pseudo first order rate coefficients at a flow rate of 50 mL min<sup>-1</sup> and at fixed pH.

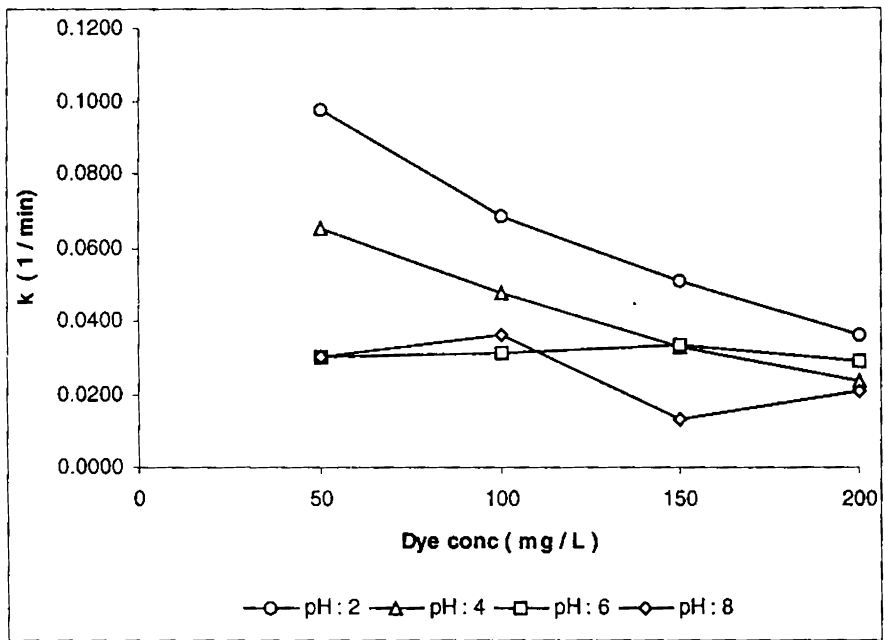


Figure 2.131.  
Direct Green - B  
Influence of dye concentration on pseudo first order rate coefficients at a flow rate of  $60 \text{ mL min}^{-1}$  and at fixed pH.

### 2.9.5. Yellow – 5GL

It was observed that the data fit well into linear first order plots and the influence of the initial dye concentrations has been studied by monitoring the variation in the pseudo-first order rate coefficients. The following figure (2.132 to 2.136) presents the first order fit of the observations.

(i) Comparison between concentration and flow rate at constant pH

Figure 2.137 illustrates the influence of dye concentration on pseudo-first order rate coefficients at pH 2 and fixed flow rates. At pH 2, random variation of the rate coefficient is observed at a flow rate of 20 mL min<sup>-1</sup>. As the flow rate was raised, the rate coefficients was found to increase with an increase in concentration up to 150 mg L<sup>-1</sup> after which it decreases for a further increase in concentration. This trend is observed at all flow rates beyond 20 mL min<sup>-1</sup> except at 50 mL min<sup>-1</sup>, where the rate coefficients were found to decrease at concentrations above 100 mg L<sup>-1</sup>.

Figure 2.138 is a representation of influence of dye concentration on pseudo first order rate coefficients at pH 4 and fixed flow rates. As the pH was raised to 4, at low flow rates (20 and 30 mL min<sup>-1</sup>) the rate coefficients were found independent of concentration. However, with increase in flow rates to 40 and 50 mL min<sup>-1</sup> the trend of decrease in rate coefficients for increase in concentration is observed only up to a concentration of 150 mg L<sup>-1</sup> after which the values were found to increase at 200 mg L<sup>-1</sup>. At a flow rate of 60 mL min<sup>-1</sup> the rate coefficients were found to increase with an increase in concentration.

Figure 2.139 illustrates the influence of dye concentration on pseudo-first order rate coefficients at pH 6 and fixed flow rates. At pH 6, the rate coefficients were found to increase linearly with an increase in concentration at a flow rate of  $20 \text{ mL min}^{-1}$ . At higher flow rates ( $30$  and  $40 \text{ mL min}^{-1}$ ), the rate coefficients were found to increase linearly with increase in concentration up to  $150 \text{ mg L}^{-1}$ , after which they become independent. The rate coefficients were found to increase with an increase in concentration up to  $100 \text{ mg L}^{-1}$ , after which it was found to become independent of concentration at a flow rate of  $50 \text{ mL min}^{-1}$ . For a further increase in flow rate ( $60 \text{ mL min}^{-1}$ ) similar trend is observed except that the rate coefficients increase with an increase in concentration rather than become independent of concentration above  $100 \text{ mg L}^{-1}$ .

Figure 2.140 is a representation of influence of dye concentration on pseudo first order rate coefficients at pH 8 and fixed flow rates. As the pH was raised to 8, for a flow rate of  $20 \text{ mL min}^{-1}$ , it is observed that after an initial increase in rate coefficients for an increase in concentration from  $50$  to  $100 \text{ mg L}^{-1}$ , the rate coefficients were found to become independent. Similar trend is also observed at a higher flow rate of  $30 \text{ mL min}^{-1}$  except that the rate coefficient is found to increase with an increase in concentration over  $150 \text{ mg L}^{-1}$ . At a flow rate of  $40 \text{ mL min}^{-1}$ , the rate coefficient was found independent of concentration up to  $150 \text{ mg L}^{-1}$  after which an increase in rate coefficient is observed as the concentration was raised to  $200 \text{ mg L}^{-1}$ . Flow rates of  $50$  and  $60 \text{ mL min}^{-1}$  showed similar trends of increase in rate coefficient for increase concentration.

(ii) Comparison between concentration and pH at constant flow rates

The relation between concentration and pH has been studied by monitoring the variation in the pseudo first order rate coefficients derived for the different pH against varying concentrations maintaining a constant flow rate.

Influence of dye concentration on the pseudo first order rate coefficients at a flow rate of  $20 \text{ mL min}^{-1}$  and fixed pH is shown in figure 2.141. At a flow rate of  $20 \text{ mL min}^{-1}$ , it was not possible to arrive at any definite conclusion because rate coefficients varied widely with out showing any apparent trend. The rate coefficients of pH 2 showed random variations. pH 4 showed a decrease in rate coefficients with increase in concentration, while for pH 6, a linear increase with increase in concentration is observed. At pH 8, after an initial increase with increase in concentration to  $100 \text{ mg L}^{-1}$  the rate coefficients were found independent of concentration.

Figure 2.142 is a representation of the influence of dye concentration on pseudo first order rate coefficients at a flow rate of  $30 \text{ mL min}^{-1}$  and fixed pH. As the flow rate was raised to  $30 \text{ mL min}^{-1}$ , the pattern tended to become more uniform. The rate coefficients at pH 2 were found to increase with an increase in concentration up to  $150 \text{ mg L}^{-1}$ , after which it decreases. At pH 4, the rate coefficients become independent of concentration. The rate coefficients of pH 6 were found to increase with an increase in concentration up to  $150 \text{ mg L}^{-1}$  after which it becomes independent of concentration. The rate coefficients after an initial increase

for increase in concentration from 50 to 100 mg L<sup>-1</sup> was found independent of concentration up to 150 mg L<sup>-1</sup>, before increasing again at 200 mg L<sup>-1</sup> for pH 8.

Influence of dye concentration on the pseudo first order rate coefficients at a flow rate of 40 mL min<sup>-1</sup> and fixed pH is shown in Figure 2.143. At a flow rate of 40 mL min<sup>-1</sup>, at pH 2, the rate coefficients were found independent of concentration up to 150 mg L<sup>-1</sup>, after which a decrease in rate coefficient is observed for an increase in concentration to 200 mg L<sup>-1</sup>. pH 4 and 8 showed similar trends of decrease in rate coefficients with increase in concentration up to 150 mg L<sup>-1</sup>, before showing an increase in the rate coefficient at a concentration of 200 mg L<sup>-1</sup>. However, pH 6 showed an increase with an increase in concentration up to 150 mg L<sup>-1</sup>, after which the rate coefficient was found independent of concentration.

Figure 2.144 is a representation of the influence of dye concentration on pseudo first order rate coefficients at a flow rate of 50 mL min<sup>-1</sup> and fixed pH. As the flow rate was raised to 50 mL min<sup>-1</sup>, the rate coefficients at pH 2 was found to increase with an increase in concentration from 50 to 100 mg L<sup>-1</sup>, after which a decrease in the rate coefficient is observed. At pH 4, the rate coefficients was found to decrease as the concentration was raised from 50 to 100 mg L<sup>-1</sup>, after which remaining independent of concentration up to 150 mg L<sup>-1</sup> an increase in rate coefficient is observed for a further increase. At pH 6, after an initial increase with increase in concentration from 50 to 100 mg L<sup>-1</sup>, the rate

coefficients become independent of concentration for further increase. At pH 8, the rate coefficient can be considered independent of concentration up to  $150 \text{ mg L}^{-1}$  before continuing to increase at higher concentration.

Influence of dye concentration on the pseudo first order rate coefficients at a flow rate of  $60 \text{ mL min}^{-1}$  and fixed pH is shown in Figure 2.145. At a flow rate of  $60 \text{ mL min}^{-1}$ , at pH 2, the rate coefficients was found independent of concentration up to  $100 \text{ mg L}^{-1}$  after which they are found to decrease with an increase in concentration. All higher pH showed more or less similar trend of an increase in the rate coefficient with an increase in concentration.



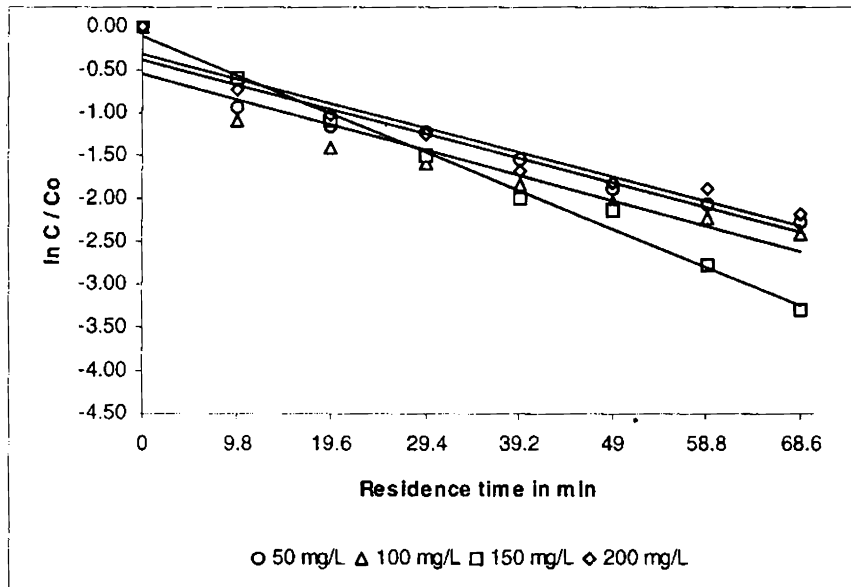


Figure 2.132  
 Yellow – 5GL  
 Plots confirming first order with respect to concentration at pH 2 and at a flow rate of 20 mL min<sup>-1</sup>

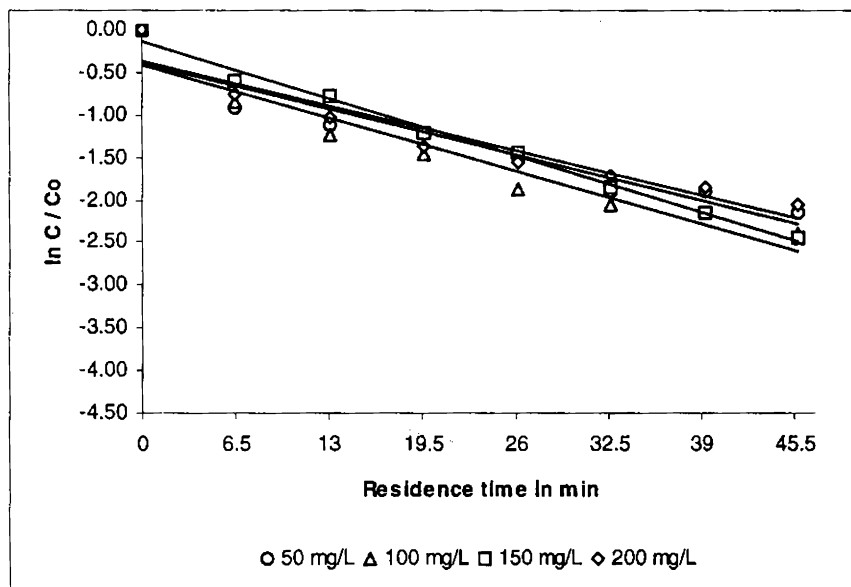


Figure 2.133  
 Yellow – 5GL  
 Plots confirming first order with respect to concentration at pH 2 and at a flow rate of 30 mL min<sup>-1</sup>

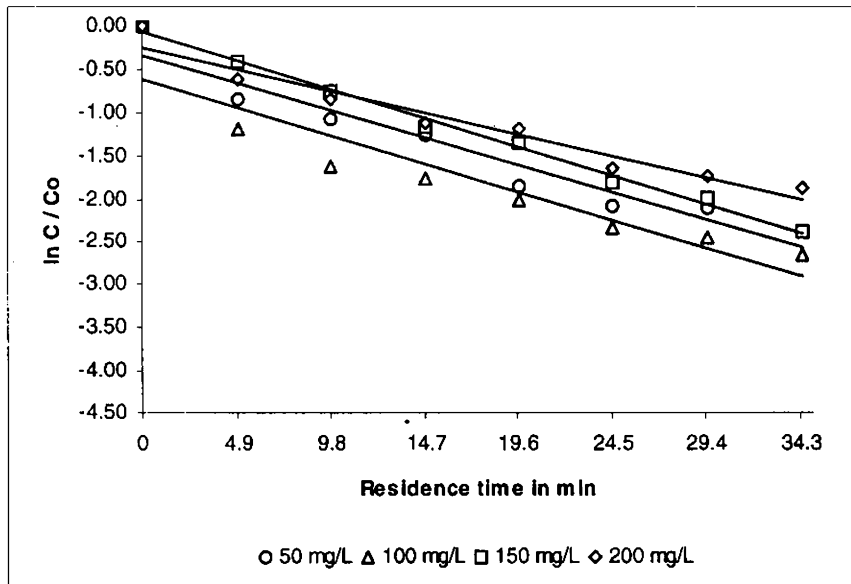


Figure 2.134  
 Yellow – 5GL  
 Plots confirming first order with respect to concentration at pH 2 and at a flow rate of 40 mL min<sup>-1</sup>

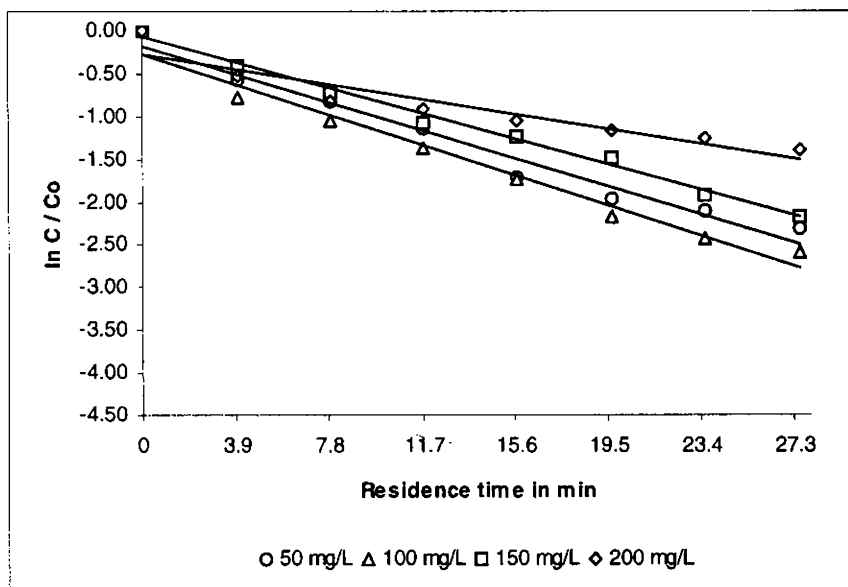


Figure 2.135  
 Yellow – 5GL  
 Plots confirming first order with respect to concentration at pH 2 and at a flow rate of 50 mL min<sup>-1</sup>

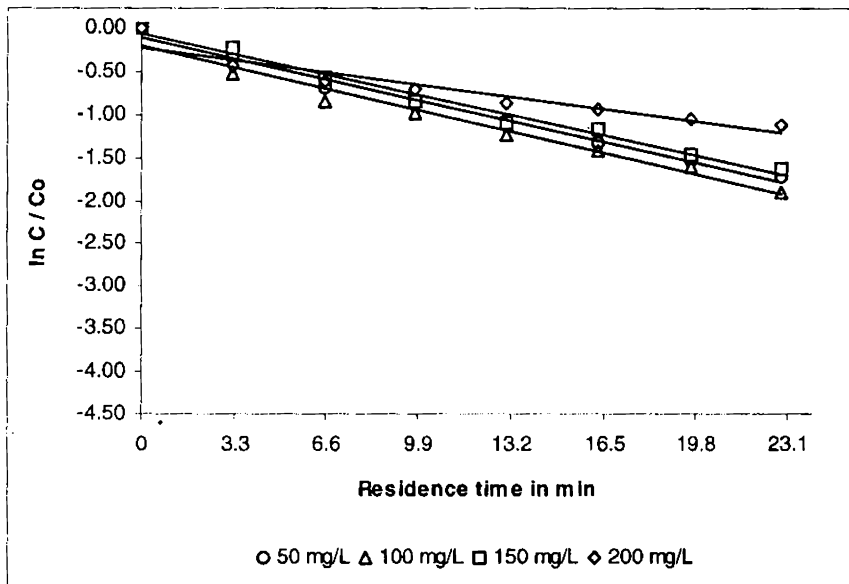


Figure 2.136  
Yellow – 5GL  
Plots confirming first order with respect to concentration at pH 2 and at a flow rate of 60 mL min<sup>-1</sup>

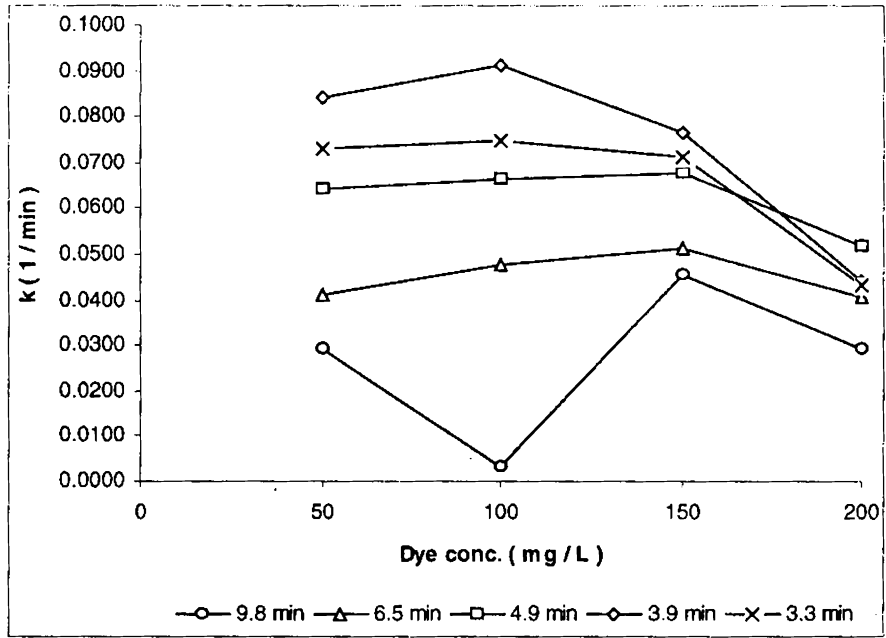


Figure 2.137  
 Direct Yellow 5GL  
 Influence of dye concentration on pseudo first order rate coefficients at pH 2 and at fixed flow rates.

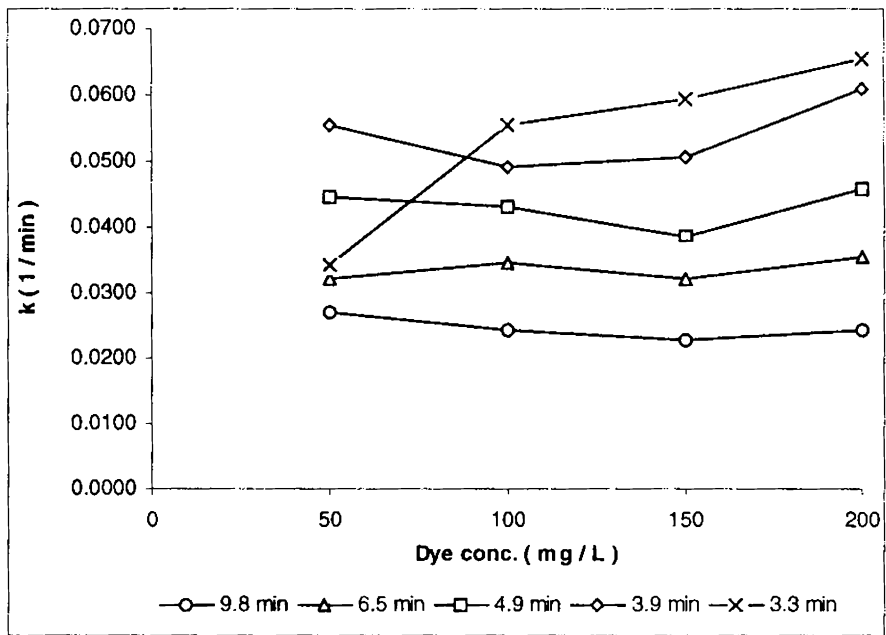


Figure 2.138  
 Direct Yellow 5GL  
 Influence of dye concentration on pseudo first order rate coefficients at pH 4 and at fixed flow rates.

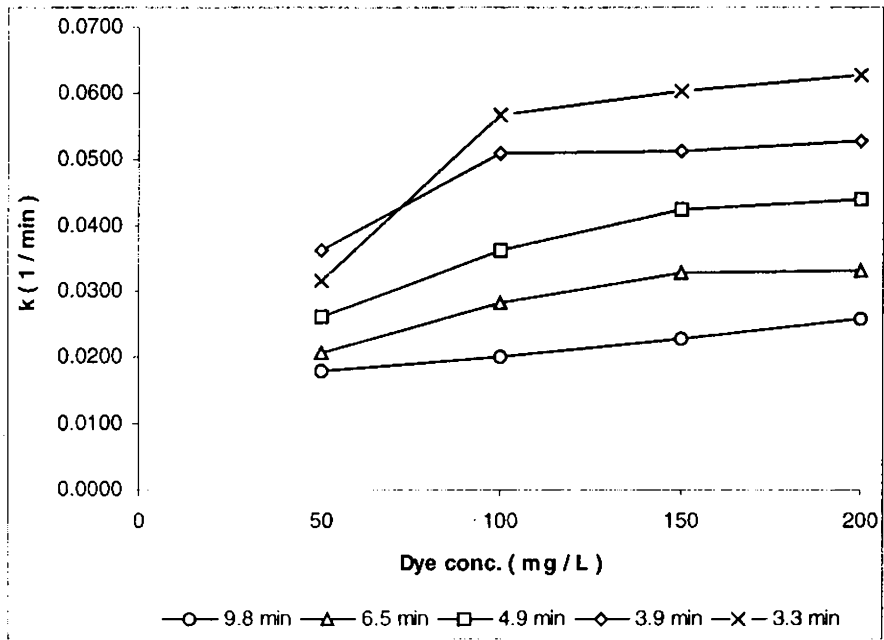


Figure 2.139  
 Direct Yellow 5GL  
 Influence of dye concentration on pseudo first order rate coefficients at pH 6 and at fixed flow rates.

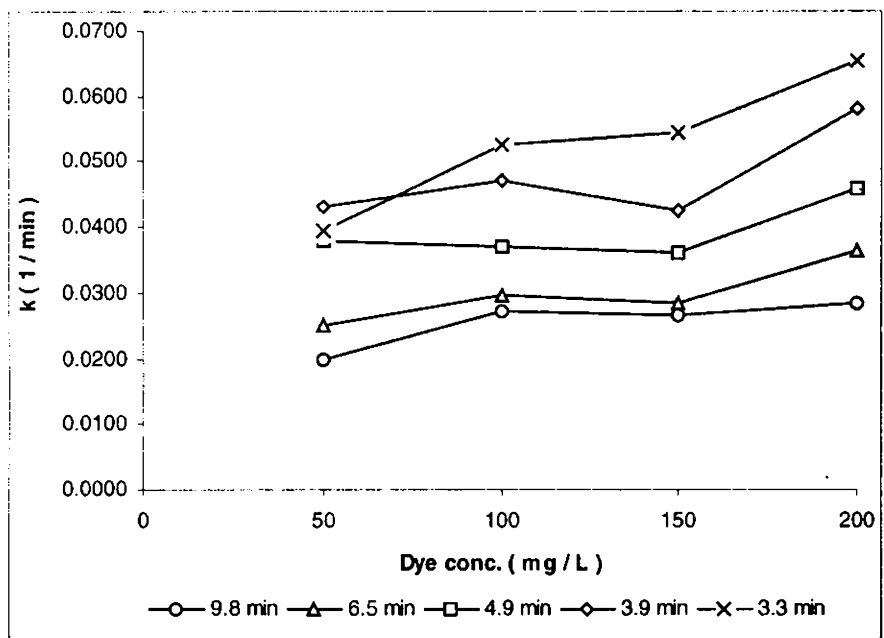


Figure 2.140  
 Direct Yellow 5GL  
 Influence of dye concentration on pseudo first order rate coefficients at pH 8 and at fixed flow rates.

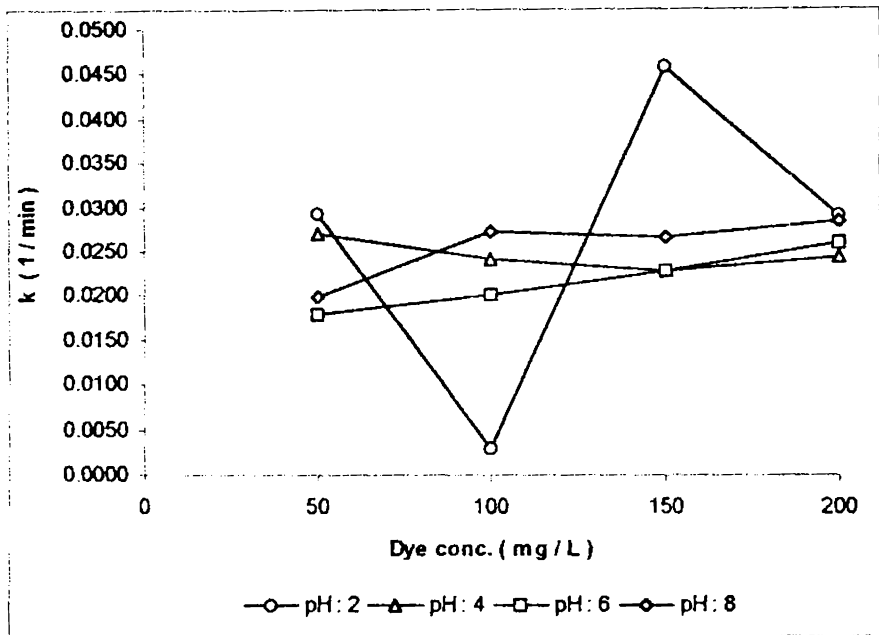


Figure 2.141  
 Direct Yellow 5GL  
 Influence of dye concentration on pseudo first order rate coefficients at a flow rate of  $20 \text{ mL min}^{-1}$  and at fixed pH.

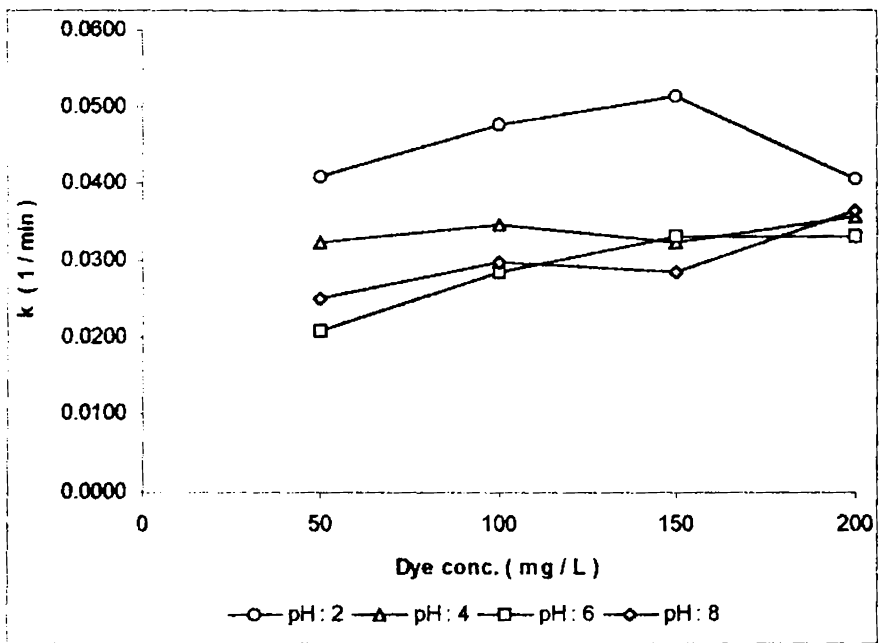


Figure 2.142  
 Direct Yellow 5GL  
 Influence of dye concentration on pseudo first order rate coefficients at a flow rate of  $20 \text{ mL min}^{-1}$  and at fixed pH.

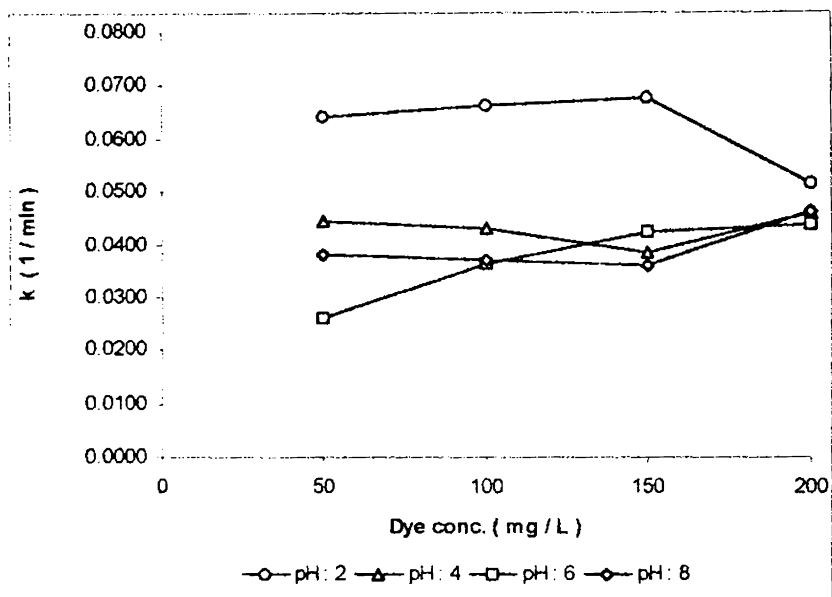


Figure 2.143  
 Direct Yellow 5GL  
 Influence of dye concentration on pseudo first order rate coefficients at a flow rate of 40 mL min<sup>-1</sup> and at fixed pH.

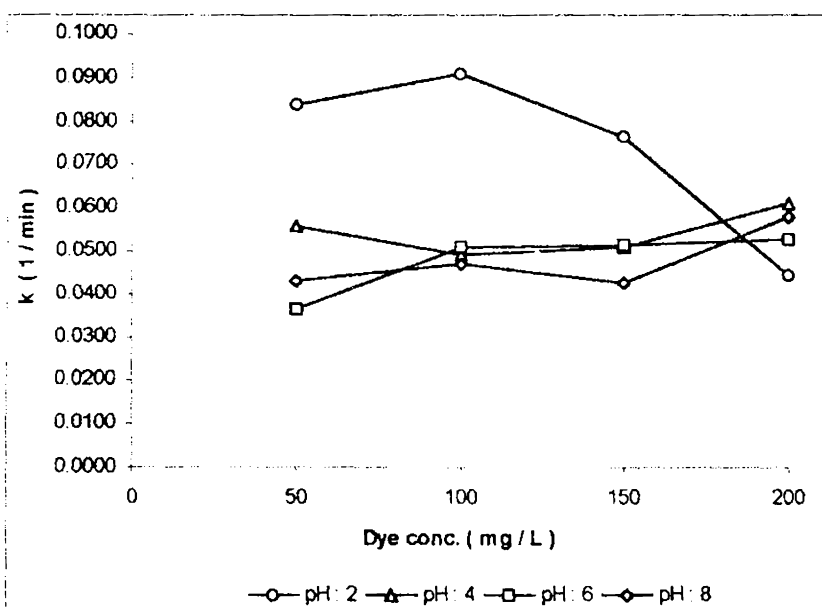


Figure 2.144  
 Direct Yellow 5GL  
 Influence of dye concentration on pseudo first order rate coefficients at a flow rate of 50 mL min<sup>-1</sup> and at fixed pH.

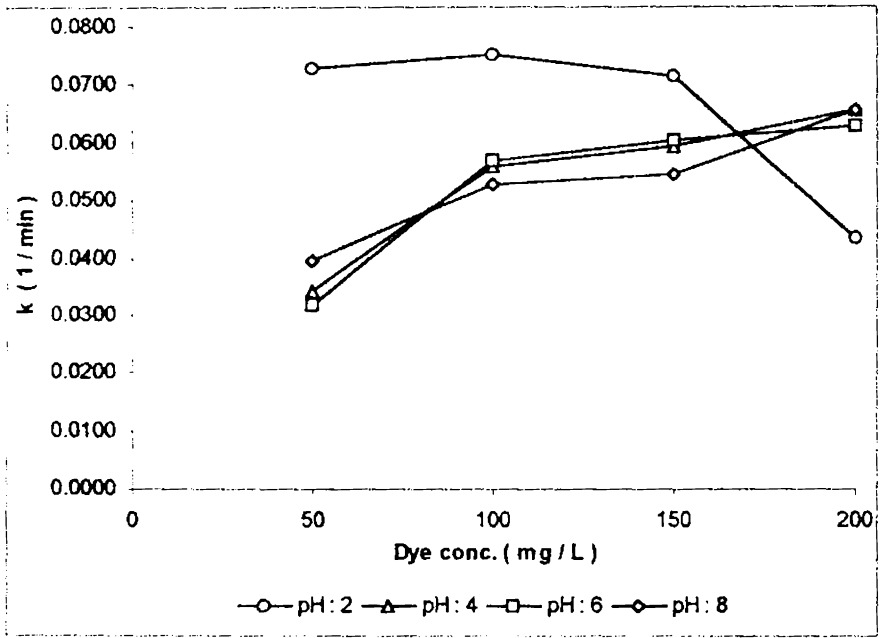


Figure 2.145  
Direct Yellow 5GL  
Influence of dye concentration on pseudo first order rate coefficients at a flow rate of  $60 \text{ mL min}^{-1}$  and at fixed pH.



### 2.10. Influence of pH

The influence of pH on the pseudo first order rate coefficients has been very characteristic showing dependence on flow rates and the initial dye concentrations. It is observed that the decrease in the dye concentration with time fit well into a first order plot suggesting that the reaction is first order with respect to pH. The influence of pH has been studied by fixing the concentration of the dye and flow rate for varying pH. The pH range encompasses both acidic as well as alkaline range. The influence of pH on reduction kinetics has been followed by monitoring the variation in the pseudo-first order rate coefficient, calculated from the slopes of the regression lines. The influence has been studied by

- (i) Comparing the rate coefficients derived for various flow rates at fixed dye concentration against varying pH conditions. This comparison gives the relation between pH and flow rates.
- (ii) Comparing the rate coefficients derived for various concentrations at fixed flow rates against varying pH conditions. This comparison gives the relation between pH and concentration.

### 2.10.1. Direct Sky Blue

It was observed that the data fit well into linear first order plots and the influence of pH on reaction kinetics has been studied by monitoring the variation in the pseudo-first order rate coefficients. The figures (2.146 to 2.150) confirm first order reaction with respect to pH.

#### (i) Comparison between pH and flow rate at constant concentration

The following observations are made by monitoring the variation in the pseudo first order rate coefficients obtained for each flow rates against varying pH with concentration remaining constant.

The influence of pH on pseudo first order rate coefficients at a dye concentration of  $50 \text{ mg L}^{-1}$  and fixed flow rates is shown in figure 2.151.

Comparisons of the pseudo first order rate coefficients indicate that for an initial dye concentration of  $50 \text{ mg L}^{-1}$  the general trend followed is a decrease in the rate coefficients with an increase in pH.

Figure 2.152 illustrates the influence of pH on the pseudo first order rate coefficients at a dye concentration of  $100 \text{ mg L}^{-1}$  and at fixed flow rates. As the initial concentration was raised to  $100 \text{ mg L}^{-1}$  it is observed that the rate coefficients decreased with an increase in pH up to 4, after which the rate coefficients become more or less independent of pH for flow rates of 20 and  $30 \text{ mL min}^{-1}$ . Higher flow rates of  $40 \text{ mL min}^{-1}$  results in a linear decrease in rate coefficients up to pH 6 after which an increase in the rate coefficient is noticed as the pH was raised to 8. At a flow rate of  $50 \text{ mL min}^{-1}$  the rate coefficients becomes independent of pH up to 6. However,

there is an increase in rate coefficients at pH 8. At a flow rate of 60 mL min<sup>-1</sup> the rate coefficient begins to show random fluctuations.

The influence of pH on pseudo first order rate coefficients at a dye concentration of 150 mg L<sup>-1</sup> and fixed flow rates is shown in figure 2.153.

As the initial dye concentration was raised to 150 mg L<sup>-1</sup> low flow rates of 20 and 30 mL min<sup>-1</sup> shows similar trends of decrease in the rate coefficient with an increase in pH from 2 to 4, after which they become independent of pH. Flow rates at 40 and 50 mL min<sup>-1</sup> showed similar trends with the rate coefficients becoming almost independent of pH up to 6 after which an increase in the value is recorded at pH 8. With an increase in flow rate to 60 ml/min the rate coefficients show random behavior.

Figure 2.154 illustrates the influence of pH on the pseudo first order rate coefficients at a dye concentration of 200 mg L<sup>-1</sup> and at fixed flow rates. At a concentration of 200 mg L<sup>-1</sup>, a linear decrease in the rate coefficient with an increase in pH is observed for both flow rates of 20 and 30 mL min<sup>-1</sup> up to pH 6 after which at these flow rates the rate coefficients were found to become independent. However, as the flow rate was raised to 40 mL min<sup>-1</sup> the rate coefficients were found independent of pH up to 4 after which it decreases at pH 6. At pH 8 there is an increase in the rate coefficient. At 50 mL min<sup>-1</sup> the rate coefficients were found to show random behavior while at a higher flow rate of 60 mL min<sup>-1</sup> the rate coefficients can be considered more or less independent of pH except for an increase at pH 4.

(ii) Comparison between pH and concentration at constant flow rates

The following observations are made by monitoring the variation in the pseudo first order rate coefficients obtained for each concentration against varying pH with the flow rates remaining constant.

The influence of pH on pseudo first order rate coefficients at a flow rate of  $20 \text{ mL min}^{-1}$  and for fixed dye concentrations is shown in figure 2.155. At a flow rate of  $20 \text{ mL min}^{-1}$ , for an initial dye concentration of  $50 \text{ mg L}^{-1}$  it was observed that the rate coefficients showed a linear decrease with an increase in pH. However, higher concentrations of 100 and  $150 \text{ mg L}^{-1}$  showed similar trends with the values becoming more or less comparable. The rate coefficients decreased as the pH was raised from 2 to 4, but beyond pH 6, the rate coefficients was found to become independent of pH. For a dye concentration of  $200 \text{ mg L}^{-1}$  the rate coefficients showed a linear decrease with an increase in pH up to pH 6, however, after which the rate coefficient was found to rise at pH 8.

Figure 2.156 represents the influence of pH on pseudo first order rate coefficients at a flow rate of  $30 \text{ mL min}^{-1}$  and for fixed dye concentrations. At a flow rate of  $30 \text{ mL min}^{-1}$ , for an initial dye concentration of  $50 \text{ mg L}^{-1}$  a decrease in the rate coefficients with increase in pH is observed. At a concentration of  $100 \text{ mg L}^{-1}$  the decrease was observed only up to pH 4 after which the rate coefficients become independent of pH. At concentrations of both 150 and  $200 \text{ mg L}^{-1}$  there was a linear decrease in the rate coefficient up to pH 6 after, which

considering the small difference, the rate coefficients can be considered to become independent of pH.

The influence of pH on pseudo first order rate coefficients at a flow rate of  $40 \text{ mL min}^{-1}$  and for fixed dye concentrations is shown in figure 2.157. At a flow rate of  $40 \text{ mL min}^{-1}$ , at an initial dye concentration of  $50 \text{ mg L}^{-1}$  a linear decrease in the rate coefficient is observed up to pH 6 after which a pronounced increase in the rate coefficient was observed at pH 8. Similar trend was also observed for a dye concentration of  $150 \text{ mg L}^{-1}$  and  $200 \text{ mg L}^{-1}$ .

Figure 2.158 represents the influence of pH on pseudo first order rate coefficients at a flow rate of  $50 \text{ mL min}^{-1}$  and for fixed dye concentrations. As the flow rate was raised to  $50 \text{ mL min}^{-1}$ , for a dye concentration of  $50 \text{ mg L}^{-1}$  a linear decrease in rate coefficient is observed with an increase in pH up to 6 after which it becomes independent of pH. Concentrations of 100 and  $150 \text{ mg L}^{-1}$  showed similar trends of being independent of pH up to 6 before recording an increase at pH 8. With an increase in concentration to  $200 \text{ mg L}^{-1}$  the rate coefficients show random fluctuations.

The influence of pH on pseudo first order rate coefficients at a flow rate of  $60 \text{ mL min}^{-1}$  and for fixed dye concentrations is shown in figure 2.159. At a flow rate of  $60 \text{ mL min}^{-1}$ , a linear decrease in the rate coefficient is observed for an increase in pH from 2 to 8 for a dye concentration of  $50 \text{ mg L}^{-1}$ . Rate coefficients for a concentration of  $100 \text{ mg L}^{-1}$  showed random variation, while that at  $150 \text{ mg L}^{-1}$  showed an initial

decrease as the pH was raised from 2 to 4 after which an increase is recorded at pH 6 before becoming independent for a further increase. As the concentration was raised to  $200 \text{ mg L}^{-1}$  the rate coefficient was found to increase with an increase in the pH from 2 to 4, which at pH 6 was found to decrease before becoming independent of pH at 8.

Irrespective of the concentrations chosen for the study a decrease in the rate coefficients with increase in pH is observed with the decrease being linear at low concentrations and at higher concentrations the rate coefficients become independent of pH after 4 or 6. Except for some minor variations rate coefficients for concentrations of 100 and 150  $\text{mg L}^{-1}$  showed similar trends with their values becoming more or less comparable at all pH conditions and flow rates. However at higher concentrations, rate coefficients do show random behaviors.

The results indicate that at low concentrations and flow rate there is a very prominent difference between the rate coefficients at the different pH studied. There is a linear decrease in the rate coefficients with an increase in the pH with a maximum recorded at pH 2 and the lowest value recorded at pH 8. This is an observed trend in a majority of the experiments. Such a trend indicates that there are two different processes operating depending on the pH chosen for the experiment. At pH 2, the rate of the reaction has been high because under acidic conditions the process is driven by chemical reaction. Under such conditions any corrosion products formed would be removed from the surface of the metal through partial dissolution, as a result of which the metal surface is free from any form of passivating

layer of corrosion products leaving a clean reduced metal surface for reacting with the dye molecules. However, under high pH conditions the metal surface when exposed to aqueous solutions and air gets oxidized resulting in the formation of a passivating layer of corrosion products mainly in the form of ferric hydroxide precipitates that form a layer preventing the transfer of electrons driving the chemical reaction but the oxide layer contain exchangeable sites that can lead to a decrease in the dye concentration by serving as sites where the dyes can be removed either by adsorption or by ion exchange. Moreover, when a comparison is made between the rate coefficients obtained at different flow rates for the same concentration, lowest rate coefficients has been recorded at  $20 \text{ mL min}^{-1}$  with the rate coefficients increasing with increased flow rates. These trends are also observed at all the four different concentrations studied. However, a point to be noted is that the linear decrease in the rate coefficient with increased pH is observed only at low concentrations of the dye. As the dye concentration is increased it has been observed that the rate coefficient values although maximum at pH 2; between pH 4, 6 and 8, the difference in these values do not appear to be significant. This suggests that under these pH's the process operating is surface mediated through adsorption on to the oxide layer formed at the metal surface. However, in a few runs a slight increase in the pseudo-first order rate coefficient with pH has been observed with a maximum at pH 8 indicating conditions where the adsorption process predominates over chemical reaction.

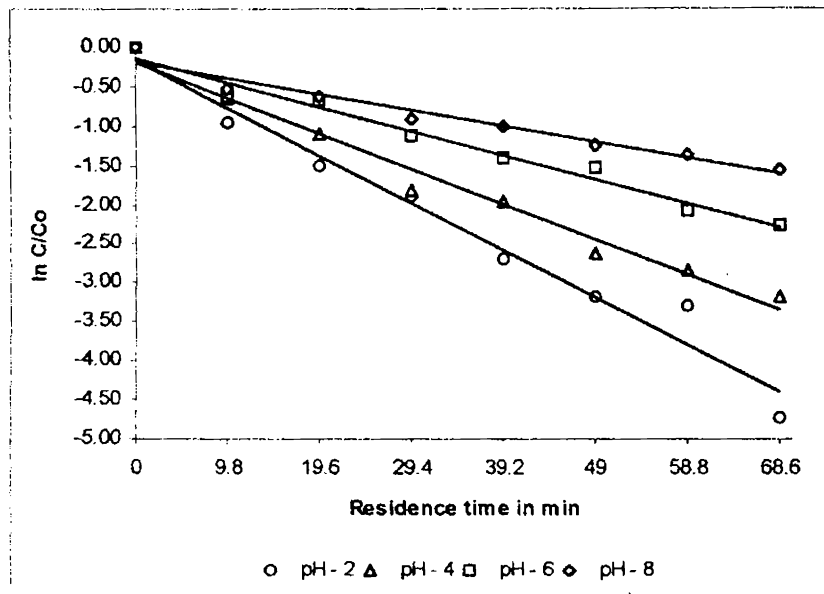


Figure 2.146  
 Direct Sky Blue  
 Influence of pH on reduction kinetics at a dye concentration of  $50 \text{ mg L}^{-1}$  and at a residence time of 9.8 min.

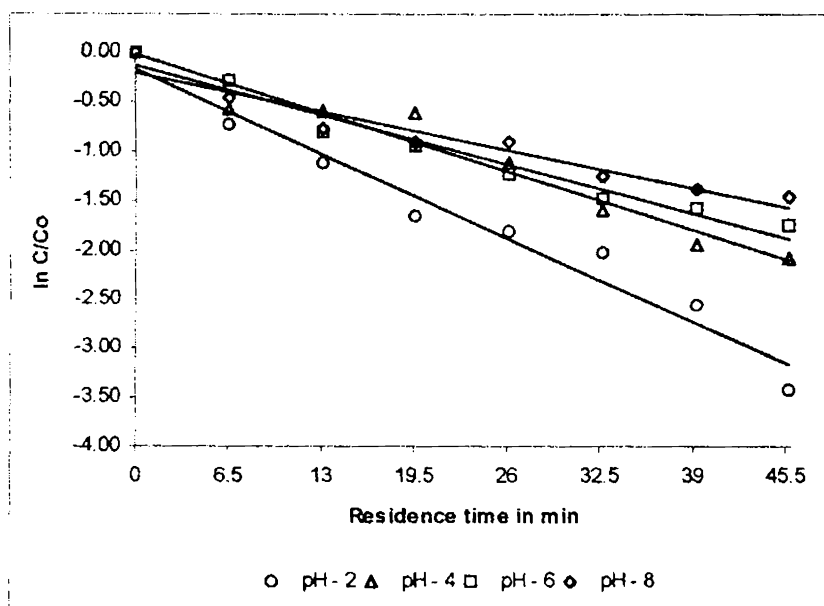


Figure 2.147  
 Direct Sky Blue  
 Influence of pH on reduction kinetics at a dye concentration of  $50 \text{ mg L}^{-1}$  and at a residence time of 6.5 min.



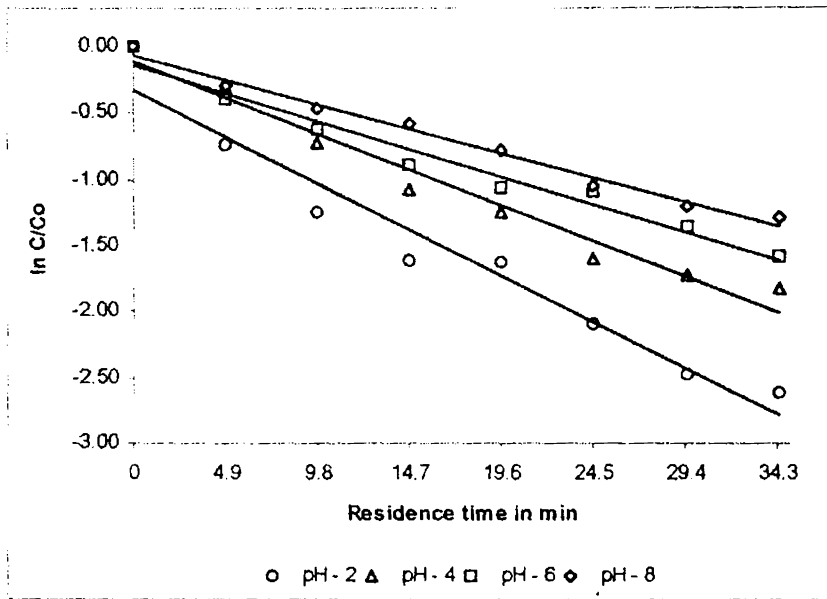


Figure 2.148  
Direct Sky Blue  
Influence of pH on reduction kinetics at a dye concentration of 50 mg L<sup>-1</sup> and at a residence time of 4.9 min

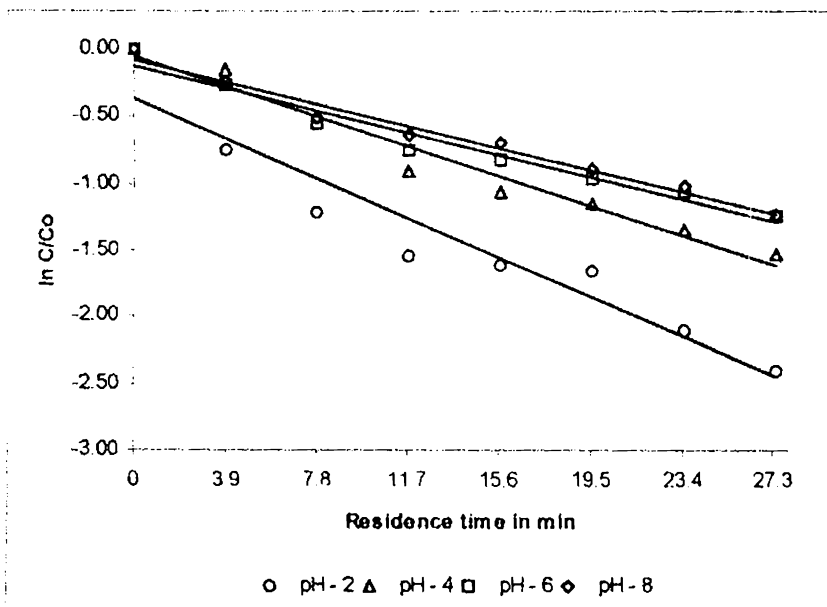


Figure 2.149  
Direct Sky Blue  
Influence of pH on reduction kinetics at a dye concentration of 50 mg L<sup>-1</sup> and at a residence time of 3.9 min.

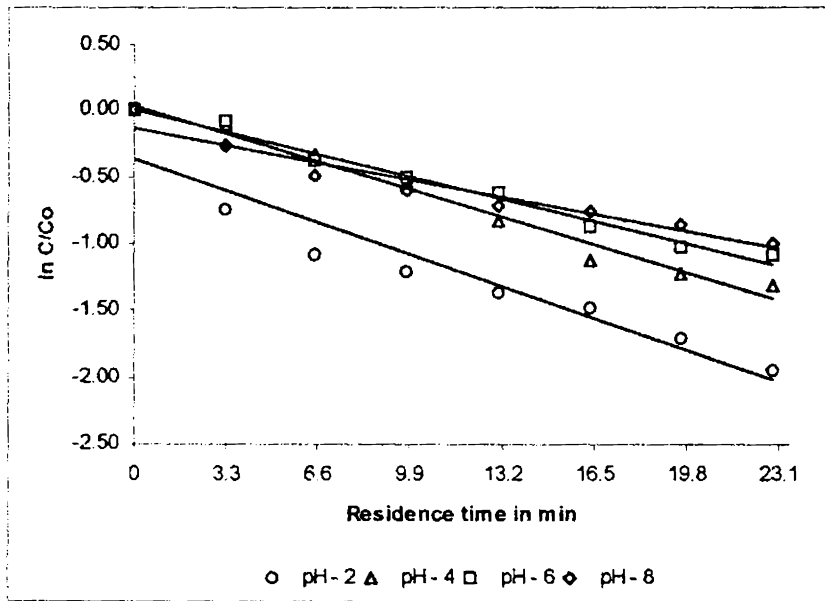


Figure 2.150  
 Direct Sky Blue  
 Influence of pH on reduction kinetics at a dye concentration of  $50 \text{ mg L}^{-1}$  and at a residence time of 3.3 min.

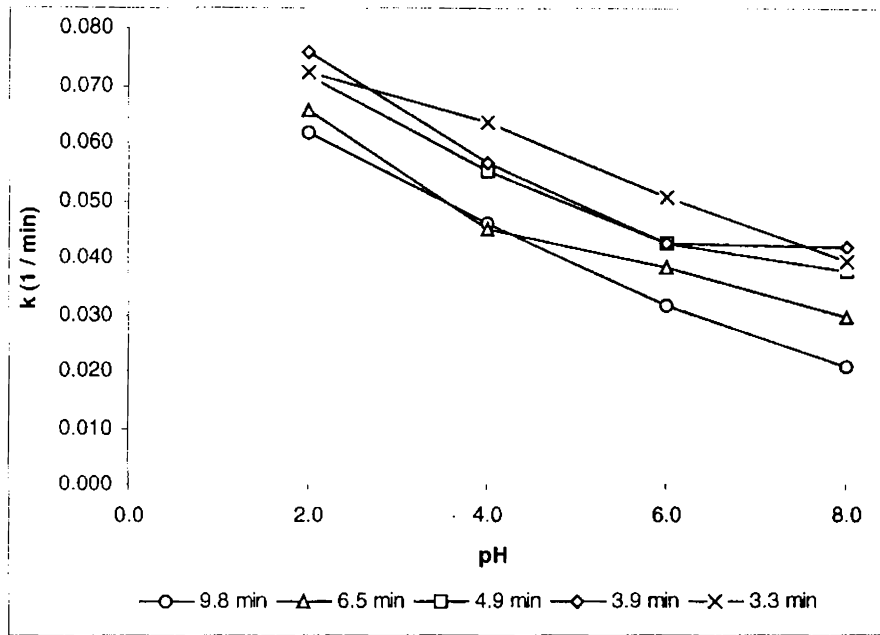


Figure 2.151  
Direct Sky Blue  
Influence of pH on pseudo first order rate coefficients at a dye concentration of 50 mg L<sup>-1</sup> and at fixed flow rates.

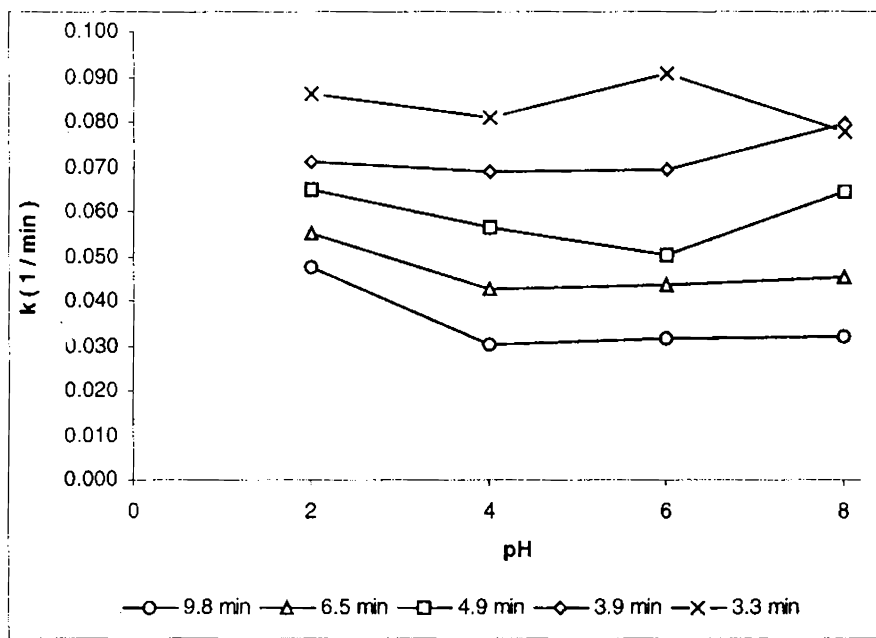


Figure 2.152  
Direct Sky Blue  
Influence of pH on pseudo first order rate coefficients at a dye concentration of 100 mg L<sup>-1</sup> and at fixed flow rates.

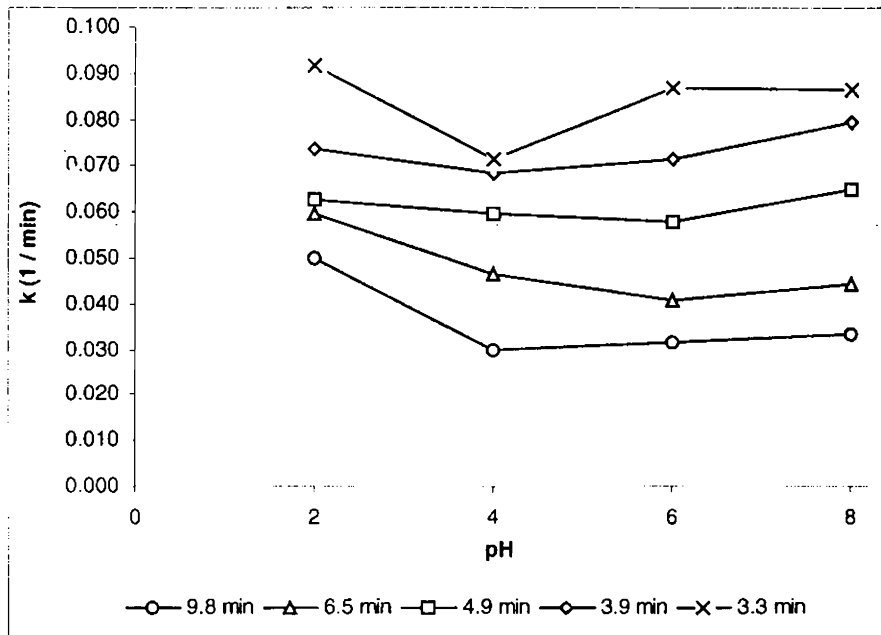


Figure 2.153  
Direct Sky Blue  
Influence of pH on pseudo first order rate coefficients at a dye concentration of  $150 \text{ mg L}^{-1}$  and at fixed flow rates.

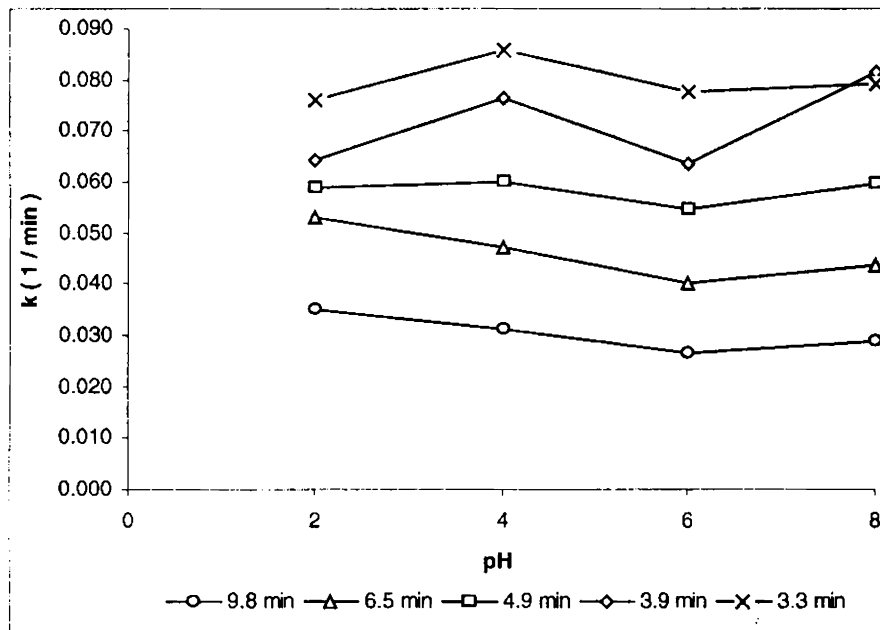


Figure 2.154  
Direct Sky Blue  
Influence of pH on pseudo first order rate coefficients at a dye concentration of  $200 \text{ mg L}^{-1}$  and at fixed flow rates.

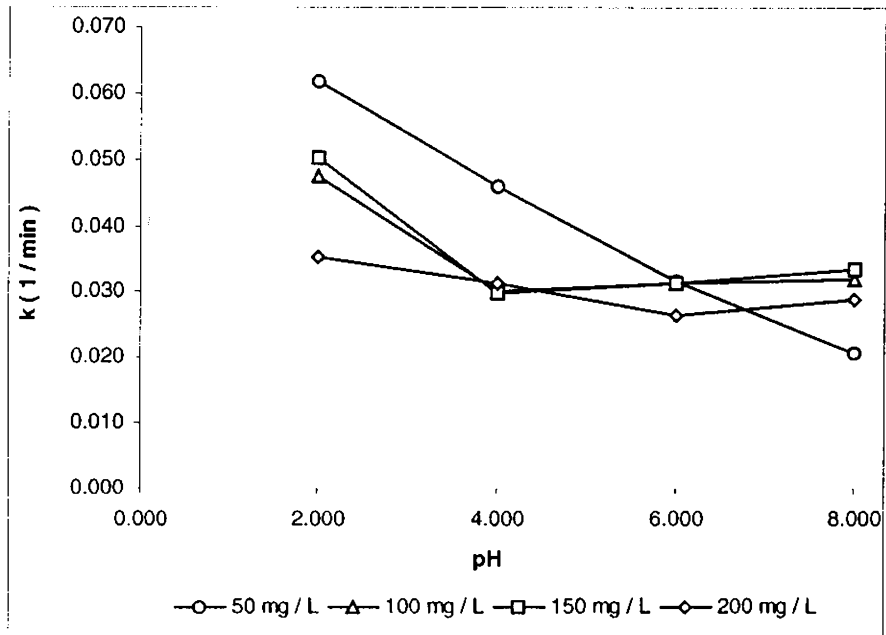


Figure 2.155  
Direct Sky Blue  
Influence of pH on pseudo first order rate coefficients at a flow rate of  $20 \text{ mL min}^{-1}$  and for fixed dye concentrations.

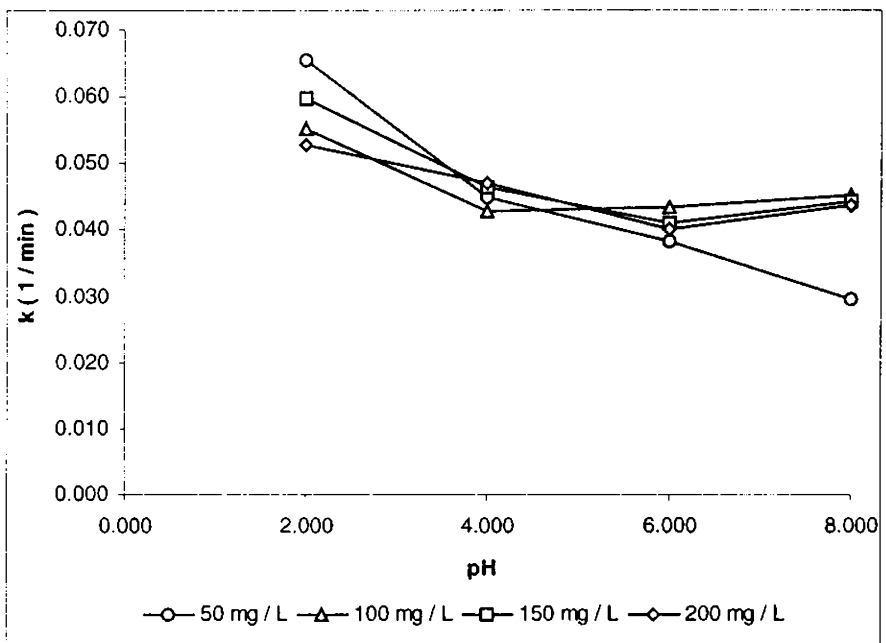


Figure 2.156  
Direct Sky Blue  
Influence of pH on pseudo first order rate coefficients at a flow rate of  $30 \text{ mL min}^{-1}$  and for fixed dye concentrations.

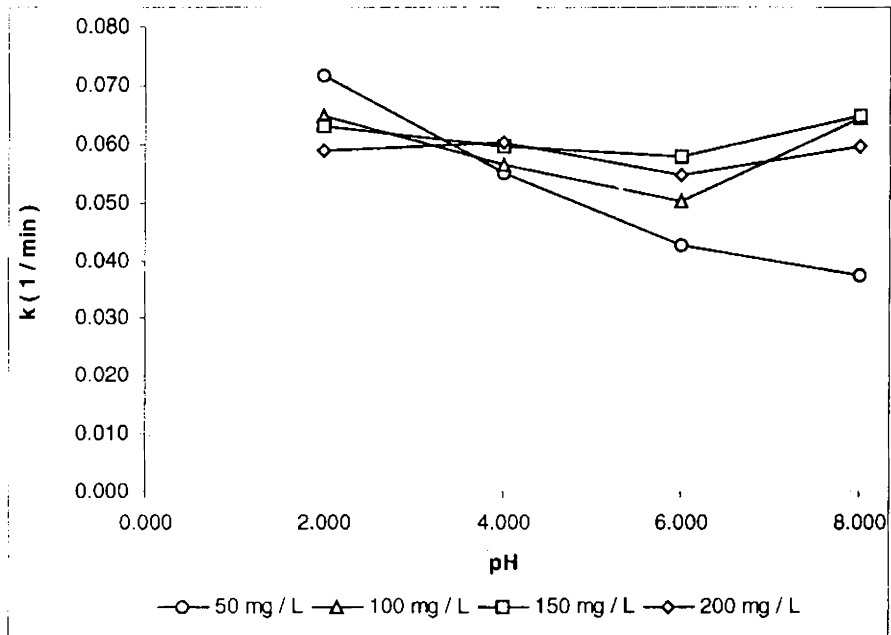


Figure 2.157  
Direct Sky Blue  
Influence of pH on pseudo first order rate coefficients at a flow rate of  $40 \text{ mL min}^{-1}$  and for fixed dye concentrations.

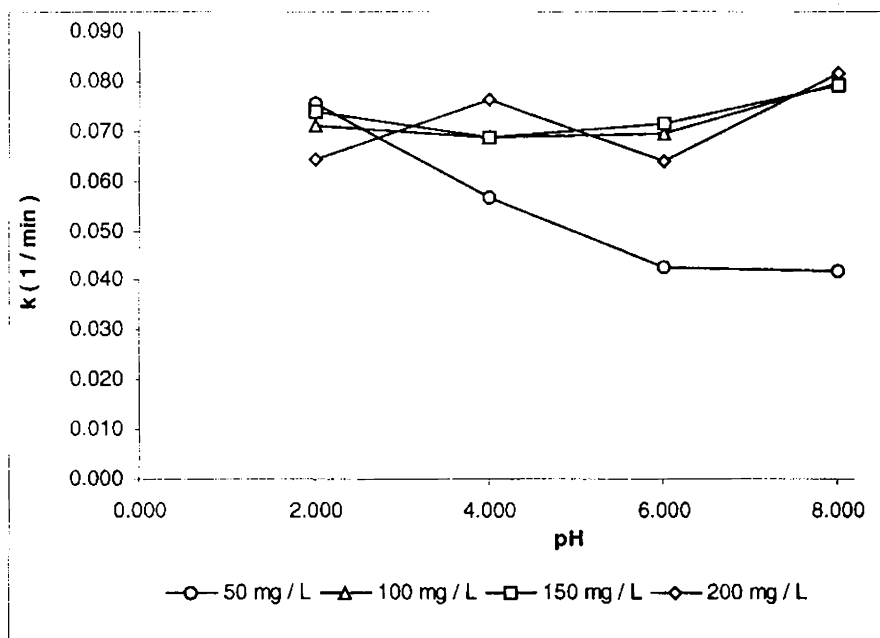


Figure 2.158  
Direct Sky Blue  
Influence of pH on pseudo first order rate coefficients at a flow rate of  $50 \text{ mL min}^{-1}$  and for fixed dye concentrations.

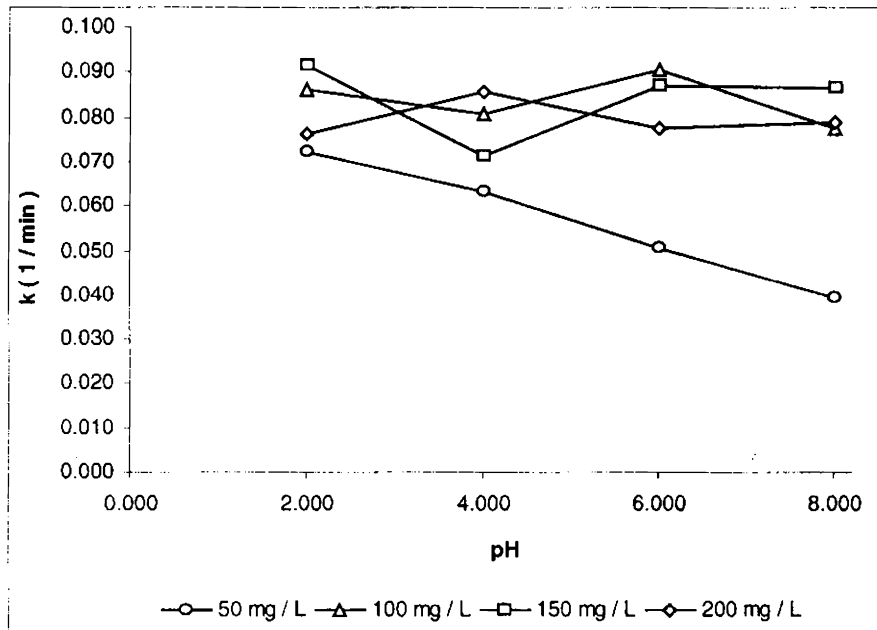


Figure 2.159  
Direct Sky Blue  
Influence of pH on pseudo first order rate coefficients at a flow rate of  $60 \text{ mL min}^{-1}$  and for fixed dye concentrations

### 2.10.2. Direct Black-EG

It was observed that the data fit well into linear first order plots and the influence of pH on reaction kinetics has been studied by monitoring the variation in the pseudo-first order rate coefficients. The figures (2.168 to 2.172) present first order fit of the observations.

(i) Comparison between pH and flow rate at constant concentration

The influence of pH on pseudo first order rate coefficients at a dye concentration of  $50 \text{ mg L}^{-1}$  and fixed flow rates is shown in figure 2.173.

For an initial dye concentration of  $50 \text{ mg L}^{-1}$ , but for a few variations which could be attributed to the inherent variation associated with the system, the rate of the reaction was found to decrease linearly with an increase in the pH over the entire range of flow rates considered for the study.

Figure 2.174 illustrates the influence of pH on the pseudo first order rate coefficients at a dye concentration of  $100 \text{ mg L}^{-1}$  and at fixed flow rates. As the initial dye concentration was raised to  $100 \text{ mg L}^{-1}$  a major decrease in the rate coefficient is observed with an increase in pH for 2 to 4. A marginal increase is observed as the pH is raised from 4 to 6, this is observed at high flow rates ( $40$  and  $50 \text{ mL min}^{-1}$ ), which can be attributed to the influence of mass transport. The rate coefficient remained steady between pH 6 and 8 indicating that at pH above 4 the rate coefficients became independent.

The influence of pH on pseudo first order rate coefficients at a dye concentration of  $150 \text{ mg L}^{-1}$  and fixed flow rates is shown in figure 2.175.



Similar trend is also observed at a higher dye concentrations of  $150 \text{ mg L}^{-1}$  as shown in figure 2.175.

Figure 2.176 illustrates the influence of pH on the pseudo first order rate coefficients at a dye concentration of  $200 \text{ mg L}^{-1}$  and at fixed flow rates. With an increase in the dye concentration to  $200 \text{ mg L}^{-1}$  there is a major decrease in the rate coefficient as the pH is raised from 2 to 4 after which the rate of the reaction tends to increase with the difference in rate coefficients between 4, 6 and 8 becoming increasingly significant with increase in flow rates. The rate coefficient at pH 8 was found higher than that at pH 6, which was in turn greater than pH 4. This trend is observed for all flow rates from  $20$  to  $50 \text{ mL min}^{-1}$ , however, at a flow rate of  $60 \text{ mL min}^{-1}$  although the increase in the rate coefficients continues, at pH 6 and 8 they become comparable.

(ii) Comparison between pH and concentration at constant flow rate

The influence of pH on pseudo first order rate coefficients at a flow rate of  $20 \text{ mL min}^{-1}$  and for fixed dye concentrations is shown in figure 2.177.

Figure 2.178 represents the influence of pH on pseudo first order rate coefficients at a flow rate of  $30 \text{ mL min}^{-1}$  and for fixed dye concentrations.

The influence of pH on pseudo first order rate coefficients at a flow rate of  $40 \text{ mL min}^{-1}$  and for fixed dye concentrations is shown in figure 2.179.

Figure 2.180 represents the influence of pH on pseudo first order rate coefficients at a flow rate of  $50 \text{ mL min}^{-1}$  and for fixed dye concentrations.

The influence of pH on pseudo first order rate coefficients at a flow rate of  $60 \text{ mL min}^{-1}$  and for fixed dye concentrations is shown in figure 2.181.

Figures 2.177 to 2.181 indicate that at all flow rates the general trend is a decrease in the rate coefficient with an increase in pH with minor variations that is found concentration dependent. For a concentration of  $50 \text{ mg L}^{-1}$  there is a steady decrease in the rate coefficient up to pH 8 while at all higher concentrations the rate coefficients after a major initial decrease with an increase in pH from 2 to 4 become independent of pH as the rate coefficients are more or less comparable. However, the rate coefficients for lower dye concentration are found greater than the higher dye concentrations, indicating that at higher dye concentrations the dye exerts its influence as a corrosion inhibitor.

At high flow rates, rate coefficient for a concentration of  $200 \text{ mg L}^{-1}$ , show a tendency to increase after an initial decrease with increase in pH from 2 to 4. Increase in the rate coefficients above pH 4 after an initial decrease, observed at high concentrations and flow rates indicate a state where the physical processes such as adsorption gains prominence over chemical reaction. The fact that there is a decrease in the rate coefficient with an increase in the dye concentration clearly indicates that the dye is a corrosion inhibitor. As a result at high dye concentrations, the observed

decrease can be attributed only to physical processes such as adsorption where mass transport of the dye molecules from the bulk solution to the metal surface become limiting and not chemical reaction involving electron transfer, as the dye has already formed a passivating layer on the surface of the metal. Therefore, adsorption phenomenon becomes a prominent step at pH above 4 and at higher concentrations where the dye inhibits the corrosion of the metal. And in all surface mediated processes an increase in the rate coefficient with an increase in concentration and flow rate is expected.

All these observations lead us to assume that there are two different processes involved in the zero valent iron mediated reduction of the azo dye. At pH 2, the pseudo first order rate coefficient is representative of the inherent chemical reaction occurring through the direct electron transfer at the metal surface and at pH 6 and 8, the rate coefficients represent the decrease in dye concentration due to surface mediated process involving adsorption or diffusion limited kinetics. pH 4 represents an intermediate or a transition pH, below which the reaction is mediated by chemical reaction and above which the reaction becomes surface mediated. Therefore, the pseudo first order rate coefficient measured at pH 4 actually represents the sum of the two processes leading to a decrease in the dye concentration, both due to chemical reaction and surface mediated phenomenon such as adsorption.

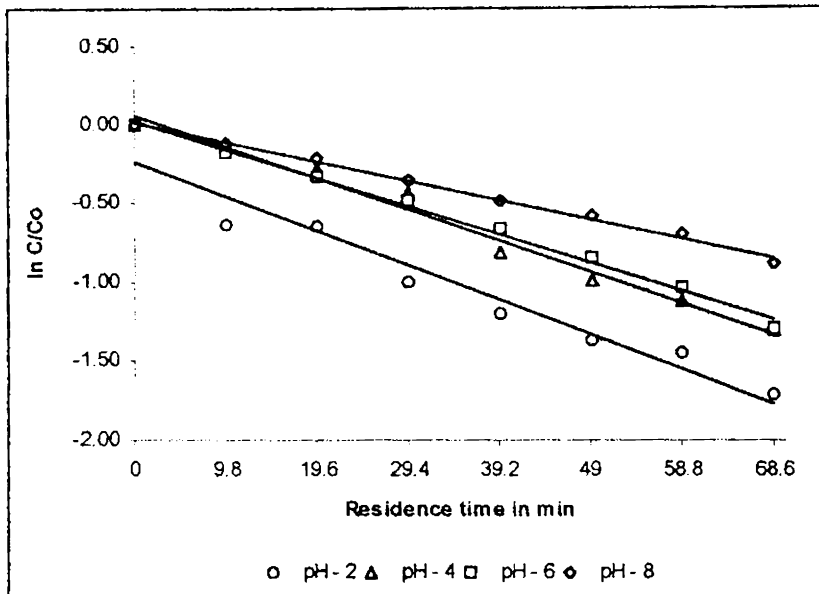


Figure 2.168  
 Direct Black EG  
 Influence of pH on reduction kinetics at a dye concentration of 50 mg L<sup>-1</sup> and  
 at a residence time of 9.8 min.

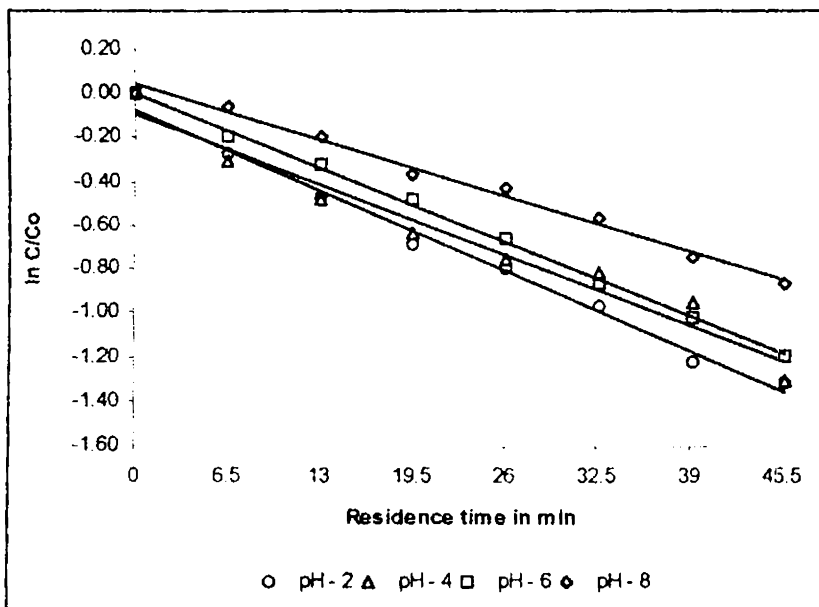


Figure 2.169  
 Direct Black EG  
 Influence of pH on reduction kinetics at a dye concentration of 50 mg L<sup>-1</sup> and  
 at a residence time of 6.5 min.

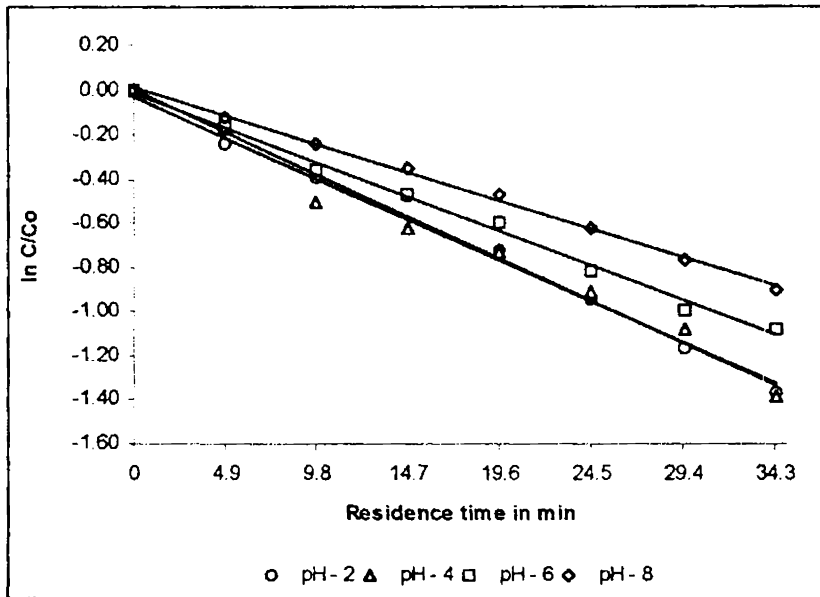


Figure 2.170  
 Direct Black EG  
 Influence of pH on reduction kinetics at a dye concentration of 50 mg L<sup>-1</sup> and at a residence time of 4.9 min.

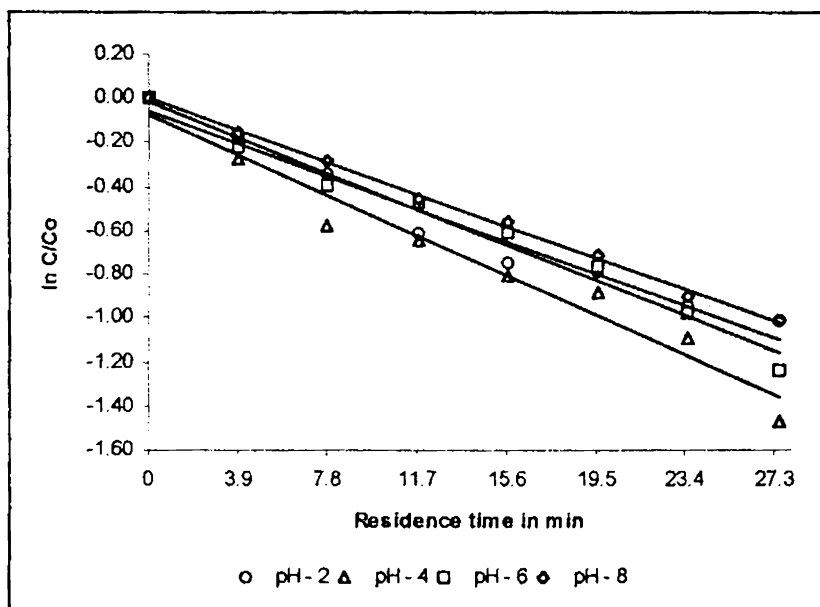


Figure 2.171  
 Direct Black EG  
 Influence of pH on reduction kinetics at a dye concentration of 50 mg L<sup>-1</sup> and at a residence time of 3.9 min.

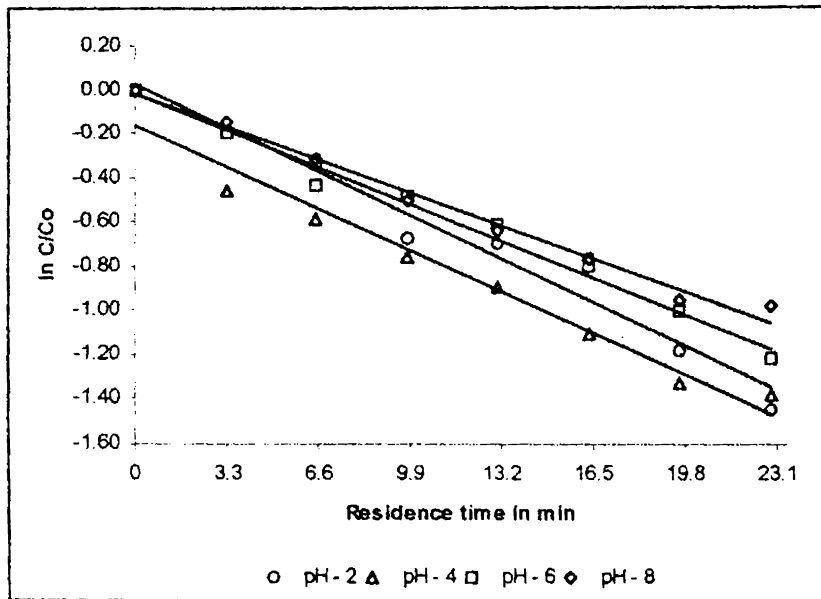


Figure 2.172  
 Direct Black EG  
 Influence of pH on reduction kinetics at a dye concentration of  $50 \text{ mg L}^{-1}$  and at a residence time of 3.3 min.

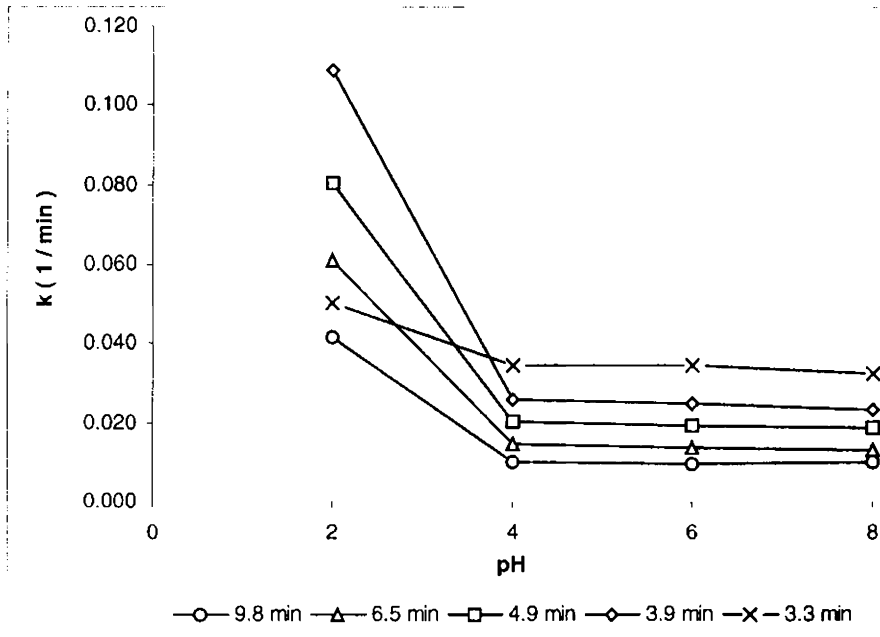


Figure 2.175  
Direct Black EG  
Influence of pH on pseudo first order rate coefficients at a dye concentration of 150 mg L<sup>-1</sup> and at fixed flow rates.

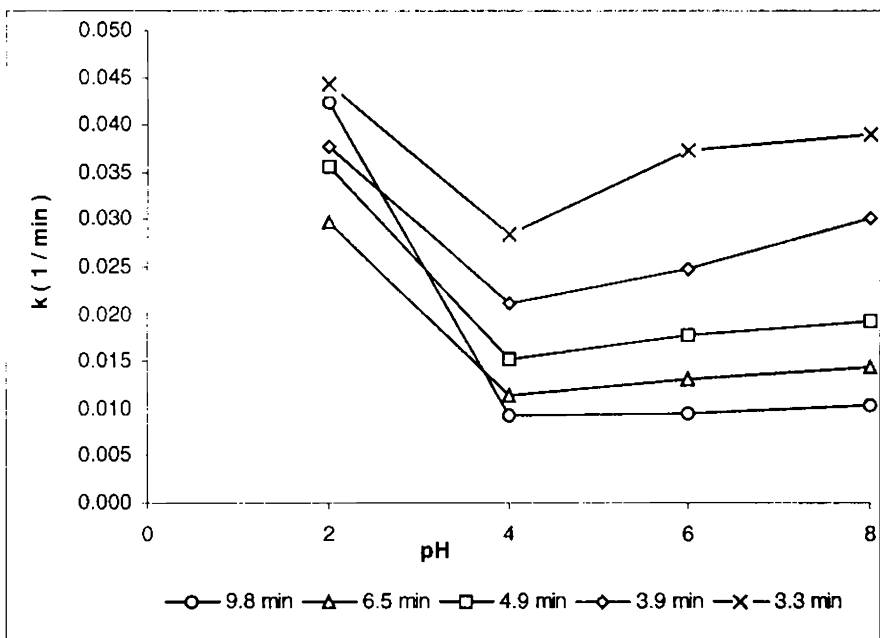


Figure 2.176  
Direct Black EG  
Influence of pH on pseudo first order rate coefficients at a dye concentration of 200 mg L<sup>-1</sup> and at fixed flow rates.

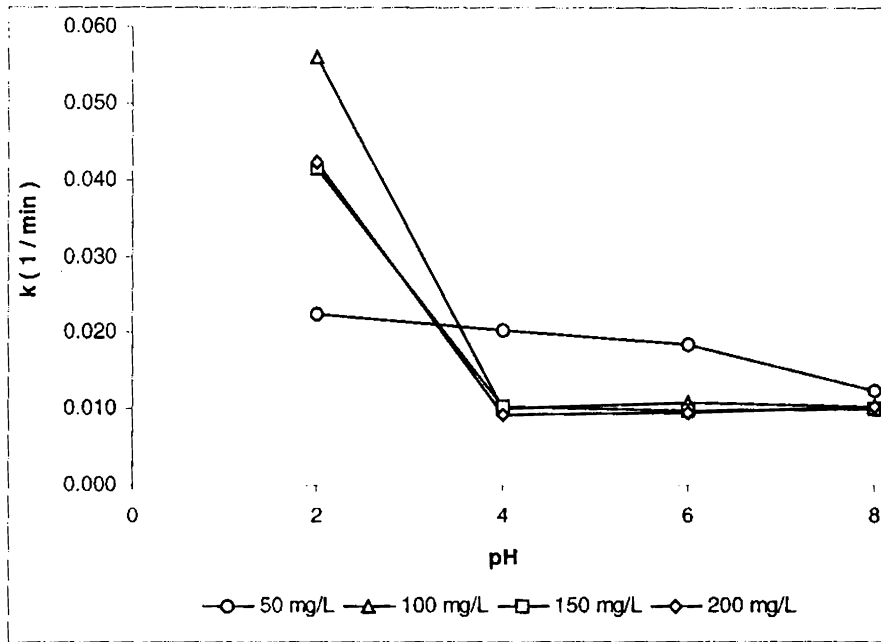


Figure 2.177  
 Direct Black EG  
 Influence of pH on pseudo first order rate coefficients at a flow rate of 20 mL min<sup>-1</sup> and for fixed dye concentrations.

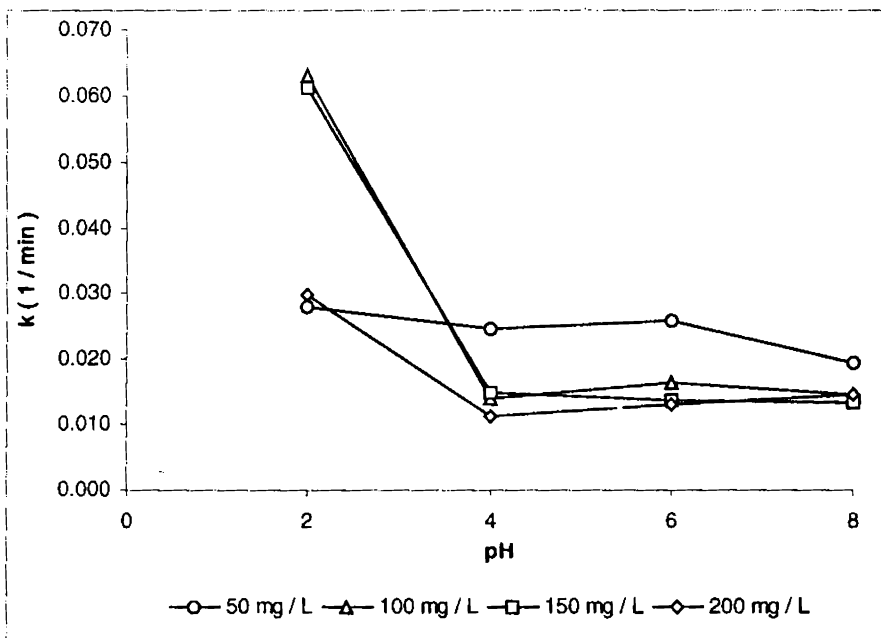


Figure 2.178  
 Direct Black EG  
 Influence of pH on pseudo first order rate coefficients at a flow rate of 30 mL min<sup>-1</sup> and for fixed dye concentrations.



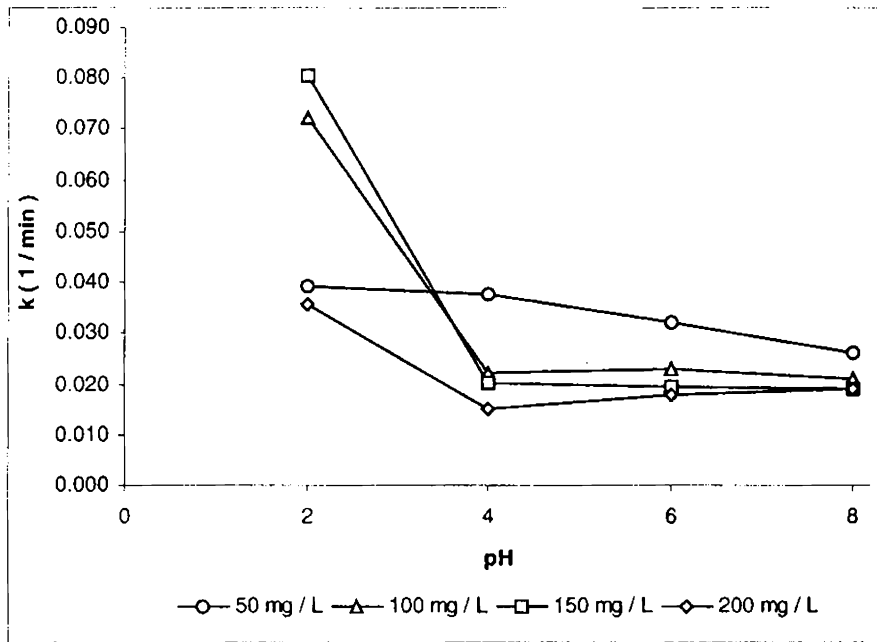


Figure 2.179  
Direct Black EG  
Influence of pH on pseudo first order rate coefficients at a flow rate of 40 mL min<sup>-1</sup> and for fixed dye concentrations.

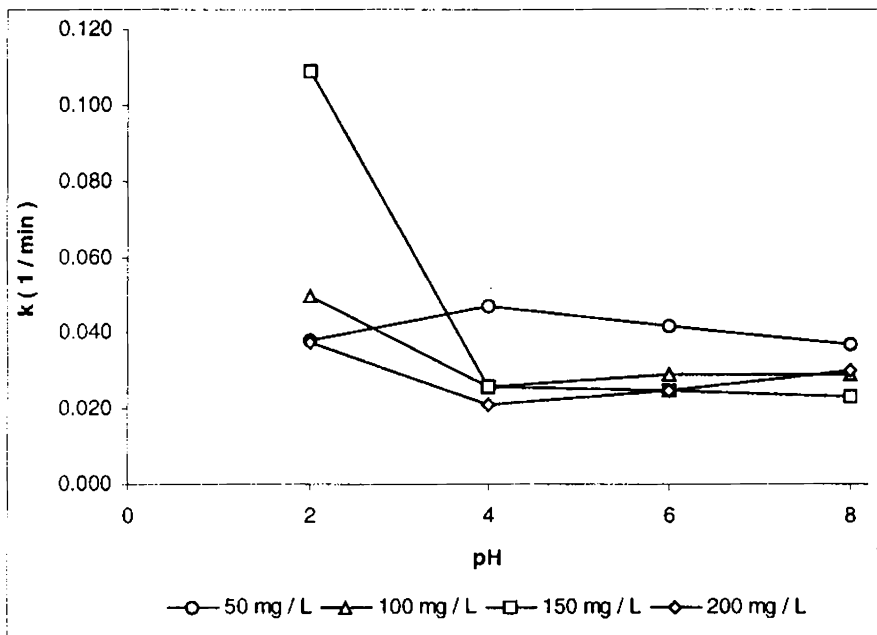


Figure 2.180  
Direct Black EG  
Influence of pH on pseudo first order rate coefficients at a flow rate of 50 mL min<sup>-1</sup> and for fixed dye concentrations.

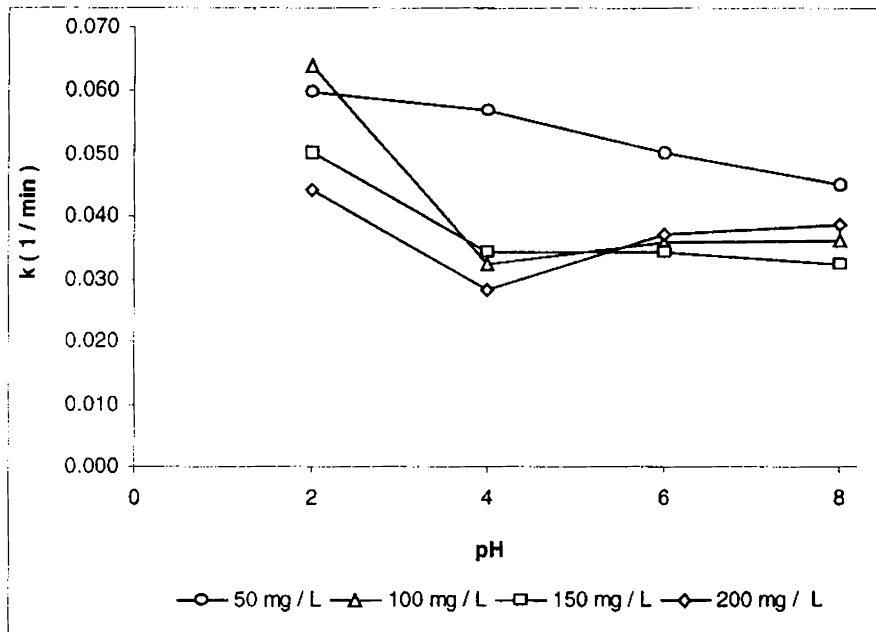


Figure 2.181  
Direct Black EG  
Influence of pH on pseudo first order rate coefficients at a flow rate of  $60 \text{ mL min}^{-1}$  and for fixed dye concentrations.

### 2.10.3. Direct Catachine Brown

It was observed that the data fit well into linear first order plots and the influence of pH on reaction kinetics has been studied by monitoring the variation in the pseudo-first order rate coefficients. The figures (2.182 to 2.186) confirm first order reaction with respect to pH.

(i) Comparison between pH and Flow rate at constant concentration

The influence of pH on pseudo first order rate coefficients at a dye concentration of  $50 \text{ mg L}^{-1}$  and fixed flow rates is shown in figure 2.187.

For an initial dye concentration of  $50 \text{ mg L}^{-1}$ , the general trend observed is that the rate coefficients show a remarkable decrease as the pH is increased from 2 to 4. From here on, the rate coefficients begin to show variations that are found flow rate dependent. At flow rates of 20 and  $50 \text{ mL min}^{-1}$  the rate coefficients were found to decrease with an increase in pH, while at 30 and  $40 \text{ mL min}^{-1}$  they were found independent of pH between 4 and 6 after which a decrease in the rate coefficient is observed. Flow rate of  $60 \text{ mL min}^{-1}$  showed a linear decrease with an increase in pH over the range studied.

Figure 2.188 illustrates the influence of pH on the pseudo first order rate coefficients at a dye concentration of  $100 \text{ mg L}^{-1}$  and at fixed flow rates. With an increase in the dye concentration to  $100 \text{ mg L}^{-1}$ , a decrease in the rate coefficient with an increase in pH is observed with the rate coefficient being maximum at pH 2. However, this decrease is observed only up to pH 6, after which they become independent of pH. The variation

of these rate coefficients at any particular pH was found dependent on flow rates.

The influence of pH on pseudo first order rate coefficients at a dye concentration of  $150 \text{ mg L}^{-1}$  and fixed flow rates is shown in figure 2.189. Similar trend is observed even for a higher dye concentration of  $150 \text{ mg L}^{-1}$ , but at higher flow rates there is a decrease in the rate coefficient at all pH ranges in contrast to lower concentrations ( $50$  and  $100 \text{ mg L}^{-1}$ ) where they become independent of pH above 6.

Figure 2.190 illustrates the influence of pH on the pseudo first order rate coefficients at a dye concentration of  $200 \text{ mg L}^{-1}$  and at fixed flow rates.

As the dye concentration is increased to  $200 \text{ mg L}^{-1}$ , the rate coefficients showed a significant drop for all flow rates for an increase in the pH from 2 to 4, after which they were found to become independent of pH. However, at a flow rate of  $20 \text{ mL min}^{-1}$ , the rate coefficients after being independent of pH up to 4 were found to decrease for a further increase in pH. This could be because the increased contact time between the dye molecule and the metal surface resulted in increased removal through adsorption.

(ii) Comparison between pH and concentration at constant flow rate

Comparison between rate coefficients derived for the various concentrations and pH for a specific flow rate indicate trends discussed below.

The influence of pH on pseudo first order rate coefficients at a flow rate of  $20 \text{ mL min}^{-1}$  and for fixed dye concentrations is shown in figure 2.191.

At a flow rate of  $20 \text{ mL min}^{-1}$ , dye concentration at  $50 \text{ mg L}^{-1}$  seems to attain an equilibrium at pH 4, after which the rate coefficients were found to become independent of pH. For higher concentrations of 100 and  $150 \text{ mg L}^{-1}$  the decrease in rate coefficients were found to continue over the entire range of pH studied. However, at a concentration of  $200 \text{ mg L}^{-1}$  they become independent of pH up to 4 before recording a decrease for a further increase.

Figure 2.192 represents the influence of pH on pseudo first order rate coefficients at a flow rate of  $30 \text{ mL min}^{-1}$  and for fixed dye concentrations.

The influence of pH on pseudo first order rate coefficients at a flow rate of  $40 \text{ mL min}^{-1}$  and for fixed dye concentrations is shown in figure 2.193.

Figure 2.194 represents the influence of pH on pseudo first order rate coefficients at a flow rate of  $50 \text{ mL min}^{-1}$  and for fixed dye concentrations.

Figures 2.192 to 2.194 indicates that flow rates of 30, 40 and  $50 \text{ mL min}^{-1}$  showed similar trends; with the rate coefficients at the two extremes of concentrations ( $50$  and  $200 \text{ mg L}^{-1}$ ) showing an initial decrease as the pH is raised from 2 to 4, after which they become independent of pH up to 6 before continuing to decrease for a further increase in pH to 8. Between

concentrations of 100 and 150 mg L<sup>-1</sup> the decrease in rate coefficients for an increase in pH continued up to pH 6 after which they become independent of pH at a concentration of 100 mg L<sup>-1</sup> while, at a concentration of 150 mg L<sup>-1</sup> a continued decrease with increase in pH is observed.

The influence of pH on pseudo first order rate coefficients at a flow rate of 60 mL min<sup>-1</sup> and for fixed dye concentrations is shown in figure 2.195.

Overlooking the minor discrepancies observed as the inherent behavior of the system, the general conclusion that can be drawn from these experiments is that there is a general decrease in the rate of the reaction for an increase in pH, with the rate coefficients being higher at pH 2 and no significant difference between that of pH 6 and 8. At low concentrations there is a significant difference in rate coefficients between the various flow rates at all pH ranges. However, with an increase in concentration, but for the difference between pH 2 and 4, no significant difference is observed, indicating that at pH beyond 4 the reduction process becomes independent of both pH and flow rates.

All these observations, point to the fact that the zero valent iron mediated reduction of Direct Catachine Brown is a two-stage process, which is pH dependent. This is clearly indicated by the high rate coefficients at pH 2 to the relatively lower values obtained at higher pH of 4, 6 and 8, with no significant difference between them. The rate coefficients are high at pH 2 because under acidic conditions the process operating is

chemical reaction mediated by direct electron transfer between the metal surface and the dye molecule in bulk solution. However, at pH 4, 6 and 8 the likely process operating could be surface mediated processes such as adsorption of the dye molecules on to the ferric hydroxide layer produced as a result of corrosion. The rates of chemical reduction being much greater than that of the surface mediated processes such as adsorption accounts for the significant difference between the rate coefficients of pH 2 and 4, while the difference between the rate coefficients of pH 4, 6 and 8 are more or less comparable as under these pH conditions adsorption is the primary removal mechanism.

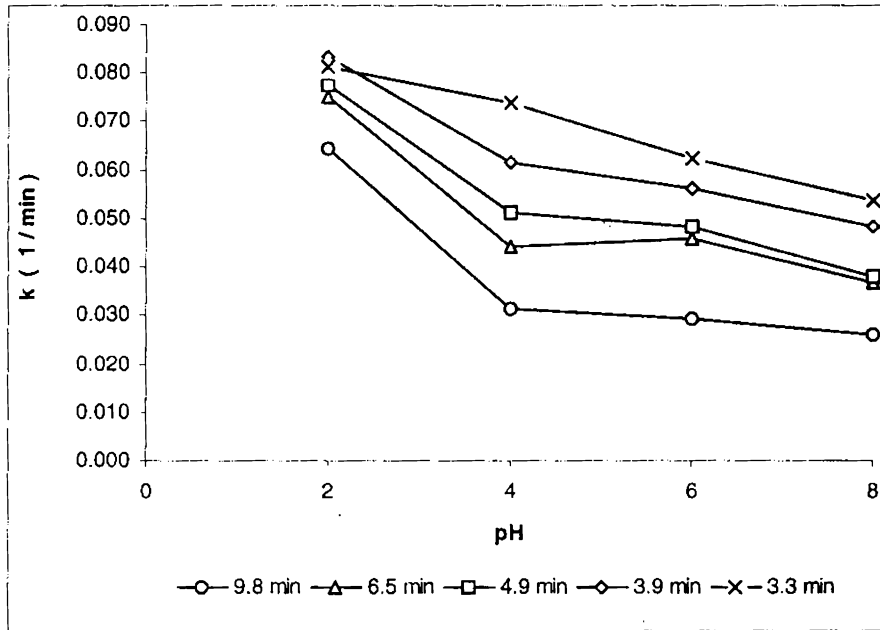


Figure 2.187  
 Direct Catachine Brown  
 Influence of pH on pseudo first order rate coefficients at a dye concentration of  $50 \text{ mg L}^{-1}$  and at fixed flow rates.

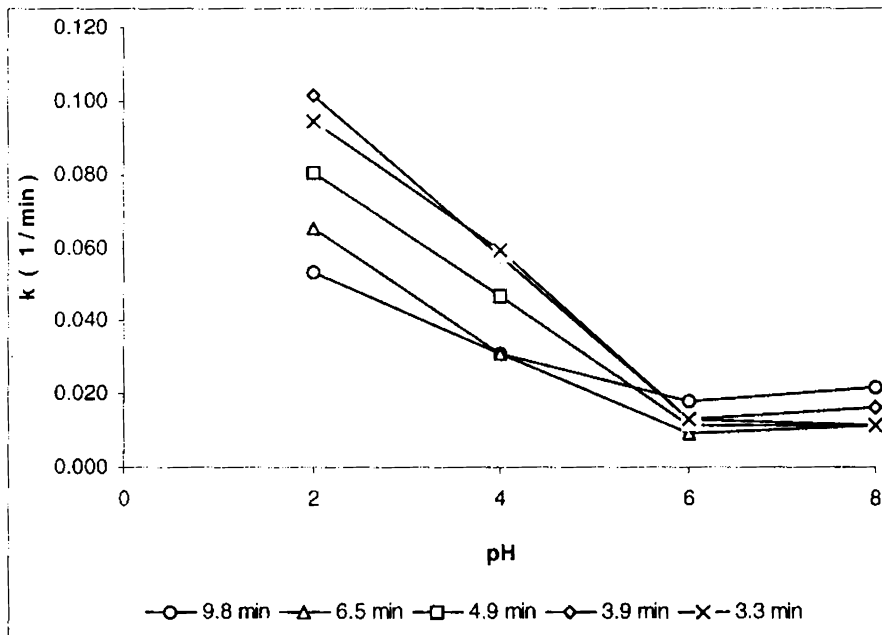


Figure 2.188  
 Direct Catachine Brown  
 Influence of pH on pseudo first order rate coefficients at a dye concentration of  $100 \text{ mg L}^{-1}$  and at fixed flow rates.



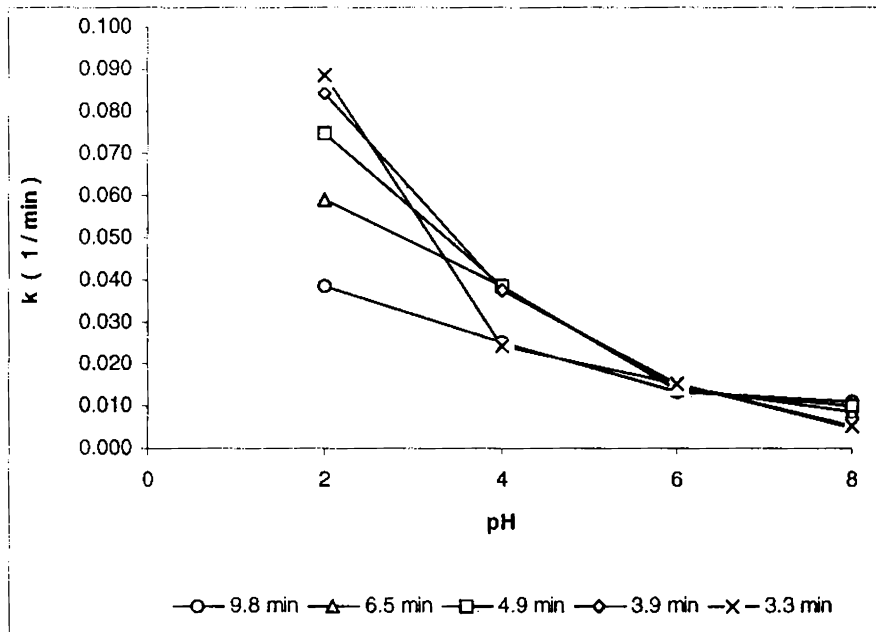


Figure 2.189  
 Direct Catachine Brown  
 Influence of pH on pseudo first order rate coefficients at a dye concentration of 150 mg L<sup>-1</sup> and at fixed flow rates.

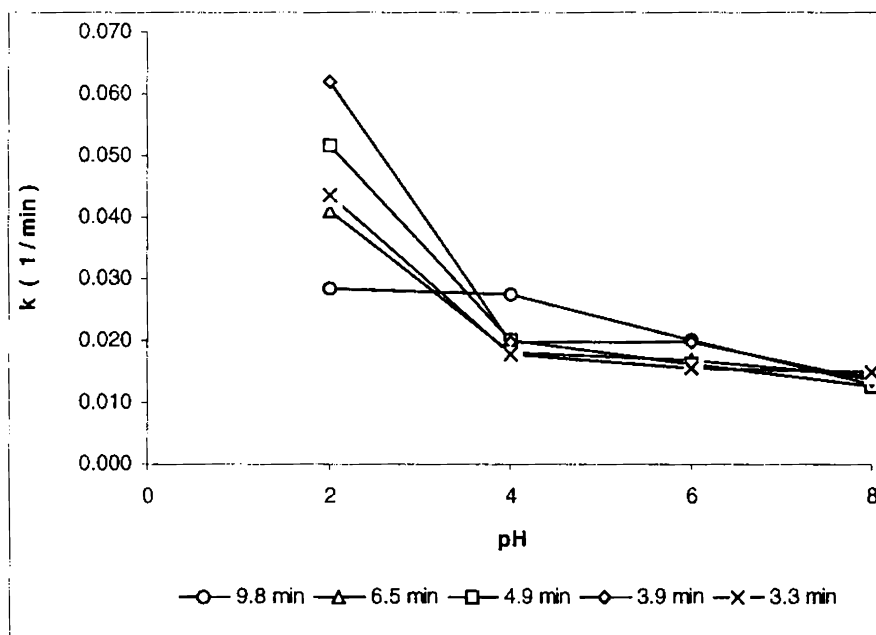


Figure 2.190  
 Direct Catachine Brown  
 Influence of pH on pseudo first order rate coefficients at a dye concentration of 200 mg L<sup>-1</sup> and at fixed flow rates.

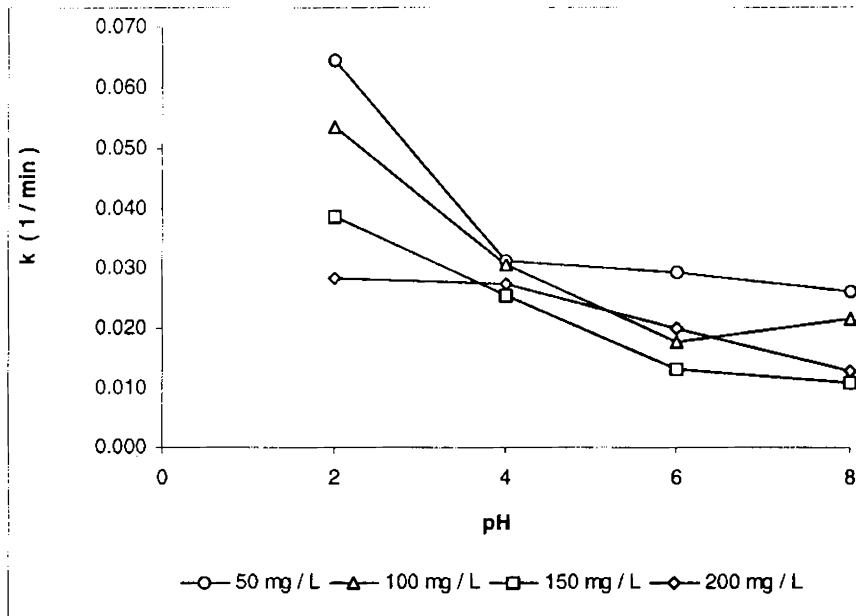


Figure 2.191  
 Direct Catachine Brown  
 Influence of pH on pseudo first order rate coefficients at a flow rate of  $20 \text{ mL min}^{-1}$  and for fixed dye concentrations.

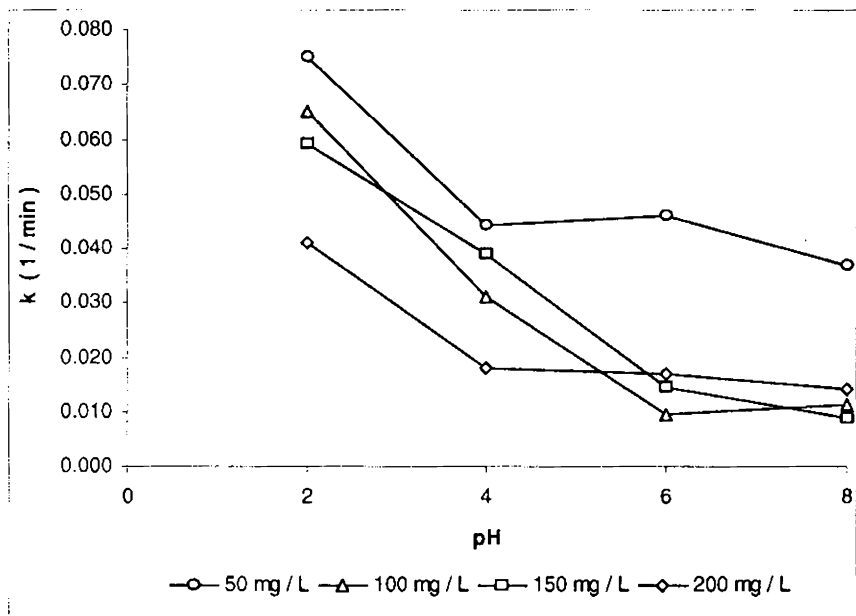


Figure 2.192  
 Direct Catachine Brown  
 Influence of pH on pseudo first order rate coefficients at a flow rate of  $30 \text{ mL min}^{-1}$  and for fixed dye concentrations.

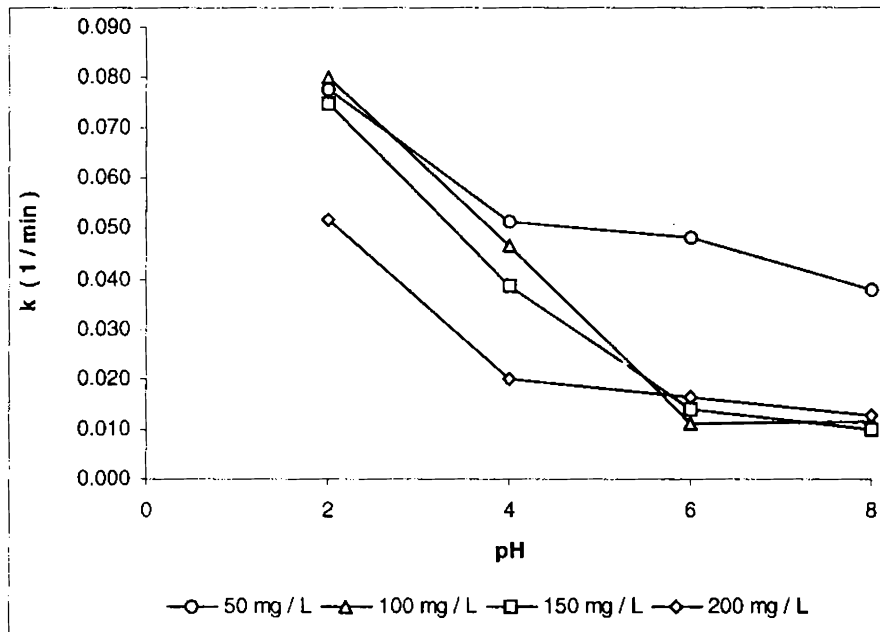


Figure 2.193  
 Direct Catachine Brown  
 Influence of pH on pseudo first order rate coefficients at a flow rate of 40 mL min<sup>-1</sup> and for fixed dye concentrations.

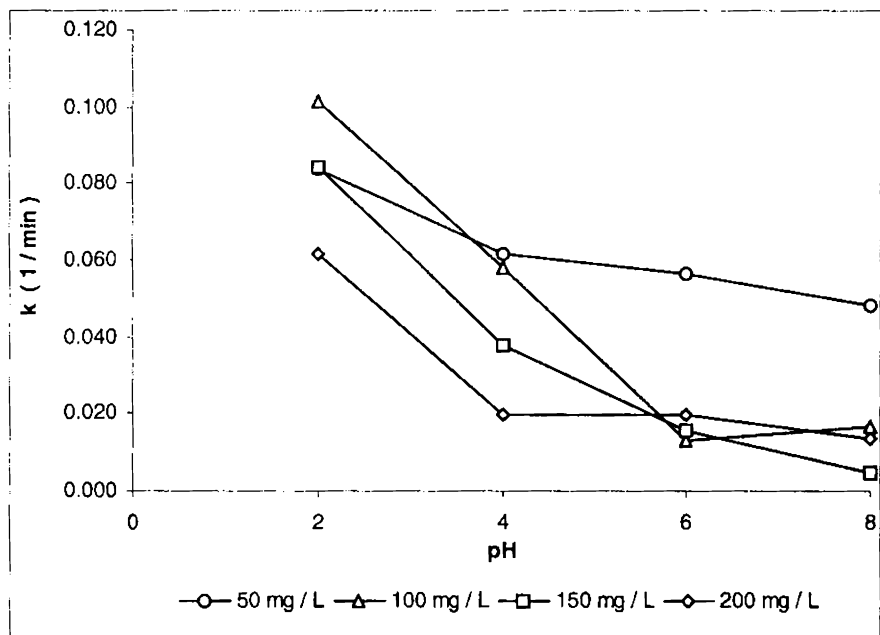


Figure 2.194  
 Direct Catachine Brown  
 Influence of pH on pseudo first order rate coefficients at a flow rate of 50 mL min<sup>-1</sup> and for fixed dye concentrations.

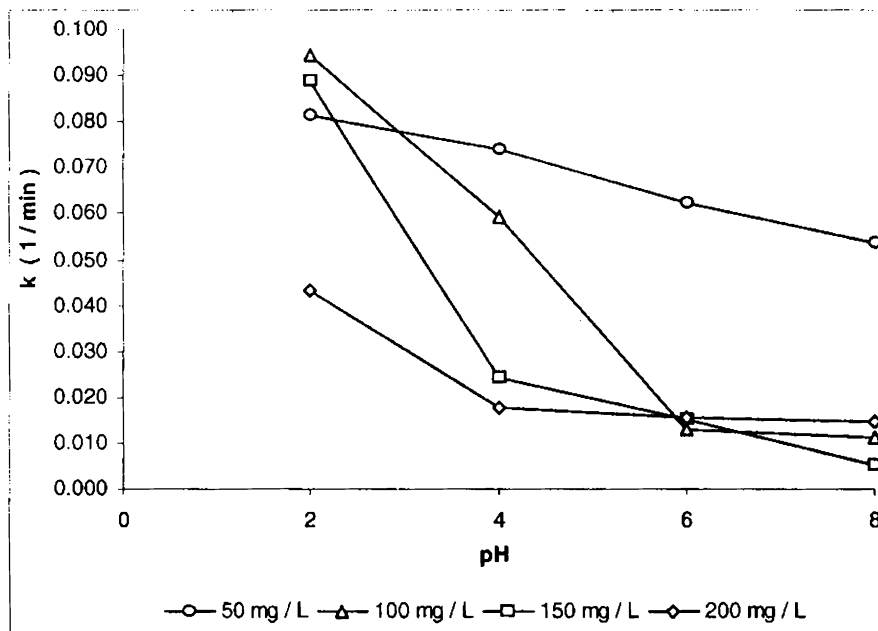


Figure 2.195  
Direct Catachine Brown  
Influence of pH on pseudo first order rate coefficients at a flow rate of  $60 \text{ mL min}^{-1}$  and for fixed dye concentrations.

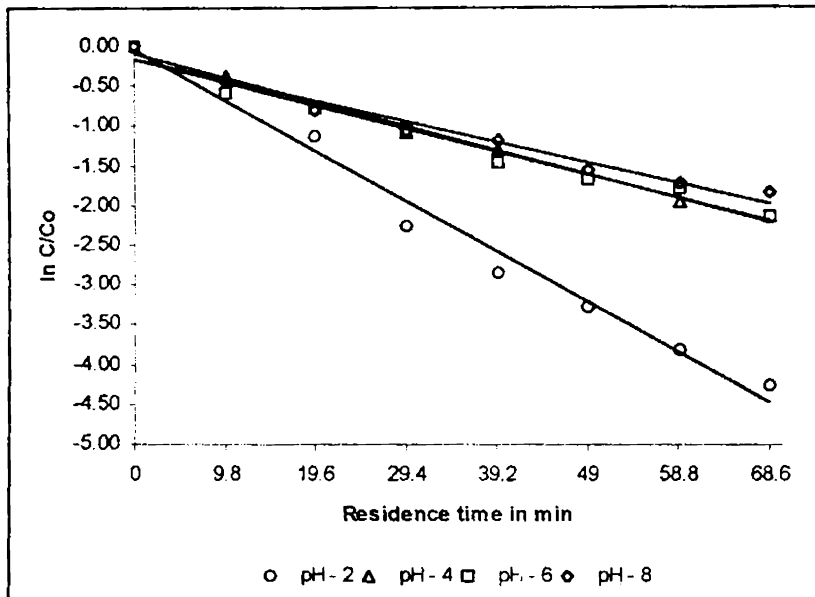


Figure 2.182  
 Direct Catachine Brown  
 Influence of pH on reduction kinetics at a dye concentration of  $50 \text{ mg L}^{-1}$  and at a residence time of 9.8 min.

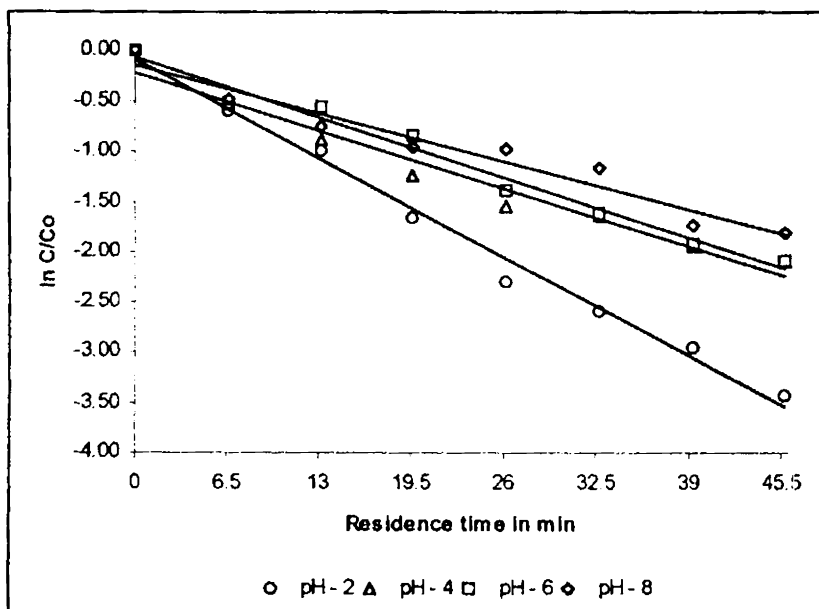


Figure 2.183  
 Direct Catachine Brown  
 Influence of pH on reduction kinetics at a dye concentration of  $50 \text{ mg L}^{-1}$  and at a residence time of 6.5 min.

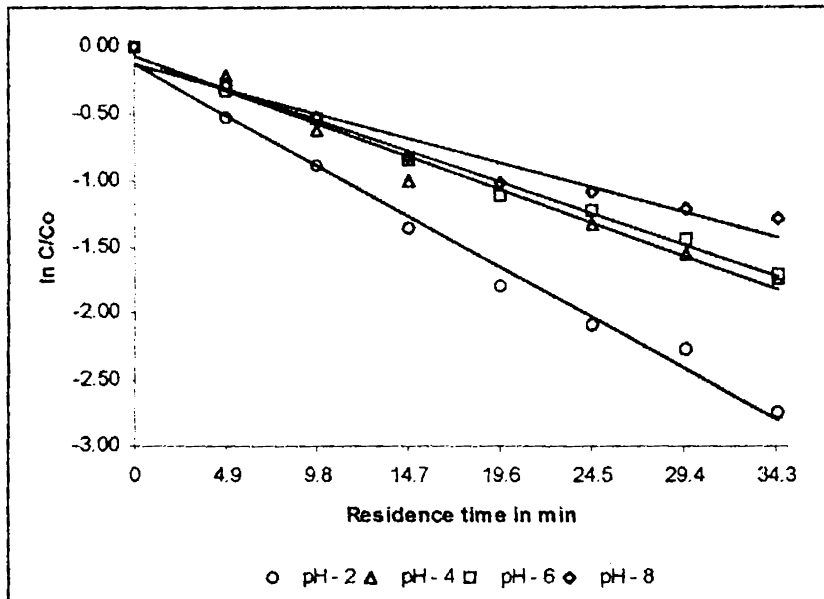


Figure 2.184  
Direct Catachine Brown  
Influence of pH on reduction kinetics at a dye concentration of 50 mg L<sup>-1</sup> and at a residence time of 4.9 min.

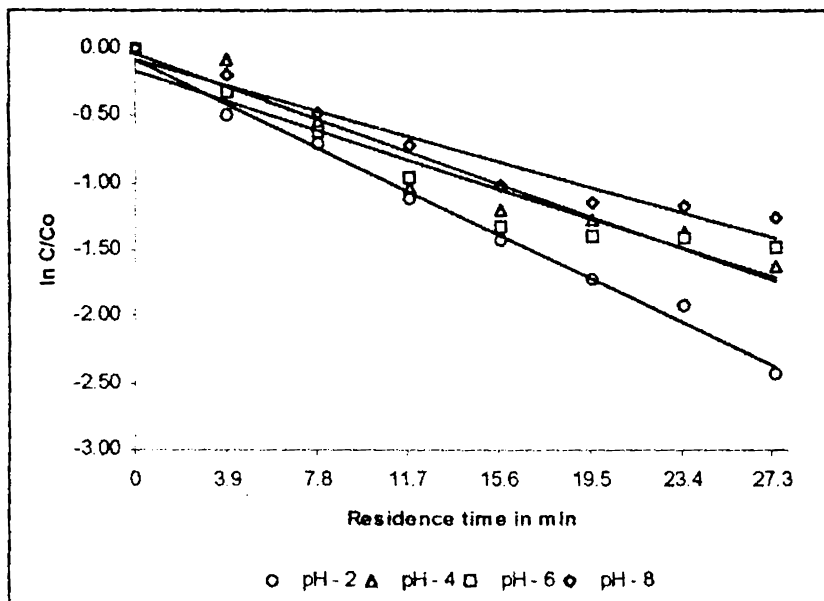


Figure 2.185  
Direct Catachine Brown  
Influence of pH on reduction kinetics at a dye concentration of 50 mg L<sup>-1</sup> and at a residence time of 3.9 min.

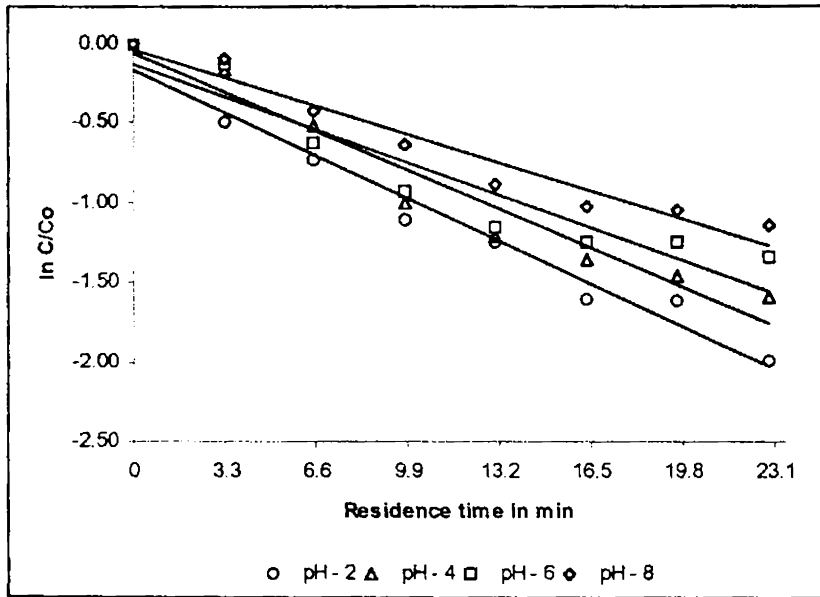


Figure 2.186  
 Direct Catachine Brown  
 Influence of pH on reduction kinetics at a dye concentration of  $50 \text{ mg L}^{-1}$  and  
 at a residence time of 3.3 min

#### 2.10.4. Direct Green – B

It was observed that the data fit well into linear first order plots and the influence of pH on reaction kinetics has been studied by monitoring the variation in the pseudo-first order rate coefficients. The figures 2.196 to 2.200 confirm first order reaction with respect to pH.

(i) Comparison between pH and flow rate at constant concentration

The relationship has been studied by monitoring the variation of pseudo first order rate coefficients derived for several flow rates under study at a specific concentration against the entire range of pH. An attempt has been made to investigate any possible correlation between the rate coefficients at different pH to flow rate.

The influence of pH on pseudo first order rate coefficients at a dye concentration of  $50 \text{ mg L}^{-1}$  and fixed flow rates is shown in figure 2.201. For an initial concentration of  $50 \text{ mg L}^{-1}$ , it is observed that there is a decrease in the rate of the reaction with an increase in pH, with the rate coefficients being maximum for pH 2 and subsequently decreasing, attaining a minimum value at pH 8. At a flow rate of  $20 \text{ mL min}^{-1}$ , after the initial decrease in the rate coefficients as the pH is raised from 2 to 4, the rate coefficients were found to become independent of pH. Beyond which up to a flow rate of  $50 \text{ mL min}^{-1}$  a decrease in the rate coefficient with an increase in pH is observed over the entire range of pH studied. However, at a higher flow rate of  $60 \text{ mL min}^{-1}$ , after an initial decrease in rate coefficient for an increase in pH from 2 to 6, the rate coefficient become independent of pH.



Figure 2.202 illustrates the influence of pH on the pseudo first order rate coefficients at a dye concentration of  $100 \text{ mg L}^{-1}$  and at fixed flow rates. As the concentration was raised to  $100 \text{ mg L}^{-1}$ , it is observed that the variations in rate coefficients with pH do show a dependence on flow rates. At a flow rate of  $20 \text{ mL min}^{-1}$ , the rate coefficients showed an initial decrease as the pH was raised from 2 to 4 and then remaining steady at pH 6 decreases at pH 8. As the flow rate was raised to  $30 \text{ mL min}^{-1}$ , the rate coefficients decreased linearly with an increase in pH from 2 to 6 after which it became independent of pH at 8. With an increase in flow rate to  $40 \text{ mL min}^{-1}$ , an increase in the rate coefficient is observed as the pH was raised to 4, before decreasing at pH 6 and then becoming independent of pH for further increase. At a flow rate  $50 \text{ mL min}^{-1}$ , the rate coefficients remained steady up to pH 4, before decreasing at pH 6 and then increasing at pH 8. However, at a flow rate of  $60 \text{ mL min}^{-1}$ , a linear decrease in the rate coefficient is observed for an increase in pH from 2 to 6 after which an increase is observed at pH: 8. This could be because, at low flow rates, the turbulence generated is not sufficient enough to remove the layer of adsorbed dye from the metal surface. Under such conditions a decrease in the rate coefficients is observed, but as the flow rate is increased to  $60 \text{ mL min}^{-1}$ , the turbulence effect generated is at its maximum, which is sufficient to remove the layer of dye formed at the metal surface thereby resulting in an increase in the rate coefficient after an initial decrease.

The influence of pH on pseudo first order rate coefficients at a dye concentration of  $150 \text{ mg L}^{-1}$  and fixed flow rates is shown in figure 2.203.

An increase in the dye concentration to  $150 \text{ mg L}^{-1}$  revealed that but for a random observation at pH 6, the general trend is a decrease in the rate coefficient with an increase in pH. However, at some flow rates the rate coefficient were found to become independent of pH, as observed at flow rate of  $30 \text{ mL min}^{-1}$ , where the rate coefficients become independent of pH beyond 4, and at a flow rate of  $60 \text{ mL min}^{-1}$ , where they become independent of pH between 4 and 6.

Figure 2.204 illustrates the influence of pH on the pseudo first order rate coefficients at a dye concentration of  $200 \text{ mg L}^{-1}$  and at fixed flow rates. At a concentration of  $200 \text{ mg L}^{-1}$ , the trend of decrease in rate coefficient with increase in pH continues with minor variations. Except for a flow rate of  $30 \text{ mL min}^{-1}$  where the rate coefficients become independent of pH beyond 4, at all other flow rates, after an initial decrease in rate coefficient with an increase in pH from 2 to 4, the rate coefficients were found to increase at pH 6 before continuing to decrease at pH 8, this increase could be due to the increased adsorption of the dye molecules over the metal surface at pH 6.

(ii) Comparison between pH and concentration at constant flow rate

In order to compare the relation between pH and concentration the rate coefficients derived for various concentrations at fixed flow rates have been compared against the range of pH studied.

The influence of pH on pseudo first order rate coefficients at a flow rate of  $20 \text{ mL min}^{-1}$  and for fixed dye concentrations is shown in figure 2.205. At a flow rate of  $20 \text{ mL min}^{-1}$ , all concentrations showed a decrease

in the rate coefficients as the pH was increased was raised from 2 to 4. At pH 4, the rate coefficients for all concentrations become comparable. Rate coefficients for concentrations of 50 and 100 mg L<sup>-1</sup> were found to become independent of pH after the initial decrease at 4. However, concentrations of 150 and 200 mg L<sup>-1</sup> showed an increase in the rate coefficients at pH 6 before recording a minimum value at pH 8.

Figure 2.206 represents the influence of pH on pseudo first order rate coefficients at a flow rate of 30 mL min<sup>-1</sup> and for fixed dye concentrations. As the flow rate was raised to 30 mL min<sup>-1</sup>, the rate coefficients was found to decrease with an increase in pH for all concentrations studied. Between concentrations, the rate coefficients of 100 and 200 mg L<sup>-1</sup> become comparable at pH 2. At pH 6, the rate coefficients of 50, 100 and 150 mg L<sup>-1</sup> become comparable, while at pH 8 the values of 100 and 150 mg L<sup>-1</sup> become comparable indicating that at the specified flow rate (30 mL min<sup>-1</sup>) dye concentrations of 100 and 150 mg L<sup>-1</sup> the rate coefficients become independent of pH above 6. However, at pH 4 the influence of concentration becomes quite apparent with the rate coefficients being greater at 50 mg L<sup>-1</sup> and lowest at 200 mg L<sup>-1</sup>. Concentrations of 150 and 200 mg L<sup>-1</sup> become independent of pH 4 while 100 mg L<sup>-1</sup> become independent of pH after 6. At an initial dye concentration of 50 mg L<sup>-1</sup>, the influence of pH was most prominent recording a decrease with an increase in pH.

The influence of pH on pseudo first order rate coefficients at a flow rate of 40 mL min<sup>-1</sup> and for fixed dye concentrations is shown in figure

2.207. But for an increase in the rate coefficients at pH 4 for a concentration of  $100 \text{ mg L}^{-1}$ , at a flow rate of  $40 \text{ mL min}^{-1}$  the general trend observed is a decrease in the rate coefficient with an increase in pH, with the values at concentrations of 100 and  $200 \text{ mg L}^{-1}$  becoming comparable at pH 6 and 50 and  $100 \text{ mg L}^{-1}$  becoming comparable at pH 8.

Figure 2.208 represents the influence of pH on pseudo first order rate coefficients at a flow rate of  $50 \text{ mL min}^{-1}$  and for fixed dye concentrations. As the flow rate was raised to  $50 \text{ mL min}^{-1}$ , the trend of decrease in rate coefficients for increase in pH is observed only for a concentration of  $50 \text{ mg L}^{-1}$ , with minor variations observed at higher concentrations. At a concentration of  $100 \text{ mg L}^{-1}$  the rate coefficients was found independent of pH up to 4, after which the rate coefficient was found to decrease as the pH was raised to 6, followed by an increase at pH 8. At a concentration of  $150 \text{ mg L}^{-1}$  the rate coefficients were found independent of pH between pH 4 and 6 before continuing to decrease to pH 8. At pH 4 the rate coefficients at 50 and  $100 \text{ mg L}^{-1}$  become comparable. At pH 6 there is only a marginal variation between concentrations. At pH 8 the rate coefficients of 150 and  $200 \text{ mg L}^{-1}$  become comparable.

The influence of pH on pseudo first order rate coefficients at a flow rate of  $60 \text{ mL min}^{-1}$  and for fixed dye concentrations is shown in figure 2.209. At a flow rate of  $60 \text{ mL min}^{-1}$ , but for the rate coefficients for  $150 \text{ mg L}^{-1}$  becoming independent of pH above pH 4, the general observation is that the rate coefficients decreases with an increase in pH for all the concentration range studied up to pH 6. After which, the rate coefficients

for concentrations of 50 and 100 mg L<sup>-1</sup> showed a marginal increase with the increase in pH to 8, but, for higher concentrations of 150 and 200 mg L<sup>-1</sup> the rate coefficients continued to decrease with increase in pH. However, since, the increase in rate coefficients at concentrations of 50 and 100 mg L<sup>-1</sup> is only marginal, they can be considered independent of pH over 6.

The general conclusion that can be drawn is that, there is a decrease in the rate coefficient with increase in pH, with the rate coefficients being maximum at pH 2 and a progressive decrease in the rate coefficients with an increase in pH to 4, 6 and 8. In some of the experiments it is observed that between these pH ranges the rate coefficients become comparable particularly between pH 6 and 8. The high rate coefficients obtained at pH 2 and significantly lower values at pH 4, 6 and 8 suggest that the iron mediated reduction of the azo dyes involve two processes that tend to shift depending on the pH conditions. Since, the rate coefficients at pH 4 was in most cases observed to be greater than that of pH 6 and 8, pH 4 can be considered as the transition pH below which i.e., at pH 2, the reaction is chemical reduction involving direct transfer of electrons from the metal surface to the dye molecule. Under such conditions, the reactive site present at the metal surface plays a major role in influencing the overall reaction kinetics. This clearly indicates the influence of, the condition of the metal surface on the reduction kinetics. Although an iron surface when exposed to air or aqueous solution will develop an oxide layer, under acidic conditions this oxide layer under-

dissolution and the system being a flow through system the oxide layer even if formed would be washed out of the system. As a result only a clean and reduced metal surface is available for reaction with the dye molecule. Under such conditions electrons produced as a result of iron corrosion would be transferred to the azo linkages results in its cleavage and the dye molecule getting reduced to form amines or hydra azo derivatives (depending on the number of electrons transferred) which in either case is colorless. However, when the pH is above 4, the oxide layer formed as a result of corrosion will remain on the surface of the metal. This oxide layer is corrosion products in the form of ferric hydroxide precipitates that contain exchangeable sites where the dye molecule can be actively adsorbed. This layer of corrosion products is the non-reactive site, which at pH over 4 influence the removal mechanism by adsorption of the dye molecules at its surface. Under such conditions the dye molecule do not under go mineralization but they simply remain adsorbed on to the surface of the metal. Now the reaction becomes a surface mediated phenomenon with the transfer of the dye molecules from the bulk solution to the metal surface becoming the rate limiting step and mass transport influencing the over all reaction kinetics. The results indicate that the rate coefficient for chemical reaction, mediated by the direct transfer of electrons from the metal surface to the dye molecule is found much higher (as indicated by the higher rate coefficients obtained for pH 2, than that of the surface mediated processes as indicated by the lower rate coefficient values for pH 6 and 8). On the other hand, the rate coefficients for pH 4 was found lower than that of pH 2,

but greater than that of pH 6 and 8; as at pH 4 the rate coefficients measured is the sum of both chemical reaction as well as surface mediated process such as adsorption while at pH 6 and 8 it is only adsorption.

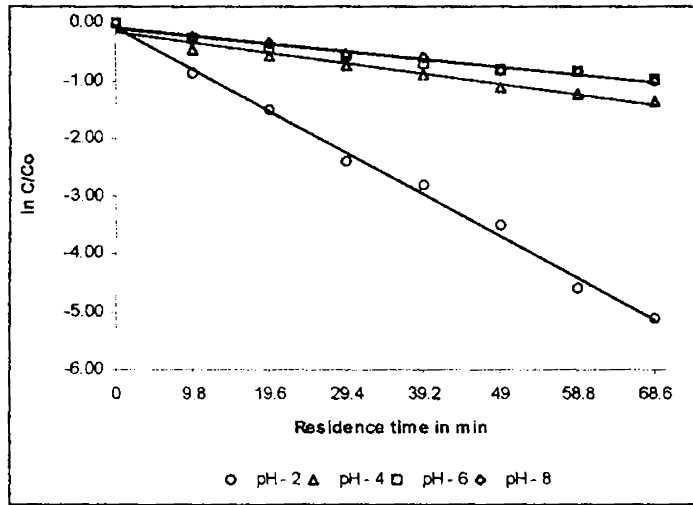


Figure 2.196  
Direct Green B  
Influence of pH on reduction kinetics at a dye concentration of  $50 \text{ mg L}^{-1}$  and at a residence time of 9.8 min.

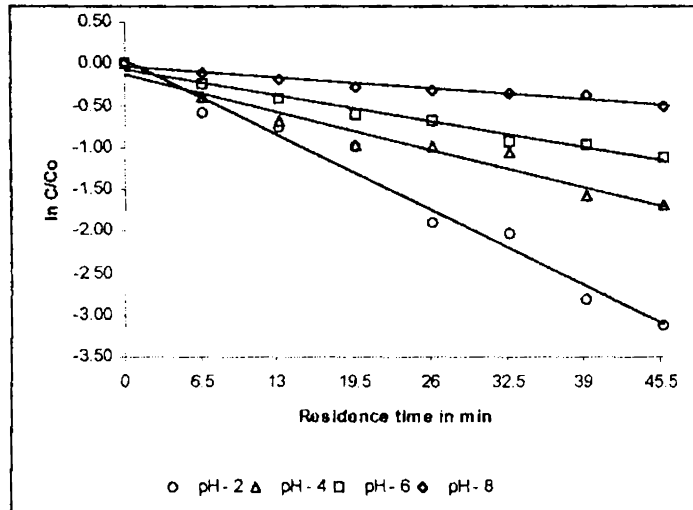


Figure 2.197  
Direct Green B  
Influence of pH on reduction kinetics at a dye concentration of  $50 \text{ mg L}^{-1}$  and at a residence time of 6.5 min.



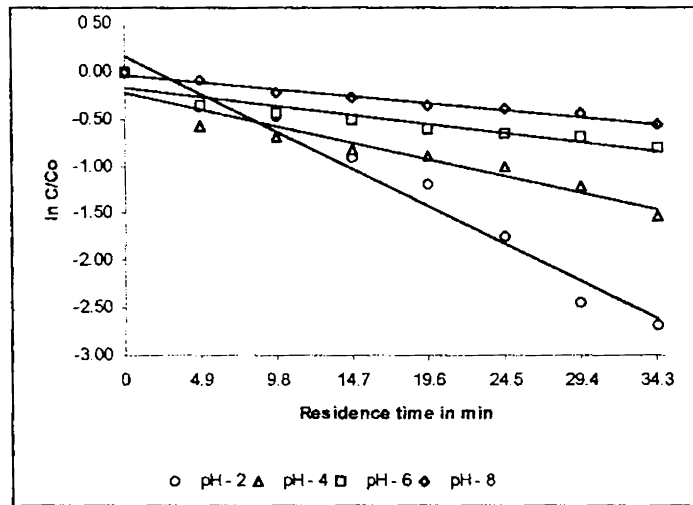


Figure 2.198  
Direct Green B  
Influence of pH on reduction kinetics at a dye concentration of 50 mg L<sup>-1</sup> and at a residence time of 4.9 min.

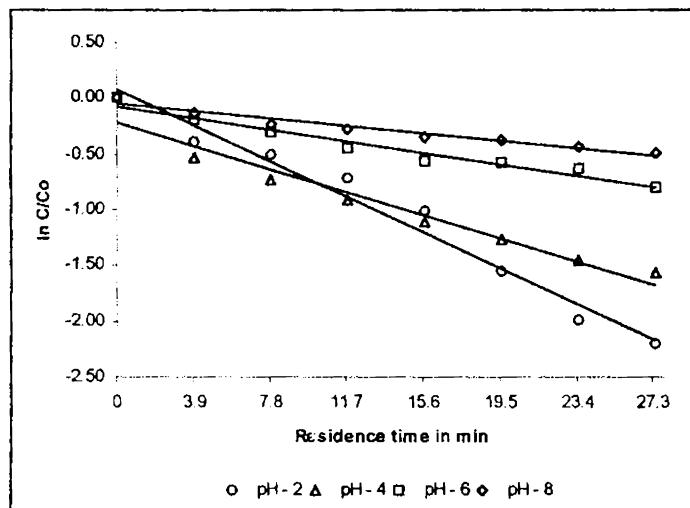


Figure 2.199  
Direct Green B  
Influence of pH on reduction kinetics at a dye concentration of 50 mg L<sup>-1</sup> and at a residence time of 3.9 min.

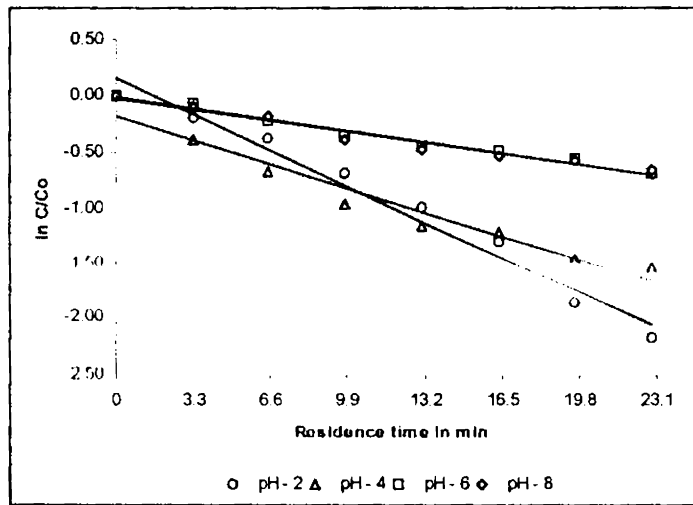


Figure 2.200  
 Direct Green B  
 Influence of pH on reduction kinetics at a dye concentration of  $50 \text{ mg L}^{-1}$  and  
 at a residence time of 3.3 min.

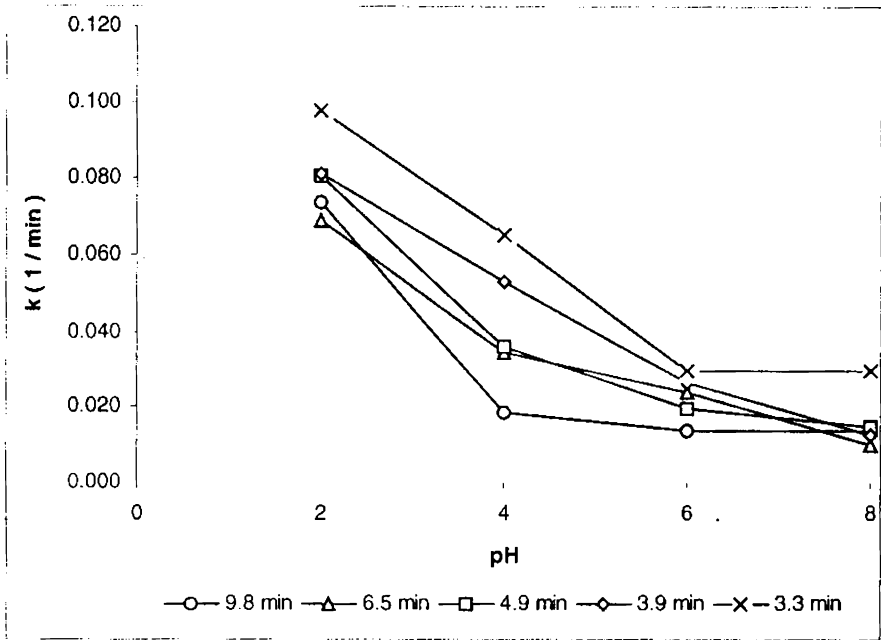


Figure 2.201  
 Direct Green - B  
 Influence of pH on pseudo first order rate coefficients at a dye concentration of 50 mg L<sup>-1</sup> and at fixed flow rates.

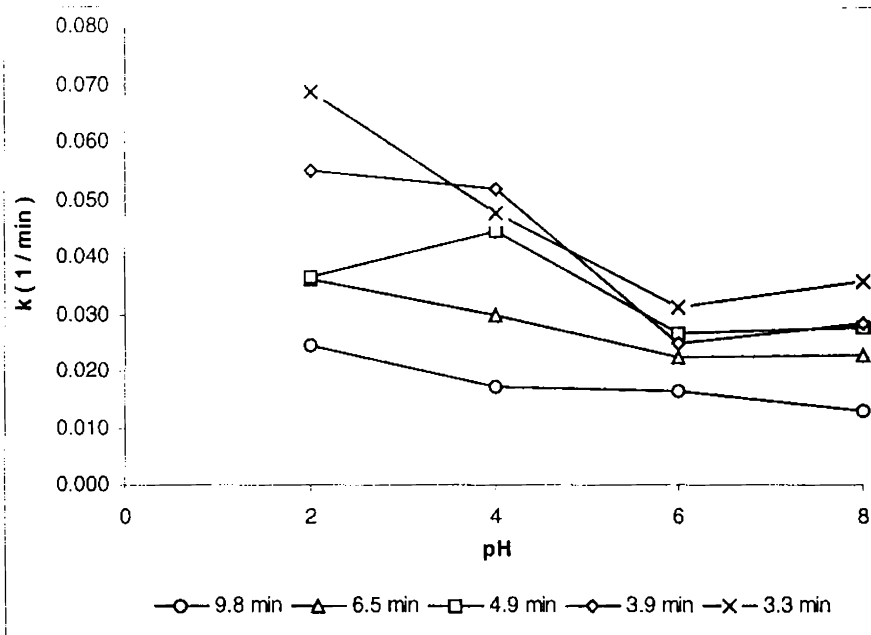


Figure 2.202  
 Direct Green - B  
 Influence of pH on pseudo first order rate coefficients at a dye concentration of 100 mg L<sup>-1</sup> and at fixed flow rates.

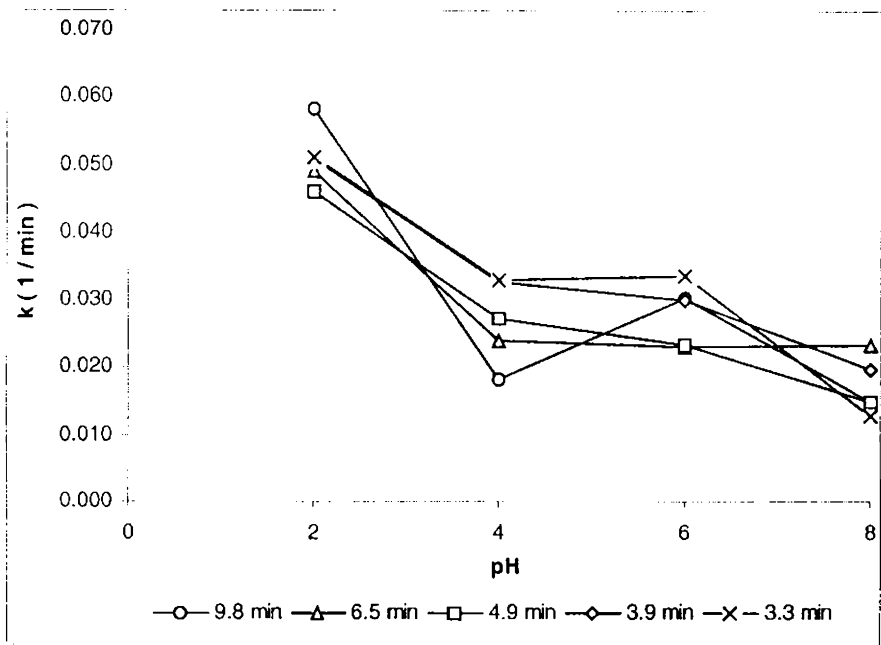


Figure 2.203  
 Direct Green - B  
 Influence of pH on pseudo first order rate coefficients at a dye concentration of 150 mg L<sup>-1</sup> and at fixed flow rates.

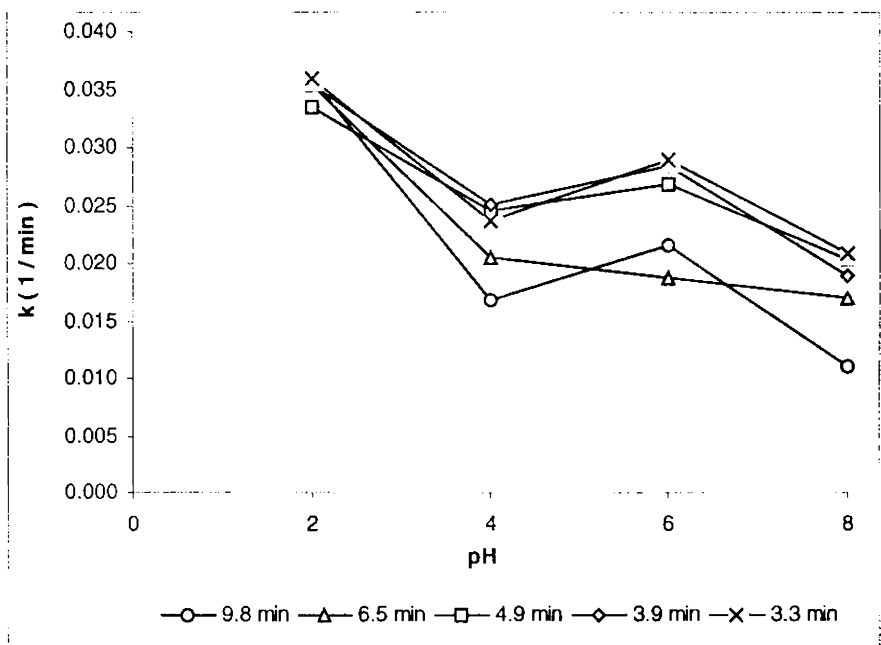


Figure 2.204  
 Direct Green - B  
 Influence of pH on pseudo first order rate coefficients at a dye concentration of 200 mg L<sup>-1</sup> and at fixed flow rates.

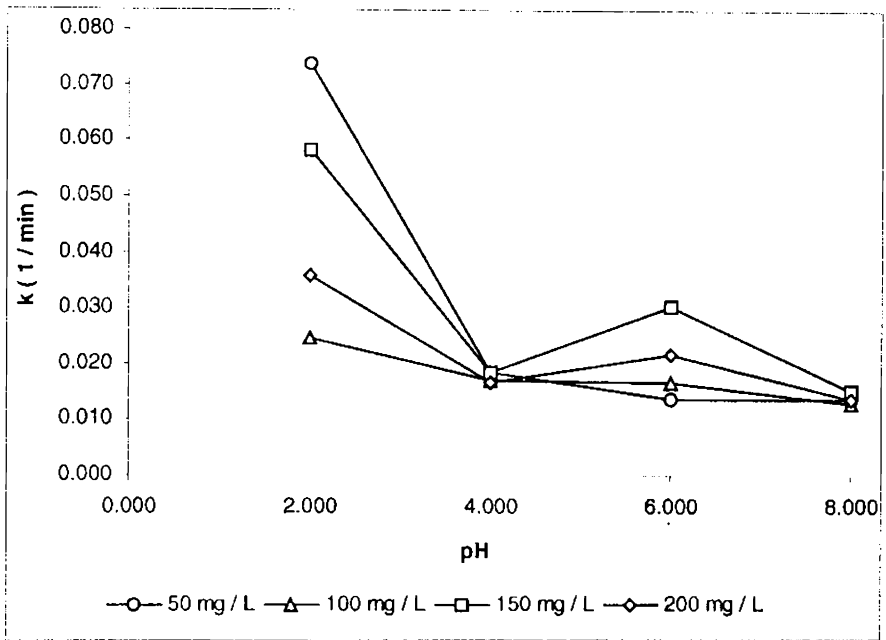


Figure 2.205  
Direct Green - B  
Influence of pH on pseudo first order rate coefficients at a flow rate of 20 mL min<sup>-1</sup> and for fixed dye concentrations.

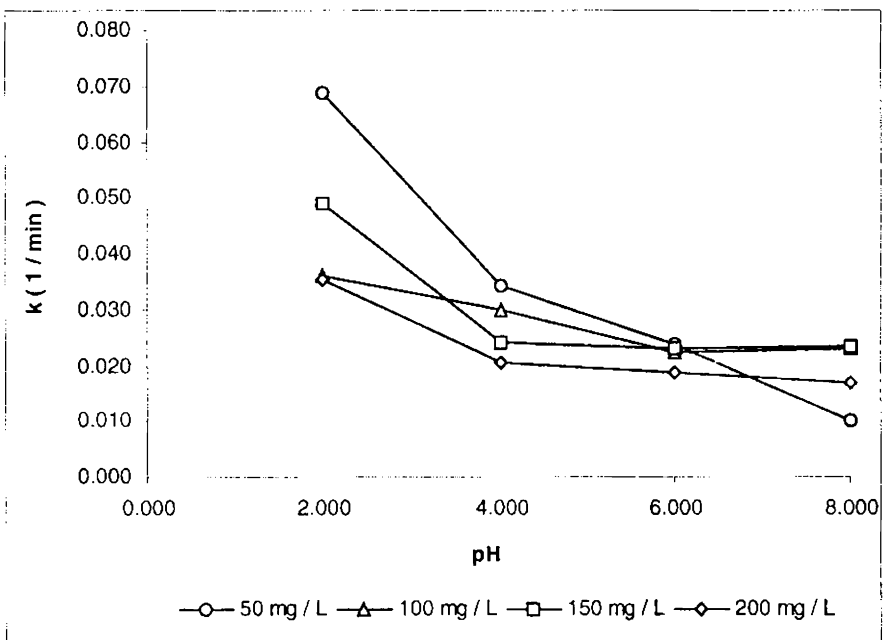


Figure 2.206  
Direct Green - B  
Influence of pH on pseudo first order rate coefficients at a flow rate of 30 mL min<sup>-1</sup> and for fixed dye concentrations.

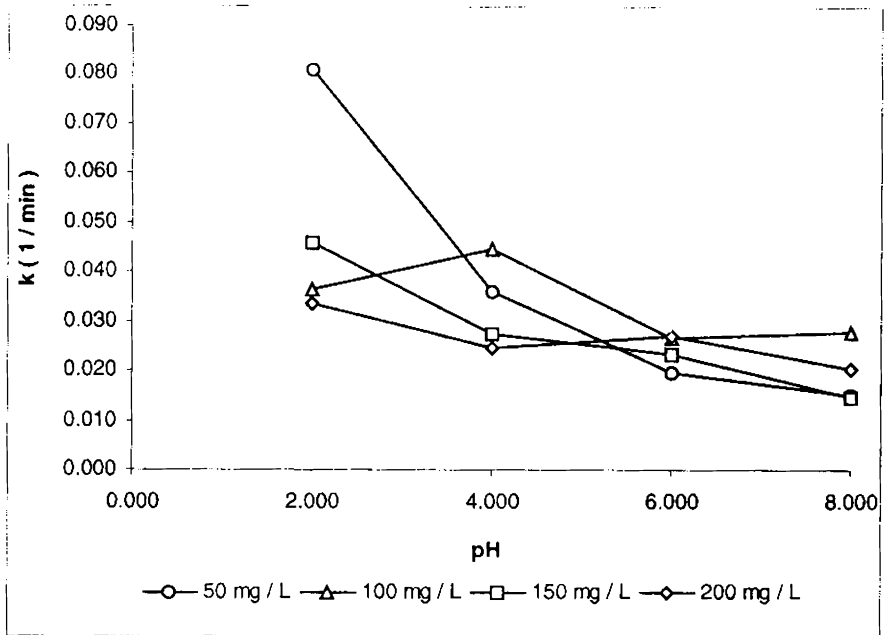


Figure 2.207  
 Direct Green - B  
 Influence of pH on pseudo first order rate coefficients at a flow rate of 40 mL min<sup>-1</sup> and for fixed dye concentrations

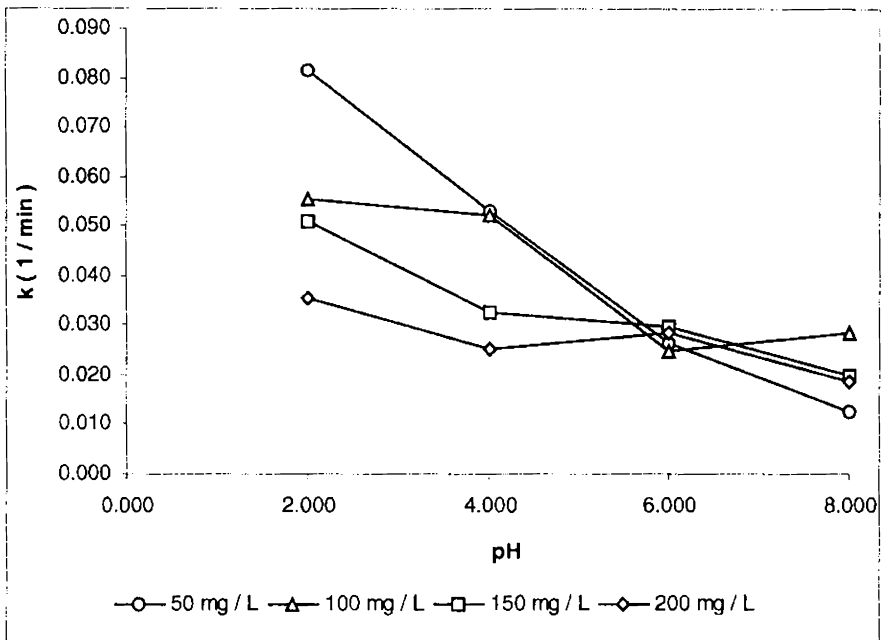


Figure 2.208  
 Direct Green - B  
 Influence of pH on pseudo first order rate coefficients at a flow rate of 50 mL min<sup>-1</sup> and for fixed dye concentrations

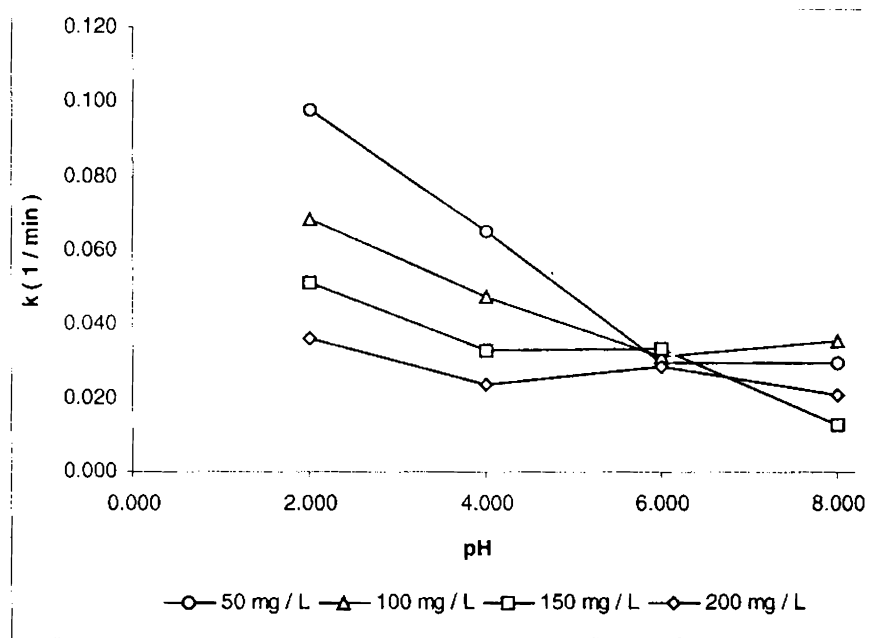


Figure 2.209  
 Direct Green - B  
 Influence of pH on pseudo first order rate coefficients at a flow rate of  $60 \text{ mL min}^{-1}$  and for fixed dye concentrations.

### 2.10.5. Yellow-5GL

It was observed that the data fit well into linear first order plots and the influence of pH on reaction kinetics has been studied by monitoring the variation in the pseudo-first order rate coefficients. The figures (2.210 to 2.214) confirm first order reaction with respect to pH.

(i) Comparison between pH and concentration at constant flow rates

The variation in the pseudo first order rate coefficient derived for the entire range of pH studied at a fixed flow rate and for several fixed concentrations to study the relation between pH and concentration.

The influence of pH on pseudo first order rate coefficients at a Flow rate of  $20 \text{ mL min}^{-1}$  and for fixed dye concentration is shown in figure 2.215. At a flow rate of  $20 \text{ mL min}^{-1}$ , the general trend observed is that at low dye concentration of  $50 \text{ mg L}^{-1}$  the rate coefficients decrease with an increase in pH up to 6, after which it becomes independent of pH. At  $100 \text{ mg L}^{-1}$ , the rate coefficients were found to decrease linearly with an increase in pH up to 6, after which for further increase in pH a decrease is observed. Concentrations of 150 and  $200 \text{ mg L}^{-1}$  indicate almost similar trends with the rate coefficients decreasing with an increase in pH to 4, after which it becomes independent of pH up to 6 before recording an increase at pH 8 for  $150 \text{ mg L}^{-1}$ ; while for  $200 \text{ mg L}^{-1}$  after an initial decrease in rate coefficient as the pH is raised to 4, a marginal increase with an increase in pH is observed. At pH 2, it is observed that the rate coefficients for dye concentrations of 50, 100 and  $200 \text{ mg L}^{-1}$  are comparable with out any major difference between them. At pH 4, the values at concentrations



above  $50 \text{ mg L}^{-1}$  become comparable which is also observed at pH 8, but there is a significant difference between the rate coefficients at pH 6. This increase in rate coefficients after an initial decrease was found dependent on concentration. When the concentration was low ( $50$  and  $100 \text{ mg L}^{-1}$ ) the rate coefficients was found to decrease up to pH 6. But at high concentrations of  $150$  and  $200 \text{ mg L}^{-1}$ , the rate coefficients showed a decrease only up to pH 4. In all the cases after the initial decrease an increase in rate coefficients is observed for an increase in pH (above 4 or 6), which is indicative of surface mediated processes such as adsorption becoming dominant.

Figure 2.216 illustrates the influence of pH on pseudo first order rate coefficients at a Flow rate of  $30 \text{ mL min}^{-1}$  and for fixed dye concentrations. As the flow rate was raised to  $30 \text{ mL min}^{-1}$ , it is observed that at concentrations of  $50$ ,  $100$  and  $200 \text{ mg L}^{-1}$ , the rate coefficient was found to decrease linearly with an increase in pH up to 6, after which in all the three cases, an increase in rate coefficient is observed with an increase in pH to 8. However, at  $250 \text{ mg L}^{-1}$  the rate coefficients were found to decrease with an increase in pH only up to pH 4, after which becoming independent of pH up to 6, decreases at pH 8.

The influence of pH on pseudo first order rate coefficients at a Flow rate of  $40 \text{ mL min}^{-1}$  and for fixed dye concentration is shown in figure 2.217. With an increase in flow rate to  $40 \text{ mL min}^{-1}$ , it was found that the rate coefficients at  $50 \text{ mg L}^{-1}$  decreased linearly with an increase in pH up to 6, after which an increase in the rate coefficient is observed as the pH was

raised to 8. At  $100 \text{ mg L}^{-1}$ , the rate coefficients showed a decrease as the pH was raised to 6 after which they become independent of pH. At  $150 \text{ mg L}^{-1}$  the rate coefficients decreased as the pH was raised to 4, but then increased at pH 6, before decreasing at pH 8. This behavior is similar to the observations made at a flow rate of  $30 \text{ mL min}^{-1}$  for the same concentration, however, since the difference between the rate coefficients of pH 4 and 8 is marginal, it is assumed that the increase observed at pH 6 is random and the rate coefficient is considered to become independent of pH. At pH 2 and 8, the rate coefficients were found independent of concentration up to  $150 \text{ mg L}^{-1}$ , as the difference between them is only marginal. Variation between values has been observed at pH 6 and 8.

Figure 2.218 illustrates the influence of pH on pseudo first order rate coefficients at a Flow rate of  $50 \text{ mL min}^{-1}$  and for fixed dye concentrations. At a flow rate of  $50 \text{ mL min}^{-1}$ , the trends observed for the dye concentration of  $50 \text{ mg L}^{-1}$  is similar to the observations made at the preceding flow rate. However, at  $100$  and  $150 \text{ mg L}^{-1}$ , the rate coefficients decreased as the pH was raised to 4 and then remains independent of pH at 6 before recording a decrease at pH 8. At pH 4 and 6, the rate coefficients for  $100$ ,  $150$  and  $200 \text{ mg L}^{-1}$  become comparable, while at pH 8, concentrations of  $50$  and  $150 \text{ mg L}^{-1}$  were found to have almost similar values. For a concentration of  $200 \text{ mg L}^{-1}$ , an increase in the rate coefficient is observed up to pH 4, after which they become independent of pH.

The influence of pH on pseudo first order rate coefficients at a Flow rate of  $60 \text{ mL min}^{-1}$  and for fixed dye concentration is shown in figure 2.219.

For an increase in flow rate to  $60 \text{ mL min}^{-1}$ , it is observed that concentrations up to  $150 \text{ mg L}^{-1}$  showed a decrease in the rate coefficient with an increase in pH up to 4, after which it remains more or less steady at pH 6. However, from this point the behavior of the rate coefficients were found concentration dependent. For  $50 \text{ mg L}^{-1}$  an increase in the rate coefficient is observed at pH 8, while for both  $100$  and  $150 \text{ mg L}^{-1}$ , a decrease is observed.  $200 \text{ mg L}^{-1}$  showed trends similar to that observed at a flow the lower flow rate ( $50 \text{ mL min}^{-1}$ ).

The general conclusion that can be drawn is that for a dye concentrations up to  $150 \text{ mg L}^{-1}$ , there is a definite decrease in the rate coefficient as the pH is raised from 2 to 4, after which a trend which show dependence on flow rate is observed. At low flow rate ( $20 \text{ mL min}^{-1}$ ), the rate coefficients show an increase at pH 8, after recording a decrease up to pH 6. While at higher concentrations they become more or less independent of pH. As the flow rate is raised further concentrations up to  $150 \text{ mg L}^{-1}$  continue with the previously observed trends but at  $200 \text{ mg L}^{-1}$  the rate coefficients at pH 2 was found to become lower than pH 4 after which they become independent of pH. This indicates that the dependence on pH is prominent under conditions of low flow rate and concentration. But there is a systematic variation of the rate coefficients with pH showing definite dependence on concentration. In order to explore this possibility the variation in rate coefficients derived for flow rates with pH at fixed concentration has been analyzed.

(ii) Comparison between pH and flow rates at constant concentration

The variation in rate coefficients derived for various pH at a fixed Concentration and for several fixed flow rates have been compared thereby determining the relation between pH and flow rates.

The influence of pH on pseudo first order rate coefficients at a dye concentration of  $50 \text{ mg L}^{-1}$  and fixed flow rates is shown in figure 2.220. At an initial concentration of  $50 \text{ mg L}^{-1}$ , the general trend observed is that at a flow rate of  $20 \text{ mL min}^{-1}$  the rate coefficients were found independent of pH between 2 and 4, and 6 and 8. However, a decrease in rate coefficient is observed as the pH is raised from 4 to 6. At all higher flow rates up to  $50 \text{ mL min}^{-1}$ , the rate coefficients were found to linearly decrease with an increase in pH up to 6 after which the rate coefficients was found to increase as the pH was raised to 8. At a flow rate of  $60 \text{ mL min}^{-1}$ , the rate coefficients were found to decrease with an increase in pH from 2 to 4 after which remaining independent of pH up to 6 an increase is observed at pH 8.

Figure 2.221 illustrates the influence of pH on the pseudo first order rate coefficients at a dye concentration of  $100 \text{ mg L}^{-1}$  and at fixed flow rates. With an increase in concentration to  $100 \text{ mg L}^{-1}$ , up to a flow rate of  $40 \text{ mL min}^{-1}$ , the rate coefficients were found to decrease with an increase in pH up to 6, after which at low flow rates of  $20 \text{ mL min}^{-1}$ , the increase in rate coefficient observed with an increase in pH from 6 to 8 give way to the rate coefficients becoming independent of pH.

The influence of pH on pseudo first order rate coefficients at a dye concentration of  $150 \text{ mg L}^{-1}$  and fixed flow rates is shown in figure 2.222. Trends observed at a dye concentration of  $150 \text{ mg L}^{-1}$  are similar to that of the trends at  $100 \text{ mg L}^{-1}$ .

Figure 2.223 illustrates the influence of pH on the pseudo first order rate coefficients at a dye concentration of  $200 \text{ mg L}^{-1}$  and at fixed flow rates. At an initial dye concentration of  $200 \text{ mg L}^{-1}$ , the rate coefficients continue to show trends similar to those observed at lower concentrations except that at a higher flow rate of  $50 \text{ mL min}^{-1}$  random variation in the rate coefficient is observed, while at  $60 \text{ mL min}^{-1}$  after an initial increase in the rate coefficient with an increase in pH from 2 to 4, they were found to become independent of pH. Schultz and Grundl, (2000) studied the reduction of 4-chloronitrobenzene by Fe(II)/Montmorillonite in batch systems over the range of pHs from 6 to 8. The authors observed that the reduction process followed first order kinetics. The reaction rates increased with an increase in pH from 6 to 8. This was found to correlate to the increase in  $\text{FeOH}^+$  which was found to be the primary reductant at high pH. This was attributed to both an increase in concentration of the  $\text{FeOH}^+$  ion and to the sorption of Fe(II) at high pH. Ferrous=ferric oxide sorption complexes on the surface of ferric oxides are analogous to  $\text{FeOH}^+$  complexes in aqueous phase. The authors state that ferric oxyhydroxide precipitates formed during the reaction are a source of mediating surfaces that could potentially control the reaction. Investigating the effectiveness of electrochemical reduction for the removal of trichloroethene (TCE) and

carbon tetrachloride ( $\text{CCl}_4$ ) Li and Farrell, (2000), observed that the half-lives increased by a factor of three between a pH of 4 and 10 indicating that hydrogen was involved in the TCE reduction by iron electrode.

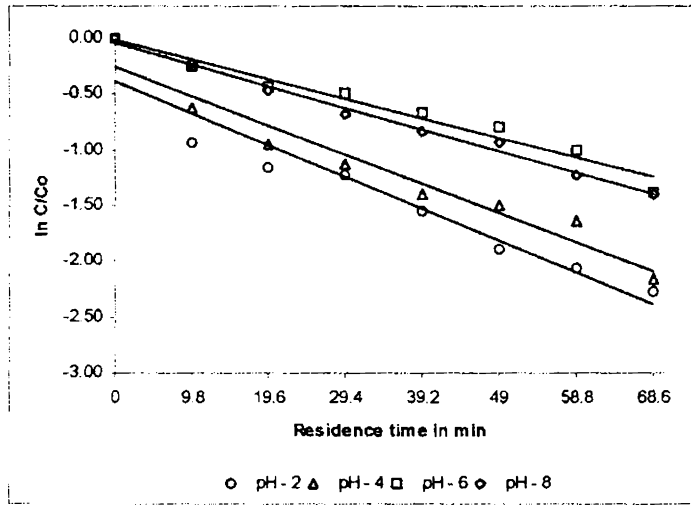


Figure 2.210  
 Yellow 5GL  
 Influence of pH on reduction kinetics at a dye concentration of  $50 \text{ mg L}^{-1}$  and at a residence time of 9.8 min.

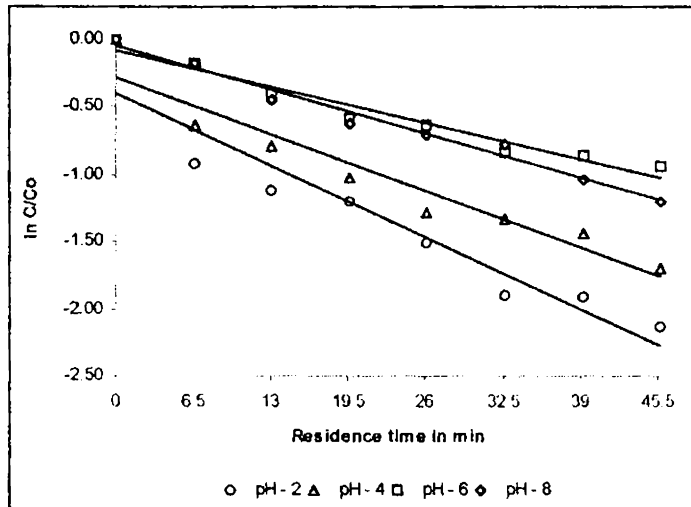


Figure 2.211  
 Yellow 5GL  
 Influence of pH on reduction kinetics at a dye concentration of  $50 \text{ mg L}^{-1}$  and at a residence time of 6.5 min.

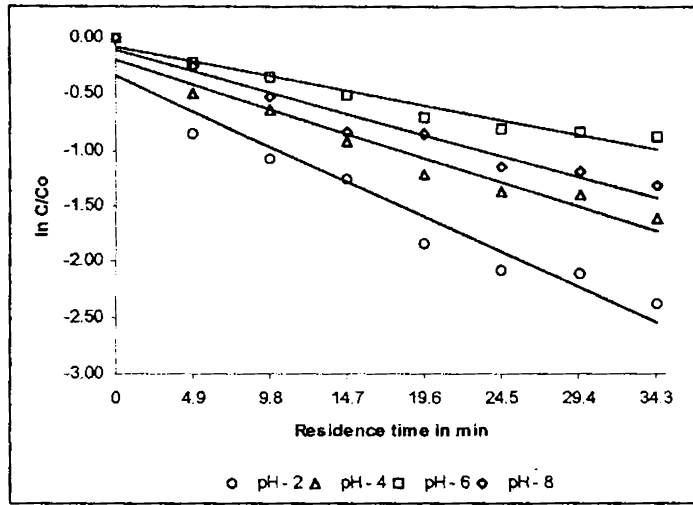


Figure 2.212  
 Yellow 5GL  
 Influence of pH on reduction kinetics at a dye concentration of  $50 \text{ mg L}^{-1}$  and at a residence time of 4.9 min.

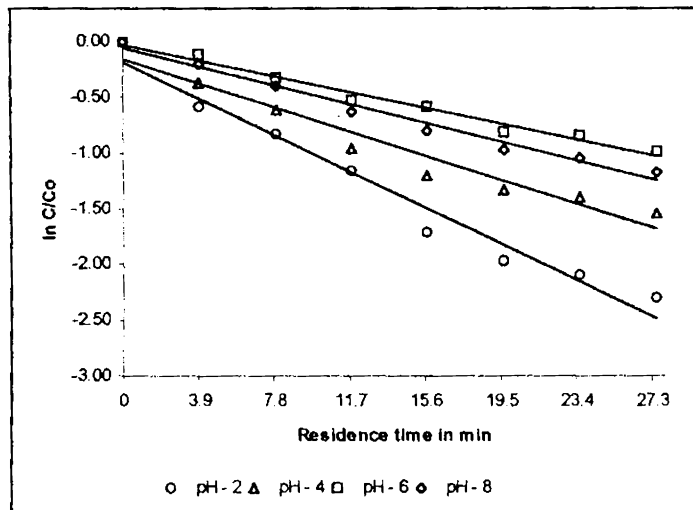


Figure 2.213  
 Yellow 5GL  
 Influence of pH on reduction kinetics at a dye concentration of  $50 \text{ mg L}^{-1}$  and at a residence time of 3.9 min.



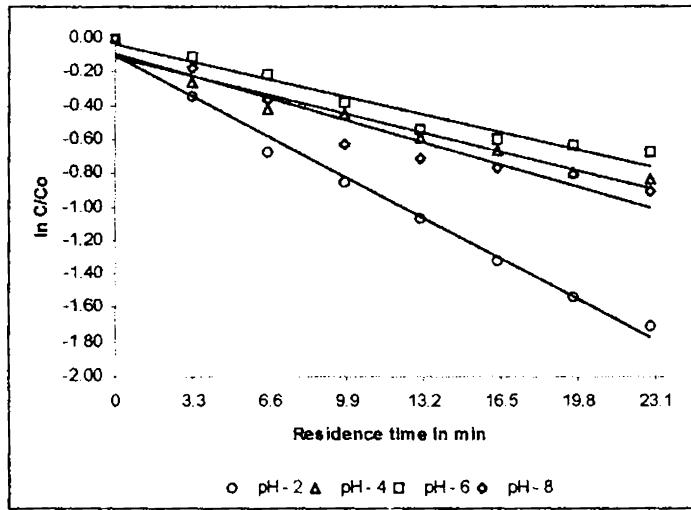


Figure 2.214  
Yellow 5GL  
Influence of pH on reduction kinetics at a dye concentration of 50 mg L<sup>-1</sup> and at a residence time of 3.3 min.

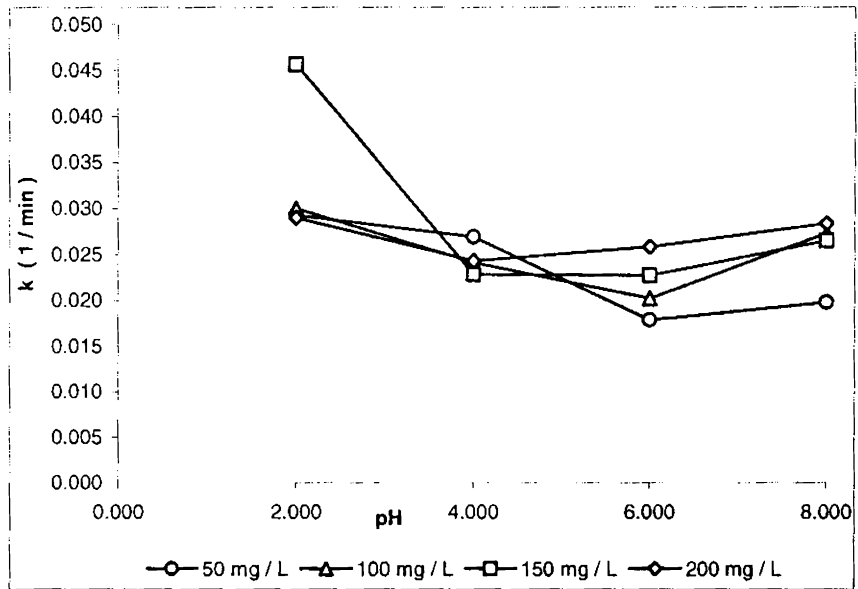


Figure 2.215  
 Direct Yellow 5GL  
 Influence of pH on pseudo first order rate coefficients at a flow rate of  $20 \text{ mL min}^{-1}$  and for fixed dye concentrations

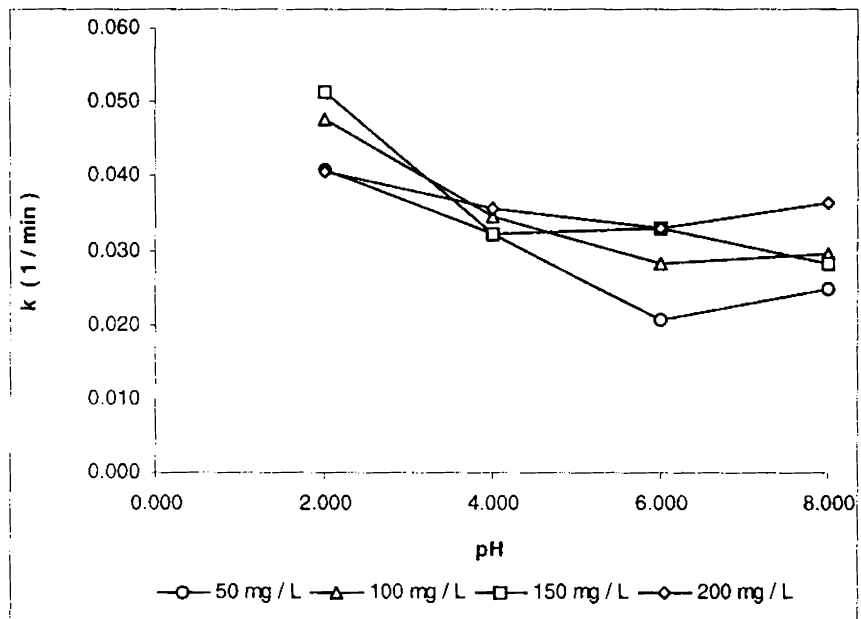


Figure 2.216  
 Direct Yellow 5GL  
 Influence of pH on pseudo first order rate coefficients at a flow rate of  $30 \text{ mL min}^{-1}$  and for fixed dye concentrations

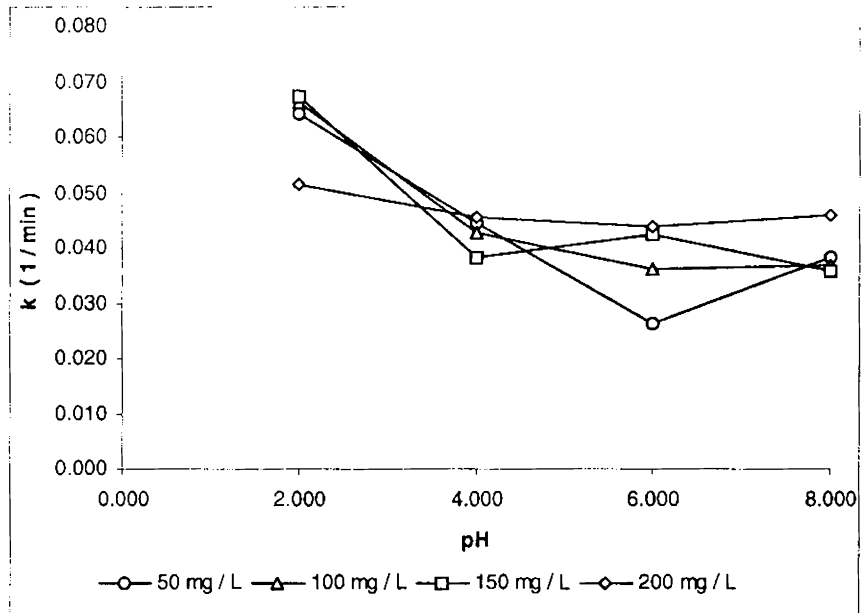


Figure 2.217  
 Direct Yellow 5GL  
 Influence of pH on pseudo first order rate coefficients at a flow rate of  $40 \text{ mL min}^{-1}$  and for fixed dye concentrations

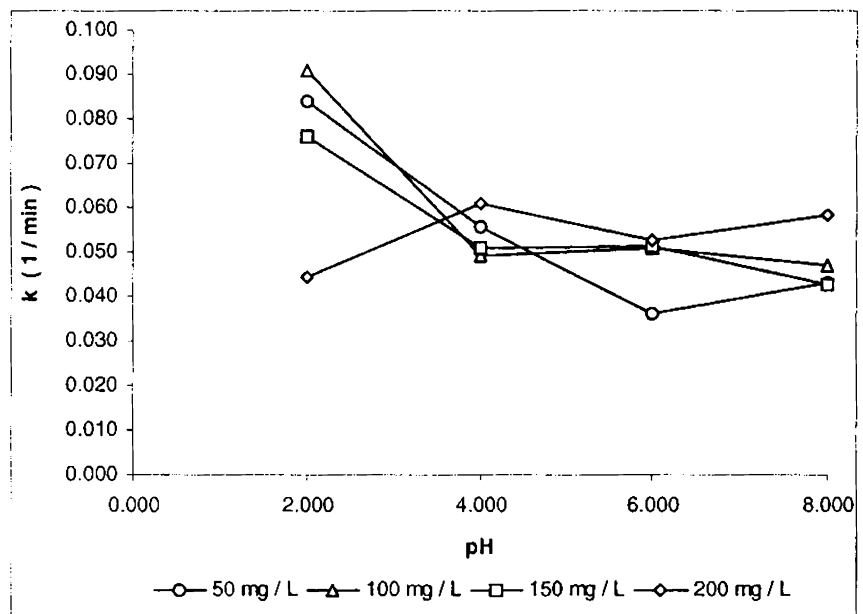


Figure 2.218  
 Direct Yellow 5GL  
 Influence of pH on pseudo first order rate coefficients at a flow rate of  $50 \text{ mL min}^{-1}$  and for fixed dye concentrations.

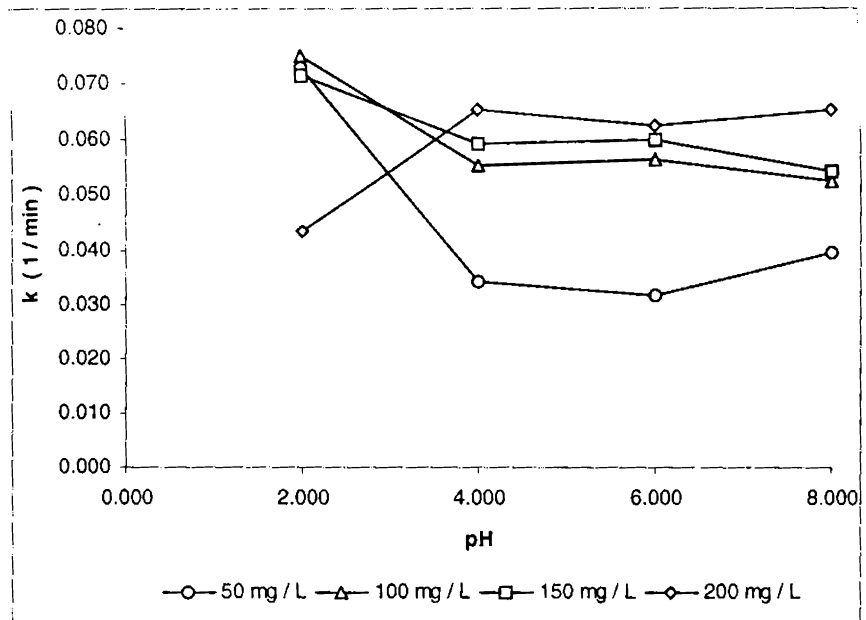


Figure 2.219  
Direct Yellow 5GL  
Influence of pH on pseudo first order rate coefficients at a flow rate of  $60 \text{ mL min}^{-1}$  and for fixed dye concentrations.

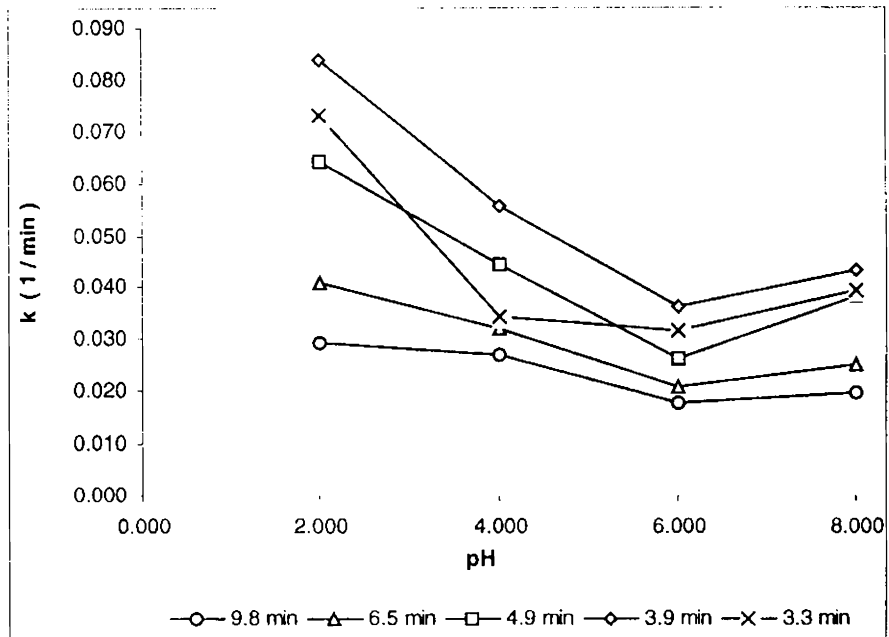


Figure 2.220  
 Direct Yellow 5GL  
 Influence of pH on pseudo first order rate coefficients at a dye concentration of 50 mg L<sup>-1</sup> and at fixed flow rates.

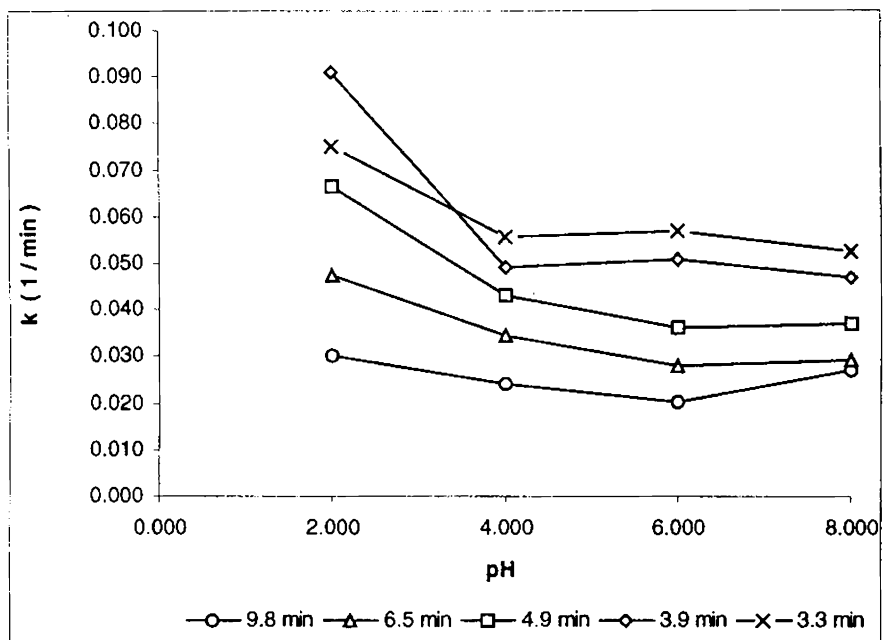


Figure 2.221  
 Direct Yellow 5GL  
 Influence of pH on pseudo first order rate coefficients at a dye concentration of 100 mg L<sup>-1</sup> and at fixed flow rates.

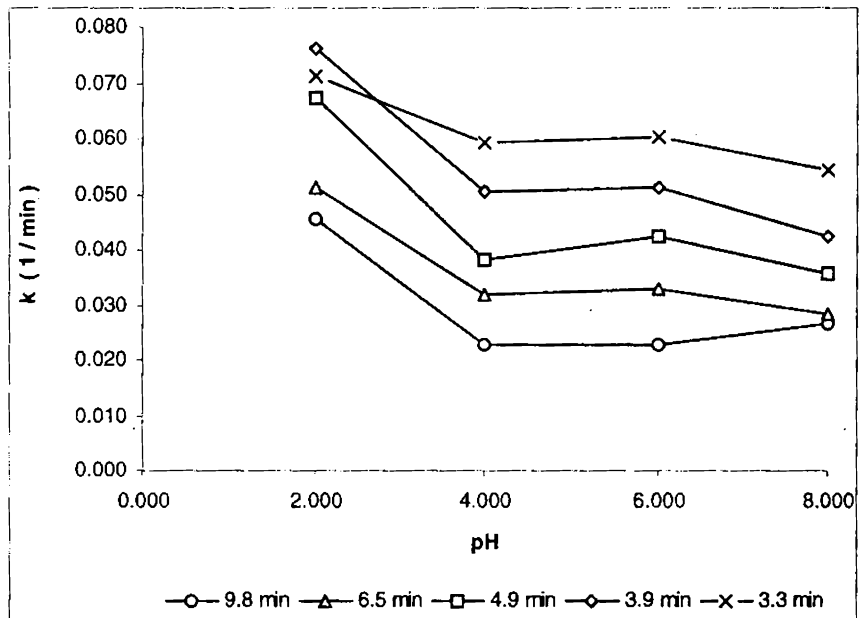


Figure 2.222  
Direct Yellow 5GL  
Influence of pH on pseudo first order rate coefficients at a dye concentration of 150 mg L<sup>-1</sup> and at fixed flow rates

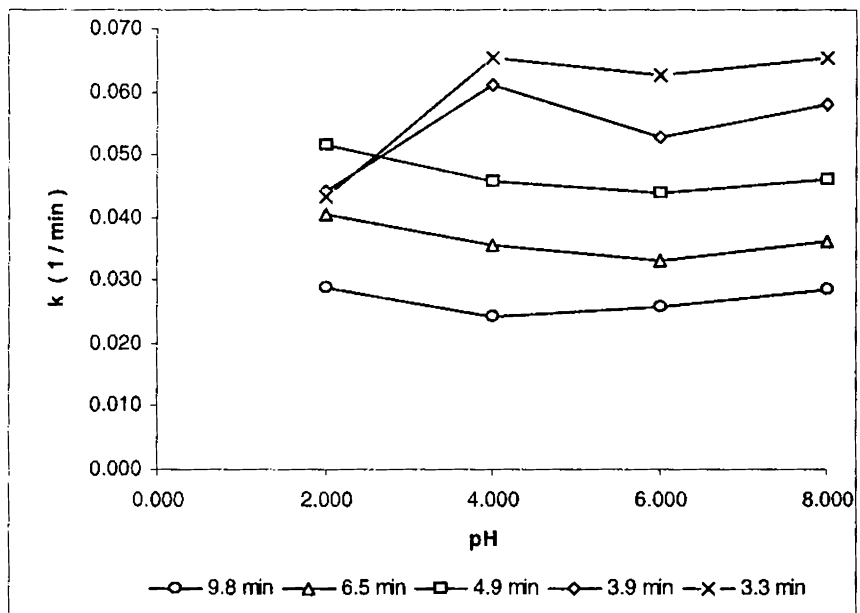


Figure 2.223  
Direct Yellow 5GL  
Influence of pH on pseudo first order rate coefficients at a dye concentration of 200 mg L<sup>-1</sup> and at fixed flow rates

## 2.11. Statistical analysis and conclusion

From the above experiments it can be observed that although definite trends have been established with respect to certain variables, trends with respect to certain others tend to vary widely making it difficult to arrive at a definite conclusion. Hence to explicitly account for the trends, results have been subjected to statistical analysis using a four factor ANOVA.

The objective was to statistically analyze the effect of four variables namely concentration, pH, flow rate and column height on the decolorization of the five azo dyes viz., Direct Sky Blue, Direct Black EG, Direct Catachine Brown, Direct Green B and Yellow 5GL in dynamic flow through column tests. Percentage decolorization has been chosen as a criterion to assess the reduction mechanism.

The ANOVA tables for various dyes studied are shown below:

Table 2.1. ANOVA table for Direct Sky Blue

Source	Sum of squares	Degrees of freedom	Mean square	F	Level of Significance
Total	530457.3	639			
b/w conc.	891.281	3	297.09	7.08	p < 0.001
b/w pH.	1489.158	3	496.39	11.82	p < 0.001
b/w FR.	11545.11	4	2886.28	68.75	p < 0.001
b/w C.ht.	490420.4	7	70060.06	1668.91	p < 0.001

Table 2.2. ANOVA table for Direct Black EG

Source	Sum of squares	Degrees of freedom	Mean square	F	Level of Significance
Total	376733.6	639			
b/w conc.	10194.42	3	3398.1	38.6	p < 0.001
b/w pH.	52368.2	3	17456.1	198.3	p < 0.001
b/w FR.	2642.0	4	660.5	7.5	p < 0.001
b/w C.ht.	36682.7	416.7	36682.7	416.7	p < 0.001

Table 2.3. ANOVA table for Direct Catachine Brown

Source	Sum of squares	Degrees of freedom	Mean square	F	Level of Significance
Total	579388.4	639			
Between conc.	68621.45	3	22873.82	153.05	$p < 0.001$
Between pH.	102571.7	3	34190.56	228.77	$p < 0.001$
Between FR.	26948.96	4	6737.24	45.08	$p < 0.001$
Between C.ht.	288284.1	7	41183.45	275.55	$p < 0.001$

Table 2.4. ANOVA table for Direct Green B

Source	Sum of squares	Degrees of freedom	Mean square	F	Level of Significance
Total	395680.6	639			
b/w conc.	7592.8	3	2530.9	32.3	$p < 0.001$
b/w pH.	39241.0	3	13080.3	167.1	$p < 0.001$
b/w FR.	21655.6	4	5413.9	69.2	$p < 0.001$
b/w C.ht.	278499.6	7	39785.7	508.2	$p < 0.001$

Table 2.5. ANOVA table for Direct Yellow 5GL

Source	Sum of squares	Degrees of freedom	Mean square	F	Level of Significance
Total	483763.9	639			
Between conc.	1906.477	3	635.49	13.74	$p < 0.001$
Between pH.	43132.43	3	14377.48	310.79	$p < 0.001$
Between FR.	6322.654	4	1580.66	34.17	$p < 0.001$
Between C.ht.	403628.4	7	57661.20	1246.45	$p < 0.001$

From the ANOVA tables, it can be inferred that there is a significant difference between concentrations ( $p < 0.001$ ), between pH, between flow rates ( $p < 0.001$ ), and between column height ( $p < 0.001$ ) at 5% level.

To separate out significant treatments in concentrations, flow rates; column heights and pH, Least Significant Difference (LSD) at 0.1% level were worked out.



### 2.11.1. Least Significant Difference for various pH

- (i) Least Significant Difference for Direct Sky Blue at various pH was found to be 2.17.

Table 6. Least Significant Difference in pH for Direct Sky Blue

pH	Average	Difference
pH - 2	60.31	0
pH - 4	56.58	3.73
pH - 6	56.90	3.41
pH - 8	56.92	3.38

Among pH, percentage decolorization of the dye at pH 2 was found to be significantly higher than pH's 4, 6 and 8. However, between pH 4, 6 and 8 there was no significant difference.

- (ii) The Least Significant Difference for Direct Black EG at various pH was found to be 3.15.

Table 7. Least Significant Difference in pH for Direct Black EG

pH	Average	Difference
pH - 2	50.6	0
pH - 4	29.6	21
pH - 6	30.5	20.1
pH - 8	29.1	21.5

Among pH, percentage decolorization of the dye was maximum at pH 2 followed by pH 4, 6 and 8. The difference between pH 2 and pH 4 was found to be highly significant however, the difference between pH 4, 6 and 8 was found to be insignificant.

- (iii) The Least Significant Difference for Direct Catachine Brown at various pH was found to be 4.10.

Table 8. Least Significant Difference in pH for Direct Catachine Brown

pH	Average	Difference
2	59.66	0
4	45.28	14.37
6	31.49	28.17
8	27.43	32.23

From the above table it can be seen that among pH the treatment efficiency was found to be maximum at pH 2 and minimum at pH 8. Between pH also gave a significant difference in treatment efficiency at all levels.

- (iv) The Least Significant Difference for Direct Green B at various pH was found to be 2.97.

Table 9. Least Significant Difference in pH for Direct Green B

pH	Average	Difference
pH - 2	51.6	0
pH - 4	41.3	10.3
pH - 6	37.2	14.4
pH - 8	29.9	21.6

Among pH, the treatment efficiency at pH 2 was found to be significantly higher than that at pH 4, 6 and 8 with the treatment efficiency being lowest at pH 8. Similarly the difference in the reaction rate between pH 4, 6 and 8 are also significant, indicating that the reduction of Direct Green – B was strongly influenced by pH.

- (v) The Least Significant Difference for Direct Yellow 5GL at various pH was found to be 2.28.

Table 10. Least Significant Difference in pH for Direct Yellow 5GL

pH	Average	Difference
2	65.7	0
4	52.2	13.5
6	45.9	19.8
8	45.4	20.4

Among pH, percentage decolorization was found to be significantly higher at pH 2 than at pH 4, 6 and 8. The reaction rate was found to be maximum at pH 2 followed by pH 4. However, between pH 6 and pH 8 there was no significant difference.

#### Discussion

The general conclusion that could be drawn on the basis of results obtained is that among pH, percentage decolorization of the dye at pH 2 was found to be significantly higher than pH's 4, 6 and 8. In most cases the difference in rate coefficients between pH 2 and pH 4 was found to be highly significant (statistically) however between pH 4, 6 and 8 the difference was not statistically significant. This observation clearly indicates that there are two pH dependent processes operating on the system. Under acidic pH conditions (pH 2), the process involved is chemical reaction mediated by direct electron transfer from the metal surface to the dye. Under such conditions the reactive sites on the metal surface play an important role in influencing the reduction kinetics. These electrons would in turn reduce the azo linkages to form the corresponding hydrazo or amine

derivative (depending on the number of electrons involved in the transfer), which in either case is colorless. Such processes are irreversible as the dye molecule loses its identity as a result of cleavage at the azo linkages. This accounts for the observed increase in the rate coefficients at pH 2. However, at pH 4, 6 and 8 the process leading to an observed decrease in the dye concentration is adsorption at the non-reactive sites present on the metal surface. An iron surface when exposed to air or aqueous solutions would develop a surface oxide layer that mainly comprises of the corrosion products. Under acidic conditions although these products are formed they do not accumulate at the metal surface as at low pH conditions they tend to get dissolved. Moreover, the system being flow through they get washed out of the column thus leaving a clean and reduced metal surface for reaction with the dye molecules. However, at high pH conditions (above pH 4), the oxide layer of corrosion products contains exchangeable sites at which removal can occur through adsorption. Under such conditions, the non-reactive sites present on the metal surface in the form of the accumulated corrosion products influence the removal mechanism. The dyes do not lose their identity, as there is no chemical reaction involved under such conditions as they simply remain bound on the surface of the metal by physical process such as adsorption. In the case of Yellow 5GL the rate coefficient values at pH 4 although significantly lower than pH 2, was significantly greater than that of pH 6 and 8. This could be attributed to the fact that at pH 4, the measured rate coefficients is a combination of both chemical reaction as well as adsorption while at pH 6 and 8 the

measured rate coefficients are indicative of only the surface process. Hence, the difference between rate coefficients at pH 6 and 8 becomes comparable, as at these two pH conditions it is the same physical process of adsorption that is operative. According to Hakanen and Lindberg (1992), there is an exchangeable site on the hydrous metal oxide at the hydrous iron substrate or on its detached corrosion product. Depending on the solution pH, the surface site may have a net positive charge ( $>OH_2^+$ ) or negative ( $>O^-$ ) charge. The exchange of protons to and from the oxide surface creates specific sorption sites. For most iron containing minerals, the solution pH value that results in no net charge on the mineral (i.e., point of zero charge or pzc) is in the range of approximately 6-8. As the solution pH falls below the pzc of the substrate, the net surface charge becomes positive, favoring the sorption of anionic species. On the other hand as the pH is increased above the pzc of the substrate, the net surface charge becomes negatively charged favoring the sorption of cationic species. At pH 6, the iron surface would contain equal amounts of negative and positive charge because the pH is close to the pzc of the iron substrate. Since both charges exist on the iron surface at this pH, sorption of a positively charged species can occur on the negatively charged oxide layer. When pH is higher than 6, the conditions become detrimental due to the production of hydroxyl ions and favors sorption. Under such conditions sorption becomes the most significant removal mechanism rather than reduction. Working on similar lines, Su and Puls (2001) report that corrosion products of  $Fe^0$  such as magnetite, hematite and goethite form a

passivated layer on the  $\text{Fe}^0$  surface thereby affecting its interaction with organic compounds. According to them pH plays an important role in adsorption on iron hydroxide. The pH effect is described in terms of the zero point of charge (zpc) of the adsorbent. Hematite a common iron oxide has a zpc of 7.1. Under low pH conditions, the iron oxide undergoes surface protonation. Surface protonation diminishes as the pH increases to above 5, and approaches 0 at pH 7 resulting in maximum adsorption. When the pH is above 9 the oxide surface becomes negatively charged, resulting in electrostatic repulsion and decreased adsorption. Gillham and O'Hannesin, (1994) studied the degradation of halogenated aliphatics by zero-valent iron and report up to ten fold increase in the rates for a decrease in pH by 2 units, indicating that the reduction rates were strongly influenced by pH. Agrawal and Tratnyek, (1996) in a study carried out on the reduction of nitro aromatic compounds by zero-valent iron metal report that changes in pH can cause changes in the nitro reduction rates through three processes. Firstly by the direct influence of  $\text{H}^+$  in the contributing reactions. Secondly, mass transport limitations imposed by the precipitation of a passive film on the metal surface, and lastly by mass transport limitations determined by the thickness of the Nernst layer between the passive film and the bulk electrolyte. Hung et al (2000), during the reductive degradation of Nitrobenzene by elemental iron in the presence of Ultrasound and Su and Puls (2001) during their study on arsenate and arsenite removal by zero-valent iron observed an increase in pH as the reaction progressed. Similar observations were also reported by

Matheson and Tratnyek (1994) during the reductive dehalogenation of chlorinated methanes by iron metal. The authors points out that this pH increase favors the formation of iron hydroxide precipitates, which may eventually form a surface layer on the metal that inhibits its further dissolution. Li and Farrell (2001) studied the reductive dechlorination of trichloroethene and carbon tetrachloride using iron and palladized-iron cathode observed that the half-lives increased by a factor of three between a pH of 4 and 10 indicating that hydrogen was involved in the TCE reduction by iron electrode. Alessi and Li (2001), studied the degradation of perchloroethylene (PCE) by zero-valent iron and observed that high pH significantly reduced the degradation rate. Williams and Scherer (2001), studied the kinetics of Cr(VI) reduction by carbonate green rust and observed that an increase in pH from 5-9 resulted in a 5-fold decrease in the reaction rate. Similar observations have also been reported by Alowitz and Scherer (2002) during the kinetics of nitrate, nitrite and Cr (VI) reduction by iron metal. The authors observed that an increase in pH resulted in a decrease in the reduction rates. These observations indicate that pH was a major factor responsible for driving the reduction reaction.

### 2.11.2. Least Significant Difference for various concentrations

- (i) In the case of Direct Sky Blue the Least Significant Difference for various concentrations was 2.17. The results are summarized in table 2.11.

Table 2.11. Least Significant Difference in concentration for Direct Sky Blue

Conc. (mg L <sup>-1</sup> )	Average	Difference
50	56.14	3.17
100	59.31	0
150	58.15	1.16
200	57.11	2.2

Among concentrations, the maximum percentage of decolorization occurred at 100 mg L<sup>-1</sup> and it is at this concentration that the treatment efficiency was found to be significantly higher when compared to the concentrations of 50 and 200 mg L<sup>-1</sup>. Between 100 and 150 mg L<sup>-1</sup> there is no significant difference.

These results coincide with the observation that the rate coefficients were found to increase with an increase in concentration from 50 to 100 mg L<sup>-1</sup> after which it remains almost steady through 150 mg L<sup>-1</sup> before decreasing at a concentration of 200 mg L<sup>-1</sup>. This indicates that the dyes tend to exert its influence as a corrosion inhibitor only from concentrations above 100 mg L<sup>-1</sup>.



- (ii) The Least Significant Difference for various concentrations of Direct Black EG was found to be 3.15.

Table 2.12. Least Significant Difference in concentration for Direct Black EG

Conc. (mg L <sup>-1</sup> )	Average	Difference
50	41.5	0
100	34.5	7.0
150	33.3	8.1
200	30.7	10.8

Among concentrations, percentage decolorization of the dye was found to be highest at 50 mg L<sup>-1</sup> and lowest at 200 mg L<sup>-1</sup>. The percentage decolorization was found to be significantly higher at 50 mg L<sup>-1</sup> than at 100, 150 and 200 mg L<sup>-1</sup>. However, between 100 and 150 mg L<sup>-1</sup> there is no significant difference. The result substantiate our view that at high dye concentrations, there can be a decrease in the rate coefficient as the dye become corrosion inhibitors by forming a passivating layer at the metal surface that prevents electron transfer. At a concentration of 50 mg L<sup>-1</sup> the dye could be effectively reduced, as at this concentration it is not inhibiting the corrosion process. It is at higher concentration of 100, 150 and 200 mg L<sup>-1</sup> that the dye becomes inhibitory.

- (iii) With respect to Direct Catachine Brown the Least Significant Difference for various dye concentrations was 4.10.

Table 2.13. Least Significant Difference in concentration for Direct Catachine Brown

Conc. (mg L <sup>-1</sup> )	Average	Difference
50	57.23	0
100	42.65	14.58
150	32.38	24.85
200	31.59	25.64

Among concentrations, the treatment efficiency has been found to be maximum at a lowest concentration of 50 mg L<sup>-1</sup> and minimum treatment efficiency has been observed at the maximum concentration of 200 mg L<sup>-1</sup> clearly indicating the dependence of the reaction on the concentration of the dye. However, between concentrations it is observed that there is a significant difference between 50, 100 and 150 mg L<sup>-1</sup>, however, between 150 mg L<sup>-1</sup> and 200 mg L<sup>-1</sup> the difference in treatment efficiency was found to be insignificant.

Since the percentage removal of the dye is maximum at the lowest concentration and decreases with further increase in concentration points to the possibility of the dyes functioning as corrosion inhibitors at higher concentrations thereby forming a passivating layer over the surface of the metal that prevents transfer of electrons required to carry out the reduction reaction.

(iv) The Least Significant Difference for various concentrations of Direct Green B was found to be 2.97.

Table 2.14. Least Significant Difference in concentration for Direct Green B.

Conc. (mg L <sup>-1</sup> )	Average	Difference
50	44.8	0
100	41.4	3.5
150	39.2	6.6
200	35.6	9.2

With respect to concentration, the treatment efficiency was found to be maximum at the lowest concentration of 50 mg L<sup>-1</sup>. Between concentrations the treatment efficiency was found to be significantly different only up to a concentration of 150 mg L<sup>-1</sup>. This observation

supports the assumption that the dye or its reduction products could be a corrosion inhibitor, as indicated by the decrease in dye removal at higher dye concentrations. The results indicate that the dye could be exerting its influence as a corrosion inhibitor only at concentrations above  $150 \text{ mg L}^{-1}$ . This accounts for the insignificant difference in rate coefficients at concentrations beyond it.

- (v) In the case of Yellow 5GL the Least Significant Difference for various dye concentrations was found to be 2.28.

Table 2.15. Least Significant Difference in concentration for Direct Yellow 5GL

Conc. ( $\text{mg L}^{-1}$ )	Average	Difference
50	50.88	3.8
100	54.71	0
150	50.45	4.3
200	53.14	1.6

Among concentrations, the percentage of decolorization was found to be highest at  $100 \text{ mg L}^{-1}$  followed by  $150 \text{ mg L}^{-1}$  and  $50 \text{ mg L}^{-1}$ ; however, at  $200 \text{ mg L}^{-1}$ , the percentage of decolorization was found to be insignificant. Between  $50$  and  $150 \text{ mg L}^{-1}$  there is no significant difference. The percentage decolorization at  $200 \text{ mg L}^{-1}$  is significantly higher than  $50 \text{ mg L}^{-1}$  and  $150 \text{ mg L}^{-1}$ , but there is no significant difference between  $100$  and  $200 \text{ mg/L}$ . However,  $100 \text{ mg L}^{-1}$  gives significantly higher percentage decolorization compared to  $50$  and  $150 \text{ mg L}^{-1}$ .

## Discussion

With respect to the variation in the pseudo first order rate coefficients with concentration, three types of behavior has been observed:

- (i) The rate coefficients behave randomly with no specific trend. Being a heterogeneous system it is associated with a number of random errors. Such errors could possibly lead to plots where no discernable trends have been observed.
- (ii) In several instances, there is an increase in pseudo first order rate coefficients up to a concentration of  $100 \text{ mg L}^{-1}$  followed by a decrease. This can be attributed the fact that these dyes at high concentrations can function as corrosion inhibitors by forming a passivating layer over the metal surface. Moreover, amines such as aniline generated through the cleavage at the azo linkages can function as corrosion inhibitors by coating the surface of the metal thereby preventing the electron transfer required for the reduction reaction. Hence, at high dye concentrations there could be a build up of the dye as well as its reduction products such as amines resulting in a decrease in the rate coefficients.
- (iii) In some cases, the rate coefficients have been found independent of the dye concentration. This is a clear indication of the dye functioning as a corrosion inhibitor. Once the dye forms a coating over the iron surface the reactive sites at the metal surface would get saturated. For the reactive sites to become available for the reaction with the dye molecule, it is

necessary that these adsorbed dye coatings would have to diffuse out, which does not occur once the dye has formed the passivating layer over the metal surface, thereby resulting in a decrease in the rate coefficients with increase in dye concentration. However, the system being a flow through one can result in the partial removal of these passivating layers over the metal surface by the shear force produced as a result of turbulence created under conditions of high flow rate. Therefore, under conditions of low flow rates there would be an observed decrease in the rate coefficients with increase in dye concentration. However, with increasing flow rates resulting in the partial removal of oxide layer can lead to an observed increase in rate coefficients. This probably accounts for an increase in the rate coefficients after an initial decrease. The decrease in the pseudo-first order rate coefficients with increasing initial concentration indicates the saturation of the reactive sites. Moreover, this phenomenon of increase in rate coefficients after an initial decrease is observed only at high pH ranges (above 4) or at high dye concentrations (beyond 100 mg L<sup>-1</sup>) or at high flow rates (above 40 mL min<sup>-1</sup>) where each of these conditions favour surface mediated processes such as adsorption where the transport of the dye molecules from the bulk solution to the metal surface becomes the rate limiting step.

Farrell et al., (2001) in electrochemical and spectroscopic study of arsenate removal from water using zero-valent iron reported that at low concentrations, the ratio of dissolved compounds to the available (uncomplexed) iron hydroxide is sufficiently low. As a result there is no competition between the dissolved substances for the complexation sites. Under such conditions the removal kinetics follows first order and may be representative of both complex formation, or may result from diffusional mass transfer limitations within the iron oxide phase. As the concentration is increased, the ratio of the dissolved organics to the complexation sites increases, leading to competition for the complexation sites. With increasing competition, the generation of new sites for complexation becomes the rate-limiting step. Under such conditions the reaction would follow zero order kinetics. Agrawal et al., (2002) studied the kinetics of dechlorination of 1,1,1-trichloroethane by zero valent iron and observed that the reduction kinetics followed first order until Cr(IV) enhanced corrosion after which they become zero order, when Cr(IV) caused surface passivation. Farrell et al (2000) investigated the reductive dechlorination of trichloroethylene using zero-valent iron and observed that although initially the reduction followed first order kinetics, at later stages shifted to zero order kinetics indicating saturation of the reactive sites. Orth and Gillham (1996) during their investigation on dechlorination of trichloroethene in aqueous solution using  $\text{Fe}^0$  observed that there would be some upper limit in the concentration of the substrate where the reactive sites get saturated and then the reaction would no longer be pseudo-first order. Wust et al

(1999) in their study on degradation of TCE and cis-DCE with commercial iron observed that the data could not be explained using pseudo-first order kinetics. At high aqueous concentrations, the degradation kinetics became pure zero-order whereas for low concentrations the kinetics was first order. The observed zero-order was attributed to the build up of iron oxides. This called for an enhanced model and it was observed that a combined zero and first order model could successfully account for their observations. This was attributed to the reason that pure order fits partially account for the mixed kinetics in the transition zone. Increase in flow rates resulted in an increase in the rate constant indicating that diffusion from bulk solution to the iron surface contributed to the overall kinetics. Variations in the kinetic parameters of combined zero-and first-order model suggested that both transport and sorption to reactive sites contributed to kinetic control. Sayles et al (1997) investigated the dechlorination of DDT, DDD and DDE by zero-valent iron in the presence and absence of nonionic surfactant and report that Initial first order transformation rates were used since the data set did not fit satisfactorily to either zero or first order or Langmuir adsorption isotherm. Ponder et al (2000) studied the reduction of Cr(VI) and Pb(II) in aqueous solutions using "Ferragels". The authors report that the reduction kinetics was complex and included both reaction and adsorption. Once the active sites on the metal surface were saturated, the reduction reaction tends to proceed at slower rates, limited by mass transfer. The authors observed that the reaction was dependent both on the initial iron concentration as well as the concentration of the substrate.

At times irrespective of the contaminant species or concentration the sorption of the contaminant on to the iron occurred at a much faster rate than the rate at which it was reduced. This indicates that the mechanism is physical. As a result the reaction could not be accounted by the simple first order kinetics alone and required complicated mixed order models to explain the observed trends. Melitas et al (2001) studied the kinetics behind removal of soluble chromium from contaminated water by zero-valent iron and observed that the reactivity of sites on zero-valent iron decreased with increasing concentration of chromium. This was attributed to the passivating effect of a corrosion inhibitor like chromium. The chromium removal rates was affected by both the ability of Cr(VI) to penetrate the passivating oxides and by the ability of iron to release  $\text{Fe}^{2+}$  at the anodic site. The authors report that although removal kinetics fitted well to zero-order rate law the process cannot be described by simple zero, first or fractional order kinetic models, as they do not account for surface passivation of iron.



### 2.11.3. Least Significant Difference for various flow rates

- (i) The Least Significant Difference for various flow rates in the case of Direct Sky Blue was found to be 2.43.

Table 2.16. Least Significant Difference in flow rates for Direct Sky Blue

Flow rates (mL min <sup>-1</sup> )	Average	Difference
20	64.3	0
30	60.1	4.2
40	57.4	6.9
50	54.5	9.7
60	52.1	12.2

With respect to flow rates, the maximum treatment efficiency was observed at 20 ml min<sup>-1</sup> followed by 30, 40, 50 and 60 ml min<sup>-1</sup>. The percentage decolorization of the dye was found to be minimum at a flow rate of 60 ml min<sup>-1</sup>.

The inference that can be drawn is that there is a definite indication that the iron mediated reduction of the diazo dye direct sky blue could also be a surface process influenced by hydro dynamic mass transport limitations as indicated by the increase in the rate of the reaction with increase in flow rates. However, with regard to treatment efficiency the contact time between the dye molecule and metal surface happen to play a major role in decolorization of the dye. This is indicated by the increased percentage removal at lower flow rates along with a progressive decrease in the removal efficiency as the flow rate is increased.

- (ii) In the case of Direct Black EG, Least Significant Difference for various flow rates was found to be 3.52.

Table 2.17. Least Significant Difference in flow rates for Direct Black EG

Flow rates (mL min <sup>-1</sup> )	Average	Difference
20	39	0
30	34.6	4.4
40	33.8	5.2
50	33.7	5.3
60	33.9	5.1

Among flow rates, the maximum treatment efficiency was observed at a flow rate of 20 ml min<sup>-1</sup> that was significantly higher than all the rest. Between flow rates of 30, 40, 50 and 60 ml min<sup>-1</sup> no significant difference in the percentage decolorization of the dye was observed.

This observation clearly indicates the influence of contact time between the dye and iron on the iron-mediated reduction of the azo dye. It is at a flow rate of 20 ml min<sup>-1</sup> that the residence time is maximum (9.8 min), with a progressive decrease in the residence time with increase in the flow rate. On the contrary, the rate of the reaction was found to increase with an increase in flow rates suggesting that the reaction is a surface mediated process also as influenced by mass transport.

- (iii) For Direct Catachine Brown the Least Significant Difference for various Flow rates was found to be 4.58.

Table 2.18. Least Significant Difference in flow rates for Direct Catachine Brown

Flow rates (mL min <sup>-1</sup> )	Average	Difference
20	51.8	0
30	43.7	8.1
40	39.3	12.5
50	37.3	14.5
60	32.7	19.1

Among flow rates, the treatment efficiency has been found to be maximum at  $20 \text{ ml min}^{-1}$  and minimum at  $60 \text{ ml min}^{-1}$ . Although there is a difference in the treatment efficiency between flow rates, it is observed that between  $40 \text{ ml min}^{-1}$  and  $50 \text{ ml min}^{-1}$  the difference has not been significant.

The fact that maximum treatment efficiency is observed at lower flow rates clearly indicate the influence of residence time i.e., the average time the dye molecules spends with in the column in contact with the metal surface. With an increase in the flow rates there is a decrease in the contact time between the dye and metal leading to a decrease in the percentage decolorization of the dye. However, one observation made is that with an increase in the flow rates there is a definite increase in the rate coefficients and in some cases the rate coefficients have also been found to increase linearly with an increase in flow rates suggesting that the iron mediated reduction of the azo dye could be a surface mediated process also influenced by mass transport limitations.

- (iv) The Least Significant Difference at various Flow rates for Direct Green B was found to be 3.3.

Table 2.19. Least Significant Difference in concentration for Direct Green B

Flow rates ( $\text{mL min}^{-1}$ )	Average	Difference
20	49.4	0
30	43.6	5.9
40	38.0	11.4
50	35.6	13.5
60	33.1	16.3

With respect to flow rate, the treatment efficiency was found to be maximum at the lowest flow rate of  $20 \text{ ml min}^{-1}$  and the lowest treatment efficiency was observed at  $60 \text{ ml min}^{-1}$ . This could probably be because of the increased contact time between the dye and the metal surface at lower flow rates. However, between flow rates a significant difference has been observed only up to  $40 \text{ ml min}^{-1}$  after which for further increase in flow rates the difference in treatment efficiency has been found to be insignificant indicating that the reduction of the tri azo dye-Direct Green B was found influenced by mass transport only up to a flow rate of  $40 \text{ ml min}^{-1}$ , as observed in some batch of the experiments where the rate coefficients were not found to increase with increase in flow rates beyond certain levels.

- (v) In the case of Yellow 5GL, the Least Significant Difference for various flow rates was found to be 2.55.

Table 2.20. Least Significant Difference in concentration for Direct Yellow 5GL

Flow rates ( $\text{mL min}^{-1}$ )	Average	Difference
20	56.45	0.00
30	54.51	1.94
40	52.40	4.05
50	50.82	5.64
60	47.30	9.16

Among flow rates, the percentage removal was found to be maximum at  $20 \text{ ml min}^{-1}$  with no significant difference between  $20$  and  $30 \text{ ml min}^{-1}$ . However, as the flow rate increased the difference become significant. The lowest percentage decolorization was observed at a flow

rate of  $60 \text{ ml min}^{-1}$ . However, between  $40 \text{ ml min}^{-1}$  and  $50 \text{ ml min}^{-1}$  no significant difference has been observed.

In most of the experiments it has been observed that there is an increase in the pseudo first order rate coefficients with increase in flow rates. However, there have been few variations where an increase in the rate coefficients have been observed only up to a flow rate of 40 or 50  $\text{mL min}^{-1}$  with a decrease in the rate coefficients at higher flow rates. Such deviations have been observed at low dye concentrations i.e., at  $50 \text{ mg L}^{-1}$  at all the four pH and at  $150 \text{ mg L}^{-1}$  (pH 2) and at  $200 \text{ mg L}^{-1}$  (pH 2). In all these cases it has been observed that the increase is linear only up to a flow rate of  $50 \text{ mL min}^{-1}$ . However, in some cases it was observed that the percentage removal become independent of flow rates between 20 and 30  $\text{ml min}^{-1}$  and between 40 and 50  $\text{ml min}^{-1}$  indicating that between these flow rates there is no significant difference in treatment efficiency.

## Discussion

The fact that maximum treatment efficiency is observed at lower flow rates, clearly indicate the influence of residence time i.e., the average time the dye molecules spends with in the column in contact with the metal surface. It is at a flow rate of  $20 \text{ ml min}^{-1}$  that the residence time is maximum (9.8 min). This accounts for maximum treatment efficiency being observed at low flow rates. With an increase in the flow rate there is a decrease in the residence time leading to a decrease in percentage decolorization of the dye. However, another observation made is that with

an increase in flow rates there is a definite increase in the pseudo first order rate coefficients. In some cases the rate coefficients have also increased linearly with increase in flow rates suggesting that iron mediated reduction of the azo dyes could be a surface mediated process influenced by hydro dynamic mass transport limitations. The iron metal-aqueous dye system is a heterogeneous system in which it is necessary that the dye molecules must come in contact with the metal surface for it to be reduced at the reducible functional groups i.e., the azo linkages. Therefore, with an increase in the flow rate there would be an increase in the number of dye molecules that interact with the reactive sites at the metal surface. This could contribute to an increase in the rate coefficients. However, when the flow rate is increased over an optimum a decrease in the rate coefficients can be expected due to the decreased contact time between the reactive sites and the dye molecules. The findings observed are also substantiated by the reports from several other related works. Scherer et al., (2001) in their study on the influence of mass transport on the reduction kinetics of Nitrobenzene by iron metal have reported that the degree to which mass transport determines the overall rate of reduction by  $\text{Fe}^0$ , was difficult to resolve because of a multitude of indirect effects (both physical and chemical processes) that may occur in batch and column reactors. The layer of granular  $\text{Fe}^0$  becomes covered by a layer of oxide formed by the accumulation of corrosion products at the metal surface. Mass transport through the oxide layer as well as external diffusion give rise to three potential domains:

- i. Mass transport limited kinetics, where  $\text{ArNO}_2$  diffuses to the surface more slowly than it reacts at the surface.
- ii. Reaction limited kinetics, where  $\text{ArNO}_2$  reacts at the surface more slowly than it diffuses to the surface.
- iii. Intermediate kinetics, where mass transport and surface reaction occur on similar time-scales.

Behavior typical of mass transport limited kinetics (e.g. faster rates with increased mixing intensity) may occur from indirect physical effects such as abrasion of the oxide layer making it difficult to confirm whether the observed kinetics are measuring diffusion rates, reaction rates, or a combination of both.

Wust et al., (1999) in their study on the degradation of TCE and cis-DCE with commercial iron using batch experiments indicate that transport of the chlorinated compounds to the iron surface may contribute to the kinetic control. In column experiments, the effect of flow velocity on degradation rate varied from insignificant to a 3-fold increase with doubling of the flow rate indicating that diffusion from bulk solution to the iron surface contributed to the overall kinetics. Variations in the kinetic parameters of combined zero-and first-order model suggested that both transport and sorption to reactive sites contributed to kinetic control. All these evidence indicated that iron mediated reduction could be a surface process. Hung et al., (2000) in their study on the kinetics and mechanism of the enhanced reductive degradation of Nitrobenzene by elemental iron in the presence of Ultrasound report that the reaction rate increased with increase in mixing

indicating the influence of mass transfer kinetics. Scherer et al.,(2001) studied the effect of mass transport on the kinetics of Nitrobenzene reduction by iron metal and suggested that mass transport was an important parameter to be considered in the design of reactive barriers. Agarwal and Tratnyek., (1996) in their study on the reduction of nitro aromatic compounds by zero-valent iron metal report a linear increase in the reduction rate with iron surface area. A linear correlation was also observed with square root of mixing rates indicating that mass transfer of NAC to the metal surface controlled the reaction rates. Zhang et al., (2002) studied the reduction of perchloroethylene in dynamic flow through column systems using surfactant-modified zeolite/zero-valent iron and observed that the PCE reduction rate constants increased with an increase in the flow rate suggesting that in flow through systems reduction of PCE was a surface phenomenon limited by mass transport.



#### 2.11.4. Least Significant Difference for various column heights

- (i) In case of Direct Sky Blue the Least Significant Difference for various column heights was found to be 3.07.

Table 2.21. Least Significant Difference in column height for Direct Sky Blue

Column height (cm)	Average	Difference
0	0.0	85.7
10	30.8	54.8
20	50.1	35.6
30	63.2	22.5
40	71.3	14.3
50	77.7	8.0
60	82.7	3.0
70	85.7	0.0

Column heights have been found to strongly influence percentage decolorization of the dye, with the treatment efficiency being maximum at 70 cm and minimum at the point of inlet. This observation again emphasizes the importance of the contact time between the dye molecule and the metal surface with greater contact established at higher heights. However, between column heights it is observed that there is a significant difference in decolorization only up to a height of 60 cm, beyond which no significant difference was observed, suggesting that the effective height could be fixed at 60 cm.

- (ii) Least Significant Difference at various column heights for Black EG was found to be 4.5.

Table 2.22. Least Significant Difference in column height for Direct Black EG

Column height (cm)	Average	Difference
0	0.0	60.3
10	13.1	47.1
20	23.1	37.1
30	34.4	25.8
40	43.1	17.1
50	50.1	10.2
60	55.9	4.4
70	60.2	0

With respect to the column height, the maximum treatment efficiency has been observed at 70 cm and a minimum at the point of inlet. There is a significant difference in the treatment efficiency at lower column heights. However, between 60 and 70 cm no significant difference in the treatment efficiency has been observed, indicating that the effective column height up to which reduction process is influenced by the column height is 60 cm.

- (iii) In the case of Direct Catachine Brown the Least Significant Difference for various column heights was found to be 5.80.

Table 2.23. Least Significant Difference in column height for Direct Catachine Brown

Column height (cm)	Average	Difference
0	0.00	64.8
10	18.4	46.4
20	32.0	32.8
30	43.5	21.3
40	51.1	13.7
50	57.1	7.6
60	60.9	3.9
70	64.7	0

Among column heights, the maximum treatment efficiency has been observed at 70 cm and the minimum treatment efficiency is observed at the

point of inlet. This clearly indicates the dependence of the reaction on column height. This is expected because with an increase in the column height there would be an increase in the contact time between the dye molecule and the metal surface. The column height has been related to flow rate through residence time. However, between column heights, there was no significant difference between 60 cm and 70 cm indicating that the effective height can be fixed at 60 cm.

(iv) Direct Green B had a Least Significant Difference of 4.2 for various the various column heights studied.

Table 2.24. Least Significant Difference in column height for Direct Green B

Column height (cm)	Average	Difference
0	0.0	64.8
10	18.1	46.7
20	31.5	33.3
30	41.8	23.1
40	48.7	16.1
50	54.7	10.2
60	60.4	4.4
70	64.8	0

Among column heights, the treatment efficiency was found to be maximum at 70 cm and minimum at the point of inlet. Between column heights, there was a significant difference in treatment efficiency at all levels. The influence of column height and flow rate can be grouped under residence time. At higher column lengths greater treatment efficiency is achieved because of the increased contact between the dye and the metal surface.

- (v) For Yellow 5GL the Least Significant Difference for various column heights was 3.23.

Table 2.25. Least Significant Difference in column height for Direct Yellow 5GL

Column height (cm)	Average	Difference
0	0.00	78.38
10	28.84	49.54
20	44.53	33.84
30	56.28	22.10
40	64.77	13.60
50	70.72	7.66
60	74.85	3.52
70	78.38	0.00

With respect to column height, percentage decolorization was found to be maximum at a height of 70 cm and minimum at the initial point of inlet. Between column heights, there was no significant difference between 60 cm and 70 cm indicating that the effective column height up to which significant treatment is achieved is 60 cm.

#### Discussion

Column heights have been found to strongly influence percentage decolorization of the dye, with the treatment efficiency being maximum at 70 cm and minimum at the point of inlet. This observation again emphasizes the importance of the contact time between the dye molecule and the metal surface with greater contact established at higher heights. However, between column heights it is observed that there is a significant difference in decolorization only up to a height of 60 cm, beyond which no significant difference was observed, suggesting that the effective column height could be fixed at 60 cm. Column height therefore decides the

residence time of the dye at a particular flow rate. Hence, it is infact the optimal residence time as indicated by the optimal column height.

## **Chapter III**

### **Fenton Oxidation Of Dyes**

### 3.1. Introduction

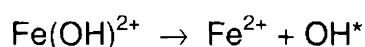
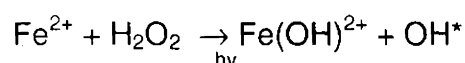
Recently there has been a renewed interest in the use of Advanced Oxidation Process (AOP) as a viable treatment option for the removal of refractory organics, color and substantial COD and TOC from industrial effluents. A common feature that all of them share is the generation of highly reactive Hydroxyl radicals ( $\text{OH}^\cdot$ ) which in turn degrade organic pollutants, usually to carbon dioxide and water. Hydroxyl radicals are ubiquitous in the environment and are present in low concentrations under normal conditions in surface water (Hoigne, 1990) and in the atmosphere (Atkinson (1989)). They are among the most reactive oxidants known and are responsible for the degradation of many environmental contaminants such as  $\text{NO}_2$ , PAHs (Atkinson, 1989) and for formation of organic polymers (Larson et al., 1991). In the natural waters hydroxyl radicals are generated by photolysis of nitrate, which could in turn cause the degradation of trace organic pollutants (Mabury and Crosby, 1994). However, the natural generation of hydroxyl radical is slow and much of it is scavenged through competitive reactions with different kinds of Dissolved Natural Organic Matter (DNOM), bicarbonate or carbonate, bromide and even hydrogen peroxide (Hoigne, 1997). Therefore, if these hydroxyl radicals could be generated synthetically and at will, its immense oxidation potential could be directed towards oxidizing many toxic and refractory organics. The Advanced Oxidation Processes (AOP) achieves this objective. Hydroxyl radicals can be generated through chemical and photochemical processes.

In the chemical process, reaction between ferrous or ferric salt with hydrogen peroxide produces hydroxyl radicals, while in photochemical reaction,  $\text{OH}^\cdot$  is produced via photolysis of hydrogen peroxide, or through a combination of  $\text{TiO}_2$  and UV or a combination of Ozone and UV or Ozone-hydrogen peroxide and UV combinations. In addition surface adsorbed hydroxyl radicals are the oxidants that possibly occur on passivated anodes and on illuminated semi-conductors. The most commonly used AOP's include hydrogen peroxide, ozone or oxygen as the bulk oxidant (Legrini et al., 1993). The common feature that all the Advanced Oxidation Processes (AOP's) such as  $\text{TiO}_2/\text{UV}$ ,  $\text{O}_3/\text{UV}$ ,  $\text{O}_3/\text{H}_2\text{O}_2$  and  $\text{O}_3/\text{H}_2\text{O}_2/\text{UV}$  share is the generation of a principal active species, the hydroxyl radical ( $\text{OH}^\cdot$ ). These hydroxyl radicals being non-specific in its reactions, is useful for degrading a variety of environmental pollutants (Spadaro et al., 1994). One method of producing the hydroxyl radical from hydrogen peroxide is through the Fenton reaction ( $\text{Fe}^{2+}/\text{Fe}^{3+}-\text{H}_2\text{O}_2$ ) (Barb et al., 1951; Walling, 1975). This method is effective in removing organic pollutants (Sedlak and Andren, 1991 and Arnold et al., 1995) but requires stoichiometric amounts of ferrous ions. The method of ferrous-hydrogen peroxide oxidation is also known as Fenton's reagent method.

Fenton reaction can also be made catalytic, by photo reducing the ferric ions in the near UV region in the presence of hydrogen peroxide. The combined process is known as the photo-assisted Fenton or photo-

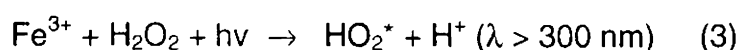
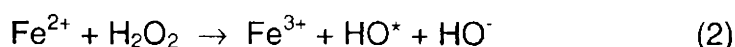
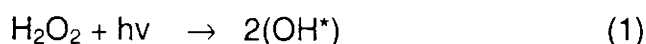


Fenton reaction and yields a more effective system for oxidative degradation (Pignatello, 1992).



The photo-Fenton reaction is optimum at pH 2.8 (Pignatello, 1992) where approximately half of the ferric is present as ferrous ion and half as  $\text{Fe}(\text{OH})^{2+}$  ion, the photoactive species. Below this pH the concentration of  $\text{Fe}(\text{OH})^{2+}$  declines and at higher pH the ferric ions precipitates as oxyhydroxide. The  $\text{Fe}(\text{OH})^{2+}$  ions absorb light at wavelengths up to about 410 nm. Hence, the reaction can be carried out efficiently with longer wavelength light than other AOP's such as  $\text{O}_3/\text{UV}$  or  $\text{H}_2\text{O}_2/\text{UV}$ , which require wavelengths below 300 nm. The ferric ions catalyst can be removed by raising the pH of the solution.

The hydroxyl radical formation in the Advanced Oxidation processes, involving UV light,  $\text{H}_2\text{O}_2$  and Fe(II) or Fe(III) salts can be represented by the following simplified reaction scheme (Prousek, 1995).



Reaction (2) takes place both in the presence and absence of light, and the concentration of ferrous ions is low as long as there is sufficient  $\text{H}_2\text{O}_2$  in the reactor. The drawback of the dark reaction is that when all the

ferrous ions are converted to ferric ions, generation of hydroxyl radicals considerably slows down, due to the slow rate of reduction of ferric to ferrous in the dark (Oliveros et al., 1997). On the other hand, although reaction (3) can be facilitated by UV/Visible light, the depletion or scarcity of hydrogen peroxide may result in an undesired accumulation of ferrous ions in the reactor. The initial rate of mineralization is reported to be faster with Fe(II)/H<sub>2</sub>O<sub>2</sub> (Fenton reagent), than Fe(III)/H<sub>2</sub>O<sub>2</sub> (Fenton-like reagent), due to the immediate formation of hydroxyl radicals with Fenton reagent. Further, the presence of Fenton-like reagents is reported to increase the chain length by the formation of Fe(III)-hydroxy complexes, resulting in a more complete destruction of the organic compounds (Ruppert et al., 1993) and as in this case dyestuffs.

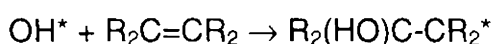
Several researchers have explored the photo-Fenton reaction as a possible wastewater treatment method. Rate enhancement of Fe(II)/H<sub>2</sub>O<sub>2</sub> degradation of 4-nitrophenol by UV irradiation has been reported (Lipezyska-Kochany, 1991). Sun and Pignatello (1993a) showed that the photo-Fenton reaction completely mineralizes 2,4-dichlorophenoxyacetic acid (2,4-D) and 2,4,5-trichlorophenoxyacetic acid (2,4,5-T). Sun and Pignatello (1993b) studied the oxidation of pesticides like metolachlor and methyl parathion under mild conditions. Pignatello and Sun (1995) and Muszkat et al., (1992) used sunlight to the Fe(III)/H<sub>2</sub>O<sub>2</sub> system in a survey of the destruction of various herbicides, several aliphatic and aromatic halogenated compounds. Detailed mechanistic studies have also been carried out with compounds such as phenol (Chen and Pignatello, 1997)

and 4-chlorophenol (Bauer, 1994; Ruppert et al., 1993), 2-and 4-nitrophenols (kiwi et al., 1994), di-n-butyl-ortho-phthalate (Halmann, 1992), polychlorinated biphenyls (PCBs) (Pignatello and Chapa, 1994) and perhalogenated alkanes (Huston and Pignatello, 1996). High concentrations of suspended solids limits the efficiency of photocatalytic oxidation processes due to the limited depth of photon penetration (Venkatadri and Peters 1993).

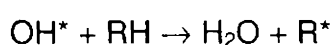
The advantage of Fenton's reagent over conventional chemical oxidation processes and other Hydroxyl radical ( $\text{OH}^*$ ) generating systems is its simplicity and being environmentally benign are easy to handle. As the chemicals are commonly available and inexpensive there is no need for special equipments like UV lamps, complex reaction vessels,  $\text{TiO}_2$  particles or ozone generators (Scott et al., 1995). In addition these processes are characterized by the absence of kinetic limitations and generation of highly reactive free radicals, which are  $10^6$  to  $10^9$  times faster than the strongest chemical oxidants known, such as ozone and hydrogen peroxide (Bicher et al., 1997) Ozonation can also be used as a wastewater treatment option, but the major disadvantages are its low reactivity (Neta et al., 1988) and selective degradation (Dowideit et al., 1995). Therefore, when a more general oxidant is required, the OH radical is the chosen one. A comparison of redox potentials show that hydroxyl radicals having a redox potential of 2.8 V is much higher than that of ozone which is 2.07 V (Carey, 1992) Sequentially these hydroxyl radicals come next only to Fluorine,

which has a redox potential of 2.87 V (Johannes, 1985). There are two mechanisms by which the  $\text{OH}^*$  reacts with organic matter (Von Sonntag, 1987):

(i) By addition to the C=C bond.



(ii) By abstracting a carbon-bound H-atom.



The addition to double bonds is generally faster than the hydrogen abstraction.

The second order rate constants of the hydroxyl radicals with compounds containing C-H or unsaturated C-C typically are of the order of  $10^7$  to  $10^{10}$   $\text{L mol}^{-1}\text{s}^{-1}$  (Buxton et al., 1988). According to Jurg Hoigne. (1997) a typical second-order rate constant for medium sized or large organic molecules is  $5 \times 10^9 \text{ M}^{-1} \text{ s}^{-1}$  or  $2.5 \times 10^9 \text{ M}^{-1} \text{ s}^{-1}$  (typical for small sized organic molecules). Reaction of hydroxyl radicals with aromatic compounds occurs almost at the diffusion-controlled rate. Continued reaction of the hydroxylated compounds with the hydroxyl radicals leads to aromatic ring cleavage. Products arising from ring cleavage are subsequently oxidized. This means that many compounds are potentially mineralized to carbon dioxide, water and inorganic ions. All these features make the Advanced Oxidation Processes (AOP) one of the most sought after and potentially important as a viable treatment option.

Two components go into the making of Fenton's reagent; namely ferrous ions ( $\text{Fe}^{2+}$ ) and hydrogen peroxide. The use of both iron and hydrogen peroxide in the field of wastewater treatment is not new. The most important environmental application of iron to date involves wastewater treatment via coagulation, which culminates in the association of solute particles to form flocculated agglomerates (Shaw, 1968) Iron salts such as  $\text{FeCl}_3$ ,  $\text{Fe}_2(\text{SO}_4)_3$  and  $\text{FeSO}_4$  are used alone or in combination with other coagulated inorganic salts such as calcium hydroxide (lime), calcium sulfate, magnesium hydroxide, magnesium sulfate and aluminium sulfate (alum). Iron salts are added to wastewater containing toxic heavy metals (e.g. Chromium (III), lead and arsenic) to form ferric hydroxide precipitates. The toxic metals are trapped within and adsorbed onto the precipitate leaving a purified effluent Eilbeck (1987).

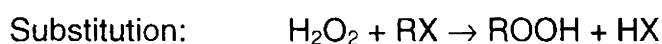
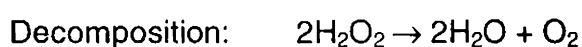
Another approach to removing toxic metals from wastewater involves adsorptive filtration. First, soluble heavy metals are removed from aqueous media by adsorption onto a thin layer of ferrihydrite that has been immobilized on the surface of sand particles. Then, the sand is filtered. Because the resulting ferrihydrite remains trapped on the sand particles, the adsorbent is later regenerated in a back washing step (USEPA, 1987) and Benjamin and Slettin (1993). Toxic metals have been removed from industrial wastewater electrolytically. Wastewater is recirculated between two iron electrodes and an electric current is passed between the electrodes when it begins to slowly remove iron from the anode in the form

of  $\text{Fe}^{2+}$ . The ferrous ions generated combine with hydroxide ions produced at the cathode to give  $\text{Fe}(\text{OH})_2$ . The iron hydroxide and adsorbed substances are then removed by flocculation and filtration (Reife, 1993; and Wilcock et al., 1996).

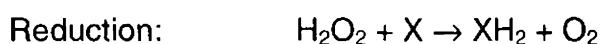
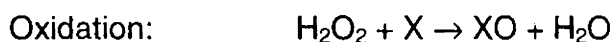
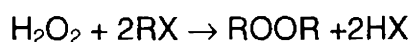
Iron salts are effective coagulants for removing phosphates, providing a potential solution to the problem of phosphate-induced eutrophication of lakes, streams and rivers. Taking advantage of this property, iron salts have also been used to remove phosphate ions from organic dye filtrates following the synthesis of azo dyes in a medium containing phosphoric acid (USEPA, 1987).

The second component of the Fenton's reagent is hydrogen peroxide. Hydrogen peroxide is a potent source of free radicals, has a redox potential of 1.78V and being a powerful oxidant its use in the environmental systems is not new. Hydrogen peroxide is considered to be a "clean" reagent since any of it that is not consumed in oxidation of the pollutant quickly decomposes to form only water and oxygen as products. Hydrogen peroxide is used to oxidize sulphides with respect to odour control, notably in pulp and paper manufacture and textile plant wastes. Sulphide corrosion of waste pipes may be controlled by the addition of hydrogen peroxide to wastewater (Cadena and Peters, 1988) Hydrogen peroxide can also be used as an additional oxygen source for overloaded activated sludge plants (Houtmeyers et al., 1977) and controlling filamentous bulking (Saayman et al., 1996 and Saayman et al., 1998)

Peroxide is used in paper manufacture (Prat et al., 1988) and during de-inking in waste paper recycling (Grayson and Eckroth, 1981) Peroxide is used in the removal of colour and it is applied extensively as a bleaching agent in the textile industry. Ince (1999) showed the cost-effectiveness in using peroxide for the photochemical degradation of dyes. Lin and Peng (1995) reported that the efficiency of the Fenton oxidation to remove COD was dependent on the hydrogen peroxide concentrations used. Hydrogen peroxide also finds wide application in the form a pretreatment option for refractory organics. The partial oxidation of recalcitrant compounds may also be advantageous in combined chemical/biological wastewater treatment processes. Two chlorinated aromatics tested by Carberry and Bensing (1991) showed enhanced biodegradability after pre-oxidation at molar ratios of peroxide to pollutant between 2:1 and 6:1, with an optimum at 4:1. The reactions related to hydrogen peroxide can be summarized into five main reactions (Snell and Etre, 1971):



Or



Hydrogen peroxide may react either directly or after it has first ionized or dissociated into free radical. In spite of the powerful oxidizing

ability of hydrogen peroxide, it acts as a reductant when reacting with stronger oxidizing agents such as chlorine, potassium permanganate and potassium dichromate. The reaction mechanism is very complex and may be affected by the reaction conditions and the type of the catalyst. Some of the factors influencing stability of hydrogen peroxide are concentration, temperature, pH, concentration of the stabilizer and presence of contaminants such as chromium, copper, iron and zinc (Grayson, 1981).

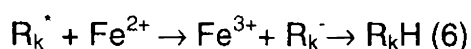
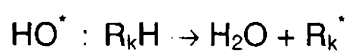
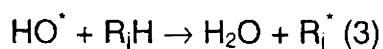
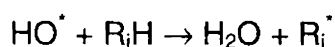
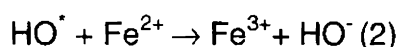
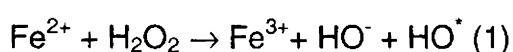
These apart, a major application of hydrogen peroxide and the ferrous salts combined is however, in the Advanced Oxidation Process, after it was observed that the high oxidative power of hydrogen peroxide could be further increased through a combination with UV radiation or metal salts. Several metals like titanium, vanadium, manganese, cobalt or nickel catalyze the decomposition of hydrogen peroxide. However, iron is the cheapest and least questionable of these metals making it the most preferred.

### **3.1.1. Mechanism of Fenton Oxidation**

Historically, Fe/H<sub>2</sub>O<sub>2</sub> oxidations have been of interest mostly from a synthetic or mechanistic perspective, their relevance to enzyme reactions and free-radical damage to cells. Recently, their potential for waste water treatment have been realized and reactions that generate hydroxyl radical (OH<sup>•</sup>) in solution at low temperature have attracted interest for destruction of toxic organic compounds in wastewaters (Joseph J. Pignatello., 1992).



In 1894, H.J.H. Fenton reported that ferrous ion strongly promoted the oxidation of malic acid by hydrogen peroxide. The  $\text{Fe}^{2+}/\text{H}_2\text{O}_2$  system is often referred to as Fenton's reagent (Fenton, 1894). In the Fenton's mechanism reactions with  $\text{H}_2\text{O}_2$ , cycle iron between the +II and +III oxidation states, yielding hydroxyl ( $\text{OH}^*$ ) radicals and other byproducts.  $\text{OH}^*$  is a powerful indiscriminate oxidant that reacts with many compounds at near diffusion controlled rates (Walling, 1975; Haag and Yao 1992). The basis of all Fenton based Advanced Oxidation Processes is that, when hydrogen peroxide is added to an aqueous system containing an organic substrate and excess  $\text{Fe}^{2+}$  at pH 0-2, the hydroxyl radicals generated attack the substrate and the subsequent course of the reaction and stoichiometry (moles of  $\text{Fe}^{2+}$  oxidized pre mole of  $\text{H}_2\text{O}_2$  added,  $\Delta[\text{Fe}^{2+}] / \Delta[\text{H}_2\text{O}_2]$ ) depend upon the fate of the organic radicals so produced. For a system containing a variety of C-H bonds, the postulated reaction steps are (Walling, 1975):



Unsaturated molecules (3) may also represent stoichiometrically equivalent addition reactions, but in either case it is assumed that the resulting radicals belong to three distinct classes:

Those oxidized by  $\text{Fe}^{3+}$ ,  $\text{R}_i^{\bullet}$

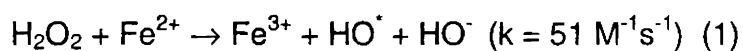
Those which are inert and dimerize,  $\text{R}_j^{\bullet}$ , and

Those which undergo reduction by  $\text{Fe}^{2+}$ ,  $\text{R}_k^{\bullet}$

Thus, in the above reaction that follows between ferrous iron and hydrogen peroxide in the presence of organic compounds but in the absence of complexing ligands other than water, decomposition of hydrogen peroxide in homogeneous aqueous solution involves the formation of organic radicals which react with molecular oxygen forming oxyl radicals namely the hydroxyl ( $\text{OH}^{\bullet}$ ) radicals and the hydroperoxyl ( $\text{HO}_2^{\bullet}$ radicals). Compared to the hydroxyl radical, the hydroperoxyl radical is much less reactive and its conjugate base  $\text{O}_2^{\bullet-}$  ( $\text{pK}_a$  4.8) is practically unreactive as a free radical (Frimer, 1988). These can in turn react with molecules of the organic compounds present, leading to a chain auto-oxidation of the compound with the formation of considerable quantities of peroxides and peroxide radicals which can react with ferrous ions or with hydrogen peroxide or they may decompose spontaneously. The carbon centered radicals generated by the oxyl radical attack may react with oxygen if present to form organoperoxy radicals ( $\text{ROO}^{\bullet}$ ) which can decompose to form hydroperoxyl radical ( $\text{HO}_2^{\bullet}$ ) or ultimately non-radical oxygenated products (Von Sonntag et al., 1997). Organo radicals may in

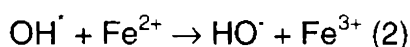
some cases be reduced by ferrous iron or be oxidized by ferric iron. The formation of hydroxyl radical ( $\text{OH}^\bullet$ ) is considered to be the primary step in peroxide-iron reaction (Walling, 1975).

The Fenton's reaction has been the subject of a plethora of studies and many mechanisms derived from spectrophotometric and kinetic studies have been proposed. Haber and Weiss (1934) proposed a mechanism, with hydroxyl radicals as the actual oxidant species. Their initial hypothesis was subsequently proved by many techniques including ESR spectroscopy. The hypothesis states that under acidic conditions the reaction is

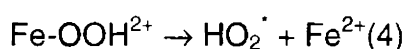


resulting in the formation of hydroxyl radicals, which are highly unstable but have a very high oxidation potential. They react with organic substances either by hydrogen abstraction or electrophilic addition to double bonds. Reacting with molecular oxygen, they initiate a non-selective sequence of oxidative reactions (dehydrogenation and or hydroxylation), resulting in destruction of the organic pollutants and conversion to  $\text{CO}_2$  and simple inorganic compounds with very high rate constants that approach diffusion controlled limits. Hydroxyl radicals ( $\text{OH}^\bullet$ ) are consumed with a rate constant of about  $10^5 \text{ s}^{-1}$  i.e., they have a mean lifetime of only about ten microseconds (Hoigne, 1997).

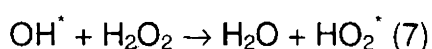
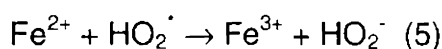
The hydroxyl radical so formed may be scavenged by reaction with another  $\text{Fe}^{2+}$  according to the reaction



or the presence of excess hydrogen peroxide, the reaction that takes place is given by



Since reaction (4) is generally much slower than reaction (1)  $[\text{Fe}^{2+}]$  is small relative to  $[\text{Fe}^{3+}]$



Reaction (7) is an additional mechanism for hydroxyl ( $\text{OH}^\cdot$ ) radical scavenging.

It should be noted that the concentration of peroxide employed in the oxidation process should be carefully controlled, as excess peroxide is involved in non-productive internal reactions and efficiency of oxidation can actually decrease with increased peroxide levels. Peyton and Glaze (1986) reported that if excess hydrogen peroxide is used the hydroxyl radicals will produce hydroperoxyl radicals which are much less reactive than hydroxyl radicals and therefore reduce the efficiency of the Advanced Oxidation Process.

Organic radicals formed by any of these reactions may quickly add a dissolved oxygen molecule to form reactive peroxy type intermediates.

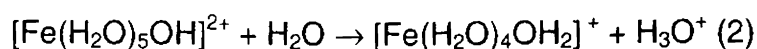
These react further to form hydroperoxyl ( $\text{HO}_2^*$ ) radicals, hydrogen peroxide and a series of different peroxides, aldehydes, acids etc. The primary requirement for the generation of hydroxyl radicals is that the concentration of ferrous ions must be sufficient enough so as to ensure that there is sufficient hydrogen peroxide in the reactor. On the other hand, the depletion or scarcity of hydrogen peroxide may result in an undesired accumulation of Fe(II) in the reactor. The initial rate of mineralization is reported to be faster with Fe(II)/ $\text{H}_2\text{O}_2$  (Fenton reagent), than Fe(III)/ $\text{H}_2\text{O}_2$  (Fenton-like reagent), due to the immediate formation of hydroxyl radicals with Fenton reagent (Ruppert et al., 1993). Further, in the presence of Fenton-Like reagents the chain length is increased by the formation of Fe(III)-hydroxy complexes, resulting in a more complete destruction of the organic compound (Ruppert et al., 1993) in this case the dye molecule.

The reaction between hydrogen peroxide and ferrous iron in dilute solution in the presence of oxygen and organic compounds leads to induced oxygen oxidation of ferrous iron. The extent of the induced oxidation may be quite large, particularly in oxygen-saturated solutions of the order of  $10^{-3}$  M in peroxide and iron, in which the concentration of oxygen is relatively high. The amount of ferrous iron oxidized by the induced reaction may be two to three times as great as the amount oxidized by the stoichiometric reaction under certain circumstances. When the reaction between ferrous iron and hydrogen peroxide is carried out in the presence of various organic compounds, organic radicals are formed

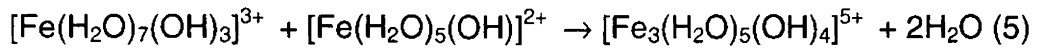
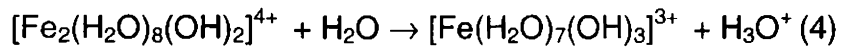
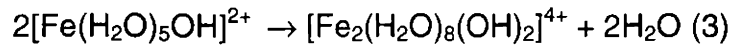
which can react with oxygen forming oxyl radicals namely the hydroxyl ( $\text{OH}^*$ ) radicals and the hydroperoxyl ( $\text{HO}_2^*$ ) radicals. These can in turn react with molecules of the organic compound present, leading to a chain auto-oxidation of the compound, with the formation of considerable quantities of peroxides or the peroxide radicals may react with three ferrous ions or with hydrogen peroxide or they may decompose spontaneously.

In the presence of oxygen it is stated that all the organic compounds show qualitatively similar behavior, without distinction between “Promoting” and “Suppressing” compounds. On the other hand, in the Fenton reaction chloride ion is a suppressing agent in the presence or absence of oxygen.

In aqueous solutions  $[\text{FeIII}]^{3+}$  is the predominant species at pH less than 2. At pH greater than 2, Fe(III)-hydroxy complexes  $[\text{FeIII}(\text{OH})_2]^+$  and  $[\text{Fe}_2\text{III}(\text{OH})_2]^{4+}$  may also catalyze the decomposition of  $\text{H}_2\text{O}_2$ . The Fenton's process employs ferrous ions and hydrogen peroxide. Under acidic pH the strong oxidative hydroxyl radical is produced and the ferrous ions are oxidized to ferric ions (Fenton, 1894; Walling and Kato, 1971). The ferric ions that is generated may form ferric hydroxo complexes with hydroxide ions as in the following two equations



These complexes have a pronounced tendency to polymerize at pH 6.5 to 7, according to the following equations (3) – (5). (Stumm et al., 1962)



Fenton's oxidation possesses the dual advantageous of both oxidation and coagulation in addition to increasing the amount of oxygen in water (Chin and Hicks, 1970; Kang and Chang, 1997).

### 3.2. Review on Fenton Oxidation:

Lin and Chen (1997)., studied a combination of electrochemical and chemical coagulation along with ion exchange for treating textile wastewater for reuse. The primary objective was to lower colour, turbidity and COD through electrochemical method and coagulation while ion exchange was primarily to further lower the COD concentration and reduce iron conductivity and total hardness of the wastewater. They observed that pH (optimum pH observed around 3) of the wastewater was an important operating factor that influenced the performance characteristics of electrochemical process. Addition of hydrogen peroxide was highly beneficial in enhancing the efficiency of electrochemical method. The efficiency enhancement was attributed to the presence of dissolved iron from the electrodes, which in the presence of hydrogen peroxide initiated a Fenton like reaction.

Kuo (1992), studied decolorization using the Fenton's reagent for five types of simulated dye wastewater prepared with disperse, reactive, direct, acid and basic dyes. The optimum pH was found below 3.5 and temperature enhanced the rate of decolorization. While the Fenton's reagent resulted in 97% decolorization for all the dye types studied the percentage decolorization was found to be structure dependent and on an average resulted in 90% COD removal.

Prat et al., (1988), examined the use of hydrogen peroxide in combination with ultraviolet radiation for the treatment of wastewaters from chlorination and alkaline extraction stages of paper-pulp bleaching. They



found that for a similar reaction time color reduction in the effluent was maximum at basic pH and that residual hydrogen peroxide would not be detrimental to the posterior biological processes. A combination of hydrogen peroxide and ultraviolet radiation, although achieved a greater reduction of color in the effluent it did not turn out to be economically competitive.

Pitroff et al., (1992), studied the decolorization of textile wastewaters by UV-radiation and hydrogen peroxide. They observed the degradation rate of the dye to be heavily dependent on the UV radiator output. The efficiency of the process although increased with higher dye concentrations, had a limit as increased dye concentration resulted in decreased permeability of the UV radiation. Reactive dyes were found to be easily decolorized with exceptions of yellow and green dyes. The green dyes required relatively longer treating time. The study also reported that UV/H<sub>2</sub>O<sub>2</sub> treatment reduced toxicity (bacterial inhibition). Similar study was conducted by Shu et al., (1995), for the decolorization of eight azo dyes. The system was found to be a very efficient treatment method for colour removal. Chang et al., (1996), used a modified Nernst equation to describe the decolorizing reaction using the oxidation-reduction potential (ORP) as an on-line monitoring and control parameter of the chemical reaction. The study utilized sodium hypochlorite to reduce the colour of wastewater spiked with five dyes, namely methyl red(MR), methyl violet (MV), methyl blue (MB), malachite green (MG) and methyl orange (MO). The ascending order of decolorization was MG>MV>MO>MT>MB.

Yang et al., (1998), explored the potential of ultraviolet light/hydrogen peroxide photochemical oxidation technology for treating textile-dyeing effluent. The effects of dye class and structure, dyebath concentration, radiation intensity and hydrogen peroxide level on a UV/H<sub>2</sub>O<sub>2</sub> system's ability to decompose and decolorize dyes were studied. Results indicated that acid, direct, basic and reactive dyes appeared to be viable candidates for photochemical oxidation, however, the limited solubility seemed to hinder the UV/H<sub>2</sub>O<sub>2</sub> degradation of disperse and vat dyes.

Bekbolet et al., (1998), studied the photocatalytic color removal of humic acid in the presence of some inorganic anions. The results showed that the removal rates could be explained in terms of Langmuir-Hinshelwood kinetics and the presence of common inorganic anions such as chloride, nitrate, sulfate and phosphate ions retarded the photocatalytic removal rate. Chloride, nitrate and sulphate although reduced the color removal rate of humic acid in water, the photocatalytic oxidation rates were found to be fast enough. However, phosphate ions retarded the rate significantly. First order equation was not found to satisfactorily explain the removal kinetics. Freundlich adsorption isotherm was found helpful in explaining the adsorption effect of anions on the photocatalytic removal rate. The authors observed that both Color<sub>436</sub> and Color<sub>400</sub> could be used as parameters to follow the decolorization of humic acids in natural waters.

Namboodri and Walsh, (1996), investigated the optimization and decolorization of spent reactive dyebath water with ultraviolet radiation in

the presence of hydrogen peroxide using both batch and continuous circulation processes. For a given concentration of the dye, under similar radiation intensity and peroxide concentration the continuous operation was found more efficient, due to the improved circulation and radiation exposure in the column.

Rodriguez et al., (1999) studied the treatment of pulp mill effluent using Fenton-type reactions assisted by 2,3-dihydroxybenzoic acid, 3,4-dihydroxybenzoic acid and 1,2-dihydroxybenzene. Efficiency of the treatment process was evaluated by the removal of absorbable organochloride compounds and toxicity reduction. Dihydroxybenzenes were found to increase the oxidative efficiency while 3,4-dihydroxybenzoic acid and 1,2-dihydroxybenzene inhibited Fenton reaction.

Solozhenko et al., (1995), studied the optimization and intensification of monoazo dye decolorization by Fenton's reagent. They observed that a hydrogen peroxide concentration of 17 mg/L resulted in 95 – 97% decolorization. The decolorization system was greatly affected by pH and occurred only in an acidic medium. The efficiency of decolorization increased under the influence of solar radiation or by an increase in the reaction temperature. The effectiveness of hydrogen peroxide was found dependent on the initial dye concentration with the consumption of hydrogen peroxide increasing with an increase in the initial dye concentration.

Wanpeng et al., (1996), studied the application of ferrous ion-peroxide oxidation combined with coagulation as a pretreatment option for

treating wastewater from H-acid manufacturing process rich in various substituted derivatives of naphthalene. The optimum pH value was below 4 and at suitable ferrous ion and peroxide dosage the overall COD removal reached 90% or more. The groups on naphthalene ring, such as nitrite and sulphide were substituted by hydroxyl free radical, and resulted in ring cleavage during oxidation process. The oxidation of H-acid by Fenton's reagent was a three-step process. First, hydroxyl radical substituted passive groups on naphthalene ring. It made the naphthalene ring activable. Secondly, naphthalene ring was oxidized and broken down, producing elementary unsaturated fatty acid. Thirdly, unsaturated fatty acid decomposed into inorganic substances. The authors reported that  $[Fe^{2+}]$ ,  $[H_2O_2]$  and  $[OH\cdot]$  were all the rate determining factors that directly influenced the concentration of hydroxyl free radical generated in aqueous system.

Spadaro et al., (1994), studied the degradation of azo dyes by hydroxyl radicals. The study demonstrated that  $Fe^{3+} - H_2O_2$  treatment degraded a substantial portion of azo dyes to water-soluble products and carbon dioxide. The study indicated a definitive evidence for the generation of benzene when azo dyes with a phenyl azo substitution were degraded with  $Fe^{3+} - H_2O_2$ .

Ince and Tezcanli (1999), investigated the effect of process parameters such as temperature, pH and alkalinity to optimize the treatability of textile dye-bath effluents by advanced oxidation. Fenton ( $Fe(II)/H_2O_2$ ) and Fenton-like ( $Fe(III)/H_2O_2$ ) reagent in the presence and

absence of UV light, was used to oxidize a reactive azo dye (Procion Red HE7B), and typical dye bath constituents. They reported that when the system was operated at pH 3 and with a  $\text{H}_2\text{O}_2/\text{Fe(II)}$  molar ratio of 20:1, with in 20 minutes of irradiation complete color removal accompanied by a 79% reduction in total organic carbon and a 50% reduction in TDS was obtained. The color removal was found unaffected by variations in the molar ratios under dark conditions, whereas degradation was found 0.75 time faster at higher molar ratios, when the solution was irradiated. Under UV irradiation, complete color removal was possible in 20 min, as opposed to 90 minutes in dark. The authors report that the reaction occurred in two stages, a fast step followed by a slow step during which the reaction was found to follow first order kinetics. An increase in the molar ratio was found more effective for TOC degradation. It is reported that pH 6 to 4 did not show any effect on decolorization, but a significant increase in the decolorization was observed as the pH was lowered to 3 and more so as it was further lowered to 2. This observation was attributed to the reduction in the solubility of ferrous sulphate at increased pH, resulting in inhibition of the Fenton reactions. However, the authors suggest the use of an appropriate membrane system to remove the dissolved solids to make the treated effluent reusable.

Sewekow and Leverkusen., (1993), studied Fenton oxidation of reactive dye effluent. The authors observed that wastewater treatment with Fenton's reagent destroyed residual colour and AOX in the effluent. Heavy metals introduced by metal-complex dyes precipitated out together with

iron hydroxide in the neutralization stage. Apart from a reduction in the COD, Fenton oxidation was found to enhance the degradability of the residues.

Tang and Chen., (1996), Investigated the oxidation kinetics and mechanism of three dyes in a well-mixed batch reactor. The optimal pH ranged from 2.0 to 3.0. The optimal ratio of  $H_2O_2$  to iron metal was 0.001M to  $1g\ L^{-1}$ . The initial oxidation rates were obtained according to pseudo-first-order kinetics and dye structure was found to influence oxidation kinetics. Dimerization occurred at high dye concentrations. The  $H_2O_2$ / iron powder system was found to be better than the Fenton's reagent system due to the continuous dissolution of iron powder.

Kang et al., (2002), evaluated Fenton process, involving oxidation and coagulation, for the removal of color and chemical oxygen demand from synthetic textile wastewater containing polyvinyl alcohol and a reactive dye. The variables studied included dosages of iron salts and hydrogen peroxide, oxidation time, mixing speed and organic content. Fenton oxidation primarily removed color (95% with in 5 minutes) while COD was removed by Fenton coagulation.

Bandara et al., (1997), studied the effectiveness of Fenton's reagent to degrade orange II under light and dark conditions. They observed the degradation to be strongly dependent on initial pH of the solution. Significant mineralization rates were observed only at pH below 5. Degradation of the dye was found to depend on the speciation of iron in solution, dissociation of hydrogen peroxide and the photolytic equilibria of

the dye each of which was a function of pH. Under irradiation the dye was completely mineralized in 40 minutes as indicated by the formation of carbon dioxide, water, nitrates, ammonia and sulfate. The  $\text{Fe}^{+3}/\text{H}_2\text{O}_2/h\nu$  system was found to be catalytic instead of stoichiometric in iron.

Bandara et al., (1996) investigated the degradation of Orange II by Fenton type reagent aided by sunlight. They observed that concentrated solutions (2.9 mM) of the azo dye Orange II could be mineralized to 95% in less than 8 hours by the Fenton's reagent in the presence of sun light. This indicated that light and thermal processes associated with UV component of natural sunlight was sufficient to promote degradation of the dye. The author's reported that the thermodynamic potential for the redox couple in Fenton like process is not the only process involved. The highly stable iron complexes in combination with hydrogen peroxide and the near surface radical formation are also processes actively responsible for the abatement of the dye. Since no activation energy was detected during the mineralization the authors suggest the involvement of a radical mechanism in the reaction.

Balanosky et al., (2000), reported the treatment of textile wastewaters from nano-filtration of biologically treated secondary textile effluents by Fenton and photo-assisted Fenton treatment. The influence of hydrodynamic and chemical parameters affecting the degradation of non-biodegradable residues of the textile waters were studied in both batch and flow reactors. Copper and ferric or ferrous ions mediated the oxidation process under irradiation analogous to the Haber-Weiss cycle and were

found to be suitable to degrade the recalcitrant part in the textile waters after the initial biological treatment. Hydrogen peroxide was effective only in the presence of ferrous or ferric ions. At lower hydrogen peroxide concentrations the reaction proceeded slowly since the oxidant concentration was not sufficient. The effect observed on the degradation kinetics upon variation of light intensity showed that ferric ion is the active chromophore absorbing the light for the solutions. The optical absorption of the iron-chromophore and the spectral emission of the light source used were identified as the most important factor determining the kinetics and efficiency of the treatment and not the intensity of the applied light. The TOC curves against time followed a near exponential decay law and a single polynomial exponential expression was constructed for TOC that could integrate the numerical values found during the degradation.

Fung et al., (1999), studied the treatability of cuprophenyl yellow RL in wastewater by UV/H<sub>2</sub>O<sub>2</sub>/Ultrasonication process. The effects of pH, hydrogen peroxide dosage and ultrasonication on the oxidation process was investigated on a bench-scale reactor and their performance on colour removal were evaluated. Improved generation of hydroxyl radicals was observed at higher pH. The oxidation efficiency could be enhanced by increasing the amount of hydrogen peroxide, however high concentrations had little positive effects on dye removal due to the competitive reaction of hydrogen peroxide with the hydroxyl radicals. Dye degradation was found to be an oxygen consuming process and ultrasonication was found to dramatically increase the oxidation efficiency. The dye was found to follow



pseudo-first order kinetics at different pH and hydrogen peroxide concentrations. The rate constants were linearly correlated with the pH but fitted better into a second order polynomial expression.

Fung et al., (2001), studied the effect of flow rate, and feeding rate of  $H_2O_2$  on a dyeing wastewater containing reactive dye under the influence of UV and Ultrasonic light. The decoloration process was found to follow first order kinetics. UV light was the most significant factor in comparison to Ultra-sonic light. The degradation rates increased at low flow rates and high feeding rate of the oxidant.

Fernandez et al., (1999), the study for the first time showed the use of immobilized iron clusters on membrane supports as being catalytically active in the decomposition of  $H_2O_2$  during the photo assisted degradation of the dye i.e., the highly dispersed Fe ions supported onto dissolved Nafion membranes were found to have similar effect as Fe ions on the decomposition of  $H_2O_2$  in homogeneous solution. The treatment was found to proceed via Fenton-like process with out sludge production due to the selective decomposition of  $H_2O_2$  on the iron ions exchanged on the membrane. The variables studied include,  $H_2O_2$  concentration, solution pH, azo dye concentration and light intensity.

Kang et al., (1997), evaluated the use of hydrogen peroxide to improve Fenton's coagulation for COD and color removal from textile effluents. It was found that hydrogen peroxide could enhance ferrous coagulation. The study indicated that the optimum pH for ferrous coagulation and Fenton's pre-oxidation ranged between 8.0-10.0 and 3.0 -

5.0 respectively. The rate of colour removal was faster than COD removal. For the same ferrous dosage, the ratio of COD removal for Fenton's coagulation versus ferrous coagulation, range from 1.4 to 2.3 and for color removal ranges from 1.1 to 1.9.

Lin and chen., (1997) studied the treatment of waste water from secondary treatment plant of dyeing and finishing mill using a combination of Fenton process, chemical coagulation and ion exchange. Results indicated that the combined system was very effective in elevating the water quality thereby suggesting the possibility for reuse.

Nadtochenko and kiwi., (1997) using steady state and pulsed laser photolysis studied the effect of added oxalate on the activity of Fenton's reagent ( $\text{Fe}^{2+}/\text{Fe}^{3+}\text{-H}_2\text{O}_2$ ). The authors reported dark and light reactions during the decolorization of Orange II. The study indicated that the excited states of  $\text{Fe}(\text{OX})_3^{3-}$  or the (FeIII)-Orange II) complexes were the active species during decolorization of the dye. Based on a radical theory of Fenton catalysis and direct evidence obtained from laser spectroscopy, the authors demonstrated the formation of  $\text{OH}^*$  adducts for Orange II as the initial degradation step leading to oxidation of the dye.

Lin and Lo., (1997) studied the influence of pH, temperature, treatment time and COD removal efficiency of a simulated desizing wastewater using Fenton oxidation along with chemical coagulation. Chemical coagulation using polyaluminium chloride and polymers were found to complement the Fenton treatment process by reducing the floc

settling time, enhancing color removal and reducing the ferrous ion concentration.

Pulgarin et al., (1996) studied the photocatalytic degradation of Tinopal CBS-X (1 disodium 4,4'-bis (2-Sulfostyryl) 1 biphenyl) via the Fenton reaction. 90% degradation was observed in 2 hours and complete degradation took about 4 hours. The variables studied included substrate concentration,  $\text{Fe}^{3+}$  ions, the contribution of the dark reaction and the presence of hydrogen peroxide. In all cases the fluorescence intensity decreased as the Fenton reaction proceeded, but the shape of the spectra did not change indicating that the degradation products were not fluorescent. The Photo-Fenton process enhanced the adsorption of Tinopal CBS-X on activated sludge.

Kaique et al., (1998) studied the oxidation of malachite green using  $\text{Fe}^{3+}$  and  $\text{H}_2\text{O}_2$  in the presence of visible light and compared it to the reaction in dark. The results indicated that visible irradiation could significantly accelerate the Fenton degradation of dyes. Similar observations were reported by Wu et al., (1999) on Malachite green.

Ince and Stefan, (1997) studied the oxidation and toxicity reduction of an azo dye - Remazol black by a UV/ $\text{H}_2\text{O}_2$  oxidation system. Although the dye was completely mineralized in 30 minutes only 44% of the organic carbon was mineralized. The toxicity reduction was 68%. The authors observed that beyond an effective concentration, the influence of hydrogen peroxide was found inhibitory.

Anat and Deshpande., (1996) studied the influence of pH, concentrations of ferrous sulphate and hydrogen peroxide as well as different ratios of ferrous sulphate to hydrogen peroxide during the Fenton oxidation of reactive dyes. The authors report that the initial reaction period for cleaving the dye molecule was almost instantaneous accompanied by reduction in toxicity.

Lin et al., (1998) used Fenton oxidation aided with sulphur oxidizing bacteria and granular activated carbon. During the process sulfur compounds were completely oxidized to sulfate and the biodegradable organics were simultaneously degraded at a removal of 55%. The combination of sulfur oxidizing bacteria and granular activated carbon treatment transformed any refractory toxic compounds present into biodegradable organics with a 95% removal of dissolved organic carbon.

Liao et al., (1999) studied the effects of light intensity, concentrations of ferrous and hydrogen peroxide and pH on the oxidation of effluents from a dye manufacturing unit. The oxidation process was enhanced for a higher intensity of radiation and increased concentration of ferrous ions during the initial reaction periods. However as the reaction progressed with an increase in the ferrous ions the removal profiles leveled off due to the lack of hydrogen peroxide residue. The authors also observed that an increased concentration of hydrogen peroxide did not necessarily mean increased removal rates of COD and color. The optimum pH was 3 and 4 for the removal of COD and color respectively.

Park et al., (1999) achieved 91.2%, 18.1% and 45.7% decolorization efficiencies for red and yellow wastewater and final effluent respectively during the Fenton oxidation of pigment wastewater. The BOD/COD ratio was increased from 0.04 to 0.36 indicating that Fenton oxidation enhanced biodegradability.

Herrera et al., (1999) studied the Photo-Fenton oxidation of Remazol brilliant blue and Uniblue - A through Laser flash photolysis and report that electron transfer between the excited dye and  $\text{Fe}^{3+}$  was found to be the initiating step, either as a bimolecular process ( $\text{D}^* + \text{Fe}^{3+} = \text{D}^{0+} + \text{Fe}^{2+}$ ) or through a dye - iron complex ( $\text{D}^* + \text{Fe}^{3+} = \text{D}\dots\text{Fe}^{3+}$ ) which again forms ( $\text{D}^{0+} + \text{Fe}^{2+}$ ). A radical chain reaction was observed between  $\text{Fe}^{3+}/\text{H}_2\text{O}_2$  during the initiation step. Photo dissociation reaction of the  $\text{D}\dots\text{Fe}^{3+}$  complex was found to be more important in the initiation of the chain reaction rather than bimolecular quenching between  $\text{D}^*$  and  $\text{Fe}^{3+}$ .

Balcioglu et a., (2001) compared the treatment efficiency of  $\text{TiO}_2/\text{UV}$ , dark and UV- light assisted Fenton and Fenton like processes of an azo dye and copper phthalocyanine dye in acidic medium. All the oxidation processes completely detoxified the azo dye, which had initially showed 70% inhibition to a marine alga *Dunaliella Tertiolecta*. The copper phthalocyanine dye underwent only limited oxidative degradation and abatement was primarily through adsorption on the photocatalyst surface or coagulative effect of ferric or ferrous ions.

Sevimil and Kinaci., (2002) investigated the effect of some operational parameters on the efficiency of Ozonation and Fenton's

process for the decolorization and COD removal of Acid Red 337 and Reactive Orange 16. Ozonation resulted in 60 to 91% color removal, while COD removal was 9-17%. The influence of pH, temperature, dosage of ferrous and hydrogen peroxide and the ratio of ferrous to hydrogen peroxide were the variables studied on the Fenton's process. pH had a profound influence while temperature was not found to influence either the color or COD removal. Increased concentration of hydrogen peroxide and ferrous sulphate resulted in increased color and COD removal. The optimum ratio of  $\text{Fe(II)/H}_2\text{O}_2$  was between 0.5 and 0.83.

Kang et al., (2002) studied the influence of dosages of iron salts and hydrogen peroxide, oxidation time, mixing speed and organic content on Fenton's process involving oxidation and coagulation for the removal of color and COD from synthetic textile wastewater containing polyvinyl alcohol and a reactive dye. When color removal was attributed to Fenton oxidation, COD removal was low and attributed to Fenton coagulation. The Fenton process was found to be more efficient for color removal rather than COD and the ratio of removal efficiency between Fenton process and ferric coagulation was 5.6 for color removal and 1.2 for COD removal.

Kang et al., (2000) observed that color removal was strongly related to generation of hydroxyl radical. The optimum pH for both hydroxyl radical generation and color removal was observed at 3.5. Up to 96% decolorization was achieved with in 30 minutes.

Bogatu et al., (2000) studied Fenton oxidation of four azo dyes and proposed that the reaction took place in three steps: first, breakage of the

azo bond leading to color removal; second, oxidation and partial cleavage of benzene and triazine rings; third, advanced oxidation and mineralization of organic nitrogen (approx. 80%).

Yang et al., (2001) observed 95.8% color removal and 72.7% COD after 60 min. reaction. The optimum  $\text{Fe}^{2+}:\text{H}_2\text{O}_2$  ratio was 1:20.

Salem and Maazawi ., (2000) observed that Fenton oxidation was first order with respect to Methylene blue and with respect to hydrogen peroxide and ferrous sulphate the order was found to be dependent on the concentration range. At low hydrogen peroxide concentrations, the reaction was found to be first order, which becomes zero order with increase in hydrogen peroxide concentration before becoming negative. Formation of colored intermediate on the surface of the catalyst was observed, which had an inhibiting effect on the rate of color removal. The rate of the reaction was strongly influenced by pH and ionic strength of the solution.

Swaminathan et al., (2003) observed that the initial oxidation reaction was found to fit into first order kinetics and the rate of oxidation of H – acid was found to be higher than the dyes. The authors observed the release of chloride and sulfate from H – acid indicating that the Fenton oxidation of dyes proceeded through cleavage of the substituent group.

Pignatello and Sun., (1995) suggests that non-selectivity of the reaction and ability to achieve complete mineralization within a reasonable time period make photo-assisted Fenton oxidation a mild and effective remedy for treating dilute pesticide wastes.

Huston and Pignatello., (1999) studied the destruction of pesticide active ingredients like alachlor, aldicarb, atrazine, azinphos-methyl, captan, carbofuran, dicamba, disulfoton, glyphosate, malathion, methoxychlor, metolachlor, picloram and simazine . In most cases complete loss of the active ingredients occurred in less than 30 min. and took over 120 min. for mineralization. This was evidenced by the appearance of inorganic ions and the decline in total organic carbon of the solution. The results suggest that many pesticides and their commercial formulations in dilute aqueous solution are amenable to photo-Fenton treatment. Longer reaction time, higher initial peroxide concentration, or additional amendments of peroxide could enhance mineralization. As mineralization proceeds carbon acquired higher oxidation states, while the organic compounds remaining in solution become less reactive with the hydroxyl radicals. This results in decay of the hydroxyl radical due to scavenging by hydrogen peroxide or self-reaction or scavenging by the ferrous ion.

Scott et al., (1995) studied the degradation of Atrazine by Fenton's reagent as a function of reagent concentration, ratios and pH in batch treatments. The optimal ratio of  $\text{FeSO}_4:\text{H}_2\text{O}_2$  was found to be 1:1 at which Atrazine was completely degraded in  $\leq 30\text{s}$ . Increase in pH from 3 to 9 resulted in a decrease from 99% degradation to 37% degradation.

Joseph J. Pignatello, (1992) studied the degradation of two herbicides 2,4-D and 2,4,5-T in acidic aerated solutions of  $\text{H}_2\text{O}_2$  and  $\text{Fe}^{2+}$  or  $\text{Fe}^{3+}$ . Complete mineralization was achieved using  $\text{Fe}^{3+}/\text{H}_2\text{O}_2$  and the transformation was found to be pH sensitive. The optimum pH was



between 2.7-2.8. Methanol and chloride ions were found to inhibit the reaction due to scavenging of the active oxidant and by sulfate due to complexation with  $\text{Fe}^{3+}$ . Visible light above 300 nm accelerated degradation with complete mineralization in < 2h.

Sun and Pignatello., (1993) presented a detailed investigation on the mineralization of 2,4-dichlorophenoxy acetic acid (2,4-D) by  $\text{Fe}^{3+}/\text{H}_2\text{O}_2/\text{UV}$  system, focusing on photochemical reactions that contribute to enhancement. The authors report that one contributing reaction to photo enhancement is photolysis of aquated ferric ions. The photo reduced iron then becomes a precursor to a second hydroxyl radical when peroxide is present via the Fenton reaction. Several species of  $\text{Fe}^{3+}$  are known to be photoactive, and their importance depends on pH and wavelength of the emitted light. It is reported that the oxidation process occurred in two stages. The first stage, where there is dechlorination and conversion of approx. 40% of ring and carboxy carbon of 2,4-D is mostly due to hydroxyl radical reactions generated under irradiation. The remaining 60% of carbon mineralization where hydroxyl radical play no significant role occurs almost exclusively by photolysis or decarboxylation of  $\text{Fe}^{3+}$  complexes of degradation intermediates probably ring-opened products coordinated via carboxyl and hydroxyl groups. The study reveal that hydroxyl radical is ineffective in oxidizing the organic intermediates remaining after the completion of the first stage, most likely due to the lower reactivity of the highly oxygenated intermediates toward the hydroxyl radical and competition for the hydroxyl radical by other solutes. The hydroperoxyl

radical produced by the reaction between hydrogen peroxide and the ferrous ion was found incapable of producing any CO<sub>2</sub> from the ring, indicating the poor reactivity of the hydroperoxyl radical (HO<sub>2</sub><sup>\*</sup>) compared to the Hydroxyl radical (OH<sup>\*</sup>). Oxygen played an important role in these reactions.

Kalpana and Ann, (1998) studied the degradation of pesticides by hydroxyl radicals generated from reaction between hydrogen peroxide and electrochemically generated ferrous iron. Multiple addition of hydrogen peroxide in smaller doses was found to enhance the degradation compared to a single dose. Small molar excess of hydrogen peroxide to iron increased the degradation of atrazine. The optimum ratio of hydrogen peroxide to iron was 5:1.

Herve et al., (1998) studied the oxidation of Atrazine by Fenton's reagent over pH ranging from 1-8. Oxidation was found to follow the mechanism proposed by Barb et al., (1951) only when the pH was less than 3. Results suggested that the reaction of hydrogen peroxide with ferrous ion involves an intermediate which leads to the formation of another intermediate that in turn reacts with Fe(II) to give Fe(III) without the formation of OH<sup>\*</sup>.

Lu et al., (1997) report that Fenton's reaction is extremely sensitive to anions and phosphate ions in particular suppress the oxidation reaction. This was attributed to complex formation by phosphate ions either with ferrous or ferric iron. The reported sequence of anions suppressing the reaction is given as H<sub>2</sub>PO<sub>4</sub><sup>-</sup> >> Cl<sup>-</sup> > NO<sub>3</sub><sup>-</sup> = ClO<sub>4</sub><sup>-</sup>. The rate of oxidation after

the addition of ferrous ions was found greater than that of ferric ions. An increased concentration of ferrous ions resulted in an increase in the oxidation rate of Dichlorvos.

Lu et al., (1997) studied the Fenton oxidation of Dichlorvos. The authors observed that oxidation of Dichlorvos were a two-stage reaction with the first stage where the decomposition was high being over with in 30s. This stage was attributed to a  $\text{Fe}^{2+}/\text{H}_2\text{O}_2$  reaction. The second stage was slow and attributed to  $\text{Fe}^{3+}/\text{H}_2\text{O}_2$  reaction. The optimum pH range was 3-4. The decomposition rate of Dichlorvos was found to increase with an increase in the concentration of ferrous ions or hydrogen peroxide.

Balmer and Sulzberger., (1999) observed that both oxalate concentration and pH greatly influenced the rate of Atrazine transformation. At all pH values, the rates were considerably higher at higher oxalate concentrations and no degradation occurred at  $\text{pH} > 7$ .

Takemura et al., (1994) studied the decomposition of tetrachloroethylene used in dry cleaning in both static and circulating experiments. Reticulated iron was chosen as the test material after comparison of several kinds of iron as an iron source. Although the organic chlorine compounds added in pure water were easily decomposed by Fenton's reaction on the reticulated iron in aqueous phase, the system could not achieve high efficiency in the case of wastewater from the actual laundry process. The reason given was the coexistence of high COD residuals, such as dirt and organic acids. A combination of circulation and air bubble agitation was found to enhance the removal of trichloroethylene.

Sedlak and Andren. , (1991) investigated the degradation of chlorobenzene and its oxidation products by Fenton's reagent. The primary step associated with degradation was hydroxylation followed by ring cleavage and mineralization. Another possible reaction pathway involved the formation of dimers and colored aromatic polymers, which were oxidized subsequently by hydroxyl attack. Depending on the presence or absence of oxygen marked differences in the reaction products have been reported during Fenton's oxidation. In the absence of oxygen, chlorophenols, dichlorobiphenyls and phenolic polymers were the predominant initial products. In the presence of oxygen, there was marked decrease in the yields of dichlorobiphenyls, which was further oxidized to chlorinated and non-chlorinated diols. The highest yield of product formed per mole of hydrogen peroxide consumed was observed in the pH range of 2-3. pH dependence and product distributions led the authors to suggest that complexes of aromatic intermediate compounds with iron and oxygen played a key role in regulating the reaction pathways.

Huston and Pignatello. , (1996) carried out kinetic and product studies to elucidate the mechanism and role of oxygen during the degradation of carbon tetrachloride and hexachloroethane in UV-illuminated (300-400 nm) acidic oxic or anoxic solutions containing Fe(III) and oxalate. The authors found the addition of ferrioxalate as a photo-Fenton precursor to be advantageous because it strongly absorbed visible light up to 550 nm and had a high quantum yield for the generation of

Fe(II). This addition, apart from generating hydroxyl radical had an added advantage of requiring lower energy of irradiation.

Sedlak and Andren., (1991) observed that hydroxyl radical generated by Fenton's reagent could rapidly oxidize polychlorinated biphenyls in aqueous solutions via addition of a hydroxyl group to one of the non-halogenated sites.

Walter and Huang, (1996) evaluated the effect of chlorine content on the oxidation kinetics of chlorinated phenol by Fenton's reagent. The reactivity of chlorophenols decreased with increasing chlorine substitution on the aromatic ring. Under conditions of excess hydrogen peroxide and ferrous ions the pseudo first order rate coefficients were found to be proportional to the number of unsubstituted positions, whereas no correlation was observed between dechlorination constants and the number of unoccupied sites on the aromatic ring. At constant hydrogen peroxide and ferrous concentrations, initial dechlorination rates were not found to change significantly suggesting that the generation of hydroxyl radical was the rate-limiting step in Fenton chemistry.

Tang and Huang. , (1997) studied the stoichiometry of Fenton's reagent in the oxidation of dichloroethylene, trichloroethylene, tetrachloroethylene and dichloroethane. The optimal ratio between Hydrogen peroxide and ferrous was 5-11 and the optimum pH was observed at 3.5. The amount of hydrogen peroxide required to oxidize an organic compound and the accumulation of chloride ions released was found to be dependent on the initial concentration, and followed the order

of TCE, Tetra-CE < DCE << DCEA. The amount of chloride ions detected at a constant concentration of hydrogen peroxide followed the order DCEA << DCE < TCE < Tetra-CE.

Tang and Huang., (1996) studied the effect of pH and concentrations of hydrogen peroxide, ferrous sulphate and substrate concentration on both oxidation and dechlorination kinetics of 2,4-DCP. The study used a mathematical model to describe the oxidation kinetics and chloride ion production at constant concentration of hydrogen peroxide and ferrous sulphate.

Tang and Huang., (1996) developed an oxidation kinetic model of TCE by Fenton's reagent based upon transition state theory. According to which hydroxylated active complexes was assumed to be the transition state after the hydroxyl radicals had attached to the organic compound. The complex either disproportionate or return to their original reactants. Both  $\text{OH}^*$  and the active complexes were highly reactive. The model indicated that Fenton oxidation was first order with respect to the concentration of organic substrate. The degree of oxidation was found dependent on the dosage of  $\text{H}_2\text{O}_2$  and  $\text{Fe}^{2+}$ . The authors also stated that because both  $\text{Fe}^{2+}$  and  $\text{H}_2\text{O}_2$  can react with  $\text{OH}^*$ , neither of them should be overdosed if the maximum reaction rate was to be achieved. Another observation made is that during the Fenton Oxidation of chlorinated compounds an increase in the chlorine content would bring about a decrease in the reactivity of the Fenton's reagent.

Tang and Huang., (1996) based on the rate constants derived the authors reported that chlorine positions of mono, di and trichlorophenol had a significant effect on the dechlorination kinetics during Fenton oxidation. They observed that closer the location of chlorine atoms on the aromatic ring, the more difficult is the dechlorination process. Dechlorination kinetics during the Fenton's oxidation was found to be affected both by directory effects of OH and Cl groups, as well as by steric hindrance of the chlorine atoms.

Wang et al., (1998) report that compared to other organic chelators pyrophosphate was found to be more stable and could significantly increase the concentration of iron in aqueous solutions. This enhanced the dechlorination of tetra chloroethene (PCE) by Fenton reaction. A decrease in the dechlorination rate was observed with time, which was attributed to both the conversion of Fe(II) to Fe(III) and the decrease of aqueous iron.

Prouslek and Duriskova., (1998) studied the oxidation of PEG and 6-Caprolactam by Fenton and Photo-Fenton reactions. They observed a COD reduction ranging from 72-84% and found the photo-Fenton reaction more efficient than the Fenton reaction.

Li et al., (1996) used furnace slag along with hydrogen peroxide to degrade 2,4-dichlorophenol. Under acidic conditions the slag dissociated to produce ferrous ions that react with hydrogen peroxide to produce hydroxyl radical which in turn degraded 2,4-dichlorophenol by Fenton- like mechanism. The results show that 100 mg L<sup>-1</sup> of 2,4-dichlorophenol and its

oxidation intermediates could be totally decomposed within 2 hours. The observed optimum pH was 2.8.

Kuo and Lo., (1999) reported that the optimum pH for degradation and mineralization of chlorobiphenyl was 3. The reaction was found to be first order with respect to hydrogen peroxide and with respect to Fe(II) concentration it was a saturation type reaction.

Margaret et al., (1999) reported that saturated aqueous solutions of Creosote and PCP could be effectively treated by Photo-assisted Fenton reaction. Acute toxicity of the treated solution to Fathead minnows was nearly eliminated and reduced the acute toxicity to Daphnia.

Brain et al., (1998) observed that in aqueous solution TNT rapidly degraded after three sequential additions of hydrogen peroxide and ferrous sulphate in a molar ratio of 25:15:1 ( $\text{H}_2\text{O}_2$ :  $\text{Fe}^{2+}$ : TNT) at pH between 2.5 and 3.

Chen and Pignatello., (1997) examined the oxidation of phenol by Fenton systems in dark and under UV/Visible light. Reactions were conducted at an initial pH of 2.8, with the hydrogen peroxide concentration in excess and iron in catalytic concentrations. In all cases, the reactions displayed autocatalysis. An important finding of the study was that quinones served as electron-transfer catalysts between dihydroxycyclohexadienyl radical – the  $\text{OH}^*$  adduct of phenol – and  $\text{Fe}^{3+}$  by way of a semiquinone radical thus, playing an important catalytic role in Fenton oxidation of aromatic compounds.



Esther et al. (1995) the study was carried out to find if  $\text{OH}^*$  are formed in the reactions of divalent iron complexes  $\text{Fe (II) L}$ ;  $\text{L} = \text{EDTA}$ ,  $\text{HEDTA}$  and  $\text{TCMA}$  in neutral and slightly acidic solutions using the  $\beta$ -elimination reaction as an assay for the formation of  $\text{OH}^*$ . The results showed the formation of an Iron (II) peroxide intermediate complex which at  $\text{pH} < 5.5$  decomposes to yield free hydroxyl radical indicating that the non-participating ligand-L has an appreciable effect on the mechanism of reaction of the metal center with hydrogen peroxide.

Sychev and Isak, (1995) report that high peroxide concentrations could also be detrimental to the degradation kinetics since after the initiation step the propagation step would be hindered by an excess hydrogen peroxide acting as a scavenger of the hydroxyl radical.

Jurg Hoigne, (1997) experimentally quantified and compared the efficiencies of various hydroxyl radical sources following the oxidation of inter-calibrated probe compounds that react during the process only with the  $\text{OH}$  radicals. However, water quality parameters control the lifetime of the  $\text{OH}$  radicals via scavenging reactions by pollutants and other solutes, must be quantified before the results can be applied.

Sonntag et al., (1997) report that with a few exceptions, such as phenoxyl radicals; radicals formed as a result of the hydroxyl radical attack on organic matter react with oxygen yielding peroxy radicals whose formation and decay contributes decisively to the oxidative degradation of Dissolved Organic Carbon. The authors claim that in the application of Advanced Oxidation Processes it must be ensured that oxygen should not

be depleted because the  $\text{HO}_2^*$  or  $\text{O}_2^{*-}$  radical liberated in the various peroxy radical reactions would rapidly react with oxygen to generate the  $\text{OH}^*$ .

Isak et al., (1996) studied the oxidation of formaldehyde, isobutyraldehyde, benzaldehyde and anisaldehyde in the presence of  $\text{Fe}^{2+}/\text{H}_2\text{O}_2/\text{H}^+$  and observed that the oxidation was first order with respect to hydrogen peroxide for aliphatic aldehydes and 0.5 order for aromatic aldehydes.  $\text{Fe}^{2+}$  played the role of a catalyst dissociating  $\text{H}_2\text{O}_2$  to  $\text{OH}^*$  and  $\text{OH}^-$ . An increase in the rate of the reaction was observed when ascorbic acid capable of reducing  $\text{Fe}^{3+}$  to  $\text{Fe}^{2+}$  was added.

Ansari et al., (1996) studied the oxidation of hydrogen sulphite to sulfate through three different routes. Fenton and photo-Fenton reactions were used to carry out the oxidation process while;  $\gamma\text{-FeOOH}$  was used in order to promote the photocatalytic oxidation. According to them intermediate species like  $\text{HSO}_5$  and or  $\text{SO}_5^*$  generated during the oxidation was involved in the autocatalytic mechanism.

Zakharov and Kumpan., (1996) found benzoic acid and acetyl salicylic acid to function as inhibitors of the radical chain decomposition of hydrogen peroxide catalyzed with iron ions in aqueous solution leading to the formation of a singlet oxygen dimmer which in turn resulted in chemiluminescence that become intense in the presence of oxygen. The inhibition was accounted for by the decay of  $\text{OH}^*$  and  $\text{HO}_2^*$ .

Aldershof et al., (1997) showed that there was no difference in the decomposition rates of different types of commercially available hydrogen

peroxide solutions in spite of the differences in the types and amounts of the added proprietary stabilizers.

Lloyd et al., (1997) used both  $\text{H}_2\text{O}_2$  and water labeled with  $^{17}\text{O}$ , together with ESR spin trapping, to detect the formation of hydroxyl radical. The authors report that the hydroxyl radical was derived exclusively from  $\text{H}_2\text{O}_2$  and there was no exchange of  $\text{O}_2$  atoms between  $\text{H}_2\text{O}_2$  and the solvent water. The reaction with ordinary  $\text{H}_2\text{O}_2$  and  $^{17}\text{O}$  labeled water also showed that none of the  $\text{OH}^*$  was derived from water.

Scott et al., (1998) Used the spin trap compound  $\alpha$ -(4-Pyridyl-1-Oxide) – N-tert-butyl nitron (4-POBN), as a probe to establish the activity of Fenton derived hydroxyl radical. The rate of disappearance of the probe was used to analyze the system kinetics and oxidation efficiency. The authors observed that the reaction of hydrogen peroxide with hydroxyl radical was an appreciable sink for the hydroxyl radical, but the reaction did not contribute significantly to the depletion of hydrogen peroxide. Non-productive reactions involving hydrogen peroxide (those that did not contribute to the production of hydroxyl radicals) represented a significant source of overall reaction inefficiency.

Leonard et al., (1998) report that chelation of  $\text{Co(II)}$  by biological chelators such as glutathione altered its oxidation-reduction potential and makes  $\text{Co(II)}$  capable of generating  $\text{OH}^*$  via a  $\text{Co(II)}$  – mediated Fenton like reaction.

Nadtochenko and Kiwi., (1998) examined primary photochemical reactions in water solutions of ferric chloride complexes in the presence

and absence of hydrogen peroxide by laser photolysis using Xylidine as the pulse molecule. The Xylidine radical formed by the oxidation of Xylidine by  $\text{Cl}^*$  or  $\text{Cl}_2^*$  was found to decay within 2 minutes in a second order reaction. An increase in the oxidant concentration resulted in an increase in the concentration of  $\text{XYL}^+$ , indicating that hydrogen peroxide competes with  $\text{Cl}^-$  and  $\text{XYL}$  for the available  $\text{Cl}^*$  in solution.

Nadtochenko and Kiwi, (1998) observed a decrease in the photodegradation of Xylidine in the presence of  $\text{Cl}^-$  anion in comparison to sulfate or perchlorate ions. The photoactive iron complex intermediates that formed in the dark and not the organic intermediates were found responsible for  $\text{XYL}$  degradation after the initial induction period.

Kiwi et al., (2000) studied photo-assisted Fenton oxidation of Orange II, in the presence of chloride anion. The authors observed that the hydroxyl radical originated from photolysis of  $\text{Fe}(\text{OH})_2$  complexes while  $\text{Cl}_2$  radical was the product of photolysis of  $\text{FeCl}_2$  complexes. The rate of decolorization decreased with increase in  $\text{Cl}^-$  concentration.

William et al., (1996) reported that Fenton's reagent removed chlorinated organics more effectively than hydrogen peroxide alone. The optimum range was 2.5-4. Reaction rates appeared to be highest at the lowest peroxide to iron ratio.

Herera et al., (1998) observed that p-coumaric acid undergoes accelerated degradation via photo-assisted Fenton reactions. The authors report that the Fenton's reagent form precursor intermediates that are susceptible to degradation under light. Degradation experiments

performed via alternate light and dark cycles showed the importance of the dark precursor species.

Anthony and Emily, (1998) report that hydroxyl radical can be generated independently of Fe or other transition metal in reactions involving hydrogen peroxide and nitric oxide.

Ali et al., (1997) Identified lactic acid as an ingredient in *Chlorella T-1* which was found to enhance the formation of DMPO-OH which did not serve as a source for OH\* but accelerated the Fenton reaction.

Sawyer, (1997) established that the Fenton chemistry involves the formation of hydroperoxide (ROOH) adducts of reduced transition metals [Fe(II), Cu(I) and Co(II) ] via nucleophilic addition. These reactive intermediates react with excess catalyst to form  $L_xFe^{(III)}OH$  (R) or with excess ROOH to form  $O_2$ ,  $H_2O$  and ROH or with excess hydrocarbon (RH) to form ROH (Fenton chemistry) or with ambient dioxygen to form adducts  $[L_x[Fe^{(II)}- OOR, BH+]$

Alexei and Kiwi, (1997) reports the transient kinetics for the species observed on application of pulsed laser to Quinoline, Quinoline and  $Fe^{3+}$  and quinoline solutions in the presence of Fenton's reagent. The authors report the formation of intermediates having a transient lifetime of less than  $4\mu s$ . The intermediates were affected by reagent concentration, concentration of the oxidant, pH and energy of the laser pulse.

Alexei and Kiwi, (1997) studied and compared the degradation of Quinoline solutions in homogeneous Fenton like reactions and heterogeneous photocatalytic  $TiO_2$ -mediated degradation and found that

the heterogeneous photocatalytic degradation proceeds at a slower rate than the homogenous reactions. Quinoline degradation was possible both under light and dark conditions. Complex formation occurred during photodegradation with Fenton like reagents, such as  $\text{Cr}^{6+}$  or  $\text{Cu}^{2+}$  ions and combinations of  $\text{Cu}^{2+}$  and  $\text{Fe}^{3+}$  ions, in the presence of hydrogen peroxide.

Sara and Dan., (1999) report that radicals may be formed via reactions that do not involve the formation of either  $\text{OH}^*$  or  $\text{OR}^*$  radicals.

Yoon et al., (2001) investigated characteristics of the Fenton system using high concentrations of iron (1-10 mM). The authors found that high ferrous enhanced the production of hydroxyl radicals that led to faster consumption of hydrogen peroxide. The possible draw backs associated with the system is the scavenging of hydroxyl radical by ferrous ions, changes in the oxidation products due to oxygen depletion and precipitation of ferric ions.

Huling et al., (2001) studied the influence of peat on Fenton systems. Increased concentration of peat was found to enhance the production of hydroxyl radical. This was attributed to the ability of organic matter to reduce ferric to ferrous ions.

Tachiev et al., (2000) proposed a kinetic model for free iron catalyst assuming the formation of a reversible complex ( $\text{Fe} - \text{H}_2\text{O}_2$ ) followed by irreversible decomposition using the pseudo-steady-state hypothesis. The reaction was found first order at low hydrogen peroxide concentrations, while at high hydrogen peroxide concentrations the reaction was found to be zero order. The rate constants were determined by the initial rate

method. pH had a significant influence on the reaction. At low pH the ferrous iron was mostly uncomplexed and in the free form, while high pH ranges (6 - 9) resulted the formation of Fe(III) complexes. Fenton's reagent (free iron catalyst) had a significant level of activity only in pH range from 2 – 4, while the complexed iron catalysts were found to be effective in the pH range from 2 – 10.

Perez and Arias., (1999) observed that both chromium(VI) and copper(II) were efficient catalysts for the decomposition of hydrogen peroxide. However, when present jointly the two catalysts exert mutual inhibition effect on the catalytic activity of the other. The inhibition effect produced by chromium (VI) on the catalytic activity of Cu(II) was found to be more pronounced than that of Cu(II) on Cr(VI).

Kremer., (1999) observed the formation of a new intermediate, which was identified as  $[\text{FeOFe}]^{5+}$ . The existence of free radicals in the system was not found to be compatible with the data and proposed a new mechanism for the reaction involving  $\text{FeO}^{2+}$  as the key intermediate.

Pignatello et al., (1999) suggested the involvement of a high-valent oxo iron complex (ferryl) in addition to the hydroxyl radical in the oxidation of organic compounds. The authors observed that hydrogen peroxide formed a complex with iron,  $\text{Fe}(\text{O}_2\text{H})^{2+}$ , that absorbs in the visible region, which could be the precursor of the ferryl complex.

Lindsey and Tarr., (2000) observed that the hydroxyl radical formation increased linearly with hydrogen peroxide concentration.

Brillas et al., (1996) studied the mineralization of aniline in acidic solution using the electro-Fenton method.  $\text{OH}^{\bullet}$  was produced at the anode by the oxidation of water and the bulk solution via Fenton reaction between  $\text{Fe}^{2+}$  and the electro generated  $\text{H}_2\text{O}_2$ . The process was found to be highly efficient and the efficiency could be enhanced when irradiated with UV light ( $\lambda_{\text{max.}} = 360 \text{ nm}$ ).

Sanchez et al., (1996) investigated the oxidation of 2,4-D using ZnO as photo-catalyst in the presence of in-situ photogenerated Fenton reagent. The photo-degradation process was dependent on the mass of the semi-conductor and light intensity. The reaction was found independent of pH except at the point of zero charge of the semi-conductor. Results showed that the photo-degradation followed Langmuir-Hinshelwood kinetics and addition of small amounts of Fe(II) increased the rate of photo-degradation.

UV-enhanced oxidation of organic compounds in aqueous low-level mixed waters at the INEL(In. Mixed waste, Proc. Bienn. Symp., 3<sup>rd</sup> 1995, Ed.Moghissi A. Alan, Love Betty R., Blauvelt Richard. K. ,1995). studied the effectiveness of UV-enhanced oxidation of organic pollutants, which included Methylene chloride, Freon 113 and EDTA in water in bench-scale oxidation using photo-assisted Fenton. Results showed that photo-assisted Fenton system provided the best performance to oxidize organic compounds.

Specht et al., (1996) report that a combination of biological and chemical oxidation by the Fenton's reagent could be used to oxidize PAH in



water to yield biodegradable products. Zambrowski et al (1997) and Evelyn et al., (1997) have also reported similar observations.

Miller et al., (1996) studied the chemical and microbiological response of pendimethalin contaminated soils after treatment with Fenton's reagent. The authors observed that the efficiency of oxidation was highest for soils with low organic matter and neutralizing capacity, in accordance with the role of organic matter as a free radical scavenger and the optimum formation of the free radical at low pH. Before treatment with the Fenton's reagent, the Heterotrophic activity as measured by glucose mineralization decreased with increasing pendimethalin concentration indicating its inhibitory effect, however, this effect was removed after the Fenton's treatment. The oxidation products were found to be biologically amenable serving as substrates for subsequent microbial growth.

Lei et al., (1998) observed that effective degradation of polyvinyl alcohol was achieved by the application of photochemically enhanced Fenton Oxidation. Oxidation was effective when low iron(II) concentrations of approximately 1 equivalent of iron(II) per 20 PVA units was employed.

Fernando et al., (1998) studied the Fenton oxidation of three polynuclear aromatic hydrocarbons, fluorine, phenanthrene and acenaphthene. The variables studied were reactant concentration, pH and the presence of humic bicarbonate ions and substances. The results indicated that the hydroxyl radical generation was higher than those from other advanced oxidation systems involving  $O_3$ , UV radiation and  $H_2O_2$ .

The decreasing order of reactivity was reported as phenanthrene > fluorine > acenaphthene.

Ralf et al., (1999) studied the kinetics of light induced degradation of TNT and 16 other nitro aromatic compounds in aqueous  $\text{TiO}_2$  slurries and in homogeneous solutions containing Fenton reagent. Reaction rates of photo-Fenton reaction were found higher than that of  $\text{TiO}_2$ -mediated photocatalytic reactions. The rate of the reaction was found to be enhanced by the addition of potassium oxalate and depended on the kind and number of substituents attached to the aromatic ring. The nitro groups were found electron withdrawing with the reaction rate decreasing with an increase in the number of nitro groups attached to the aromatic ring.

Bin et al., (2001) investigated the degradation of nitroaromatics using four different AOP's. Of these Ozonation and Fenton oxidation was found to be the most effective.

Lee and Hosomi., (2001) compared the biodegradability between Benz(a)anthracene contaminated soil and Benz(a)anthracene contaminated soil after Fenton oxidation. When 98% of Benz(a)anthracene was degraded after 63 days following Fenton oxidation only 12% was found to be degraded in soil without Fenton oxidation indicating that Fenton oxidation enhanced biodegradability. Similar observations were made by the same authors on Benzo(a)pyrene.

Turan and Gurol., (2002) studied the oxidation of diethylene glycol by ozone and modified Fenton process in aqueous solution. They observed that both the oxidation processes could effectively oxidize high

concentrations of diethylene glycol (DEG). The stepwise addition of hydrogen peroxide and ferric salt resulted in a much higher removal than the one-time pulse addition of chemicals. Increased concentrations of hydrogen peroxide and ferrous sulphate enhanced the oxidation of diethylene glycol. Oxygen consumption per mole of DEG was found higher for Fenton oxidation than for ozone.

Lu et al., (1994) compared experiments using ferric ions instead of ferrous ion for catalytically oxidizing phenol-containing wastewater. The variables tried were concentration of hydrogen peroxide, ferric and initial pH. The results indicated that under acidic conditions the reduction of phenol, COD and TOC were excellent when using both  $\text{Fe}^{3+}$  and  $\text{Fe}^{2+}$  as catalysts, but at pH 7.0 the catalytic activity of both the ferric and ferrous ions was distinctly lower.

Lin et al., (2000) used Fenton oxidation in combination with Ultra sonic to remove 2-chlorophenol from wastewater. The combination was found to enhance the decomposition efficiency by decreasing the reaction time. More than 99% of 2-chlorophenol was decomposed and 86% was mineralized. The oxidation kinetics of 2-chlorophenol was found to be pseudo first order and the rate constants were found to increase with an increase in the concentration of the Fenton's reagent.

Kuo et al., (1998) studied the oxidation of 2,4-chlorophenol and 2,4,6-trichlorophenol in aqueous solution using the Photo-Fenton process. The oxidation was found to be first order. The study was conducted in two parts. The first part explored the treatment efficiency and reaction rate

expression. The second part identified the products intermediates and observed that some of the intermediates were more toxic than the primary compound.

Enric et al., (1998) studied the degradation of 4-Chlorophenol in acidic solution by different electrochemical methods involving  $H_2O_2$  electro-generation from an oxygen diffusion cathode. The authors found electro-Fenton and photoelectro-Fenton to be more efficient than peroxy coagulation.

Basu and Wei., (1998) studied the effect oxidant and catalyst in the Fenton's oxidation of 2,4,6-trichlorophenol. Progress of the reaction was monitored in terms of TCP removal, release of chloride ions from the organic structure, changes in pH and reductions in COD and TOC. The authors also studied the effects of various reaction parameters such as temperature, pH, oxidation state of the catalyst, mode of addition of oxidant to the reactor and the presence of dissolved oxygen. The optimum molar ratio of the oxidant to the substrate was found to be 5.5:1 and for that of the catalyst to the oxidant was 0.10:1. Rate of the reaction was found to increase with an increase in temperature from 15-35°C and the utilization of hydrogen peroxide could be enhanced by the addition in smaller increments. The optimum pH range was 2-3.5 and dissolved oxygen was found to accelerate the reaction rate.

Wang et al., (1999) compared several Fenton-related oxidative processes to isolate one that could effectively remove 2,4-dinitrophenol from industrial wastewater. The authors found that initially the Photo-

Fenton process gives the same oxidation ability as the Fenton process, however gradually the Photo-Fenton process begin to out-rank the other treatment options as irradiation stimulates the regeneration of ferrous ion, resulting in enhanced generation of hydroxyl radicals.

Gun et al., (1999) studied the effect of hydrogen peroxide concentration, p-chlorophenol and chloride level on the Fenton oxidation of p-chlorophenol. The authors observed that the optimum pH range was between 2 - 4. The process was a two-step process. A fast initial stage, which was found to be first order with the rate constants proportional to the initial levels of  $\text{Fe}^{2+}$  and  $\text{H}_2\text{O}_2$ . The slow step was primarily attributed to the depletion of  $\text{Fe}^{2+}$  caused by Fe-organic complex formation. The effect of chloride on oxidation was found to be pH dependent and increased with an increase in concentration.

Bier et al., (1999) reported that RDX could be oxidized using Fenton's reagent. The extent of transformation and mineralization was enhanced in the presence of UV irradiation.

Javier et al., (1999) Observed that the oxidation of 2,4,6-trichlorophenol followed pseudo first order kinetics.

Kang et al., (1999) applied Fenton's reagent to decolorize and degrade 2,4-dinitrophenol. The variables studied were concentration of ferrous ion, hydrogen peroxide and dissolved oxygen. At low dosages of ferrous ions and hydrogen peroxide, a linear increase in the initial removal rates of DNP and color is observed. High dosages of ferrous ions (>1mm) led to insignificant response of the initial removal rate of DNP, while that of

color was not affected and kept increasing constantly. Because of the non-selective feature of the hydroxyl radical, leveling off in the initial removal rates was observed at high hydrogen peroxide concentrations.

Lu., (2000) observed that the oxidation rate of 2-chlorophenol in a reaction where the decomposition of hydrogen peroxide was catalyzed by goethite increased with decreasing goethite particle size. The mechanism of oxidation was attributed to catalysis of ferrous ions and goethite surface.

Kwon et al., (1999) studied Fenton oxidation of p-chlorophenol and observed that the oxidation was a two-step process. An initial fast step that resulted in a significant oxidation within a few minutes followed by a slow step. The initial fast rate was found first order with respect of p-chlorophenol and its rate constant was proportional to the initial level of  $\text{Fe}^{2+}$  and hydrogen peroxide. The occurrence of the slow phase was attributed to the depletion of ferrous ions caused by the formation of Fe – organic complex. The extent of oxidation was limited by hydrogen peroxide.

Banerjee et al., (1995) showed that landfill leachate with an initial COD concentration of  $390 \text{ mg L}^{-1}$  could be reduced to below the discharge limit ( $35 \text{ mg L}^{-1}$ ) by using the Fenton's reagent or a combination of UV/ $\text{H}_2\text{O}_2$ /catalyst.

Kim et al., (1997) investigated the treatment of landfill leachate by a combination of the classical Fenton reaction with UV light (Photo-assisted Fenton reaction). The degradation rate was found to be influenced by the amount of hydrogen peroxide, Fe(II) added, pH value and radiation

intensity. The optimum conditions observed were  $1 \times 10^{-3}$  mole  $L^{-1}$  Fe(II), pH 3 and a molar ratio of COD:H<sub>2</sub>O<sub>2</sub> of 1:1.

Gau and Chang., (1996) instead of using the traditional Fenton method and ferric chloride coagulation, a 2-stage Fenton process accompanied by Fenton method with powdered activated carbon was studied. Molecular weight chromatography was used to evaluate the fraction of organic removal. The study indicated that a proper combination of the two stage Fenton process with activated carbon was found advantageous as Fenton coagulation could remove low molecular weight better than FeCl<sub>3</sub> with activated carbon efficiently adsorbing oxidation resistant organics.

Kim and Vogel, (1998) studied the degradation of landfill leachate by utilizing combinations of Fe(II)/H<sub>2</sub>O<sub>2</sub>/UVA and Fe(III) oxalate/H<sub>2</sub>O<sub>2</sub>/UVA. Degradation rates were found to be dependent on the concentrations of hydrogen peroxide, iron catalyst, pH and the concentration of dissolved oxygen. The Photo-Fenton process gave a higher COD reduction.

Choi et al., (1998) Showed that the Fenton's reagent could effectively treat landfill leachate and removed all humic material and over 99% of fulvic material.

Yoon et al., (1998) compared Fenton reaction with coagulation in removing landfill leachate organics. When both the processes were found effective in removing the organics a relation was observed with respect to the molecular weight of organic compounds. Coagulation removed 59-73% of organics with molecular weight greater than 500 and less than 18% for

compounds with molecular weight less than 500. Fenton process removed 72-89% of organics with molecular weight greater than 500 and less than 43% of organics with molecular weight less than 500. The efficiency of removal was higher for Fenton reaction.

Li et al., (1997) observed that Fenton's reagent effectively oxidized TNT in a soil slurry (1.5 wt/vol. Soil:H<sub>2</sub>O) containing 4300 mg TNT kg<sup>-1</sup>. The process was influenced by factors such as temperature, dissolved organic matter and clay mineralogy and was more efficient with the sequential addition of hydrogen peroxide rather than a single batch addition. In spite of both fulvic acid and humic acid capable of effectively reducing ferric to ferrous ions, the TNT mineralization rate was not greatly affected by either of them.

Peterson et al., (1997) combined Fenton oxidation and soil washing to remediate TNT contaminated soil to test whether it was possible to grow plants on the washed soil. Complete destruction of TNT in the wash solutions with .40% mineralization was achieved by Fenton oxidation. No significant reduction in germination or early seeding development was observed in *Festuca arundinacea* schreb. The study reported that an integrated treatment combining soil washing, Fenton oxidation and phytoremediation could be used for treating TNT contaminated sites.

Li et al., (1997) determined the potential of Fenton's reagent to remediate TNT contaminated in water, aqueous extracts of contaminated soil and soil-water slurries. The transformation and mineralization rates were evaluated in terms of the variables such as concentrations of Fe<sup>2+</sup>



and  $\text{H}_2\text{O}_2$ , solution pH, temperature and initial TNT concentration. The authors reported a marked influence of irradiation on mineralization with 40% mineralization occurring in the dark and subsequent exposure to light resulting in 90% mineralization. The primary mechanism of TNT oxidation was reported to be oxidation of the methyl group followed by decarboxylation (indicated by the formation of 2,4,6-trinitrobenzoic acid and 1,3,5-trinitrobenzene). Subsequent transformation involved the removal of nitro moiety with ring hydroxylation and cleavage (indicated by the formation of oxalic acid).

Rose and Peter., (1995) developed an efficient solar photocatalytic reactor to degrade chemical warfare agents and toxic byproducts in aqueous solutions and then compared its efficiency with that of the conventional  $\text{TiO}_2$  slurry photocatalysis. The study reported that the Photo-Fenton reaction (80% mineralization within 2 hours) was more efficient than the  $\text{TiO}_2$  mediated photocatalysis (No mineralization).

Li et al., (1998) studied UV - catalyzed Fenton oxidation of mono, di and tri Nitrotoluene in aqueous solution. The number and position of nitro substitutions was found to influence the oxidation rate. The UV – catalyzed Fenton oxidation mineralized more than 95% of TNT in aqueous extracts of contaminated soils.

Arienzo, (1999) used solid pyrite in place of ferrous sulphate to clean water contaminated with 2,4,6-trinitrotoluene. The study showed that unlike the classical Fenton reaction, an increased addition of hydrogen peroxide did not show an increase in the pseudo first order rate constant.

Compared to the classical Fenton reaction the modified Fenton was a slower process.

Kaiqun et al., (1999) compared Photo-Fenton oxidation (aided by visible light) of Malachite Green with the dark reaction. The authors report that visible light enhanced the generation of hydroxyl radical and Electron transfer from the excited dye by visible light into  $\text{Fe}^{3+}$  was a probable mechanism for the oxidation of Malachite Green.

Poulios and Aetopoulou., (1999) observed the disappearance of the dye to follow pseudo first order kinetics according to Langmuir-Hinshelwood model.

Barburinski and Helena., (1997) studied Fenton oxidation of an industrial wastewater producing maleic acid anhydride and observed that an increase in the concentration of both hydrogen peroxide and ferrous ions resulted in increased COD removal and caused no inhibition of microbial activity or disadvantageous changes in the structure of activated sludge flocs.

Oliveros et al., (1997) studied the oxidation of industrial wastewater containing toxic aromatic amines and observed that Fenton's reagent in the presence of UV/Vis irradiation was found to significantly enhance the degradation rates of xyldine.

Hornig et al., (1996) assessed the treatability of high strength wastewater from a Brewery plant using anaerobic and aerobic process accompanied by Fenton oxidation. The operating parameters were

$\text{COD}/\text{H}_2\text{O}_2 = 1$ ,  $\text{Fe}^{2+}/\text{H}_2\text{O}_2 = 2$  pH = 2-3 and reaction time 1h. The COD and suspended solids removal efficiency was 90 and 75% respectively.

Bowers et al., (1989) evaluated the possibility of using hydrogen peroxide as a pretreatment option prior to biological oxidation of refractory organic compounds viz., 2,4-dichlorophenol, dinitro-ortho-cresol and two unknown phenolic wastewaters of industrial origin. The treatment efficiency was evaluated by subjecting the residual by-products to toxicity (Microtox) tests. In all cases the by-products were an order of magnitude less toxic than the initial compounds. The hydrogen peroxide pretreatment process, coupled with biological treatment, resulted in substantial savings in the required oxidant dosage for further chemical oxidation.

Bauer and Fallman., (1997) compared the treatment efficiency of the various Advanced Oxidation Processes and observed that the Photo-Fenton system driven by sunlight was the most cost effective treatment process.

Kittis et al., (1999) studied the effectiveness of the Fenton's reagent as a pretreatment option for recalcitrant non-ionic surfactants. The authors found that Fenton's oxidation was an effective pretreatment option as it enhanced the biodegradability of both ethylene oxide and propylene glycol.

Yoo et al., (2001) evaluated the use of coagulation combined with Fenton oxidation to treat refractory organics in leachate. The authors observed a 9% increase in COD removal and a 50% reduction in the sludge to be disposed by recirculating the sludge generated from the Fenton oxidation to a coagulation process. Stepwise addition of the

reagents in Fenton oxidation increased the COD removal by 5% and a 25% reduction in chemical consumption.

Clarke et al., (1997) proposed a method that included providing a potential difference across the medium to cause the peroxide and the ferrous ions to migrate towards and react with the contaminants to form non-toxic byproducts of the organic contaminants.

Chien et al., (1998) observed that Fenton's reagent could completely mineralize soils contaminated with 2-methyl naphthalene, n-hexadecane and diesel fuel, provided enough hydrogen peroxide is added. The process was found effective at neutral pH.

Richard et al., (1999) studied the ability of iron containing minerals like hematite and magnetite to oxidize PCP in soil through a Fenton like oxidation. Magnetite catalyzed reactions provided the most efficient oxidation, however a decrease in oxidation efficiency was reported with time, attributed to the formation of an amorphous layer of iron oxide on the surface.

## Abstract

Fenton's reagent is very efficient in degrading almost any refractory organic substance. The list includes compounds like phenol (Smis, 1981), chlorophenols (Sedlak and Andren, 1991), municipal wastewater (Bishop et al., 1968) and printing and dyeing wastewater (Smis, 1983). Hydrogen peroxide and iron have been used to generate  $\text{OH}^*$  and oxidize undesirable contaminants in soils and aquifers (Watts et al., 1993; Ravi Kumar and Gural 1994; Yeh and Novak, 1995). Several investigators have reported that Fenton's oxidation can reduce effectively refractory organics, such as color and COD in synthetic textile wastewaters (Kuo, 1992; Gregor, 1994 and Solozhenko et al., 1995) and real textile wastewaters (Lin and Peng, 1995 a, b). Organic substances in the dye intermediate wastewater are often aromatic compounds substituted by some groups, such as  $-\text{NH}_2$ ,  $-\text{NO}_2$ ,  $-\text{SO}_3^-$  etc. They have strong toxicity to organisms. The biological processes cannot effectively degrade these substances and decolorize the wastewater (An Huren, Qian Yi. (1994). The  $\text{Fe}^{2+}$ - $\text{H}_2\text{O}_2$  treatment has been suggested as an alternative method for removing dyes from industrial effluent (Bigda et al., 1992; Moore et al., 1993 and Kuo, 1992). To compare their effects on specified target compounds it is therefore necessary to have data to predict the rates with which they react with such target compounds relative to the rate with which they are consumed or scavenged by the other compounds present.

The objective of this study was to investigate the oxidation kinetics of a few commercially available dyes by an Advanced Oxidation Process

(AOP) involving hydrogen peroxide and ferrous sulphate under ambient light and temperature conditions. The study involved preparation of a synthetic dye bath to simulate a conventional batch dyeing process. Monitoring the effluents for residual dye concentration tested the effectiveness of the Advanced Oxidation Process. Three operating variables namely concentration of hydrogen peroxide, ferrous sulphate and the dye concentration on the performance of Fenton Oxidation was investigated with an aim of determining their optimum conditions in the oxidation of the dyes. The study also involves kinetic aspects of the oxidation reaction and the kinetic rate coefficients based on the observed data derived from the batch experiments have been established.

### 3.3. Fenton Oxidation of Dyes

The objective of this study was to investigate the treatability of a strongly colored azo dye (C.I. Direct Brown 3B, Direct Catachine Brown), a reactive dye (C.I. Yellow-6, Reactive Yellow), a basic dye (C.I. Basic blue 9, Methylene Blue) and an Acid dye (C.I. Acid Orange AO – 9, Acid Orange) by an Advanced Oxidation Process (AOP) involving Fenton's reagent under ambient light and temperature conditions. Monitoring the effluents for residual dye concentration tested the effectiveness of Fenton's oxidation.

Azo dyes can also be significantly decolorized by the reduction of its azo linkages. However, such a process would lead to the formation of aromatic amines which are generally not considered as environmentally safe end products, as they are suspect carcinogens and mutagens. This study was conducted to show that the Fenton oxidation leads to the mineralization of the azo dyes without the formation of toxic amines.

Reactive dyes are used for dyeing cotton. The strong nitrogen bond and ring structure of these dyes makes biological oxidation difficult and at times incomplete.

Basic dyes have been used extensively for dyeing silk and cellulose acetate. However, these dyes have poor fastness leading to their gradual decline. Leather and paper still continue to be dyed with basic dyes. The first basic dye to be synthesized was Mauve, by Perkin in 1856. Since then many new dye structures have been synthesized. In addition to mauve

there is also a whole range of other synthetic basic dyes such as fuchsine, methyl violet, aniline blue etc. available to dye natural vegetable products as straw, raffia and jute. The use of Basic dyes gained advantage during the mid-1950 with the synthetic fiber material polyacrylonitrile hitting the market. The advantage of this fiber was that the positively charged colored ion of the basic dye i.e., the cation, was attracted strongly by the negatively charged ions in the acrylic fiber and this combination had unusually good light and wash fastness.

The name "Acid dye" is derived from the dyeing process. These dyes are applied to wool, silk and polyamides in the presence of an organic or inorganic acid and hence are called acid dyes. The term acid dye denotes a large group of anionic dyes with relatively low molecular weights that carry from one to three sulfonic acid groups. Chemically, acid dyes belong to such various subclasses as nitro, nitroso, monoazo, diazo, triphenyl methane, xanthene, azine, quinoline, ketone-imine and anthraquinone. When dissolved in water, they produce colored anions ( $\text{RSO}_3^-$ ) and colorless sodium cations ( $\text{Na}^+$ ). On the basis of their application and wet-fastness properties, acid dyes can be divided into three groups namely leveling dyes, milling dyes and super milling dyes. Leveling dyes are usually applied either to wool or to nylon. Leveling dyes for wool have low molecular weights and usually require highly acidic dyebath for good exhaustion. Leveling dyes for nylon are of high molecular weight and they are applied at a neutral or weakly acidic pH. Milling dyes on the other hand has a higher molecular weight than leveling dyes. These dyes are



applied from weakly acidic liquor in the pH range of 5.2 to 6.2; and they are usually applied with acetic acid. Super milling dyes are applied from neutral solutions. The application of such dyes requires utmost care as they have comparatively high molecular weights. They are often referred to as fast acid dyes or acid milling types because originally they were used in wool fabrics, which were to be subjected to severe wet treatments in processing (milling) to improve the fabric density.

The study is divided into two parts:

- Part 1: Deals with determining the optimum concentration of ferrous sulphate and hydrogen peroxide required to decolorize the dye to over two half lives and to optimize the operating conditions for maximum color removal.
- Part 2: Investigates the effect of process variables such as the concentration of ferrous sulphate, hydrogen peroxide and the dye, to elucidate the reaction mechanism behind the Fenton oxidation of the dye.

The results obtained have been interpreted using the initial rate method.

### 3.3.1. Materials and methods

#### (i) Reagents and supplies

The dyes whose structure and other related features are shown in figures 3.1 to 3.4 were obtained from M/s. Dhaval Dye Chem., Mumbai, India. This dye is chosen for the study as it happens to be the most widely used dye among the class of Direct dyes finding applications in the textile industry where it is used to dye cotton and also in the coir dyeing units of the Alappuzha district, in Kerala, India. The commercially available dye samples were used for the study with out any further purification.

Analytical grade Hydrogen peroxide used in the experiments obtained from Qualigens (India) was 30% (W/W).

Ferrous sulphate heptahydrate (99.5% purity) from Merck (India) was used for the study.

The strength of both hydrogen peroxide and ferrous sulphate was determined every day by permagnometry prior to starting the experiment.

Fenton's reagent was prepared by the sequential addition of ferrous sulphate and hydrogen peroxide.

Reagent grade hydrochloric acid and sodium hydroxide was used for pH adjustments. Conventionally Fenton Oxidation is carried out in sulphuric acid medium, however, for our experiments hydrochloric acid is used as solar salts are in most cases widely used in the dye bath.

#### (ii) Instruments and experimental set up

Optical absorption spectra of the dye in dilute solutions were recorded using a Varian UV/Vis. Cary – 50 single beam spectrophotometer

and  $\lambda_{\text{max}}$  of the dye was determined. This was followed by determining the residual dye concentration in the reaction mixture using a 1 mm quartz cell against a calibration diagram.

All observations have been drawn from well-mixed batch experiments carried out in 1L glass beakers in a multiple spindle constant speed stirrer rotating at 75 rpm.

pH measurements have been made using a Systronics pH meter.

### 3.3.2. Experimental Procedure

UV-Vis spectrum of the dye in aqueous medium was recorded and absorption maximum of the dye in the visible region was identified. A calibration curve of the dye was prepared at this wavelength, thereby; the decrease in optical density could be directly related to the decrease in dye concentration. All experiments were carried out at dye concentrations where the absorbance values at the respective  $\lambda_{\text{max}}$  of the dye ranged between 0.2 and 3 absorbance units.

Stock solution of the dye was prepared by weighing out appropriate amounts of the dye in distilled water. The solution was then heated to near boiling, which was then cooled and filtered. Working standards and calibration curve for the dye was prepared from such solutions.

In typical experiment aliquots of the stock dye solution was mixed with appropriate concentration of ferrous sulphate. pH of the reaction mixture was adjusted to  $2 \pm 0.1$ . The reaction was initiated by the addition of hydrogen peroxide to the reaction mixture followed by stirring (75 rpm).

Test samples were withdrawn at regular time intervals and the residual dye concentration was determined through comparison with the calibration diagram.

Preliminary runs were carried out to arrive at a minimum workable concentration of ferrous sulphate and hydrogen peroxide. The concentrations were chosen in such a manner that the reaction proceed at a rate that could be monitored by spectrophotometry. A ferrous sulphate to hydrogen peroxide mole ratio of 1:15 was found ideal to monitor the reaction. Hence, in all preliminary tests the mole ratio has been maintained at 1:15. From these preliminary experiments the minimum concentration of ferrous sulphate and hydrogen peroxide to follow the reaction to at least three half-lives was determined. In subsequent experiments the influence of hydrogen peroxide was determined by fixing the concentration of ferrous sulphate found optimum through preliminary tests for varied concentrations of hydrogen peroxide and for a fixed concentration of the dye. The criterion behind fixing the dye concentration was half the maximum concentration of the dye at which the  $\lambda_{\max}$  gave an absorbance value of less than 3 absorbance units. From this experiment the minimum concentration of hydrogen peroxide to take the reaction to over three half-lives was chosen as the optimum. Fixing the hydrogen peroxide concentration at this obtained optimum for varied concentrations of ferrous sulphate established the optimum concentration of ferrous sulphate which was again the minimum concentration required to take the reaction to over three half lives.

Fixing both hydrogen peroxide and ferrous sulphate concentrations at the obtained optimum for varying dye concentrations established the influence of dye on Fenton oxidation.

There are several reports, which suggests that the optimum pH for Fenton's oxidation is around 3 (Barbeni et al., 1987). In our experiments it is observed that even at pH 3, high ferrous sulphate concentrations could result in precipitation of ferric hydroxide. Since, the reaction losses its efficiency during the oxidation of ferrous to ferric ions and there is a shift from the classical Fenton mechanism ( $\text{Fe}^{2+}$ -  $\text{H}_2\text{O}_2$  system) to Fenton-like mechanism ( $\text{Fe}^{3+}$  -  $\text{H}_2\text{O}_2$  system) it was considered ideal to carry out all experiments at pH 2. At this pH no precipitate formation was observed even when moderately high ferrous sulphate concentrations was employed. Ince and Tezcanli (1999) report that the rate of colour degradation and total colour removed at pH 2 and 3 were found to be nearly the same ( $k=0.16 \text{ min}^{-1}$  and  $k=0.15 \text{ min}^{-1}$  estimated by regression analysis using the data of the first ten minutes of treatment; where degradation kinetics was linear, and the percentage decolorization was 99% and 98%). All the experiments have been conducted at pH 2.

### 3.4. Results and Discussion

3.4.1. Molecular structures and other related features of various dyes used in the study are shown in figures 3.1 to 3.4.

(i) Molecular structure of Catachine brown is shown in figure 3.1.

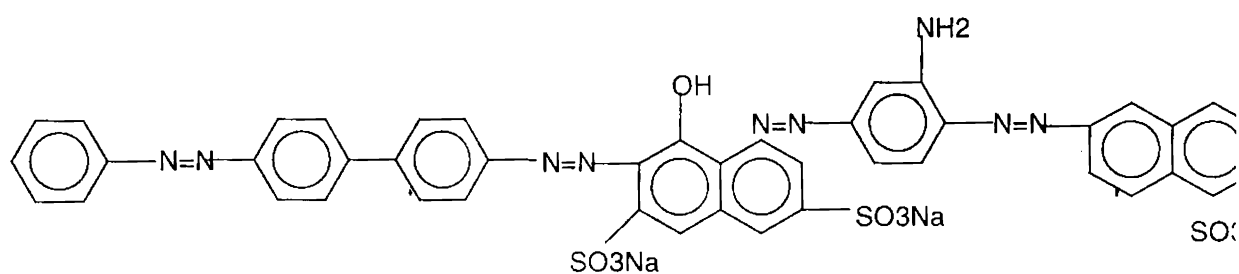


Figure 3.1. Molecular structure of C.I. Direct Brown 3B

C.I. General name:	C.I. Direct Brown 3B
C.I. Constitution number:	35520
Commercial Name:	Catachine Brown
Application class:	Direct
Chemical class:	Tetra azo

(ii) The molecular structure of Reactive Yellow is shown in figure 3.2.

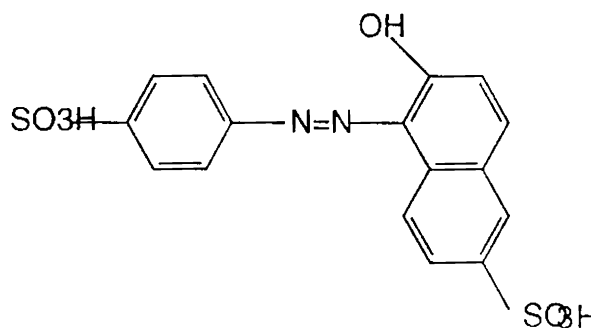


Figure 3.2. Molecular structure of Reactive Yellow

C.I. Name:	Yellow-6
C.I. No:	15985
Commercial Name:	Reactive Yellow
Application class:	Reactive
Chemical Class:	Azo

(iii) The molecular structure of Methylene Blue is shown in figure 3.3.

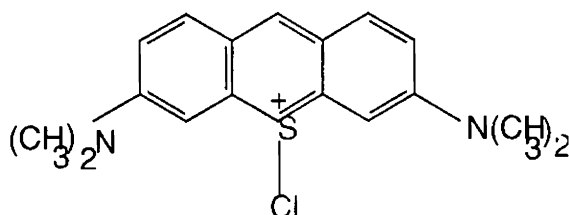


Figure 3.3 Molecular structure of Methylene Blue

C.I. Generic name Basic blue 9

C.I. Constitution No. 52015

Commercial name: Methylene Blue

Classification based on mode of application: Basic

Classification based on chemical structure: Thiazine dye.

(iv) The molecular structure of Acid Orange is shown in figure 3.4

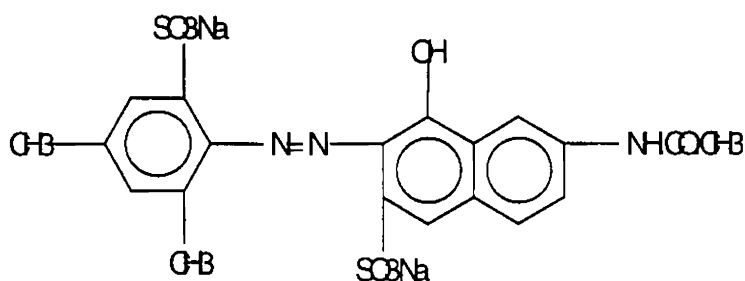


Figure 3.4. Molecular structure of Acid Orange

C.I. General name: C.I. Acid Orange AO - 9

C.I. Constitution number 17925

Commercial Name: Acid Orange

Application class: Acid

Chemical class: Mono azo

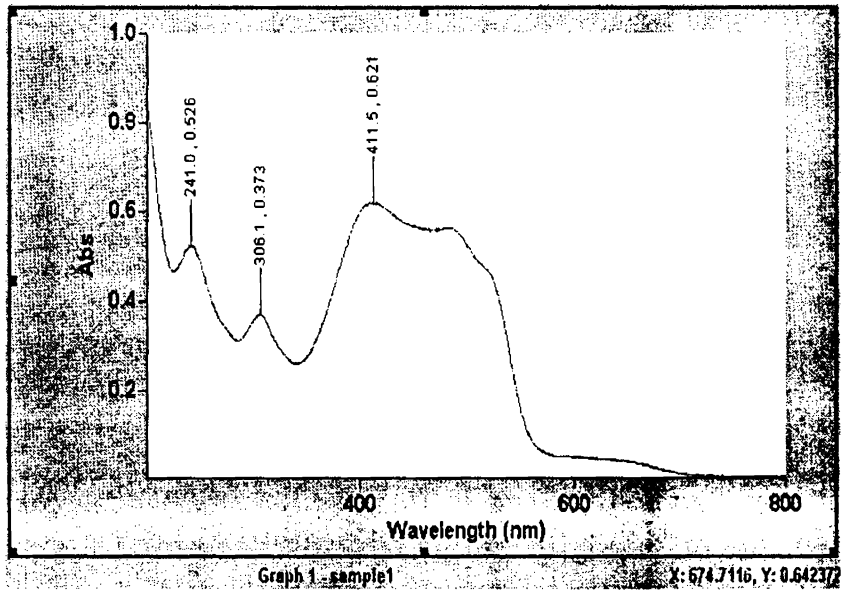


Figure 3.5  
 UV-Vis absorption spectrum of Direct Catachine Brown (DCB) in water.  
 Concentration of the dye 100 mg/L, path length 10 mm.

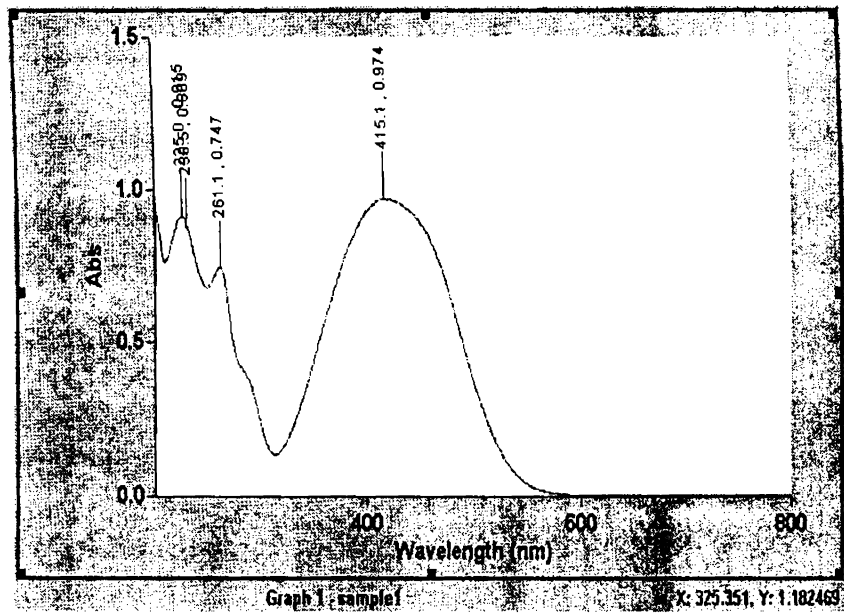


Figure 3.6  
 UV-Vis absorption spectrum of Reactive Yellow (RY) in water.  
 Concentration of the dye 50 mg/L, path length 10 mm.



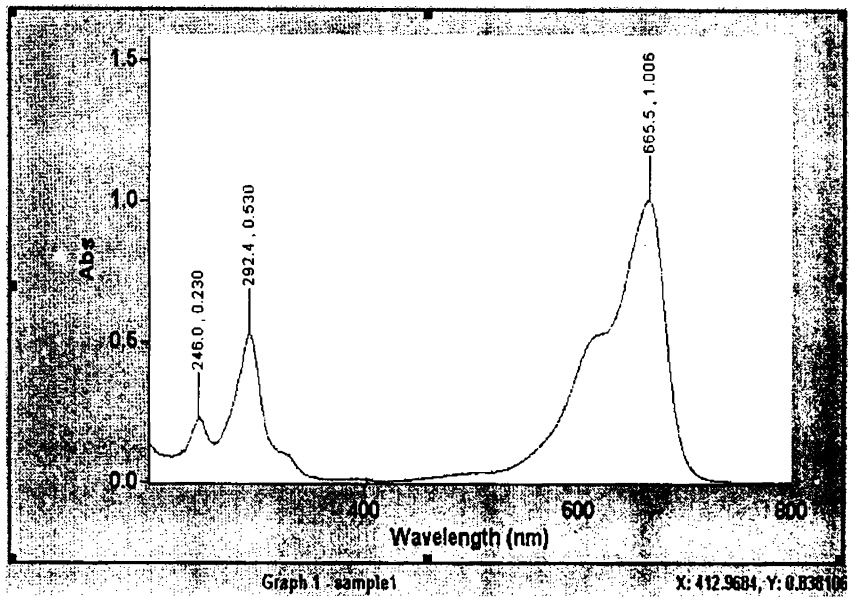


Fig. 3.7.  
 UV-Vis absorption spectrum of Methylene Blue (MB) in water.  
 Concentration of the dye 10 mg/L, path length 10 mm.

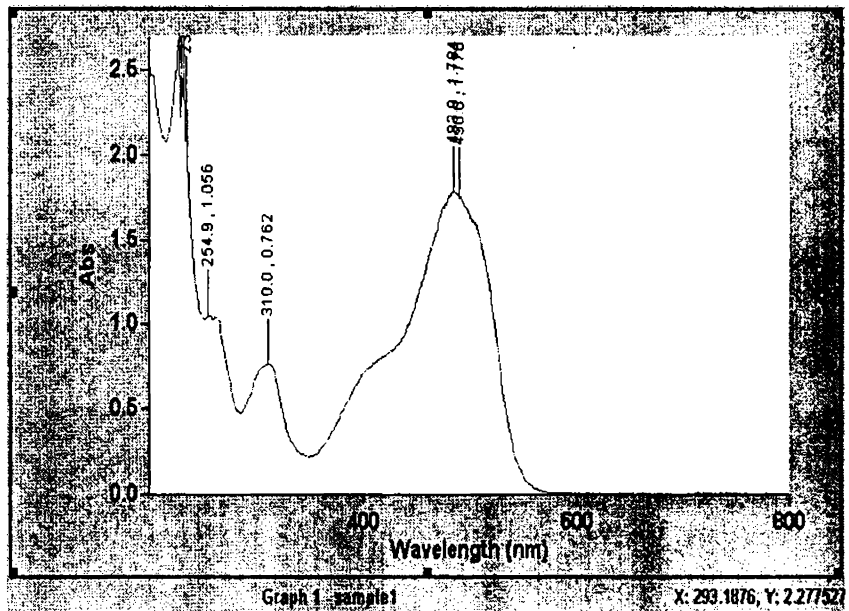


Fig. 3.8  
 UV-Vis absorption spectrum of Acid Orange (AO) in water.  
 Concentration of the dye 50 mg/L, path length 10 mm.

3.4.2. UV-Vis spectrum of the different dyes studied is shown in figures 3.5 to 3.8.

(i) Two main peaks characterize the absorption spectrum of an acidified solution of Direct Catachine Brown, as shown in figure 3.5. One in the visible range ( $\lambda_{\text{max.}} = 411.5 \text{ nm}$ , Abs.= 0.621) and another in the UV region ( $\lambda_{\text{max.}} = 241 \text{ nm}$ , Abs.= 0.526). The visible band is due to the long conjugated  $\pi$  system of aromatic rings connected by the two azo groups, whereas the UV band at 241 nm is characteristic of the two adjacent rings (Silverstein et al., 1991).

(ii) The absorption spectrum of the acidified solution of Reactive Yellow is characterized by a single peak in the visible region with wavelength of maximum absorption at 415 nm ( $\lambda_{\text{max}} = 415 \text{ nm}$ , Abs.= 0.974) as shown in figure 3.6.

(iii) Absorption spectrum of an aqueous solution of Methylene Blue at pH 2 is shown in figure 3.7. The spectrum is characterized by a single peak in the visible region with the wavelength of maximum absorption at 665.5 nm ( $\lambda_{\text{max}} = 665.5 \text{ nm}$ , Abs.= 1.006).

(iv) The absorption spectrum of an aqueous solution of Acid Orange at pH 2 is given in figure 3.8 indicates a single peak in the visible region ( $\lambda_{\text{max}} = 483.9 \text{ nm}$ , and Abs. = 1.784).

3.4.3. Calibration curves for all the dyes used in the study is shown in figures 3.9 to 3.12.

Calibration curve for Direct Catachine Brown was prepared at 411.5 nm. The dye solution obeys Beer-Lambert's law in the concentration range from 0 to 400 mg L<sup>-1</sup> and the calibration curve is shown in figure 3.9. Concentration of the dye chosen for the experiments covered the entire range up to which the dye obeyed Beer-Lambert's law. The residual dye concentration in the samples drawn was determined by comparison with the calibration curve.

A calibration curve for Reactive Yellow was prepared at 415 nm. The dye solution obeyed Beer-Lambert's law over the concentration range from 0 to 150 mg L<sup>-1</sup> and the calibration curve is shown in figure 3.10. Residual dye concentration was determined by comparison with the calibration curve.

Calibration curve for Methylene Blue was prepared at a wavelength of 665.5 nm. The dye solution obeys Beer-Lambert's law in the concentration range from 0 to 20 mg L<sup>-1</sup>. The calibration curve is shown in figure 3.11. The residual dye concentration in samples was determined by comparison with the calibration curve.

Calibration curve for Acid Orange was prepared at a wavelength of 483.9 nm and is shown in figure 3.12. The dye solution obeys Beer-Lambert's law in the concentration range from 0 to 100 mg L<sup>-1</sup>. Concentrations of the dye chosen for the experiments covered the range up to which the dye obeyed Beer-Lambert's law.

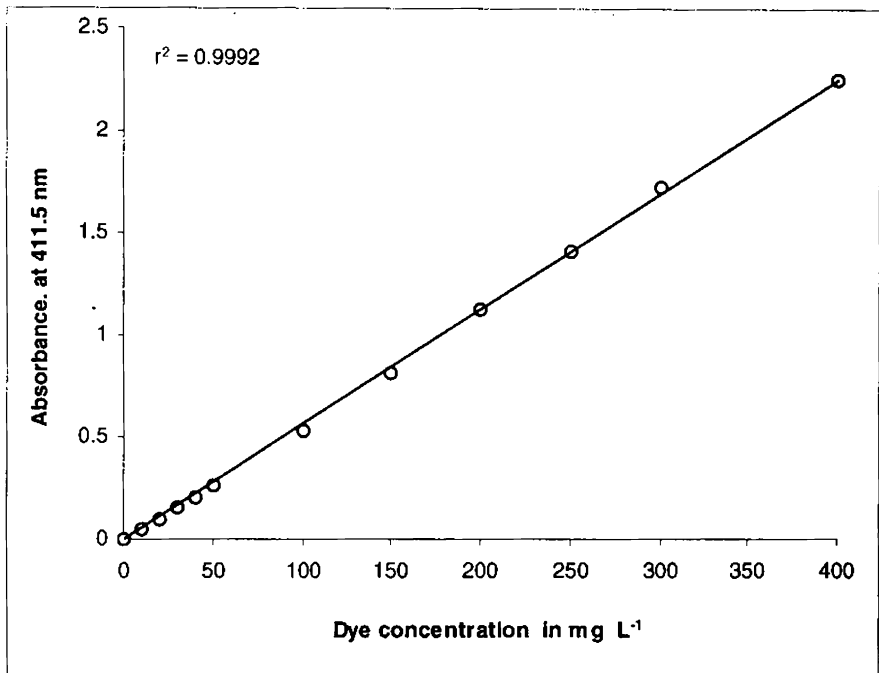


Figure 3.9  
Calibration curve according to Beer Lambert's law for Direct Catachine Brown (DCB)  
(Conc. range 0 to 400 mg L<sup>-1</sup>), path length 10 mm, analytical wavelength 411.5 nm

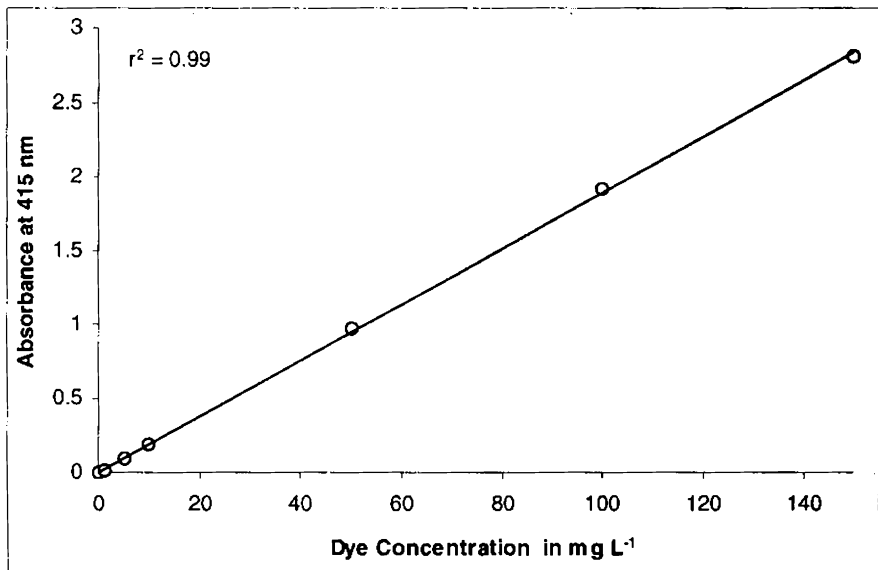


Figure 3.10  
Calibration curve according to Beer Lambert's law for Reactive Yellow (RY)  
(Conc. range 0 to 150 mg L<sup>-1</sup>), path length 10 mm, analytical wavelength 415 nm

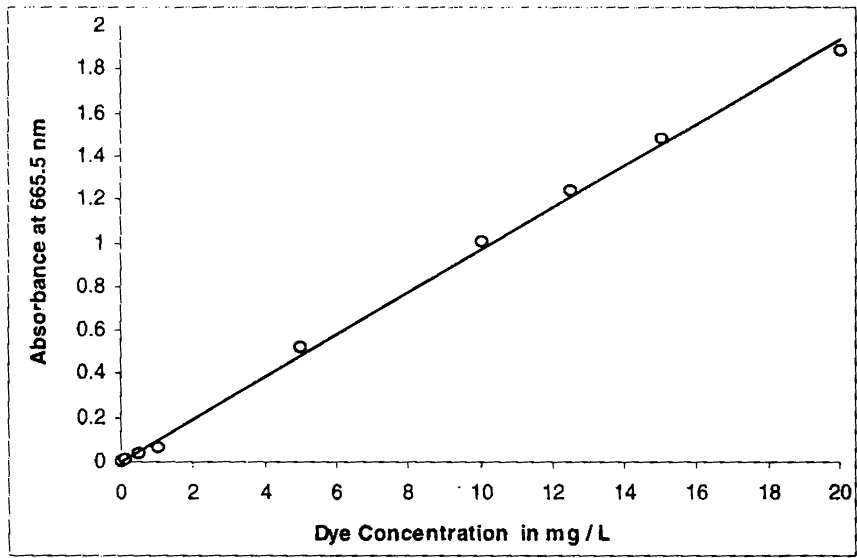


Figure 3.11  
Calibration curve according to Beer Lambert's law for Methylene Blue (MB)  
(Conc. range 0 to 20 mg L<sup>-1</sup>), path length 10 mm, analytical wavelength 665.5 nm ( $r^2 = 0.99$ )

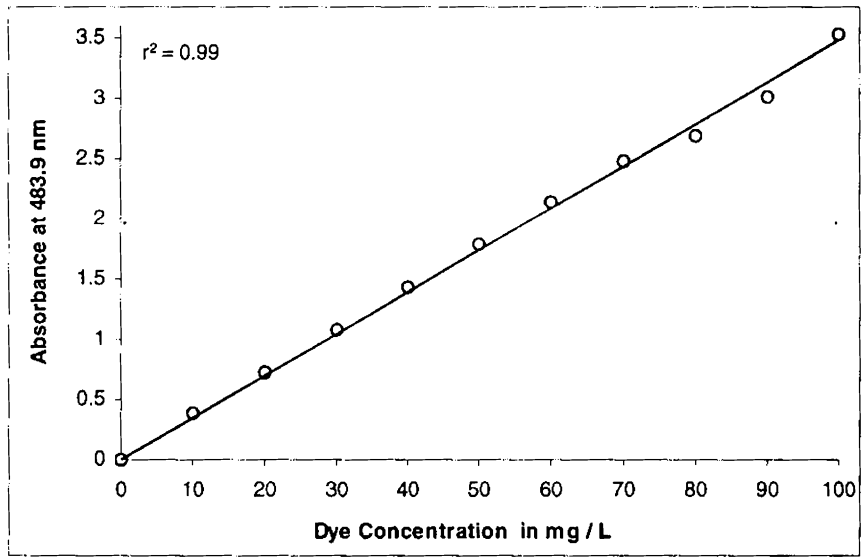


Figure 3.12  
Calibration curve according to Beer Lambert's law for Acid Orange (AO)  
(Conc. range 0 to 100 mg L<sup>-1</sup>), path length 10 mm, analytical wavelength 483.9 nm

### 3.5. Optimization studies

#### 3.5.1. Optimization of hydrogen peroxide

To define the influence of hydrogen peroxide on the oxidation of Catachine Brown, a series of experiments were carried out in which the concentration of hydrogen peroxide exceeded the dye concentration ( $150 \text{ mg L}^{-1}$ ). The extent of oxidation was monitored by following the decrease in absorbance at  $411.5 \text{ nm}$  as a function of time. The concentration of hydrogen peroxide was varied according to its mole ratio with respect to ferrous sulphate. The mole ratios ranged from 1:15 to 1:90. Figure 3.13 shows the results of a typical experiment carried out to study the influence of hydrogen peroxide on the kinetics of Fenton oxidation of the dye.

As can be seen from figure 3.13, there is an increase in oxidation of the dye with an increase in hydrogen peroxide concentration. However, there is an optimum concentration ( $367 \text{ mg L}^{-1}$ ) beyond which a further increase in hydrogen peroxide concentration did not result in any significant increase in oxidation of the dye.

In the case of Reactive Yellow, the effect of hydrogen peroxide on Fenton's oxidation was studied by fixing concentration of the dye at  $75 \text{ mg L}^{-1}$  and ferrous sulphate at  $60 \text{ mg L}^{-1}$  over a range of hydrogen peroxide concentrations. The extent of oxidation was monitored by following decrease in absorbance at  $415 \text{ nm}$  as a function of time. The results are shown in figure 3.14.

The general inference drawn is that there is a definite increase in the rate of the reaction with an increase in concentration of hydrogen peroxide.

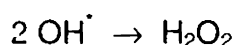
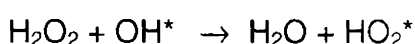


This increase continues only up to an optimum concentration above which a further increase in hydrogen peroxide concentration does not significantly enhance the oxidation. At low hydrogen peroxide concentrations (above a critical minimum) the reaction followed zero order kinetics (indicated by a linear decrease in dye concentration with time). This could be because the concentration of hydroxyl radicals produced is proportional to the concentration of both hydrogen peroxide and ferrous sulphate. At low concentrations of hydrogen peroxide the concentration of hydroxyl radicals produced is also low. The excess of ferrous ions present scavenges the hydroxyl radical leading to formation of hydroperoxyl radical. Being of lower reactivity than the hydroxyl radical the hydroperoxyl radical probably participates in the oxidation through an extremely slow step, which is represented by zero order kinetics.

The optimum concentration of hydrogen peroxide required to oxidize Reactive Yellow at a concentration of  $75 \text{ mg L}^{-1}$  is fixed at  $110 \text{ mg L}^{-1}$ , as a further increase did not show any significant influence on oxidation of the dye.

The effect of hydrogen peroxide on Fenton oxidation of Methylene Blue has been studied by fixing the dye concentration at  $10 \text{ mg L}^{-1}$ , ferrous sulphate at  $35 \text{ mg L}^{-1}$  and for varying concentrations of hydrogen peroxide. The extent of oxidation was monitored by following the decrease in absorbance at  $665.5 \text{ nm}$  as a function of time. Preliminary experiments indicated that the optimum concentration of hydrogen peroxide was observed at around  $65 \text{ mg L}^{-1}$ , the concentration of hydrogen peroxide was

varied in such a manner that there were two concentrations below the optimum one concentration close to optimum and two concentrations above optimum. The results are depicted in figure 3.15. The figure indicates that up to an optimum hydrogen peroxide concentration there is an increase in the amount of dye oxidized with increase in concentration of hydrogen peroxide. However, for a further increase in the hydrogen peroxide concentration above optimum the amount of dye removed tends to level off, before recording a decrease. This behavior can be explained because an increase in the hydrogen peroxide concentration would result in the generation of hydroxyl radicals, which would in turn lead to oxidation of the dye. From figure 3.15, It is observed that this phenomenon continues up to a hydrogen peroxide concentration of  $60 \text{ mg L}^{-1}$ ; probably up to which the ratio of ferrous sulphate to hydrogen peroxide to generate hydroxyl radicals are in balance. For a further increase in hydrogen peroxide concentration, the ferrous ions tend to become limiting. This leads to an excessive build up of hydroxyl radicals, which associate between them and get scavenged to form hydroperoxyl radicals ( $\text{HO}_2^*$ ), having lower reactivity. The possible reaction involved is shown in below



Liao et al. (1999) used photo-Fenton oxidation for the simultaneous removal of COD and color from dye wastewater. The authors observe that an increased concentration of hydrogen peroxide does not necessarily mean increased removal rates of COD and color. Fig. 3.15. shows that the

optimum concentration of hydrogen peroxide to oxidize Methylene Blue at a concentration of  $10 \text{ mg L}^{-1}$  is  $60 \text{ mg L}^{-1}$ .

The effect of hydrogen peroxide on the Fenton oxidation of Acid Orange was studied by fixing both the dye (at  $50 \text{ mg L}^{-1}$ ) as well as ferrous sulphate concentration (at  $40 \text{ mg L}^{-1}$ ) for varying concentrations of hydrogen peroxide. The extent of oxidation was monitored by following the decrease in absorbance at  $483.9 \text{ nm}$ , as a function of time. The concentration of hydrogen peroxide was varied in such a manner that there were two concentrations below the optimum (obtained from preliminary experiments), one concentration at the optimum and two concentrations above optimum. Results of a typical experiment to highlight the influence of hydrogen peroxide are shown in figure 3.16.

Results of the study indicate that, oxidation of the dye could be enhanced by increasing the concentration of hydrogen peroxide. However, there exists an optimum beyond which a further increase does not significantly enhance the oxidation. Fig. 3.16 indicates that the optimum hydrogen peroxide concentration is  $91.7 \text{ mg L}^{-1}$ .

The results indicate that by increasing the concentration of hydrogen peroxide an increase in oxidation of the dye could be achieved at a fixed concentration of ferrous sulphate. Experiments were carried out to find if oxidation of the dye could be enhanced even if one of the reagents were held at low concentrations with the other in excess. The results indicated that an increased oxidation of the dye occurred even for a lower concentration of ferrous sulphate provided the concentration of hydrogen

peroxide was raised. Similarly, a lower concentration of hydrogen peroxide could also produce the same effect provided the concentration of ferrous sulphate is increased. These results suggest the flexibility of Fenton oxidation. Thus, effect of these two reagents was found complementary. However, an increase in the hydrogen peroxide concentration above a particular optimum did not significantly enhance the oxidation of the dye. On the other hand elevated hydrogen peroxide concentration could decrease the amount of dye oxidized. This means that although the formation of hydroxyl radical propagates according to the reaction proposed by Haber and Weiss (1934)



The generation of the hydroxyl radical does not follow the stoichiometry suggested Haber and Weiss (1934). After initiation of the reaction the hydroxyl radical generation propagates through a free radical mechanism. An increase in hydrogen peroxide concentration initially increases the oxidation of the dye at lower hydrogen peroxide concentrations. Further increase in its concentration above an optimum adversely affected the reaction. This observation clearly indicates that at higher hydrogen peroxide concentrations a non-productive reaction that leads to scavenging of hydroxyl radical occurs. The results indicate a decrease in the amount of dye decolorized. Similar observations of on decrease in decolorization of the dye at increased concentrations of

hydrogen peroxide were reported. (Kang et al., 2002 and Solozenko et al.1995).

Sychev and Isak (1995), in studies on the mechanisms of the homogeneous catalysis of the activation of  $O_2$  and  $H_2O_2$  and the oxidation of organic substrates report that higher peroxide concentrations can also be detrimental to the degradation kinetics since after the initiation step the propagation step would be hindered by an excess hydrogen peroxide acting as a scavenger of the hydroxyl radical.

An explanation of this phenomenon has been attempted in the second part of this study that deals with the elucidation of the reaction mechanism.

The general inference drawn is that there is a definite increase in the rate of the reaction with an increase in concentration of hydrogen peroxide. This increase continues only up to an optimum concentration above which a further increase in hydrogen peroxide concentration does not significantly enhance the oxidation. At low hydrogen peroxide concentrations (above a critical minimum) the reaction followed zero order kinetics (indicated by a linear decrease in dye concentration with time). This could be because the concentration of hydroxyl radicals produced is proportional to the concentration of both hydrogen peroxide and ferrous sulphate. At low concentrations of hydrogen peroxide the concentration of hydroxyl radicals produced is also low. The excess of ferrous ions present scavenges the hydroxyl radical leading to formation of hydroperoxyl radical. Being of lower reactivity than the hydroxyl radical the hydroperoxyl radical probably

participates in the oxidation through an extremely slow step, which is represented by zero order kinetics.

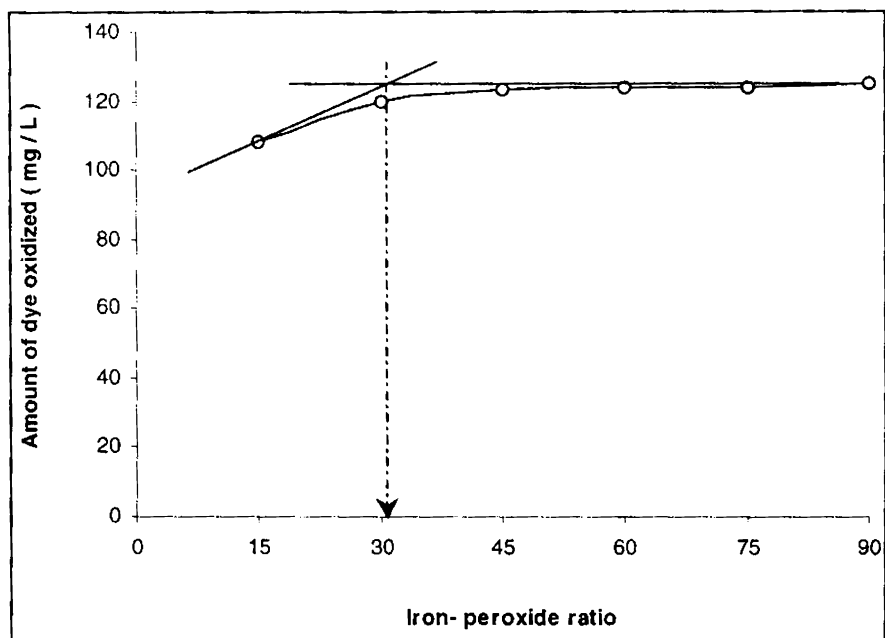


Figure 3.13

Influence of mole ratio of  $\text{Fe}^{2+}$  to  $\text{H}_2\text{O}_2$  on the oxidation of Direct Catachine Brown (DCB)  
 $[\text{FeSO}_4] = 100 \text{ mg L}^{-1}$ ,  $[\text{DCB}] = 150 \text{ mg L}^{-1}$ , pH 2, vol. 1L, stirring rate 75 rpm,  
 $[\text{H}_2\text{O}_2]$  varied 183.5, 367, 550, 735, 917.5 and  $1101 \text{ mg L}^{-1}$ .

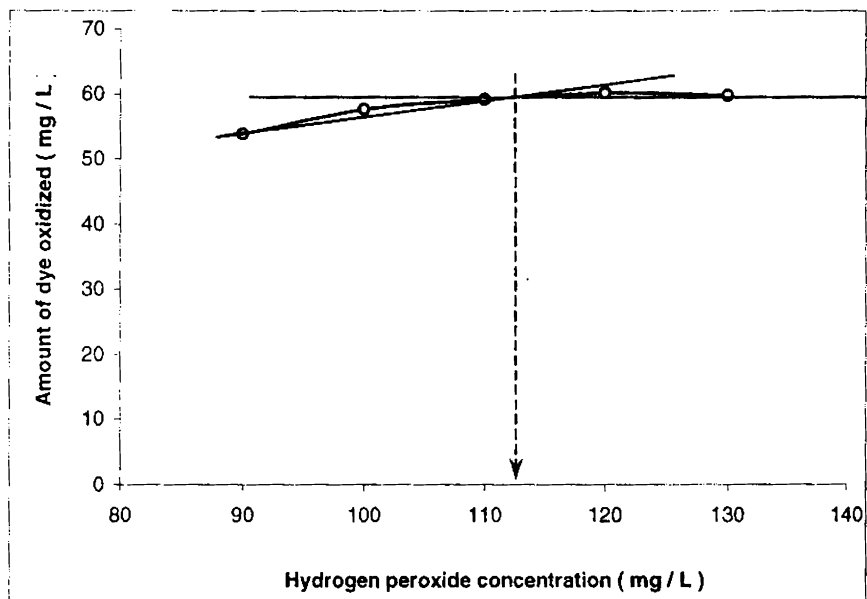


Figure 3.14  
Influence of  $\text{H}_2\text{O}_2$  on the oxidation of Reactive Yellow (RY)  
[ $\text{FeSO}_4$ ] =  $60 \text{ mg L}^{-1}$ , [RY] =  $75 \text{ mg L}^{-1}$ , pH 2, vol. 1L, stirring rate 75 rpm,  
[ $\text{H}_2\text{O}_2$ ] varied 90, 100, 110, 120 and 130  $\text{mg L}^{-1}$ .



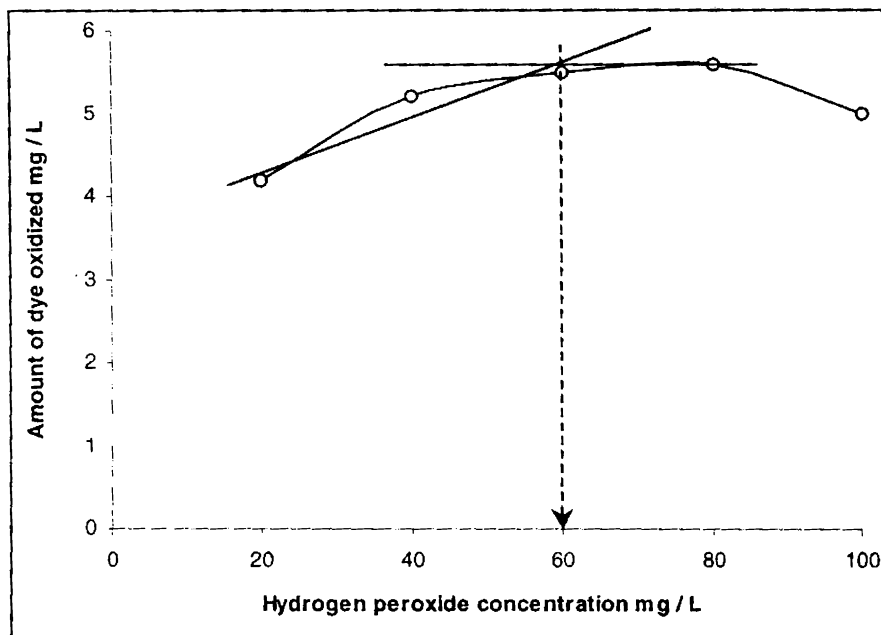


Figure 3.15

Influence of H<sub>2</sub>O<sub>2</sub> on the oxidation of Methylene Blue (MB)

[FeSO<sub>4</sub>] = 35 mg L<sup>-1</sup>, [MB] = 10 mg L<sup>-1</sup>, pH 2, vol. 1L, stirring rate 75 rpm,

[H<sub>2</sub>O<sub>2</sub>] varied 20, 40, 60, 80 and 100 mg L<sup>-1</sup>.

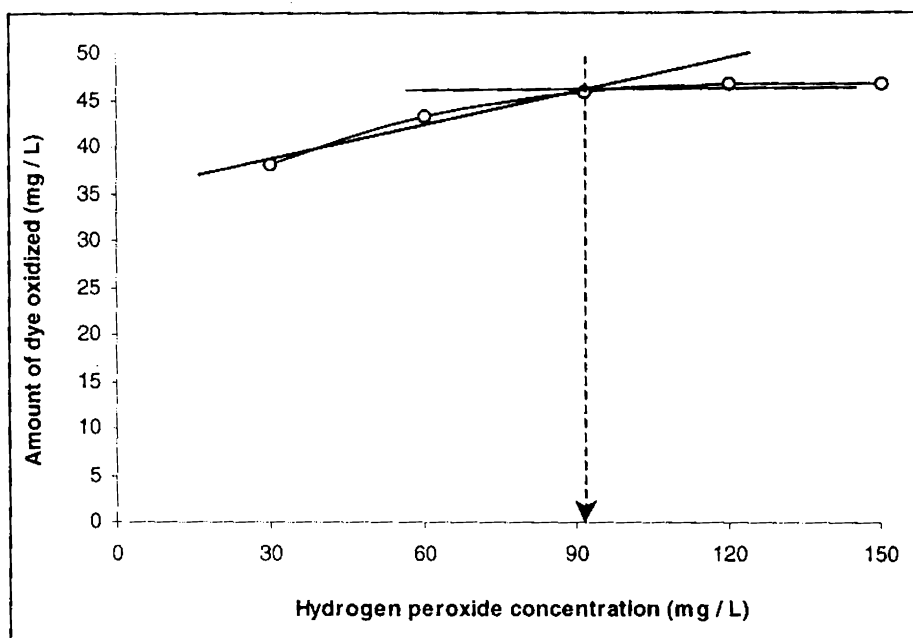


Figure 3.16

Influence of  $H_2O_2$  on the oxidation of Acid Orange (AO)

$[FeSO_4] = 50 \text{ mg L}^{-1}$ ,  $[MB] = 40 \text{ mg L}^{-1}$ , pH 2, vol. 1L, stirring rate 75 rpm,

$[H_2O_2]$  varied 30, 60, 91.7, 120 and 150  $\text{mg L}^{-1}$ .

### 3.5.2. Optimization of Ferrous Sulphate

Experiments to determine the influence of ferrous sulphate on the oxidation of Direct Catachine Brown was carried out by fixing the concentration of both hydrogen peroxide (at optimum) and the dye but for varying concentrations of ferrous sulphate. The results are shown in figure 3.17.

The results indicate that for the range of concentration of ferrous sulphate concentrations studied ( $90\text{-}130\text{ mg L}^{-1}$ ) there is an increase in the oxidation of the dye up to about  $100\text{ mg L}^{-1}$ . Beyond this point addition of ferrous sulphate did not significantly enhance the oxidation of the dye. This behavior is similar to that of hydrogen peroxide, where an increased concentration above a certain limit does not significantly improve the oxidation of the dye.

The effect of ferrous sulphate on Fenton oxidation of Reactive Yellow was studied by fixing concentration of the dye at  $75\text{ mg L}^{-1}$ , hydrogen peroxide at  $110\text{ mg L}^{-1}$  and for varying concentrations of ferrous sulphate. Figure 3.18 shows the results obtained and indicate that an increase in the ferrous sulphate concentration clearly enhances the amount of dye oxidized. At low ferrous sulphate concentrations the reaction was found to be zero order as a linear decrease in dye concentration with time was observed. Higher ferrous sulphate concentrations beyond an optimum, does not cause any significant improvement in oxidation of the dye. Zero order kinetics can be accounted for, as at low concentrations of ferrous sulphate, the small concentrations of hydroxyl radicals generated

are not sufficient to carry out the oxidation reaction. Excess hydrogen peroxide, leading to the formation of hydroperoxyl radicals, rapidly scavenges the hydroxyl radical. The hydroperoxyl radicals being of lower reactivity results in decreased oxidation of the dye. Fig. 3.18 indicates that the optimum concentration of ferrous sulphate is  $60 \text{ mg L}^{-1}$ .

The influence of ferrous sulphate on the oxidation of Methylene Blue was studied for a fixed concentration of the dye at  $10 \text{ mg L}^{-1}$ , hydrogen peroxide at  $60 \text{ mg L}^{-1}$  (obtained as the optimum concentration in step 3.3) and for varying concentrations of ferrous sulphate. Preliminary experiments showed that the optimum ferrous sulphate concentration was about  $35 \text{ mg L}^{-1}$ . Therefore, the range of ferrous sulphate concentrations was chosen in such a manner that there were two concentrations below optimum, one concentration at optimum and two concentrations above it. The decrease in dye concentration with time was monitored at  $665.5 \text{ nm}$ . Figure 3.19 show results of the experiment carried out to determine the influence of ferrous sulphate for a fixed concentration of dye and hydrogen peroxide. Results show that increased ferrous sulphate concentrations enhance the oxidation of the dye and can significantly reduce the concentration of hydrogen peroxide required for reaction. In other words, the amount of dye oxidized can be increased even for a lower concentration of hydrogen peroxide provided concentration of ferrous sulphate is high. Increased addition of ferrous sulphate had a positive effect on oxidation kinetics of Methylene Blue as it not only resulted in

almost complete oxidation but also significantly reduced the concentration of hydrogen peroxide and the time required for oxidation.

Tang and Huang (1996) studied the oxidation kinetics of unsaturated chlorinated aliphatic compounds by Fenton's reagent. Based on the transition state theory, hydroxylated active complexes were assumed to be the transition state after hydroxyl radicals attached to the organic compound. The complex either disproportionate or returns to their original reactants. Both  $\text{OH}^*$  and the active complexes had extremely high reactivity. The model indicates that Fenton oxidation was first order with respect to the concentration of organic substrate. The degree of oxidation was found dependent on the dosage of  $\text{H}_2\text{O}_2$  and  $\text{Fe}^{2+}$ . The authors also state that because both  $\text{Fe}^{2+}$  and  $\text{H}_2\text{O}_2$  can react with  $\text{OH}^*$  neither of them should be overdosed if the maximum reaction rate is to be achieved. Figure 3.19 indicates that the optimum concentration of ferrous sulphate is  $40 \text{ mg L}^{-1}$ .

Influence of ferrous sulphate on the oxidation of Acid orange was studied for a fixed concentration of dye and hydrogen peroxide but for varying concentrations of ferrous sulphate. The dye concentration was fixed at  $50 \text{ mg L}^{-1}$  and concentration of hydrogen peroxide at  $91.7 \text{ mg L}^{-1}$  (as obtained in step 5.1). The decrease in dye concentration with time was monitored at the  $\lambda_{\text{max}}$ . Results of the experiment for different concentrations of ferrous sulphate are shown in figure 3.20. From the figure it can be seen that the ferrous sulphate concentration has an influence on oxidation of the dye with the amount of dye oxidized

increasing with an increase in the ferrous sulphate concentration. However, similar to hydrogen peroxide there exists an optimum concentration beyond which no significant influence on oxidation of the dye was observed. A higher concentration of ferrous sulphate resulted in rapid oxidation of the dye at a rate that could not be effectively monitored by spectrophotometry. On the other hand, at low ferrous sulphate concentrations amount of dye oxidized was negligible and the oxidation kinetics followed zero order (indicated by a linear decrease in the dye concentration with time). Figure 3.20 indicates that the optimum concentration of ferrous sulphate is  $40 \text{ mg L}^{-1}$ .

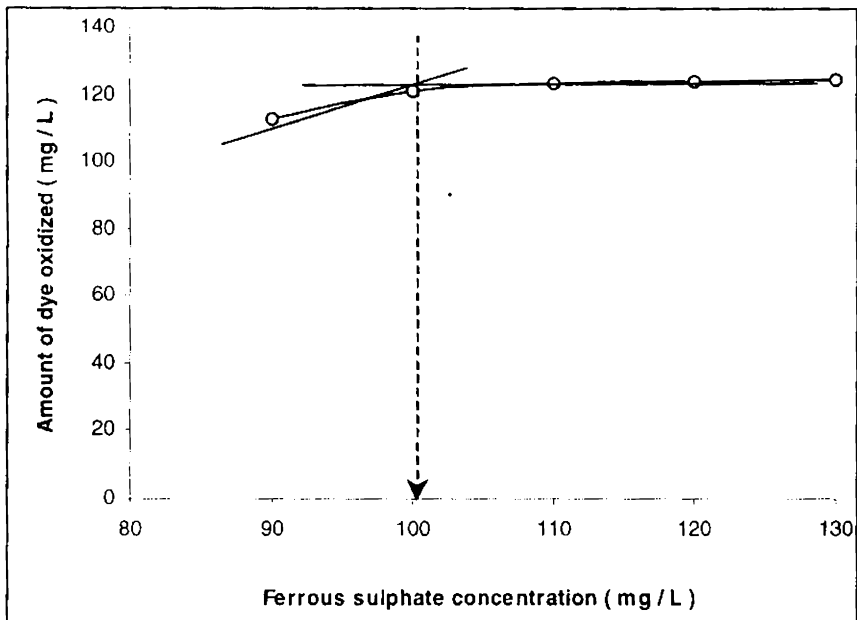


Figure 3.17  
Influence of ferrous sulphate concentration on the oxidation of Direct Catachine Brown in aqueous solution.  
[H<sub>2</sub>O<sub>2</sub>]= 367 mg L<sup>-1</sup>, [DCB] = 150 mg L<sup>-1</sup>, pH 2, vol. 1L, stirring rate 75 rpm,  
[FeSO<sub>4</sub>] = varied 90, 100, 110, 120 and 130 mg L<sup>-1</sup>

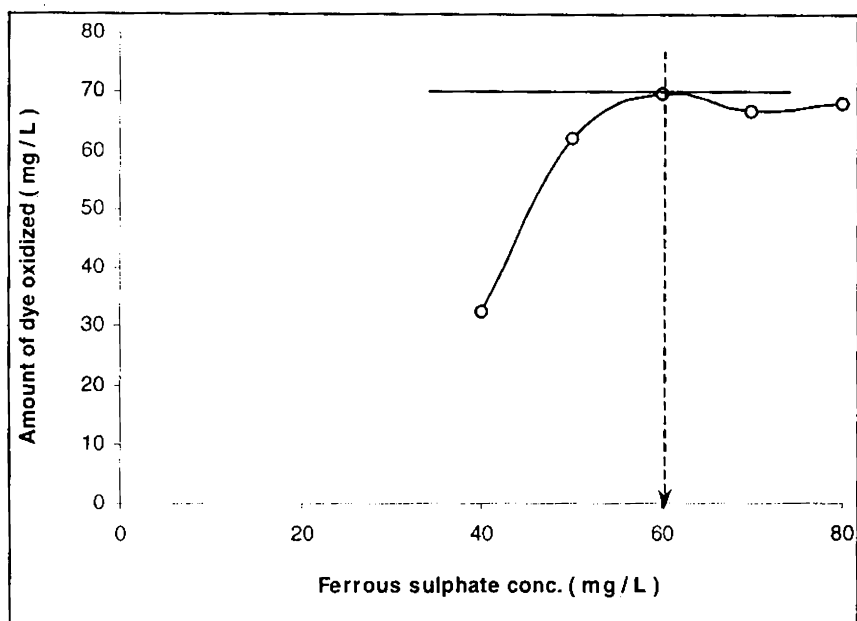


Figure 3.18  
Effect of ferrous sulphate concentration on the oxidation of Reactive Yellow [RY] in aqueous solution.  
[H<sub>2</sub>O<sub>2</sub>] = 110 mg L<sup>-1</sup>, [RY] = 75 mg L<sup>-1</sup>, pH 2, vol. 1L, stirring rate 75 rpm,  
[FeSO<sub>4</sub>] = varied 40, 50, 60, 70 and 80 mg L<sup>-1</sup>



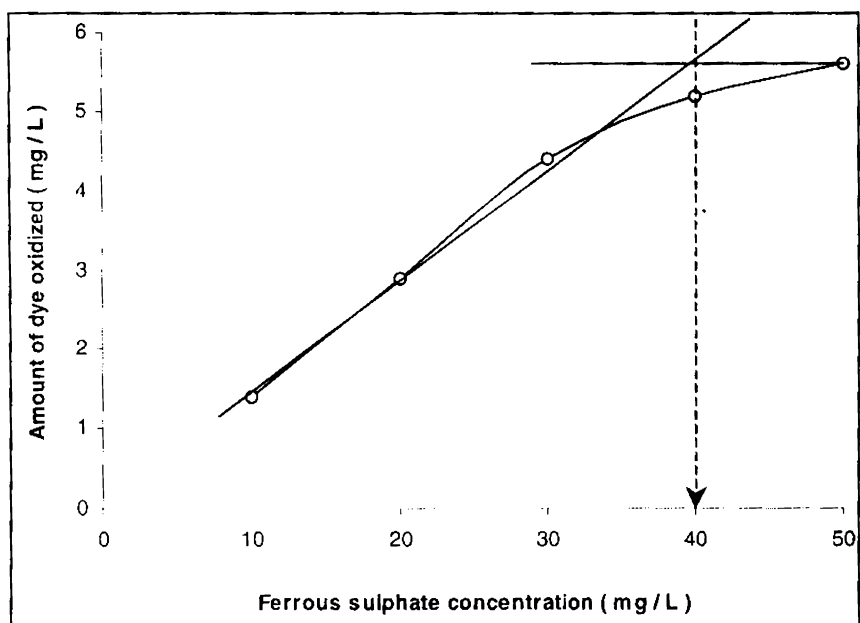


Figure 3.19

Effect of ferrous sulphate concentration on the oxidation of Methylene Blue [MB] in aqueous solution.

$[\text{H}_2\text{O}_2] = 60 \text{ mg L}^{-1}$ ,  $[\text{MB}] = 10 \text{ mg L}^{-1}$ , pH 2, vol. 1L, stirring rate 75 rpm,

$[\text{FeSO}_4] = \text{varied } 10, 20, 30, 40 \text{ and } 50 \text{ mg L}^{-1}$

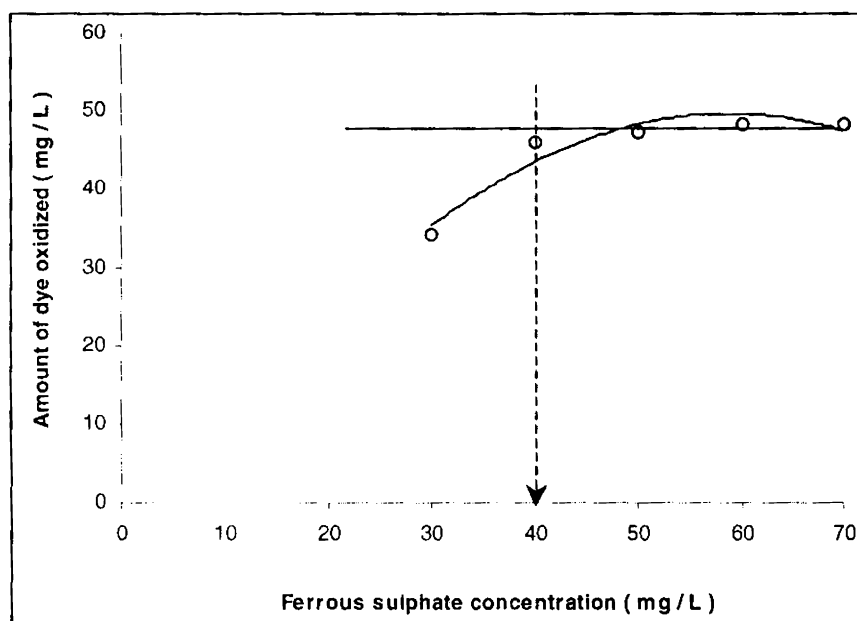


Figure 3.20

Effect of ferrous sulphate concentration on the oxidation of Acid Orange [AO] in aqueous solution.  $[\text{H}_2\text{O}_2] = 91.7 \text{ mg L}^{-1}$ ,  $[\text{AO}] = 50 \text{ mg L}^{-1}$ , pH 2, vol. 1L, stirring rate 75 rpm,  $[\text{FeSO}_4] = \text{varied } 30, 40, 50, 60 \text{ and } 70 \text{ mg L}^{-1}$

### 3.5.3. Influence of dye concentration

The Influence of dye concentration on Fenton oxidation of Direct Catachine Brown was studied for fixed concentrations of hydrogen peroxide ( $367 \text{ mg L}^{-1}$ ) and ferrous sulphate ( $100 \text{ mg L}^{-1}$ ) at optimum concentrations obtained from figure 3.13 and 3.17 and for varying dye concentrations. Experiments were carried out for the dye concentrations of 50, 100, 200, 300 and  $400 \text{ mg L}^{-1}$ . The results are depicted in figure 3.21.

The results obtained indicate that oxidation of the dye is more efficient at higher concentrations than for dilute solutions. When the concentration of dye was  $50 \text{ mg L}^{-1}$  (the lowest concentration studied) a ferrous sulphate concentration of  $100 \text{ mg L}^{-1}$  and a hydrogen peroxide concentration of  $367 \text{ mg L}^{-1}$  could oxidize  $43 \text{ mg L}^{-1}$  of the dye. However, for the same concentration of the Fenton's reagent,  $272 \text{ mg L}^{-1}$  of the dye could be oxidized for a concentration of  $400 \text{ mg L}^{-1}$ . The results obtained clearly indicate that the oxidation efficiency is enhanced at higher dye concentrations. However, this trend is likely to approach a limit.

This behavior can be explained on the basis of the self-scavenging action of hydroxyl radicals at low concentrations of the dye. As the dye concentration increases there is an increase in the concentration of these radicals reacting with the dye rather than reacting among themselves. This reaches a maximum stoichiometric limit when  $[\text{H}_2\text{O}_2]: [\text{Dye}]$  reaches 0.9.

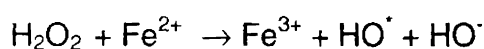
In order to determine whether a higher concentration of the dye could be oxidized even at lower concentrations of ferrous sulphate by increasing the concentration of hydrogen peroxide, experiments were

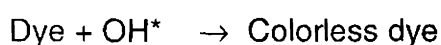
carried out by choosing a particular concentration of the dye and then varying both ferrous sulphate and hydrogen peroxide, maintained at a constant mole ratio of 1:15. The results are summarized in Table 3.1.

Table 3.1. Conditions of experiments carried out to determine the optimum for the oxidation of Direct Catachine Brown - dye concentration of 150 mg/L and varying concentrations of the Fenton's reagent, mole ratio of ferrous sulphate to hydrogen peroxide 1:15.

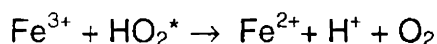
Dye mg/L	FeSO <sub>4</sub> mg/L	FeSO <sub>4</sub> mM/L	H <sub>2</sub> O <sub>2</sub> mg/L	H <sub>2</sub> O <sub>2</sub> mM/L	Fe:H <sub>2</sub> O <sub>2</sub> Mole ratio	Amount of Dye oxidized. mg/L
150	20	0.072	36.7	1.08	1:15	20
150	40	0.14	73.4	2.16	1:15	42
150	60	0.21	110.1	3.24	1:15	45
150	80	0.29	146.8	4.32	1:15	84
150	100	0.36	183.5	5.39	1:15	108
150	120	0.43	220.2	6.47	1:15	104
150	140	0.5	256.9	7.55	1:15	120
150	160	0.58	293.6	8.63	1:15	122
150	180	0.65	330.3	9.71	1:15	123
150	200	0.72	367	10.8	1:15	126

The amount of dye oxidized increased with an increase in the concentration of the Fenton's reagent. However, the data points out two features. First, although a ferrous sulphate to hydrogen peroxide mole ratio of 1:15 is found optimum, the ratio of the oxidant to the dye is important in driving the oxidation to completion. Secondly, when the concentration of the Fenton's reagent is not sufficient, the data points show a random behavior. This may be due to slow reaction at reduced concentration of the reagent, where the reaction pathway changes, according to some probable reactions involving the derived species.





at low concentrations of  $\text{H}_2\text{O}_2$ , or when  $\text{Fe}^{2+}$  is depleted the reaction switches over to



Both ferrous ions and hydrogen peroxide are integral components of Fenton's reagent generating hydroxyl radicals. Lower concentrations of either of them would result in decreased generation of the free radical thereby leading to a decrease in rate of the reaction resulting in the poor dye removal.

Walter and Huang (1996) evaluated the effect of the chlorine content of chlorinated phenols on their oxidation kinetics by Fenton's reagent. The reactivity of chlorophenols decreased with increasing chlorine substitution on the aromatic ring. They observed that at constant hydrogen peroxide and ferrous concentrations, initial dechlorination rates did not change significantly. This suggests that the generation of hydroxyl radical was the rate-limiting step

From table 3.1 it is observed that there is an increase in the amount of the dye oxidized with increase in the concentration of the Fenton's reagent. However, beyond a ferrous sulphate concentration of  $140 \text{ mg L}^{-1}$  and a hydrogen peroxide concentration of  $256.9 \text{ mg L}^{-1}$  the increase was not significant. A comparison of the second order rate coefficients obtained for the different concentrations of the Fenton's reagent shows that beyond a ferrous sulphate concentration of  $180 \text{ mg L}^{-1}$  and a hydrogen peroxide

concentration of  $330 \text{ mg L}^{-1}$ , increase in the concentration of the Fenton's reagent decreased the rate of oxidation of the dye. This indicates scavenging of the hydroxyl radicals by excess ferrous ions.

Table 3.1 shows that at a ferrous sulphate concentration of  $100 \text{ mg L}^{-1}$  and a hydrogen peroxide concentration of  $183.5 \text{ mg L}^{-1}$ , the amount of dye oxidized was  $108 \text{ mg L}^{-1}$ . Table 3.2 summarize the results of the experiments to show that the oxidation efficiency could also be increased by increasing the concentration of hydrogen peroxide even for low concentrations of ferrous sulphate.

Table 3.2. Influence of increased hydrogen peroxide concentration.

Dye $\text{mg L}^{-1}$	$\text{FeSO}_4$ $\text{mg L}^{-1}$	$\text{FeSO}_4$ $\text{mM L}^{-1}$	$\text{H}_2\text{O}_2$ $\text{mg L}^{-1}$	$\text{H}_2\text{O}_2$ $\text{mM L}^{-1}$	Fe: $\text{H}_2\text{O}_2$ Mole ratio	Amount of Dye oxidized $\text{mg L}^{-1}$
150	100	0.36	367	10.8	1:30	120.0
150	100	0.36	550	16.2	1:45	123.0
150	100	0.36	735	21.6	1:60	124.5
150	100	0.36	917.5	27.0	1:75	124.5
150	100	0.36	1101	32.4	1:90	124.5

A comparison of Tables 3.1 and 3.2 show that the lower concentration of ferrous sulphate is offset by increasing the concentration of hydrogen peroxide, leading to an increased oxidation of the dye. This means that both ferrous sulphate and hydrogen peroxide are integral components of the Fenton's reagent. Reduced concentration of any one of them would result in decreased production of the hydroxyl radicals. Hydrogen peroxide is the oxidant and ferrous ions being required in an optimum stoichiometry. Kinetic studies have been carried out at a fixed

concentration of ferrous sulfate ( $100 \text{ mg L}^{-1}$ ) and the hydrogen peroxide concentration at  $367 \text{ mg L}^{-1}$ .

The effect of dye concentration on Fenton's oxidation of Reactive Yellow was determined by fixing the concentration of hydrogen peroxide at  $110 \text{ mg L}^{-1}$  and ferrous sulphate concentration at  $60 \text{ mg L}^{-1}$  (optimum concentrations obtained from figure 3.14 and 3.18) for varying concentrations of the dye. The concentrations chosen ranged from 25 to  $125 \text{ mg L}^{-1}$ . The results obtained are shown in figure 3.22 and indicate that the oxidation efficiency of Fenton's reagent is higher at higher concentrations of the dye. When the initial dye concentration was  $25 \text{ mg L}^{-1}$ ,  $21.3 \text{ mg L}^{-1}$  of dye was oxidized at a ferrous sulphate concentration of  $60 \text{ mg L}^{-1}$  and a hydrogen peroxide concentration of  $110 \text{ mg L}^{-1}$ . The same concentration of Fenton's reagent resulted in oxidizing  $116.7 \text{ mg L}^{-1}$  of the dye at a concentration of  $125 \text{ mg L}^{-1}$ . This indicates that it was difficult to oxidize lower dye concentrations than concentrated solutions. The observations are summarized in Table 3.3.

Table 3.3. Optimum stoichiometric concentrations of the Fenton's reagent for various dye concentrations.

[Dye] ( $\text{mg L}^{-1}$ )	$\text{FeSO}_4$ ( $\text{mg L}^{-1}$ )	$[\text{H}_2\text{O}_2]$ ( $\text{mg L}^{-1}$ )	mg $\text{H}_2\text{O}_2$ / mg dye	Exposure (h)	mg of dye oxidized
25	60	110	4.40	2	21.3
50	60	110	2.20	2	44.7
75	60	110	1.50	2	67.0
100	60	110	1.10	2	80.7
125	60	110	0.88	2	116.7

The oxidation efficiency of Fenton's reagent for various dye concentrations is shown in figure 3.22.

Effect of dye concentration on Fenton's oxidation of Methylene Blue was determined for a fixed concentration of both hydrogen peroxide and ferrous sulphate at 60 and 40 mg L<sup>-1</sup> respectively. The dye concentrations were varied and the concentrations studied ranged from 0 to 20 mg L<sup>-1</sup>. Results are shown in figure 3.23. The results reveal that Fenton's oxidation is more efficient at higher rather than for lower dye concentrations. The results obtained are summarized in Table 3.4.

Table 3.4. Optimum stoichiometric concentrations of Fenton's reagent for various dye concentrations.

[Dye] (mg L <sup>-1</sup> )	FeSO <sub>4</sub> (mg L <sup>-1</sup> )	[H <sub>2</sub> O <sub>2</sub> ] (mg L <sup>-1</sup> )	mg H <sub>2</sub> O <sub>2</sub> / mg dye	Exposure (h)	mg of dye oxidized
4	40	60	15	2	2.7
8	40	60	7.5	2	7.5
12	40	60	5.0	2	11.5
16	40	60	3.8	2	14.8
20	40	60	3.0	2	18.9

Figure 3.23 and table 3.4 further strengthen the view that Fenton's reagent is effective for treating concentrated rather than dilute dye solutions. This observation has an attractive practical implication, as it is cost effective to treat the concentrated effluent followed by a second treatment of the residual dye and finally dilution with non-colored stream. Increased oxidation efficiency at higher dye concentrations indicate that deactivation of hydroxyl radical is an important mechanism lowering the treatment efficiency at low dye concentration while, at higher dye concentrations the reaction between hydroxyl radical and dye molecules dominate resulting in an observed increase in treatment efficiency.



Effect of dye concentration on Fenton's oxidation of Acid orange was studied by maintaining the concentration of ferrous sulphate and hydrogen peroxide at 40 mg L<sup>-1</sup> and 91.7 mg L<sup>-1</sup> respectively (optimum concentrations obtained in figures 3.16 and 3.20), and for varying concentrations of the dye. Dye concentrations chosen included the range up to which it followed Beer-Lamberts law. Results of the experiment are summarized in table 3.5.

Table 3.5. Optimum stoichiometric concentrations of the Fenton's reagent for various dye concentrations.

[Dye] (mg L <sup>-1</sup> )	FeSO <sub>4</sub> (mg L <sup>-1</sup> )	[H <sub>2</sub> O <sub>2</sub> ] (mg L <sup>-1</sup> )	mg H <sub>2</sub> O <sub>2</sub> / mg dye	Exposure (h)	mg of dye oxidized
20	40	91.7	4.6	2	20
40	40	91.7	2.3	2	38.5
60	40	91.7	1.5	2	56.7
80	40	91.7	1.1	2	75.5
100	40	91.7	0.9	2	92.5

For the same concentration of Fenton's reagent, when the dye was completely decolorized at a concentration of 20 mg L<sup>-1</sup>; there was a progressive increase in the amount of dye oxidized at all higher concentrations. This indicates that the Fenton oxidation is a process that works best at higher dye concentrations. This observation is of much practical utility in onsite conditions.

The oxidation efficiency of the Fenton's reagent for various concentrations of Acid Orange is shown in Figure 3.24 which indicates a linear increase in amount of dye oxidized for the same concentration of Fenton's reagent irrespective of its initial concentration and decreased oxidant consumption at increased dye concentrations support the

observation that it is economical to treat concentrated rather than dilute dye solutions.

### 3.6. Kinetic Studies

The kinetic experiments have been carried out with the objective of elucidating the influence of the concentration of the of the following on the oxidation kinetics of the dye:

- (i) Hydrogen peroxide
- (ii) Ferrous sulfate
- (iii) Dye

The experimental approach is described in section 3.3.2.

The integral method is usually adopted only under isolation condition i.e., when the parameter that is to be monitored is kept at very low concentrations, so that the rate of the reaction would be dependent upon this isolated parameter. However, since, both ferrous sulphate and hydrogen peroxide are critical components of the Fenton's system if the concentration of any one of the constituents is made too low the reaction would not proceed. Hence, it is not possible to isolate either hydrogen peroxide or ferrous sulphate to study the reaction mechanism. Under such conditions the differential method (initial rate) is applied.

In the initial rate method the rate of the reaction is determined directly from the concentration versus time plots considering only the first few points after the start of the experiment.

In our studies the kinetic data has been interpreted using the initial rate method where rather than following the reaction to completion, observations are based on the first few initial points of decrease i.e., for the first half of the experiment. This takes into account only the reactions

before secondary reactions begin to have any discernible effect on oxidation of the dye.

A common feature observed in all experiments is that there is a first initial dip immediately on addition of hydrogen peroxide. The intensity of this initial dip can be pronounced and can achieve from less than 10% to 100% oxidation instantaneously, depending on the concentration of hydrogen peroxide and ferrous sulphate chosen for the experiment. However, it is after this initial dip, that the reaction begins to show interpretable trends. The initial concentration was determined after pH correction of the reaction mixture containing the desired concentration of ferrous sulphate. This point does not take into account the effect on addition of hydrogen peroxide. Moreover, it has been observed that when the trend line is extrapolated to the Y-axis from the point of first measurement, the intercept on Y-axis suggest that a considerable portion of the dye gets oxidized immediately on addition of hydrogen peroxide. Farley and Hunter (1996) made similar observation during the Fenton oxidation of 1,2,3-trichloropropane. The oxidation kinetics followed pseudo first order after an initial period of higher and variable reaction kinetics.

Sun and Pignatello (1993) investigated the mineralization of 2,4-dichlorophenoxy acetic acid (2,4-D) by  $\text{Fe}^{3+}/\text{H}_2\text{O}_2/\text{UV}$  system. They reported that the oxidation occurred in two stages. The first stage was attributed to reaction of free radicals generated under irradiation. In subsequent reaction the hydroxyl radical does not play any significant role. The reaction is exclusively due to photolysis or due to decarboxylation of  $\text{Fe}^{3+}$  complexes

of degradation intermediates. The study reveals that the hydroxyl radical is ineffective in oxidizing the organic intermediates remaining after the first stage. This is most likely due to the lower reactivity of the highly oxygenated intermediates toward the hydroxyl radical or competitive consumption of hydroxyl radicals by other solutes. This argument is not tenable in the present context since there is a significant concentration of the dye in the medium at this point. The hydroperoxyl radical ( $\text{HO}_2^*$ ) produced by the reaction between hydrogen peroxide and the ferrous ion is less reactive than hydroxyl radicals. The slow acting residual hydroperoxide radical may also give such slow reaction.

Lu et al. (1997) studied the oxidation of Dichlorvos insecticide by Fenton's reagent. They observed that the oxidation was a two-stage reaction. The first stage is a rapid decomposition, which is over with in 30s. This stage was attributed to a  $\text{Fe}^{2+}/\text{H}_2\text{O}_2$  reaction leading to the formation of hydroxy radicals. The second much slower stage was attributed to the  $\text{Fe}^{3+}/\text{H}_2\text{O}_2$  reaction.

Ince and Tezcanli (1999) studied the treatability of textile dye-bath effluents by advanced oxidation and its preparation for reuse. They found that the reaction occurs in two stages, a fast step followed by a slow step. The slow step reaction followed first order kinetics.

Anat and Deshpande (1996) studied the decolorization of wastewater containing reactive dyes by Fenton's reagent and found that the initial step is instantaneous. They attributed this to the rapid cleaving of

the dye molecule. However, they did not provide any proof as to the pattern cleavage.

Working on the oxidation of p-chlorophenol by Fenton's reagent Gun et al. (1999) reported that the process involved two steps. A fast initial stage, which obeyed first order rate law and a second slow stage which is attributed to the depletion of  $\text{Fe}^{2+}$  by Fe-organic complex formation. Here also no proof was provided.

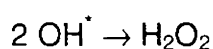
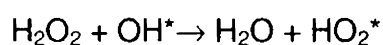
Kwon et al. (1999) studied the oxidation of p-chlorophenol by Fenton's reagent. They observed that the oxidation was a two-step process. The initial step was fast and resulted in significant oxidation within a few minutes. This was followed by a slow step. The initial fast rate was found first order with respect of p-chlorophenol. The slow phase was attributed to the depletion of ferrous ions caused by the formation of Fe – organic complex.

### 3.6.1. Influence of hydrogen peroxide on oxidation kinetics

The influence of hydrogen peroxide concentration on the rate of oxidation of the dye has been studied by maintaining a constant concentration of dye and ferrous sulphate but for varying concentrations of hydrogen peroxide. Five different concentrations of hydrogen peroxide were tried. The concentrations have been fixed in such a manner that there were two concentrations above optimum (as obtained from preliminary experiments), one concentration at the optimum and two concentrations below optimum. The results are depicted in figure 3.25.

Balanosky et al. (2000) studied the performance of a reactor in the oxidative degradation of textile waste. He also confirmed hydrogen peroxide was effective only in the presence of ferrous or ferric ions, and at lower hydrogen peroxide concentrations the reaction proceeded only slowly.

Figure 3.25 show that the initial rates for the decolorization reaction increased linearly with an increase in the concentration of hydrogen peroxide up to 390 mg L<sup>-1</sup> beyond which there was a drop in the initial rates. This is because high hydrogen peroxide concentrations results in recombination of hydroxyl radicals among themselves to form hydroperoxyl radicals, according to the following reactions



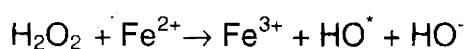
Although hydroperoxyl radical is an oxidant it is much less reactive than the hydroxyl radicals (Legrini et al., 1993).

The results support the view that increased hydrogen peroxide concentrations decrease the rate of oxidation of the dye beyond an optimum value.

A plot of the initial rate against dye concentration is linear passing through the origin indicating that the reaction is first order with respect to hydrogen peroxide.

Kang et al. (2002) studied the pre-oxidation and coagulation of textile wastewater by the Fenton process observed 95% decolorization with in five minutes.

The influence of hydrogen peroxide on oxidation kinetics of Reactive Yellow was studied for a fixed ferrous sulphate concentration of 60 mg L<sup>-1</sup> and a dye concentration of 75 mg L<sup>-1</sup>. Concentrations of hydrogen peroxide chosen for the experiment were 90, 100, 110, 120 and 130 mg L<sup>-1</sup>. The results obtained are shown in figure 3.26 and indicate that the initial rates were found to increase linearly with an increase in hydrogen peroxide concentration with an intercept at the origin. This indicates that the reaction is first order with respect to hydrogen peroxide. Reaction pathway followed can be represented by the following equation



Similar observations have been reported by Isak et al., (1996) during the oxidation of aldehydes by Fenton's reagent.

Lindsey and Tarr (2000) studied the generation of hydroxyl radical during Fenton oxidation following a single addition of iron and hydrogen



peroxide. The authors observed a linear increase in hydroxyl radical formation with the concentration of hydrogen peroxide.

The influence of hydrogen peroxide on kinetics of Fenton oxidation of Methylene Blue was studied by fixing the concentrations of ferrous sulphate at  $35 \text{ mg L}^{-1}$  and dye at  $10 \text{ mg L}^{-1}$ . The concentration of hydrogen peroxide was varied. Five concentrations of hydrogen peroxide were chosen in such a manner that there was two concentrations below optimum, one concentration at optimum and two concentrations above optimum. The variation in initial rates for different concentrations of hydrogen peroxide is shown in figure 3.27. Results indicate that an increase in the initial rate with an increase in hydrogen peroxide concentration up to  $2.35 \text{ mM}$  after which the initial rates decrease. This is probably the concentration of hydrogen peroxide where the ratios of ferrous ions to hydrogen peroxide are in balance to initiate the generation of hydroxyl radicals, which in turn oxidize the dye.

Similar observations have also been observed in the case of Acid Orange. Experiments to establish the influence of hydrogen peroxide on Fenton's oxidation of Acid Orange was performed by fixing the concentration of dye at  $50 \text{ mg L}^{-1}$ , the ferrous sulphate concentration at  $40 \text{ mg L}^{-1}$  (as obtained in the preliminary experiments) for varying the concentrations of hydrogen peroxide. Five different concentrations of hydrogen peroxide were chosen in such a manner that there were two concentrations below optimum, one concentration at the optimum and two concentrations above optimum. Thereby, obtaining influence of hydrogen

peroxide concentrations at both extremes relative to the optimum concentration. The results obtained are shown in figure 3.28.

As the concentration of hydrogen peroxide was increased the initial rates tend to increase in an exponential manner. Under such conditions the concentration of hydrogen peroxide is sufficient enough to be decomposed by the ferrous ions acting as a catalyst to generate the hydroxyl radicals. William et al., (1996) report that reaction rates appeared to be highest at the lowest peroxide to iron ratio. Gradually a stage is reached where the concentration of hydrogen peroxide exceeds the concentration of ferrous sulphate. Under such conditions the excess hydrogen peroxide would involve in non-productive internal reactions that lead to scavenging of the hydroxyl radicals ( $\text{OH}^*$ ) to form hydroperoxyl ( $\text{HO}_2^*$ ) radicals. These hydroperoxyl radicals have a lower reactivity when compared to the peroxy radicals. The reactions mediated by hydroperoxyl radicals after the hydroxyl radical has been scavenged, results in lowering the initial rates. This accounts for the curvature observed in figure 3.27 and 3.28.

Lloyd et al. (1997) studied the origin of hydroxyl radical  $\text{O}_2$  in the Fenton reaction and report that hydroxyl radical was derived exclusively from  $\text{H}_2\text{O}_2$ . However, at higher hydrogen peroxide concentrations there is an excess of hydrogen peroxide over the ferrous ions. Excess peroxide involves in non-productive internal reactions that leads to scavenging of the hydroxyl radicals ( $\text{OH}^*$ ) by formation of hydroperoxyl radicals ( $\text{HO}_2^*$ ). Compared to the hydroxyl radical, the hydroperoxyl radical has a much

lower reactivity. After hydroxyl radicals are scavenged which is the most likely situation at hydrogen peroxide concentrations above 2.35 mM, oxidation of the dye is promoted by hydroperoxyl radical. The hydroperoxyl radical being of lower reactivity results in a decrease in the initial rates. Scott et al. (1998) measured Hydroxyl radical activity in soil slurry using the spin trap agent  $\alpha$ -(4-Pyridyl-1-Oxide) – N-tert-butylNitron. They observed that non-productive reactions involving hydrogen peroxide (those that did not contribute to the production of hydroxyl radicals) represented a significant source for the overall decrease in reaction efficiency.

Sun and Pignatello, (1993) studied the oxidation of 2,4-D by  $\text{Fe}^{3+}/\text{H}_2\text{O}_2/\text{UV}$  system and reports similar observations. The authors report that the hydroxyl radical is ineffective in oxidizing organic intermediates remaining after completion of the first stage. This was attributed to the low reactivity of highly oxygenated intermediates to hydroxyl radical and competition for the hydroxyl radical by other solutes. The hydroperoxyl ( $\text{HO}_2^*$ ) radical was incapable of producing any  $\text{CO}_2$  from the ring, indicating its poor reactivity in comparison to Hydroxyl radical ( $\text{OH}^*$ )

Liao et al. (1999) studied the removal of COD and color from dye manufacturing process wastewater using Photo-Fenton oxidation process. The author's reported that increased concentration of hydrogen peroxide does not necessarily mean increased removal rates of COD and color.

Ince and Stefan (1997) studied the degradation and toxicity reduction of a textile azo dye Remazol Black – B using  $\text{UV}/\text{H}_2\text{O}_2$ . The

authors observed that beyond an effective concentration, the influence of hydrogen peroxide was found inhibitory.

Sychev and Isak (1995) studied Iron compounds and the mechanisms of homogeneous catalysis. They report that higher peroxide concentrations could be detrimental to degradation kinetics since after initiation step, the propagation step would be hindered by excess hydrogen peroxide acting as a scavenger of the hydroxyl radical.

Huston and Pignatello. (1999) used photo-assisted Fenton reaction to degrade selected pesticide active ingredients in water. The authors state that at longer reaction time, higher initial peroxide concentration could result in greater mineralization. As mineralization proceeds the carbon acquires higher oxidation states, however, the organic compounds remaining in solution typically become less reactive with the hydroxyl radicals. This results in the decay of hydroxyl radical through scavenging by hydrogen peroxide or self-reaction or scavenging by ferrous ion.

A plot of the initial rates against hydrogen peroxide concentration fit well into a second order polynomial expression giving a curve as shown in Figures 3.27 and 3.28; indicating that there is a possible chance for complexation with hydrogen peroxide.

Fung et al. (1999) studied the treatability of organic and colour removal in desizing/dyeing wastewater by UV/US system combined with hydrogen peroxide. The authors observed that increasing the amount of hydrogen peroxide could enhance the oxidation efficiency. However high concentrations had little positive effects on dye removal due to the

competitive reaction of hydrogen peroxide with the hydroxyl radicals. The dye was found to follow pseudo-first order kinetics at different pH and hydrogen peroxide concentrations. The rate constants were linearly correlated with pH but fitted better into a second order polynomial expression.

One way of confirming this observation is by a double reciprocal plot in which the inverse of initial rates is plotted against inverse of hydrogen peroxide concentration. Such a plot is presented in figure 3.29 and 3.30.

The double reciprocal plot for Methylene Blue at different concentrations of hydrogen peroxide is shown in figure 3.29. The resulting plot is linear up to the limiting concentration with a positive intercept at the Y-axis confirming the involvement of a complexation step in Fenton oxidation of Methylene Blue. Since, concentrations of ferrous sulphate and the dye were maintained constant for varying concentrations of hydrogen peroxide, complexation between hydrogen peroxide and the dye is most likely.

Figure 3.28 show that the variation in initial rates fits a second order polynomial expression representing a curve in the case of Acid Orange. The observation is similar to that of Fung et al., (1999) where the rate constants fitted better into a second order polynomial expression. The curve is an indication of complexation with hydrogen peroxide. A double reciprocal plot can prove this observation. Figure 3.30 suggest a linear variation in the double reciprocal of the initial rate against the hydrogen peroxide concentration with an intercept at the Y-axis. Since,

concentrations of ferrous sulphate and the dye were maintained constant for varying concentrations of hydrogen peroxide, the observation confirms the involvement of a complexation step with hydrogen peroxide during Fenton oxidation of Acid Orange.

Salem and Maazawi (2000) studied the kinetics and mechanism of color removal of Methylene Blue with hydrogen peroxide catalyzed by supported alumina surfaces. The authors observed that at low hydrogen peroxide concentrations, the reaction was first order, which becomes zero order with increase in hydrogen peroxide concentration before becoming negative. They observed the formation of colored intermediate on the surface of the catalyst. Pignatello et al. (1999) showed evidence for an additional oxidant in photo assisted Fenton reaction. The authors observed that hydrogen peroxide formed a complex with iron,  $\text{Fe}(\text{O}_2\text{H})^{2+}$ , that absorbs in the visible region, which could be the precursor of ferryl complex.

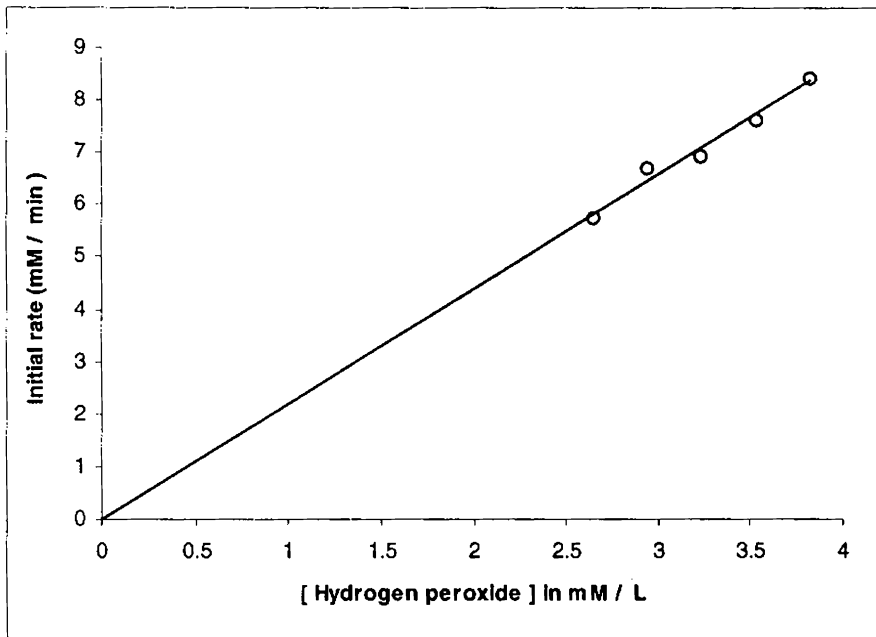


Figure 3.25  
Direct Catachine Brown  
Variation of initial rates with hydrogen peroxide concentration  
[DCB] = 150 mg L<sup>-1</sup>, [FeSO<sub>4</sub>] = 100 mg L<sup>-1</sup>, pH 2, vol. 1L, stirring rate 75 rpm,  
[H<sub>2</sub>O<sub>2</sub>] = varied 300, 330, 367, 390 and 420 mg L<sup>-1</sup>

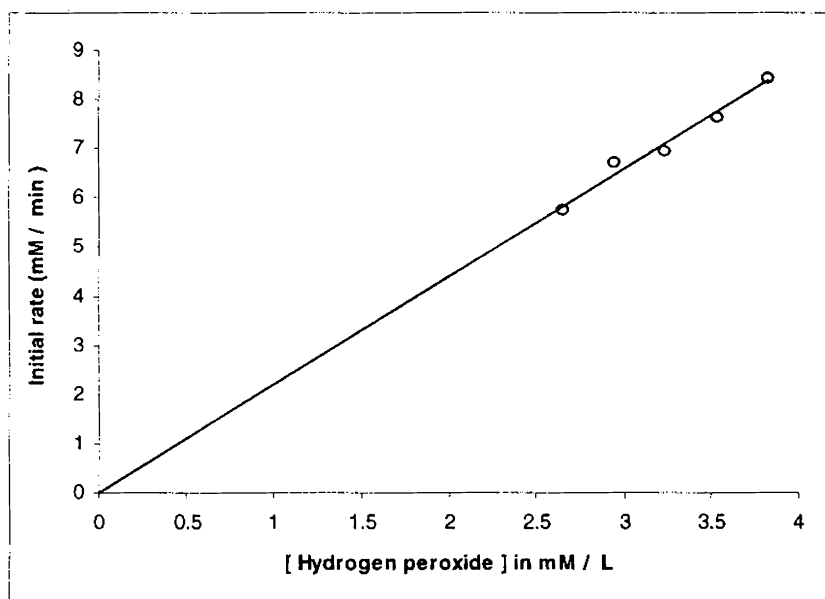


Figure 3.26

Reactive Yellow (RY)

Variation of initial rates with hydrogen peroxide concentration

[RY] = 75 mg L<sup>-1</sup>, [FeSO<sub>4</sub>] = 60 mg L<sup>-1</sup>, pH 2, vol. 1L, stirring rate 75 rpm,

[H<sub>2</sub>O<sub>2</sub>] = varied 2.6, 2.94, 3.23, 3.53 and 3.82 mM L<sup>-1</sup>



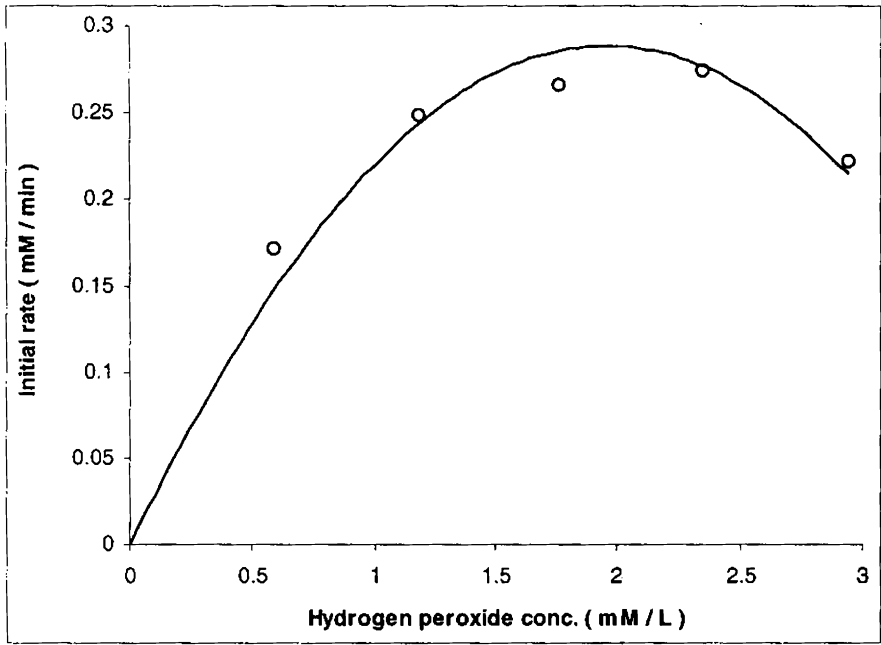


Figure 3.27  
Methylene Blue (MB)  
Variation of initial rates with hydrogen peroxide concentration  
[MB] =  $10 \text{ mg L}^{-1}$ , [FeSO<sub>4</sub>] =  $35 \text{ mg L}^{-1}$ , pH 2, vol. 1L, stirring rate 75 rpm,  
[H<sub>2</sub>O<sub>2</sub>] = varied 0.59, 1.18, 1.76, 2.35 and 2.94  $\text{mM L}^{-1}$

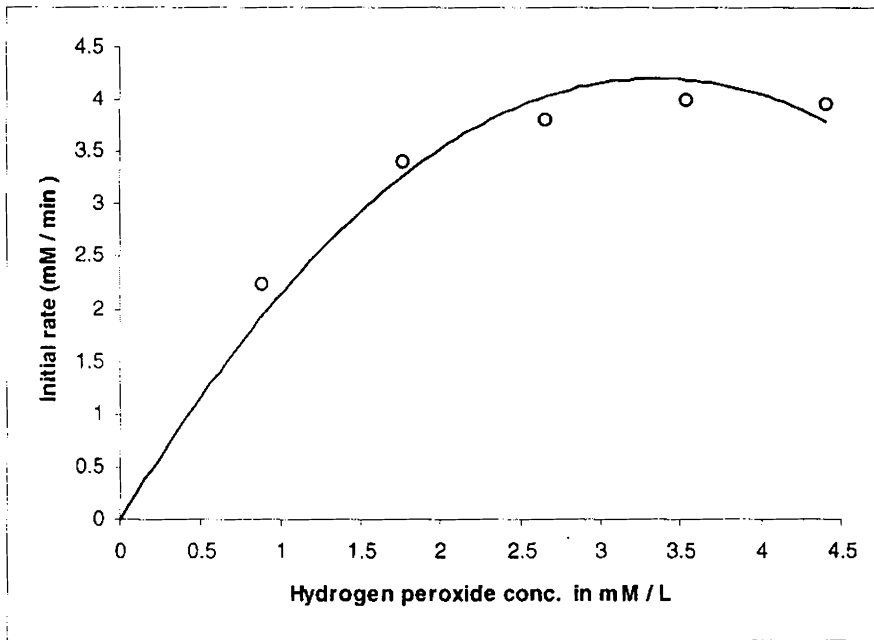


Figure 3.28

Acid Orange ( AO )

Variation of initial rates with hydrogen peroxide concentration

[AO] = 50 mg L<sup>-1</sup>, [FeSO<sub>4</sub>] = 40 mg L<sup>-1</sup>, pH 2, vol. 1L, stirring rate 75 rpm,

[H<sub>2</sub>O<sub>2</sub>] = varied 0.88, 1.76, 2.7, 3.53 and 4.4 mM L<sup>-1</sup>

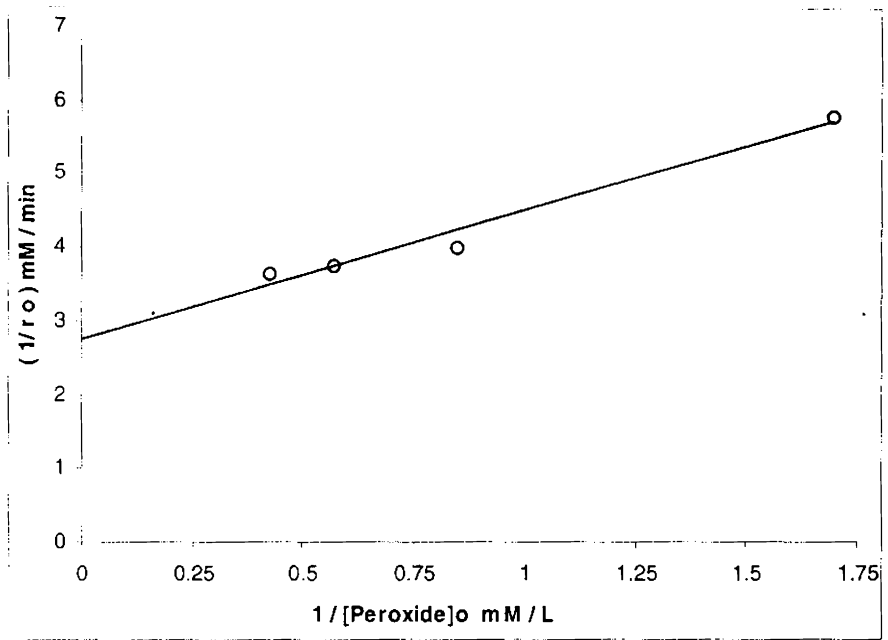


Figure 3.29

Methylene Blue (MB)

Double reciprocal plot of initial rates and hydrogen peroxide concentration  
[MB] =  $10 \text{ mg L}^{-1}$ ,  $[\text{FeSO}_4] = 35 \text{ mg L}^{-1}$ , pH 2, vol. 1L, stirring rate 75 rpm,  
 $[\text{H}_2\text{O}_2] =$  varied 0.59, 1.18, 1.76, 2.35 and  $2.94 \text{ mM L}^{-1}$

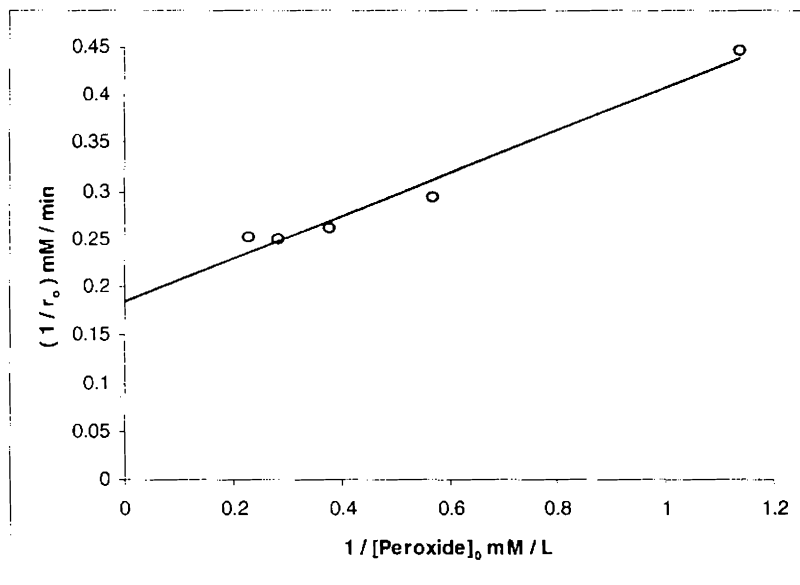


Figure 3.30

Acid Orange (AO)

Double reciprocal plot of initial rates and hydrogen peroxide concentration  
[AO] =  $50 \text{ mg L}^{-1}$ ,  $[\text{FeSO}_4] = 40 \text{ mg L}^{-1}$ , pH 2, vol. 1L, stirring rate 75 rpm,  
[H<sub>2</sub>O<sub>2</sub>] = varied 0.88, 1.76, 2.7, 3.53 and  $4.4 \text{ mM L}^{-1}$

### 3.6.2. Influence of ferrous sulphate on the oxidation kinetics

The influence of ferrous sulphate concentration on the oxidation of Direct Catachine Brown was studied by fixing the concentrations of hydrogen peroxide and the dye at  $367 \text{ mg L}^{-1}$  and  $150 \text{ mg L}^{-1}$  respectively. The concentration of ferrous sulphate was varied. The results are shown in figure 3.31. Variation of initial rates with Ferrous sulphate concentration gives a linear plot passing through the origin indicating that the reaction is first order with respect to ferrous sulphate.

Results indicate that the initial rates increased linearly with increasing ferrous sulphate concentration up to  $120 \text{ mg L}^{-1}$ . Further increase resulted in a decrease in the initial rates. Since, the concentration of ferrous sulphate was varied at a constant concentration of hydrogen peroxide, the fall in initial rates could be due to the hydrogen peroxide concentration becoming limiting. This results in an increased accumulation of ferrous ions in solution. Of the two it is hydrogen peroxide, which is the de facto oxidant. Ferrous ions only function as catalyst that facilitates the homolysis of hydrogen peroxide. The excess ferrous ions would react with hydrogen peroxide at a very fast rate to yield hydroxyl radicals until all the hydrogen peroxide present in the reactor is utilized. It is up to this point that the rate coefficient values would continue to increase with an increase in the concentration of ferrous ions. Beyond a certain limit further increase in ferrous sulphate concentration leads to accumulation without an active role for catalysis.

The influence of ferrous sulphate on the oxidation kinetics of Reactive Yellow was studied by fixing the concentration of dye at  $75 \text{ mg L}^{-1}$  and hydrogen peroxide at  $110 \text{ mg L}^{-1}$  for varied concentrations of ferrous sulphate. The ferrous sulphate concentrations chosen for the experiments were 40, 50, 60, 70 and  $80 \text{ mg L}^{-1}$ . The results are shown in figure 3.32.

From figure 3.32 it can be seen that as the concentration of ferrous sulphate is increased there is a linear increase in the initial rate up to a concentration of  $70 \text{ mg L}^{-1}$  after which the initial rates show a decrease. This indicates the negative influence of excess ferrous sulphate concentration. Bandara et al., 1996 investigated the degradation of Orange II by Fenton type reagent aided by sunlight. They observed that stable iron complexes in combination with hydrogen peroxide and the near surface radical formation are processes actively responsible for abatement of the dye. A plot of initial rates against the concentration of ferrous sulphate is a linear up to the limiting concentration indicating that the reaction is first order with respect to ferrous sulphate.

This indicates that when the concentration of ferrous ions is lesser than that of hydrogen peroxide concentration the decomposition of hydrogen peroxide will be catalyzed by ferrous ions generating hydroxyl radicals. Under such conditions hydroxyl radicals would mediate oxidation of the dye. This is indicated by an increase in the initial rates. This phenomenon would continue up to an optimum ferrous sulphate concentration. However, as the concentration is raised above the optimum, ferrous ions begin to exceed the concentration of hydrogen peroxide. The

small amounts of hydrogen peroxide present would be immediately decomposed by ferrous ions and the remaining excess ferrous ions would accumulate in the medium. This is undesirable, as excess ferrous ions are known to scavenge hydroxyl radicals to form hydroperoxyl radicals of lower reactivity. These hydroperoxyl radicals resulting in a decrease in the initial rates would now mediate oxidation of the dye. Ferric ions produced by the oxidation of ferrous ions can also scavenge hydroperoxyl radicals.

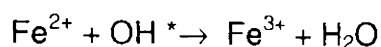
Influence of ferrous sulphate on Fenton's oxidation of Acid Orange was studied by fixing the concentration of hydrogen peroxide at  $91.7 \text{ mg L}^{-1}$  (obtained optimum) and the dye at  $50 \text{ mg L}^{-1}$ , for varying concentrations of ferrous sulphate. The ferrous sulphate concentration was varied in such a manner that there was one concentration below the observed optimum, one concentration at the optimum and three concentrations above the optimum. Figure 3.33 shows the variation in initial rates with concentration of ferrous sulphate.

From the figure (3.33) it can be seen that the initial rate increases with an increase in the concentration of ferrous sulphate up to a limiting concentration of  $60 \text{ mg L}^{-1}$  after which a further increase results in a decrease in the initial rates. Indicating that at high ferrous sulphate concentrations the excess ferrous ions scavenge the hydroxyl radicals. This is similar to the observation made by Tang and Huang (1996), who state that because both  $\text{Fe}^{2+}$  and  $\text{H}_2\text{O}_2$  can react with  $\text{OH}^*$ , so neither of them should be overdosed if the maximum reaction rate is to be achieved. Wang et al., (1998) observed a decrease in the dechlorination rate of tetra

chloroethene with time during Fenton oxidation. This was attributed to the conversion of Fe (II) to Fe (III).

Up to an optimum ferrous sulphate concentration of 60 mg L<sup>-1</sup>, the initial rates increased linearly with the regression line passing through origin indicating that the reaction is first order with respect to ferrous sulphate.

Fig. 3.33 indicates that both low and high ferrous sulphate concentrations can have a negative impact on oxidation rate of the dye. This is because when the concentration of ferrous sulphate is lower than the concentration of hydrogen peroxide, ferrous ions would catalyze the decomposition of hydrogen peroxide to form highly reactive hydroxyl radicals. These hydroxyl radicals in turn oxidize the dye. Under such conditions, rate of the reaction would show an increase with an increase in the ferrous sulphate concentration up to an optimum (which is at 60 mg L<sup>-1</sup>). Further increase would result in the concentration of ferrous ions exceeding that of hydrogen peroxide. So initially hydrogen peroxide would be rapidly decomposed by ferrous ions, after which the remaining ferrous ions would simply accumulate in the reaction mixture. This increased accumulation of ferrous ions is undesirable as they lead to scavenging of hydroxyl radicals and form hydroperoxyl radicals thereby decreasing the reaction rate (Huston and Pignatello., 1999) according to the equation.



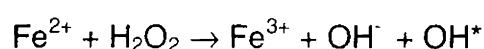


From Fig. 3.33 it can be seen that the initial rates increased linearly with an increase in ferrous sulphate up to a limiting concentration of 60 mg L<sup>-1</sup>. The plot is linear and passes through origin indicating that the reaction is first order with respect to ferrous sulphate.

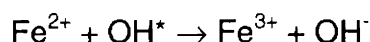
One common feature observed irrespective of the dye class (Direct, Reactive and Acid dye) is that although there is an initial increase in the rate of oxidation with an increase in ferrous sulphate concentration, beyond an optimum, the increased concentration was found to negatively influence the rate of reaction by actually decreasing the reaction rate for further increase. These observations made with respect to the three dyes namely Direct Catachine Brown, Reactive Yellow and Acid Orange can be accounted for by considering observations made by other authors working in similar or related fields.

Yoon et al. (2001) investigated the reaction pathway of OH radicals produced by Fenton oxidation in wastewater treatment. They observed that high concentrations of ferrous ions enhanced the production of hydroxyl radicals that led to faster consumption of hydrogen peroxide. A possible draw back associated with such a system is the scavenging of hydroxyl radical by the ferrous ions. They did not report the optimal concentrations.

On the basis of the above discussion the probable mechanism followed could be summarized as



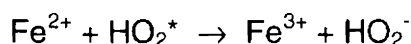
This step would continue up to an optimum concentration of ferrous ions. Under conditions of an excess of ferrous ions the hydroxyl radicals formed are scavenged according to the reaction



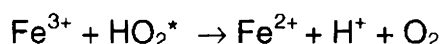
Or, the hydroxyl radical can undergo a dismutation reaction



Or, the hydroperoxyl radical may be scavenged by the ferrous ions according to the reaction



The ferric ions may be recycled to ferrous ions by the reaction



These reactions can contribute to a decrease in the initial rates at excessive concentrations of ferrous ions.

Wang et al. (1998) investigated the effect of pyrophosphate on the dechlorination of tetrachloroethene by Fenton's reagent. A decrease in the dechlorination rate was observed with time. This was attributed to the conversion of Fe (II) to Fe (III) and complexation of Fe (III) with pyrophosphate.

Kang et al. (1999) applied Fenton's reagent to degrade 2,4-dinitrophenol. At low dosages of ferrous ions and hydrogen peroxide, a linear increase in the initial removal rate of DNP is observed while at higher dosages of ferrous ions (>1mM) the effect was insignificant.

Liao et al. (1999) studied the effects of ferrous, hydrogen peroxide and pH on the oxidation of effluents from a dye-manufacturing unit. Oxidation increased with concentration of ferrous ions during the initial reaction periods. However as the reaction progressed with an increase in the ferrous ions the removal profiles leveled off due to the lack of hydrogen peroxide residue.

The influence of ferrous sulphate on oxidation kinetics of Methylene Blue was studied by fixing the concentrations of hydrogen peroxide at 60 mg/L and dye concentration at 10 mg L<sup>-1</sup>. The concentration of ferrous sulphate was varied from 10 to 50 mg L<sup>-1</sup>.

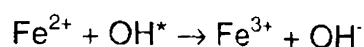
The variation in initial rates for different ferrous sulphate concentrations is shown in figure 3.34.

Kang et al. (1999) observed a linear increase in the initial degradation rates of DNP and color at low dosages of ferrous ions and hydrogen peroxide. At High concentration of ferrous ions (>1mm) the response was insignificant.

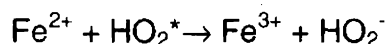
Liao et al. (1999) observed that during the initial reaction periods the rate of oxidation process increased at higher intensity of radiation and concentration of ferrous ions. As the reaction progressed with an increase in the ferrous ions the removal profiles leveled off due to the lack of hydrogen peroxide residue.

Wang et al. (1998) studied the Fenton oxidation of tetrachloroethene and observed a decrease in the dechlorination rate with time. This was attributed to the conversion of Fe (II) to Fe (III).

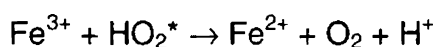
Figure 3.34 indicates that the initial rates increased with an increase in the concentration of ferrous sulphate up to 0.14 mM after which the initial rates leveled off. This trend indicates that a further increase in the ferrous sulphate concentration could lead to a decrease in the initial rates. Isak et al. (1996) studied the oxidation kinetics of aldehydes by Fenton's reagent and observed that  $\text{Fe}^{2+}$  played the role of a catalyst dissociating  $\text{H}_2\text{O}_2$  to  $\text{OH}^*$  and  $\text{OH}^-$ . Liao et al. (1999) studied the use of Photo-Fenton oxidation for the removal of COD and color from dye wastewater. The oxidation process was enhanced for increased concentration of ferrous ions during the initial reaction periods. However as the reaction progressed, with an increase in the ferrous ions the removal profiles leveled off due to the lack of hydrogen peroxide residue. This is a very likely phenomenon, as ferrous sulphate at high concentrations decrease the rate of oxidation of the dye by scavenging hydroxyl radicals. Initially, ferrous sulphate added would catalyze the oxidation of hydrogen peroxide in the medium. Yoon et al., (2001) investigated the reaction pathway of  $\text{OH}^-$  radicals produced by Fenton oxidation in wastewater treatment. The authors found that high concentrations of ferrous ions enhanced the production of hydroxyl radicals and led to faster consumption of hydrogen peroxide. An increase in the ferrous sulphate concentration beyond an optimum leads to undesirable and excessive accumulation of ferrous ions in the reaction mixture. These ferrous ions scavenge the hydroxyl radical through the following equation



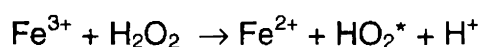
The little of the hydroperoxyl radical that is formed would also react with the excess of ferrous ions according to the following reaction and get scavenged.



$\text{Fe}^{3+}$  formed in the above step can also scavenge the hydroperoxyl radical according to the following equation



The  $\text{Fe}^{3+}$  formed can also react with hydrogen peroxide according to the equation



However, the hydroperoxyl radical formed has a lower reactivity.

Ferrous ions are generated in low concentrations and the absence of hydroxyl radical does not permit any reaction to take place between the two. This could lead to a decrease in the initial rates.

The initial rates when plotted against ferrous sulphate concentrations fitted well into a second order polynomial expression representing a curve as shown in figure 3.34. This indicates that there could be a complexation step involved with respect to ferrous sulphate also. Therefore, a double reciprocal plot was carried out. The results are shown in figure 3.35.

The double reciprocal plots of initial rates for oxidation of Methylene Blue at different concentrations of ferrous sulphate are shown in figure 3.35. Where  $r_0$  is the initial rates obtained for different ferrous sulphate concentrations and  $[\text{FeSO}_4]_0$  is the initial ferrous sulphate

concentration. The plot was found to be linear with a positive intercept. Since, the concentration of hydrogen peroxide and the dye was maintained constant for varying concentrations of ferrous sulphate a complexation between ferrous sulphate and the dye is most likely. Figure 3.35 confirms complexation with ferrous sulphate.

Joseph J. Pignatello. (1992) studied photo assisted Fenton to catalyze the degradation of chlorophenoxy herbicides. The authors observed that scavenging of the active oxidant and complexation with  $\text{Fe}^{3+}$  could inhibit the reaction.

Herve et al. (1998) studied oxidation of Atrazine by Fe (II)/ $\text{H}_2\text{O}_2$  system. They suggested that the reaction of hydrogen peroxide with ferrous ion involves an intermediate which leads to the formation of another intermediate which reacts with Fe (II) to give Fe (III) with out the formation of  $\text{OH}^*$ .

Sedlak and Andren. (1991) studied the oxidation of chlorobenzene with Fenton's reagent. The authors suggest that complexes of aromatic intermediate compounds with iron and oxygen may play a role in regulating the reaction pathways.

Herrera et al. (1998) studied photo-oxidation of concentrated p-coumaric acid in homogeneous solution and report that Fenton's reagent form precursor intermediates that are susceptible to degradation under light.

Alexei and Kiwi (1997) studied transient intermediate species active during the Fenton – mediated degradation of Quinoline. The authors report

formation of intermediates having a transient lifetime of less than 4 $\mu$ s. The intermediates were affected by reagent concentration, concentration of the oxidant and pH.

Tachiev et al. (2000) studied the Kinetics of hydrogen peroxide decomposition with complexed and "free" iron catalysts. At low pH the ferrous iron was mostly uncomplexed and in the free form, while high pH ranges (6 - 9) resulted in the formation of Fe (III) complexes.

Kwon et al. (1999) studied the oxidation of p-chlorophenol by Fenton's reagent. Occurrence of the slow phase was attributed to depletion of ferrous ions caused by the formation of Fe – organic complex.

Nadtochenko and kiwi (1997) studied photo induced adduct formation between orange II and Fe<sup>3+</sup> (aq) or Fe(OX)<sub>3</sub><sup>3-</sup>H<sub>2</sub>O<sub>2</sub> using steady state and pulsed laser photolysis. They reported that the excited states of Fe(OX)<sub>3</sub><sup>3-</sup> or the (FeIII)-Orange II) complexes are the active species during the decolorization of the dye. Based on a radical theory of Fenton catalysis and direct evidence obtained from laser spectroscopy, the authors established the formation of OH\* adducts for Orange II as the initial degradation step leading to observed oxidation of the dye.

Herrera et al. (1999) studied the photochemical decolorization of Remazol Brilliant Blue and Uniblue A in the presence of Fe<sup>3+</sup> and H<sub>2</sub>O<sub>2</sub> through Laser flash photolysis. The authors report that electron transfer between the excited dye and Fe<sup>3+</sup> was found to be the initiating step, either as a bimolecular process ( $D^* + Fe^{3+} = D^{0+} + Fe^{2+}$ ) or through a dye - iron complex ( $D^* + Fe^{3+} = D \dots Fe^{3+}$ ) which again forms ( $D^{0+} + Fe^{2+}$ ). A radical

chain reaction is observed between  $\text{Fe}^{3+}/\text{H}_2\text{O}_2$  during the initiation step. Photo dissociation reaction of the  $\text{D}\dots\text{Fe}^{3+}$  complex is found to be more important in the initiation of chain reaction rather than bimolecular quenching between  $\text{D}^*$  and  $\text{Fe}^{3+}$ .

Esther et al. (1995) studied the Reactions of low transition metal complexes with hydrogen peroxide. The results indicated the formation of an Iron (II) peroxide intermediate complex which at  $\text{pH} < 5.5$  decompose to yield free hydroxyl radical. This indicated that the non-participating ligand-L had an appreciable effect on the reaction mechanism of the metal center with hydrogen peroxide.

Sawyer (1997) studied Metal Hydro peroxide induced activation of dioxygen ( $\text{O}_2$ ) for the ketonization of hydrocarbons by Fenton reagent. The authors established that Fenton chemistry involves the formation of hydro peroxide ( $\text{ROOH}$ ) adducts of reduced transition metals [ $\text{Fe}$  (II),  $\text{Cu}$  (I) and  $\text{Co}$  (II)] via nucleophilic addition. These reactive intermediates react with excess catalyst to form  $\text{L}_x\text{Fe}^{(\text{III})}\text{OH}$  (R) or with excess  $\text{ROOH}$  to form  $\text{O}_2$ ,  $\text{H}_2\text{O}$  and  $\text{ROH}$  or with excess hydrocarbon (RH) to form  $\text{ROH}$  (Fenton chemistry) or with ambient dioxygen to form adduct  $[\text{L}_x^- [\text{Fe}^{(\text{III})} - \text{OOR}, \text{BH}^+]$ .



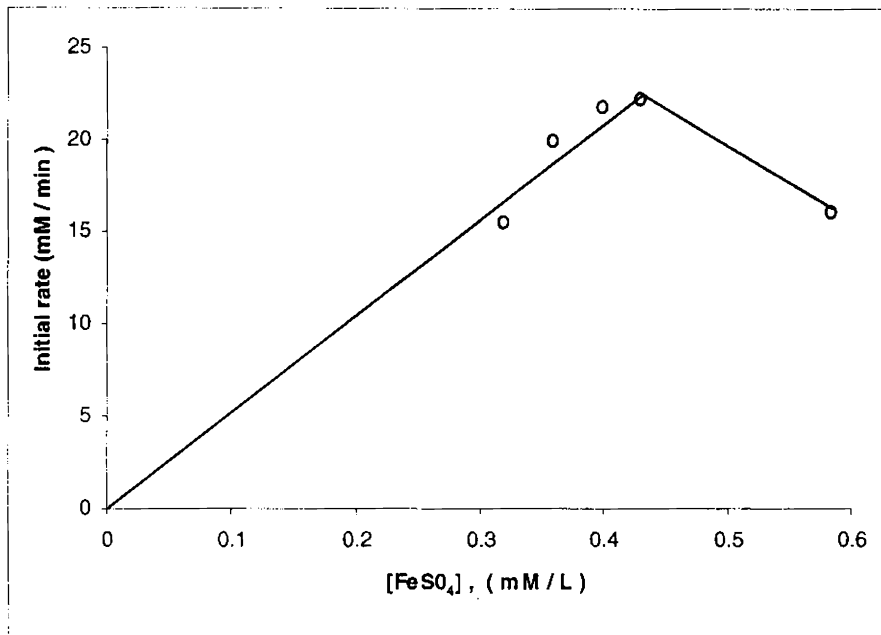


Figure 3.31

Direct Catachine Brown ( DCB )

Variation of initial rates with ferrous sulphate concentration

$[\text{DCB}] = 150 \text{ mg L}^{-1}$ ,  $[\text{H}_2\text{O}_2] = 367 \text{ mg L}^{-1}$ , pH 2, vol. 1L, stirring rate 75 rpm,

$[\text{FeSO}_4] = \text{varied } 0.32, 0.36, 0.40, 0.43 \text{ and } 0.47 \text{ mg L}^{-1}$

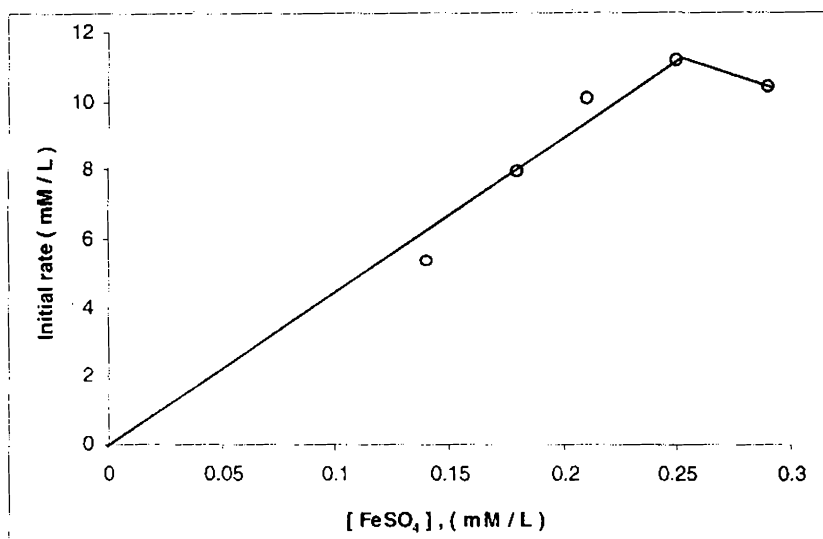


Figure 3.32

Reactive Yellow ( RY )

Variation of initial rates with ferrous sulphate concentration

[RY] = 75 mg L<sup>-1</sup>, [H<sub>2</sub>O<sub>2</sub>] = 110 mg L<sup>-1</sup>, pH 2, vol. 1L, stirring rate 75 rpm,

[FeSO<sub>4</sub>] = varied 0.14, 0.18, 0.21, 0.25 and 0.29 mM L<sup>-1</sup>

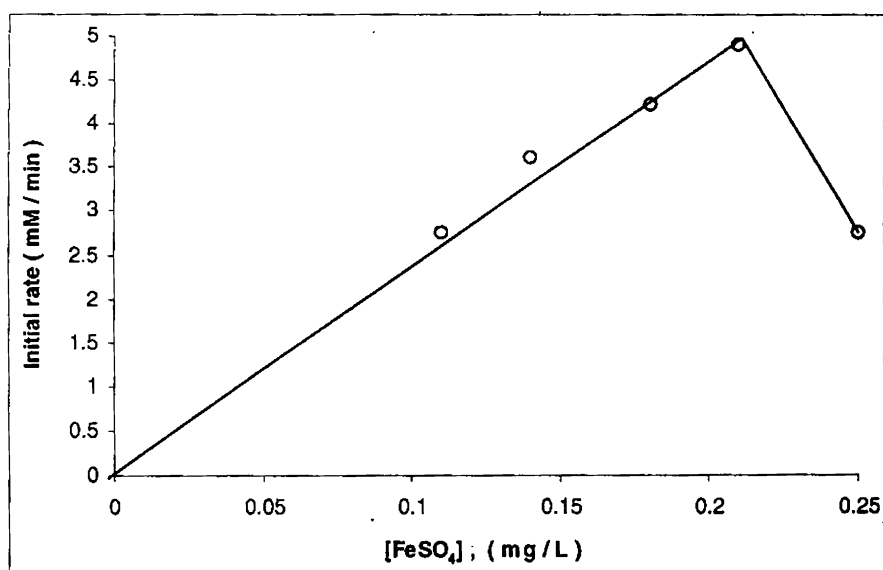


Figure 3.33

Acid Orange ( AO )

Variation of initial rates with ferrous sulphate concentration

[AO] = 50 mg L<sup>-1</sup>, [H<sub>2</sub>O<sub>2</sub>] = 91.7 mg L<sup>-1</sup>, pH 2, vol. 1L, stirring rate 75 rpm,

[FeSO<sub>4</sub>] = varied 0.11, 0.14, 0.18, 0.21 and 0.25 mM L<sup>-1</sup>

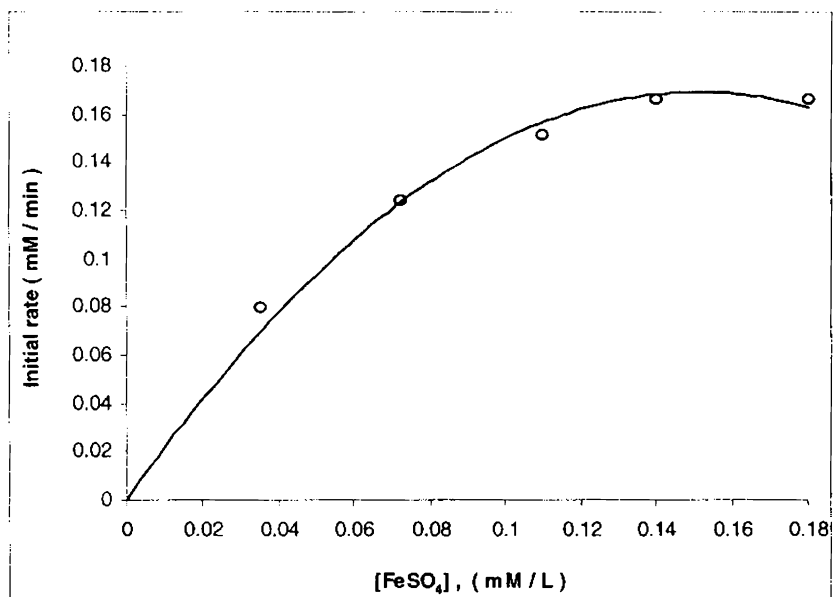


Figure 3.34

Methylene Blue ( MB )

Variation of initial rates with ferrous sulphate concentration

[MB] = 10 mg L<sup>-1</sup>, [H<sub>2</sub>O<sub>2</sub>] = 60 mg L<sup>-1</sup>, pH 2, vol. 1L, stirring rate 75 rpm,

[FeSO<sub>4</sub>] = varied 0.035, 0.072, 0.11, 0.14 and 0.18 mM L<sup>-1</sup>

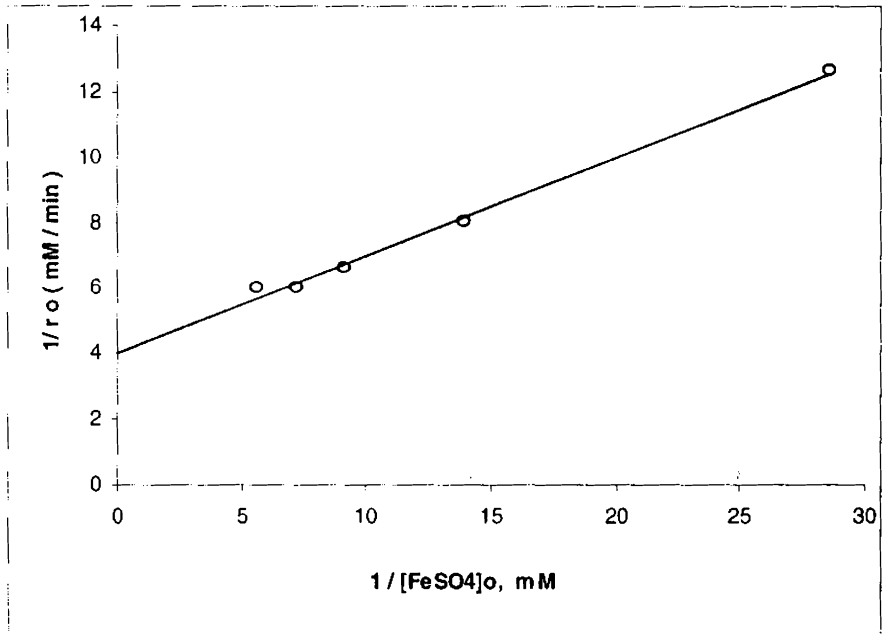


Figure 3.35

Methylene Blue ( MB )

Double reciprocal plot of initial rate against ferrous sulphate concentration

$[\text{MB}] = 10 \text{ mg L}^{-1}$ ,  $[\text{H}_2\text{O}_2] = 60 \text{ mg L}^{-1}$ , pH 2, vol. 1L, stirring rate 75 rpm,

$[\text{FeSO}_4] = \text{varied } 0.035, 0.072, 0.11, 0.14 \text{ and } 0.18 \text{ mM L}^{-1}$

### 3.6.3. Influence of dye concentration on oxidation kinetics

Influence of concentration of the dye on kinetics of Fenton's oxidation of Direct Catachine Brown was studied by fixing the concentration of hydrogen peroxide at  $367 \text{ mg L}^{-1}$  and ferrous sulphate at  $100 \text{ mg L}^{-1}$ . The concentrations of the dye ranged from 50 to  $400 \text{ mg L}^{-1}$ . The variation in initial rates for different concentrations of Direct Catachine Brown is shown in figure 3.36.

The initial rates were found to increase linearly with an increase in the concentration of the dye up to  $300 \text{ mg L}^{-1}$ . However, the observed decrease in initial rates when the concentration of the dye was raised to  $400 \text{ mg L}^{-1}$  could be due to inhibition of the hydroxyl radical formation due to the reaction between ferrous ions and hydrogen peroxide.

The influence of dye concentration on the Fenton oxidation of Reactive Yellow has been established by fixing the concentration of hydrogen peroxide and ferrous sulphate at 110 and  $60 \text{ mg L}^{-1}$  (the obtained optimum concentrations) respectively for varying dye concentrations. The dye concentrations studied ranged from  $25 \text{ mg L}^{-1}$  to  $125 \text{ mg L}^{-1}$ . Fig. 3.37 illustrates the results obtained. On the basis of the obtained results it is inferred that the initial rates showed a linear variation with an increase in the dye concentration. Indicating that the reaction can be considered first order with respect to the dye. This can be accounted, as at increased concentrations there is an increased collision between dye molecules and the hydroxyl radicals produced, leading to an increase in initial rates.

Influence of dye concentration on the kinetics of Fenton oxidation of Methylene Blue was studied for different concentrations of the dye ranging from  $4 \text{ mg L}^{-1}$  to  $20 \text{ mg L}^{-1}$  keeping ferrous sulphate and hydrogen peroxide concentrations fixed at the observed optimums of  $40$  and  $60 \text{ mg L}^{-1}$  respectively. Variation in initial rates for different concentrations of the dye is shown in figure 3.38. Results indicate that the variation in initial rates with dye concentration is linear indicating that the reaction is first order with respect to Methylene Blue.

Salem and Maazawi (2000) studied the Kinetics and mechanism of color removal of Methylene Blue with hydrogen peroxide catalyzed by supported alumina surfaces. The authors observed that Fenton oxidation was first order with respect to Methylene Blue and with respect to hydrogen peroxide and ferrous sulphate the order was found to be dependent on the concentration range.

Influence of dye concentration on Fenton's oxidation of Acid Orange has been studied by fixing the concentration of hydrogen peroxide (at  $91.7 \text{ mg L}^{-1}$ ) and ferrous sulphate (at  $40 \text{ mg L}^{-1}$ ) as obtained through the optimization experiments for varying concentrations of the dye. Concentration range chosen for the experiment ranged from  $0$  to  $100 \text{ mg/L}$ . Fig. 3.39 illustrates the influence of concentration of Acid Orange on Fenton oxidation. The study indicated that the initial rates increased linearly with dye concentration up to  $80 \text{ mg L}^{-1}$ .

One common feature observed irrespective of the dye class, is that the initial rates increased linearly with an increase in the dye

concentration. This can be accounted for by the collision theory, according to which, with an increase in the dye concentration there would be an increased collision between the dye molecules and hydroxyl radicals leading to an increase in the rate of the reaction. However exceptions have been observed in the case of Direct Catachine Brown and Acid Orange where although at lower dye concentrations the increase in the rate of the reaction is linear, at higher dye concentrations (300 and 80 mg L<sup>-1</sup> respectively), a decrease in rate of the reaction with an increase in the dye concentration has been observed. This could be because, increased dye concentrations probably interferes with the reaction between ferrous ions and hydrogen peroxide thereby inhibiting the activity of hydroxyl radicals.



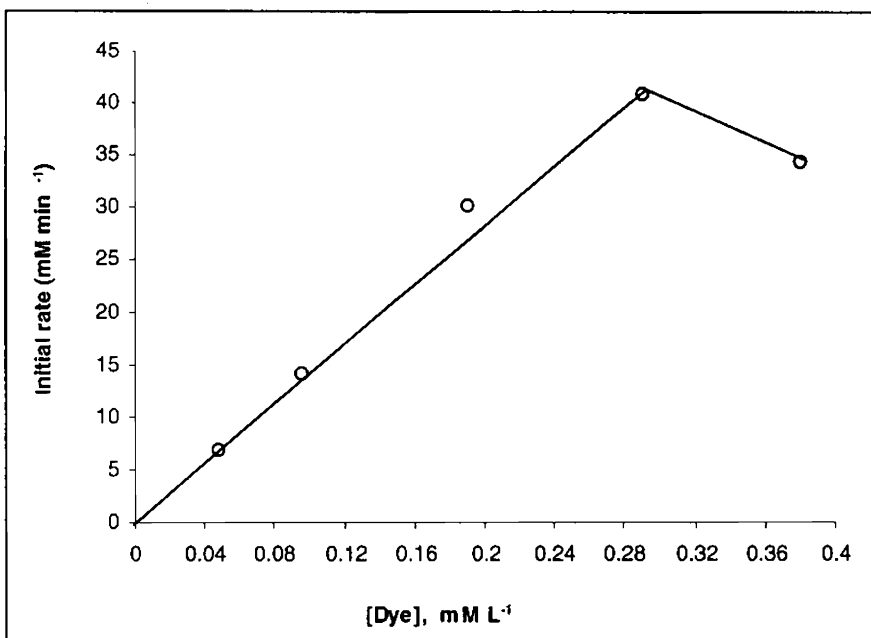


Figure 3.36

Direct Catachine Brown

Variation of initial rates with hydrogen peroxide concentration

[H<sub>2</sub>O<sub>2</sub>] = 367 mg L<sup>-1</sup>, [FeSO<sub>4</sub>] = 100 mg L<sup>-1</sup>, pH 2, vol. 1L, stirring rate 75 rpm,

[DCB] = varied 0.048, 0.096, 0.19, 0.29 and 0.38 mM L<sup>-1</sup>

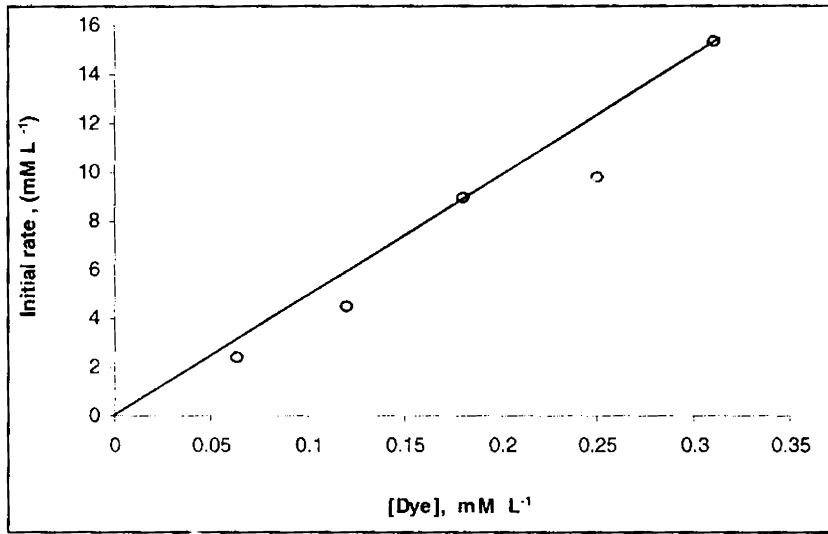


Figure 3.37

Reactive Yellow

Variation of initial rates with hydrogen peroxide concentration

[H<sub>2</sub>O<sub>2</sub>] = 110 mg L<sup>-1</sup>, [FeSO<sub>4</sub>] = 60 mg L<sup>-1</sup>, pH 2, vol. 1L, stirring rate 75 rpm,

[RY] = varied 0.063, 0.12, 0.18, 0.25 and 0.31 mM L<sup>-1</sup>

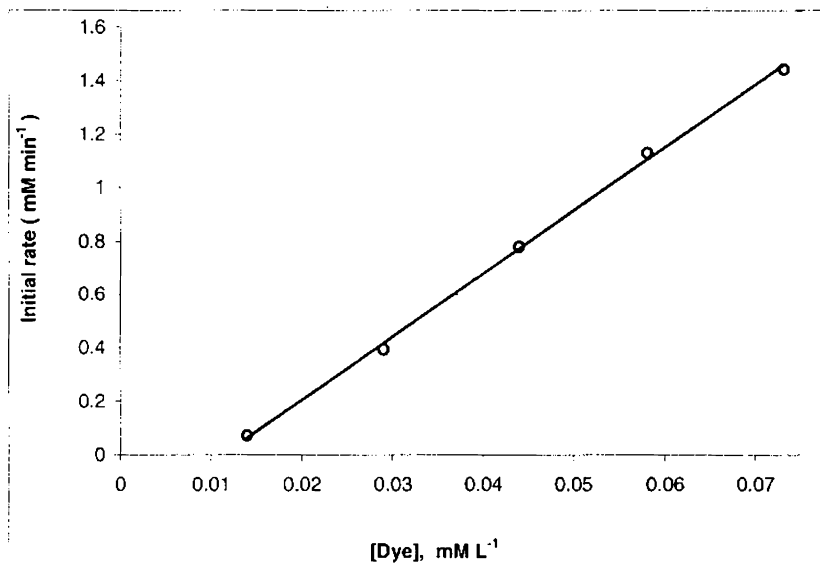


Figure 3.38

Methylene Blue (MB)

Variation of initial rates with hydrogen peroxide concentration

$[\text{H}_2\text{O}_2] = 60 \text{ mg L}^{-1}$ ,  $[\text{FeSO}_4] = 40 \text{ mg L}^{-1}$ , pH 2, vol. 1L, stirring rate 75 rpm,

$[\text{MB}] = \text{varied } 0.0125, 0.025, 0.0375, 0.05 \text{ and } 0.0625 \text{ mM L}^{-1}$

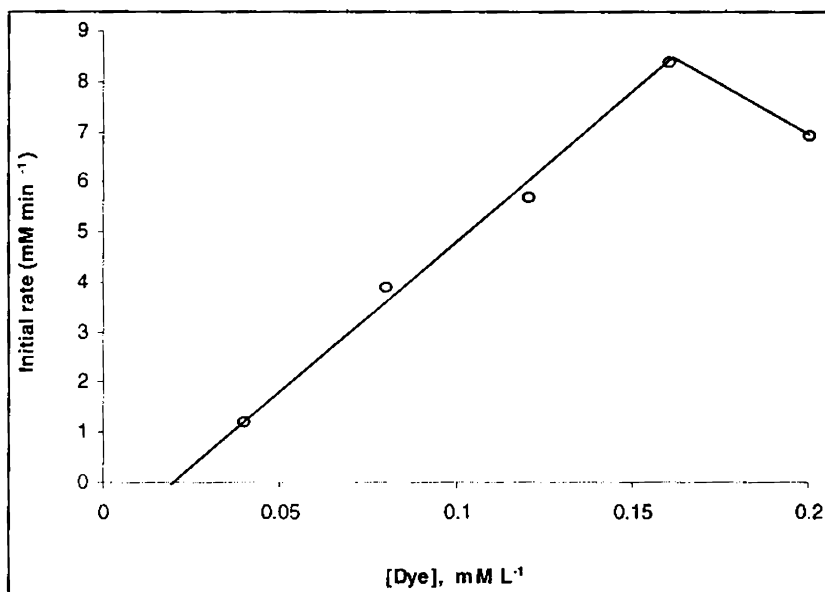


Figure 3.39

Acid Orange (AO)

Variation of initial rates with hydrogen peroxide concentration

[H<sub>2</sub>O<sub>2</sub>] = 60 mg L<sup>-1</sup>, [FeSO<sub>4</sub>] = 40 mg L<sup>-1</sup>, pH 2, vol. 1L, stirring rate 75 rpm,

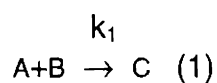
[AO] = varied 0.04, 0.08, 0.12, 0.16 and 0.20 mM L<sup>-1</sup>

### 3.6.4. Reaction mechanisms

- (i) Where the reaction is first order with respect to [Dye], [H<sub>2</sub>O<sub>2</sub>] and [FeSO<sub>4</sub>]

If we assume that the reaction comprises of two equations.

Equation (1) represents the fast step and equation (2) represents the slower one.



$$\text{Rate} = k_2[C] [D]$$

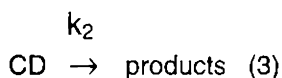
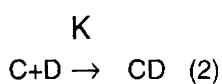
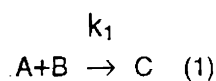
$$[C] = k_1[A] [B]$$

$$\text{Rate} = k_1k_2[A] [B] [D]$$

$$\text{Rate} = K[A] [B] [D]$$

Where [A] represents concentration of ferrous sulphate  
 [B] represents concentration of hydrogen peroxide  
 [C] represents concentration of hydroxyl radical formed  
 as a result of the reaction between [A] and [B]  
 [D] represents dye concentration  
 k<sub>1</sub> and k<sub>2</sub> represents rate constants  
 K represents equilibrium constant.

- (ii) Where there is complex formation both with respect to  $[\text{H}_2\text{O}_2]$  and  $[\text{FeSO}_4]$  but first order with respect to dye



$$\text{Rate} = k[\text{CD}]_e = kK[\text{C}]_e [\text{D}]_e$$

$$K = \frac{[\text{CD}]_e}{[\text{C}]_e [\text{D}]_e}$$

$$[\text{D}]_t = [\text{D}]_e + K[\text{C}]_e [\text{D}]_e$$

$$[\text{D}]_e = \frac{[\text{D}]_t}{1+K[\text{C}]_e}$$

$$\text{Rate} = \frac{kK[\text{C}]_e [\text{D}]_t}{1+K[\text{C}]_e}$$

$$\text{Rate} = \frac{kK k_1 [\text{A}] [\text{B}] [\text{D}]}{1+ k_1 K [\text{A}] [\text{B}]}$$

At constant D and B

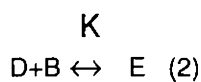
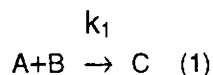
$$\text{Rate} = \frac{\text{const. } [\text{A}]}{1+ \text{const. } [\text{A}]}$$

At constant D and A

$$\text{Rate} = \frac{\text{const. } [\text{B}]}{1+ \text{const. } [\text{B}]}$$

- where  $[\text{A}]$  represents concentration of ferrous sulphate  
 $[\text{B}]$  represents concentration of hydrogen peroxide  
 $[\text{C}]$  represents concentration of hydroxyl radical formed as a result of the reaction between  $[\text{A}]$  and  $[\text{B}]$   
 $[\text{D}]$  represents dye concentration  
 $[\text{E}]_e$  represents an intermediate complex  
 $k_1$  and  $k_2$  represents rate constants  
 $K$  represents equilibrium constant.

- (iii) Where there is complex formation with respect to  $[H_2O_2]$  and first order with respect to  $[FeSO_4]$  and dye



$$[C] = k_1[A][B]$$

$$[E]_e = K[D]_e[B]_e$$

$$\text{Rate} = k[E]_e[C]_e$$

$$\text{Rate} = kK[D]_e[B]_e[C]$$

$$[D]_t = [D]_e + [E]_e$$

$$= [D]_e + K[D]_e[B]_e$$

$$= [D]_e\{1 + K[B]_e\}$$

$$[D]_e = \frac{[D]_t}{1 + K[B]_e}$$

If  $[B]$  is large,  $[B]_e = [B]_t$

$$[D]_e = \frac{[D]_t}{1 + K[B]_t}$$

$$\text{Rate} = \frac{kK k_1 [D]_t [B]_t [C]}{1 + K[B]_t}$$

Where  $[A]$  represents concentration of ferrous sulphate  
 $[B]$  represents concentration of hydrogen peroxide  
 $[C]$  represents concentration of hydroxyl radical formed as a result of the reaction between  $[A]$  and  $[B]$   
 $[D]$  represents dye concentration  
 $[E]_e$  represents an intermediate complex  
 $k_1$  and  $k_2$  represents rate constants  
 $K$  represents equilibrium constant.

### 3.6.5. Conclusions

1. Findings reported on kinetic profile during oxidation of dyes with Fenton's reagent are in good agreement with observations of earlier workers on other organic substrates. This work goes a step further. Critical concentration of the dye at which the reaction mechanism undergoes transition has been identified. Fenton oxidation of all the dyes studied occurred in two distinct stages:

- (i) An initial fast step where the percentage decolorization can range from less than 10% to 100% depending on the concentration of ferrous sulphate and hydrogen peroxide chosen for the experiment. This part of the reaction was too rapid to be effectively monitored.
- (ii) A slow step, which begins from the point of initial dip and then takes the reaction to completion at a rate that is slower and can be controlled by a judicious choice of ferrous sulphate and hydrogen peroxide concentrations. This slow step can be monitored.

2. The oxidation of Reactive Yellow showed that the initial rates for decolorization increased linearly with an increase in hydrogen peroxide concentration over the range studied. Since the initial rates increased linearly with an intercept at origin, the oxidation reaction was considered to follow first order kinetics. In the case of Direct Catachine Brown the initial rates although increased linearly at lower



hydrogen peroxide concentrations, beyond an optimum concentration resulted in a decrease in the initial rates, as excessive hydrogen peroxide concentrations results in a decrease in the oxidation rate due to scavenging of hydroxyl radicals. However up to the point of increase the initial rates increased linearly with an intercept at the origin indicating that the reaction is first order with respect to hydrogen peroxide. In the case of Acid Orange and Methylene Blue the variation in initial rates fitted a first order polynomial representing a curve, which in turn gave a linear fit for the double reciprocal plot with a positive intercept. These observations confirm that of a complexation step is involved in the Fenton oxidation of Acid Orange and Methylene Blue.

3. Fenton oxidation of all dyes except Methylene Blue showed that the initial rates increased linearly with an in the ferrous sulphate concentration. This increase was observed only up to an optimum concentration beyond which further increase resulted in a decrease in the initial rates. Variation of initial rates with Ferrous sulphate concentration resulted in a linear plot passing through the origin indicating that the reaction is first order with respect to ferrous sulphate. However in the case of Methylene Blue the initial rates when plotted against ferrous sulphate concentrations fitted well into a second order polynomial expression representing a curve. This indicates that there could be a complexation step involved with

respect to ferrous sulphate. A linear plot with positive intercept in the double reciprocal plot of initial rates against hydrogen peroxide concentration confirmed complexation.

4. Fenton oxidation is first order with respect to the dye concentration irrespective of the dye class, as a linear increase in initial rates with increase in dye concentration was observed. However a few exceptions have been noticed. In the case of Reactive Yellow and Methylene Blue when the initial rates increased with increase in the dye concentration over the entire concentration range chosen for the experiments, in the case of Direct Catachine Brown and Acid Orange although a linear increase in initial rates was observed at low dye concentrations, higher concentrations were found to inhibit the activity of hydroxyl radicals and thereby resulting in a decrease in the initial rates.

## **References**

## References (Chapter – I)

Abraham Reife and Harold S. Freeman. (1996). Carbon adsorption of dyes and selected intermediates. In. *Envtl. Chemistry of Dyes and Pigments*, Eds. John Wiley and Sons, Inc.

Ajmal and Khan. (1985) Effect of textile factory effluent on soil and crop plant. *Environ. Pollut. Ser. A*. **37**, 131-148

Alves, Ana Maria Brites; De Pinho and Maria Norberta (2000) Ultra filtration for color removal of tannery dyeing wastewaters. *Desalination*, **130**(2), 147-154.

Bailey P.S. Ozonation In Organic Chemistry. Vol. I, Academic Press, New York, 1978.

Bailey P.S. Ozonation In Organic Chemistry. Vol. II, Academic Press, New York, 1982.

Beydilli M.I., Pavlostathis S.G. and Tincher W.C. (1998) Decolorization and toxicity screening of selected reactive azo dyes under methanogenic conditions. *Wat. Sci. Tech.* **38**(4-5), 225-232.

Boe R.W. Pilot-Scale Study on anaerobic-aerobic treatment of textile dye wastewater, M.S. Thesis, VPI&SU, Oct. 1993.

Boe R.W., Boardman G.D., Dietrich A.M., Milchelsen D.L. and Pudali M. Pilot Scale Study On Anaerobic Treatment Of A Textile Wastewater. Prepared for the 25<sup>th</sup> Mid-Atlantic Industrial and Hazardous Waste Conference. Univ. of Maryland, college park, July 1993.

Brown D. and Hamburger B. (1987) The degradation of dyestuffs: Part-III- investigations of their ultimate degradability. *Chemosphere*, **16**(7), 1539-1553.

Buffle J. Complexation Reactions In Aquatic Systems, Ellis Horwood Ltd., Chichester, 1988.

Carriere J., Mourato D and Jones J.P. Answers To Textile Wastewater Problems: Membrane Filtration And Membrane Bio-reactor Systems, AATCC Book of papers, 1993 International Conference And Exhibition, Montreal, Quebec, Oct, 3-6, 1993, p. 224.

Cheremisinoff P.N., Ellerburch F., eds., Carbon Adsorption Handbook, Ann Arbor Science, Ann Arbor, MI, 1978.

Cho, Nam-Seok; Lee, Jae-Won; Park, Jong-Moon; Choi, Tac-Ho; Leonowicz, Andrzej (1999) Decolorization of kraft pulp bleaching effluent by white-rot fungi. *Polpu, Chongi Gisul*, **31**(4),361-763.

Chou E.C., Wiegere B.W., Huggins D.K. and Wiewiorowski E.I. U.S.Patent 4,544,541, 1984.

Ciorba, George A., Radovan, Ciprian, Vlaicu, Ilie and Iovi, Aurel (2001) Colour removal from simulated dye wastewaters by electrochemical treatment. Proceedings -Electrochemical Society, 2001-23 (Energy and Electrochemical Processes for a Cleaner Environment), 35-44.

Conneely A., Smyth W.F. and McMullan G. (1999) A study of microbial degradation of metal pthalocyanine textile dyes by HPLC and Atomic Absorption. *J. Phorphyrins Pthalocyanines*. **617**, 5521-5529.

Cook M.M., Ulman J.A., Iraclidis A., Stennick R.S. and Barratt D.A. Abstracts of papers, 203<sup>rd</sup> National Meeting of the American Chem. Society, San. Francisco, C.A, 1992, Environmental Chemistry Division.

Coupal B. and Lalancette J.M. (1976) The treatment of waste waters with peat moss. *Wat. Res.* **10**, 1071-1076.

Davies R.A., Kaempf H.J. and Clemens M.M. (1973) Removal of organic material by adsorption on activated carbon from chemical and industrial effluents. *Textile Chem. Col.* **9**, 827-832.

Davis G.M., Koon J.H. and Adams C.E. (1982) Treatment Of Two Textile Dye House Wastewaters. Proc. 37<sup>th</sup> Industrial Waste Conference, pp 981-997, Purdue Univ., West Lafayette, Ind.

De John P.B. and Hutchins R.A. Treatment of dye wastes with Granular Activated Carbon, AATCC Book of papers, 1975, International Conference and Exhibition, 327.

Dohanyos M., Medera V. and Sedlaeck M. (1978) The adsorption of dyes on activated sludge. *Prog. Nat. Tech.* **10**(5-6), 559.

El Gundi M.S., (1991). Color removal from textile effluents by Adsorption techniques. *Wat. Res.* **25**, 271-273.

Erswell A., Brouckaert C.J. and Buckley C.A. (1988) The reuse of reactive dye liquours using charged ultrafiltration membrane technology. *Desalination*, **70**, 157-167.

Figueiredo, S. A.; Boaventura, R. A.; Loureiro, J. M. (2000) Color removal with natural adsorbents: modeling, simulation and experimental. *Sep. Purif. Technol.*, **20**(1), 129-141.

Friar L.B. and Smith K.M. U.S. Patent. 4, 279, 64, 1980. Chem. Abstr. 95, 223522j (1981).

Gaddis J.L. and Spencer H.G. Proc. Symp. Text. Ind. Tech. EPA – 600/2-79 – 104, U.S. Environmental Protection Agency, Cincinnati, 1979, p. 107.

Ganjidoust, H.; Vosoughi, M. and Ayati, M (2000). Effect of polymers on cellulose wastewater treatment and their comparison with chemical coagulants. *Iran. J. Polym. Sci. Technol.* **13**(1), 37-43. ,

Gardner D.A., Holdsworth T.J., Shaul G.M., Dostal K.A. and Betowski D.L. Aerobic and Anaerobic treatment of C.I. Disperse Blue 79. Prepared by Radian Corporation under contract No. 68-03-3371 for the USEPA office of Research and Development. Cincinnati, Ohio-Document No. EPA/600/2-89/05/Aand B.

Gardiner D.G. and Borne B.J. (1978) Textile wastewater treatment and environmental effects. *J. Soc. Dyers Col.* **94**(8), 339-348.

Ger. Offen. DE 3,148,878 (June 23, 1983), Kroll J., Mols H.H., Ditzer R., Martiny and Steiner K.H. (to Bayer A-G).

Ger. Offen. DE 3, 148,878 (June 23, 1983) Pohlmann H., Gruenbein W., Walch A., Wildhard J., Meininger F., Opitz K and Junghanns E (to Hoechst A-G).

Gordon McKay., Michel. S. Otterburn and Jamal A. Aga. (1985). Fullers earth and fired clay as adsorbents for dye stuffs. Equilibrium and rate studies. *Water, Air and Soil Pollution.* **24**, 307-322.

Gordon McKay. (1980) Color removal by adsorption. *J. Soc. Dyers Col.* **21**(3), 41-44, 66.

Gosh M.M., Woodard F.E., Sproul O.J., Knowlton P.B. and Guertin P.D. (1978) Chlorination of dye house effluents. *J.W.P.C.F.* **50**, 1776-1780.

G.S.Gupta, G.Barad & V.N.Singh (1990) Removal of chrome dye from aqueous solution by mixed adsorbents: fly ash & coal. *Wat. Res.* **24**(1), 45-50.

Grau P., (1991). Textile Industry Wastewaters Treatment. *Wat. Sci. Tech.* **24**(1), 97-103.

Groves G.R., Buckley C.A and Treffry-Goatley K. (1988) A Guide For The Planning, Design And Implementation Of Wastewater Treatment Plants In The Textile Industry- Part II: Effluent Treatment/Water Recycle Systems For Textile Dyeing And Printing Effluents, Water Research Commission, Pretoria, YSBN 0-908356-66-8.

Gruszecka Klaudyna and Jankowski Tomasz. (1998). Treatment of mixed dyes and municipal wastewaters by activated sludge. *Environ. Prot. Engg.* **24**(3-4), 41-52.

Hall S.G. Ph.D. thesis. The adsorption of dispersed dyes on powdered activated carbon. Univ. of North Carolina, Greensboro, North Carolina, 1975, Univ. Microfilms, Ann Arbor, Michigan.

Hitz H.R., Huber W. and Reed R.H. (1978) The adsorption of dyes on activated sludge. *J. Soc. Dyers Col.* **94**, 71-75.

Hitz H.R., Huber W. and Reed R.H. (1978) Publication sponsored by ETAD The adsorption of dyes on Activated sludge. *J.Soc. Dyers. Col.* **2**, 71-76.

Horning R.H. (1997) Crompton and Knowles Corporation for the American Dye Manufacturers Institute (ADMI). *Textile chem. Col.* **9**(3), 24-28 (1997).

Horning R.H. (1978)Textile Dyeing Wastewaters-characterization End Treatment. U.S. Environmental Protection Agency, EPZ-600/2-78-098, Washington, D.C., 1978.

Hu T.L. (1998) Degradation of azo dye RP<sub>2</sub>B by *Pseudomonas Luteola*. *Wat. Sci. Tech.* **38**(4-5), 299-306.

Huag W., Schmidt A., Nortemann B., Hempel D.C., Stolz A. and Knackmuss H.J. (1991) Mineralization of the sulfonated azo dye mordant yellow 3 by a 6-aminonaphthalene-2-sulfonate degrading bacterial consortium. *Appl. Environ. Microbiol.* **57**, 3144 - 3149.

Hutton D.G. and Robertaccio F.L. U.S. Patent 3,904,518, Sept. 9, 1975.

Ibrahim N.A., El-Awady M.H. and M.H. Abo-Shosha (1998) Removal of anionic dyestuffs from aqueous and effluent liquors using cement kiln dust. *Colourage*, **2**, 29-34, 1998.

Ince, N. H.; Hasan, D. A.; Ustun, B. and Tezcanli, G. (2002) Combinative dyebath treatment with activated carbon and UV/H<sub>2</sub>O<sub>2</sub>: A case study on Everzol Black-GSP. *Wat. Sci. Tech.* **46**(4-5) 51-58.

Irvine E., Welch D., Grose A. B. F. and Donn A. (2000) Nanofiltration for colour removal - 7 years operational experience in Scotland. Spec. Publ. - R.Soc.Chem., 249 (Membrane Technology in Water and Wastewater Treatment), 41-48.

Jpn. Pat. 62186986 (Aug. 15, 1987), Henz A. and Pfenninger H. (to Ciba-Geigy A-G)

Kabdash I., Tunay O., Artan R and Orhon D. (1995) Acrylic Dyeing Wastewaters Characterization And Treatability. Prep. 3<sup>rd</sup> Int. Conference *Appropriate Waste Management Technologies for developing countries*, pp 339-348, Nagpur, India.

Kadirvelu, K.; Palanival, M.; Kalpana, R.; Rajeswari, S. (2000) Activated carbon from an agricultural by-product, for the treatment of dyeing industry wastewater. *Bioresour. Technol.*, **74**(3), 263-265.

Khattri, S. D. and Singh, M. K. (2000) Colour removal from synthetic dye wastewater using a bioadsorbent. *Water, Air, Soil Pollut.*, **120**(3-4), 283-294.

Koprivanac, N.; Papic, S.; Bozic, A. Loncaric; Cafuk, I. (1998). Waste color removal from dye industry effluents. Warsaw '98, Int. Symp. Exhib. Environ. Contam. Cent. East. Eur., Symp. Proc., 4th, 1097-1102.

Kosarek L.J. Removal of various toxic metals and cyanide from water by membrane processes. In W.J.Cooper, ed., " Chemistry for water reuse – Vol. 1", Ann Arbor Science, Ann Arbor, MI, 1981, p. 261.

Koyuncu, I.; Yalcin, F. and Ozturk, I. (1999) Color removal of high strength paper and fermentation industry effluents with membrane technology. *Wat. Sci. Tech.* **40**(11-12), 241-248.

Krull R., Hemmi M., Otto P and Hempel D.C. (1998) Combined biological and chemical treatment of highly concentrated residual dyehouse liquors. *Wat. Sci. Tech.* **38**(4-5), 339-346.

Kuo W. (1992). Decolorizing dye wastewater with Fenton's reagent. *Wat. Res.* **26**(7), 881-886.

Laszlo J.A. (1994) Removing acid dyes from textile wastewater using biomass for decolorization. *Am. Dyest. Rep.* **83**(8), 17-21.

Lopez A., Ricco G., Tiravanti G., Pipinto A.C. and Passino R. (1998). Biodegradability enhancement of refractory pollutants by ozonation. A laboratory investigation on an azo dye intermediate. *Wat. Sci. Tech.* **38**(4-5), 239-248.



Lores C. and Moore R.B., U.S.Patent 3, 770, 423, 1973. Chem. Abstr. 80, 137055t (1974).

Loyd K.C., Boardman G.D. and Michelsen D.C. Anaerobic/Aerobic Treatment Of A Textile Dye Wastewater. Preprinted for the mid-Atlantic Industrial Waste Conference, Morgan Town, WV, July 15-17, 1992.

Luangdilok W and Panswad T. (2000) Effect of chemical structures of reactive dyes on color removal by an anaerobic-aerobic process. *Wat. Sci. Tech.* **42**(3-4), 377-382.

Malik, P. K.; Bhowal, S. K. and Sanyal, S. K.(2001). Removal of colour from textile dyeing wastewater utilizing inorganic coagulants alone and in conjugation with a cationic polyelectrolyte. *Journal of Surface Science and Technology*, **17**(3-4), 181-189.

Matsui M., Kobayashi K., Shibata K. and Takase Y. (1981). Ozonation of dyes (II) - Ozone treatment of 4-phenyl azo-1-naphthol. *J.Soc.Dye.Chem.Col.* **97**, 210-213.

Matsui M., Kimura T., Nambu T., Shibata K and Takase Y. (1984) Reaction of water-soluble dyes with ozone. *J.Soc.Dye.Chem.Col.*, **100**(4), 125-127.

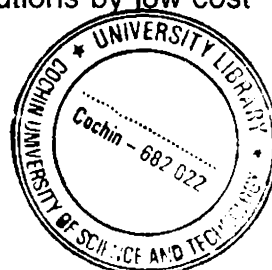
McClung S. and Lemley A. Electrochemical Treatment Of Acid Dye Wastewater, Preprint Extended Abstract, American Chemical Society Division Of Environmental Chemistry, Washington D.C. August 23, 1992.

McClung S. and Lemley A. Electrochemical treatment of Acid dye wastewater. Pre print extended abstract, American Chemical Society, Washington, D.C., August 23, 1992.

McCurdy M.W., Boardman G.D., Michelsen D.L. and Woodby R.M. Chemical Reduction And Oxidation Combined With Biodegradation For The Treatment Of A Textile Dye Wastewater. Proceedings of the 46<sup>th</sup> Purdue Industrial waste conference., Purdue Univ. W.Lafayette, Indiana, May, 1991.

Mckay G., Otterburn M.S. and Sweeny A.G. (1980). Removal of color from effluents using various adsorbents – III Silica: Rate process. *Wat. Res.* **15**, 14 -18.

Mckay G., Ramprasad G. and Pratapa Mowli P. (1986). Equilibrium studies for the adsorption of dyestuffs from aqueous solutions by low cost materials. *Water Air and Soil Pollution.* **29**, 273-283.



Mckay G., Porter J.F. and Prasad G. (1985). The removal of dye colors from aqueous solutions by adsorption on low-cost materials. *Water, Air and Soil Pollution*. **114**(3-4), 423-438.

Mckay G., El-Geundi M.S. and Nassar M.M. (1988) External mass transport processes during the adsorption of dyes onto bagasse pith. *Wat. Res.* **22**, 1527-1533.

Mehrotra R., Prasad S and Srivastav B.K. (1995) Acrylic Dyeing Wastewaters Characterization And Treatability. Prep. 3<sup>rd</sup> Int. Conference Appropriate Waste Management Technologies For Developing Countries, pp 617-629, Nagpur, India.

Meidl J.A. and Wilhelmi A.R. PACT-An economical solution in treating contaminated groundwater and leachate. Paper presented at the New England water pollution control Association Meeting. January 27-29, 1986.

Meyer V., Carlsson F.H.H. and Ollermann R.A. (1992). Decolorization of textile effluents using a low cost natural adsorbent material. *Wat. Sci. Technol.* **26**(5/6), 1205-1211.

Michelsen D.L., Fulk L.L., Wooby R.M. and Boardman G.D. (1992) Adsorptive and chemical pretreatment of reactive dye discharges, ACS Symposium Series 518, Emerging technologies in hazardous waste management III, Washington, D.C. pp. 119-136.

Minke R. and Rott U. (1999) Anaerobic treatment of split flow wastewater and concentrates from the textile processing industry. *Wat. Sci. Tech.* **40**(1), 169-176.

Mohan, S. Venkata and Karthikeyan, J. (2000) Removal of diazo dye from aqueous phase by algae *Spirogyra* species. *Environ Toxicol.. Chem.*, **74**(3-4), 147-154.

Nicolet, L. and Rott, U. (1999) Recirculation of powdered activated carbon for the adsorption of dyes in municipal wastewater treatment plants. *Wat. Sci. Technol.*, **40**(1), 191-198.

Nicola Willmott, Jim Grechrie and Gordon Nelson. (1989) The biotechnology approach of color removal from textile effluent. *J. Soc. Dyer. Col.* **114**(2), 1998.

Pagga U. and Brown D. (1986) The biodegradation of dyestuffs in aerobic biodegradation test. *Chemosphere*, **15**(4), 479-491.

Pagga U. and Taeger K. (1994) Development of a method for adsorption of dyestuffs on activated sludge. *Wat. Sci. Tech* **28** (5), 1051-1057.

Panswad T. and Wongchaisuwan S. (1986) Mechanisms of dye wastewater colour removal by magnesium carbonate-hydrated basic. *Wat. Sci. Tech.* **18**(3), 139-144.

Park and Shore (1984) Water for the dye house, supply consumption, recovery and disposal. *J. Soc. Dyers and Col.* **100**, 383-397.

Perkins W., Judkins J and Perry W (1980). Renovation of dyebath water by chlorination or ozonation. Part I: reaction of dyes. *Textile. Chem. Color.* **12**, 182-187.

Poon C.P.C and Virgadamo P.P. Anaerobic-Aerobic treatment of textile wastes with Activated carbon, prepared for the USEPA office of research and monitoring, Washington, D.C., EPA-RZ-73-248, May, 1973.

Poots V.J.P., McKay G and Healy J.J. (1976a) The removal of acid dye from effluent using naturally occurring adsorbents- I. Peat . *Wat. Res.* **10**, 1061-1066.

Poots V.J.P., McKay G and Healy J.J. (1976b) The removal of acid dye from effluent using naturally occurring adsorbents-II. Wood. *Wat. Res.* **10**, 1067-1072.

Porter J.J. and Sneider E.I. (1976). Long-term biodegradability of textile chemicals. *J. Wat. Pollut. Control. Fed.* **48**(9), 2198-2210.

Porter J.J. (1990) Membrane filtration techniques used for recovery of dyes, chemicals and energy. *Text. Chem. Color.* **22**(6), 21-25.

Powell W.W., Michelsen P.C., Boardman G.D., Dietrich A.H. and R.N.Woodby. Removal of color and TOC from segregated dye discharges using ozone and Fenton's reagent. Prepared and presented at chemical oxidation technologies for the nineties. Second International Symposium, Feb., 1992.

Powell W.W. The removal of color and DOC from segregated dye waste streams using ozone and Fenton's reagent followed by biotreatment. M.S.Degree, VPI & SU February, 1992.

Pratt H.D. Jr. A study of the degradation of some Azo Disperse Dyes in waste Disposal systems, Georgia Institute of Technology. M.S. Thesis, September, 1968.

Priyantha, N.; Keerthiratna, S.; Lokuge, I.; Gajanayake, H. (2000) Removal of blue coloration from industrial effluents by burnt-brick particles. *Journal of the National Science Foundation of Sri Lanka*, 28(4), 287-299.

Reife A. Waste treatment of soluble azo acid, direct and reactive dyes using a sodium hydrosulfite pretreatment followed by carbon adsorption, AATCC Book of papers, 1990. International conference and exhibition. October 1-3, 1990. Philadelphia.

Reife A. Reduction Of Toxic Components And Wastewaters Of Disperse Blue 79, 41<sup>st</sup> Southeast Regional American Chemical Society Meeting. October 9-11, 1989, Raleigh, NC.

Reife A. Kirk – Othmer Encyclopedia of chem. Technology, 4<sup>th</sup> Ed. 8, 1993, 753.

Reife A. (1993) Dye, Environmental chemistry. Kirk-Othmer Encyclopedia of Chemical Technology. 4<sup>th</sup> edition John Wiley and Sons, Inc., New York, 8, 753-784.

Ribeiro, Rosa Maria; Bergamasco, Rosangela; Gimenes, Marcelino Luiz (2002) Membranes synthesis study for color removal of a textile effluent. *Desalination*, 145(1-3), 61-63.

Rott U and Minke R (1999) Overview of wastewater treatment and recycling in the textile processing industry. *Wat. Sci. Tech.* 40(1), 137-144.

Sanglet P.R. U.S. Patent 4, 859, 448, 1989.

Sasaki, Hiroaki., Nanba Akira., Hirano Ryuichi. Mitsubishi Gas Chem. Co. Ltd. Japan. *Jpn. Kokai Tokkyo Koho JP 11 253, 974 (99, 253, 974)* 21 Sept. 1999, Appl. 1998/56,940. Method for treating dye containing wastewater.

Sewekow U. Minimizing Effluent Load In Reactive Dyeing. AATCC Book of papers, 1993. International conference and exhibition, Montreal, Quebec, Oct. 3-6, 1993, p. 235.

Sharma, Pragya; Kaur, Amarjeet; Markenday, D. K. (1999) Biosorption of the dye by various low cost adsorbent - a lab scale investigation. *Indian J. Environ. Prot.* 19(6), 442-445.

Shaul G.M., Dempsey C.R. and Dostal K.A. Fate of Water Soluble Azo Dyes In Activated Sludge Process, USEPA water Engineering Research Laboratory, Cincinnati, Ohio, August, 1987.

Shriver L.E. and Dague R.R. (1978) Dye waste treatment and reuse. *Am. Dyest. Repr.* **67**, 34-42.

Sheng H. Lin and Cheng L. Lai. (1999). Catalytic oxidation of dye wastewater by metal oxide catalyst and granular activated carbon. *Environ. Int.* **25** (4), 497-504.

Shintani, Noboru; Sugano, Yasushi; Shoda, Makoto (2002) Decolorization of kraft pulp bleaching effluent by a newly isolated fungus, *Geotrichum candidum* Dec 1. *Journal of Wood Science*, **48**(5), 402-408.

Singer P.C. and Little L.W. (1975) Characterization and treatment of textile dyeing wastewater. *J. Wat. Pollut. Control. Fed.* **47**(10), 1205-1211.

Sneider E.H. and Porter J.J. (1974). Ozone destruction of selected dyes in wastewater. *Am.Dyest. Repr.* **63** (8), 36-48.

Srinivasan, S. V.; Murthy, D. V. S.(1999) Color removal from bagasse-based pulp mill effluent using a white rot fungus. *Bioprocess Eng.*, **21**(6), 561-564.

Stahr R.W., Boepple C.P. and Knocke W.R. (1980) Textile waste treatment: Color Removal And Solids Handling Characteristics. Proc. 35<sup>th</sup> industrial waste conference, pp 186-199, Purdue University, West Lafayette, Ind.

Sung Ki Lee, Inventor, Andco Incorporation, Assignee, Electrochemical Contaminant removal from aqueous media. U.S. Pat. 3,926,754. Oct. 16, 1973.

Susan J. Hobbs (1989) Acquisition and use of data for assessment of the environmental impact of colorants. 355-352. Vol. 105 Oct. 1989.

Szpyrkowicz Lidia, Juzzolino Claudia, Kaul Santosh N., Daniele,Salvatore and De Faveri, Marco D. (2000) Electrochemical Oxidation of Dyeing Baths Bearing Disperse Dyes. *Ind. Eng. Chem. Res.*, **39**(9), 3241-3248.

Taebi, A., Esmaeilian, M. and Amirshahi, S. H. (2000) Application of chitosan as an adsorbent for decolorization of textile industry wastewaters. *Iran. J. Polym. Sci. Technol.* **12**(4), 237-246.

Tincher W.C., Weinberg M and Stephens S. Removal of dyes and chemicals from textile wastewater, Book of papers, International conference and exhibition, Nashville, TN; AAT CC, 1988, P.No. 25.

Tincher W.C. Survey of the Coosa Basin for organic contaminants from carpet processing. Contract No. 3-27-630 for the environmental protection Division, Dept. of Nat. Resources, State of Georgia, 1978.

Tsuchida Tatsuo., Ke Maki. and Kirura Takuhira. Toray industries, Inc. Japan. Jpn. Kokai Tokkyo Koho JP 11 262, 775 (99 262, 775). Decolorization of dyeing wastewater by using Saccharide caramelization.

Tzitzis, M., Vayenas D.V., Lyberatos G. (1994) Pretreatment of textile industry wastewaters with ozone. *Wat. Sci. Tech.* **29**(9), 151-160.

Uhrich K.D. Inventor, Andco Environmental Processes, Inc., Assignee, Method for removing dye stuffs from wastewater. U.S. Pat. 4,880,510. Nov. 14. 1989.

Ulman J.A. and Cook M.M. Abstracts of papers, 204<sup>th</sup> National Meeting of the American Chemical Society, Washington DC, 1992, Environmental Chemistry Division.

U.S.Pat.4,523,924 (June 18, 1985), Lacroix R. (to Ciba-Geigy Corp).

U.S.Pat.4,500,321 (Feb. 19, 1985), Hugelshofer P., Bruttel B., Pfenninger H. and Lacroix R. (to Ciba-Geigy Corp).

U.S.Pat. 4,436,523 (May 13, 1984), Hugelshofer P., Zbinden P. and Koli Z (to Ciba-Geigy Corp).

U.S.Pat.4,329,145 (May 11, 1982) Kroll J., Mob H.H., Hornle R., Schuffenhaeur E., Brandt H., Bremer R., Wolf K and Schiwly W. (to Bayer A-G).

Vlyssides, A. G., Loizidou, M., Karlis, P. K. and Zorpas, A. A. (1999) Textile dye wastewater treatment with the use of an electrolysis system. *Hazard. Ind. Wastes*, **31**, 147-156.

Voyksner R.D., Straaub R., Keever J.T., Freeman H.S. and Hum W.N. (1993) *Environ. Sci. Technol.* **27**, 1665.

Walker, G. M. and Weatherley, L. R. (2000) Biodegradation and biosorption of acid anthraquinone dye. *Environ. Pollut.*, **108**(2), 219-223.

Walsh G.E., Bahner L.H. and Horning W.B. (1980) Toxicity of textile mill effluents to fresh water and estuarine algae, crustaceans and fishes, *Env. Pollut. Ser. A*, **21**, 169-179.

Weber E.J. and Wolfe N.C. (1987) Kinetic studies of the reduction of aromatic azo compounds in anaerobic sediment/water systems. *Environ. Toxicol. Chem.* **6**, 911-916.

Weeter D.W. and Hodgson A.G. (1977) Dye wastewater alternatives for biological waste treatment. Proc. 32<sup>nd</sup> Industrial Waste Conference, pp 1-9, Purdue University, West Lafayette, Ind.

Weinberg M.K. Effectiveness Of The Andco Electrochemical Treatment Process And Its Application In Textile Wastewater Treatment, Georgia Institute of Technology, M.S.Thesis. 1989.

Wilcock A., Tibbens J., Fuss F., Wagner J and Brewster M. (1992). Using electrochemical technology to treat textile wastewater : 3 – case studies. *Am. Dyest. Reprtr.* **8**, 15-22.

Wilcock A., Tibbens J., Fuss F., Wagner J and Brewster M. (1992). Using electrochemical technology to treat textile wastewater.

## References (Chapter –II)

Abinash Agrawal and Paul G. Tratnyek. 1996, Reduction of nitro aromatic compounds by zero-valent iron metal. *Environ. Sci. Technol.* **30**(1), 153-160.

Agrawal A., Ferguson W.J., Gardner B.O., Christ J.A., Bandstra J.Z. and Tratnyek P.G. 2002 Effects of carbonate species on the kinetics of dechlorination of 1,1,1-trichloroethane by zero valent iron. *Environ. Sci. Technol.* **36**(20), 4326-4333.

Alessi D.S. and Li Z.H. Synergistic effect of cationic surfactants on perchloroethylene degradation by zero-valent iron. *Environ. Sci. Technol.* **35**(18), 3713-3717.

Allen R. Pratt., David W. Blowes and Carol J. Ptacek. 1997 Kinetics of chromate reduction on proposed subsurface remediation material. *Environ. Sci. Technol.* **31**(9), 2492-2498.

Alowitz M.J. and Scherer M.M. 2002 Kinetics of nitrate, nitrite and Cr(VI) reduction by iron metal. *Environ. Sci. Technol.* **36**(3), 299-306.

Bockris J O'M.; Reddy A.K. *Modern Electrochemistry*, Vol. 2, Plenum press; New York, 1970.

Carina Grittini., Mark Malcomson., Quintus Fernando and Nic Korte. Rapid dechlorination of polychlorinated biphenyls on the surface of a Pd/Fe bimetallic system. *Environ. Sci. Technol.* **29**(11), 1995.

Casey F.X.M., Ong S.K. and Horton R. 2000 Degradation and transformation of trichloroethylene in miscible displacement experiments through zero-valent metals. *Environ. Sci. Technol.* **34**(23), 5023-5029.

Chin F. Chew and Tian C. Zhang. 1998 In-situ remediation of nitrate contaminated ground water electrokinetics/iron wall process. *Wat. Sci. Tech.* **38**(7), 135-142.

Christopher A. Schultz and Timothy J. Grundl. 2000 pH dependence on reduction rate of 4-chloronitrobenzene by Fe(II)/Montmorillonite systems. *Environ. Sci. Technol.* **34**(17), 3641-3648.

Chunming Su and Robert W. Puls. 2001 Arsenate and Arsenite removal by zero-valent iron: kinetics, redox transformation and implications for in situ ground water remediation. *Environ. Sci. Technol.* **35**(7), 1487-1492.



Chunming Su and Robert W. Puls. 1999 Kinetics of Trichloroethene reduction by zerovalent iron and tin: pretreatment effect, apparent activation energy and intermediate products. *Environ. Sci. Technol.* **33**(1), 163-168.

Chunming Su and Robert W. Puls. 2001 Arsenate and Arsenite removal by zero-valent iron: Effects of phosphate, silicate, carbonate, borate, sulfate, chromate, molybdate and nitrate relative to chloride. *Environ. Sci. Technol.* **35**(22), 4562-4568.

Clarke E.A., Anilker R. In Handbook of environmental chemistry, Vol. 3, Part A, Anthropogenic Compounds; Hutzinger, O., Ed.; Springer-Verlag; Berlin and Heidelberg, 1980; pp 181-215.

Cornell R.M., Schwertmann U. *The Iron Oxides*; VCH publishers: New York, 1996.

Cornell R.M. and Schwertmann U. *The iron oxides*; VCH publishers: New York 1996.

Cunningham J.A. and Reinhard M. 2002 Injection-extraction treatment well pairs: An alternative to permeable reactive barriers (PRB). *Ground Water.* **40**(6), 599-607.

David R. Burris., Timothy J. Campbell and Valipuram S. Manoranjan. 1996 Sorption of Trichloroethylene and tetrachloroethylene in batch reactive metallic iron-water system. *Environ. Sci. Technol.* **29**(11), 2850-2855.

David W. Blowes., Carol J. Ptacek and John L. Jambor. 1997 In-situ remediation of Cr(VI)- contaminated groundwater using permeable reactive walls: laboratory studies. *Environ. Sci. Technol.* **31**(12), 3348-3357.

Eric J. Weber. 1995 Chemical and sediment mediated reduction of the azo dye Disperse Blue 79. *Environ. Sci. Technol.* **29**(5), 1163-1170.

Eric J. Weber. 1996 Iron-mediated reductive transformations: investigation of reaction mechanism. *Environ. Sci. Technol.* **30**(2), 716-719.

Geiger C.L., Ruiz N.E., Clausen C.A., Reinhart D.R. and Quinn J.W. 2002 Ultrasound pretreatment of elemental iron: kinetic studies of dehalogenation reaction enhancement and surface effects. *Wat. Res.* **36**(5), 1342-1350.

George L. Baughman and Eric J. Weber. 1994 Transformation of dyes and related compounds in anoxic sediment: Kinetics and products. *Environ. Sci. Technol.* **28**(2), 267-276.

Gerald R. Eykholt and Douglas T. Davenport. 1998 Dechlorination of chloroacetanilide herbicides Alachlor and Metolachlor by iron metal. *Environ. Sci. Technol.* **32**(10), 1482-1487.

Ghauch A. 2001 Degradation of benomyl, picloram and dicamba in a conical apparatus by zero-valent iron powder. *Chemosphere.* **43**(8), 1109-1117.

Gillham R.W. and O'Hannesin. 1994 Enhanced degradation of halogenated aliphatics by zero-valent iron. *Ground Water* **32**(6), 958-967.

Gregory D. Sayles., Guanrong You., Maoxiu Wang and Margaret J. Kupferle. 1997 DDT, DDD and DDE dechlorination by zero-valent iron. *Environ. Sci. Technol.* **31**(12), 3448-3454.

Gu B., Liang L., Dickey M.J., Yin X. and Dai S. 1998 Reductive precipitation of Uranium (VI) by zero-valent iron. *Environ. Sci. Technol.* **32**(21), 3366-3373.

Huang Y.H. and Zhang T.C. Kinetics of nitrate reduction by iron at near neutral pH. *J. Environ. Eng.-ASCE.* **128**(7), 604-611.

Hudlicky M. *Reductions in Organic Chemistry*; J.Wiley and Sons; New York, 1986; pp 69-76.

Hueper W.C. *Occupational and Environmental Cancers of the Urinary System*; Yale university press; New Haven, 1969.

Hakanen M. and Lindberg A. *Sorption of Uranium on rocks in anaerobic groundwater*. Report JYT-92-25; Nuclear Waste Commission Of Finnish Power Companies; Helsinki, Finland, 1992.

Hozalski R.M. Zhang L. and Arnold W.A. 2001 Reduction of haloacetic acids by Fe<sup>0</sup>: implications for treatment and fate. *Environ. Sci. Technol.* **35**(11), 2258-2263.

Hui Ming Hung., Frank H. Ling and Michael R. Hoffmann. 2000 Kinetics and mechanism of the enhanced reductive degradation of Nitrobenzene by elemental iron in the presence of Ultrasound. *Environ. Sci. Technol.* **34**(9), 1758-1763.

*IARC Monographs on the Evaluation of the Carcinogenic Risk of Chemicals to Man*; IARC: Lyon, 1975; Vol. 8.

James Farrell., Jianping Wang., Peggy O'Day and Martha Conklin. 2001 Electrochemical and spectroscopic study of arsenate removal from

water using zero-valent iron media. *Environ. Sci. Technol.* **35**(10), 2026-2032.

James Farrell., Mark Kason., Nicos Melitas and Tie Li. 2000 Investigation of the long-term performance of zero-valent iron for reductive dechlorination of trichloroethylene. *Environ. Sci. Technol.* **34**(3), 514-521.

James Farrell., Nikos Melitas., Mark Kason and Tie Li. 2000 Electrochemical and column investigation of iron-mediated reductive dechlorination of trichloroethylene and perchloroethylene. *Environ. Sci. Technol.* **34**(12), 2549-2556.

James Farrell., Jianping Wang., Peggy O'Day and Martha Conklin. 2001 Electrochemical and spectroscopic study of arsenate removal from water using zero-valent iron media. *Environ. Sci. Technol.* **35**(10), 2026-2032.

Jiasheng Cao., Liping Wei., Quingguo Huang., Liansheng Wang and Shuokui Han. 1999 Reducing degradation of azo dye by zero-valent iron in aqueous solution. *Chemosphere*, **38**(3), 565-571.

John F. Devlin., Jorg Klausen and Rene P. Schwarzenbach. 1998 Kinetics of nitroaromatic reduction on granular iron in recirculating batch experiments. *Environ. Sci. Technol.* **32**(13), 1941-1947.

Joseph N. Fiedor., William D. Bobstick., Robert J. Jarabek and James Farrell. 1998 Understanding the mechanism of Uranium removal from groundwater by zero valent iron using X-ray photoelectron spectroscopy. *Environ. Sci. Technol.* **32**(10), 1466-1473.

Kulkarni, S.V., Blackwell C.D., Blackard A.L., Stackhouse C.W. and Alexander M.W. *Textile Dyes And Dyeing Equipment: Classification, Properties And Environmental Aspects*; U.S.E.P.A: Research Triangle Park, NC, 1985; EPA – 600/2-85/010.

Kim Y.H. and Carraway E.R. 2003 Rapid dechlorination of TCE by zero-valent bimetals. *Environ. Technol.* **24**(1), 69-75.

Klausen J., Ranke J. and Schwarzenbach R.P. 2001 Influence of solution composition and column aging on the reduction of nitroaromatic compounds by zero-valent iron. *Chemosphere*. **44**(4), 511-517.

Leah J. Matheson and Paul G. Tratnyek. 1994 Reductive dehalogenation of chlorinated methanes by iron metal. *Environ. Sci. Technol.* **28**(12), 2045-2053.

Lien H.L., and Zhang W.X. 2002 Enhanced dehalogenation of halogenated methanes by bimetallic Cu/Al. *Chemosphere*. **49**(4), 371-378.

Li T. and Farrell J. 2001 Electrochemical investigation of the rate-limiting mechanisms for trichloroethylene and carbon tetrachloride reduction at iron surfaces. *Environ. Sci. Technol.* **35**(17), 3560-3565.

Loraine G.A., Burriss D.R., Li L.X. and Schoolfield J. 2002 Mass transfer effects on kinetics of 1,2-dibromoethane reduction by zero-valent iron in packed bed reactors. *J. Environ. Eng.-ASCE*. **128**(1), 85-93.

Mantha R., Biswas N., Taylor K.E. and Bewtra J.K. 2002 Removal of nitroaromatics from synthetic wastewater using two-step zero-valent iron reduction and peroxidase-catalyzed oxidative polymerization. *Wat. Environ. Res.* **74**(3), 280-287.

Michelle M. Scherer., Kathleen M. Johnson., John C. Westall and Paul G. Tratnyek. 2001 Mass transport effect of the kinetics of Nitrobenzene reduction by iron metal. *Environ. Sci. Technol.* **35**(13), 2804-2811.

Michelle M. Scherer., Barbara A. Balko., David A. Gallagher and Paul G. Tratnyek. 1998 Correlation analysis of rate constants for dechlorination by zero-valent iron. *Environ. Sci. Technol.* **32**(19), 3026-3033.

Michelle M. Scherer., John C. Westall., Margaret Ziomek Moroz and Paul G. Tratnyek. 1997 Kinetics of carbon tetrachloride reduction at an oxide free iron electrode. *Environ. Sci. Technol.* **31**(8), 2385-2391.

Morrison S.J., Metzler D.R. and Carpenter C.E. 2001. Uranium precipitation in a permeable reactive barrier by progressive irreversible dissolution of zero-valent iron. *Environ. Sci. Technol.* **35**(2), 385-390.

Naomi L. Stock., Julie Peller., Vinodgopal K. and Prashant V. Kamat. 2000 Combinative sonolysis and photocatalysis of textile dye degradation. *Environ. Sci. Technol.* **34**(9), 1747-1750.

Nikos Melitas., Ouafra Chuffe Moscoso and James Farrell. 2001 Kinetics of soluble chromium removal from contaminated water by zero-valent iron media: corrosion inhibition and passive oxide effects. *Environ. Sci. Technol.* **35**(19), 3948 – 3953.

Nikos Melitas. and James Farrell. 2002 Understanding chromate kinetics with corroding iron media using tafel analysis and electrochemical impedance spectroscopy. *Environ. Sci. Technol.* **35**(19), 3958 – 3963.

Nikolaidis N.P., Dobbs G.M. and Lackovic J.A. 2003 Arsenic removal by zero-valent iron: field, laboratory and modeling studies. *Wat. Res.* **37**(6), 1417-1425.

Oh B.T., Just C.L. and Alvarez P.J. 2001 Hexahydro-1,3,5-trinitro-1,3,5-triazine (RDX) mineralization by zero-valent iron and mixed anaerobic cultures. *Environ. Sci. Technol.* **35**(21), 4341-4346.

Oh S.Y., Cha D.K., Kim B.J. and Chiu P.C. 2002 Effect of adsorption to elemental iron on the transformation of 2,4,6-trinitrotoluene and hexahydro-1,3,5-triazine in solution. *Environ. Toxicol. Chem.* **21**(7), 1384-1389.

Oh S.Y., Cha D.K. and Chiu P.C. 2002 Graphite mediated reduction of 2,4-dinitrotoluene with elemental iron. *Environ. Sci. Technol.* **36**(10), 2178-2184.

Perey J.R., Chiu P.C., Huang C.P. and Cha D.K. 2001 Zero-valent iron pretreatment for enhancing the biodegradability of azo dyes. *Wat. Env. Res.* **74**(3), 221-225.

D.H. Phillips., B. Gu., D.B. Watson., Y. Roh., L. Liang and S.Y. Lee. 2000 Performance evaluation of a zero-valent iron reactive barrier: Mineralogical characteristics. *Environ. Sci. Technol.* **34**(19), 4169-4176.

Ramkrishna Mantha., Keith E. Taylor., Nihar Biswas and Jatinder K. Bewtra. 2001 A continuous system for Fe<sup>0</sup> reduction of nitrobenzene in synthetic wastewater. *Environ. Sci. Technol.* **35**, 3231-3236.

Ramaswami A., Tawachsupa S and Isleyuen M. 2001 Batch-mixed iron treatment of high arsenic waters. *Wat. Res.* **35**(18); 4474-4479.

Richardson J.P. and Nicklow J.W. 2002 In-situ permeable reactive barriers for groundwater contamination. *Soil and Sediment Contamination.* **11**(2), 241-268.

Ritter K., Odziemkowski M.S. and Gillham R.W. 2002 an In-situ study of the role of surface films on granular iron in the permeable iron wall technology. *J. Contam. Hydrol.* **55**(1-2), 87-111.

Robert D. Voyksner, Rolf Straub and Jeffrey T. Keever. 1993 Determination of aromatic amines originating from azo dyes by chemical reduction combined with liquid chromatography/mass spectrometry. *Environ. Sci. Technol.* **27**(8), 1665-1672.

Roh Y., Lee S.Y. and Elless M.P. Characterization of corrosion products in the permeable reactive barriers. *Envtl. Geol.* **40**(1-2), 184-194.

Sangkil Nam and Paul G. Tratnyek. 2000 Reduction of Azo dyes with zero valent iron. *Wat. Res.* **34**(6), 1837 – 1845.

Schneider P., Neitzel P.L., Osenbruck K., Noubacteb C., Merkel B. and Hurst S.(2001) In-situ treatment of radioactive mine water using reactive materials – Results of laboratory and field experiments in uranium ore mines in Germany. *Acta Hydrochemica et Hydrobiologica* **29**(2-3), 129-138.

W.Scott, Orth and Robert W. Gillham. 1996 Dechlorination of trichloroethene in aqueous solution using Fe<sup>0</sup>. *Environ. Sci. Technol.* **30**(1), 66-71.

Searle C.E., Ed. *Chemical Carcinogenesis*; ACS Monograph; American Chemical Society; Washington, DC, 1976.

Sherman M. Ponder., John G. Darab and Thomas E. Mallouk. 2000 Remediation of Cr(VI) and Pb(II) aqueous solutions using supported, nanoscale zero-valent iron. *Environ. Sci. Technol.* **34**(12), 2564-2569.

Sibel Uludag-Demirer and Alan R.Bowers. 2000 Adsorption/reduction reactions of trichloroethylene by elemental iron in the gas phase: The role of water. *Environ. Sci. Technol.* **34**(20), 4407-4412.

.Singh J., Comfort S.D. and Shea P.J. 1999 Iron-mediated remediation of RDX contaminated water and soil under controlled Eh/pH. *Environ. Sci. Technol.* **33**(9), 1488-1494.

Thomas Astrup., Stripp L.S. and Thomas H. Christensen. 2000 Immobilization of chromate from coal fly ash leachate using an attenuating barrier containing zero-valent iron. *Environ. Sci. Technol.* **34**(19), 4163-4168.

Thomas B. Hofstetter., Cornelis G. Heijman., Stefan B. Haderlein., Christof Holliger and Bene P. Schwarzenbach. 1999 Complete reduction of TNT and other (poly) nitroaromatic compounds under iron-reducing subsurface conditions. *Environ. Sci. Technol.* **33**(9), 1479-1487.

Tie Li and James Farrell., 2000. Reductive dechlorination of trichloroethene and carbon tetrachloride using iron and palladized-iron cathode. *Environ. Sci. Technol.* **34**(1), 173 – 179.

Timothy L. Johnson., Michelle M. Scherer and Paul G.Tratnyek. 1996 Kinetics of halogenated organic compound degradation by iron metal. *Environ. Sci. Technol.* **30**(8), 2534-2640.

Todd A. Martin and J. Houston Kempton. 2000 In situ stabilization of metal-contaminated groundwater by hydrous ferric oxide: An experimental and modeling investigation. *Environ. Sci. Technol.* **34**(15), 3229-3234.

Tratnyek P.G., Scherer M.M., Deng B.L. and Hu S.D. 2001 Effects of natural organic matter, anthropogenic surfactants and model quinones on the reduction of contaminants by zero-valent iron. *Wat. Res.* **35**(18), 4435-4443.

Uhlig, H.H. and Revie, R.W. Corrosion and Corrosion control, 3<sup>rd</sup> ed.; John Wiley: New York, 1985.

Uludag-Demirer S. and Bowers A.R. 2001 Gas phase reduction of chlorinated VOCs by zero-valent iron. *J. Environ. Sci. Health, Part A: Toxic / Hazard. Subst. Environ. Eng., A* **36**(8), 1535-1547.

Uludag-Demirer and S. Bowers A.R. 2003 Effects of surface oxidation and oxygen on the removal of trichloroethylene from gas phase using elemental iron. *Water Air and Soil Pollution.* **142** (1-4), 229-242.

Westerhoff P. and James J. 2003 Nitrate removal in zero-valent iron packed columns. *Wat. Res.* **37**(8), 1818-1830.

Wildman M.J. and Alvarez P.J.J. 2001 RDX degradation using an integrated Fe<sup>0</sup>-microbial treatment approach. *Wat. Sci. Technol.* **43**(2). 25-33.

William A. Arnold and A. Lynn Roberts. Pathways and kinetics of chlorinated ethylene and chlorinated acetylene reaction with Fe<sup>0</sup> particles. *Environ. Sci. Technol.* **34**(9), 1784-1805.

Williams A.G.B and Scherer M.M. 2001 Kinetics of Cr(VI) reduction by carbonate green rust. *Environ. Sci. Technol.* **35**(17), 3488-3494.

Wolfgang F. Wust., Ralf Kober., Oliver Schlicker and Andreas Dahmke. 1999 Combined zero and first order kinetic model of the degradation of TCE and cis-DCE with commercial iron. *Environ. Sci. Technol.* **33**(23), 4304-4309.

Xiong Y. and Karlsson H.T. 2001 Approach to a two-step process of dye wastewater containing acid red B. *J. Environ. Sci. Health, Part A: Toxic / Hazard. Subst. Environ. Eng., A* **36**(3), 321-331.

Yoshida O., Miyakawa M., Okada Y., Ohshiro K., Harada T., Machida S., Kato T. In *Decomposition Of Toxic And Nontoxic Organic Compounds In Soils*; Overcash, M.R., Ed.; Ann Arbor Science: Ann Arbor, MI, 1981.

Young – Hun Kim and Elizabeth R. Carraway. 2000 Dechlorination of pentachlorophenol by zero valent iron and modified zero valent irons. *Environ. Sci. Technol.* **34**(10), 2014-2017.

Zhang P.F., Tao X., Li Z.H. and Bowman R.S. 2002 Enhanced perchloroethylene reduction in column systems using surfactant-modified zeolite/zero-valent iron. *Environ. Sci. Technol.* **36**(16), 3597-3603.



### References (Chapter – III)

Aldershof Brian K., Dennis Ronald M. and Kunitsky Craig J. (1997) Study of the decomposition of four commercially available Hydrogen peroxide solutions by Fenton's reagent. *Water Env. Res.* Vol. **69**(5), pp. 1052-1056.

Alexei Nedolonjko and Kiwi John. (1997) Transient intermediate species active during the Fenton – mediated degradation of quinoline in oxidative media: Pulsed Laser Spectroscopy. *J. Photochem. Photobiol., A.* Vol. **110**(2), pp. 141-148.

Alexei Nedolonjko and Kiwi John. (1997) Parameters affecting the homogeneous and heterogeneous degradation of quinoline solutions in light activated processes. *J. Photochem. Photobiol., A.* Vol. **110**(2), pp. 149-157.

Anat A. Lev. and Vithal V. Deshpande. (1996) Design of Advanced Oxidation Process for decolorization of reactive dye wastewater stream using Fenton's reagent. *Chem. Oxid.* **6**, pp. 13-18.

An Huren, Qian Yi. (1994) Biodegradabilities of dyes under the aerobic conditions. *Chin. J. Environ. Sci.* **15**(6), 16-19.

Ansari, Anas., Pearl Jose., Domenech, Xavier, Oxidation of S(IV) to S(VI) under Fenton, Photo-Fenton and  $\gamma$ -FeOOH photocatalysed conditions. (1996) *J. Mol. Catal. A:chem.* **112**(2), pp. 269-276.

Anthony Nappi J., Emily Vass. (1998) Hydroxyl radical formation resulting from the interaction of nitric oxide and hydrogen peroxide. *Biochim. Biophys. Acta.* **1380**(1), pp. 55-63.

Arienzo M. (1999) Decontamination of TNT-polluted water by modified Fenton. In. *5<sup>th</sup> Int. In-situ on-site Biorem Symp.* Vol. **7**, pp. 197-202.

Arnold S.M., Hickey W.J. and Harris R.F. (1995) Degradation of atrazine by Fenton's reagent: condition optimization and product quantification. *Environ. Sci. Technol.* Vol. **29**, pp. 2083 –2089.

Atkinson R. (1989) Kinetics and mechanisms of the gas phase reactions of the hydroxyl radical with organic compounds. *J. Phys. Chem. Ref. Data, Monograph 1.* American Chemical Society, American Institute of physics, and the National Institute of Standards and Technology; New York, N.Y.

Balanosky E., Herrera F., Lopez A. and Kiwi J. Oxidative degradation of textile waste modeling reactor performance. (2000) *Wat. Res.* **34**(2), pp. 582-596.

Balcioglu I.A., Arslan I. and Sacan M.T. (2001) Homogenous and heterogeneous advanced oxidation of two commercial reactive dyes. *Environ. Technol.* **22**(7), pp. 813 – 822.

Balmer M.E. and Sulzberger B. (1999) Atrazine degradation in irradiated iron oxalate systems: Effects of pH and oxalate. *Environ. Sci. Technol.* **33**(14), pp. 2418 – 2424.

Bandara J., Nadtochenko V., Kiwi J and Pulgarin C. Dynamics of oxidant addition, as a parameter in the modeling of dye mineralization (Orange II) via advanced oxidation technologies. (1997) *Wat. Sci. Tech.* **35**(4), pp. 87-93.

Bandara J., Morrison C., Kiwi J., Pulgarin C., Peringer P. (1996) Degradation and decolorization of concentrated solution of Orange II. Kinetics and quantum yield for sun light induced reactions via Fenton type reagents. *J. Photochem. Photobiol. A.* **99**(1), pp. 57-66.

Banerjee Kashi., O'Toole and Thomas J. (1995) Reduction of COD in leachate from a hazardous waste landfill adjacent to a coke-making facility. *In. Iron making conference proc.* 1995, **54**, pp. 347-357.

Barb W.G., Baxendale J.H., George P. and Hargrave K.R. (1951) Reactions of ferrous and ferric ions with hydrogen peroxide. *Trans. Faraday Soc.* **47**, pp. 462-500.

Barburinski A. Krzysztof., Koscielniak Helena. (1997) Degradation of industrial contaminants by the Fenton reaction. *Chem. Inz. Ekol.* **4**(2), pp. 153-162.

Bauer Rupert and Fallman Hubert. (1997) The photo-Fenton oxidation - a cheap and efficient wastewater treatment method. *Res.Chem.Intermed.* **23**(4), pp. 341-354.

Bauer R. (1994) Applicability of solar irradiation for photochemical wastewater treatment. *Chemosphere*, **29**, pp.1225-1233.

Bekbolet, M., Boyacioglu, A and Ozakaraova, B. (1998) The influence of solution matrix on the photocatalytic removal of color from natural waters. *Wat. Sci. Tech.* **38**(6), pp.155-162.

Benjamin M.M., Slettin R.S. Emerging Technology Report: Metals Treatment at Superfund Sites. Adsorptive Filtration; June 1993; EPA Report 540/R-93/515.

Bensing T.M. and Carberry J.B. (1991) Peroxide pre-oxidation of recalcitrant toxic waste to enhance biodegradation. *Wat. Sci. Tech.* **23**, pp. 367-376.

Bier Eleanor L., Jasbir Singh., Li Zheng M., Comfort, S.D., and Patricik Shea. (1999) Remediating hexahydro-1,3,5-trinitro-1,2,5-triazine contaminated water and soil by Fenton oxidation. *Environ. Toxicol. Chem.* **18**(6), pp. 1078-1084.

Bigda, R.J.; Elizardo, K.P. *Abstracts of Papers, 204<sup>th</sup> ACS National Meeting*, Washington, DC; American Chemistry Society: Washington, DC, 1992; pp 259-262.

Bircher K.G., Lem W., Simms K.M. and Dussert B.W. (1997) Combination of UV oxidation with other treatment technologies for the remediation of contaminated water. *J. Adv. Oxid. Technol.* **2**(3), pp. 435-441.

Bin A.K., Machniewski P., Sakowicz R, Ostrowska J. and Zielinski Z. (2001) Degradation of nitroaromatics (MNT, DNT and TNT) by AOP's. *Ozone Sci. Eng.* **23**(5), pp. 343 – 349.

Bishop, D.B., Stern G., Fleischman M. and Marshall L.S. (1968) Hydrogen peroxide catalytic oxidation of refractory organics in municipal wastewater. *I&EC Process Design and Development*, **7**, pp. 110-117.

Bogatu., D., Gheju M., Viorica Dalea., Lovi A. and Negrea P. (2000) Study of azo dyes oxidation with Fenton Reagent by use of UV-Vis spectroscopy. In *Proceedings of the 5<sup>th</sup> International Symposium and Exhibition on Environmental Contamination in Central and Eastern Europe*. Prague, Czech Republic, Sept. 12-14, 2000.

Bowers A.R., Gaddipati P., Eckenfelder Jr. W.W. and Monsen R.M. (1989) Treatment of toxic or refractory wastewaters with hydrogen peroxide. *Wat. Sci. Tech.* **21**, pp. 477-486.

Brain M. Sherman., Herbert E. Allen and Huang C.P. (1998) Catalyzed hydrogen peroxide treatment of 2,4,6-trinitrotoluene in soils. *Hazard. Ind. Wastes.* **30**, pp. 765 – 774.

Brillas Enrique, Mur Eva and Casado Juan. (1996) Iron (II) catalysis of the mineralization of aniline using a carbon-PTFE O<sub>2</sub>-fed cathode. *J. Electrochem. Soc.* **143**(3), pp. L49-L53.

Buxton G.V., Greenstock C.L., Helman W.P. and Ross A.B. (1988) Critical review of rate constants for reactions of hydrated electrons, hydrogen atoms and hydroxyl radicals (OH<sup>•</sup>/ O<sup>•</sup>) in aqueous solution. *J. Phys. Chem. Ref. Data.* Vol. **17**, pp. 513-586.

Cadena F. and Peters R.W. (1988) Evaluation of chemical oxidizers for hydrogen Sulphide control. *J.W.P.C.F.* **60**, pp. 367-376.

Carey J.H. (1992) An introduction to advanced oxidation processes for the destruction of organics in water. *Water Poll. Res. Canada.* **27**(1), pp. 1-21.

Chen R. and Pignatello J.J. (1997) Role of quinone intermediates as electron shuttles in Fenton and photo assisted Fenton oxidation of aromatic compounds. *Environ. Sci. Technol.* **31**, pp. 2399-2406.

Cheves Walling (1975). Fenton's Reagent Revisited. *Acc. of chem. res.* **8**, 125-131.

Chin C. and Hicks M.G. (1970) Hydrogen peroxide studies of oxygen demand. *J.WPCF.* **42**, pp. 1327-1342.

Clarke Robert L., Smedley Stuart I. and Kimmel Stan. (1997) In situ electrochemical remediation of organically contaminated soil, sediments and ground water using electrochemically generated and delivered Fenton's reagent. *PCT. Int.Appl. WO 97*, **28**, 294.

Claustre Prat , Manuel Vincente and Santhago Esplugas. (1987) Treatment of bleaching waters in the paper industry by hydrogen peroxide and ultraviolet radiation. *Wat. Res.* **6**, pp. 663-668.

Clemens Von Sonntag, Peter Dowideit, Xingwang Fang, Ralf Mertens, Xianming Pan, Man Nien Schuchmann and Heinz-Peter Schuchmann. (1997) The fate of peroxy radicals in aqueous solution. *Wat. Sci. Tech.* **35**(4), pp. 9-15.

Chien Chen T., Anthony Tafuri N., Maqsd Rahman and Mary B. Foerst. (1998) Chemical oxidation treatment of petroleum contaminated soil using Fenton's reagent. *J. Environ. Sci. Health, Part A: Toxic/Hazard. Subst. Environ. Eng. A.* **33**(6), pp. 987-1008.

Cheng-Nan Chang, Jih-Gaw Lin, Allen C.Char and Chu-sung Liu. (1996) Modified Nernst model for on-line control of the chemical oxidation decoloring process. *Wat. Sci. Tech.* **34**(3-4), pp.151-157.

Choi Heung Jin., Huang C.P., Cazano Pasquale S. and Robin Roddy M. (1998) Pilot plant evaluation of landfill leachate treatment using Fenton's reagent. *Hazard. Ind. Wastes*. **30**, pp. 757-764.

David L.Sedlak and Anders W.Andren. (1991) Oxidation of chlorobenzene with Fenton's reagent. *Environ. Sci. Technol.* **25**(4), pp. 777-782.

David L.Sedlak and Anders W. Andren. (1991) Aqueous-phase oxidation of polychlorinated biphenyls by hydroxyl radicals. *Environ. Sci. Technol.* **25**(8) 1419-1427.

Donald T. Sawyer. (1997) Metal [Fe(II), Cu(I), Co(II), Mn(III)]Hydroperoxide induced activation of dioxygen (O<sub>2</sub>) for the ketonization of hydrocarbons by oxygenated Fenton chemistry. *Co-Ord. Chem. Rev.* Vol. 165, pp. 297-313.

Dowideit P., Von Sonntag C and Leitzke O. (1995) *Abbau von chlorierten Olefinen durch Ozon und Ozon/Wasserstoffperoxid. gwf Wasser-Abwasser*. In press.

Eilbeck W.J., Mattock G. *Chemical Process in Waste Water Treatment*. Wiley: New York, 1987.

Enric Brillas., Roser Sauleda and Juan Carado. (1998) Degradation of 4-chlorophenol by anodic oxidation, electro-Fenton, Photoelectro-Fenton and peroxy-coagulation process. *J. Electrochem. Soc.* **145**(3), pp. 759-765.

Evelyn N., Prince Roger C. and Douglas Gregory S. (1997) In. Situ on-site bioremediation., Pap.Int. In situ on-site Bioremediation symposium., 4<sup>th</sup>, (4), 487-492.

Fenton H.J.H. (1894) Oxidation of tartaric acid in the presence of iron. *Chem. Soc. J. Lond.* **65**, 899-910.

Fernandez J., Bandara J., Lopez A., Buffat Ph. and Kiwi J. (1999) Photoassisted Fenton degradation of nonbiodegradable azo dye (Orange II) in Fe-free solutions mediated by cation transfer membranes. *Langmuir*. **15**(10), pp. 185-192.

Fernando Beltran J., Manuel Gonzalez., Francisco Rivas J. and Pedro Alvarez. (1998) Aqueous oxidation of three polynuclear aromatic hydrocarbons in water. *Water, Air, Soil Pollut.* **105** (3-4), pp. 685-700.

Fung P.C., Huang Q., Tsui S.M. and Poon C.S. (1999) Treatability study of organic and colour removal in desizing/dyeing wastewater by

UV/US system combined with hydrogen peroxide. *Wat. Sci. Tech.* **40**(1), pp. 153-160.

Fung P.C., Poon C.S., Chu C.W. and Tsui S.M. (2001) Degradation kinetics of reactive dye by UV/H<sub>2</sub>O<sub>2</sub>/US process under continuous mode operation. *Wat. Sci. Technol.* **44**(6), pp. 67-72.

Gau S.H., and Chang F.S., (1996) Improved Fenton method to remove recalcitrant organics in landfill leachate. *Wat. Sci. Tech.* Vol. **34**(7-8), Water Quality International. **196**(Part - 4), pp. 455-462.

Grayson M. and Eckroth D. (1981) *Kirk-Othmer Encyclopedia of Chemical Technology*, **13**, pp. 12-36. J.Wiley and Sons, New York.

Grayson M. (1981) *Kirk-Othmer Encyclopedia of Chemical Technology*, 3<sup>rd</sup> edition, Vol. 13, pp. 12-29. Wiley Interscience, New York.

Gregor K.H. (1994) Oxidative decolorization of textile wastewater with advanced oxidation processes. In *Chemical Oxidation Technologies for the Nineties*, Vol. 2, Eckenfelder, Jr., W.W., Bowers A.R. and Roth J.A. (Eds). Technomic Publishing Co. Inc., pp. 161-193.

Gun Kwon Bum., Le Dong Soo., Kang Namgoo and Yoon Jeyong. (1999) Characteristics of p-chlorophenol oxidation by Fenton's reagent. *Wat. Res.* **33**(9), pp. 2110-2118.

Gurnham C.F. (Ed) (1965) *Industrial Waste Control*. Academic Press, New York.

Haag, W.R., and Yao, C.C.D. (1992). "Rate constants for reaction of hydroxyl radicals with several drinking water contaminants". *Environ. Sci. Technol.*, **26**(5), 1005-1013.

Halmann M. (1992) Photo degradation of di-n-butyl-ortho-ohthalate in aqueous solutions. *J. Photochem. Photobiol. A: Chem.* **66**, pp. 215-223.

Herrera F., Kiwi J., Lopez A and Nadtochenko V. (1999) Photochemical decolorization of Remazol Brilliant Blue and Uniblue A in the presence of Fe<sup>3+</sup> and H<sub>2</sub>O<sub>2</sub>. *Environ. Sci. Technol.* **33**(18), pp. 3145 – 3151.

Herrera F., Pulgarin C., Nadtochenko V and Kiwi J. (1998) Accelerated photo-oxidation of concentrated p-coumaric acid in homogeneous solution. Mechanistic studies, intermediates and precursors formed in the dark. *J.Appl. Catal., B*, **17** (1-2), pp. 141-156.

Hoigne J. (1990) Formulation and calibration of environmental reaction kinetics: Oxidations by aqueous photo oxidants as an example. In *Aquatic chemical Kinetics, Reaction Rates of Processes in Natural Waters*, Stumm, W. (Ed). Wiley Interscience, New York, pp. 43-70.

Hornng Ken-Yang., Perng Ming-Jing., Tzou Wen-Yuang., Chen Chin-Hwa and Cheng, sheng-shung. (1997) A case study of a brewery factory wastewater treatment by anaerobic/aerobic and Fenton process. In. *Proc-WEFTEC' 96*, 3, pp. 531-538.

Houtmeyers J., Poffe R. and Verachert H. (1977) Hydrogen peroxide as a supplemental oxygen source for activated sludge: microbial investigations. *European J. Appl. Microbiol.* 4, pp. 295-305.

Huling S.G., Arnold R.G., Sierka R.A. and Miller M.R. (2001) Influence of peat on Fenton oxidation. *Wat. Res.* 35(7), pp. 1687 – 1694.

Huston P.L. and Pignatello J.J. (1996) Reduction of perchloroalkanes by ferrioxalate-generated carboxylate radical preceding mineralization by the photo-Fenton reaction. *Environ. Sci. Technol.* 30, pp. 3457-3463.

Herve Gallard., Joseph de Laat and Bernard Legube. (1998) Effect of pH on the rate of oxidation of organic compounds by Fe(II)/H<sub>2</sub>O<sub>2</sub>. Reaction mechanisms and modeling. *New J. Chem.* 22(3), pp. 263-268.

Hung-Yee Shu, Ching-Rong Huang. (1995) Ultraviolet enhanced oxidation for color removal of azo dye wastewater. *Amer. Dyest. Reprtr.* 20, pp. 30-34.

Huling Scott G., Arnold Robert G., Sierka Raymond A. and Miller Mathew R. (1998) Measurement of Hydroxyl radical activity in a soil slurry using the Spin Trap  $\alpha$ -(4-Pyridyl-1-Oxide) – N-tert-butylnitron. *Environ. Sci. Technol.* 32(21), pp. 3436-3441.

Ince N.H. and G.Tezcanli. (1999) Treatability of textile dye-bath effluents by advanced oxidation: preparation for reuse. *Wat. Sci. Tech.* Vol. 40(1), pp. 183-190.

Ince N.H., Stefan M.I. and Bolton J.R. (1997) UV/H<sub>2</sub>O<sub>2</sub> degradation and toxicity reduction of textile azo dyes: Remazol Black-B, a case study. *J. Adv. Oxid. Technol.* 2(3), pp. 442-448.

Ince N.H. (1999) "Critical" effect of hydrogen peroxide in photochemical dye degradation. *Wat. Res.* 33(4), 1080-1084.

Isak V.G., Sychev A.Ya. and Anikina (1996) Kinetics of oxidation of aldehydes by the Fenton reagent. *Fiz.Khim.* 70(8), pp. 1534-1536.

Jack T. Spadaro, Lorne Isabelle, and V.Renganathan. (1994) Hydroxyl radical mediated degradation of azo dyes: Evidence for benzene generation. *Environ. Sci. Technol.* **28** (7), pp. 1389-1393.

Jaime Rodriguez, David Contreras, Carolina Parra, Juanita Freet, Jaime Baeza and Nelson Duran. (1999) Fenton oxidation of pulp mill effluents. *Wat. Sci. Tech.* **40**(11-12), pp. 351-355.

Javier F. Benitez., Beltran Heredia Jesus., Juan L. Acerio., Javer F. Rubio. (1999) Chemical decomposition of 2,4,6-trichlorophenol by ozone, Fenton's reagent and UV radiation. *Ind. Eng. Chem. Res.* **38**(4), pp. 1341-1349.

Johannes. (1985) Decomposition of ozone in water in presence of organic solutes action as promoters and inhibitors of radical reaction. *Environ. Sci. Technol.* **19**, pp. 1206-1213.

Joseph J. Pignatello. 1992 Dark and photo assisted  $\text{Fe}^{3+}$  catalyzed degradation of chlorophenoxy herbicides by hydrogen peroxide. *Environ. Sci. Technol.* **26**(5), pp. 944-951.

Joseph J. Pignatello and Yunfu Sun. (1995) Complete oxidation of metolachlor and methyl parathion in water by the photoassisted Fenton reaction. *Wat. Res.* **29**, No.8, pp. 1837-1844.

Joseph J. Pignatello. (1992) Dark and photoassisted  $\text{Fe}^{3+}$  catalyzed degradation of chlorophenoxy herbicides by hydrogen peroxide. *Environ. Sci. Technol.* **26**(5), 944-951.

Jurg Hoigne. (1997) Inter-calibration of OH radical sources and water quality parameters. *Wat. Sci. Tech.* **35**(4), pp. 1-8.

Kaiqun Wu., Yinde Xie., Zhao Jincai and Hidaka Hisao. (1999) Photo-Fenton degradation of dye under visible light. *J. Mol. Catal. A: Chem.* **144**(1), pp. 77-84.

Kalpana Pratap and Ann Lemley T.J. (1998) Fenton electrochemical treatment of aqueous atrazine and metolachlor. *J. Agric. Food Chem.* **46**(8), pp. 3285-3291.

Kang S.F., Liao C.H. and Chen M.C. (2002) Pre-oxidation and coagulation of textile wastewater by the Fenton process. *Chemosphere.* **46**(6), pp. 923 – 928.

Kang S.F., Liao C.H. and Po S.T. (2000) Decolorization of textile wastewater by photo-Fenton oxidation technology. *Chemosphere*, **41**(8), pp. 1287 – 1294.



Kang Shyh Fang., Wang Tea Hsiu and Lin Yen Han. (1999) Decolorization and degradation of 2,4-dinitrophenol by Fenton's reagent. *J. Environ. Sci. Health, Part A : Toxic/Hazard Subst. Environ. Eng. A.* **34** (4), pp. 935 – 950.

Kim Soo M., Geissen Sven U. and Vogelpohl Alfons. (1997) Landfill – leachate treatment by a photoassisted Fenton reaction. *Wat. Sci. Technol.* **35**(4), pp. 239-248.

Kim Soo Myung and Vogel Pohl Afons. (1998) Degradation of organic pollutants by the photo-Fenton process. *Chem. Eng. Technol.* **21**(2), pp. 187-191.

Kitis M., Adams C.D. and Daigger G.T. (1999) The effects of Fenton's reagent pretreatment on the biodegradation of non-ionic surfactants. *Water Res.* **33**(11), pp. 2561-2568.

Kiwi J., Lopez A. and Nadtochenko V. (2000) Mechanism and kinetics of the OH – radical intervention during Fenton oxidation in the presence of a significant amount of radical scavenger (Cl<sup>-</sup>). *Environ. Sci. Technol.* **34**(11), pp. 2162 – 2168.

Kiwi J., Pulgarin C. and Peringer P. (1994) Effect of Fenton and photo-Fenton reactions on the degradation and biodegradability of 2 and 4-nitrophenols in water treatment. *Appl.Catal.B: Environ.* **3**, pp. 335-350.

Kremer M.L. (1999) Mechanism of the Fenton reaction. Evidence for a new intermediate. *Phys. Chem. Chem. Phys.* **1**(15), pp. 3595 – 3605.

Kuo W.G. (1992) Decolorizing dye wastewater with Fenton's reagent. *Wat. Res.* **26**, pp. 881-886.

Kuo chao-Yin., Lo Shang-Lien and Chan Min-Tse. (1997) Oxidation of aqueous chlorophenols with photo-Fenton process. *J. Environ. Sci. Health, Part B*, **33**(6), pp. 723 – 747.

Kuo Chao Yin and Lo shang Lien. (1999) Oxidation of aqueous chlorobiphenyls with Photo-Fenton process. *Chemosphere*, Vol. **38**(9), pp. 2041-2051.

Kwon B.G., Lee D.S., Kang N. and Yoon J. (1999) Characteristics of p-chlorophenol oxidation by Fenton's reagent. *Wat. Res.* **33**(9), pp. 2110 – 2118.

Larson R.A., Schlauch M.B. and Marley K.A. (1991) Ferric ion promoted photodecomposition of triazines. *J. Agric. Fd. Chem.* **39**, 2057-2062.

Lee B.D. and Hosomi M. (2001) A hybrid Fenton oxidation – microbial treatment for soil highly contaminated with Benz(a)anthracene. *Chemosphere*, **43**(8), pp. 1127 – 1132.

Lee B.D. and Hosomi M. (2001) Fenton oxidation of ethanol-washed distillation-concentrated benzo(a)pyrene: Reaction product identification and biodegradability. *Wat. Res.* **35**(9):2314-2319.

Legrini O., Oliveros E. and Braun A.M. (1993) Photochemical processes for water treatment. *Chem.Rev.* **93**, pp. 671-698.

Lei Lecheng., Hu Xijun., Lock Yue, Pl., Bossmann Stefan H., Gob Sabine and Braun Andre M. (1998) Oxidative degradation of polyvinyl alcohol by the photochemically enhanced Fenton reaction. *J. Photochem. Photobiol. A.* **116**(2), pp. 159-166.

Leonard Stephen., Gannet Peter M., Rojanarakul You., Schwegler – Berry Diane., Castranova Vince., Vallyathan Val. and Shi Xianghin. J. (1998) Cobalt mediated generation of reactive O<sub>2</sub> species and its possible mechanism. *J Inorg. Biochem.* **70**(3/4), pp. 239-244.

Li Z.M., Comfort S.D. and Shea P.J. (1997) Destruction of 2,4,6-Tri Nitro Toluene by Fenton oxidation. *J. Environ. Qual.* **26**(2), pp. 480-487.

Li Z.M., Shea P.J. and Comfort S.D. (1997) Fenton oxidation of 2,4,6-TNT in contaminated soil slurries. *Environ. Eng. Sci.* **14**(1), pp. 55-66.

Li.Z.M., Shea P.J. and Comfort S.D. (1998) Nitrotoluene destruction by UV-catalyzed Fenton oxidation. *Chemosphere.* **36**(8), pp. 1849-1865.

Liao Chih Hsiang., Kang Shyh Fang and Hung Pin. (1999) Simultaneous removal of COD and color from dye manufacturing process wastewater using Photo-Fenton oxidation process. *J. Environ. Sci. Health, Part A: Toxic / Hazard. Subst. Environ. Eng., A.* **34**(4), pp. 989-1012.

Lin sheng H. and Chen Mogul. (1997) Purification of textile wastewater effluents by a combined Fenton process and ion exchange. *Desalination.* **109**(2), pp. 121-130.

Lin sheng H., Lo Choc. (1997) Fenton process for the treatment of desizing wastewater. *Wat.Res.* 1997, **31**(8), pp. 2050-2056.

Lin Binle., Yamaguchi R., Hosami M and Murakami A. (1998) A new treatment process for photo-processing waste using a sulfur oxidizing bacteria/granular activated carbon system followed by Fenton oxidation. *Wat. Sci. Tech.* **38**(4-5), pp. 163 – 170.

Lindsey M.E. and Tarr M.A. (2000) Quantitation of hydroxyl radical during the Fenton oxidation following a single addition of iron and peroxide. *Chemosphere*, **41**(3), pp. 409 – 417.

Lloyd Roger V., Hanna Phillip M. and Maron Ronald P. (1997) The origin of the hydroxyl radical  $O_2$  in the Fenton reaction. *Free Radical Biol. Med.* **22**(5), pp. 885-888.

Lin Jin-Graw., Chao Allen C. and Ma Ying Shih. (2000) Oxidation of 2-chlorophenol from wastewater with the ultrasonic and Fenton process. *J. Environ. Eng. ASCE.* **125**(2), pp. 130 – 137.

Lu Jun, Gilbert Eberle S.H. (1994) Oxidation of wastewater containing phenol by catalytic oxidation with  $H_2O_2$  and ferric ion as catalyst. *Shanghai Huavjing Kexue* 1994, **13**(7), pp. 16-19.

Lu M.C. (2000) Oxidation of chlorophenols with hydrogen peroxide in the presence of goethite. *Chemosphere.* **40**(2), pp.125 – 130.

Lu Ming- Chun., Chen Jong – Nan and Chang chen – Ping. (1997) Effect of inorganic ions on the oxidation of dichlorvos insecticide with Fenton's reagent. *Chemosphere.* **35**(10), pp. 2285-2293.

Lu Ming- Chun., Chen Jong – Nan and Chang chen – Ping. (1997) Factors affecting the oxidation of Dichlorvos insecticide by Fenton's reagent. *Hazard. Ind. Wastes.* **30**, pp. 899-908.

Li Yuan shen., You Young Hao and Chung Hsin Yu. (1996) Degradation of 2,4-dichlorophenol wastewater by hydrogen peroxide in the presence of basic oxygen furnace slag. *Environ. Eng. Sci.* **16**(4), pp. 275-285.

Lin S.H. and Peng C.F. (1996) Continuous treatment of textile wastewater by combined coagulation, electrochemical oxidation and activated sludge. *Wat. Res.* **30**(3), pp. 587-592.

Lin S.H. and Peng C.F. (1995a) Treatment of textile wastewater by Fenton's reagent. *J. Environ. Sci. Health.* **A 30**(1), pp. 541-560.

Lin S.H. and Peng C.F. (1995b) A continuous Fenton's process for treatment of textile wastewater. *Environ. Technol.* **16**, pp. 693-699.

Lin S.H. and Peng C.F. (1995) Treatment of textile water by Fenton's reagent. *J. Environ. Sci. Health.* **30**, pp. 89-98.

Lipezynska-Kochany E. (1991) Novel method for a photo-catalytic degradation of 4-nitrophenol in homogeneous aqueous solution. *Environ. Technol.* **12**, pp. 87-92

Little L.W. (1977) Acute toxicity of selected commercial dyes to the fathead minnow and evaluation of biological treatment for reduction of toxicity. *Proc. Purdue. Indust. Wastes Conf.*

Mabury S.A. and Crosby D.G. (1994) The relationship of hydroxyl reactivity to pesticide persistence. In *Aquatic and Surface Photochemistry*, Eds. G.R. Helz, R.G.Zepp and D.G. Crosby, pp. 149-161. Lewis Publishers, Ann Arbor.

Margaret A. Engwall., Joseph J. Pignatello and Domencio Grasso. (1999) Degradation and detoxification of the wood preservative Creoste and pentachlorophenol in water by photo-Fenton reaction. *Water Res.* **33**(5), pp. 1151-1158.

Michael Pittroff, Dr.Karl Heinz Gregor, Hollriegelskreuth. (1992) Decolorization of textile wastewaters by UV-radiation with hydrogen peroxide. *Melliand Textilberichte.* **73**, 1992, pp. E-245.

Miller Christopher M., Valentine Richard L., Roehl Marc E and Alvarez Pedro. (1996) Chemical and microbiological assessment of pendimethalin contaminated soil after treatment with Fenton's reagent. *Wat. Res.* **30**(11), pp. 2579-2586.

Mixed waste, Proc. Bienn. Symp., 3<sup>rd</sup> (1995), Ed.Moghissi A.Alan, Love Betty R., Blauvelt Richard. K. 1995.

Moore, S.B.; Antenucci, A. *Abstracts of Papers, ACS National Meeting*, Denver, CO; American Chemical Society: Washington, DC, 1993; pp.465-466.

Muszkat L., Halmann M., Raucher D. and Bir L. (1992) Solar photo degradation of xenobiotic contaminants in polluted well water. *J. Photochem. Photobiol. A: Chem.* **65**, pp. 409-417.

Nadtochenko V. and Kiwi J. (1997) Photoinduced adduct formation between orange II and  $\text{Fe}^{3+}$  (aq) or  $\text{Fe}(\text{OX})_3^{3-}\text{H}_2\text{O}_2$ . *J. Chem. Soc., Faraday Trans.* **93**(14), pp. 2373 – 2378.

Nadtochenko V. and Kiwi. J. (1998) Primary photochemical reactions in the Photo-Fenton system with Ferric chloride: 1 A case study

of Xylidine oxidation as a model compound. *Environ. Sci. Technol.* **32**(21), pp. 3273-3281.

Nadtochenko V. and Kiwi. J. (1998) Photoinduced mineralization of Xylidine by the Fenton Reagent:2 Implications of the precursors formed in the dark. **32**(21), pp. 3282-3285.

Namboodri, C.G., and Walsh, W.K. (1996) Ultraviolet light / Hydrogen peroxide system for decolorizing spent reactive dye bath wastewater. *Amer.Dyest.Reptr.* **23**(4), pp.15-24.

Neta P., Huie R.E and Ross A.B. (1988) Rate constants for reactions of inorganic radicals in aqueous solution. *J. Phys. Chem. Ref. Data*, **17**, pp. 1027-1284.

Oliveros E., Legrini O., Hohl M., Muller T. and Braun A.M. (1997) Large scale development of a light-enhanced Fenton reaction by optimal experimental design. *Wat. Sci.Tech.* **35**(4), pp. 223-230.

Oliveros Esther, Legrini Omar., Hohl Mathias., Muller Thomas and Braun Andre M. (1997) Industrial wastewater treatment: Large scale development of light-enhanced Fenton's reagent. *Chem. Eng. Process.* **36**(5), pp. 397-405.

Park T.J., Lee K.H., Jung E.J. and Kim C.W. (1999) Removal of refractory organics and color in pigment wastewater with Fenton Oxidation. *Wat. Sci. Tech.* **39**(10-11), pp. 189-192.

Patrick L.Huston and Joseph J.Pignatello. (1999) Degradation of selected pesticide active ingredients and commercial formulations in water by the photo-assisted Fenton reaction. *Wat. Res.* **33**(5), pp. 1238-1246, 1999.

Patrick L.Huston and Joseph J.Pignatello. (1996) Reduction of Perchloroalkanes by ferrioxalate-generated carboxylate radical preceding mineralization by the photo-Fenton reaction. *Environ. Sci. Technol.* **30**(12), pp. 55-60.

Perez Benito J.F. and Arias C. (1999) Mutual catalyst inhibition in the Chromium (VI) – copper (II) – hydrogen peroxide reacting system. *New J. Chem.* **23**(9), pp. 945 – 949.

Peterson M.M., Comfort S.D., Horst G.L., Shea P.J. and Oh B.T. (1997) Remediating TNT-contaminated soil-by-soil washing and Fenton oxidation. *Sci. Total Environ.* **204**(2), pp. 107-115.

Pignatello J.J., Liu D. and Huston P. (1999). Evidence for an additional oxidant in the photoassisted Fenton reaction. *Environ. Sci. Technol.* **33**(11), pp. 1832 – 1839.

Poulios I and Aetopoulou I. (1999) Photocatalytic degradation of the textile dye reactive orange 16 in the presence of TiO<sub>2</sub> suspensions. *Environ. Technol.* **20**(5), pp. 479-487.

Prousek J. and Duriskova I. (1998) Oxidative degradation of polyethylene glycols (PEG) by the Fenton and Photo-Fenton reactions. *Chem. Listy.* **92**(3), pp. 218-220.

Pulgarin Cesar O., Peringer Paul A. and Kiwi John T. (1996) Efficient visible light induced degradation of the brightener Tinopal CBS-X. Accelerated bacterial adsorption observed after photocatalytic treatment. *J. Adv. Oxid. Technol.* **1**(1), pp. 85-93.

Perkins W.S., Judkins J.F. Jr. and Perry W.D. (1980) Renovation of dyebath water by chlorination or Ozonation. Part I: reaction of dyes. *Textile Chem. Color.* **12**, pp. 182-187.

Peyton G.R. and Glaze W.H. (1986) Mechanism of photolytic Ozonation. In *Photochemistry of Environmental Aquatic Systems*, Eds R.G.Zika and W.J.Cooper, *ACS Symposium Series 327*. Am.Chem.Soc, Washington DC, pp. 76-88.

Pignatello J.J. (1992) Dark and photo assisted Fe<sup>3+</sup> catalyzed degradation of chlorophenoxy herbicides by hydrogen peroxide. *Environ. Sci. Technol.* **26**, pp. 944-951.

Pignatello J.J. and Chapa G. (1994) Degradation of PCBs by ferric ion, hydrogen peroxide and UV light. *Environ.Toxicol. Chem.* **13**, pp. 423-427.

Pignatello J.J. and Sun Y. (1995) Complete oxidation of metolachlor and methyl parathion in water by the photo assisted Fenton reaction. *Wat. Res.* **29**,pp. 1837-1844.

Porter J.J. (1972) Treatment of textile waste with activated carbon. *Am. Dyestuff. Rep.* **61**, pp. 8-12.

Prat C., Vincente M. and Espillugas S. (1988) Treatment of bleaching wastes in the paper industry by hydrogen peroxide and ultraviolet radiation. *Wat. Res.* **22**, pp. 663-668.

Prousek J. (1995) Fenton reaction after a century. *Chemicke Listy.* **89**(1), pp. 11-21.

Ralf Dillert., Jorg Huppertz., Arne Renwanz., Ulrike Siebers and Detlef Bahemann. (1999) Light-induced degradation of nitroaromatic compounds in aqueous systems: comparison between titanium dioxide photocatalysis and photo-Fenton reaction. *J. Adv. Oxid. Technol.* **4**(1), pp. 85-90.

Reife A. *Kirk-Othmer Encyclopedia of Chemical Technology*, 4<sup>th</sup> ed., Wiley: New York. 1993; **8**, pp. 753-783.

Richard J. Watts., Mathew D. Udell., Simgho Kong and Solomon W. Leung. (1999) Fenton – like soil remediation catalyzed by naturally occurring iron minerals. *Environ. Eng. Sci.* **16**(1), pp. 93-103

Rose timothy L. and Marren Peter J. (1993) Destruction of agent simulants by the Photo-Fenton reaction. *Proc. ERDEC Sci.Conf.Chem.Biol.Def.Res.* pp. 847-853.

Ruppert G., Bauer R and Heisler G. (1993) The photo-Fenton reaction - an effective photochemical wastewater treatment process. *J. Photochem. Photobiol. A: Chem.*, **73**, pp. 75-78.

Salem I.A. and El Maazawi M.S. (2000) Kinetics and mechanism of color removal of Methylene blue with hydrogen peroxide catalyzed by some supported alumina surfaces. *Chemosphere.* **41**(8), pp. 1173 – 1180.

Sanchez Laura., Pearl Jose., Domenech Xavier. (1996) Degradation of 2,4-Dichlorophenoxy acetic acid by in-situ photogenerated Fenton reagent. *Electrochim Acta.* **41**(13), 1981-1985.

Sara Goldstein and Dan Meyerstein. (1999) Comments on the mechanism of the "Fenton-like" reaction. *Acc. Chem. Res.* **32**(7), pp. 547-550.

Scott M.Arnold., William J.Hickey and Robin F.Harris. (1995) Degradation of Atrazine by Fenton's reagent: condition optimization and product quantification. *Environ. Sci. Technol.* **29**(8), pp. 2083 – 2089.

Sevimil M.F. and Kinaci C. (2002) Decolorization of textile wastewater by Ozonation and Fenton's process. *Wat. Sci. Tech.* **45**(12), pp. 279 – 286.

Sewekow and Leverkusen. (1993) Treatment of reactive dye effluents with hydrogen peroxide/iron(II) sulphate. *Melliand Textilberichte.* **74**(2), pp. 153 (E-69).

Sheng H.Lin and Ming L. Chen. (1997) Treatment of textile wastewater by chemical methods for reuse. *Wat. Res.* Vol. **31**, pp. 868-876.

Shyh-Fang Kang and Huey-Min Chang. (1997) Coagulation of textile secondary effluents with Fenton's reagent. *Wat. Sci. Tech.* **36**(12), pp. 215-222.

Shyh-Fang Kang, Chih-Hsaing Liao and Mon-Chu Chen. (2002) Pre-oxidation and coagulation of textile wastewater by the Fenton process. *Chemosphere.* **46**, pp. 923-928.

Sychev Y and Isak V. (1995) Iron compounds and the mechanisms of the homogeneous catalysis of the activation of O<sub>2</sub> and H<sub>2</sub>O<sub>2</sub> and the oxidation of organic substrates. *Russ. Chem Rev.* Vol. **64**, pp. 1105-1129.

Somnath Basu and Irvine Wei. W. (1998) Advanced Oxidation Process of 2,4,6-trichlorophenol in aqueous phase by Fenton's reagent. Part – I Effects of the amounts of oxidant and catalyst on the treatment reaction. *Chem. Eng. Commun.* **164**, pp. 111-137.

Somnath Basu and Irvine Wei. W. (1998) Advanced Chemical Oxidation of 2,4,6-trichlorophenol in aqueous phase by Fenton's reagent. Part – 2 Effects of the amounts of oxidant and catalyst on the treatment reaction. *Chem. Eng. Commun.* **164**, pp. 139-151.

Specht a., Bents S., Kohnemann M., Lichtenberg T. and Siefert E. (1996) Biological decomposition of Polycyclic Aromatic Hydrocarbon in combination with chemical oxidation. *Hamb.Ber.* 1996.

Swaminathan K., Sandhya S., Sophia A.C., Pachhade K. and Subrahmanyam Y.V. (2003) Decolorization and degradation of H – acid and other dyes using ferrous-hydrogen peroxide system. *Chemosphere.* **50**(5), pp. 619 – 625.

Solozhenko, E.G., Soboleva., N.M. and Goncharuk, V.V. (1995) Decolorization of azo dye solutions by Fenton's oxidation. *Wat. Res.* **29**(9), pp. 2206-2210.

Saayman G.B., Schutte C.F. and Van Leeuwen J. (1996) The effect of chemical bulking control on biological nutrient removal in a full-scale activated sludge plant. *Wat. Sci Tech.* **34**(34), pp. 275-282.

Saayman G.B., Schutte C.F. and Van Leeuwen J. (1998) Chemical control of filamentous sludge bulking in a full-scale biological nutrient removal activated sludge plant. *Ozone Science Engineering.* **20**(1), pp. 1-15.



Schuchmann M.N. and Von Sonntag. (1988) The rapid hydration of the acetyl radical. A pulse radiolysis study of acetaldehyde in aqueous solution. *J. Am. Chem. Soc.* **110**, 5698-5701.

Scott M.Arnold., William J.Hickey and Robin F.Harris. 1995 Degradation of Atrazine by Fenton's reagent: condition optimization and product quantification. *Environ. Sci. Technol.* **29**(8), pp. 2083 – 2089.

Sedlak D.L. and Andren A.W. (1991) Aqueous phase oxidation of polychlorinated biphenyls by hydroxyl radicals. *Environ. Sci. Technol.*, **25**, pp. 1419-1427.

Sedlak, D.L. and Andren. A.W. (1991) Oxidation of chlorobenzene with Fenton's reagent. *Environ. Sci. Technol.* **25**, pp. 777-782.

Shaw D.J. *Introduction of colloid and surface chemistry*, Butterworths: London, U.K., 1968.

Smis A.F.E. (1981) Phenol oxidation with hydrogen peroxide. *J. Effluent and Water Treatment*, **3**, pp. 109-112.)

Smis A.F.E. (1983) Industrial effluent treatment with hydrogen peroxide. *Chemistry and Industry*. **18**, pp. 555-558.

Snell F.D. and Etre L.S. (1971) *Encyclopedia of Industrial Chemical Analysis*. **14**, pp. 427, Interscience, New York.

Solozhenko E.G., Soboleva N.M. and Goncharuk V.V. (1995) Decolorization of azodye solutions by Fenton's oxidation. *Wat. Res.* **29**(9), pp. 2206-2210.

Stumm W. and Morgan J.J. (1962) Chemical aspects of coagulation. *J. Am. Wat. Wks Ass.* pp. 971-992.

Sun Y. and Joseph J. Pignatello. (1993a) Photochemical reactions involved in the total mineralization of 2,4-D by  $\text{Fe}^{3+}/\text{H}_2\text{O}_2$  and  $\text{Fe}^{3+}/\text{H}_2\text{O}_2$  /UV. *Environ. Sci. Technol.* **27**, pp. 304-310.

Sun Y. and Pignatello J.J. (1993b) Organic intermediates in the degradation of 2,4-dichlorophenoxy acetic acid by  $\text{Fe}^{3+}/\text{H}_2\text{O}_2$  and  $\text{Fe}^{3+}/\text{H}_2\text{O}_2$  /UV. *J.Agric.Food Chem.* **41**, pp. 1139-1142.

Tachiev G., Roth J.A. and Bowers A.R. (2000) Kinetics of hydrogen peroxide decomposition with complexed and "free" iron catalysts. *Int. J. Chem. Kinet.* **32**(1), pp. 24-35.

Tang Walter, Huang C.P., (1996) Effect of chlorine content of chlorinated phenols on their oxidation kinetics by Fenton's reagent. *Chemosphere*, **33**(8), pp. 1621-1635.

Tang W.Z. and Huang C.P. (1997) Stoichiometry of Fenton's reagent in the oxidation of chlorinated aliphatic organic pollutants. *Environ. Technol.* **18**(1), pp. 13-23.

Tang W.Z. and Huang C.P. (1996) 2,4-Dichlorophenol-oxidation kinetics by Fenton's reagent. *Environ. Technol.* **17**(12), 1371-1378.

Tang Walter Z., Huang C.P. (1996) An oxidation kinetic model of unsaturated chlorinated aliphatic compounds by Fenton's reagent. *J. Environ. Sci. Health, Part A.* **31**(10), pp. 2755-2775.

Tang Walter Z., Huang C.P. (1996) Effect of chlorine position of chlorinated phenols on their dechlorination kinetics by Fenton's reagent. *Waste Management.* **18**(8), pp. 615-622.

Turan Ertaş T and Gürol M.D. (2002) Oxidation of diethylene glycol with ozone and modified Fenton processes. *Chemosphere.* **47**(3), pp. 293 – 301.

U.S. Environmental Protection Agency. Recovery of Metals from sludges and wastewater; September 1991; EPA Report 1600/52-91/041.

U.S. Environmental Protection Agency. "Phosphorus Removal"; September 1987; EPA Report 625/1-87/001.

Venkatadri, R. and Peters, R.W. 1993 Chemical oxidation technologies: Ultraviolet light/Hydrogen peroxide, Fenton's reagent and Titanium dioxide-assisted photo catalysis. *Haz. Waste and Mat.* Vol. **10**, pp. 107-149.

Von Sonntag C., Dowideit P., Fang X., Mertens R., Pan X., Schuchmann M.N. and Schuchmann P.H. (1997) The fate of peroxy radicals in aqueous solution. *Wat. Sci. Tech.* **35**(4), pp. 9-15, 1997.

Von Sonntag C. (1987) *The Chemical Basis of Radiation Biology*, Taylor & Francis, London.

Walling C. and Kato S. (1971) The oxidation of alcohols by Fenton's reagent: the effect of copper ion. *J. Am. Chem. Soc.* **93**, pp. 4275-4283.

Walling C.H. (1975) Fenton's reagent revisited. *Acc. Chem. Res.* **8**, pp. 125-131.

Wang Teh Hsiu., Kang Shyh Fang and Lin yen Han. (1999) Comparison among Fenton-related processes to remove 2,4-dinitro phenol. *J. Environ. Sci. Health, Part A: Toxic/Hazard. Subst. Environ. Eng. A.* **34**(6), pp.1267-1281.

Wang Xiaojiang., Brusseau and Mark L. (1998) Effect of Pyrophosphate on the dechlorination of tetrachloroethene by the Fenton reaction. *Environ. Toxicol. Chem.* **17**(9), pp. 1689 – 1694.

Walter Z.Tang and Rena Z.Chen. (1996) Degradation kinetics and mechanisms of commercial dyes by H<sub>2</sub>O<sub>2</sub>/Iron powder system. *Chemosphere.* **32**(5) pp. 947-958.

Watts, R.J., Udell, M.D., and Mosen, R.M. (1993) Use of iron minerals in optimizing the peroxide treatment of contaminated soils. *Water Envir. Res.*, **65**(7), pp. 839-844.

William J.Walker., Timothy Holbrook B. and Dale W. Evans. (1996) Destruction of chlorinated organic compounds in soil and water with hydrogen peroxide. In *Proc., Annu. Meet – Air and waste Manage. Assoc.* **89<sup>th</sup>**, pp. 4-6.

Wilcock A.E., Brewster M., Peck G. In *Environmental Chemistry of Dyes and Pigments*: Reife A., Freeman H.S. Eds., Wiley New York, 1996, p. 61.

Wu K.Q., Sie Y.D., Zhao J.C. and Hidaka H. (1999) Photo-Fenton degradation of a dye under visible light irradiation. *J. Mol. Catal. A – Chem.* **144**(1), pp. 77 – 84.

Yang Yue-Ping., Wu Xing Yi., Xu Xin Hua and Wang Da Hui. (2001) Treatment of dyeing wastewater by photo-assisted Fenton system. *Gaoxiao Huaxue Gongcheng Xuebao.* **15**(3), pp. 242 – 247.

Yeh, C.K., and Noval, J.T. (1995) The effect of hydrogen peroxide on the degradation of methyl and ethyl tert-butyl ether in soils. *Water Envir. Res.* **67**(5), pp. 828-834.

Yoon J., Cho S., Cho Y and kim S. (1998) Characteristics of coagulation of Fenton reaction in the removal of landfill leachate organics. *Wat. Sci. Tech.* **38**(2), pp. 209-214.

Yoon J., Lee Y. and Kim S. (2001) Investigation of the reaction pathway of OH radicals produced by Fenton oxidation in wastewater treatment. *Wat. Sci. Technol.* **44**(5), pp. 15 – 21.

Yoo H.C., Cho S.H. and Ko S.O. (2001) Modification of coagulation and Fenton oxidation processes for cost-effective leachate treatment. *J. Environ. Sci. Health, Part A: Toxic/Hazard. Subst. Environ. Eng. A.* **36**(1), pp. 39 – 48.

Yozo Takemura, Kengo Seno-0, Tatsuo Mukai and Motoyuki Suzuki. (1994) Decomposing organic chlorine compounds in dry cleaning wastewater by Fenton's reaction on reticulated iron. *Wat. Sci. Tech.* **30**(3), pp. 129-137.

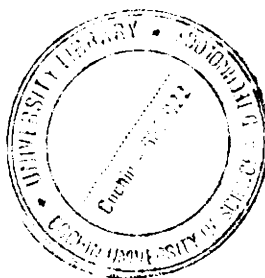
Yiqi Yang, David Travis Wyatt and Michael Bahorsky. (1998) Decolorization of dyes using UV/H<sub>2</sub>O<sub>2</sub> photochemical oxidation. *Textil. Chem. Col.* **30**(4), pp. 27-34.

Yunfu Sun and Joseph J. Pignatello. (1993) Photochemical reactions involved in the total mineralization of 2,4-D by Fe<sup>3+</sup>/H<sub>2</sub>O<sub>2</sub>/UV. *Environ. Sci. Technol.* **27**(2), pp. 304-310.

Zakharov I.V., Kumpan Yu.V. (1996) Inhibiting and chemiluminescent properties of benzoic acid and acetyl salicylic acid in the Fenton reagent. *Kinet. Catal.* (Translation of kinet. catal.) **37**(2), pp. 174-178.

Zambrowski Mark., Killion Holly., Miller Glenn. and Seiber James. (1997) The use of Fenton's reagent in the oxidation of contaminated hydrocarbon in drilling muds. In *Prepr. Pap. ACS Natl. Meet.*, Am.Chem.Soc., Div. Environ. Chem. **37**(2), 285-287.

Zhu Wanpeng, Yang Zhihua and Wang Li. (1996) Application of ferrous-hydrogen peroxide for the treatment of H-acid manufacturing process wastewater. *Wat. Res.* **30** (12), pp.2949-2954.



## **ERRATA**

Abraham Reife and Harold S. Freeman. (1996). Carbon adsorption of dyes and selected intermediates. In. *Envtl. Chemistry of Dyes and Pigments*, Eds. John Wiley and Sons, Inc.

Agrawal A., and Tratnyek P.G., (1996) Reduction of nitro aromatic compounds by zero-valent iron metal. *Environ. Sci. Technol.* **30**(1), 153-160.

Astrup T., Stripp L.S. and Thomas H. Christensen. (2000) Immobilization of chromate from coal fly ash leachate using an attenuating barrier containing zero-valent iron. *Environ. Sci. Technol.* **34**(19), 4163-4168.

Blowes W., Carol J. Ptacek and John L. Jambor. (1997) In-situ remediation of Cr(VI)- contaminated groundwater using permeable reactive walls: laboratory studies. *Environ. Sci. Technol.* **31**(12), 3348-3357.

Burris D.R., Campbell T.J., and Manoranjan V.S. (1995) Sorption of trichloroethylene and tetrachloroethylene in a batch reactive metallic iron-water system. *Environ. Sci. Technol.* **29**(11), 2850-2855.

Chew F and Tian C. Zhang. (1998) In-situ remediation of nitrate contaminated ground water electrokinetics/iron wall process. *Wat. Sci. Tech.* **38**(7), 135-142.

D.Tegtmeyer (1993) Possibilities and opportunities for membrane treatment of wastewater in textile dyeing. **74**(2), E-66, 148-151.

Demirer U., and S. Bowers A.R. (2000) Effects of surface oxidation and oxygen on the removal of trichloroethylene from gas phase using elemental iron. *Water Air and Soil Pollution.* **142** (1-4), 229-242.

Demirer U., and S. Bowers A.R. (2001) Effects of surface oxidation and oxygen on the removal of trichloroethylene from gas phase using elemental iron. *Water Air and Soil Pollution.* **142** (1-4), 229-242.

Devlin F., Jorg Klausen and Rene P. Schwarzenbach. (1998) Kinetics of nitroaromatic reduction on granular iron in recirculating batch experiments. *Environ. Sci. Technol.* **32**(13), 1941-1947.

Eykholt G.R., and Davenport D.T. (1998) Dechlorination of chloroacetanilide herbicides Alachlor and Meolachlor by iron metal. *Environ. Sci. Technol.* **32**(10), 1482-1487.

Farrell J., Mark Kason., Nicos Melitas and Tie Li. (2000) Investigation of the long-term performance of zero-valent iron for reductive dechlorination of trichloroethylene. *Environ. Sci. Technol.* **34**(3), 514-521.

Fiedor N., William D. Bobstick., Robert J. Jarabek and James Farrell. (1998) Understanding the mechanism of Uranium removal from groundwater by zero valent iron using X-ray photoelectron spectroscopy. *Environ. Sci. Technol.* **32**(10), 1466-1473.

Grittini C., Mark Malcomson., Quintus Fernando and Nic Korte. (1995) Rapid dechlorination of polychlorinated biphenyls on the surface of a Pd/Fe bimetallic system. *Environ. Sci. Technol.* **29**(11), 2055-2060.

Henz A. and Pfenninger H. (to Ciba-Geigy A-G) Jpn. Pat. 62186986 (Aug. 15, 1987).

Hobbs J.S. (1989) Acquisition and use of data for assessment of the environmental impact of colorants. 355-352. Vol. 105 Oct. 1989.

Hofstetter B., Cornelis G. Heijman., Stefan B. Haderlein., Christof Holliger and Bene P. Schwarzenbach. (1999) Complete reduction of TNT and other (poly) nitroaromatic compounds under iron-reducing subsurface conditions. *Environ. Sci. Technol.* **33**(9), 1479-1487.

Hugelshofer P., Zbinden P. and Koli Z (to Ciba-Geigy Corp) U.S.Pat. 4,436,523 (May 13, 1984).

Hung M., Frank H. Ling and Michael R. Hoffmann. (2000) Kinetics and mechanism of the enhanced reductive degradation of Nitrobenzene by elemental iron in the presence of Ultrasound. *Environ. Sci. Technol.* **34**(9), 1758-1763.

Ince N.H. and Tezcanli G. (1999) Treatability of textile dye-bath effluents by advanced oxidation: preparation for reuse. *Wat. Sci. Tech.* Vol. **40**(1), pp. 183-190.

Johnson L., Michelle M. Scherer and Paul G. Tratnyek. (1996) Kinetics of halogenated organic compound degradation by iron metal. *Environ. Sci. Technol.* **30**(8), 2534-2640.

Kroll J., Mols H.H., Ditzer R., Martiny and Steiner K.H. (to Bayer A-G) Ger. Offen. DE 3,148,878 (June 23, 1983).

Kulla H.G.; Klausener F; Meyer U; Ludeke B; Leisinger T *Arch. Microbiol.* (1983) **135**. 1-7.

Li T., and Farrell J., (2000) Reductive dechlorination of trichloroethene and carbon tetrachloride using iron and palladized-iron cathode. *Environ. Sci. Technol.* **34**(1), 173 – 179.

Lloyd K.C., Boardman G.D. and Michelsen D.C. (1992) Anaerobic/Aerobic Treatment Of A Textile Dye Wastewater. Preprinted for the mid-Atlantic Industrial Waste Conference, Morgan Town, WV, July 15-17, 1992.

Mantha R., Biswas N., Taylor K.E. and Bewtra J.K. (2001) Removal of nitroaromatics from synthetic wastewater using two-step zero-valent iron reduction and peroxidase-catalyzed oxidative polymerization. *Wat. Environ. Res.* **74**(3), 280-287.

Martin A., and J. Houston Kempton. (2000) In situ stabilization of metal-contaminated groundwater by hydrous ferric oxide: An experimental and modeling investigation. *Environ. Sci. Technol.* **34**(15), 3229-3234.

Matheson and Tratnyek P.G. (1994) Reductive dehalogenation of chlorinated methanes by iron metal. *Environ. Sci. Technol.* **28**(12), 2045-2053.

Melitas N., Ouafra Chuffe Moscoso and James Farrell. (2001) Kinetics of soluble chromium removal from contaminated water by zero-valent iron media: corrosion inhibition and passive oxide effects. *Environ. Sci. Technol.* **35**(19), 3948 – 3953.

Ponder M., John G. Darab and Thomas E. Mallouk. (2000) Remediation of Cr(VI) and Pb(II) aqueous solutions using supported, nanoscale zero-valent iron. *Environ. Sci. Technol.* **34**(12), 2564-2569.

Porter J.J. and Rozelle (1990) Membrane filtration techniques used for recovery of dyes, chemicals and energy. *Text. Chem. Color.* **22**(6), 21-25.

Pratt M., David W. Blowes and Carol J. Ptacek. (1997) Kinetics of chromate reduction on proposed subsurface remediation material. *Environ. Sci. Technol.* **31**(9), 2492-2498.

Prousek J. (1995) Fenton reaction after a century. *Chemické Listy.* **89**(1), pp. 11-21.

Sayles G.D., Guanrong You., Maoxiu Wang and Margaret J. Kupferle. (1997) DDT, DDD and DDE dechlorination by zero-valent iron. *Environ. Sci. Technol.* **31**(12), 3448-3454.

Scherer M. M., Kathleen M. Johnson., John C. Westall and Paul G. Tratnyek. (2001) Mass transport effect of the kinetics of Nitrobenzene reduction by iron metal. *Environ. Sci. Technol.* **35**(13), 2804-2811.

Sivavec T.M., and Horney, D.P., Reductive dechlorination of chlorinated ethenes by iron metal., 208<sup>th</sup> National Meeting, American Chemical Society, Anaheim, C.A., *Environmental Division Extended Abstracts*; American Chemical Society; Washington D.C. 1995; 695-698.

Spiro M. (1989) In *Chemical Kinetics*, Vol.28, Reactions at the Liquid-Solid Interphase; Compton, R.G., Ed.; Elsevier: Amsterdam, 1989: pp 69-166.

Su C., and Puls R.W., (2001) Arsenate and Arsenite removal by zero-valent iron: kinetics, redox transformation and implications for in situ ground water remediation. *Environ. Sci. Technol.* **35**(7), 1487-1492.

Su C., and Robert W. Puls. (1999) Kinetics of Trichloroethene reduction by zerovalent iron and tin: pretreatment effect, apparent activation energy and intermediate products. *Environ. Sci. Technol.* **33**(1), 163-168.

Thomas A.O., Drury D.M., Norris G., O'Hannesin S.F., Vogan J.L. (1995) In *Contaminated Soil*; Van den Brink, S.J., Rosman R., Ahrend R., Eds., Kluwer:Amsterdam: The Netherlands, 1995: pp 1083-1091.

Walker G.M. and Weatherley L.R. (2000) Biodegradation and biosorption of acid anthraquinone dye. *Environ. Pollut.* **108**(2), 219-223.

Weber E.J. and Wolfe N.C. (1987) Kinetic studies of the reduction of aromatic azo compounds in anaerobic sediment/water systems. *Environ. Toxicol. Chem.* **6**, 911-916.

Willetts J.R.M. and Ashbolt N.J. (2000) Understanding anaerobic decolorisation of textile dye wastewater: mechanism and kinetics. *Wat. Sci. Tech.* **42**(1-2), 409-415.

Wust F.W., Ralf Kober., Oliver Schlicker and Andreas Dahmke. (1999) Combined zero and first order kinetic model of the degradation of TCE and cis-DCE with commercial iron. *Environ. Sci. Technol* **33**(23), 4304 - 4309.